IMPACT OF AEROSOLS (SAHARAN DUST AND MIXED) ON THE EAST MEDITERRANEAN OLIGOTROPHIC ECOSYSTEM, RESULTS FROM EXPERIMENTAL STUDIES

EDITED BY: Paraskevi Pitta, Barak Herut and Tatiana M. Tsagaraki
PUBLISHED IN: Frontiers in Marine Science

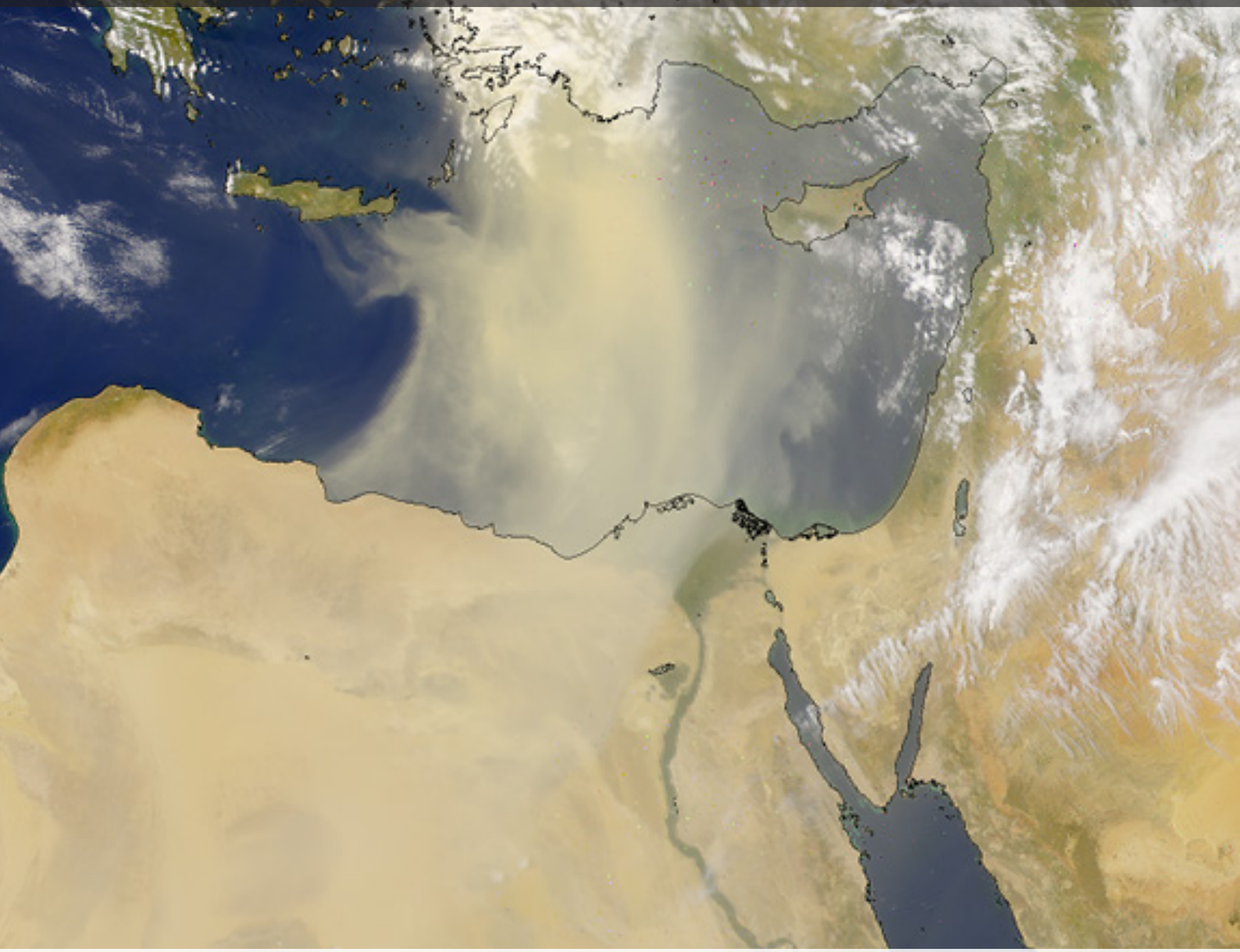

frontiers Research Topics

frontiers

ISSN 1664-8714
ISBN 978-2-88945-319-1
DOI 10.3389/978-2-88945-319-1

About Frontiers

Frontiers is more than just an open-access publisher of scholarly articles: it is a pioneering approach to the world of academia, radically improving the way scholarly research is managed. The grand vision of Frontiers is a world where all people have an equal opportunity to seek, share and generate knowledge. Frontiers provides immediate and permanent online open access to all its publications, but this alone is not enough to realize our grand goals.

Frontiers Journal Series

The Frontiers Journal Series is a multi-tier and interdisciplinary set of open-access, online journals, promising a paradigm shift from the current review, selection and dissemination processes in academic publishing. All Frontiers journals are driven by researchers for researchers; therefore, they constitute a service to the scholarly community. At the same time, the Frontiers Journal Series operates on a revolutionary invention, the tiered publishing system, initially addressing specific communities of scholars, and gradually climbing up to broader public understanding, thus serving the interests of the lay society, too.

Dedication to Quality

Each Frontiers article is a landmark of the highest quality, thanks to genuinely collaborative interactions between authors and review editors, who include some of the world's best academicians. Research must be certified by peers before entering a stream of knowledge that may eventually reach the public - and shape society; therefore, Frontiers only applies the most rigorous and unbiased reviews.
Frontiers revolutionizes research publishing by freely delivering the most outstanding research, evaluated with no bias from both the academic and social point of view.
By applying the most advanced information technologies, Frontiers is catapulting scholarly publishing into a new generation.

What are Frontiers Research Topics?

Frontiers Research Topics are very popular trademarks of the Frontiers Journals Series: they are collections of at least ten articles, all centered on a particular subject. With their unique mix of varied contributions from Original Research to Review Articles, Frontiers Research Topics unify the most influential researchers, the latest key findings and historical advances in a hot research area! Find out more on how to host your own Frontiers Research Topic or contribute to one as an author by contacting the Frontiers Editorial Office: **researchtopics@frontiersin.org**

IMPACT OF AEROSOLS (SAHARAN DUST AND MIXED) ON THE EAST MEDITERRANEAN OLIGOTROPHIC ECOSYSTEM, RESULTS FROM EXPERIMENTAL STUDIES

Topic Editors:
Paraskevi Pitta, Institute of Oceanography, Hellenic Centre for Marine Research, Greece
Barak Herut, Israel Oceanographic and Limnological Research, Israel
Tatiana M. Tsagaraki, University of Bergen, Norway

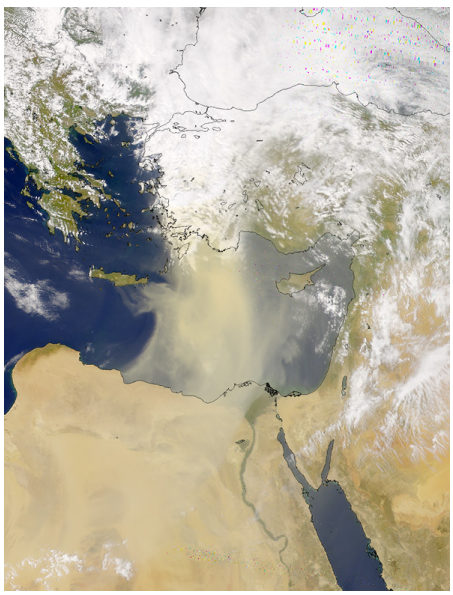

Intense dust event over the Eastern Mediterranean.

Image provided by the SeaWiFS Project, NASA/Goddard Space Flight Center, and ORBIMAGE, available at: https://visibleearth.nasa.gov/view.php?id=55469.

In oligotrophic environments, dust and nutrient inputs via atmospheric routes are considered important sources of macro-nutrients and micro-trace metals fuelling primary and secondary production. Yet, the impact of these dust inputs on the microbial populations is not fully investigated in the Eastern Mediterranean Sea (EMS). The response of oligotrophic systems to dust inputs, whether as positive or negative feedbacks to autotrophic and heterotrophic production and thus to biogeochemical cycling, is important to examine further.

Experimental studies have explored nutrient additions in various combinations to determine the limiting resource to productivity or N2 fixation. Recent experimental studies have applied dust enrichments to bottle or mesocosm incubations of seawater from different oceanic regions.

This research topic presents two Eastern Mediterranean dust addition mesocosm experiments using, for the first time, real aerosol additions, pure Saharan dust and mixed aerosols (a natural mixture of desert dust and polluted European particles), as well as other EMS aerosol experimental studies.

The topic includes manuscripts introducing results on: a) the impact of Saharan dust vs mixed aerosols on the autotrophic and heterotrophic surface microbial populations in the EMS, b) the impact of single vs multi-pulses of Saharan dust introduction into the pelagic environment of the EMS and c) other experimental studies of aerosol impacts on the EMS ecosystem.

Citation: Pitta, P., Herut, B., Tsagaraki, T. M., eds. (2017). Impact of Aerosols (Saharan Dust and Mixed) on the East Mediterranean Oligotrophic Ecosystem, Results from Experimental Studies. Lausanne: Frontiers Media. doi: 10.3389/978-2-88945-319-1

Table of Contents

frontiers in Marine Science

EDITORIAL
published: 21 August 2017
doi: 10.3389/fmars.2017.00264

Editorial: Impact of Aerosols (Saharan Dust and Mixed) on the East Mediterranean Oligotrophic Ecosystem, Results from Experimental Studies

Paraskevi Pitta[1]*, *Barak Herut*[2] *and Tatiana M. Tsagaraki*[3]

[1] Institute of Oceanography, Hellenic Centre for Marine Research, Crete, Greece, [2] Israel Oceanographic and Limnological Research, National Institute of Oceanography, Haifa, Israel, [3] Department of Biology, University of Bergen, Bergen, Norway

Keywords: Sharan dust, aerosols, eastern Mediterranean, mesocosm experiments, planktonic food web

Editorial on the research topic

Impact of Aerosols (Saharan Dust and Mixed) on the East Mediterranean Oligotrophic Ecosystem, Results from Experimental Studies

In oligotrophic environments, dust and nutrient inputs via atmospheric deposition are considered important sources of macro-nutrients and micro-trace metals fueling primary and secondary production. Yet, the impact of these dust inputs on the microbial populations has so far been partially investigated in the Eastern Mediterranean Sea (EMS). The objective of this special issue was to study the influence of dust deposition on the biological productivity, structure, and function of plankton and microbial communities in the Eastern Mediterranean. It is a collection of papers presenting the results of: (a) the impact of Saharan dust vs. mixed aerosols on the autotrophic and heterotrophic surface microbial populations in the EMS, (b) the impact of single vs. multi-pulses of Saharan dust introduction into the pelagic environment of the EMS, and (c) other experimental and field studies of aerosol impacts on the EMS ecosystem.

What is unique about the papers of this volume is that they focus on biological aspects covering a wide range of the pelagic food web, from viruses to copepods, using large-scale experimental approaches and using naturally collected aerosols, not dust analogs.

Two large-scale mesocosm experiments took place in Crete, Greece, in 2012 and 2014, at the HCMR mesocosm facility CretaCosmos (www.cretacosmos.eu). During the 2012 "ATMOMED" experiment, the addition of either natural pure Saharan dust or mixed aerosol (desert dust and polluted particles) in a single pulse into the ultra-oligotrophic environment of the Eastern Mediterranean took place. The 2014 "ADAMANT" experiment studied the effect of Saharan dust deposition on the pelagic microbial food web of the Eastern Mediterranean when added in multiple, successive dust pulses.

Seven papers (from the 2012 experiment, single addition) focus on the impact of atmospheric deposition (natural/Saharan dust vs. anthropogenic/mixed aerosol) on different parts of the pelagic microbial food web from viruses up to copepods. Herut et al. present an overview and rationale of this experiment with detailed information on the chemical characteristics of the aerosols (Saharan dust and polluted) used in 2012. Tsagaraki et al. present the overall response of the entire planktonic food web, from viruses to zooplankton, to the addition of Saharan dust and mixed aerosol. Rahav et al. study the impact of atmospheric deposition on N_2 fixation. Guo et al. focus on the bacterial community and investigate how the atmospheric input affects metabolic activities and community

OPEN ACCESS

Reviewed by:
Angel Borja,
AZTI Pasaia, Spain

***Correspondence:**
Paraskevi Pitta
vpitta@hcmr.gr

Specialty section:
This article was submitted to Marine Ecosystem Ecology, a section of the journal Frontiers in Marine Science

Received: *24 July 2017*
Accepted: *02 August 2017*
Published: *21 August 2017*

Citation:
Pitta P, Herut B and Tsagaraki TM (2017) Editorial: Impact of Aerosols (Saharan Dust and Mixed) on the East Mediterranean Oligotrophic Ecosystem, Results from Experimental Studies. Front. Mar. Sci. 4:264. doi: 10.3389/fmars.2017.00264

dynamics. Tsiola et al. concentrate on the impact of viral lysis and grazing by flagellates on bacterioplankton production. Meador et al. track variations in the lipidome associated with dust fertilization. Christou et al. describe the changes in the mesozooplankton community and evaluate the feeding response of the dominant copepod species.

Krom et al. present data from a microcosm experiment conducted in parallel with the 2012 mesocosm experiment. This microcosm experiment studies the effects of acid processes acting on Saharan dust in the atmosphere on primary and bacterial productivity and biomass.

Three papers present results from the second mesocosm experiment (multiple dust addition), conducted in Crete in 2014. Pitta et al. present the response of the whole microbial food web to the Saharan dust additions while also presenting data on the chemical signature of this dust. Lagaria et al. focus on the response of phytoplankton populations to Saharan dust depositions. In Tsiaras et al. a biogeochemical model is customized to simulate the 2014 mesocosm experiment.

Finally, there are three more papers; one on the effect of dust-associated airborne microbes deposited into the sea on marine autotrophic and heterotrophic production (Rahav et al.), one on the impact of dry deposition on the sea surface microlayer (Astrahan et al.) and a last one describing a long term flux of Saharan dust to the suburban area of Athens, Greece (Vasilatou et al.).

The mesocosm experiments were funded by two projects, the EU-FP7 project "MESOAQUA" (grant agreement no. 228224) and the project "ADAMANT" (nr code/MIS: 383551), co-financed by the European Union and Greek national funds. Additional funding to the authors is mentioned at the end of each paper. The captain and the crew of the R/V Philia as well as the scientific, technical and administrative staff that made these experiments happen are also thanked.

Finally, we would like to acknowledge the contribution of the handling editor as well as of numerous reviewers to the completion of the present special issue.

AUTHOR CONTRIBUTIONS

All authors listed have made a substantial, direct and intellectual contribution to the work, and approved it for publication.

Conflict of Interest Statement: The authors declare that the research was conducted in the absence of any commercial or financial relationships that could be construed as a potential conflict of interest.

frontiers in Marine Science

ORIGINAL RESEARCH
published: 15 November 2016
doi: 10.3389/fmars.2016.00226

The Potential Impact of Saharan Dust and Polluted Aerosols on Microbial Populations in the East Mediterranean Sea, an Overview of a Mesocosm Experimental Approach

Barak Herut[1], Eyal Rahav[1,2]*, Tatiana M. Tsagaraki[3,4], Antonia Giannakourou[5], Anastasia Tsiola[3], Stella Psarra[3], Anna Lagaria[5], Nafsika Papageorgiou[3], Nikos Mihalopoulos[6], Christina N. Theodosi[6], Kalliopi Violaki[6], Eleni Stathopoulou[7], Michael Scoullos[7], Michael D. Krom[8,9], Anthony Stockdale[8], Zongbo Shi[10], Ilana Berman-Frank[2], Travis B. Meador[11], Tsuneo Tanaka[12] and Pitta Paraskevi[3]*

[1] Israel Oceanographic and Limnological Research, National Institute of Oceanography, Haifa, Israel, [2] Mina and Everard Goodman Faculty of Life Sciences, Bar-Ilan University, Ramat-Gan, Israel, [3] Institute of Oceanography, Hellenic Centre for Marine Research, Heraklion, Crete, Greece, [4] Department of Biology, University of Bergen, Bergen, Norway, [5] Institute of Oceanography, Hellenic Centre for Marine Research, Anavyssos, Attiki, Greece, [6] Department of Chemistry, University of Crete, Heraklion, Crete, Greece, [7] Laboratory of Environmental Chemistry, Department of Chemistry, University of Athens, Athens, Greece, [8] School of Earth and Environment, University of Leeds, Leeds, UK, [9] Department of Marine Biology, Charney School of Marine Sciences, Haifa University, Haifa, Israel, [10] Department of Geography, Earth and Environmental Sciences, Birmingham University, Birmingham, UK, [11] MARUM Center for Marine Environmental Sciences, Bremen, Germany, [12] Laboratoire d'Océanographie Physique et Biogéochimique, Université de la Méditerranée, Marseille, France

OPEN ACCESS

Edited by:
Cosimo Solidoro, National Institute of Oceanography and Experimental Geophysics, Italy

Reviewed by:
Ursula Scharler, University of KwaZulu-Natal, South Africa
Maurizio Ribera D'Alcala', Stazione Zoologica Anton Dihrn, Italy

***Correspondence:**
Barak Herut
barak@ocean.org.il
Eyal Rahav
eyal.rahav@ocean.org.il

Specialty section:
This article was submitted to Marine Ecosystem Ecology, a section of the journal Frontiers in Marine Science

Received: *29 July 2016*
Accepted: *27 October 2016*
Published: *15 November 2016*

Citation:
Herut B, Rahav E, Tsagaraki TM, Giannakourou A, Tsiola A, Psarra S, Lagaria A, Papageorgiou N, Mihalopoulos N, Theodosi CN, Violaki K, Stathopoulou E, Scoullos M, Krom MD, Stockdale A, Shi Z, Berman-Frank I, Meador TB, Tanaka T and Paraskevi P (2016) The Potential Impact of Saharan Dust and Polluted Aerosols on Microbial Populations in the East Mediterranean Sea, an Overview of a Mesocosm Experimental Approach. Front. Mar. Sci. 3:226. doi: 10.3389/fmars.2016.00226

Recent estimates of nutrient budgets for the Eastern Mediterranean Sea (EMS) indicate that atmospheric aerosols play a significant role as suppliers of macro- and micro- nutrients to its Low Nutrient Low Chlorophyll water. Here we present the first mesocosm experimental study that examines the overall response of the oligotrophic EMS surface mixed layer (Cretan Sea, May 2012) to two different types of natural aerosol additions, "pure" Saharan dust (SD, 1.6 mg l^{-1}) and mixed aerosols (A—polluted and desert origin, 1 mg l^{-1}). We describe the rationale, the experimental set-up, the chemical characteristics of the ambient water and aerosols and the relative maximal biological impacts that resulted from the added aerosols. The two treatments, run in triplicates (3 m^3 each), were compared to control-unamended runs. Leaching of ~2.1–2.8 and 2.2–3.7 nmol PO_4 and 20–26 and 53–55 nmol NO_x was measured per each milligram of SD and A, respectively, representing an addition of ~30% of the ambient phosphate concentrations. The nitrate/phosphate ratios added in the A treatment were twice than those added in the SD treatment. Both types of dry aerosols triggered a positive change (25–600% normalized per 1 mg l^{-1} addition) in most of the rate and state variables that were measured: bacterial abundance (BA), bacterial production (BP), *Synechococcus* (Syn) abundance, chlorophyll-a (chl-*a*), primary production (PP), and dinitrogen fixation (N_2-fix), with relative changes among them following the sequence BP>PP≈N2-fix>chl-a≈BA≈Syn. Our results show that the "polluted" aerosols triggered a relatively larger biological

change compared to the SD amendments (per a similar amount of mass addition), especially regarding BP and PP. We speculate that despite the co-limitation of P and N in the EMS, the additional N released by the A treatment may have triggered the relatively larger response in most of the rate and state variables as compared to SD. An implication of our study is that a warmer atmosphere in the future may increase dust emissions and influence the intensity and length of the already well stratified water column in the EMS and hence the impact of the aerosols as a significant external source of new nutrients.

Keywords: mesocosm experiments, dust, aerosols, nutrients, trace metals, Eastern Mediterranean Sea

INTRODUCTION

In low-nutrient low-chlorophyll (LNLC) marine environments, nutrient and trace metal inputs via atmospheric aerosols are considered important sources of macro and micro nutrients (Duce et al., 1991, 2008; Jickells et al., 2005; Kanakidou et al., 2012), fueling microbial production and influencing the bacterioplankton community structure (Moore et al., 2013; Guieu et al., 2014a; Chien et al., 2016; Rahav et al., 2016a). The Eastern Mediterranean Sea (EMS), located in the so-called dust-belt (Astitha et al., 2012), is considered extremely oligotrophic (reviewed in Siokou-Frangou et al., 2010) and is strongly influenced by natural desert sources that contain some of the highest atmospheric dust (mineral aerosol) concentrations near the Earth's surface (Klingmüller et al., 2016). The EMS region has been identified in the last decade as a hot-spot of climate change, showing a decrease in precipitation and an increase in the temperature and annual number of unusually hot days (Hoerling et al., 2012; Lelieveld et al., 2012; IPCC, 2014). It is suggested that the increasing temperatures together with the decreasing relative humidity of the last decade, have promoted soil drying, leading to increased dust emissions in the EMS, a process that is expected to continue in the future due to climate change (Klingmüller et al., 2016) and consequently supply more macro and micro nutrients into its surface oligotrophic water.

The EMS is also exposed to relatively high pollution levels of aerosols (Lelieveld et al., 2002), which interact with the already high background levels of natural mineral particles. The bioavailability of nutrients and trace metals from aerosols is related to both, the original aerosol chemical and mineralogical composition and the interactions and chemical transformations during atmospheric transport (Baker et al., 2006; Baker and Jickells, 2006; Mackey et al., 2015). Recent studies have shown that the exposure to acid processes in the atmosphere can also change the phosphorus (P) bioavailability of dust/aerosols (Nenes et al., 2011; Bougiatioti et al., 2016).

Atmospheric deposition of nutrients to LNLC provinces is particularly important in regions where there is little input of new nutrients from other external sources (e.g., Jickells et al., 2005; Duce et al., 2008), as is the case in the EMS (Herut et al., 1999, 2002; Krom et al., 2004). Such inputs are more significant during stratified periods, as they enable new production in a period of generally low autotrophic production (Guieu et al., 2010). In addition to new production, it has been shown that leachable nutrients from atmospheric inputs may enhance N_2 fixation, changes in phytoplankton species composition and carbon sequestration (e.g., Mills et al., 2004; Guo et al., 2012; Moore et al., 2013; Bressac et al., 2014; Guieu et al., 2014b; Rahav et al., 2016a). While a low availability of macronutrients (N, P) and metal micronutrients (e.g., Fe, Co) can limit or co-limit phytoplankton growth in the ocean (e.g., Moore et al., 2013), high concentrations of some metals (e.g., Cu or Al) can be toxic to phytoplankton (e.g., Paytan et al., 2009; Jordi et al., 2012; Krom et al., 2016). Yet, the impact of these dust inputs on microbial populations has not been fully investigated in the EMS. The response of oligotrophic systems to dust inputs, whether as positive or as negative feedbacks to autotrophic and heterotrophic production (and thus to biogeochemical cycling), must therefore be further examined (Guieu et al., 2014a).

To date, these influences were assessed in the EMS mainly by on-board dust enrichment microcosm experiments (Herut et al., 2005; Ternon et al., 2011) or *in situ* observations (Rahav et al., 2016a), which showed an increase in primary production and in heterotrophic bacterial activity, while no previous mesocosm experiment has been performed. The use of large-scale mesocosms may be particularly important to reduce the effects of bottle enclosure that may change the autotrophic-heterotrophic biomass ratio, especially in oligotrophic regions such as the EMS (Calvo-Díaz et al., 2011). Similarly, a mesocosm experiments in the Western Mediterranean Sea examined the addition of a dust analog (treated Saharan soil) to surface seawater (Guieu et al., 2014b). In that experiment, the Saharan dust amendment strongly stimulated primary production and algal biomass and altered the autotrophic phytoplankton communities (Guieu et al., 2014b). Furthermore, these additions affected the structure, diversity and functioning of the microbial food web (Pulido-Villena et al., 2014) while also increasing the N_2 fixation rates (Ridame et al., 2013).

Here we present an overview of a mesocosm experimental study that examines the microbial response of the oligotrophic EMS surface mixed layer (Cretan Sea, May 2012) to two different types of natural aerosol additions; "pure Saharan dust" and "mixed aerosols" (a natural mixture of desert dust and polluted particles). To the best of our knowledge, this is the first mesocosm study in which naturally collected aerosols were used in the Mediterranean Sea. The added particles were designed to mimic the impact of an intense dry atmospheric deposition to the upper mixed layer (1–1.5 mg of dust l^{-1}) on the physiology and biomass of the ambient microbial populations of the EMS, using natural aerosols collected across the Levantine basin (Crete and

Israel). The two aerosol types were compared to control runs in triplicates for a total duration of 8 days.

This article provides a brief overview of the design, rationale, characteristics of the aerosols and the principal responses of the microbial variables in the mesocosm experiment, as part of a Research Topic entitled "Impact of aerosols (Saharan dust and mixed) on the East Mediterranean oligotrophic ecosystem, results from experimental studies." Other components of the mesocosm experiment, including microbial community structure and temporal dynamics, microbial biodiversity and function are discussed in other articles of this special issue (Guo et al., 2016; Rahav et al., 2016b; and others in this special issue).

MATERIALS AND METHODS

Mesocosm Experimental Design and Sampling

An aerosol-enrichment mesocosm experiment was performed at the CRETACOSMOS facility of the Hellenic Centre for Marine Research (HCMR, www.cretacosmos.eu) in Crete, Greece, during the 10–18 of May 2012. The facility consists of a 350 m^3 land-based concrete pond, 5 m deep, supplied with continuous seawater flow-through in order to maintain ambient surface water temperature. The experiment was carried out using surface (∼10 m depth) seawater that was collected using a rotary submersible pump placed onboard the R/V Philia from a location 5 nautical miles north of Heraklion (Crete, Greece, 35° 24.957 N, 25° 14.441 E) at a bottom depth of 170 m during the 8–9 of May 2012. The collected seawater was equally distributed by gravity into nine food-grade polyethylene mesocosm bags to ensure the homogeneity of the collected seawater between bags. The mesocosms were mounted on aluminum frames (1.12 m diameter) attached to the pool's walls. Each mesocosm had a total volume of 3 m^3 (**Figure 1**). The mesocosms were gently mixed throughout the experiment, using an airlift pump to avoid stratification. The mesocosms were covered with a two-layer lid in order to protect them from natural atmospheric aerosol depositions during the experiment and mimic the light conditions at a 10 m water depth. HOBO data loggers (ONSET Corporation) were installed to measure the temperature and light (irradiation) in each bag as well as in the main pond.

On May 10th at 08:30, samples were collected from all the mesocosms prior to the dust/aerosol additions to serve as reference conditions. At 11:45, the dust/aerosols were added to the mesocosms and the first sampling was carried out 3 h later at 14:45. Each mesocosm was sampled daily during the morning (08:30) from May 11th to 15th, 2012, and then once every 2 days until May 18th, apart from parameters that required more frequent monitoring, which were sampled every day throughout the experiment. Acid-washed silicone tubes were used for transferring the samples collected at about 50 cm depth into similarly treated 20 L Nalgene containers.

Two different types of natural additions were performed in triplicates: "pure" Saharan dust, (labeled as SD) and mixed aerosol containing a natural mixture of desert dust and polluted European particles (labeled as A). The additions of SD and A resulted in a final concentration of 1.6 and 1 mg l^{-1}, respectively, in the mesocosm bags (**Table 1**). Triplicate control (labeled C) mesocosm treatments were run in parallel. Each replicate addition was performed by pouring a concentrated mixture of the aerosol/dust with filtered (0.2 μm) seawater into the bags. This mixture was prepared just prior to the addition in pre-cleaned (10% hydrochloric acid washed) 100 ml polyethylene bottles. In order to mimic an intense dust storm effect, it was decided to add quantity equivalent to final concentration of 1.6 mg l^{-1} of aerosols in the mesocosm bags. Previous studies yielded a deposition of ∼1 mg of dust l^{-1} in the upper 5 m mixed layer during dust storm events in the EMS (Herut et al., 2005; Rahav et al., 2016a). Yet, due to the limited mass availability of aerosols representing an European origin (**Figure 2**), we prepared a mixture of desert/mineral dust and polluted aerosols (treatment A), allowing for an addition equivalent to only 1 mg l^{-1} in the relevant mesocosms (**Table 1**, **Figure 1**). *Aerosol chemical composition*—Analyses of the chemical compositions of SD and A aerosols were carried out after total digestion with HF and aqua regia, following the procedure of ASTM (1983) and Herut et al. (2001). The digested samples were diluted in 25 ml with Milli-Q water and filtered through a Whatman 42 filter paper. Briefly, 1 ml of aqua regia solution and 4 ml of hydrofluoric acid were added to ca. 0.15 g of dry aerosol in 125 ml plastic bottles (that can withstand temperatures of up to 1300°C on a sand bath). Prior to dilution, 5 ml of saturated boric acid was added to the resultant solution. The concentrations of trace elements were measured using an Agilent 280FS atomic absorption spectrometer, a graphite furnace Agilent 240Z AA and ICP-MS. Major elements were measured on an ICP-AES. The bottle blanks were usually less than 2% of the measured concentrations. The accuracy of the method was evaluated based on analyses of International Certified Reference Materials: MESS-4, SRM 2702, and IAEA 158. All elements gave results within 94–110% of the certified values, except for Cd, which gave an 80% recovery.

Aerosol Collection and Leaching Experiments

Dry deposited material was collected in Crete (Heraklion and Sambas) and Israel (Beit Yannay and Tel Shikmona, see Herut et al., 2002) during major Saharan dust storms and during periods that showed the transport of air masses was from Europe (**Table 1**, **Figure 2**). These two sites represent aerosols across the Levantine basin in the SE Mediterranean Sea. Aerosol origin and route was tracked by calculating 3-day back trajectories using the NOAA HYSPLIT model from the Air Resources Laboratory at 1000 and 3000 m altitude levels (**Figure 2**). We needed between 9 and 15 g of material for the additions to the different mesocosm replicates to obtain the final concentrations in the mesocosm bags (1 and 1.6 mg l^{-1}), and therefore material collected on different sampling dates was pooled, representing the two types of treatments (**Table 1**). However, while for the SD treatment sufficient material was collected, only a limited amount could be collected to represent a clear dominated polluted European

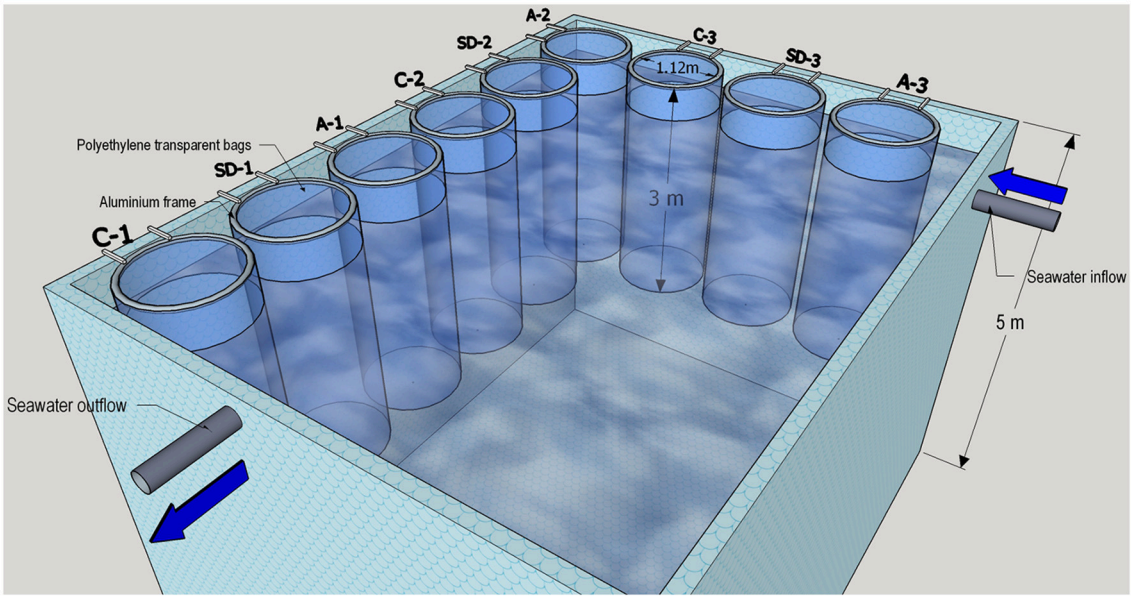

FIGURE 1 | A schematic illustration of the experimental mesocosm setup facility held in May 10-18 2012 in Crete. Two treatments (SD and A) and an unamended control (C) were run in triplicate 3 m^3 mesocosm bags.

TABLE 1 | Summary of the dust/aerosol origin and collection in this study.

	Saharan dust (SD)	Mixed polluted aerosols (A)
Location	Heraklion/Sambas (13.9 g) Beit Yannay (1.58 g)	Heraklion—(6.9 g) Haifa (2.8 g)
Sampling dates	3 May 2007; 8, 16, 22, 24, 25, 28 April 2012	8 May 2012; 6 April 2011; 1, 2, 12, 18 April 2012
Airflow sector*	Saharan dominated	European + desert component
Total amount collected prior the experiment (g)	14.7	9.5
Material added to mesocosms (mg l^{-1})	1.6	1.0-1.1

See also –Figure 2**.*

derived aerosols. Therefore, treatment A represents a mixture of European as well as desert aerosols (**Table 1**).

Leaching experiments were performed according to two different methodologies using sterile surface seawater from different origins, in the nutrient laboratories of the Israel Oceanographic and Limnological Research (Haifa) and at the University of Leeds (**Figure S1**). In Haifa, 250 ml plastic containers were pre-cleaned with 10% hydrochloric acid and washed afterwards with Milli-Q water. Each bottle was filled with filtered (0.2 μm), aged and poisoned (with 50 μL chloroform) SE Mediterranean surface seawater (collected with the R/V Shikmona, 40 km off the Israeli coast), to which 30 mg of SD or A powder was added. The bottles were covered with aluminum foil and shaken at room temperature for a total of 48 h. Subsamples (10 ml) collected at 0, 0.75, 2, 6, 24, and 48 h were pipetted using pre-cleaned (10% HCl) syringes through a 0.2 μm filter and immediately analyzed for nitrate+nitrite and phosphate concentrations. Nutrients were measured with a Seal Analytical AA-3 system (Kress et al., 2014; Ozer et al., in press). The precision level for nitrate+nitrite and phosphate was 0.02 and 0.003 μM, respectively. All analytical results were corrected against unamended blanks. The limit of detection (2 times the standard deviation of the blank) for the procedures was 0.075 μM for nitrate+nitrite and 0.008 μM for phosphate. For simplicity, we refer in the text to nitrate+nitrite as NO_x and to ortho-phosphate as P. The quality assurance of the nutrient measurements was confirmed by the results of inter-comparison exercises (NOAA/NRC, JAPAN, QUASIMEME).

In Leeds, prior to the leaching of phosphate, 120 ml plastic containers were coated with iodine by adding a crystal or two of elemental iodine and placed in an oven at 40°C for 10 min. The containers were then cooled to room temperature (22°C) and swilled with Milli-Q water to remove all the excess I_2. For the nitrate leaching, uncoated 250 ml plastic containers were used. For the phosphate leaching experiment, 50 ml of sterile seawater was added to each container in a biological safety cabinet. ~6 mg of accurately weighed dust was then added and the containers were placed on a shaking table for 30 min, 2, 6, 24, and 49 h situated in a light proof box. The duration of the leaching experiment was based on the study of Mackey et al. (2012), which found an increasing amount of leached P after 24–48 h, and assumed stabilization. At each sampling, ~7 ml were removed by

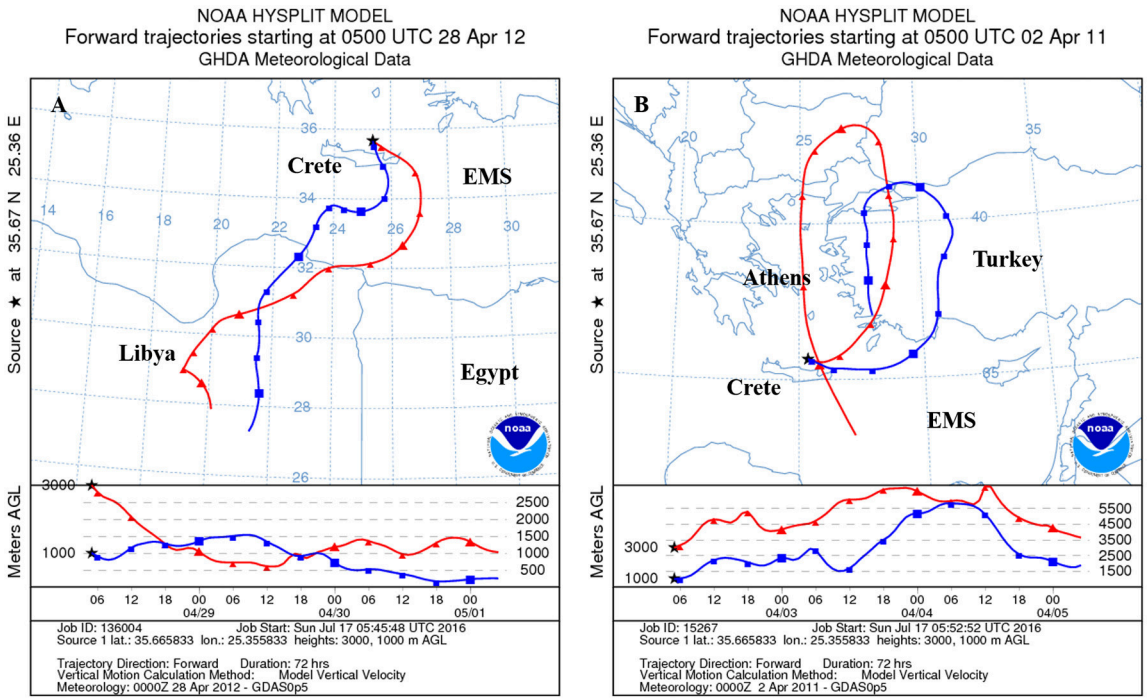

FIGURE 2 | Representative air mass back trajectories derived from the backward trajectories model NOAA/ARL HYSPLIT-4 (www.noaa.gov), showing the origin and track of the Saharan-dominated population (A) and the anthropogenic-dominated population **(B)** over the 3 days that preceded their collection at Crete and Israel.

syringe from the sample, filtered through 0.45 μm polycarbonate filters and stored at 4°C for subsequent analysis. For the nitrate leaching experiment, 100 ml of sterile seawater were used and sampled in the same way as the other determinants, after 30 min of leaching. The analysis of all the nitrate and phosphate samples was carried out after the 48 h sample was collected. A series of 6 blank samples were run through the sampling procedure and the average values were subtracted from each sample analyzed (mean blank values were -3 ± 4 nmol P l^{-1} and 48 ± 50 nmol NO_x l^{-1}). Nutrient content was determined by standard SEAL AA-3 automated methods for phosphate (using the molybdate blue method), nitrate (as nitrite after Cd column reduction) and ammonium (using a fluorescence method). The precision of the replicate analysis was 1.8 ± 0.01 μM for phosphate, 6.0 ± 0.05 μM for nitrate and 5.75 ± 0.05 μM for ammonium.

Measurement of $^{33}PO_4$ Uptake

Samples (10 ml) for PO_4 turnover times were collected every day and measured using ^{33}P-orthophosphate (Thingstad et al., 1993). Carrier-free ^{33}P-orthophosphate (PerkinElmer, specific activity: 370 MBq ml^{-1}) was added to the samples at a final concentration of 20–79 pM. Samples used for the subtraction of the background and abiotic adsorption were fixed with 100% trichloroacetic acid (TCA) (final conc. 0.5%) before the isotope's addition. The samples were then incubated under subdued (laboratory) illumination. The incubation time varied between 1 and 20 min: short enough to assure a linear relationship between the fractions of the isotope adsorbed vs. the incubation time but long enough to reliably detect any isotope uptake above the background levels. Incubation was terminated by a cold chase of 100 mM KH_2PO_4 (final conc. 1 mM). Subsamples (3.3 ml) were filtered in parallel onto 25 mm polycarbonate filters with 2, 0.6, and 0.2 μm pore sizes. All filters were placed on a Millipore 12 place manifold with Whatman (GF/C) glass fiber filters saturated with 100 mM KH_2PO_4 as support. After filtration, the filters were placed in polyethylene vials with an Ultima Gold (Packard) scintillation cocktail and radio-assayed. After the radio-activities of the filter were corrected for those of the blank filter obtained from fixed samples, the phosphate turnover time ($T_{[PO4]}$: h) was calculated as $T_{[PO4]} = -t/\ln(1-f)$, where f is the fraction (no dimension) of added isotope collected on the 0.2 μm filter after the incubation time (t: h).

Phosphate Concentrations in the Mesocosm Bags

Water samples were collected and analyzed immediately for their phosphate concentrations using the MAGIC method (Rimmelin and Moutin, 2005). The detection limit was 1.6 nM for phosphate.

Chlorophyll *a*

Seawater samples (500 ml) were passed through a Whatman GF/F filter (~0.7 μm pore size) and extracted overnight (16 h) in 10 ml of 90% acetone solution in the dark (Holm-Hansen et al., 1965). Chlorophyll *a* concentrations were determined by the non-acidification method (Welschmeyer, 1994) using a

TD700 fluorometer equipped with 436 nm excitation and 680 nm emission filters.

Picophytoplankton and Heterotrophic Bacterial Abundance

Samples for determining the picophytoplankton and heterotrophic bacterial abundance were collected every day throughout the experiment's duration. The samples were fixed with 0.2 μm filtered glutaraldehyde (a final concentration of 0.5%), kept at 4°C for ∼45 min, flash-frozen in liquid nitrogen and then transferred to a −80°C refrigerator until further processing. Frozen samples were thawed at room temperature and sub-samples were stained with SYBR Green I and incubated for 10 min in the dark, according to Vaulot and Marie (1999). Samples for picophytoplankton abundance were analyzed based on their auto-fluorescence signals, without pre-staining, using a FACSCalibur (Becton Dickinson) flow cytometer equipped with an air-cooled laser at 488 nm and a standard filter set-up. Flow cytometry data were acquired and processed with the Cell Quest Pro software (Becton Dickinson). An average estimated flow rate of 58 μL min^{-1} was used. The picophytoplankton carbon biomass was calculated from cell counts, assuming 175 fg C $cell^{-1}$ for *Synechococcus* cells, 53 fg C $cell^{-1}$ es (Campbell and Yentsch, 1989).

Primary Productivity (PP)

Photosynthetic carbon fixation rates were estimated using the ^{14}C incorporation method (Steemann-Nielsen, 1952). For each mesocosm, three light and one dark 320-mL polycarbonate bottles were filled with sample water during morning time (09:00–10:00 a.m.), inoculated with 5 μCi of $NaH^{14}CO_3$ tracer (Perkin-Elmer) and incubated in a land-based tank for 3 h. At the end of the incubation, the spiked seawater samples were filtered through 0.2 μm polycarbonate filters (47 mm diameter) under low vacuum pressure (<150 mmHg) and the filters were collected for the determination of primary production rate. The filters were placed in 5-ml scintillation vials and were acidified with 1 ml of 0.1 N HCL in order to remove excess ^{14}C-bicarbonate overnight. After the addition of 4 ml scintillation cocktail (ULTIMA-GOLD), the radioactivity of the samples (disintegrations per minute, dpm) was measured in a Liquid Scintillation Counter (Packard Tri-Card 4000). Primary production rates were calculated by subtracting the dpm of the dark bottles from the respective light ones. We used a value of 26,400 mg C m^{-3} for the concentration of dissolved inorganic carbon (Triantaphyllou et al., 2010) and a value of 1.05 for the isotopic discrimination factor (Lagaria et al., 2011).

Bacterial Productivity (BP)

BP was estimated by the 3H-leucine method (Kirchmann et al., 1986), as modified by Smith and Azam (1992). For each mesocosm, duplicate SD, A and control samples were incubated with a mixture of L-[45 3H]-leucine (Perkin Elmer, 115 Ci $mmol^{-1}$) and non-radioactive leucine to a final concentration of 20 nM. Samples were incubated for 2 h in the dark at the *in-situ* temperature, after which they were fixed and treated following the micro-centrifugation protocol (Smith and Azam, 1992), as described in detail by Van Wambeke et al. (2008). In brief, incubations were terminated after 2 h by the addition of trichloroacetic acid (TCA). Samples were then centrifuged at 16,000 × g and the resulting cell pellet was washed twice with 5% TCA and with 80% ethanol. Incorporation of 3H- leucine into the TCA-insoluble fraction was measured by liquid scintillation counting (Packard Tri-Carb 4000TR) after resuspension of the cell pellet in scintillation cocktail (Ultima-Gold). Bacterial production was calculated according to Kirchmann (1993), from 3H-leucine incorporation rates. Duplicate incubations had an analytical error <10%. Concentration kinetics optimization was also performed to ensure that the bacterial growth was not limited by the concentration of leucine.

Dinitrogen (N_2) Fixation Rates

$^{15}N_2$ uptake measurements were performed using the ^{15}N-enriched seawater protocol described by Mohr et al. (2010), with minor modifications for the EMS (Rahav et al., 2013). The detailed methodology is presented in Rahav et al. (2016a) this Special Issue.

Dissolved Trace Metal Analysis

The samples used for the analysis of trace metals (each 1 L in volume) were collected in PTFE bottles (pre-treated overnight with 2N HNO_3 and rinsed afterwards with ultrapure Milli-Q water), and within 12 h from their collection the samples were filtered through pre-weighted nitrocellulose membrane filters (Millipore 0.45 μm pore size) under a clean laminar hood (class 100) in order to separate the particulate form from the dissolved form of the metals. The dissolved metals in the filtered samples were determined immediately after filtration through a process of pre-concentration accomplished by passing the sample through Chelex-100 resin columns for retaining the metals and by eluting them using 10 ml nitric acid 2N s.p. under the clean laminar hood (the pre-concentration factor = 100). The pre-concentration procedure is a slight modification (Scoullos et al., 2007) of the procedure proposed by Riley and Taylor (1968) and Kingston et al. (1978).

Trace metal concentrations (Cu, Pb, Zn, Mn, Al, Fe) in the eluates were determined by employing a Varian SpectrAA 200 Flame Atomic Absorption Spectrophotometer (FAAS) for Zn, Al and Fe and a Varian SpectrAA-640Z Graphite Furnace Atomic Absorption Spectrophotometer (GFAAS) with Zeeman background correction for Cu, Pb and Mn. The relative standard deviation ($Sr = (S/\chi) \times 100$) of the measurements that resulted from replicate (3–4) determinations and standard addition experiments was <5%.

Statistical Analyses

The tests of statistical significance was carried out using a one-way analysis of variance (ANOVA) followed by a Fisher LSD means comparison test. Prior to analyses, the ANOVA assumptions, namely the normality and the heterogeneity of variances of the data, were examined. These tests were used

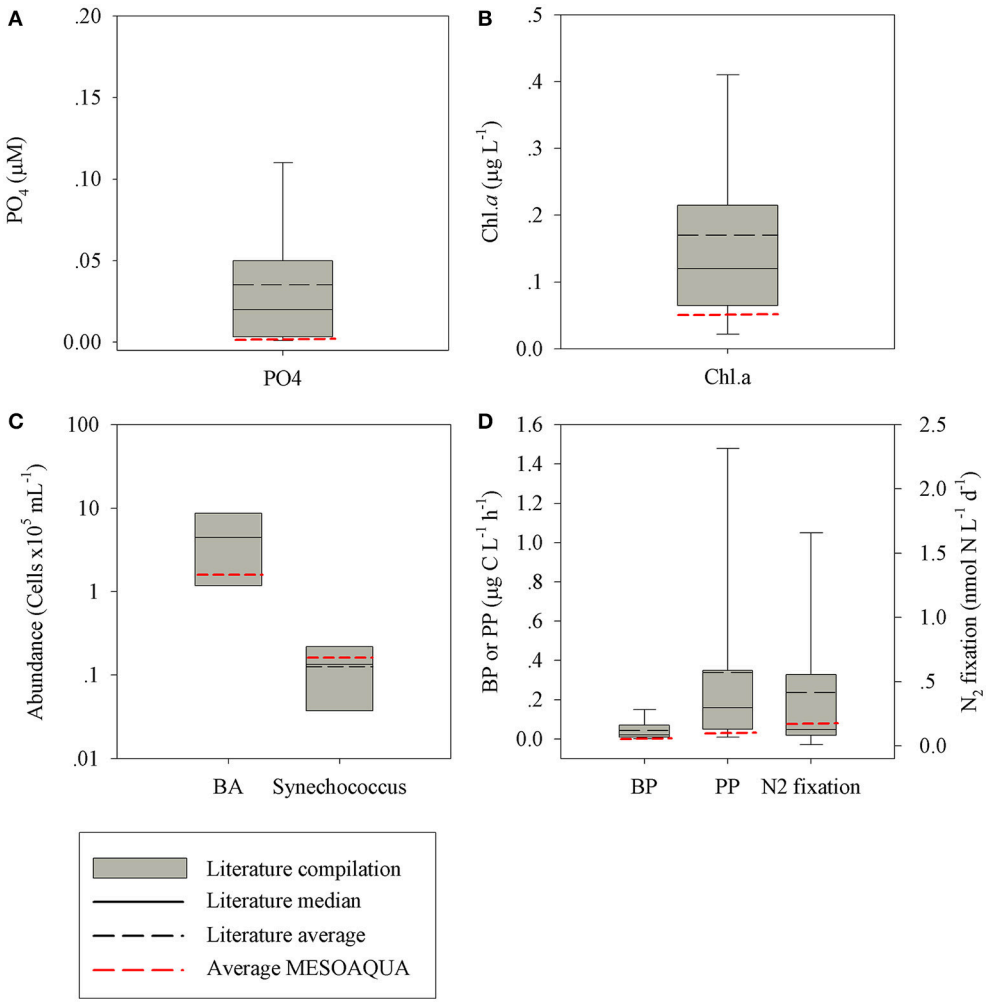

FIGURE 3 | A box plot distribution of phosphorus (A), chl-*a* **(B)**, microbial cell abundances **(C)**, and microbial production rates **(D)**, as reported for oligotrophic marine environments worldwide (Azov, 1986; Zohary and Robarts, 1998; Herut et al., 2000; Pinhassi and Hagström, 2000; Ignatiades et al., 2002; Wu et al., 2003; Krom et al., 2005; Pulido-Villena et al., 2008; Foster et al., 2009; Fernández et al., 2010; Christaki et al., 2011; Van Wambeke et al., 2011; Watkins-Brandt et al., 2011; Moisander et al., 2012; Rahav et al., 2013, 2015, 2016b; Tanhua et al., 2013; Kress et al., 2014; Keuter et al., 2015; Raveh et al., 2015; Tsiola et al., 2016). The black line represents the median (solid) and average (dashed) value. In red: the average values measured during this study (MESOAQUA).

to compare between the controls and the different treatments ($P < 0.05$) at the conclusion of the mesocosm experiment or between the results measured here and those compiled from the literature (**Figures 5**, **6**). All tests were performed using the XLSTAT.

RESULTS

The Ambient Water and Initial Conditions

The characteristics of the ambient surface (10 m) water collected during the 8–9 of May north of the Island of Crete and the initial conditions of the experiment (1 day prior to the additions) were typical oligotrophic, representing the EMS offshore waters (Kress et al., 2014; Pitta et al., 2016) as well as other LNLC systems. All the measured state and rate parameters showed values typical of oligotrophic systems (**Figure 3**), which are consistent with previous observations of the spring conditions in the EMS (references in **Figure 3**). The chlorophyll *a* (chl-*a*) concentrations, primary production (PP) and bacterial production (BP) were at the lower range of the oligotrophic systems; $0.06 \pm 0.00\,\mu g\ l^{-1}$, $0.42 \pm 0.02\,\mu g\ C\ l^{-1}\ h^{-1}$, and 15.59 ± 7.57 ng C l^{-1} h^{-1}, respectively. Bacterial abundance (BA, 4.2×10^5 cells ml^{-1}), *Synechococcus* abundance (Syn., 2.3×10^4 cells ml^{-1}) and dinitrogen fixation (N_2-fix, 0.21 ± 0.01 nmol N l^{-1} d^{-1}) were within the oligotrophic range. The phosphate and phosphate turnover time were also characteristic to oligotrophic conditions, $0.012\,\mu M$ and ~1 h, respectively. The seawater temperature during the experiment was in the range of 19–20°C, with no marked stratification of the water column inside the mesocosms.

TABLE 2 | The elemental composition of the trace metals from the SD and A treatments.

Element	Unit	SD	A	A/SD
Al	%	4.7	4.0	0.87
Fe	%	3.19	2.28	0.71
P	%	0.04	0.07	1.60
S	%	0.14	0.31	2.27
Si	%	17.38	17.95	1.03
Ti	%	0.22	0.22	0.99
Ca	%	8.01	9.10	1.14
Mg	%	1.36	1.45	1.07
Mn	ppm	476	432	0.91
Cu	ppm	47	59	1.25
Pb	ppm	19	23	1.20
Zn	ppm	162	190	1.17
Cd	ppm	0.21	0.32	1.55
Ni	ppm	27	24	0.92

Samples were digested with HF and aqua regia according to the procedure of ASTM (1983) and Herut et al. (2001).

The Chemical Composition and Nutrient Leachability of the Aerosols

The heavy metal concentrations were enriched in the SD compared to A, while the major element concentrations show similar values (**Table 2**). The Si/Al ratios were at the upper range found in northern African mineral dusts, while the Fe/Ca ratios were relatively low (Formenti et al., 2011, 2014). The latter indicate a certain depletion in Al and Ca compared to typical African mineral dust. The Mn/Fe, Pb/Fe, Ni/Fe, and Cd/Fe ratios were similar to the equivalent ratios in the African aerosols sampled by Chien et al. (2016), while the Cu/Fe ratios in this study are somewhat higher. The Mn/Fe and P/Fe ratios (wt./wt.) in SD were similar to the Saharan soil used by Guieu et al. (2010) (0.015 vs. 0.015 for Mn/Fe and 0.014 vs. 0.017 for P/Fe) and to those measured by Chien et al. (2016) in African aerosols. The P/Fe, Pb/Fe, Cd/Fe, and Cu/Fe ratios in A were higher than in SD by 2.2, 1.7, 2.2, and 1.75, respectively, indicating enrichment in these elements probably due to a larger anthropogenic fraction.

The amount of P leached was 2.1–2.7 and 2.2–3.7 nmol PO_4 per mg of SD and A, respectively (**Table 3**; **Figure S1**), representing an addition of ∼25–50% of the ambient concentrations. Similar P leached values were observed in other studies: 1.9 nmol phosphate per mg Saharan dust (Ridame and Guieu, 2002); 2.6–2.7 nmol phosphate per mg of Saharan dust (Chien et al., 2016); 4.2 nmol phosphate per mg of total suspended particles (TSP) sampled in the Red Sea (Mackey et al., 2012). The amount of nitrate leached was 20–26 and ∼54 nmol NO_x per mg of SD and A, respectively (**Table 3**; **Figure S1**). The average leached N and P resulted in a distinctly lower N:P ratio in treatment SD (∼9:1) than in A (∼18:1) or 7:1 vs. 15:1, considering the larger leachability of P by Leeds laboratory (**Table 3**). The higher leachable values of P obtained in Leeds compared to those retrieved in Haifa (∼30 and ∼75% for SD and A, respectively, **Table 3**; **Figure S1**) were probably attributed to the coating with iodine done in Leeds, which prevented adsorption into the walls of the containers. These leaching experiments were performed using sterile seawater, at different particle concentrations than those used in the mesocosm experiments. They also represent higher particle concentrations than those naturally found at the surface mixed layer after dust storms/aerosol depositions. Such differences, both in the seawater's biological reactivity and in the particle concentrations, may impact the amount of nutrient release (e.g., Ridame and Guieu, 2002; Mackey et al., 2012) and hence the leaching dynamics of N, P and other micronutrients. We therefore consider the experimental leaching amounts of N and P as an approximation of the total amount released in the mesocosms using the average values.

The turnover time of phosphorus (∼1 h), regardless of the treatment, represents extreme oligotrophic P starved conditions. The P released from the dust/aerosols was probably immediately consumed, as no increase in Tt was recorded even 3 h after addition.

Dissolved Trace Metal Concentrations

The presented dissolved trace metal concentrations were measured in the initial conditions (prior to additions) and also 3 and 24 h after addition. The amount of trace metals added to the experimental mesocosm after the SD and A additions is presented in **Table 4**. Fast enrichment (3 h after addition) was observed for Mn in both the SD and A treatments compared to the initial conditions and the control. A relatively fast enrichment of Ni, Fe, and Pb was observed in the SD treatment. Such a fast release of trace metals coincides with the observations in other studies (Baker et al., 2006; Séguret et al., 2011). Generally, the dissolved concentrations of Mn, Ni, and Cu were similar to the values reported in Chien et al. (2016), while the Fe and Pb concentrations were enriched. The dissolved trace metal concentrations were similar to the range of values measured at the EMS offshore Israel (**Figure 4**).

Mn increased by ∼4 nM following the SD and ∼1 nM in the A treatments. This represents an increase by a factor of ∼2 and 1.3 in the ambient concentrations, respectively. Ni increased by ∼ 2 nM following the SD treatment. Pb and Fe increased by ∼1 and ∼6 nM in SD, respectively.

Biological Parameters

Both types of treatments triggered a positive change (relative to the unamended control mesocosms) in most of the performed rate and state measured parameters such as BA and BP, Syn abundance, chl-*a*, PP, and N_2-fix. These changes are in agreement with other dust microcosm/mesocosm additions from the Mediterranean Sea and are presented as the maximal difference (treatment minus control, **Figures 5A–E**) or normalized to 1 mg l^{-1} of SD or A addition (**Figures 6A,B**). The added aerosol/dust concentrations (1 and 1.6 mg l^{-1}) in our experiment fall within the linear dose-response range previously studied in the EMS (e.g., Herut et al., 2005; 0.2–4.9 mg l^{-1}) and therefore supports a linear normalization. Overall, the maximal observed changes in the two treatments for the different parameters ranged from 25

TABLE 3 | Summary of the leached NO_x and PO_4 from the SD and A treatments.

Type of Dust	Laboratory	NO_3+NO_2 (NO_x)		PO_4		NO_x/PO_4
		nmol leached per mg dust	nmole added to 1 L mesocosm seawater	nmol leached per mg dust	nmole added to 1 L mesocosm seawater	mol/mol
SD	Haifa	26		2.1		12
	Leeds	20		2.8		7
	Average	23	36.8	2.4	3.9	9
Aerosol	Haifa	53		2.2		24
	Leeds	55		3.7		15
	Average	54	54.0	3.0	3.0	18

*Leaching experiments were carried in Haifa and Leeds as detailed in the Materials and Methods section and in **Figure S1**.*

TABLE 4 | Summary of the trace metal concentrations in the different mesocosms 24 h after the SD or A additions.

Treatment	Time (h)	Mn (nM)	Cu (nM)	Ni (nM)	Pb (nM)	Fe (nM)	Zn (nM)
C	0	2.2	0.9	3.1	0.8	9.3	41.2
C	3	2.2 ± 0.3	0.8 ± 0.3	3.1 ± 0.2	3.7 ± 2.1	13.2 ± 2.3	28.2 ± 2.5
C	24	2.3	0.6	3.2	3.2	N.A	15.6
SD	0	1.6	1.2	3.2	1.4	11.9	19.3
SD	3	5.9 ± 0.8	1.3 ± 0.2	5.2 ± 0.8	2.1 ± 0.2	17.5 ± 2.2	37.8 ± 10.4
SD	24	5.7 ± 1.0	2.1 ± 0.7	5.4 ± 0.6	3.2 ± 0.8	18.3 ± 1.1	43.0 ± 2.7
A	0	2.1	1.3	3.6	1.5	12.2	30.7
A	3	3.1 ± 0.2	1.0 ± 0.1	3.2 ± 0.2	1.6 ± 0.3	10.9 ± 3.1	24.4 ± 7.1
A	24	3.3 ± 0.3	1.0 ± 0.0	3.5 ± 0.1	1.7 ± 0.4	12.6 ± 2.3	24.5 ± 0.2

Values are presented as averages and their corresponding standard deviation.

to 660% per 1 mg l^{-1} of dust/aerosol addition (**Figure 6A**). For SD treatment, the maximal change (increase) was observed after 48 h for BP (98%, 11.8 ± 1.2 ng C l^{-1} h^{-1}), chl-*a* (27%, 33.6 ± 3.3 ng l^{-1}) and N_2-fix (223%, 0.21 ± 0.03 nmol N l^{-1} d^{-1}) and 72 h for PP (61%, 0.28 ± 0.05 μg C l^{-1} h^{-1}) and Syn. (23%, 2.75 ± 0.64 μg C l^{-1}). BA showed a progressive increase (from 25%; 2.78 ± 0.43 μg C l^{-1} after 24 h to 48% at day 8) along the experiment. For A treatment, an immediate maximal change (increase) was observed after 3 h for BP (660%, 24.2 ± 8.5 ng C l^{-1} h^{-1}), after 1 day for chl-*a* (47%, 33.2 ± 3.8 ng l^{-1}), after 2 days for PP (102%, 0.29 ± 0.08 μg C l^{-1} h^{-1}) and N_2-fix (141%, 0.09 ± 0.03 nmol N l^{-1} d^{-1}) and after 3 days for Syn.(41%, 2.89 ± 0.89 μg C l^{-1}). BA showed a progressive increase (from 39%; 2.53 ± 0.46 ng C l^{-1} after 24 h to 63% at day 8) along the experiment.

DISCUSSION

Here we assess the impact of pure Saharan dust vs. mixed aerosols on the surface seawater autotrophic and heterotrophic microbial populations, mimicking the potential effects of an intense Saharan dust storm and a relatively intense mixed aerosol deposition. While the EMS is exposed to a relative high frequency of Saharan and other desert dust storms (Koçak et al., 2004; Ganor et al., 2010), which will probably increase in the future due to climate change (Lelieveld et al., 2016), anthropogenic aerosols were found to be enriched in dust when it arrived at sampling sites after passing through populated and industrialized urban areas (Koçak et al., 2012). It has been observed that the anthropogenic component increased the trace metal content and changed their speciation in EMS aerosols (Kocak et al., 2010), and that such aerosols are enriched in nitrate compared to bioavailable phosphate (e.g., Chien et al., 2016). Therefore, any increase in anthropogenic aerosol deposition in the future and hence in the relative fraction of N deposition may influence the phytoplankton community structure in LNLC areas (Chien et al., 2016). Such a trend, of a relatively higher release of nitrate vs. phosphate, was observed here. While in the SD treatment more phosphate (by ∼34%) was added to the mesocosms compared to the A treatment, the opposite trend was observed for nitrate. The A treatment added more nitrate (by ∼40%) than the SD treatment. Consequently, the nitrate/phosphate ratios added in the A treatment were twice than those added in the SD treatment, 18 vs. 9 using the average or 15 vs. 7 considering a larger release of P (**Table 3**).

The phosphate turnover time prior to the additions of dust/aerosol was ∼1 h, a typical value of P deficiency in the EMS (Zohary and Robarts, 1998; Flaten et al., 2005; Tanaka et al., 2011). The SD and A additions did not trigger an increase in the phosphate turnover time caused by the release of phosphate from the dust/aerosol. By definition, the Tt equals the amount of bioavailable phosphate divided by its consumption

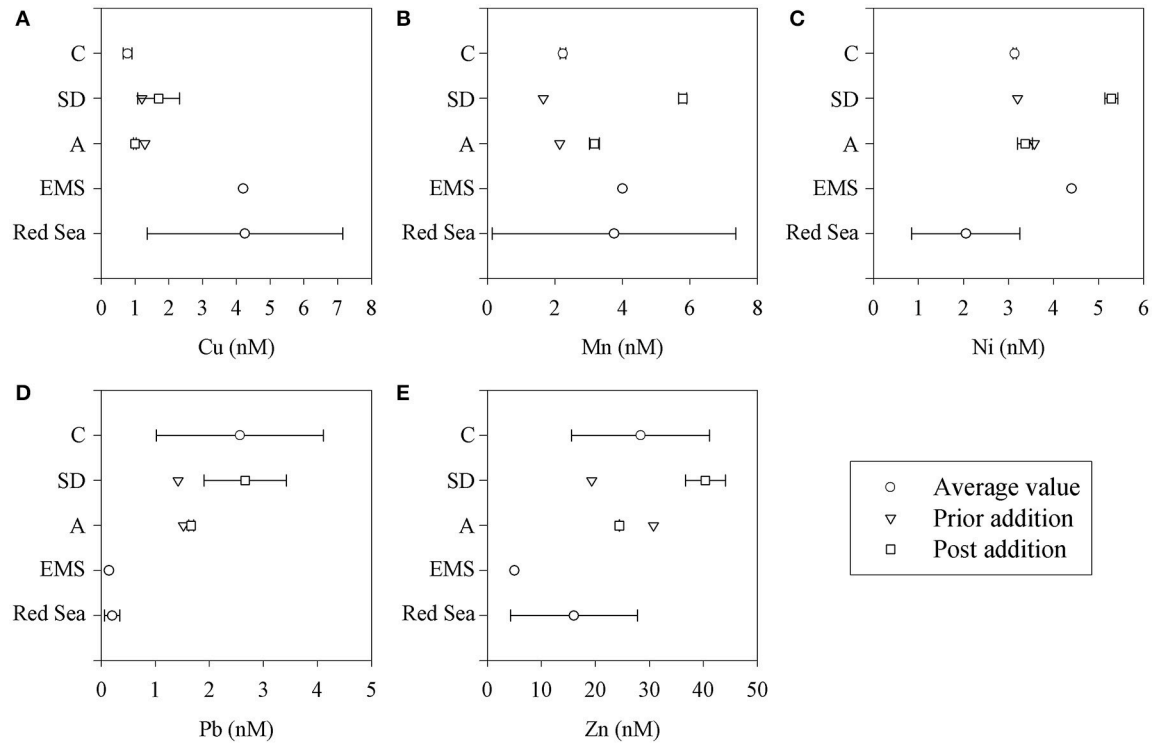

FIGURE 4 | Dissolved trace metal concentrations (A-E) in the mesocosm tanks (C, SD, and A) and in representative oligotrophic stations in the eastern Mediterranean (EMS) and Red (northern Gulf of Aqaba) Seas (Herut et al., unpublished). Values are presented in nM.

(or uptake) rate. This suggests that the amount of phosphate added to the system from the dust/aerosol through leaching was relatively small and that it was rapidly removed by the microbial community. Bioassays in which a significant amount of phosphate was released showed an increase in phosphate Tt (Herut et al., 2005; Tanaka et al., 2011).

The amount of leachable phosphate and nitrate in the SD treatment, 3.8 and ∼23 nM, respectively, corresponds to a potential increase of ∼58 ng chl-*a* l^{-1} by using P:C ratios or ∼55 ng chl *a* l^{-1} by using N:C ratios of Redfield (1:16:106) and C:chl *a* ≈ 80 (wt., Behrenfeld et al., 2005). The observed chl-*a* increase is somewhat lower, ∼30 ng chl-*a* l^{-1}. However, the highest bacterial production rate was ∼3.3 nmol C l^{-1} h^{-1}, at 24 h after addition, which corresponds to ∼1.6 nmol P $l^{-1}d^{-1}$, using a C/P ratio of 50 for bacteria (Fagerbakke et al., 1996), although the latter is not constant (Zimmerman et al., 2014; Godwin and Cotner, 2015). Assuming that out of the released phosphate ∼ 1.6 nM was used by the bacteria and 2.2 nM was used by the autotrophs, the latter corresponds to the observed increase in chl-*a* (∼30 ng l^{-1}). The lower observed chl-*a* values may also infer some grazing activity. A similar calculation for the A treatment shows a similar result, which corresponds to the observed increase in chl-*a*.

Additional trace metals, micronutrients (Fe, Zn, Mn, Co-not measured) or potentially toxic metals that have possibly been delivered by the dust were not assessed via leaching experiments in this study. However, these were measured 3 h and 1 day after the additions (**Table 4**), showing values similar to an open remote EMS station (100 km offshore Israel), to the Red Sea (Herut et al., unpublished) or, for part of the elements, to the mean ocean concentration, although the Mn, Fe and Zn values were significantly higher (Statham and Hart, 2005; Semeniuk et al., 2009; Moore et al., 2013).

The SD treatments were relatively enriched ($p < 0.05$) in dissolved Mn, Ni, and Fe concentrations compared to the A mesocosms, probably due to the larger mass addition (1.6 mg l^{-1} vs. 1 mg l^{-1}). All the measured dissolved metal concentrations were well below the ecological ambient water quality criteria for chronic levels (Buchman, 2008). Metal bioavailability may determine phytoplankton productivity, especially by iron, copper, cobalt, zinc and nickel, via scarcity or toxic effects (Huertas et al., 2014). Their specific impact, including manganese, on biological processes is mainly related to the metalloproteins state (Cvetkovic et al., 2010). The enrichment of Mn in SD and A treatments as compared to C ($p < 0.05$) may serve as a micronutrient supporting photosynthesis (Huertas et al., 2014) and/or may reverse toxicity effects of Cu and Zn (Sunda, 1987). Although the bioavailability of the measured dissolved Fe is not certain (Rue and Bruland, 1995), the amount is high enough to exclude possible Fe limitation (e.g., Statham and Hart, 2005). Assuming that particulate Fe dissolution in seawater is ∼0.06% (0.03–0.17%, Blain et al., 2004; Chien et al., 2016), a maximum amount of ∼50 nmol Fe l^{-1} (900 nmol particulate Fe l^{-1} × 0.06%) was released from

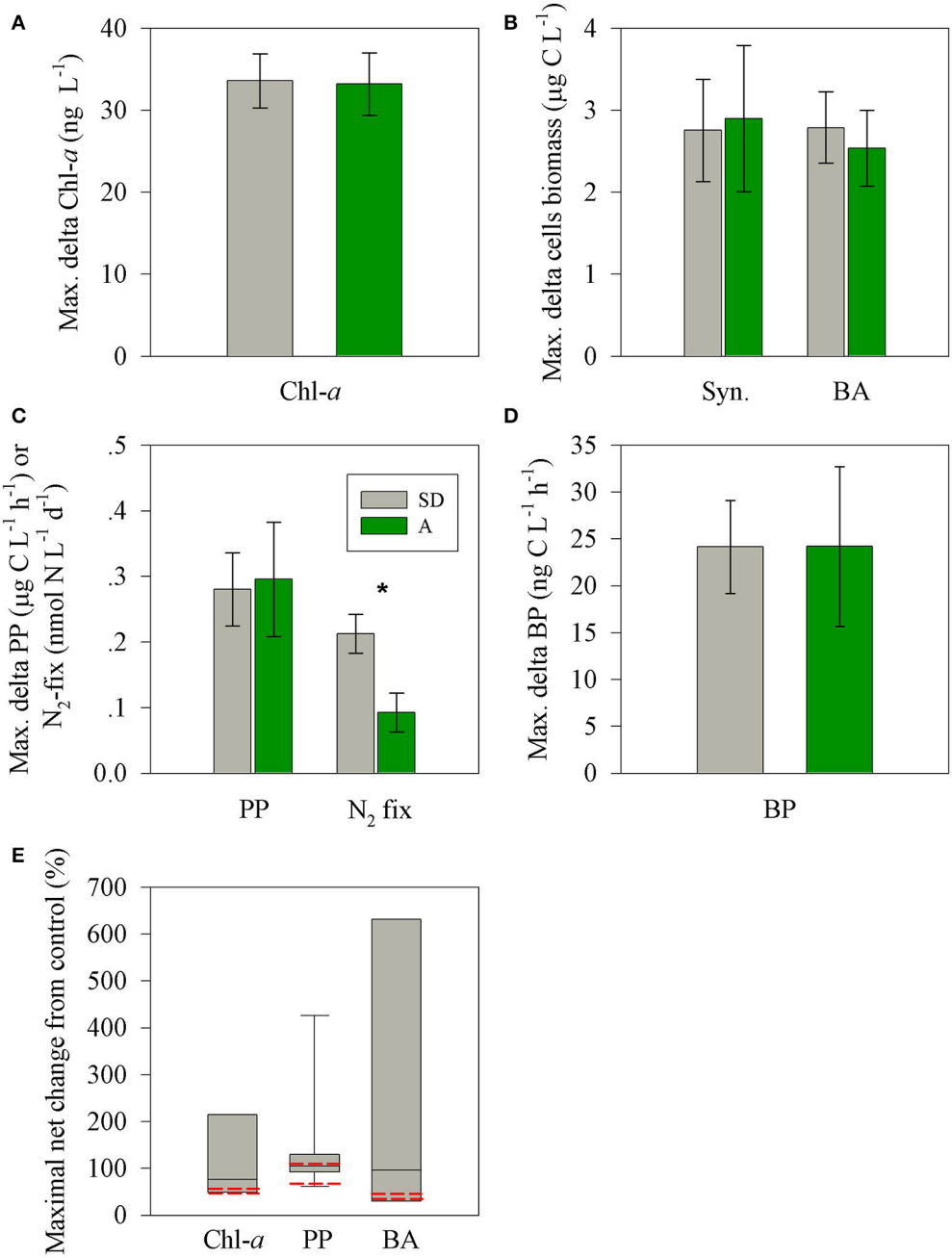

FIGURE 5 | The observed maximal net changes of for the autotrophic and heterotrophic microbial variables (A–D) following SD (gray) or A (green) additions in the surface EMS during May 2012 and a box plot distribution of the net change reported for chl-*a*, PP, and BP in Mediterranean Sea studies. Data were taken from Herut et al. (2005); Ternon et al. (2011); Ridame et al. (2013); Rahav et al. (2016b); Rahav et al., unpublished and this study **(E)**. The red lines represents the observed values measured for SD and A during this study. The asterisks above the columns represent statistically significant differences (one-way ANOVA and a Fisher LSD means comparison test, $P < 0.05$) for mean values of P additions between stations.

the SD addition, larger than in the A treatment (∼24 nmol Fe l^{-1}), and probably supplying enough bioavailable Fe^{2+}. The significantly higher ($p = 0.02$) N_2-fix rates measured in the SD treatment (Rahav et al., 2016b) may be related to a relatively larger release of Fe in this treatment and its relatively lower nitrate/phosphate ratio (∼10:1). In addition, the significantly ($p < 0.05$) higher Ni concentrations in SD as compared to A or C, is known to play an important role in the cellular physiology of diazotrophic cyanobacteria such as *Trichodesmium* (Rodriguez and Ho, 2014) and supports the latter observation and the appearance of this N_2-fixer in the SD treatment (Rahav et al., 2016b).

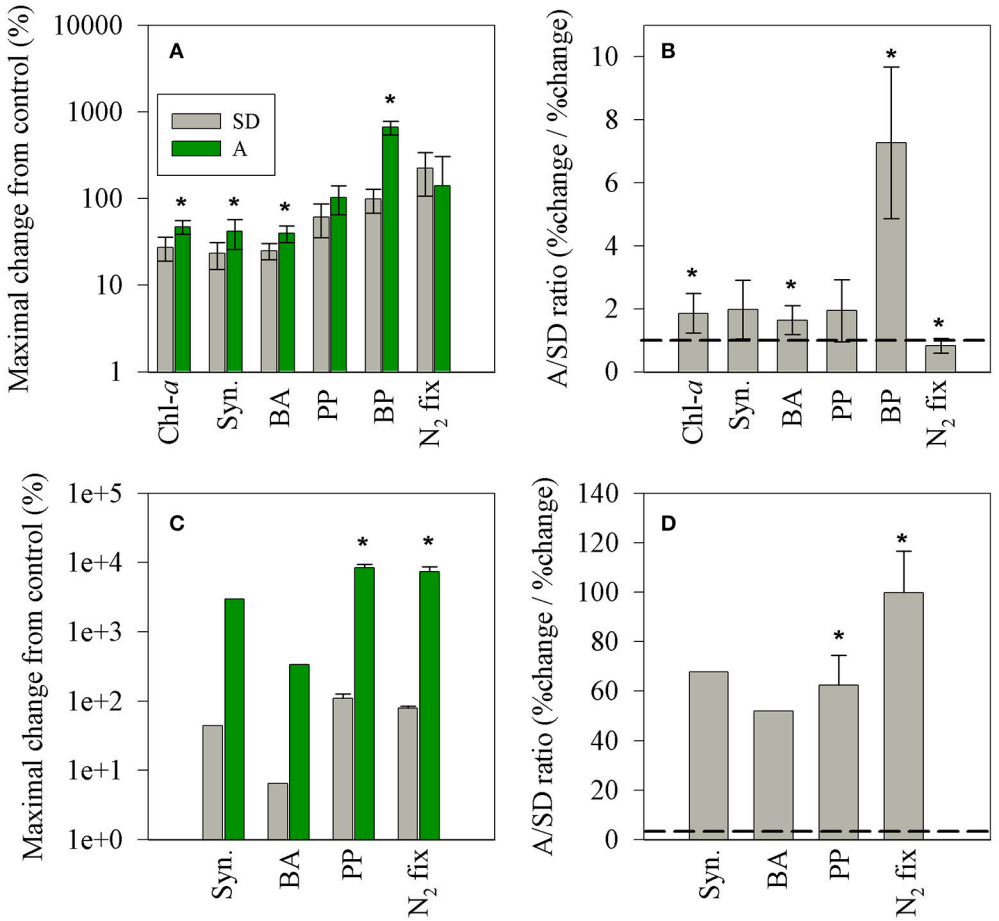

FIGURE 6 | The maximal net changes (normalized to 1 mg l^{-1} dust) in autotrophic and heterotrophic microbial populations (A,C) and the A/SD ratio **(B,D)** measured in this study **(A,B)** and that reported in the BOUM campaign (Station B, Ternon et al., 2011, **C,D)**. The black line represents a 1:1 ratio between A and SD values. The asterisks above the columns represent statistically significant differences (one-way ANOVA and a Fisher LSD means comparison test, $P < 0.05$).

Both types of dry aerosol additions (SD and A) triggered a positive change (25–600% per 1 mg/L addition) in all rate and state measurements (**Figures 5**, **6**), showing a general sequence ($p < 0.05$) of higher relative change in the rate parameters: N_2-fix > BP > PP > Chla ≈ BA ≈ Syn for SD and BP > PP ≈ N_2-fix > Chla ≈ BA ≈ Syn for A. Nevertheless, a larger normalized increase was observed in treatment A for all parameters, except for N_2-fix (**Figure 6B**). In addition, the BP dramatically increased within 3 h after addition (∼600%, yet reached 154% after 24 h), while no such response was observed for SD. The primary differences between the two treatments is the leachable molar ratio of nitrate/phosphate; almost twice in treatment A (∼15:1) than SD (∼9:1), and the additional amount of added leachable N by treatment A (∼30% more than SD) (**Table 3**). No significant changes were observed after additions and between treatments in the dissolved organic nutrients, not likely to dominate the observed change in the heterotrophic bacterial activity. These differences in the relative impact (normalized to mass), between pure mineral/desert dust and mixed aerosols, were also observed by Ternon et al. (2011) for the addition of a dust analog (manipulated Saharan soil) and aerosols (total suspended material in air) collected by low volume sampler at sea (**Figures 6C,D**). While in the latter on-board experiment lower quantities of P were release by the aerosols (0.3–1.6 nmol P l^{-1}) as compared to the Saharan analog (6 nmol P l^{-1}), in our experiment similar amounts of P were added by A and SD, but larger quantities of N were added in A (**Table 3**). Yet, only the inorganic phase of nutrients was considered here, whereas the dissolved organic pools likely to be present in aerosols (e.g., Markaki et al., 2010) were not measured and should be further considered. Apart from the increased solubility in aerosols, the smaller size particles as compared to crustal mineral aerosols, increases the particle's surface/volume ratio and solubility (Baker and Jickells, 2006), implying a larger impact per mass of a mixed character as A treatment. Our data suggest that despite the co-limitation of P and N (Kress et al., 2005; Zohary et al., 2005), the additional N released by the A treatment may have triggered the relative larger response in most of the

rate and state parameters. A similar observation was reported for the DUNE experiment in the Western Mediterranean Sea (Ridame et al., 2014) and was calculated for the data presented during the BOUM campaign across the Mediterranean Sea in which aerosol addition triggered stronger responses of the microbial community than Saharan dust (Tanaka et al., 2011; Ternon et al., 2011). Yet, the magnitude of the maximal net effect imposed by SD or A on the surface microbial populations (% change normalized to 1 mg l^{-1}) is significantly lower than that reported from a microcosm experiment in the Ionian Sea during the BOUM campaign in summer 2008 (by ∼1 order of magnitude, **Figure 6C**, Ternon et al., 2011). When normalizing the responses from the BOUM study, Saharan analog or aerosols addition resulted in a general sequence of PP ≈ N_2-fix ≈ Syn. > BA. Furthermore, the overall responses triggered by the aerosol addition in the BOUM campaign (microbial biomass and activity) were much higher than that reported for the Saharan analog amendments. This results in a high calculated aerosol/Saharan analog ratios in the BOUM study, ranging from ∼50 to 100% (**Figure 6D**). These different responses by different aerosols should be further studied in detail considering all bioavailable macro and micro nutrients or other inhibiting elements.

The role atmospheric deposition plays in influencing bacterioplankton dynamics in LNLC regions is important for understanding (observationally and via ocean biogeochemical models) the current and future functioning of LNLC regions (Guieu et al., 2014a). Increasing temperatures leading to increased dust emissions in the EMS (Klingmüller et al., 2016) and anthropogenic activities contributing to the Mediterranean atmospheric chemical composition and aerosols solubility (exposure to lower pH levels during transport), are expected to continue in the future due to climate change, and thereby supply more macro and micro nutrients into its surface oligotrophic water. A warmer atmosphere may influence the intensity and length of the already well stratified water column in the EMS and hence the impact of the atmosphere as a significant external source of new macro and micro nutrients. We show here that the above trends may lead to the alteration of the heterotrophic/autotrophic relationships.

AUTHOR CONTRIBUTIONS

Planning of the original experimental design and carrying out of experiment and sampling in the field (BH, PP, TMT, TBM). Aerosols collection (NM, BH, CNT). Aerosols chemical composition (BH). Heavy metals (ES, MS). Leaching rate of nutrients from dust (BH, ER, MDK, AS, KV, ZS). Phosphorous turnover time (TT). Chlorophyll a concentration (NP). Primary production (AL, SP). Synechococcus abundance and biomass (AT). Bacterial abundance, biomass and rate (AT, AG). Nitrogen fixation (ER, IBF, BH). Statistics (ER). Organizing the operation of mesocosm and obtaining funding (PP, TMT). Writing up manuscript (BH, ER).

ACKNOWLEDGMENTS

This work was financed by the European Union Seventh Framework Program (FP7/2007-2013) under grant agreement no. 228224, "MESOAQUA: Network of leading MESOcosm facilities to advance the studies of future AQUAtic ecosystems from the Arctic to the Mediterranean" through grants to BH, IBF, ER, ZS, and MDK. The authors wish to thank G. Piperakis for his technical assistance, A. Konstantinopoulou for assistance with bacterial production analyses, D. Podaras and S. Diliberto for assistance during the experiment and N. Sekeris for his help with constructions and ideas on technical solutions. The captain and the crew of the R/V Philia are also thanked for their assistance during the transportation of water from the sea to the CRETACOSMOS facility. Funding was also provided by the Israel Science Foundation grants (996/08) to IBF and BH. Funding was also provided by Leverhulme Trust (grant RPG 406) to MDK.

SUPPLEMENTARY MATERIAL

The Supplementary Material for this article can be found online at: http://journal.frontiersin.org/article/10.3389/fmars.2016.00226/full#supplementary-material

Figure S1 | Leached nitrate (A) and phosphate **(B)** from the SD (circle) and A (triangle) particles as retrieved in the Leeds (white) and Haifa (red) laboratories.

REFERENCES

Astitha, M., Lelieveld, J., Abdel Kader, M., Pozzer, A., and De Meij, A. (2012). Parameterization of dust emissions in the global atmospheric chemistry-climate model EMAC: impact of nudging and soil properties. *Atmos. Chem. Phys.* 12, 11057–11083. doi: 10.5194/acp-12-11057-2012

ASTM (1983). *Designation - D3683-78. Standard Test Method for Trace Elements in Coal and Coke Ash by Atomic Absorption.* Pennsylvania, PA: American Society for Testing and Materials Publisher.

Azov, Y. (1986). Seasonal patterns of phytoplankton productivity and abundance in nearshore oligotrophic waters of the Levant Basin (Mediterranean). *J. Plankton Res.* 8, 41–53. doi: 10.1093/plankt/8.1.41

Baker, A. R., French, M., and Linge, K. L. (2006). Trends in aerosol nutrient solubility along a west-east transect of the Saharan dust plume. *Geophys. Res. Lett.* 33, 10–13. doi: 10.1029/2005GL024764

Baker, A. R., and Jickells, T. D. (2006). Mineral particle size as a control on aerosol iron solubility. *Geophys. Res. Lett.* 33, 1–4. doi: 10.1029/2006GL026557

Behrenfeld, M. J., Boss, E., Siegel, D. A., and Shea, D. M. (2005). Carbon-based ocean productivity and phytoplankton physiology from space. *Global Biogeochem. Cycles* 19, 1–14. doi: 10.1029/2004GB002299

Blain, S., Guieu, C., Claustre, H., Leblanc, K., Moutin, T., Guiner, B. Q., et al. (2004). Availability of iron and major nutrients for phytoplankton in the north-east Atlantic Ocean. *Limnol. Oceanogr.* 49, 2095–2104. doi: 10.4319/lo.2004.49.6.2095

Bougiatioti, A., Nikolaou, P., Stavroulas, I., Kouvarakis, G., Weber, R., Nenes, A., et al. (2016). Particle water and pH in the eastern Mediterranean: source variability and implications for nutrient availability. *Atmos. Chem. Phys.* 16, 4579–4591. doi: 10.5194/acp-16-4579-2016

Bressac, M., Guieu, C., Doxaran, D., Bourrin, F., Desboeufs, K., Leblond, N., et al. (2014). Quantification of the lithogenic carbon pump following a simulated dust-deposition event in large mesocosms. *Biogeosciences* 11, 1007–1020. doi: 10.5194/bg-11-1007-2014

Buchman, M. F. (2008). *NOAA Screening Quick Reference Tables*, *Office of Response and Restoration Division*. Seattle, WA: National Oceanic and Atmospheric Administration.

Calvo-Díaz, A., Díaz-Pérez, L., Suárez, L. Á., Morán, X. A. G., Teira, E., and Marañón, E. (2011). Decrease in the autotrophic-to-heterotrophic biomass ratio of picoplankton in oligotrophic marine waters due to bottle enclosure. *Appl. Environ. Microbiol.* 77, 5739–5746. doi: 10.1128/AEM.00066-11

Campbell, J. W., and Yentsch, C. M. (1989). variance within homogeneous phytoplankton populations, III: analysis of natural populations. *Cytometry* 10, 605–611. doi: 10.1002/cyto.990100516

Chien, C., Mackey, K. R., Dutkiewicz, S., Mahowald, N. M., Prospero, J. M., and Paytan, A. (2016). Effects of African dust deposition on phytoplankton in the western tropical atlantic Ocean off Barbados. *Global Biogeochem. Cycles* 30, 716–734. doi: 10.1002/2015GB005334

Christaki, U., Van Wambeke, F., Lefevre, D., Lagaria, A., Prieur, L., Pujo-Pay, M., et al. (2011). Microbial food webs and metabolic state across oligotrophic waters of the Mediterranean Sea during summer. *Biogeosciences* 8, 1839–1852. doi: 10.5194/bg-8-1839-2011

Cvetkovic, A., Menon, A. L., Thorgersen, M. P., Scott, J. W., Poole, F. L., Jenney F. E., Jr., et al. (2010). Microbial metalloproteomes are largely uncharacterized. *Nature* 466, 779–782. doi: 10.1038/nature09265

Duce, R. A., LaRoche, J., Altieri, K., Arrigo, K. R., Baker, A. R., Capone, D. G., et al. (2008). Impacts of atmospheric anthropogenic nitrogen on the open ocean. *Science* 320, 893–897. doi: 10.1126/science.1150369

Duce, R. A., Liss, P. S., Merrill, J. T., Atlas, E. L., Buat-Menard, P., Hicks, B. B., et al. (1991). The atmospheric input of trace species to the world ocean. *Global Biogeochem. Cycles* 5, 193–259. doi: 10.1029/91GB01778

Fagerbakke, K. M., Heldal, M., and Norland, S. (1996). Content of carbon, nitrogen, oxygen, sulfur and phosphorus in native aquatic and cultured bacteria. *Aquat. Microb. Ecol.* 10, 15–27. doi: 10.3354/ame010015

Fernández, A., Mouriño-Carballido, B., Bode, A., et al. (2010). Latitudinal distribution of *Trichodesmium* spp. and N_2 fixation in the Atlantic Ocean. *Biogeosciences* 7, 2195–2225. doi: 10.5194/bgd-7-2195-2010

Flaten, G. A., Skjoldal, E. F., Krom, M. D., Law, C. S., Mantoura, R. F. C., Pitta, P., et al. (2005). Studies of the microbial P-cycle during a Lagrangian phosphate-addition experiment in the Eastern Mediterranean. *Deep Sea Res. II Top. Stud. Oceanogr.* 52, 2928–2943. doi: 10.1016/j.dsr2.2005.08.010

Formenti, P., Caquineau, S., Desboeufs, K., Klaver, A., Chevaillier, S., Journet, E., et al. (2014). Mapping the physico-chemical properties of mineral dust in western Africa: mineralogical composition. *Atmos. Chem. Phys.* 14, 10663–10686. doi: 10.5194/acp-14-10663-2014

Formenti, P., Schütz, L., Balkanski, Y., Desboeufs, K., Ebert, M., Kandler, K., et al. (2011). Recent progress in understanding physical and chemical properties of African and Asian mineral dust. *Atmos. Chem. Phys.* 11, 8231–8256. doi: 10.5194/acp-11-8231-2011

Foster, R., Paytan, A., and Zehr, J. P. (2009). Seasonality of N_2 fixation and *nifH* gene diversity in the Gulf of Aqaba (Red Sea). *Limnol. Oceanogr.* 54, 219–233. doi: 10.4319/lo.2009.54.1.0219

Ganor, E., Osetinsky, I., Stupp, A., and Alpert, P. (2010). Increasing trend of African dust, over 49 years, in the eastern Mediterranean. *J. Geophys. Res. Atmos.* 115, 1–7. doi: 10.1029/2009jd012500

Godwin, C. M., and Cotner, J. B. (2015). Aquatic heterotrophic bacteria have highly flexible phosphorus content and biomass stoichiometry. *ISME J.* 9, 2324–2327. doi: 10.1038/ismej.2015.34

Guieu, C., Aumont, O., Paytan, A., Bopp, L., Law, C. S., Mahowald, N., et al. (2014a). The significance of the episodic nature of atmospheric deposition to Low Nutrient Low Chlorophyll regions. *Global Biogeochem. Cycles* 28, 1179–1198. doi: 10.1002/2014GB004852

Guieu, C., Dulac, F., Desboeufs, K., Wagener, T., Pulido-Villena, E., Grisoni, J. M., et al. (2010). Large clean mesocosms and simulated dust deposition: a new methodology to investigate responses of marine oligotrophic ecosystems to atmospheric inputs. *Biogeosciences* 7, 2765–2784. doi: 10.5194/bg-7-2765-2010

Guieu, C., Dulac, F., Ridame, C., and Pondaven, P. (2014b). Introduction to project DUNE, a DUst experiment in a low nutrient, low chlorophyll ecosystem. *Biogeosciences* 11, 425–442. doi: 10.5194/bg-11-425-2014

Guo, C., Xia, X., Pitta, P., Herut, B., Rahav, E., Berman-Frank, I., et al. (2016). Shifts in microbial community structure and activity in the ultra-oligotrophic Eastern Mediterranean Sea driven by the deposition of Saharan dust and European aerosols. *Front. Mar. Sci.* 3:170. doi: 10.3389/fmars.2016.00170

Guo, C., Yu, J., Ho, T. Y., Wang, L., Song, S., Kong, L., et al. (2012). Dynamics of phytoplankton community structure in the South China Sea in response to the East Asian aerosol input. *Biogeosciences* 9, 1519–1536. doi: 10.5194/bg-9-1519-2012

Herut, B., Almogi-Labin, A., and Jannink, N. (2000). The seasonal dynamics of nutrient and chlorophyll *a* concentrations on the SE Mediterranean shelf-slope. *Oceanol Acta* 23, 771–782. doi: 10.1016/S0399-1784(00)01118-X

Herut, B., Collier, R., and Krom, M. D. (2002). The role of dust in supplying nitrogen and phosphorus to the Southeast Mediterranean. *Limnol. Oceanogr.* 47, 870–878. doi: 10.4319/lo.2002.47.3.0870

Herut, B., Krom, M. D., Pan, G., and Mortimer, R. (1999). Atmospheric input of nitrogen and phosphorus to the Southeast Mediterranean: sources, fluxes, and possible impact. *Limnol. Oceanogr.* 44, 1683–1692. doi: 10.4319/lo.1999.44.7.1683

Herut, B., Nimmo, M., Medway, A., Chester, R., and Krom, M. D. (2001). Dry atmospheric inputs of trace metals at the Mediterranean coast of Israel (SE Mediterranean): sources and fluxes. *Atmos. Environ.* 35, 803–813. doi: 10.1016/S1352-2310(00)00216-8

Herut, B., Zohary, T., Krom, M. D., Mantoura, R. F. C., Pitta, P., Psarra, S., et al. (2005). Response of East Mediterranean surface water to Saharan dust: on-board microcosm experiment and field observations. *Deep Sea Res. II Top. Stud. Oceanogr.* 52, 3024–3040. doi: 10.1016/j.dsr2.2005.09.003

Hoerling, M., Eischeid, J., Perlwitz, J., Quan, X., Zhang, T., and Pegion, P. (2012). On the increased frequency of mediterranean drought. *J. Clim.* 25, 2146–2161. doi: 10.1175/JCLI-D-11-00296.1

Holm-Hansen, O., Lorenzen, C. J., Holmes, R. W., and Strickland, J. D. H. (1965). Fluorometric determination of chlorophyll. *ICES J. Mar. Sci.* 30, 3–15. doi: 10.1093/icesjms/30.1.3

Huertas, M. J., López-Maury, L., Giner-Lamia, J., et al. (2014). Metals in cyanobacteria: analysis of the copper, nickel, cobalt and arsenic homeostasis mechanisms. *Life* 4, 865–886. doi: 10.3390/life4040865

Ignatiades, L., Psarra, S., Zervakis, V., et al. (2002). Phytoplankton size-based dynamics in the Aegean Sea (Eastern Mediterranean). *J. Mar. Syst.* 36, 11–28. doi: 10.1016/S0924-7963(02)00132-X

IPCC (2014). *Intergovernmental Panel on Climate Change, Climate Change 2013: The Physical Science Basis*. Cambridge: Cambridge University Press.

Jickells, T. D., An, Z. S., Andersen, K. K., Baker, A. R., Bergametti, G., Brooks, N., et al. (2005). global iron connections between desert dust, ocean biogeochemistry, and climate. *Science* 308, 67–71. doi: 10.1126/science.1105959

Jordi, A., Basterretxea, G., Tovar-Sánchez, A., Alastuey, A., and Querol, X. (2012). Copper aerosols inhibit phytoplankton growth in the Mediterranean Sea. *Proc. Natl. Acad. Sci. U.S.A.* 109, 21246–21249. doi: 10.1073/pnas.1207567110

Kanakidou, M., Duce, R. A., Prospero, J. M., Baker, A. R., Benitez-Nelson, C., Dentener, F. J., et al. (2012). Atmospheric fluxes of organic N and P to the global ocean. *Global Biogeochem. Cycles* 26, 1–12. doi: 10.1029/2011GB004277

Keuter, S., Rahav, E., Herut, B., and Rinkevich, B. (2015). Distribution patterns of bacterioplankton in the oligotrophic south-eastern Mediterranean Sea. *FEMS Microbiol.* 91, 1–39. doi: 10.1093/femsec/fiv070

Kingston, H. M., Barnes, I. L., Brady, T. J., Rains, T. C., and Champ, M. A. (1978). Separation of eight transition elements from alkali and alkaline earth elements in estuarine and seawater with chelating resin and their determination by graphite furnace atomic absorption spectrometry. *Anal. Chem.* 50, 2064–2070. doi: 10.1021/ac50036a031

Kirchmann, D. L. (1993). "Leucine incorporation as a measure of biomass production by heterotrophic bacteria," in *Handbook of Methods in Aquatic Microbial Ecology*, eds P. F. Kemp, B. F. Sherr, E. B. Sherr, and J. J. Cole (Boca Raton, FL: Lewis), 509–512.

Kirchmann, D. L., Newell, S. Y., and Hodson, R. E. (1986). Incorporation versus biosynthesis of leucine: implications for measuring rates of protein syntheis and biomass production by bacteria in marine systems. *Mar. Ecol. Prog. Ser.* 32, 47–59. doi: 10.3354/meps032047

Klingmüller, K., Pozzer, A., Metzger, S., Stenchikov, G. L., and Lelieveld, J. (2016). Aerosol optical depth trend over the Middle East. *Atmos. Chem. Phys.* 16, 5063–5073. doi: 10.5194/acp-16-5063-2016

Koçak, M., Kubilay, N., and Mihalopoulos, N. (2004). Ionic composition of lower tropospheric aerosols at a Northeastern Mediterranean site: implications

regarding sources and long-range transport. *Atmos. Environ.* 38, 2067–2077. doi: 10.1016/j.atmosenv.2004.01.030

Kocak, M., Kubilay, N., Tuğrul, S., and Mihalopoulos, N. (2010). Atmospheric nutrient inputs to the northern levantine basin from a long-term observation: sources and comparison with riverine inputs. *Biogeosciences* 7, 4037–4050. doi: 10.5194/bg-7-4037-2010

Koçak, M., Theodosi, C., Zarmpas, P., Séguret, M. J. M., Herut, B., Kallos, G., et al. (2012). Influence of mineral dust transport on the chemical composition and physical properties of the Eastern Mediterranean aerosol. *Atmos. Environ.* 57, 266–277. doi: 10.1016/j.atmosenv.2012.04.006

Kress, N., Frede Thingstad, T., Pitta, P., Psarra, S., Tanaka, T., Zohary, T., et al. (2005). Effect of P and N addition to oligotrophic Eastern Mediterranean waters influenced by near-shore waters: a microcosm experiment. *Deep Sea Res. II Top. Stud. Oceanogr.* 52, 3054–3073. doi: 10.1016/j.dsr2.2005.08.013

Kress, N., Gertman, I., and Herut, B. (2014). Temporal evolution of physical and chemical characteristics of the water column in the easternmost Levantine Basin (Eastern Mediterranean Sea) from 2002 to 2010. *J. Mar. Syst.* 135, 6–13. doi: 10.1016/j.jmarsys.2013.11.016

Krom, M. D., Herut, B., and Mantoura, R. F. C. (2004). Nutrient budget for the Eastern Mediterranean: implications for phosphorus limitation. *Limnol. Oceanogr.* 49, 1582–1592. doi: 10.4319/lo.2004.49.5.1582

Krom, M. D., Shi, Z., Stockdale, A., Berman-Frank, I., Giannakourou, A., Herut, B., et al. (2016). Response of the Eastern mediterranean microbial ecosystem to dust and dust affected by acid processing in the atmosphere. *Front. Mar. Sci.* 3:133. doi: 10.3389/fmars.2016.00133

Krom, M. D., Thingstad, T. F., Brenner, S., et al. (2005). Summary and overview of the CYCLOPS P addition Lagrangian experiment in the Eastern Mediterranean. *Deep Sea Res Part II Top. Stud. Oceanogr.* 52, 3090–3108. doi: 10.1016/j.dsr2.2005.08.018

Lagaria, A., Psarra, S., Lefèvre, D., et al. (2011). The effects of nutrient additions on particulate and dissolved primary production and metabolic state in surface waters of three Mediterranean eddies. *Biogeosciences* 8, 2595–2607. doi: 10.5194/bg-8-2595-2011

Lelieveld, J., Hadjinicolaou, P., Kostopoulou, E., Chenoweth, J., El Maayar, M., Giannakopoulos, C., et al. (2012). Climate change and impacts in the Eastern Mediterranean and the Middle East. *Clim. Change* 114, 667–687. doi: 10.1007/s10584-012-0418-4

Lelieveld, J., Lelieveld, J., Berresheim, H., Borrmann, S., Crutzen, P. J., Dentener, F. J., et al. (2002). Global air pollution crossroads over the mediterranean.pdf. *Science* 298, 794–799. doi: 10.1126/science.1075457

Lelieveld, J., Proestos, Y., Hadjinicolaou, P., Tanarhte, M., Tyrlis, E., and Zittis, G. (2016). Strongly increasing heat extremes in the Middle East and North Africa (MENA) in the 21st century. *Clim. Change* 137, 1–16. doi: 10.1007/s10584-016-1665-6

Mackey, K. R., Chien, C., Te Post, A. F., Saito, M. A., and Paytan, A. (2015). Rapid and gradual modes of aerosol trace metal dissolution in seawater. *Front. Microbiol.* 5:794. doi: 10.3389/fmicb.2014.00794

Mackey, K. R., Roberts, K., Lomas, M. W., Saito, M. A., Post, A. F., and Paytan, A. (2012). Enhanced solubility and ecological impact of atmospheric phosphorus deposition upon extended seawater exposure. *Environ. Sci. Technol.* 46, 10438–10446. doi: 10.1021/es3007996

Markaki, Z., Loÿe-Pilot, M. D., Violaki, K., Benyahya, L., and Mihalopoulos, N. (2010). Variability of atmospheric deposition of dissolved nitrogen and phosphorus in the Mediterranean and possible link to the anomalous seawater N/P ratio. *Mar. Chem.* 120, 187–194. doi: 10.1016/j.marchem.2008.10.005

Mills, M. M., Ridame, C., Davey, M., La Roche, J., and Geider, R. J. (2004). Iron and phosphorus co-limit nitrogen fixation in the eastern tropical North Atlantic. *Nature* 429, 292–294. doi: 10.1038/nature02550

Mohr, W., Großkopf, T., Wallace, D. W. R., and Laroche, J. (2010). Methodological underestimation of oceanic nitrogen fixation rates. *PLoS ONE* 49:e12583. doi: 10.1371/journal.pone.0012583

Moisander, P. H., Zhang, R., Boyle, E. A., et al. (2012). Analogous nutrient limitations in unicellular diazotrophs and *Prochlorococcus* in the South Pacific Ocean. *ISME J.* 6, 733–744. doi: 10.1038/ismej.2011.152

Moore, C. M., Mills, M. M., Arrigo, K. R., Berman-Frank, I., Bopp, L., Boyd, P. W., et al. (2013). Processes and patterns of oceanic nutrient limitation. *Nature Geosci* 6, 701–710. doi: 10.1038/ngeo1765

Nenes, A., Krom, M. D., Mihalopoulos, N., Van Cappellen, P., Shi, Z., Bougiatioti, A., et al. (2011). Atmospheric acidification of mineral aerosols: a source of bioavailable phosphorus for the oceans. *Atmos. Chemi. Phys.* 11, 6265–6272. doi: 10.5194/acp-11-6265-2011

Ozer, T., Gertman, I., Kress, N., Silverman, J., and Herut, B. (in press). Interannual thermohaline (1979-2014) and nutrient (2002-2014) dynamics in the Levantine surface and intermediate water masses, SE Mediterranean Sea. *Global Planet. Change* 1–8. doi: 10.1016/j.gloplacha.2016.04.001

Paytan, A., Mackey, K. R., Chen, Y., Lima, I. D., Doney, S. C., Mahowald, N., et al. (2009). Toxicity of atmospheric aerosols on marine phytoplankton. *Proc. Natl. Acad. Sci. U.S.A.* 106, 4601–4605. doi: 10.1073/pnas.0811486106

Pinhassi, J., and Hagström, Å. (2000). Seasonal succession in marine bacterioplankton. *Aquat. Microb. Ecol.* 21, 245–256. doi: 10.3354/ame021245

Pitta, P., Nejstgaard, J. C., Tsagaraki, T. M., Zervoudaki, S., Egge, J. K., Frangoulis, C., et al. (2016). Confirming the "Rapid phosphorus transfer from microorganisms to mesozooplankton in the Eastern Mediterranean Sea" scenario through a mesocosm experiment. *J. Plankton Res.* 38, 502–521. doi: 10.1093/plankt/fbw010

Pulido-Villena, E., Baudoux, A.-C., Obernosterer, I., Landa, M., Caparros, J., Catala, P., et al. (2014). Microbial food web dynamics in response to a Saharan dust event: results from a mesocosm study in the oligotrophic Mediterranean Sea. *Biogeosciences* 11, 337–371. doi: 10.5194/bgd-11-337-2014

Pulido-Villena, E., Wagener, T., and Guieu, C. (2008). Bacterial response to dust pulses in the western Mediterranean: implications for carbon cycling in the oligotrophic ocean. *Global Biogeochem. Cycles* 22, 1–12. doi: 10.1029/2007GB003091

Rahav, E., Bar-Zeev, E., Ohayon, S., Elifantz, H., Belkin, N., Herut, B., et al. (2013). Dinitrogen fixation in aphotic oxygenated marine environments. *Front. Microbiol.* 4:227. doi: 10.3389/fmicb.2013.00227

Rahav, E., Herut, B., Mulholland, M., Belkin, N., Elifantz, H., and Berman-Frank, I. (2015). Heterotrophic and autotrophic contribution to dinitrogen fixation in the Gulf of Aqaba. *Mar. Ecol. Prog. Ser.* 522, 67–77. doi: 10.3354/meps11143

Rahav, E., Paytan, A., Chien, C., Ovadia, G., Katz, T., and Herut, B. (2016a). The impact of atmospheric dry deposition associated microbes on the southeastern Mediterranean Sea surface water following an intense dust storme. *Front. Mar. Sci.* 3:127. doi: 10.3389/fmars.2016.00127

Rahav, E., Shun-Yan, C., Cui, G., Liu, H., Tsagaraki, T. M., Giannakourou, A., et al. (2016b). Evaluating the impact of atmospheric depositions on springtime dinitrogen fixation in the Cretan Sea (Eastern Mediterranean)—a mesocosm approach. *Front. Mar. Sci.* 3:180. doi: 10.3389/fmars.2016.00180

Raveh, O., David, N., Rilov, G., and Rahav, E. (2015). The temporal dynamics of coastal phytoplankton and bacterioplankton in the Eastern Mediterranean Sea. *PLoS ONE* 10:e0140690. doi: 10.1371/journal.pone.0140690

Ridame, C., Dekaezemacker, J., Guieu, C., Bonnet, S., L'Helguen, S., and Malien, F. (2014). Contrasted Saharan dust events in LNLC environments: impact on nutrient dynamics and primary production. *Biogeosciences* 11, 4783–4800. doi: 10.5194/bg-11-4783-2014

Ridame, C., and Guieu, C. (2002). Saharan input of phosphate to the oligotrophic water of the open western Mediterranean Sea. *Limnol. Oceanogr.* 47, 856–869. doi: 10.4319/lo.2002.47.3.0856

Ridame, C., Guieu, C., and L'Helguen, S. (2013). Strong stimulation of N2 fixation in oligotrophic Mediterranean Sea: results from dust addition in large *in situ* mesocosms. *Biogeosciences* 10, 7333–7346. doi: 10.5194/bg-10-7333-2013

Riley, J. P., and Taylor, D. (1968). Chelating resins for the concentration of trace elements from sea water and their analytical use in conjunction with atomic absorption spectrophotometry. *Anal. Chim. Acta* 40, 479–485. doi: 10.1016/S0003-2670(00)86764-1

Rimmelin, P., and Moutin, T. (2005). Re-examination of the MAGIC method to determine low orthophosphate concentration in seawater. *Anal. Chim. Acta* 548, 174–182. doi: 10.1016/j.aca.2005.05.071

Rodriguez, I. B., and Ho, T.-Y. (2014). Diel nitrogen fixation pattern of *Trichodesmium*: the interactive control of light and Ni. *Sci. Rep.* 4:4445. doi: 10.1038/srep04445

Rue, E. L., and Bruland, K. W. (1995). Complexation of iron(lll) by natural organic ligands in the Central North Pacific as determined by a new competitive ligand equilibration/adsorptive cathodic stripping voltammetric method. *Mar. Chem.* 5, 117–138. doi: 10.1016/0304-4203(95)00031-L

Scoullos, M. J., Sakellari, A., Giannopoulou, K., Paraskevopoulou, V., and Dassenakis, M. (2007). Dissolved and particulate trace metal levels in the Saronikos Gulf, Greece, in 2004. The impact of the primary Wastewater Treatment Plant of Psittalia. *Desalination* 210, 98–109. doi: 10.1016/j.desal.2006.05.036

Séguret, M. J. M., Koçak, M., Theodosi, C., Ussher, S. J., Worsfold, P. J., Herut, B., et al. (2011). Iron solubility in crustal and anthropogenic aerosols: the Eastern Mediterranean as a case study. *Mar. Chem.* 126, 229–238. doi: 10.1016/j.marchem.2011.05.007

Semeniuk, D. M., Cullen, J. T., Johnson, W. K., Gagnon, K., Ruth, T. J., and Maldonado, M. T. (2009). Plankton copper requirements and uptake in the subarctic Northeast Pacific Ocean. *Deep Sea Res. I Oceanogr. Res. Papers* 56, 1130–1142. doi: 10.1016/j.dsr.2009.03.003

Siokou-Frangou, I., Christaki, U., Mazzocchi, M. G., Montresor, M., Ribera d'Alcalá, M., Vaqué, D., et al. (2010). Plankton in the open Mediterranean Sea: a review. *Biogeosciences* 7, 1543–1586. doi: 10.5194/bg-7-1543-2010

Smith, D. C., and Azam, F. (1992). A simple, economical method for measuring bacterial protein synthesis rates in sea water using 3H-leucine. Mar Microb Food Webs 6: 107-114.

Statham, P. J., and Hart, V. (2005). Dissolved iron in the Cretan Sea (eastern Mediterranean). *Limnol. Oceanogr.* 50, 1142–1148. doi: 10.4319/lo.2005.50.4.1142.

Steemann-Nielsen, E. (1952). On the determination of the activity for measuring primary production. *J. Cons. Int. Explor. Mer.* 18, 117–140.

Sunda, W. G. (1987). "Neritic-oceanic trends in tracemetal toxicity to phytoplankton communities," in *Oceanic Processes in Marine Pollution*, ed Z. J. M. Capuzzo (Malabar: Krieger), 19–29.

Tanaka, T., Thingstad, T. F., Christaki, U., Colombet, J., Cornet-Barthaux, V., Courties, C., et al. (2011). Lack of P-limitation of phytoplankton and heterotrophic prokaryotes in surface waters of three anticyclonic eddies in the stratified Mediterranean Sea. *Biogeosciences* 8, 525–538. doi: 10.5194/bg-8-525-2011

Tanhua, T., Hainbucher, D., Schroeder, K., et al. (2013). The Mediterranean Sea system: a review and an introduction to the special issue. *Ocean Sci.* 9, 789–803. doi: 10.5194/os-9-789-2013

Ternon, E., Guieu, C., Ridame, C., L'Helguen, S., and Catala, P. (2011). Longitudinal variability of the biogeochemical role of Mediterranean aerosols in the Mediterranean Sea. *Biogeosciences* 8, 1067–1080. doi: 10.5194/bg-8-1067-2011

Thingstad, T. F., Skjoldal, E. F., and Bohne, R. A. (1993). Phosphorus cycling and algal bacterial competition in Sandsfjord, western Norway. *Mar. Ecol. Prog. Ser.* 99, 239–259. doi: 10.3354/meps099239

Triantaphyllou, M., Dimiza, M., Krasakopoulou, E., et al. (2010). Seasonal variation in Emiliania huxleyi coccolith morphology and calcification in the Aegean Sea (Eastern Mediterranean). *Geobios* 43, 99–110. doi: 10.1016/j.geobios.2009.09.002

Tsiola, A., Pitta, P., Fodelianakis, S., et al. (2016). Nutrient limitation in surface waters of the oligotrophic Eastern Mediterranean Sea: an enrichment microcosm experiment. *Microb. Ecol.* 71, 575–588. doi: 10.1007/s00248-015-0713-5

Van Wambeke, F., Catala, P., Pujo-Pay, M., and Lebaron, P. (2011). Vertical and longitudinal gradients in HNA-LNA cell abundances and cytometric characteristics in the Mediterranean Sea. *Biogeosciences* 8, 1853–1863. doi: 10.5194/bg-8-1853-2011

Vaulot, D., and Marie, D. (1999). Diel variability of photosynthetic picoplankton in the equatorial Pacific. *Appl. Environ. Microbiol.* 104, 3297–3310. doi: 10.1029/98jc01333

Wambeke, F. V., Obernosterer, I., Moutin, T., Duhamel, S., Ulloa, O., and Claustre, H. (2008). Heterotrophic bacterial production in the eastern South Pacific: longitudinal trends and coupling with primary production. *Biogeosciences* 5, 157–169. doi: 10.5194/bg-5-157-2008

Watkins-Brandt, K., Letelier, R., Spitz, Y., et al. (2011). Addition of inorganic or organic phosphorus enhances nitrogen and carbon fixation in the - oligotrophic North Pacific. *Mar. Ecol. Prog. Ser.* 432, 17–29. doi: 10.3354/meps09147

Welschmeyer, N. A. (1994). Fluorometric analysis of chlorophyll a in the presence of chlorophyll b and pheopigments. *Limnol. Oceanogr.* 39, 1985–1992. doi: 10.4319/lo.1994.39.8.1985

Wu, J., Chung, S.-W., Wen, L.-S., et al. (2003). Dissolved inorganic phosphorus, dissolved iron, and *Trichodesmium* in the oligotrophic South China Sea. *Global Biogeochem. Cycles* 17, 8–10. doi: 10.1029/2002GB001924

Zimmerman, A. E., Allison, S. D., and Martiny, A. C. (2014). Phylogenetic constraints on elemental stoichiometry and resource allocation in heterotrophic marine bacteria. *Environ. Microbiol.* 16, 1398–1410. doi: 10.1111/1462-2920.12329

Zohary, T., Herut, B., Krom, M. D., Fauzi, C., Mantoura, R., Pitta, P., et al. (2005). P-limited bacteria but N and P co-limited phytoplankton in the Eastern Mediterranean - A microcosm experiment. *Deep Sea Res. II Top. Stud. Oceanogr.* 52, 3011–3023. doi: 10.1016/j.dsr2.2005.08.011

Zohary, T., and Robarts, R. (1998). Experimental study of microbial P limitation in the eastern Mediterranean. *Limnol. Oceanogr.* 43, 387–395. doi: 10.4319/lo.1998.43.3.0387

Conflict of Interest Statement: The authors declare that the research was conducted in the absence of any commercial or financial relationships that could be construed as a potential conflict of interest.

frontiers in Marine Science

ORIGINAL RESEARCH
published: 04 July 2017
doi: 10.3389/fmars.2017.00210

Atmospheric Deposition Effects on Plankton Communities in the Eastern Mediterranean: A Mesocosm Experimental Approach

Tatiana M. Tsagaraki[1,2], Barak Herut[3], Eyal Rahav[3,4], Ilana R. Berman Frank[4], Anastasia Tsiola[1], Manolis Tsapakis[1], Antonia Giannakourou[5], Alexandra Gogou[5], Christos Panagiotopoulos[6], Kalliopi Violaki[7], Stella Psarra[1], Anna Lagaria[1], Epaminondas D. Christou[5], Nafsika Papageorgiou[1], Soultana Zervoudaki[5], Ma L. Fernandez de Puelles[8], Nikolaos Nikolioudakis[9,10], Travis B. Meador[11], Tsuneo Tanaka[12], Maria L. Pedrotti[13,14], Michael D. Krom[15,16] and Paraskevi Pitta[1]*

[1] Institute of Oceanography, Hellenic Centre for Marine Research, Heraklion, Greece, [2] Department of Biology, University of Bergen, Bergen, Norway, [3] Israel Oceanographic and Limnological Research, National Institute of Oceanography, Haifa, Israel, [4] Mina and Everard Goodman Faculty of Life Sciences, Bar-Ilan University, Ramat-Gan, Israel, [5] Hellenic Centre for Marine Research, Institute of Oceanography, Anavyssos Attikis, Greece, [6] Mediterranean Institute of Oceanography, Institut de Recherche pour le Développement (IRD), Centre National de la Recherche Scientifique, Université de Toulon, Aix Marseille Université, Marseille, France, [7] Environmental Chemistry Processes Laboratory, Department of Chemistry, University of Crete, Heraklion, Greece, [8] Centro de Baleares, Instituto Español de Oceanografia, Palma de Mallorca, Spain, [9] Institute of Marine Biological Resources and Inland Waters, Hellenic Centre for Marine Research, Heraklion, Greece, [10] Institute of Marine Research, Bergen, Norway, [11] MARUM Center for Marine Environmental Sciences, University of Bremen, Bremen, Germany, [12] Laboratoire d'Oceanographie Physique et Biogeochimique, University of the Mediterranean, Marseille, France, [13] Laboratoire d'Océanographie de Villefranche (LOV), Pierre-and-Marie-Curie University, Villefranche-sur-Mer, France, [14] Centre National de la Recherche Scientifique, Paris, France, [15] School of Earth and Environment, University of Leeds, Leeds, United Kingdom, [16] Department of Marine Biology, Charney School of Marine Sciences, University of Haifa, Haifa, Israel*

OPEN ACCESS

Edited by:
Angel Borja, AZTI Pasaia, Spain

Reviewed by:
Jacob Carstensen, Aarhus University, Denmark
Veljo Kisand, University of Tartu, Estonia

***Correspondence:**
Tatiana M. Tsagaraki
tatiana.tsagaraki@uib.no

Specialty section:
This article was submitted to Marine Ecosystem Ecology, a section of the journal Frontiers in Marine Science

Received: *22 December 2016*
Accepted: *16 June 2017*
Published: *04 July 2017*

Citation:
Tsagaraki TM, Herut B, Rahav E, Berman Frank IR, Tsiola A, Tsapakis M, Giannakourou A, Gogou A, Panagiotopoulos C, Violaki K, Psarra S, Lagaria A, Christou ED, Papageorgiou N, Zervoudaki S, Puelles MLFd, Nikolioudakis N, Meador TB, Tanaka T, Pedrotti ML, Krom MD and Pitta P (2017) Atmospheric Deposition Effects on Plankton Communities in the Eastern Mediterranean: A Mesocosm Experimental Approach. Front. Mar. Sci. 4:210. doi: 10.3389/fmars.2017.00210

The effects of atmospheric deposition on plankton community structure were examined during a mesocosm experiment using water from the Cretan Sea (Eastern Mediterranean), an area with a high frequency of atmospheric aerosol deposition events. The experiment was carried out under spring-summer conditions (May 2012). The main objective was to study the changes induced from a single deposition event, on the autotrophic and heterotrophic surface microbial populations, from viruses to zooplankton. To this end, the effects of Saharan dust addition were compared to the effects of mixed aerosol deposition on the plankton community over 9 days. The effects of the dust addition seemed to propagate throughout the food-web, with changes observed in nearly all of the measured parameters up to copepods. The dust input stimulated increased productivity, both bacterial and primary. Picoplankton, both autotrophic and heterotrophic capitalized on the changes in nutrient availability and microzooplankton abundance also increased due to increased availability of prey. Five days after the simulated deposition, copepods also responded, with an increase in egg production. The results suggest that nutrients were transported up the food web through autotrophs, which were favored by the Nitrogen supplied through both treatments. Although, the effects of individual events are generally short lived, increased deposition frequency and magnitude of events is expected in the area, due to predicted reduction in rainfall

and increase in temperature, which can lead to more persistent changes in plankton community structure. Here we demonstrate how a single dust deposition event leads to enhancement of phytoplankton and microzooplankton and can eventually, through copepods, transport more nutrients up the food web in the Eastern Mediterranean Sea.

Keywords: microbial food-web, dust deposition, phytoplankton, zooplankton, Eastern Mediterranean, mesocosm

INTRODUCTION

Mineral dust is an important driver of biogeochemical cycles in the surface ocean and an integral component of the land-atmosphere-ocean system (Mahowald et al., 2005, 2008; Bryant, 2013). In the atmosphere, natural sources account for ∼75% of atmospheric aerosols while anthropogenic sources account for the rest (Ginoux et al., 2012). The major component of natural aerosols is mineral dust from desert regions with the Sahara desert being the single largest source contributing 55% of global emissions (Ginoux et al., 2012). Elements leached from aerosols are an important source of biologically available nutrients, which support ocean productivity and marine ecosystem functioning especially in the offshore areas of the global ocean.

Supply of iron through atmospheric deposition to the ocean is well-documented and considered one of the main sources of this critical trace element to large ocean areas (Jickells, 2005 and references therein). It is a major reason why large areas of the global ocean are not Fe limited, as mineral dust provides sufficient iron to support primary productivity. Mineral dust can also provide an important source of P, both as labile phosphate and also as mineral apatite originating mainly from deserts (Mahowald et al., 2008). Under natural conditions, insoluble mineral apatite may drop through the surface layers without interacting with the biota but after acidification processes in the atmosphere, mainly interaction with pollutants such as NOx and SOx, it is converted into bioavailable phosphate (Nenes et al., 2011; Stockdale et al., 2016). Atmospheric input also represents a large and increasing source of anthropogenic inorganic N (mainly as NO_x from industrial sources and cars and NH_3 from agricultural sources as well as natural inputs from lightning and other sources). Atmospheric aerosols also contain important amounts of DON and DOP with largely unknown bioavailability (Markaki et al., 2010).

Atmospheric inputs (natural and polluted) are a particularly important source of external nutrients to the Mediterranean, because of its proximity to the Sahara desert to the south (Lawrence and Neff, 2009; Ganor et al., 2010) and the major anthropogenic atmospheric input from the north. Atmospheric inputs of inorganic nutrients to the Mediterranean Sea surface are considered a major nutrient influx, far exceeding riverine inputs in some regions (Guerzoni et al., 1999), representing 60% of the total external N input and 30% of the P input to the Eastern Mediterranean (Krom et al., 2004). The high mineral dust flux also results in relatively high concentrations of dissolved Fe, which prevent Fe limitation in surface waters (Statham and Hart, 2005). While the major source of atmospheric N to the Eastern Mediterranean is from anthropogenic sources, and can contain many other compounds related to anthropogenic activity (Myriokefalitakis et al., 2015), the greatest part of the P input is from mineral dust, mainly from the Sahara.

A prominent feature of the Mediterranean basin is the strong west to east gradient of primary productivity with an average of 120–131 gC m^{-2} yr^{-1} in the western Mediterranean compared to 56–76 gC m^{-2} yr^{-1} in the eastern Mediterranean (Crispi et al., 2002; Siokou-Frangou et al., 2010; Lazzari et al., 2012). There is a similar gradient in chlorophyll concentration (D'Ortenzio and Ribera d'Alcalà, 2009; Lazzari et al., 2012) and in nutrient concentrations (Pujo-Pay et al., 2011), which are also unusually low. Considering the high nitrate:phosphate molar ratios of 25–28:1 in the deep water (Krom et al., 1991) and high N:P ratios of DOM and POM, the system is often characterized as P starved (Krom et al., 2005). It has been found that P is the main limiting nutrient during the winter phytoplankton bloom (Krom et al., 1991). However, in summer conditions the surface waters of the EMS are likely N and P co-limited (Thingstad et al., 2005) and strictly N limitation has also been reported during mid-summer (Tanaka et al., 2011).

Phosphorus deposition from atmospheric sources has been estimated at ∼0.5 mM P m^{-2} y^{-1} in the eastern Mediterranean (Herut and Krom, 1996; Carbo et al., 2005), while a typical deposition event contains ∼0.05 g P L. Phosphorus input, regardless the source, has been shown to influence the community structure and production in the area (Fonnes Flaten et al., 2005; Pasternak et al., 2005; Lekunberri et al., 2010; Pitta et al., 2016). In general deposition events from the Sahara desert tend to have low leachable N:P ratios while those which include or have interacted with air masses from Europe have higher leachable N (e.g., Herut et al., 2016, this issue) and can reach very high N:P ratios (Markaki et al., 2010).

Lekunberri et al. (2010) measured a positive response to dust addition in bacterial production and abundance as well as in primary production and community respiration in a microcosm experiment in the NW Mediterranean. The response of primary producers was also documented previously in the Eastern Mediterranean by Herut et al. (2005) during a microcosm experiment and in mesocosm experiments by Rahav et al.. (2016, this issue) and by Ridame and Guieu (2002), in the eastern and western Mediterranean, respectively. During the dry deposition season (May–September), Volpe et al. (2009) found a strong positive correlation between phytoplankton (measured as chlorophyll *a* concentration) and dust on a weekly timescale. However, the authors conclude that a link between dust deposition and changes in phytoplankton biomass cannot be established during the dust storm season since the results of this study could also be attributed to oceanographic conditions, mainly upwelling, deep convection and coastal freshwater outflow. Gallisai et al. (2014) suggest a different response, using a

modeling approach, where the addition of nutrients though dust of desert origin, seems to stimulate production in the plankton community whereas when the dust is of European origin the feedbacks appear to be negative. The latter study attributes this mismatch to a high concentration of other pollutants (mainly Cu) in European origin dust, which, depending on the season can inhibit phytoplankton growth.

In a summary on the significance of this episodic nature of atmospheric deposition to low nutrient, low chlorophyll (LNLC) areas by Guieu et al. (2014), conclude that responses to any addition are not as simple as in the high nutrient areas. It is likely that the dust depositional flux containing P will increase in the Eastern Mediterranean basin as a result of the predicted decreased rainfall and increased temperature (IPCC, 2014). Furthermore, it is predicted under certain scenarios that there will also be increased flux of anthropogenic N to the basin (Lamarque et al., 2013). It is therefore an ecologically-important matter to investigate the nature of change induced by a sudden addition of nutrients from different origins (desert vs. anthropogenic origin).

The marine environment surrounding Crete in the Eastern Mediterranean is a typical example of an oligotrophic LNLC area where aeolian inputs could influence the marine pelagic ecosystem. Koçak et al. (2010) found that DIN and PO4 inputs dominated over riverine inputs. Atmospheric monitoring data show that strong dust outbreaks occur in January, February, May, and July–September, leading to deposition events in the Cretan Sea (Kalivitis et al., 2007). Our aim was to examine whether there is a direct connection between these deposition events and changes in plankton community abundance or growth rates. The mesocosm approach, utilized here, allowed us to monitor the development of the same microbial community over a number of days, while the large volume of the mesocosms (>1 m^3) allowed experimentation with trophic groups up to copepods. The questions we aimed to address with the present experiment, with regards to the Eastern Mediterranean were: (I) how does a single dry deposition event affect the microbial food web, from viruses to zooplankton; and (II) does the source of dust (desert vs. mixed aerosol) make a difference to the type and magnitude of change observed.

We expected that inputs of nutrients from deposition (both types) would be primarily used by bacteria and incorporated into biomass, from there we hypothesized that the bacteria would be either controlled by increase of viruses, minimizing the transfer up the food web or by flagellate grazers, bypassing the classical food chain and transferring energy directly through microzooplankton to copepods. Alternatively small autotrophs benefiting from the dust input, would transport energy through the classical food chain. The channeling of nutrients through grazers is faster than the classical pathway, a process illustrated in Pitta et al. (2016), where, following a phosphorus addition, copepods respond by producing eggs within 2 days, (faster response) and then again after 5 and 7 days (slower response).

We further hypothesized that the observed response to the Saharan dust addition would be stronger compared to the mixed aerosol, primarily because more nutrients would be supplied through the Saharan dust and also because the mixed aerosols contain more potentially toxic compounds (e.g., Cu, Al) that could inhibit phytoplankton growth and thus result in a response more centered on the microbial loop.

MATERIALS AND METHODS

Experimental Design and Sampling

The experiment was carried out at the mesocosm facilities of the Hellenic Centre for Marine Research (HCMR), Crete (CRETACOSMOS, http://cretacosmos.eu/). The facility consists of a 350 m^3 land-based 5 m deep concrete tank, which is filled with seawater pumped directly into the tank, while the temperature is kept stable through continuous flow of pumped seawater. The mesocosm bags were incubated in the tank for the duration of the experiment. To fill the mesocosm bags, ∼28 m^3 of subsurface water (10 m) was collected from a location north of Heraklion city with the R/V *Philia* (35° 24.957 N, 25° 14.441 E, bottom depth: 170 m) using a rotary submersible pump. The seawater was pumped into acid-cleaned 1 m^3 high density polypropylene tanks which were then transported to CRETACOSMOS. The duration of water acquisition, transportation and filling of the mesocosm bags was ∼2 h per trip, five trips were needed to acquire the required volume of seawater. The nine mesocosm bags used in the experiment had a diameter of 1.32 m, a total volume of 3 m^3 and were made of transparent food-grade polyethylene. Homogeneity during filling was ensured by distributing water from each 1 m^3 tank equally into all the bags using timed intervals while filling. Once the mesocosms were filled, they were covered with a two layer lid (PVC & a nylon mesh) in order (I) to protect them from additional undesired atmospheric aerosols during the experiment and (II) to simulate the light intensity at 10 m (*in situ* sampling conditions). Finally the mesocosm bags were left to settle overnight before the treatments commenced. An airlift system (Jacobsen et al., 1995) ensured water mixing within the mesocosms.

On May 10th, initial samples were taken from all bags prior to any manipulation as a reference. Following sampling, mixed aerosols were added to 3 bags (1.0 mg L^{-1}), Saharan dust (1.6 mg L^{-1}) to three bags and another 3 served as controls. The amount of dust added is representative of a typical deposition event in the area (Herut et al., this issue). Sampling, with acid washed silicone tubes, was carried out daily for the first 4 days and beyond that point, every second day for a total of 9 days from addition (May 19th). All containers and apparatus for filling and sampling were also acid washed daily. Triplicates of treatments were labeled as Saharan Dust (SD), Aerosol (A), and Control (C) and will be referred to as such hereon (see further details in Herut et al., this issue). All measurements are presented in the text as the mean value of 3 replicates followed by the standard error of the mean in brackets. Where no SE is presented no replicate samples from mesocosms were measured.

Nutrients Released with Aerosol Addition

Details of leached nutrients are presented in detail in Herut et al. (2016, this issue). Briefly, dust collected locally was used in order to simulate the deposition events in the area, as realistically as

possible. The dust added to the SD mesocosms released 36.8 nM inorganic nitrogen (NO_3+NO_2) and 3.9 nM PO_4. In the A mesocosms the dust added released 54 nM inorganic nitrogen (NO_3+NO_2) and 3 nM PO_4.

Dissolved Inorganic Nutrients

Water samples were collected daily and analyzed immediately for their phosphate concentrations using the MAGIC method (Rimmelin and Moutin, 2005). The detection limit was 0.8 nM for phosphate. Daily analysis of water samples for dissolved silicate, nitrite and nitrate was done according to Strickland and Parsons (1972), and for ammonium according to Ivancic and Degobbis (1984). The detection limits were 0.017 μM for nitrate and 0.019 μM for ammonium and 0.025 μM for silicate.

Dissolved Organic Carbon (DOC)

Samples for DOC analysis were transferred into dark glass bottles (precombusted at 330°C for 6 h) and then filtered through GF/F filters (precombusted at 450°C for 6 h). The filtrate was collected in 15 mL glass vials (precombusted at 450°C for 6 h) and acidified with 20 μl H_3PO_4 (85%). Samples were stored in the dark at 4°C until laboratory analysis by high-temperature combustion on a Shimadzu TOC 5000 analyzer, as described in Sohrin and Sempéré (2005). A four-point calibration curve was constructed daily using standards prepared by diluting a stock solution of potassium hydrogen phthalate in Milli-Q water. To avoid random errors associated with day-to-day instrument variability, all samples from a given treatment were analyzed in a single day. The procedural blanks (i.e., runs with Milli-Q water) ranged from 1 to 2 μM C whereas the analytical precision was within 2%. Operational average blanks related to transfer and storage of samples, filtration, and handling were 8.4 ± 2.5 μM C ($n = 7$).

Total Particulate Nutrients

Water samples collected from the mesocosms were filtered on 0.2, 0.6, 2, and 10 μm pore size polycarbonate (PC, 47 mm diameter) and Glass Fiber (GFF, 47 mm diameter) filters. The filters were air dried and stored and total particulate nutrients were measured using wavelength dispersive X-Ray Fluorescence (WDXRF) as described in Paulino et al. (2013). An S4 Pioneer XRF was used (Bruker-AXS, Karlruhe, Germany) at the department of Biology, University of Bergen. Size fractionated particulate Si, P, Fe, and Ca was measured on the PC filters and total C, N and P over 0.7 μm on the GFF filters. The detection limit is dependent on the peak-to-ground ratio of the spectral lines but the method has a detection limit for most of the elements at ∼5 ppm, detection limits are included in Paulino et al. (2013).

Uptake of $^{33}PO_4$

Samples (10 mL) for turnover time of PO_4 were collected every day and measured using ^{33}P-orthophosphate (Thingstad et al., 1993). Carrier-free ^{33}P-orthophosphate (PerkinElmer, 370 MBq mL^{-1}) was added to samples at a final concentration of 20–79 pM. Samples for the subtraction of the background and abiotic adsorption were fixed with 100% trichloroacetic acid (TCA) (final conc. 0.5%) before isotope addition. Samples were incubated under subdued (laboratory) illumination. The incubation time varied between 1 and 20 min. Incubation was stopped by a cold chase of 100 mM KH_2PO_4 (final conc. 1 mM). Subsamples (3.3 mL) were filtered in parallel onto 25 mm polycarbonate filters with 2, 0.6, and 0.2 μm pore sizes. After filtration, filters were placed in polyethylene scintillation vials with Ultima Gold (Packard), and radio-assayed. After the radioactivity of each filter was corrected for those of the blank filter obtained from fixed samples, phosphate turnover time ($T_{[PO4]}$: h) was calculated as $T_{[PO4]} = -t/\ln(1-f)$ where f is the fraction (no dimension) of added isotope collected on the 0.2 μm filter after the incubation time (t: h).

Alkaline Phosphatase Activity (APA)

Samples of APA were collected daily from every mesocosm treatment. One mL of sea water sample was added to the substrate MUF-P. The alkaline phosphatase (AP) hydrolyses the fluorogenic substrate MUF-P and yields a highly fluorescent product (methyllumbelliferon: MUF) and a phosphate group in equimolar concentrations (Rengefors et al., 2001; Sebastian et al., 2004). The MUF produced was detected as increase in fluorescence with spectrofluorometer (Hithachi F-2000, excitation-364 nm and emission-448 nm). A standard curve with MUF (Sigma Co.) was used to quantify the amount of MUF produced by APA, so the phosphate liberated in the reaction could be estimated.

Chlorophyll *a*

The amount of chlorophyll *a* corresponding to the 0.2–0.6, 0.6–2, and >2 μm size classes was measured fluorimetrically (Holm-Hansen et al., 1965). Samples for chlorophyll *a* analysis were sequentially filtered through 2, 0.6, and 0.2 μm polycarbonate filters (47 mm diameter) using moderate vacuum pressure (<200 mmHg). The filters were immediately extracted in 90% acetone at 4°C in the dark overnight (for 14–20 h). Chl *a* concentration was determined using a Turner TD-700 fluorometer. Total Chl *a* was calculated as the sum of the three size fractions.

Bacterial and Primary Production

Bacterial production (BP) was measured using the ^{3}H-leucine method, according to Kirchman et al. (1985) and modifications by Smith and Azam (1992). For each mesocosm, duplicate samples (1.5 mL) and one trichloracetic acid (TCA) killed control were incubated in 2 mL tubes with a mixture of [4,5-^{3}H] leucine (Perkin Elmer, specific activity 115 Ci $mmol^{-1}$) and non-radioactive leucine at final concentrations of 16 and 7 nM, respectively. All samples were incubated for 2 h in the dark at *in situ* temperature. Incubation was terminated with the addition of 90 μL 100% TCA. Samples were then stored at 4°C in the dark until further processing. Centrifugation was carried out at 16,000 g for 10 min. After discarding the supernatant, 1.5 mL of 5% TCA was added, samples were vigorously shaken using a vortex and then centrifuged again at the same speed and duration. After discarding the supernatant, 1.5 mL of 80% ethanol was added, samples were shaken and centrifuged again. The supernatant was then discarded and 1.5 mL of scintillation liquid (Ultima Gold) was added. The radioactivity incorporated

into the pellet was counted using a Packard Tri-Carb 4000TR scintillation counter. BP was calculated according to Kirchman et al. (1993), from the ^{3}H-leucine incorporation rates.

Primary production (PP) was measured using the ^{14}C incorporation method of Steeman-Nielsen (1952). Three light and one dark 320 mL polycarbonate bottles were filled with sample water from each mesocosm in the morning, inoculated with 5 μCi of $NaH^{14}CO_3$ tracer each, and incubated in the large concrete tank for 3 h around midday. After the incubation, samples were filtered through 0.2, 0.6, and 2 μm polycarbonate filters under moderate vacuum pressure placed in scintillation vials where 1 mL of 1% HCl solution was immediately added in order to remove excess ^{14}C-bicarbonate overnight. Then, 4 mL scintillation fluor (Ultima Gold) was added to the vials, and samples' radioactivity was counted in a scintillation counter. Primary production (μg C L^{-1} h^{-1}) was then calculated from the radioactivity (disintegrations per minute, dpm) measured in the light and dark samples.

Abundance of Viruses, Pico- and Nanoplankton and Flagellates

Samples for determining the abundance of virus-like particles (VLP), heterotrophic bacteria (HB) and picophytoplankton were collected daily and fixed with 25% 0.2 μm-filtered glutaraldehyde (0.5% final concentration). After remaining at 4°C for ∼45 min, they were flash frozen in liquid nitrogen and transferred at −80°C until further processing. Frozen samples were thawed at room temperature and sub-samples were stained for viral and bacterial enumeration, according to Brussaard (2004) and Marie et al. (1999), respectively. For more details see Tsiola et al. (this issue).

Samples for flagellate counting were collected every day, fixed with glutaraldehyde (final concentration, 1%), and kept in the dark at 48°C. Flagellate cells were concentrated to ∼10 mL^{-1} onto a 25-mm-diameter, 0.8-mm pore-sized black polycarbonate filter, stained with 406-diamidino-2-phenylindole (1 mg mL^{-1}) for 10 min and finally collected on the filter (Porter and Feig, 1980). The filters were mounted on slides and stored frozen (−20°C). Autotrophic (ANF) and heterotrophic nanoflagellates (HNF) were examined on at least 50 fields at x1,000, using UV and blue excitations under an Olympus BX60 epifluorescence microscope. All cells were sized and divided into four categories (5, 5–10, and >10 μm) using an ocular micrometer.

Eukaryotic Microplankton Abundance

Samples for microplankton enumeration (250 mL) were preserved in acid lugol solution (final concentration 4%) and stored at 4°C in the dark before being analyzed within 3 months of collection.

Prior to the microscopic analysis the samples were left to settle in the collection bottles in the dark and after 48 h 150 mL was slowly siphoned away. The remaining100 mL were sedimented and further analyzed according to Utermöhl (1958) on an inverted microscope (Olympus IX70) using an image analysis system after 24 h sedimentation. Examination of the supernatant in 5 random samples showed minimal cell loss (0–4%) during the above sample concentration process.

Zooplankton Abundance, Copepod Egg Production, and Feeding Rates

Total abundance of zooplankton larger than 45 μm was determined at the beginning and the end of the mesocosm experiment, by collection of triplicate samples from the field. At the end of the experiment, the content of each one of the mesocosms was filtered through a 45 μm net, fixed with 4% buffered formalin, and analyzed using a dissecting microscope.

Copepod egg production and feeding rates were measured four times (11, 12, 15, and 16 May 2012) in each mesocosm treatment. For the egg production and feeding experiments, adult females of the dominant copepod species *Clausocalanus furcatus*, were used. The copepods were collected from the same area as the original water for the mesocosms. Water for the incubations was collected from each replicate mesocosm early in the morning and mixed (at a ratio of three to one) according to the respective treatment. For the estimation of egg production, 3–4 females were placed in each of six 620 ml glass jars (replicates) containing well-mixed 60 μm filtered water collected from each treatment. For the feeding experiments adult copepods (ca. 10–12 females, pre-conditioned for 24 h) were added to three of the bottles (1.3 L polycarbonate), whereas the other six served as initial (three) and control (three) bottles. For more details see Christou et al. (2016, this issue).

Transparent Exopolymer Particles (TEP)

Samples for TEP analyses were collected daily from each mesocosm. Ambient seawater (10 m depth) was also collected during 3 days prior to the experiment to assess the *in situ* concentration of TEP. Water samples (400 mL) were filtered on 0.4 μm Whatman polycarbonate filters (25 mm diameter) under low and constant vacuum (<150 mmHg) to preserve TEP state. The TEP concentrations were measured spectrophotometrically according to a dye-binding assay (Engel, 2009). Briefly, material retained in the filters was stained with 500 μl of an aqueous solution of 0.06% acetic acid (pH 2.5) and 0.02% Alcian Blue (Sigma, 8GX). Filters were then transferred into 25-ml tubes and incubated for 2 h with 6 mL of sulfuric acid (H_2SO_4, 80%) was added. Absorbance of these acid solutions was measured on a spectrophotometer (Shimadzu UV-Vis; UV-2501PC) at a wavelength of 787 nm. TEP values are expressed as xanthan gum weight equivalent (X equival L^{-1}) calculated by means of a calibration curve.

Ratio of Heterotroph to Autotroph Abundance

In order to establish which of the two trophic strategies was favored by the community following the addition and if the trend was dependent on size, we compared the ratio of heterotroph and autotroph abundance. The plankton community abundance was divided into four categories: (a) the picoplankton (Heterotrophic bacteria: Synechococcus & APE), (b) HNF under 5 μm ESD: (Equivalent Spherical Diameter), ANF under 5 μm ESD, (c) HNF over 5 μm ESD: ANF over 5 μm ESD, and (d) Ciliates, Dinoflagellates, and Tintinnids: Diatoms. We assumed all dinoflagellates as potentially heterotrophic as in Loder et al. (2011). On days where abundance data was available for two or

more size classes the logged total abundance between treatments was also compared.

Statistical Analysis

Experimental results were analyzed for significant changes over time and between treatments using repeated measures analysis of variance (RM-ANOVA), with a compound symmetry correlation structure and after checking if the assumptions for performing the analysis were met. The dependent variable was the measured parameter and the independent variables were the treatment type (Control, Saharan Dust, Aerosol) and time (day number). Where the interaction term between variables was not significant, it was removed.

On individual experimental days, one-way analysis of variance (one-way ANOVA) was used to assess whether there were statistically significant differences in measured parameters between treatments, the treatment type (Control, Saharan Dust, Aerosol) was the independent variable and again, the analysis was performed when assumptions were met. Following the one-way ANOVA, the differences between groups (as mean) were explored using Tukey's HSD test.

Where the employed ANOVA analyses showed statistically significant differences, the F ratio, degrees of freedom, confidence level are given in brackets as follows (F_{df} = ratio, $p < 0.05$, eta squared). The effect size, eta squared (η^2 one-way ANOVA) and partial eta squared ($\eta_p{}^2$ RM ANOVA) are also indicated. Differences were considered significant at the 95.0% confidence level. All statistical analysis was performed using the IBM SPSS™ 22 software.

RESULTS

The initial water characteristics used prior to the aerosol additions (SD or A) are discussed in Herut et al. (2016), this issue. The results presented here pertain to measurements from the mesocosm bags after filling was completed as described in the Materials and Methods Section.

Dissolved Nutrients

Mean initial phosphate concentration in the mesocosms was 13.6 nM (±1.45). After the addition of either SD or A the PO_4 concentration decreased while no changes were observed in the C mesocosm. One-way ANOVA showed that prior to any addition, the A mesocosm bags had a significantly higher concentration of phosphate (F_2 = 1 1.05, p = 0.01, η^2 = 0.79); Average initial concentration 17.9 nM (±2.3), this difference was evident until Day 4 (**Figure 1A**).

Dissolved inorganic nitrogen (DIN) was calculated as the sum of NO_2, NO_3, and NH_4 and was initially 270 nM (±15). One-way ANOVA showed that prior to addition the DIN concentration was higher in the C and A than the SD bags ($F_2 = 11.05$, $p = 0.01$ $\eta^2 = 0.79$). On Day 3 the DIN concentration was significantly higher in the mixed A treated mesocosms than the C ($F_2 = 10.56$, $p = 0.011$, $\eta^2 = 0.78$), with a mean concentration of 289 nM (±53.2) and 268 nM (±19.9) in the mixed aerosol and Saharan dust treatment, respectively (**Figure 1B**).

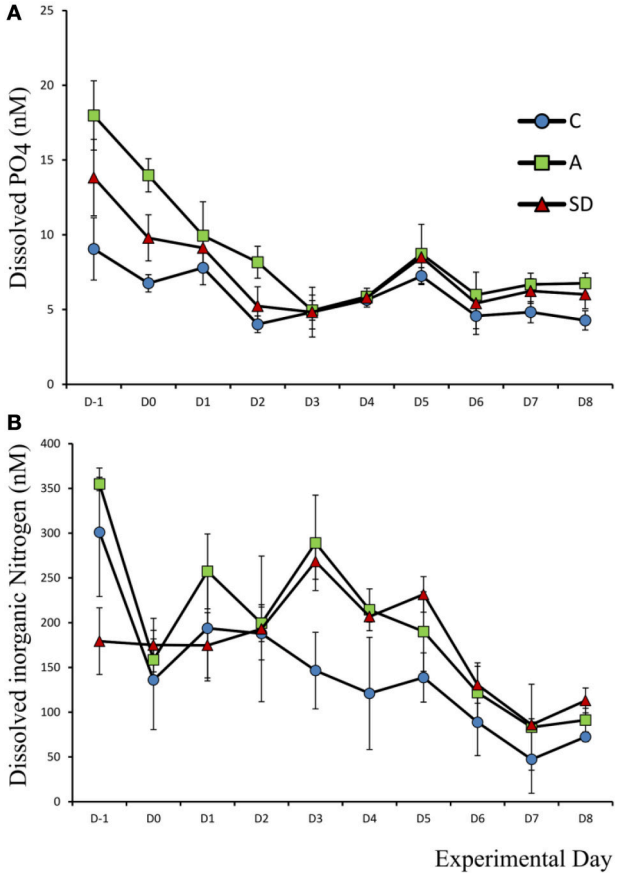

FIGURE 1 | Concentration of dissolved **(A)** phosphate and **(B)** inorganic nitrogen, in each treatment over the course of the experiment.

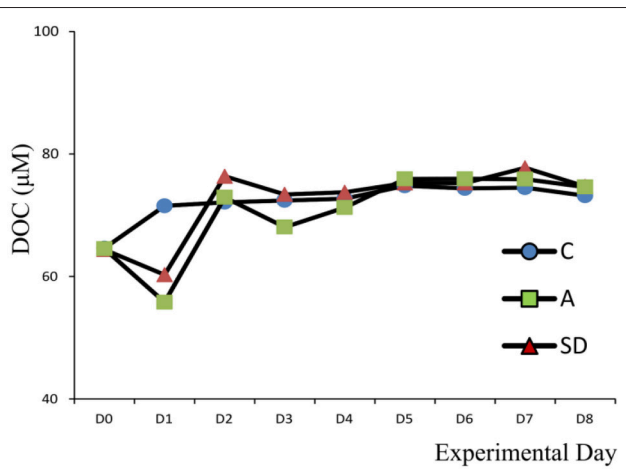

FIGURE 2 | Dissolved organic carbon (DOC) concentration in the different treatments.

Prior to additions, the mean silicate concentration in all mesocosms was 1,230 nM (±49). A peak in the C and A treatments was measured on Day 1, where the concentration increased to a mean of 1,690 nM (±207) and 1,770 nM

(±207), respectively (not shown). No significant differences were observed in silicate concentrations between treatments after the addition of dust.

Dissolved Organic Carbon (DOC)

Initial DOC concentrations for all mesocosm experiments ranged from 62 to 65 μM C. Values were lower, but close to DOC concentration at the sampling site (73 μMC) suggesting no contamination occurred during the seawater transfer. On Day 2, DOC concentrations increased by 12 and 8 μMC from their initial concentration for the SD and A mesocosms, respectively (**Figure 2**). These values are in agreement with the organic carbon content of the initial SD (8 μM C) and A (6 μM C) dust before addition to the mesocosm (data not shown). Overall, DOC concentration did not exhibit significant differences between the treatments.

Particulate Nutrients

No significant differences were found for particulate carbon and nitrogen between treatments and days. Mean particulate carbon (C_{par}) was 3.98 μM (±0.32) at the beginning of the experiment while particulate nitrogen (N_{par}) was 0.39 μM (±0.19). The corresponding particulate C:N ratio was 10:1, slightly higher than the typical Redfield ratio (6.6), suggesting a potential N limitation.

Mean particulate phosphorus (P_{par}) was 0.08 μM (±0.01) at the beginning of the experiment. One-way ANOVA on individual days showed that on Day 2 addition P_{par} was significantly higher in the SD treatment than both the A and C treatments ($F_2 = 22.9$, $p = 0.002$, $\eta^2 = 1$; **Figure 3A**). The particulate C:P ratio on D0 in the C tanks was 46.6 (±4.6), suggesting that particles were P replete (not shown).

Particulate Fe concentration changed considerably after both the SD and A additions. Initial Fe concentration was 0.037 μM (±0.006). In the A treatment, a significant increase in Fe was observed ($F_5 = 27.1$, $p = 0.001$, $\eta^2 = 1$), with values of 0.065 (±0.001) on D1 which remained at a similar concentration for one more day. In the SD mesocosms Fe_{par} increased to 0.16 (±0.004) 1 day after addition (**Figure 3B**). Based on 1 one-way ANOVA analyses, Fe_{par} differed significantly between all treatments on D1 ($F_2 = 211$, $p < 0.001$, $\eta^2 = 1$). The same applies for D2 ($F_2 = 32.3$, $p < 0.001$, $\eta^2 = 0.89$) and D4 ($F_2 = 10.3$, $p = 0.043$, $\eta^2 = 0.67$).

Phosphorus Turnover Time and Uptake

The mean turnover time $T_{[PO4]}$ of phosphorus was 1.05 (± 0.04) h in the beginning of the experiment. After aerosol addition, $T_{[PO4]}$ decreased significantly over time all mesocosms ($F_9 = 419$, $p < 0.001$, $\eta_p{}^2 = 0.57$) to reach a minimum of 0.08 (±0.003) h in both A & SD on Day 6. The turnover time was higher in the control than the dust added mesocosms on Day 3($F_2 = 34.15$, $p < 0.001$, $\eta^2 = 0.92$) and on most of the following days (**Figure 4A**).

Phosphorus uptake in the smallest fraction (0.2–0.6 μm) decreased in all treatments up to days 3–4, most of the P during these days was instead taken up by the fraction >2 μm. From the beginning, more than 50% of P uptake was mediated by the 0.6–2 μm fraction, which also displayed the smallest magnitude of change (**Figures 4B–D**).

Alkaline Phosphatase Activity

Alkaline phosphatase activity (APA) was low at the beginning of the experiment, the mean concentration was 1.90 (±0.23) nM MUF h^{-1}. APA peaked in all mesocosms toward the end of the experiment, on Day 6, at 17.71 (±0.52), 16.96 (±6.22), and 13.60 (±9.49) nM MUF h^{-1} in the C, A, and SD treatments, respectively. Activity was higher in the control and mixed aerosol mesocosms, than in the Saharan dust treatment before the dust was added ($F_2 = 9.59$, $p = 0.014$, $\eta^2 = 0.76$), the same was the case up to Day 2 (**Figure 5**).

Chlorophyll *a*

Total Chl *a* (>0.2 μm) prior to addition was 0.064 μg L^{-1}. The Chl *a* levels followed the same trend in all mesocosms, with an overall increase of 1.5-fold in all treatments up to Day 3 where it peaked. Yet, the day after both aerosol types were added (D1), Chl *a* concentration was significantly higher than the control ($F_2 = 153$, $p < 0.001$, $\eta^2 = 1$). The trend continues with higher Chl *a* concentration in the A treated mesocosms (**Figure 6A**). Chl *a* size fractionation showed that the increase observed in the dust

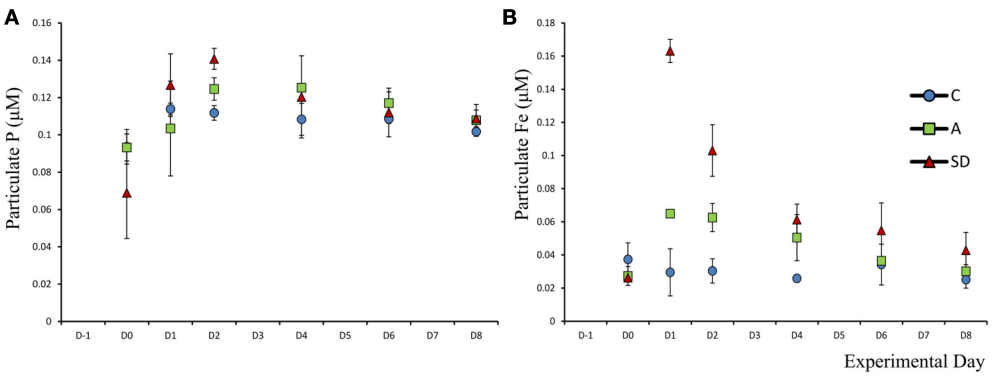

FIGURE 3 | Total particulate phosphorus (P) **(A)** and Iron (Fe) **(B)** in each treatment.

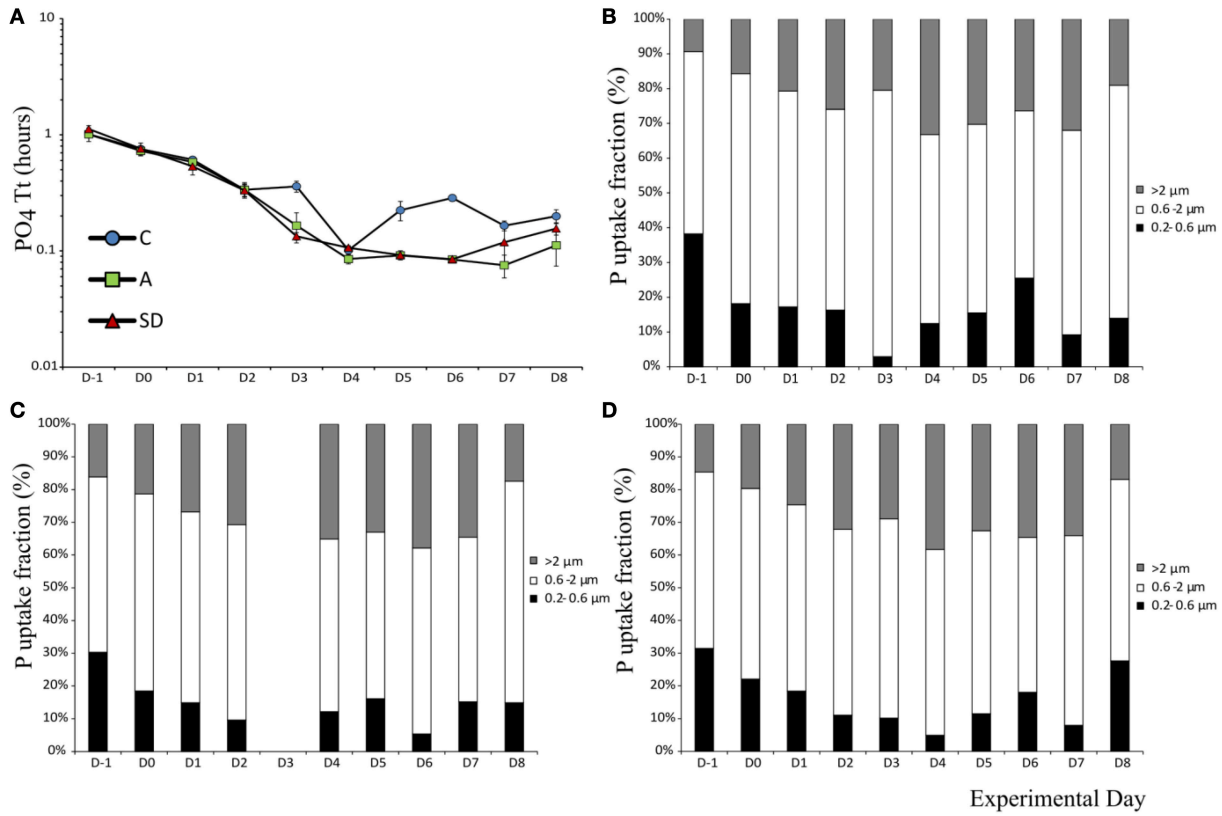

FIGURE 4 | Phosphate turnover time **(A)** and uptake in different size fractions in the control **(B)**, mixed aerosol **(C)**, and Saharan dust **(D)** treatments.

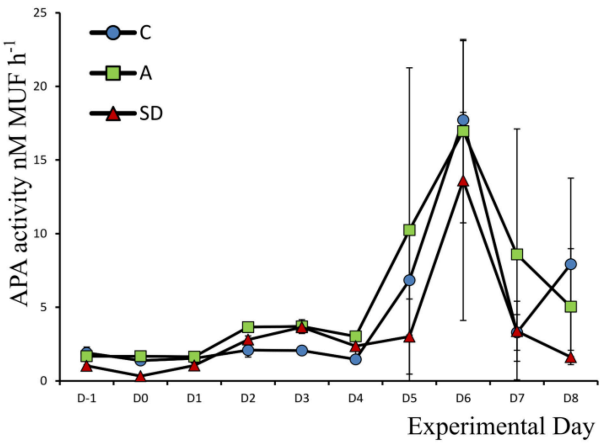

FIGURE 5 | Alkaline phosphatase activity in each treatment.

treated mesocosms was mostly due to changes in the fractions from 0.6–2 and >2 µm (**Figures 6B–D**).

Bacterial and Primary Production

Bacterial production (BP) prior to addition was 13.6 (±1.8) ng C L^{-1} h^{-1}. The response on the day of dust addition (Day 0) was very fast in the A treatment, BP increased over 150%, to 31.5 (±2.4) ng C L^{-1} h^{-1} which was significantly more ($F_2 = 104.1$, $p < 0.001$, $\eta^2 = 0.97$) than both the SD and the control (**Figure 7A**). The following day, BP peaked in the mixed aerosol treatments, again with significant differences from the control ($F_2 = 18.6$, $p = 0.003$, $\eta^2 = 0.86$), but not between treatments, following the peak BP was decreasing to Day 4 (**Figure 7A**).

Mean initial total primary production (PP), prior to addition, was 0.39 (±0.02) µg C L^{-1} h^{-1}. From Day 1, the mixed aerosol added mesocosms showed significantly higher PP rates ($F_2 = 7.1$, $p = 0.025$, $\eta^2 = 0.87$), an increase of 56% compared to Day 0. On Day 2, the PP rates in both dust treatments were higher than the control ($F_2 = 19.7$, $p = 0.002$, $\eta^2 = 0.7$) but treatments did not differ between them until Day 3, when SD displayed its maximal values of 0.58 (±0.01SE) µg C L^{-1} h^{-1}. Treatment A peaked 1 day later, reaching values of 0.68 (±0.06 SE) µg C L^{-1} h^{-1} (**Figure 7B**).

The size fractionation showed that observed differences were mostly due to changes in PP of the fractions 0.2–0.6 and 0.6–2 µm, which increased in the SD and A treatments on days 1–3. After that the fraction of PP >2 µm increased in the SD mesocosms but not in the A ones.

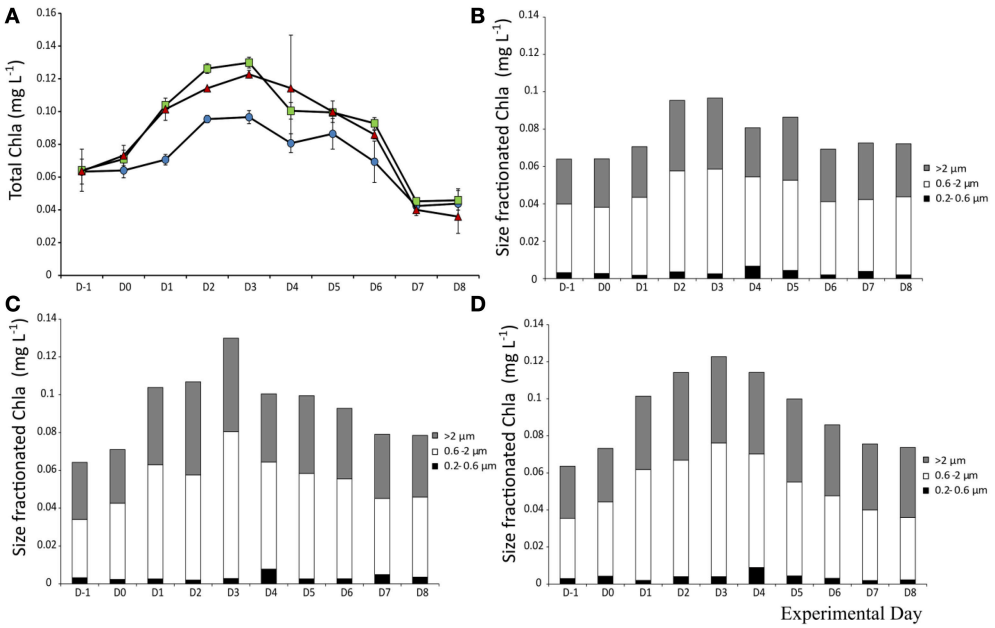

FIGURE 6 | Total Chlorophyll *a* concentration **(A)** and contribution of each size fraction to total Chla *a* in the control **(B)**, mixed aerosol **(C)**, and Saharan dust **(D)** treatments.

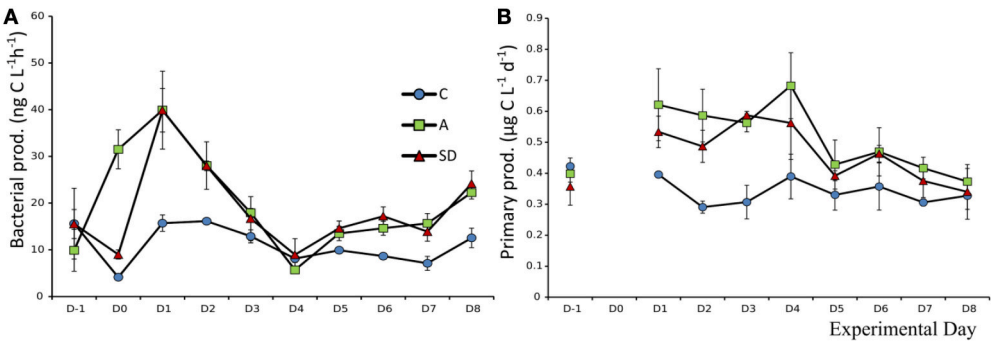

FIGURE 7 | Bacterial production **(A)** and primary production **(B)** in each treatment.

Abundance of Viruses, Pico- and Nanoplankton and Flagellates

Changes in viral abundance over time were similar in all mesocosms. Mean initial abundance was 6.6×10^6 ($\pm 2.1 \times 10^5$) individuals mL^{-1}, which changed little until the end of the experiment. After the addition of dust, on Day 1, viral abundance in the A treatment was significantly higher ($F_2 = 16.54$, $p = 0.004$, $\eta^2 = 0.85$). The same response was observed on Day 3 for the SD treatment ($F_2 = 5.51$, $p = 0.044$, $\eta^2 = 0.65$) (**Figure 8A**). The virus to bacteria ratio was higher in the controls, with an increasing trend as the experiment progressed. The increasing trend was also observed for the dust added mesocosms, with no differences between them (**Figure 8B**).

Mean heterotrophic bacteria (HB) abundance at the beginning of the experiment was 4.2×10^5 ($\pm$ 3.6×10^3) cells mL^{-1}. The abundance in control mesocosms decreased significantly over time ($F_9 = 219$, $p < 0.001$, $\eta_p{}^2 = 0.97$) to 2.3×10^5 ($\pm 4.2 \times 10^3$) cells mL^{-1} at the end of the experiment. In the aerosol treated mesocosms (SD and A), HB abundance was higher that the control on all days after addition (D1 onwards). HB peaked in A & SD on Day 1 at 5.17×10^5($\pm 1.2 \times 10^4$) and 5.14×10^5 ($\pm 2.4 \times 10^4$) cells mL^{-1}, respectively (**Figure 9A**). Abundance declined steadily until Day 5, after which it started increasing again in the dust treated mesocosms until the end of the experiment. No significant differences between dust types were detected (**Figure 9A**).

Initial mean *Synechococcus* abundance was 2.3×10^4 (± 105) cells mL^{-1}. Significant changes over time were observed in all mesocosms ($F_9 = 150$, $p < 0.001$, $\eta_p{}^2 = 0.96$). Differences were significant only after the addition of SD or A. On D1 significantly

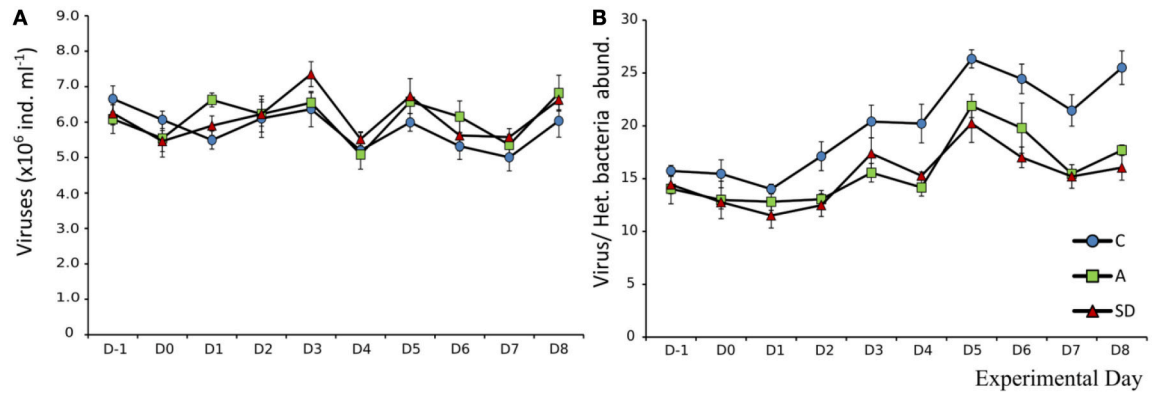

FIGURE 8 | Abundance of viruses **(A)** and ratio of viral to bacterial abundance **(B)** in each treatment.

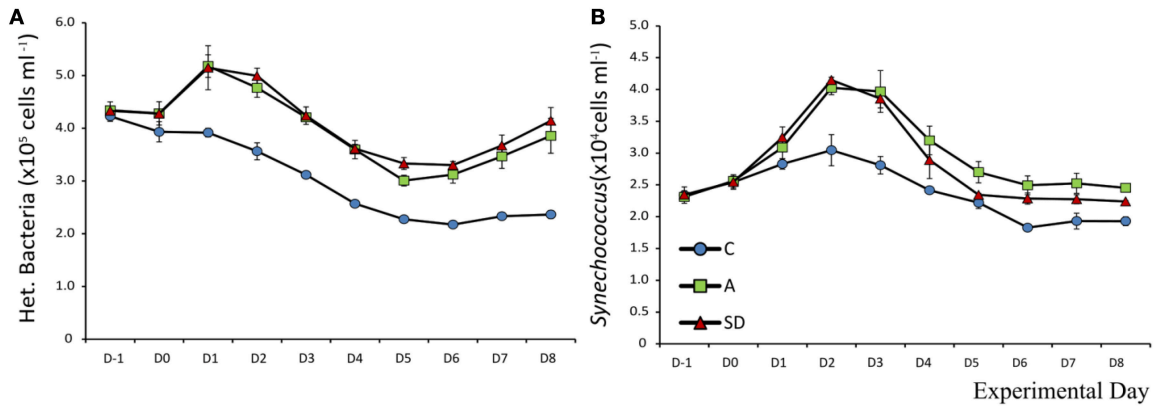

FIGURE 9 | Abundance of **(A)** heterotrophic bacteria and **(B)** *Synechococcus* sp. in each treatment.

more *Synechococcus* than the control were observed in the SD mesocosms ($F_2 = 6.1$, $p = 0.035$, $\eta^2 = 0.67$). From Day 2 onwards the abundance of *Synechococcus* in both the A and SD mesocosms was higher than the control until the end of the experiment. *Synechococcus* peaked in both treatments on D2 with a more than 70% increase from the beginning of the experiment at 4.0×10^4 (±609) and 4.1×10^4 (±257) cells mL^{-1}in the A and SD mesocosms, respectively (**Figure 9B**).

Autotrophic picoeukaryotes (APE) also changed significantly over time, again with a very similar trend between all mesocosms ($F_9 = 224$, $p < 0.001$, ${\eta_p}^2 = 0.97$). Mean initial abundance was 1,335 (±34.1) cells mL^{-1}. On Day 3 the SD mesocosms showed a significantly higher abundance than the control ($F_2 = 8.8$, $p = 0.016$, $\eta^2 = 0.75$), at 2,193 (±95) cells mL^{-1}. After Day 3 a decrease was observed, to abundances much lower than the starting day, in all mesocosms (data not shown).

The mean abundance of autotrophic nanoflagellates (ANF) at the beginning of the experiment was 1,107 (±29) cells mL^{-1}. One day after the addition significantly more ANF were observed in both A & SD mesocosms ($F_2 = 7.47$, $p < 0.05$, $\eta^2 = 0.71$). The abundance peaked on D2 at 1,741 (±183) and 2,013 (±183) cells mL^{-1} in the A and SD mesocosms, respectively (**Figure 10A**).

The size distribution of the autotrophic flagellates suggests that small flagellates were dominant in all treatments and days, with the size class under 5 μm making up more than 70% of the community total (data not shown). Heterotrophic nanoflagellates (HNF) did not display any significant differences between treatments and days. Their mean abundance at the beginning of the experiment was 3,073 (±90) cells mL^{-1}. The abundance declined up to D2 to a mean abundance of 1,177 (±40) cells mL^{-1} (**Figure 10B**).

Eukaryotic Microplankton Abundance

Diatom abundance was high at the beginning of the experiment, dominated by the chain forming diatom *Chaetoceros* sp. at the sampling site with 2,500 cells L^{-1}. The diatom population decreased during the experiment reaching a minimum of 920 cells L^{-1} in the C and A treatments on Day 8. In the SD the decline was sharper, the population halved in 2 days going from an initial abundance of 2,345 cells L^{-1} to 1,175 cells L^{-1}. Dinoflagellate abundance was 665 cells L^{-1} at the beginning of the experiment. While in the C mesocosms minimal changes were observed throughout, the SD and A additions triggered different responses with nearly doubled dinoflagellate abundance

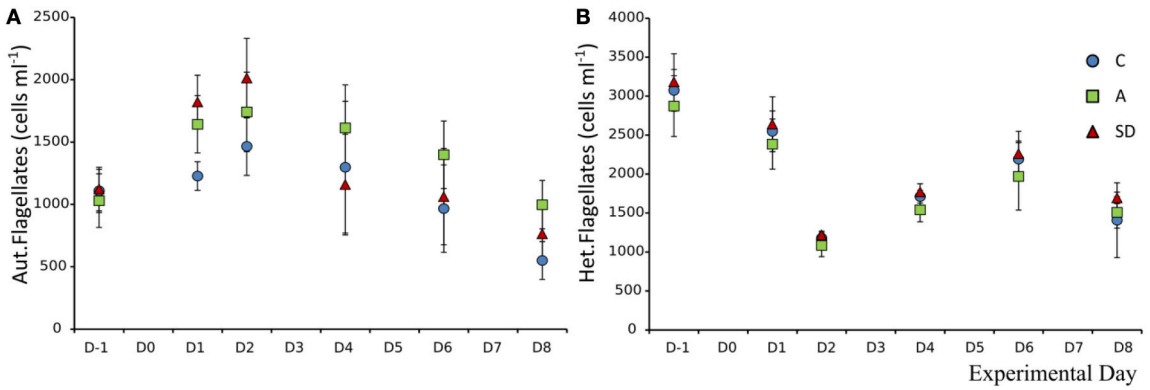

FIGURE 10 | Abundance of autotrophic nanoflagellates **(A)** and heterotrophic nanoflagellates **(B)** in each treatment.

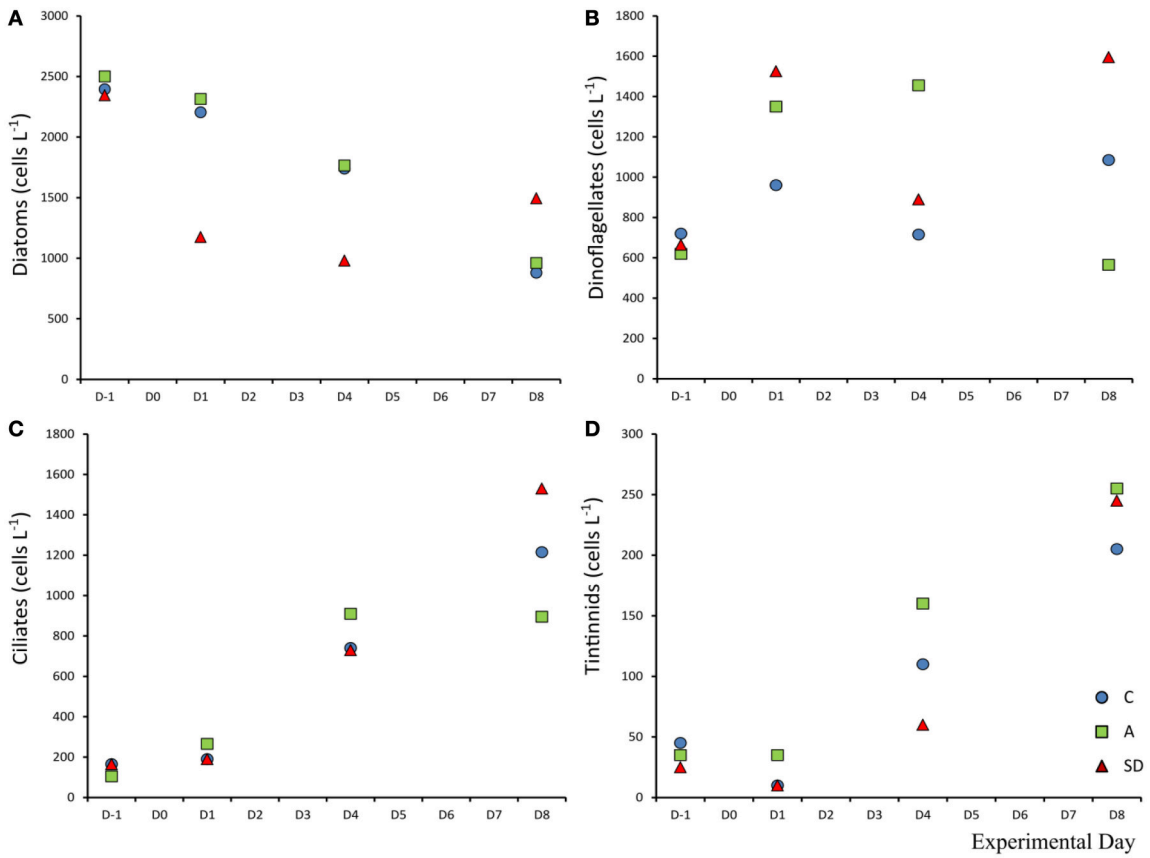

FIGURE 11 | Abundance of diatoms **(A)**, dinoflagellates **(B)**, ciliates **(C)**, and tintinnids **(D)** in each treatment.

at D1 (1,525 cells L^{-1}) in the SD treatment. Initial average ciliate abundance (D-1) was 145 cells L^{-1}, the abundance increased in all mesocosms and was highest in the SD treatment. On Day 8, in the SD mesocosms, ciliate abundance was almost 10 times higher than the start, at 1,530 cells L^{-1}, which was also the highest abundance measured. Loricate tintinnids also increased, from an initial abundance of 35 cells L^{-1} to a final abundance of 1,213 cells L^{-1} in the A treatment (**Figures 11A–D**).

Zooplankton Abundance, Copepod Egg Production, and Feeding Rates

Total zooplankton abundance in the ambient seawater samples was 188 (±40) ind. m^{-3}, at the end of the experiment mean zooplankton abundance decreased in all treatments but the differences were not statistically significant, (**Figure 12A**). Most of the zooplankton community consisted of copepods, with *Clausocalanus* sp. being the dominant genus (Christou et al.,

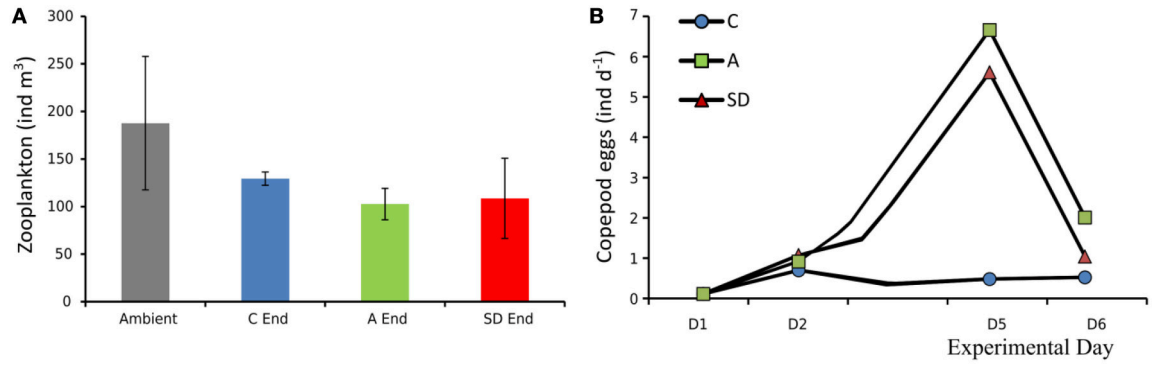

FIGURE 12 | Initial zooplankton abundance (ambient water) and at the end of the experiment **(A)**, copepod egg production in mesocosms **(B)**.

2016, this issue). In the aerosol added treatments copepod egg production increased on Day 5 from an average of 0.8 eggs per individual per day, 1 day after addition to more than 5 eggs ind. day^{-1} (**Figure 12B**). Essential feeding was detected during all experiments on ciliates and dinoflagellates, whereas grazing on Chl *a* was lower. Both ciliates and dinoflagellates were cleared at comparable rates with marginally higher clearance rates for ciliates (Ciliates: 14–152 mL cop^{-1} day^{-1}; Dinoflagellates: 22–97 mL cop^{-1} day^{-1}), Chl *a* was cleared at much lower rates in most cases (2–54 mL cop^{-1} day^{-1}; Christou et al., 2016, this issue).

Transparent Exopolymer Particles (TEP)

Transparent exopolymer particles did not display any significant differences between treatments and days. The exception was Day 6 where one way ANOVA showed significantly more TEP in the SD treated mesocosms than in the A or control mesocosms ($F_2 = 7.56$, $p = 0.023$, $\eta^2 = 0.72$). At the beginning of the experiment, mean TEP concentration was 118.5 (±5.05) xanthan eq. μg L^{-1}. Then an increase in TEP concentration was observed with maximum values of 188.4 (±15) and 203.7 (±25) xanthan eq. μg L^{-1} in SD and A mesocosms on Day 6 and Day 7, respectively. While in the control mesocosms the average was 99.1 (±4.46).

Ratio of Heterotroph to Autotroph Abundance

Overall, the ratio between autotrophic and heterotrophic abundance of plankton groups showed an interesting pattern following the addition. The results of the comparison are shown in **Figure 13**. The H:A ratio decreased in all the size classes up to microplankton after the dust addition (**Figure 13**). The decrease lasted until days 2 and 3 after which slightly different trends were observed in each treatment. In the pico-fraction the heterotrophs dominated more in the Saharan dust addition while the H:A ratio remained lower than the initial ratio until the end of the experiment (**Figure 13A**). Small nanoflagellate H:A ratio returned to initial values in the control and SD but not the A treatment (**Figure 13B**) and the same is the case for the large nanoflagellates where the heterotrophs increased earlier in the SD treatment (**Figure 13C**). In the microplankton size fraction the heterotrophs increased in all treatments, the largest increase was observed in the SD (**Figure 13D**).

DISCUSSION

The impact of Saharan dust and mixed aerosol deposition on plankton communities was examined in the Eastern Mediterranean. The deposition resulted in changes in the plankton community at different scales and magnitudes, but throughout the monitored groups, from bacteria to zooplankton. To our knowledge, this is the first experiment demonstrating the transfer of atmospheric deposition effects to a higher trophic level. The copepod egg production increased in both sets of dust added mesocosms 5 days after the addition of dust. Although a small amount of nutrients was added, this constituted an important percentage increase in the total dissolved phosphate pool. In the SD 40% additional dissolved phosphate was added in comparison to 30% for the A. This <5 nM PO_4 addition was enough to trigger a 0.04 mg L^{-1} increase in Chl *a* after 1 day (Herut et al., 2016, this issue).

Regarding our expectations for the changes in the plankton community we observed the expected transfer of energy to higher trophic levels. This transfer occurred through the classical food chain and not through a bypass of the microbial loop. It took 5 days for copepod egg production to increase, there were more autotrophs during the first 4 days of the experiment (**Figure 13E**) and the P turnover time decreased during the first 4 days. The dominance of the autotrophic pathway could be because of the high inoculum in the collected seawater, with many diatoms, ready to use the Nitrogen supply, likely co-limiting as indicated by the initial C:N ratio. The origin of dust added did not seem to change the observed community responses, thus our expectation regarding added effects of mixed aerosol was not met.

Marañón et al. (2010) demonstrated that the degree of oligotrophy influences the type of response to deposition, suggesting that in less oligotrophic conditions, since bacteria are less limited by inorganic nutrient supply, phytoplankton have a better chance of utilizing the supplied nutrients. Their results, from bioassay experiments in the Atlantic, show the bacterial response was more pronounced in ultraoligotrophic

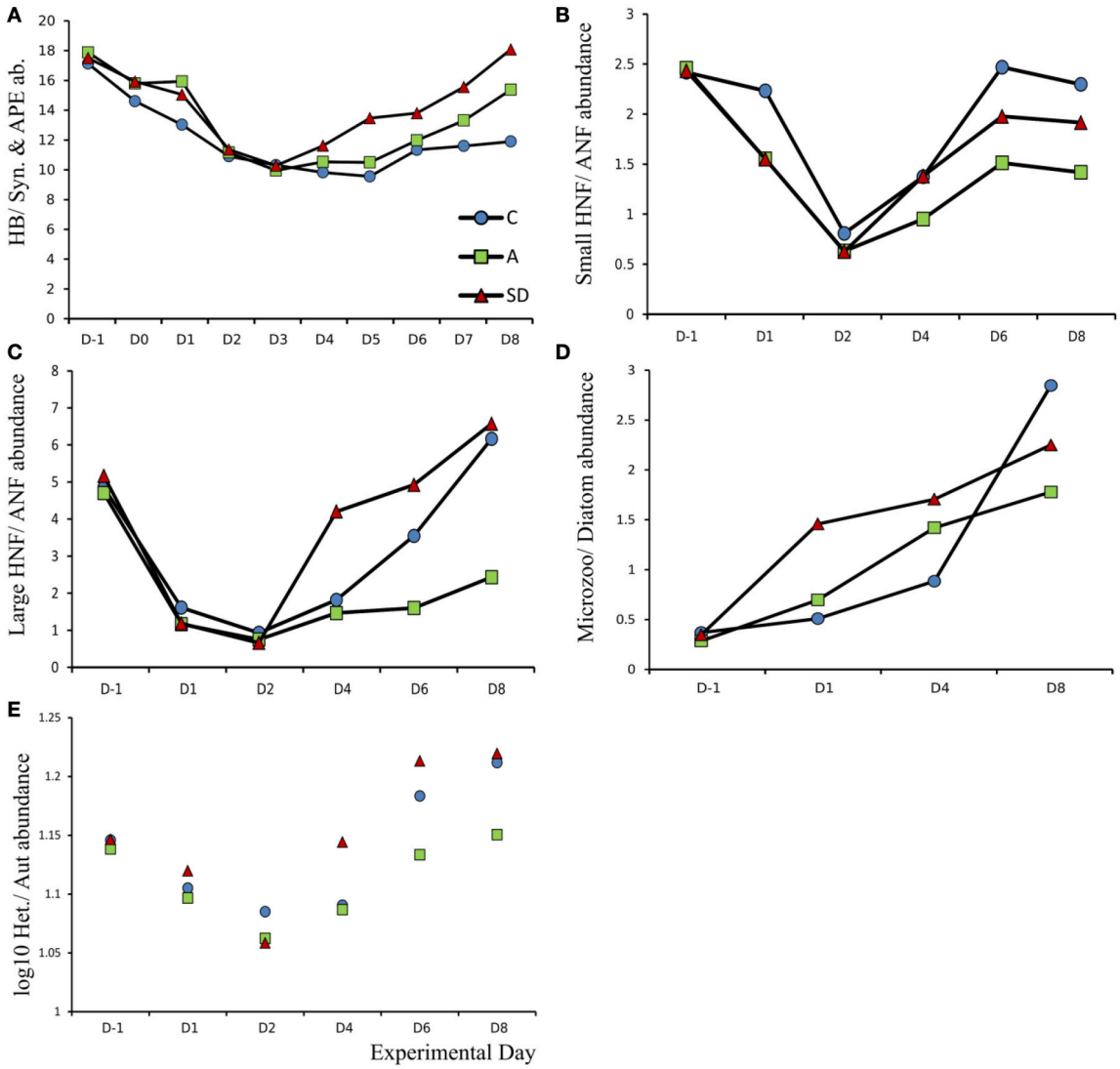

FIGURE 13 | Ratio of heterotrophic to autotrophic abundance for **(A)** Heterotrophic bacteria (HB) vs. *Synechococcus* (Syn) and autotrophic pikoeukaryotes (APE), **(B)** Small (ESD < 5 μm) heterotrophic nanoflagellates (HNF) vs. small autotrophic nanoflagellates (ANF). **(C)** Large (ESD > 5 μm) heterotrophic nanoflagellates (HNF) vs. small autotrophic nanoflagellates (ANF) **(D)** Microzooplankton (Microzoo) vs. Diatoms and **(E)** Pooled total abundance (Log10) of heterotrophs vs. autotrophs.

conditions and deposition affected the community rates more than the standing stocks while heterotrophs were more favored by autotrophs. In the present experiment, the response of bacterial production was faster and of larger magnitude than the primary production (**Figure 7**), but the autotrophs keeps being dominant in abundance for more days after addition (**Figure 13E**).

A difference in initial conditions is probably the reason for the variability in reported experimental results in other deposition effect studies. Deposition has been found to stimulate a response in abundance, community composition and rates as reviewed by Guieu et al. (2014). In a series of mesocosms in the western Mediterranean, Ridame et al. (2014) found an increase in primary production and Chl *a* concentration in response to deposition events. For heterotrophic bacteria, dust addition has been found to result in increased bacterial respiration, whereas repeating the addition in the same experiment, resulted in a decrease in bacterial abundance (Pulido-Villena et al., 2014). A decrease in bacterial abundance has also been observed in a microcosm experiment in 2008 (Pulido-Villena et al., 2008), while Herut et al. (2005) observed no changes in abundance but an increase in activity. Larger heterotrophs (nanoflagellates) did not respond to the dust deposition events in a mesocosm experiment performed in the western Mediterranean (Pulido-Villena et al., 2014). This is also highlighted in the review by Guieu et al. (2014), where the authors question whether the simple "fertilization" effect traditionally suggested as the overall response of HNLC regions, applies to LNLC regions also.

Our results suggest that sufficient nutrients were made available for both autotrophs and heterotrophs to utilize, an inference supported both by the P turnover time and the DOC results. Specifically, the turnover time decreased over the course

of the experiment (**Figure 5**), meaning that what P was added with the dust was not in excess of the consumption by the plankton community. Concurrently, DOC concentration did not increase significantly suggesting that additional carbon fixation (due to increased PP) was not of large magnitude or rapidly consumed by bacteria. TEP formation also did not occur, further suggesting that there was little organic carbon accumulation due to increased production. The supplied nutrients were nevertheless enough to sustain the changes observed in the mesocosms with alkaline phosphatase production not starting until the final days of the experiment (**Figure 6**). Despite the rapid initial response of bacteria, the fast growing smaller autotrophs followed, and tipped the trophic balance (H:A) during the first days of the experiment. Even though bacterial abundance increased, viruses did not seem to respond numerically, the bacteria population also displayed internal changes in terms of DNA content and growth rate (Tsiola et al., 2016, this issue), likely connected to changes in the community structure to which the increased bacterial production was also attributed (Guo et al., 2016, this issue). The virus to bacteria ratio was higher in the control, suggesting that it was grazing and not viruses controlling the bacterial abundance in the dust added mesocosms.

Gasol et al. (1997) found that in oligotrophic environments, a high H:A ratio can be expected while, when nutrient availability increases, the H:A ratio is expected to decrease since the autotrophic community develops faster than the heterotrophs. The changes in the H:A ratio of plankton community abundance indicate that during the peak of observed effects, i.e., a couple of days after the addition of aerosols, the community became less heterotrophic than before addition (**Figure 13E**). Heterotrophs then increase as a response to the increased availability of prey and in this instance it appears that bottom up effects from the addition of nutrients via the dust, were swiftly mediated by grazing, a response also documented in Pulido-Villena et al. (2014). The H:A ratios further indicate that the Saharan dust treatment returned to more oligotrophic conditions faster than the aerosol, along with the control. This would suggest N and P co-limitation, not present in the A treatment because of the higher amount of leached NO3 provided with the dust. At the beginning of the experiment the diatom abundance was quite high, the dominant genus, *Chaetoceros* sp. is typically large, and one of the most commonly occurring blooming species in the Mediterranean (Siokou-Frangou et al., 2010; Rigual-Hernandez et al., 2013). After addition, the diatom abundance declined, indicating that smaller autotrophs (pico- and nano-fractions) managed to outcompete their larger counterparts for mineral nutrient resources right after addition. The copepod grazing experiments showed that this group produced more eggs in the dust treated mesocosms and thus, copepods were clearly able to capitalize on the increased growth of microplankton in a few days. As the clearance rates indicate (Christou et al., 2016, this issue), copepods grazed more on microzooplankton than on phytoplankton. In an experiment from the same area, where the response of copepods was measured following different levels of phosphate additions, Pitta et al. (2016) found that copepods almost doubled their egg and nauplii production after 2 days incubation at only 10 nM addition of phosphate. This immediate response was not observed in the present experiment, where it appears copepods responded to the increase of preferred prey after some days. However, the quality/quantity of prey was not sufficient to sustain an increase in copepod abundance as previously observed in a phosphorus addition mesocosm experiment (Pitta et al., 2016). From the information provided by the standing stocks and production of the different groups we can conclude that the larger heterotrophic eukaryotes were more favored than copepods by the conditions created in the mesocosms after the addition of dust.

Overall it appeared that the response to Saharan dust addition vs. the mixed aerosol was very similar and affected most components of the plankton community. Differences in responses between treatments were subtle and faded out when moving further up the food web and/or forward in time. When comparing responses to addition of Saharan Dust to ambient deposition from samples taken from a transect across the Mediterranean, Ternon et al. (2010) also found a response to both deposition types relative to the control but no significant differences in the magnitude of the response observed between the two types of deposition. This suggests that some common components in the two aerosol types may be responsible for the changes observed, as was the case in the present study. Considering the amount of nutrients added and the magnitude of changes observed it is remarkable that a ca. 3.5 nM addition of P can trigger changes that culminate in an increase of egg production by copepods. As mentioned, the system response to atmospheric deposition highly depends on the ambient conditions and trophic status of the system at the time of deposition, as well as on the timing of the deposition event. Whether or not we can predict this response is more the subject of modeling approaches, but during previous years deposition events in the eastern Mediterranean have increased both in frequency and intensity (Pey et al., 2013). Given the frequency of events it could be hypothesized that more persisting changes resulting from deposition can occur, especially in stratified waters. The implications can be far reaching as observed in Martínez-Garcia et al. (2011), as the coupling of dust to climate patterns also connects to long term cycling of nutrients and climate mediation and could also be connected to POC export events (Ternon et al., 2010).

Our results demonstrate that a single deposition event is enough to induce changes in the microbial food web that are measureable up to zooplankton. In spring conditions this could indicate that repeated deposition would make the system more productive. Although, the differences due to source of the dust were not conclusively observable in the standing stocks, there was some indication that production rates, as indicated by the bacterial production, were triggered faster where mixed aerosol was added. Future scenarios for the Mediterranean region predict rising temperature, which will influence circulation and stratification patterns, and decrease in precipitation (Somot et al., 2006; Giorgi and Lionello, 2008). The decrease in precipitation and increase in temperature (IPCC, 2014) suggest the trend for increased dry deposition will continue, and we can expect that surface inputs via the air-sea interface will become more important in this ecosystem. The results presented, indicate that

the eastern Mediterranean system responses to deposition events, although episodic in nature, can significantly alter long term community dynamics.

AUTHOR CONTRIBUTIONS

TMT: Performed experimental work and wrote the MS. PP and BH: Designed experiment, Secured funding, performed experimental work and contributed to the MS. ER, IBF, AT, MT, AnG, CP, KV, SP, AL, EDC, SZ, NN, MLP, and MDK: Performed experimental work and contributed to the MS. AlG, NP, MF, TM, and TT: Performed experimental work.

ACKNOWLEDGMENTS

The work presented was financed by the EU-FP7 project "MESOAQUA: Network of leading MESOcosm facilities to advance the studies of future AQUAtic ecosystems from the Arctic to the Mediterranean" (grant agreement no. 228224) and by the project ADAMANT: Atmospheric deposition and Mediterranean sea water productivity (nr code/MIS: 383551), co-financed by the European Union (European Social Fund–ESF) and Greek national funds through the Operational Program "Education and Lifelong Learning" of the National Strategic Reference Framework (NSRF) (Research Funding Program: THALES). Funding for MDK was also provided by Leverhulme Trust entitled "Understanding the delivery of phosphorus nutrient to the oceans" Grant Number RPG 406.

The authors would like to thank G. Piperakis for his technical assistance throughout the experiment, and S. Zivanovic and E. Dafnomili for assistance with chemical analyses. The captain and the crew of the R/V Philia are thanked for their assistance during the transportation of water from the sea to the mesocosms.

REFERENCES

Brussaard, C. P. D. (2004). Optimization of procedures for counting viruses by flow cytometry. *Appl. Environ. Microbiol.* 70, 1506–1513. doi: 10.1128/AEM.70.3.1506-1513.2004

Bryant, R. G. (2013). Recent advances in our understanding of dust source emission processes. *Prog. Phys. Geogr.* 37, 397–421. doi: 10.1177/0309133313479391

Carbo, P., Krom, M. D., Homoky, W. B., Benning, L. G., and Herut, B. (2005). Impact of atmospheric deposition on N and P geochemistry in the southeastern Levantine basin. *Deep Sea Res. Part II Top. Stud. Oceanogr.* 52, 3041–3053. doi: 10.1016/j.dsr2.2005.08.014

Christou, E., Zervoudaki, S., Fernandez de Puelles, M., Protopapa, M., Varkitzi, I., Pitta, P., et al. (2016). Response of the calanoid copepod *Clausocalanus furcatus*, to atmospheric deposition events: outcomes from a mesocosm study. *Front. Mar. Sci.* 3:35. doi: 10.3389/fmars.2017.00035

Crispi, G., Crise, A., and Solidoro, C. (2002). Coupled Mediterranean ecomodel of the phosphorus and nitrogen cycles. *J. Mar. Syst.* 33–34, 497–521. doi: 10.1016/S0924-7963(02)00073-8

D'Ortenzio, F., and Ribera d'Alcalà, M. (2009). On the trophic regimes of the Mediterranean Sea: a satellite analysis. *Biogeosciences* 6, 139–258. doi: 10.5194/bg-6-139-2009

Engel, A. (2009). "Determination of marine gel particles," in *Practical Guidelines for the Analysis of Seawater*, ed O. Wurl (Boca Raton, FL: CRC Press), 125–142.

Fonnes Flaten, G. A., Skjoldal, E. F., Krom, M. D., Law, C. S., Mantoura, R. F. C., Pitta, P., et al. (2005). Studies of the microbial P-cycle during a Lagrangian phosphate-addition experiment in the Eastern Mediterranean. *Deep Sea Res. Part II Top. Stud. Oceanogr.* 52, 2928–2943. doi: 10.1016/j.dsr2.2005.08.010

Gallisai, R., Peters, F., Volpe, G., Basart, S., and Baldasano, J. M. (2014). Saharan dust deposition may affect phytoplankton growth in the Mediterranean sea at ecological time scales. *PLoS ONE* 9:e110762. doi: 10.1371/journal.pone.0110762

Ganor, E., Osetinsky, I., Stupp, A., and Alpert, P. (2010). Increasing trend of African dust, over 49 years, in the eastern Mediterranean. *J. Geophys. Res. Atmos.* 115. doi: 10.1029/2009jd012500

Gasol, J. M., del Giorgio, P. A., and Duarte, C. M. (1997). Biomass distribution in marine planktonic communities. *Limnol. Oceanogr.* 42, 1353–1363. doi: 10.4319/lo.1997.42.6.1353

Ginoux, P., Prospero, J. M., Gill, T. E., Hsu, N. C., and Zhao, M. (2012). Global-scale attribution of anthropogenic and natural dust sources and their emission rates based on MODIS Deep Blue aerosol products. *Rev. Geophys.* 50. doi: 10.1029/2012rg000388

Giorgi, F., and Lionello, P. (2008). Climate change projections for the Mediterranean region. *Glob. Planet. Change* 63, 90–104. doi: 10.1016/j.gloplacha.2007.09.005

Guerzoni, S., Chester, R., and Dulac, F. (1999). The role of atmospheric deposition in the biogeochemistry of the Mediterranean Sea. *Prog. Ocenogr.* 44, 147–190. doi: 10.1016/s0079-6611(99)00024-5

Guieu, C., Aumont, O., Paytan, A., Bopp, L., Law, C. S., Mahowald, N., et al. (2014). The significance of the episodic nature of atmospheric deposition to Low Nutrient Low Chlorophyll regions. *Global Biogeochem. Cycles* 28, 1179–1198. doi: 10.1002/2014GB004852

Guo, C., Xia, X., Pitta, P., Herut, B., Rahav, E., Berman-Frank, I., et al. (2016). Shifts in microbial community structure and activity in the ultra-oligotrophic eastern Mediterranean sea driven by the deposition of saharan dust and european aerosols. *Front. Mar. Sci.* 3:170. doi: 10.3389/fmars.2016.00170

Herut, B., and Krom, M. D. (1996). "Atmospheric input of nutrients and dust to the SE Mediterranean," in *Impact of Desert Dust across the Mediterranean*, eds S. Guerzoni and R. Chester (Springer Netherlands), 349–358.

Herut, B., Rahav, E., Tsagaraki, T. M., Giannakourou, A., Tsiola, A., Psarra, S., et al. (2016). The potential impact of saharan dust and polluted aerosols on microbial populations in the East Mediterranean Sea, an overview of a mesocosm experimental approach. *Front. Mar. Sci.* 3:226. doi: 10.3389/fmars.2016.00226

Herut, B., Zohary, T., Krom, M. D., Mantoura, R. F. C., Pitta, P., Psarra, S., et al. (2005). Response of East Mediterranean surface water to Saharan dust: on-board microcosm experiment and field observations. *Deep Sea Res. Part II Top. Stud. Oceanogr.* 52, 3024–3040. doi: 10.1016/j.dsr2.2005.09.003

Holm-Hansen, O., Lorenzen, C. J., Holmes, R. W., and Strickland, J. D. H. (1965). Fluorometric determination of chlorophyll. *ICES J. Mar. Sci.* 30, 3–15. doi: 10.1093/icesjms/30.1.3

IPCC (2014). *Climate Change 2014: Synthesis Report. Contribution of Working Groups I, II and III to the Fifth Assessment Report of the Intergovernmental Panel on Climate Change*. Core Writing Team eds R. K. Pachauri and L. A. Meyer (Geneva: IPCC), 151.

Ivancic, I., and Degobbis, D. (1984). An optimal manual procedure for ammonia analysis in natural waters by the indophenol blue method. *Water Res.* 18, 1143–1147. doi: 10.1016/0043-1354(84)90230-6

Jacobsen, A., Egge, J. K., and Heimdal, B. R. (1995). Effects of increased concentration of nitrate and phosphate during a spring bloom experiment in mesocosm. *J. Exp. Mar. Bio. Ecol.* 187, 239–251. doi: 10.1016/0022-0981(94)00183-E

Jickells, T. D. (2005). Global Iron connections between Desert dust, Ocean biogeochemistry, and climate. *Science* 308, 67–71. doi: 10.1126/science.1105959

Kalivitis, N., Gerasopoulos, E., Vrekoussis, M., Kouvarakis, G., Kubilay, N., Hatzianastassiou, N., et al. (2007). Dust transport over the eastern Mediterranean derived from total ozone mapping spectrometer, aerosol robotic network, and surface measurements. *J. Geophys. Res. Atmos.* 112. doi: 10.1029/2006jd007510

Kirchman, D. L., Keil, R. G., Simon, M., and Welschmeyer, N. A. (1993). Biomass and production of heterotrophic bacterioplankton in the oceanic subarctic Pacific. *Deep Sea Res. I Oceanogr. Res. Pap.* 40, 967–988. doi: 10.1016/0967-0637(93)90084-G

Kirchman, D., K'nees, E., and Hodson, R. (1985). Leucine incorporation and its potential as a measure of protein synthesis by bacteria in natural aquatic systems. *Appl. Environ. Microbiol.* 49, 599–607.

Koçak, M., Kubilay, N., Tuğrul, S., and Mihalopoulos, N. (2010). Atmospheric nutrient inputs to the northern levantine basin from a long-term observation: sources and comparison with riverine inputs. *Biogeosciences* 7, 4037–4050. doi: 10.5194/bg-7-4037-2010

Krom, M. D., Herut, B., and Mantoura, R. F. C. (2004). Nutrient budget for the Eastern Mediterranean: implications for phosphorus limitation. *Limnol. Oceanogr.* 49, 1582–1592. doi: 10.4319/lo.2004.49.5.1582

Krom, M. D., Kress, N., Brenner, S., and Gordon, L. I. (1991). Phosphorus limitation of primary productivity in the eastern Mediterranean Sea. *Limnol. Oceanogr.* 36, 424–432. doi: 10.4319/lo.1991.36.3.0424

Krom, M. D., Thingstad, T. F., Brenner, S., Carbo, P., Drakopoulos, P., Fileman, T. W., et al. (2005). Summary and overview of the CYCLOPS P addition Lagrangian experiment in the Eastern Mediterranean. *Deep Sea Res. Part II Top. Stud. Oceanogr.* 52, 3090–3108. doi: 10.1016/j.dsr2.2005.08.018

Lamarque, J. F., Dentener, F., McConnell, J., Ro, C. U., Shaw, M., Vet, R., et al. (2013). Multi-model mean nitrogen and sulfur deposition from the Atmospheric Chemistry and Climate Model Intercomparison Project (ACCMIP): evaluation historical and projected changes. *Atmos. Chem. Phys.* 13, 7997–8018.

Lawrence, C. R., and Neff, J. C. (2009). The contemporary physical and chemical flux of aeolian dust: a synthesis of direct measurements of dust deposition. *Chem. Geol.* 267, 46–63. doi: 10.1016/j.chemgeo.2009.02.005

Lazzari, P., Solidoro, C., Ibello, V., Salon, S., Teruzzi, A., Béranger, K., et al. (2012). Seasonal and inter-annual variability of plankton chlorophyll and primary production in the Mediterranean Sea: a modelling approach. *Biogeosciences* 9, 217–233. doi: 10.5194/bg-9-217-2012

Lekunberri, I., Lefort, T., Romero, E., Vázquez-Domínguez, E., Romera-Castillo, C., Marrasé, C., et al. (2010). Effects of a dust deposition event on coastal marine microbial abundance and activity, bacterial community structure and ecosystem function. *J. Plankton Res.* 32, 381–396. doi: 10.1093/plankt/fbp137

Loder, M. G. J., Meunier, C., Boersma, M., Aberle, N., Löder, M. G. J., and Wiltshire, K. H. (2011). The role of ciliates, heterotrophic dinoflagellates and copepods in structuring spring plankton communities at Helgoland Roads, North Sea. *Mar. Biol.* 158, 1551–1580. doi: 10.1007/s00227-011-1670-2

Mahowald, N. M., Baker, A. R., Bergametti, G., Brooks, N., Duce, R. A., Jickells, T. D., et al. (2005). Atmospheric global dust cycle and iron inputs to the ocean. *Global Biogeochem. Cycles* 19. doi: 10.1029/2004GB002402

Mahowald, N., Jickells, T. D., Baker, A. R., Artaxo, P., Benitez-Nelson, C. R., Bergametti, G., et al. (2008). Global distribution of atmospheric phosphorus sources, concentrations and deposition rates, and anthropogenic impacts. *Global Biogeochem. Cycles* 22. doi: 10.1029/2008GB003240

Marañón, E., Fernández, A., Mouriño-Carballido, B., Martínez-García, S., Teira, E., Cermeño, P., et al. (2010). Degree of oligotrophy controls the response of microbial plankton to Saharan dust. *Limnol. Oceanogr.* 55, 2339–2352. doi: 10.4319/lo.2010.55.6.2339

Marie, D., Brussaard, C. P. D., Thyrhaug, R., Bratbak, G., and Vaulot, D. (1999). Enumeration of marine viruses in culture and natural samples by flow cytometry. *Appl. Environ. Microbiol.* 65, 45–52.

Markaki, Z., Loÿe-Pilot, M. D., Violaki, K., Benyahya, L., and Mihalopoulos, N. (2010). Variability of atmospheric deposition of dissolved nitrogen and phosphorus in the Mediterranean and possible link to the anomalous seawater N/P ratio. *Mar. Chem.* 120, 187–194. doi: 10.1016/j.marchem.2008.10.005

Martínez-Garcia, A., Rosell-Melé, A., Jaccard, S. L., Geibert, W., Sigman, D. M., and Haug, G. H. (2011). Southern Ocean dust–climate coupling over the past four million years. *Nature* 476, 312–315. doi: 10.1038/nature10310

Myriokefalitakis, S., Daskalakis, N., Mihalopoulos, N., Baker, A. R., Nenes, A., and Kanakidou, M. (2015). Changes in dissolved iron deposition to the oceans driven by human activity: a 3-D global modelling study. *Biogeosciences* 12, 3973–3992. doi: 10.5194/bg-12-3973-2015

Nenes, A., Krom, M. D., Mihalopoulos, N., Van Cappellen, P., Shi, Z., Bougiatioti, A., et al. (2011). Atmospheric acidification of mineral aerosols: a source of bioavailable phosphorus for the oceans. *Atmos. Chem. Phys.* 11, 6265–6272. doi: 10.5194/acp-11-6265-2011

Pasternak, A., Wassmann, P., and Riser, C. W. (2005). Does mesozooplankton respond to episodic P inputs in the Eastern Mediterranean? *Deep Sea Res. Part II Top. Stud. Oceanogr.* 52, 2975–2989. doi: 10.1016/j.dsr2.2005.09.002

Paulino, A. I., Heldal, M., Norland, S., and Egge, J. K. (2013). Elemental stoichiometry of marine particulate matter measured by wavelength dispersive X-ray fluorescence (WDXRF) spectroscopy. *J. Mar. Biol. Assoc. U.K.* 93, 2003–2014. doi: 10.1017/S0025315413000635

Pey, J., Querol, X., Alastuey, A., Forastiere, F., and Stafoggia, M. (2013). African dust outbreaks over the Mediterranean Basin during 2001–2011: PM 10 concentrations, phenomenology and trends, and its relation with synoptic and mesoscale meteorology. *Atmos. Chem. Phys.* 13, 1395–1410. doi: 10.5194/acp-13-1395-2013

Pitta, P., Nejstgaard, J. C., Tsagaraki, T. M., Zervoudaki, S., Egge, J. K., Frangoulis, C., et al. (2016). Confirming the "Rapid phosphorus transfer from microorganisms to mesozooplankton in the Eastern Mediterranean Sea" scenario through a mesocosm experiment. *J. Plankton Res.* 38, 1–20. doi: 10.1093/plankt/fbw010

Porter, K. G., and Feig, Y. S. (1980). The use of DAPI for identifying and counting aquatic microflora. *Limnol. Oceanogr.* 25, 943–948. doi: 10.4319/lo.1980.25.5.0943

Pujo-Pay, M., Conan, P., Oriol, L., Cornet-Barthaux, V., Falco, C., Ghiglione, J. F., et al. (2011). Integrated survey of elemental stoichiometry (C, N, P) from the western to eastern Mediterranean Sea. *Biogeosciences* 8, 883–899. doi: 10.5194/bg-8-883-2011

Pulido-Villena, E., Baudoux, A. C., Obernosterer, I., Landa, M., Caparros, J., Catala, P., et al. (2014). Microbial food web dynamics in response to a Saharan dust event: results from a mesocosm study in the oligotrophic Mediterranean Sea. *Biogeosciences* 11, 5607–5619. doi: 10.5194/bg-11-5607-2014

Pulido-Villena, E., Wagener, T., and Guieu, C. (2008). Bacterial response to dust pulses in the western Mediterranean: implications for carbon cycling in the oligotrophic ocean. *Global Biogeochem. Cycles* 22. doi: 10.1029/2007GB003091

Rahav, E., Shun-Yan, C., Cui, G., Liu, H., Tsagaraki, T. M., Giannakourou, A., et al. (2016). Evaluating the impact of atmospheric depositions on springtime dinitrogen fixation in the Cretan Sea (Eastern Mediterranean)—A mesocosm approach. *Front. Mar. Sci.* 3:180. doi: 10.3389/fmars.2016.00180

Rengefors, K., Pettersson, K., Blenckner, T., and Anderson, D. M. (2001). Species-specific alkaline phosphatase activity in freshwater spring phytoplankton : application of a novel method. *J. Plankton Res.* 23, 435–443. doi: 10.1093/plankt/23.4.435

Ridame, C., and Guieu, C. (2002). Saharan input of phosphate to the oligotrophic water of the open western Mediterranean Sea. *Limnol. Oceanogr.* 47, 856–869. doi: 10.4319/lo.2002.47.3.0856

Ridame, C., Dekaezemacker, J., Guieu, C., Bonnet, S., L'Helguen, S., and Malien, F. (2014). Contrasted Saharan dust events in LNLC environments: impact on nutrient dynamics and primary production. *Biogeosciences* 11, 4783–4800. doi: 10.5194/bg-11-4783-2014

Rigual-Hernandez, A. S., Barcena, M. A., Jordan, R. W., Sierro, F. J., Flores, J. A., Meier, K. J. S., et al. (2013). Diatom fluxes in the NW Mediterranean: evidence from a 12-year sediment trap record and surficial sediments. *J. Plankton Res.* 35, 1109–1125. doi: 10.1093/plankt/fbt055

Rimmelin, P., and Moutin, T. (2005). Re-examination of the MAGIC method to determine low orthophosphate concentration in seawater. *Anal. Chim. Acta* 548, 174–182. doi: 10.1016/j.aca.2005.05.071

Sebastian, M., Aristegui, J., Montero, M. F., Escanez, J., and Xavier Niell, F. (2004). Alkaline phosphatase activity and its relationship to inorganic phosphorus in the transition zone of the North-western African upwelling system. *Prog. Oceanogr.* 62, 131–150. doi: 10.1016/j.pocean.2004.07.007

Siokou-Frangou, I., Christaki, U., Mazzocchi, M. G., Montresor, M., Ribera d'Alcalá, M., Vaqué, D., et al. (2010). Plankton in the open Mediterranean Sea: a review. *Biogeosciences* 7, 1543–1586. doi: 10.5194/bg-7-1543-2010

Smith, D. C., and Azam, F. (1992). A simple, economical method for measuring bacterial protein synthesis rates in seawater using 3H-leucine. *Mar. Microb. Food Webs* 6, 107–114.

Sohrin, R., and Sempéré, R. (2005). Seasonal variation in total organic carbon in the northeast Atlantic in 2000–2001. *J. Geophys. Res. Oceans* 110. doi: 10.1029/2004jc002731

Somot, S., Sevault, F., and Déqué, M. (2006). Transient climate change scenario simulation of the Mediterranean Sea for the twenty-first century using a high-resolution ocean circulation model. *Clim. Dynam.* 27, 851–879. doi: 10.1007/s00382-006-0167-z

Statham, P. J., and Hart, V. (2005). Dissolved iron in the Cretan Sea (eastern Mediterranean). *Limnol. Oceanogr.* 50, 1142–1148. doi: 10.4319/lo.2005.50.4.1142

Steeman-Nielsen, E. (1952). The use of radio-active carbon (C^{14}) for measuring organic production in the sea. *ICES J. Mar. Sci.* 18, 117–140. doi: 10.1093/icesjms/18.2.117

Stockdale, A., Krom, M. D., Mortimer, R. J. G., Benning, L. G., Carslaw, K. S., Herbert, R. J., et al. (2016). Understanding the nature of atmospheric acid processing of mineral dusts in supplying bioavailable phosphorus to the oceans. *Proc. Natl. Acad. Sci. U.S.A.* 113, 14639–14644. doi: 10.1073/pnas.1608136113

Strickland, J. D. H., and Parsons, T. R. (1972). *A Practical Handbook of Seawater Analysis*. Ottawa, ON: Fisheries Research Board of Canada.

Tanaka, T., Thingstad, T. F., Christaki, U., Colombet, J., Cornet-Barthaux, V., Courties, C., et al. (2011). Lack of P-limitation of phytoplankton and heterotrophic prokaryotes in surface waters of three anticyclonic eddies in the stratified Mediterranean Sea. *Biogeosciences* 8, 525–538. doi: 10.5194/bg-8-525-2011

Ternon, E., Guieu, C., Loÿe-Pilot, M. D., Leblond, N., Bosc, E., Gasser, B., et al. (2010). The impact of Saharan dust on the particulate export in the water column of the North Western Mediterranean Sea. *Biogeosciences* 7, 809–826. doi: 10.5194/bg-7-809-2010

Thingstad, T. F., Krom, M. D., Mantoura, R. F. C., Flaten, G. A. F., Groom, S., Herut, B., et al. (2005). Nature of phosphorus limitation in the ultraoligotrophic eastern Mediterranean. *Science* 309, 1068–1071. doi: 10.1126/science.1112632

Thingstad, T. F., Skjoldal, E. F., and Bohne, R. A. (1993). Phosphorus cycling and algal-bacterial competition in Sandsfjord, western Norway. *Mar. Ecol. Prog. Ser.* 99, 239–259. doi: 10.3354/meps099239

Tsiola, A., Tsagaraki, T. M., Giannakourou, A., Nikolioudakis, N., Yücel, N., Herut, B., et al. (2016). Bacterial growth and mortality after deposition of Saharan dust and mixed aerosols in the Eastern Mediterranean Sea: a mesocosm experiment. *Front. Mar. Sci.* 3:281. doi: 10.3389/fmars.2016.00281

Utermöhl, H. (1958). Zur vervollkommnung der quantitativen phytoplankton methodik. *Mitteilungen Internationale Vereinigung Theoretische und Angewandte Limnologie* 9, 1–38.

Volpe, G., Banzon, V. F., Evans, R. H., Santoleri, R., Mariano, A. J., and Sciarra, R. (2009). Satellite observations of the impact of dust in a low-nutrient, low-chlorophyll region : fertilization or artifact ? *Glob. Biochem. Cycles* 23, 1–14. doi: 10.1029/2008gb003216

Conflict of Interest Statement: The authors declare that the research was conducted in the absence of any commercial or financial relationships that could be construed as a potential conflict of interest.

frontiers in Marine Science

ORIGINAL RESEARCH
published: 23 September 2016
doi: 10.3389/fmars.2016.00180

Evaluating the Impact of Atmospheric Depositions on Springtime Dinitrogen Fixation in the Cretan Sea (Eastern Mediterranean)—A Mesocosm Approach

Eyal Rahav[1,2], Cheung Shun-Yan[3], Guo Cui[3], Hongbin Liu[3], Tatiana M. Tsagaraki[4,5], Antonia Giannakourou[5], Anastasia Tsiola[5], Stella Psarra[5], Anna Lagaria[5], Margaret R. Mulholland[6], Eleni Stathopoulou[7], Pitta Paraskevi[5], Barak Herut[1] and Ilana Berman-Frank[2]*

[1] Israel Oceanographic and Limnological Research, National Institute of Oceanography, Haifa, Israel, [2] Mina and Everard Goodman Faculty of Life Sciences, Bar-Ilan University, Ramat-Gan, Israel, [3] Division of Life Science, Hong Kong University of Science and Technology, Hong Kong, Hong Kong, [4] Department of Microbiology, University of Bergen, Bergen, Norway, [5] Hellenic Centre for Marine Research, Heraklion, Greece, [6] Department of Ocean, Earth and Atmospheric Sciences, Old Dominion University, Norfolk, VA, USA, [7] Laboratory of Environmental Chemistry, Department of Chemistry, University of Athens, Athens, Greece

OPEN ACCESS

Edited by:
Alberto Basset, University of Salento, Italy

Reviewed by:
Robinson W. (Wally) Fulweiler, Boston University, USA
Patrick Georges Gillet, UCO Angers, France

***Correspondence:**
Eyal Rahav
eyal.rahav@ocean.org.il

Specialty section:
This article was submitted to Marine Ecosystem Ecology, a section of the journal Frontiers in Marine Science

Received: *15 May 2016*
Accepted: *06 September 2016*
Published: *23 September 2016*

Citation:
Rahav E, Shun-Yan C, Cui G, Liu H, Tsagaraki TM, Giannakourou A, Tsiola A, Psarra S, Lagaria A, Mulholland MR, Stathopoulou E, Paraskevi P, Herut B and Berman-Frank I (2016) Evaluating the Impact of Atmospheric Depositions on Springtime Dinitrogen Fixation in the Cretan Sea (Eastern Mediterranean)—A Mesocosm Approach. Front. Mar. Sci. 3:180. doi: 10.3389/fmars.2016.00180

Large amounts of dust and atmospheric aerosols, originating from surrounding desert areas (e.g., Sahara and Middle East) are deposited annually on the surface of the Eastern Mediterranean Sea. These depositions can provide high amounts of micro (such as Fe, Zn, Co) and macro nutrients (such as P and N) to supplement nutrient-poor surface waters- that typically limit primary productivity and also dinitrogen (N_2) fixation in many marine environments. Here, we studied the impact of the atmospheric deposition of dust and aerosols on N_2 fixation in the Cretan Sea (Eastern Mediterranean Sea). Mixed polluted aerosols (hereafter A) and Saharan dust (hereafter SD) were added to nine mesocosms (3-m^3 each) containing surface mixed layer seawater (~10 m), and N_2 fixation was evaluated for 6 days during May 2012 (springtime). The addition of SD triggered a rapid (30 h) and robust (2–4-fold) increase in N_2 fixation rates that remained high for 6 days and contributed 3–8% of the primary productivity. The A addition also resulted in higher N_2 fixation rates compared to the unamended control mesocosms, although the responses were less profound (1.5–2-fold) and accounted for only 2–4% of the primary productivity. The microbial community responded differently to the two additions. Heterotrophic bacterial N_2 fixers dominated the diazotroph community in A and the control mesocosms, while the non-filamentous cyanobacterial group *Trichodesmium* prevailed in the SD treatment (68% of all the operational taxonomic units, verified by qPCR analyses). Our results indicate that the aerosol source, its route prior to deposition, and its specific chemical composition, can alter the diazotrophic diversity and activity in the Eastern Mediterranean Sea and may thus impact both the N and C dynamics in this impoverished environment.

Keywords: N_2 fixation, primary productivity, bacterial productivity, Saharan dust, aerosols

INTRODUCTION

Dinitrogen (N_2) fixation is recognized as an important pathway for bioavailable nitrogen inputs in many of the world's oceans (Gruber and Galloway, 2008; Sohm et al., 2011). This process can alter phytoplankton populations and primary production in nitrogen (N) limited marine environments (e.g., Falkowski, 1997; Carpenter et al., 2004; Sohm et al., 2011) and thus fuels the biological pump. Many physical, chemical, and biological factors can affect the magnitude of N_2 fixation in a given ecosystem. Where N_2 fixers (diazotrophs) occur, they are most often limited by phosphorus (P) (Wu et al., 2000; Sanudo-Wilhelmy et al., 2001; Dyhrman and Haley, 2006), iron (Fe) (Paerl et al., 1987; Berman-Frank et al., 2001, 2007; Moore et al., 2009), or both (Mills et al., 2004).

Wet and dry deposition of atmospheric dust can increase the availability of Fe and P in the surface ocean (Herut et al., 1999, 2005; Bonnet and Guieu, 2006; Guieu et al., 2014) thereby supplementing the requirements of primary producers (mostly N and P, Zohary et al., 2005; Rahav et al., 2016a; Tsiola et al., 2016) and N_2-fixers (Gruber and Sarmiento, 1997; Mills et al., 2004; Marañón et al., 2010). Dust enrichment enhanced N_2 fixation rates in microcosm experiments from the tropical Atlantic (Mills et al., 2004; Marañón et al., 2010), the North Atlantic (Gruber and Sarmiento, 1997), the Red Sea (Foster et al., 2009), and the tropical and subtropical western North Pacific (Kitajima et al., 2009). Furthermore, a 100-fold increase in the abundance of *Trichodesmium*, a non-filamentous cyanobacterial diazotroph, and a ∼2-fold increase in dissolved organic nitrogen were reported following dust stimulation in the West Florida Shelf (Lenes et al., 2001). However, N_2 fixation rates and high abundances of diazotrophs are not always observed in areas of the ocean where dust deposition is high. For example, the oligotrophic Mediterranean Sea receives high annual inputs of dust (20×10^6 to 50×10^6 tons y^{-1}, Guerzoni et al., 1999) characterized by relatively high dissolved Fe concentrations (∼42 μmol m^{-2} y^{-1}, Bonnet and Guieu, 2006). Yet N_2 fixation rates are typically low in surface waters and the upper mixed layer (usually <0.2 nmol N L^{-1} d^{-1}, Sandroni et al., 2007; Ibello et al., 2010; Bonnet et al., 2011; Rahav et al., 2013a; Benavides et al., 2016) relative to other marine systems (reviewed in Sohm et al., 2011).

Several studies have examined the possibility of low P availability limiting diazotrophy in the Mediterranean Sea but results have been inconclusive (see literature compilation in **Table 1**). While N_2 fixation was enhanced by ∼50% after the addition of P to surface waters in an ultraoligotrophic, P-limited anticyclonic eddy in the Eastern Mediterranean Sea during the summer of 2002 (Rees et al., 2006), no significant increases in N_2 fixation rates were observed several years later during an identical experiment at the same location and for the same incubation period (24 h) (Ridame et al., 2011). Similarly, N_2 fixation rates were not enhanced by P additions in the Levantine Basin (Eastern Mediterranean) during the summer of 2009, including within the cores of cyclonic and anticyclonic eddies (Rahav et al., 2013b).

One possible reason for the variable results from the nutrient amendment experiments above could be the relatively small volumes of the microcosm experiments (each a few liters in total). The ultra-oligotrophic conditions in the study area coupled with the short duration of the experiments (usually less than 48 h) may have been insufficient to detect active diazotrophy. In addition, the low population density may have excluded the representation of the entire microbial food web in the small incubation experiments. In ultraoligotrophic areas such as the Eastern Mediterranean Sea, larger-scale experiments conducted over longer timescales may be required to determine N_2 fixation rates and responses to additions of potentially rate-limiting elements. Mesocosms (52 m^3 bags) were recently employed to examine diazotrophic responses to dust additions in the western Mediterranean Sea (2008, 2010) (Ridame et al., 2013). During this experiment, addition of a dust analog (manipulated top-soils collected from the Sahara desert) induced a rapid (24–48 h), robust (2–5.3-fold), and lengthy (4–6 days duration) increase in N_2 fixation (**Table 1**), suggesting that dust inputs may stimulate diazotrophic activity over longer timescales (>48 h) than typical microcosm experiments.

In this study, we employed mesocosms to evaluate the impact of atmospheric deposition on diazotrophy and primary productivity during springtime in the Cretan Sea, an oligotrophic region in the Eastern Mediterranean Sea. Treatments included additions of: (1) "pure" Saharan dust (1.6 mg L^{-1}), and (2) mixed polluted and desert origin aerosols (1 mg L^{-1}). Our main objectives were to study how different aerosols affect diazotrophic diversity and N_2 fixation in the oligotrophic Cretan Sea during the spring and study whether these atmospheric inputs can relieve the nutrient limitations for diazotrophs. We hypothesized that the aerosol source and the atmospheric route prior to deposition might trigger different diazotrophic responses that would be reflected in both diversity and activity. Specifically, the two deposition types, and their consequent leached nutrients (N, P and the subsequent N:P ratio), might result in different responses of the diazotrophic community that could subsequently impact the microbial food web in the oligotrophic Cretan Sea.

MATERIALS AND METHODS

Experimental Design

Water was collected using a rotary submersible pump from the surface mixed layer (∼10 m) on May 9–10, 2012, from an area located 5 nautical miles north of Heraklion, Crete (35° 24.957 N, 25° 14.441 E). The collected seawater was brought within ∼2 h to the Hellenic Centre for Marine Research mesocosm facility (www.cretacosmos.eu), where it was homogenously distributed between pre-cleaned (10% HCl) mesocosms (see Figure 1 in Herut et al., this issue, Pitta et al., 2016). Nine 3-m^3 mesocosms were filled and chemical and biological measurements were made to fully characterize the initial properties of the water (**Table 2**). The mesocosms were prepared from transparent polyethylene

TABLE 1 | Summary of the microcosm/mesocosm experiments performed in the Mediterranean Sea aimed studying the limiting nutrients for diazotrophy.

Location	Water type	Type of addition	Sampling depth	Maximal change in N_2 fixation rates (% from control)	Reference	Comments
Levantine Basin	Anticyclonic eddy	P (~100 nM)	Surface (16 m)	+50	Rees et al., 2006	
		Fe (6 nM)		No change		
Western Basin	Anticyclonic eddy	P (30 nM)	Surface (8 m)	+200	Ridame et al., 2011	Station A
		P (30 nM)+ Fe (2 nM)		+400		
		Dust (1.1 mg L^{-1})		+130		
Ionian Sea	Anticyclonic eddy	P (30 nM)	Surface (8 m)	No change	Ridame et al., 2011	Station B
		P (30 nM)+ Fe (2 nM)		No change		
		Dust (1.1 mg L^{-1})		+210		
Levantine Basin	Anticyclonic eddy	P (30 nM)	Surface (8 m)	+200	Ridame et al., 2011	Station C
		P (30 nM)+ Fe (2 nM)		+150		
		Dust (1.1 mg L^{-1})		+430		
Levantine Basin	Coastal	P (100 nM)	Surface (~2 m)	No change	Rahav et al., 2016a	
		N (1600 nM)		No change		
		C (1000 nM)		+170		Monosaccharide
		NP		No change		
		CP		+320		
		CN		+140		
		CNP		+600		
		Xanthan Gum (300 $\mu g L^{-1}$)		+1000		Polysaccharide
Levantine Basin	Open sea	P (100 nM)	Surface (5–20 m)	No change	Rahav et al., 2013b	
	Anticyclonic eddy	P (100 nM)		No change		
	Cyclonic gyre	P (100 nM)		No change		
Levantine Basin	Open sea	Xanthan Gum (100–4500 $\mu g L^{-1}$)	Aphotic water (250 m)	+400	Rahav et al., 2013c	
Western Basin	Coastal	Dust (10 g m^{-2})	Surface (0–5 m)	+700	Ridame et al., 2013	Mesocosms
Cretan Sea	Open sea	Saharan dust (1.6 mg L^{-1})	Surface (~10 m)	+400	This study	Mesocosms
			Mixed polluted aerosol (1 mg L^{-1})	+200		

bags and were supported by aluminum frames. The mesocosms were deployed within a continuously circulating seawater 350 m^3 pool to maintain ambient temperature. Each mesocosm was 3 m deep and the seawater inside it was gently mixed using an air pump. Two experimental amendments were made (triplicate mesocosms per treatment): (1) the addition of "pure" Saharan dust (SD), collected from Heraklion and Tel-Shikmona (Haifa, Israel) during Saharan dust events, and (2) the addition of mixed aerosols (A), collected in Crete and Israel, which contained a natural mixture of desert dust and polluted European particles. The leaching nutrient values of the SD and A particles are described in details in Herut et al., (this issue). In short, the SD leached ~23.5 nmol N per mg of dust and ~2.3 nmol P per mg of dust. The A particles leached ~53.0 nmol N per mg of dust and ~2.8 nmol P per mg of dust. These leached nutrients resulted in significantly different N:P ratio of ~10 (mol:mol) in the SD and ~19 (mol:mol) in the A particles. Three mesocosms were used as controls, with no addition. All mesocosms were sampled daily at 08:30 over a 6 days period. For a detailed description of the mesocosms' setup and analyses, see Tsagaraki et al. (this issue) and Herut et al. (this issue).

Nutrient Concentrations

Water samples were collected and analyzed daily to measure phosphate concentrations using the MAGIC method that concentrate the phosphate in the samples, thus allowing a more accurately measures in oligotrophic environments such as the surface waters of the Mediterranean Sea (Rimmelin and Moutin, 2005), nitrite and nitrate concentrations (Strickland and Parsons, 1972), and ammonium concentrations (Ivancic and Deggobis, 1984). The detection limits were 0.8 nM for phosphate, 0.017 μM for nitrate+nitrite, and 0.019 μM for ammonium.

Chlorophyll *a*

Seawater samples (500 mL) were passed through a Whatman GF/F filter, and extracted overnight in 10 mL of 90% acetone

TABLE 2 | The initial chemical and biological properties of the Cretan Sea sub-surface water during May 9th 2012, before amendments were performed.

Parameter	Units	Average ± Stdev
NO_2+NO_3	nM	132 ± 27
NH_4	nM	131 ± 60
PO_4	nM	13 ± 4
Chlorophyll *a* (Chla)	$\mu g\ L^{-1}$	0.06 ± 0.01
Synechococcus	$\mu g\ C\ L^{-1}$	5.8 ± 0.2
Pico-eukaryotes	$\mu g\ C\ L^{-1}$	0.6 ± 0
Heterotrophic bacteria	$\mu g\ C\ L^{-1}$	8.5 ± 0.2
Primary productivity (PP)	$ng\ C\ L^{-1}\ h^{-1}$	393 ± 46
Bacterial productivity (BP)	$ng\ C\ L^{-1}\ h^{-1}$	13.7 ± 5.5
N_2 fixation	$nmol\ N\ L^{-1}\ d^{-1}$	0.22 ± 0.05
Contribution of N_2 fixation to PP	%	5.4 ± 1.7
Trichodesmium	*nifH* gene copies L^{-1}	81264 ± 7265

n = 3 for all analyses except for the Trichodesmium gene copies where 1 sample was analyzed.

solution in the dark. Chlorophyll *a* concentrations were determined by the non-acidification method (Welschmeyer, 1994) using a TD700 fluorometer equipped with 436 nm excitation and 680 nm emission filters.

Picophytoplankton and Heterotrophic Bacterial Abundance

Samples for determining picophytoplankton and heterotrophic bacterial abundance were collected every day during the experimental period. The samples were fixed with 0.2 μm filtered glutaraldehyde (0.5% final concentration) and held at 4°C for approximately 45 min, flash-frozen in liquid nitrogen, and then transferred to a −80°C refrigerator until further processing. Frozen samples were thawed at room temperature and sub-samples were stained with SYBR Green I and incubated for 10 min in the dark, according to Marie et al. (1997) and Vaulot and Marie (1999). Samples for picophytoplankton abundance were analyzed based on their auto-fluorescence signals, without pre-staining using a FACSCalibur (Becton Dickinson) flow cytometer equipped with an air-cooled laser at 488 nm and a standard filter set-up (Marie et al., 1997; Vaulot and Marie, 1999). Flow cytometry data were acquired and processed with the Cell Quest Pro software (Becton Dickinson). An average estimated flow rate of 58 μL min^{-1} was used. The picophytoplankton carbon biomass was calculated from cell counts, assuming 175 fg C $cell^{-1}$ for *Synechococcus* cells, 53 fg C $cell^{-1}$ for *Prochlorococcus* cells, and 2100 fg C $cell^{-1}$ for picoeukaryotes (Campbell and Yentsch, 1989).

Primary Productivity (PP)

Photosynthetic carbon fixation rates were estimated using the ^{14}C incorporation method (Nielsen, 1952). Water samples were analyzed in triplicate with dark and zero time controls. Polycarbonate (Nalgene) bottles were filled with 50 mL of sample water, inoculated with 5 μCi of $NaH^{14}CO_3$ tracer (Perkin Elmer, Boston, MA, USA), and incubated for 4 h under natural illumination and temperature. To determine the quantity of the added tracer, 50 μl samples were immediately taken out from each of the polycarbonate bottles and stored with 50 μL of ethanolamine for later analysis. Incubations were terminated by filtering the samples through a GF/F filter using a low vacuum pressure (<50 mmHg). The filters were then placed in scintillation vials (5 mL) and 50 μl of 32% hydrochloric acid solution were added to each vial in order to remove excess ^{14}C-bicarbonate overnight. After the addition of 3 mL of scintillation cocktail (ULTIMA-GOLD), the samples were counted using a TRI-CARB 2100 TR (PACKARD) scintillation counter. The hourly PP rates were also compared to daily measurements taken using the $NaH^{13}CO_3$ method as described in Mulholland and Bernhardt (2005). The positive ($R = 0.62$) and significant ($P < 0.001$) relationship between the two measuring techniques lends credibility to our results and suggest that the use of "potential" PP (4 h incubation and not daily) was accurate enough to characterize the Cretan Sea autotrophic production during the study period.

For the ^{13}C uptake rate measurements, water samples were placed in triplicate clear 4.5 L polycarbonate Nalgene bottles and amended with (99%) $NaH^{13}CO_3$ (Sigma) to obtain 1% of the ambient dissolved inorganic carbon and incubated under the same conditions and bottles as for the N_2 fixation measurements (see below more details). Triplicate parallel dark bottles were also incubated and subtracted from the light bottles to correct for dark carbon fixation. Incubations were terminated and analyzed as described for the N_2 fixation measurements. The contribution of N_2 fixation to the N demand for primary productivity was estimated using the measured particulate C: N ratio obtained for each sample. A comparison between the rates measured using the ^{13}C and ^{14}C methods can be seen in Figure S1.

Bacterial Productivity (BP)

Rates of bacterial productivity (BP) were estimated using the [4,5-^{3}H]-leucine incorporation method (Simon et al., 1990). Triplicate (1.7 mL) samples were incubated with 100 nmol L^{-1} [4,5-^{3}H]-leucine (Perkin Elmer, Boston, MA, USA) for 4 h at *in situ* temperatures in the dark, with triplicate trichloroacetic acid (TCA) killed samples serving as controls. Incubations were terminated by adding 100 μL of cold TCA (100%) to the vials and treated according to the micro-centrifugation protocol (Simon et al., 1990). After the addition of 1 mL of scintillation cocktail (ULTIMA-GOLD), the samples were counted using a TRI-CARB 2100 TR (PACKARD) scintillation counter. A conversion factor of 3.1 kg C mol^{-1} and an isotope dilution factor of 2.0 were used to estimate bacterial productivity (Simon et al., 1989).

Dinitrogen (N_2) Fixation Rates

$^{15}N_2$ uptake measurements were performed using the ^{15}N-enriched seawater protocol described by Mohr et al. (2010), with minor modifications for the Eastern Mediterranean

Sea (Rahav et al., 2013a,c). Enriched seawater was prepared daily by degassing filtered (0.2-μm) natural seawater using a degassing membrane (Liqui-Cel, MiniModule® G542) for ∼1 h. Then 1 ml of $^{15}N_2$ gas (99%) was added for every 100 ml of the degassed seawater and shaken vigorously until the bubbles disappeared (∼30 min). Aliquots of this $^{15}N_2$- sea enriched water were then added to the incubation bottles, with the enriched water constituting 5% of the total volume of the sample (i.e., 225 mL). Similar enriched seawater additions collected from the oligotrophic North Pacific Subtropical Gyre (NPSG) resulted in a final $^{15}N_2$ enrichment of 1.5 atom%, following the addition of 50 ml of $^{15}N_2$-enriched water to a 4.5 L bottle (Wilson et al., 2012). The bottles were then shaken and incubated under ambient surface seawater temperatures. Incubation bottles were either covered with neutral density screening to simulate ambient light or were kept under complete darkness for 24 h (see Rahav et al., 2013b). The incubations under ambient irradiance (representative of a full diel cycle having both light and dark cycles) recorded the activities of both autotrophic and heterotrophic diazotrophs, whereas the dark incubations reflected the activity of mainly heterotrophic diazotrophs who do not require light energy for fixing N_2 (Rahav et al., 2013b). We estimated the heterotrophic contribution to N_2 fixation by comparing the dark incubations to the bottles incubated under ambient diel irradiance.

The incubations were terminated by filtering water through pre-combusted 25 mm GF/F filters (with a nominal pore size of 0.7 μm). The filters were then dried in an oven at 60°C and stored in a desiccator until analysis. In the laboratory, samples were pelletized in tin disks and analyzed with a Europa 20/20 mass spectrometer equipped with an automated carbon and nitrogen analyzer. For isotope ratio mass spectrometry, standard curves were performed with each sample run to determine N mass. Samples were run only when the standard curves had R^2 values >0.99. At masses >4.7 μg N, the precision for the atom % ^{15}N measurement was <0.0001%, based on daily calibrations made in association with sample runs and with calibrations averaged made throughout several years. For most of the results reported here, the masses were >4.7 μg N. However, samples with <4.7 μg N were only used if the precision was 0.0001% for that sample run. Standard masses ranged between 1.2 and 100 μg N. In addition to the daily standard curves, reference standards and standards processed as samples were run every 6 to 8 samples.

DNA Sample Collection and Extraction

Seawater (3–8 L) was filtered through GF/D glass microfiber filters (2.7 μm, Whatman International Ltd.) and 0.2 μm pore-sized polyethersulfone membrane filters (Supor-200, Pall Corp.) using a peristaltic pump for a duration of 40 min. Total genomic DNA was recovered from biomass left on the membrane filters using PureLink Genomic DNA Kits (Invitrogen, Carlsbad, CA) (Kong et al. (2013). Extracted DNA was eluted into 50–60 μl of TE buffer (Tris and EDTA) and stored at −20°C until further analysis.

Nested PCR and 454-Pyrosequencing

Samples collected onto 0.2 μm filters were sequenced using a 454-pyrosequencing at −48, 48, and, 144 h after the atmospheric additions were carried out. The Genomic DNA samples collected from each of the different treatments were pooled into one sample prior to pyrosequencing, granting a representative view of the microbial microorganisms of each mesocosm type. *nifH* gene fragments were amplified from the genomic DNA samples following the nested polymerase chain reaction (PCR) protocol (Zehr and Turner, 2001). The nested PCR reaction was performed in triplicate using a Platinum Taq DNA polymerase PCR system in a volume of 12.5 μL (Invitrogen, Carlsbad, CA), which contained a 1X rxn PCR buffer, 4 mM $MgCl_2$, 400 μM dNTPs, 1 μM of primers (nifH 3 and nifH 4 for the first round and nifH 1 and nifH 2 for the second round of the nest PCR), 1 unit of Platinum Taq polymerase and 1 μL of total genomic DNA. Thirty cycles were performed for each of the nested PCR rounds. After the nested PCR cycles ended, 1 μL of the PCR products were used to run 10 cycles of PCR with sample-specific multiplex identifiers (MIDs) and adaptor-attached primers (Farnelid et al., 2011). The PCR condition was the same as that used for the nested PCR. The PCR products were then gel-purified with a Quick gel purification kit (Invitrogen, Carlsbad, CA). For 454-pyrosequencing, the MID-adaptor-labeled PCR products were mixed in the same concentrations to construct an amplicon library following the Rapid Library construction protocols (Roche, 454 Life Science). The DNA library attached beads were loaded onto a Pico TiterPlate and sequenced with a GS Junior System.

Quantitative PCR (qPCR)

Trichodesmium sp. *nifH* gene copies were quantified using a TaqMan probe qPCR analysis as described in Moisander et al. (2012). No other cyanobacterial diazotrophs were detected in any of the mesocosm bags. The qPCR reaction was 10 μL in volume, contained 1 X Premix Ex Taq (Takara), 1 μL genomic DNA or RNA, 0.5 μM reverse and forward primers and 0.25 μM probes (labled with 5′-FAM and 3′-TAMRA). The qPCR reactions were run in triplicate using the Applied Biosystems' 7500 Fast Real-Time PCR System (Applied Biosystems, CA, USA) (Moisander et al., 2012). The linear regression r^2 value of the standard curve was 0.99 for all the reactions and the efficiency of the qPCR reaction was 101%. The detection limit was 10 *nifH* gene copies L^{-1}.

Sequences Quality Control and Analysis

The sequencing quality control and analysis were conducted with Mothur (Schloss et al., 2009). Low quality sequences were removed, including short sequences (<300 bases in length), ambiguous base-containing sequences and chimeric sequences. The trimmed sequences were de-noised with 0.01 sigma value in order to reduce the effects of the PCR bias and were then aligned with the *nifH* DNA database of the Ribosomal Database Project (Wang et al., 2013). The distances between these high quality DNA sequences were then calculated and clustered at 95% similarity. Based on this similarity clustering,

operational taxonomic units (OTUs), representative sequences of each OTU, the Shannon diversity index, and the Chao richness estimator were generated using Mothur. The OTUs that contained more than 10 sequences were selected for the above analysis, whereas the rest of the OTUs were grouped as "other" species. Note that the rarefaction curves of our samples did not reach a plateau (not shown), suggesting that the sequencing depth of our study was insufficient to look at rare diazotrophic species. We therefore set a cutoff of 10 sequences to filter the less abundant OTUs (e.g., Farnelid et al., 2013). The OTU representative DNA sequences were translated into amino acid (aa) sequences using the FrameBOT pipeline in which the frameshift errors were corrected (Wang et al., 2013). The OTU representative sequences were used to search the protein sequence database in the National Center of Biotechnology Information (NCBI) via the protein BLAST webpage (McGinnis and Madden, 2004). The OTU representative sequences and the affiliated references were used to construct a Neighbor-joining phylogenetic tree (p-distance) with MEGA 6.0 (Tamura et al., 2013). The OTUs affiliated with the same reference sequences were grouped and these groups were then named with the species name of the reference sequences. To display the diazotrophic community structures, the relative abundances of these groups were calculated. For the relationships between the samples, the samples were clustered with a Thetayc calculator using an Unweighted Pair Group Method with an Arithmetic Mean (UPGMA) algorithm using Mothur. Sequence data was deposited in NCBI under accession number SRP075730.

Statistical Analysis

Data are displayed as averages; error bars signify one standard deviation ($n = 3$). A repeated measures analysis of variance (ANOVA) was used to compare differences between the control and the SD or A mesocosm treatments. Prior analyses, the ANOVA assumptions, namely the normally and the heterogeneity of variances of the data, were examined. At selected time-points throughout the experiment, a one-way ANOVA followed by Tukey's *post-hoc* test was applied ($P < 0.05$). The relationship between the N_2 fixation and the autotrophic and heterotrophic variables was determined with a Pearson correlation test ($n = 3$, $P < 0.05$). All tests were performed using the XLSTAT software.

RESULTS AND DISCUSSION

Characteristics of Cretan Sea Surface Water

The surface Cretan Sea water used for the mesocosm study exhibited typical low-nutrient, low-chlorophyll, oligotrophic Eastern Mediterranean Sea characteristics (**Table 2**; Pitta et al., 2016). The dissolved inorganic nitrite+nitrate, ammonium, and phosphorus (P) concentrations were close to their detection limits (132 ± 27, 131± 60, and 13 ± 4 nM, respectively), resulting in a high N:P ratio (~20:1). Correspondingly, low surface chlorophyll-*a* was measured prior to any addition (0.06 ± 0.01 μg L^{-1}). The picophytoplankton biomass was within the range previously reported for the Cretan Sea (Ignatiades et al., 2002; Tsiola et al., 2016), with *Synechococcus* the predominant autotrophic picoplankton (5.8 ± 0.2 μg C L^{-1}), followed by pico-eukaryotes (0.6 ± 0.2 μg C L^{-1}). The heterotrophic bacterial biomass was higher than that of the autotrophic bacterioplankton (8.5 ± 0.2 μg C L^{-1}), although it was still at the lower end of that reported for oligotrophic oceans (Cho and Azam, 1988 and see Figure 3 in Herut et al., this issue). The surface primary and bacterial productivity rates (PP and BP) were also low (393 ± 46 ng C L^{-1} h^{-1} for PP and 13.7 ± 5.5 ng C L^{-1} h^{-1} for BP), and were consistent with previous studies performed in the Cretan Sea (Gotsis-Skretas et al., 1999; Psarra et al., 2000; Tsiola et al., 2016).

Dinitrogen (N_2) fixation rates, measured using the enriched seawater method (Mohr et al., 2010), were low (0.22 ± 0.05 nmol N L^{-1} d^{-1}), and similar to the rates measured the previous spring in surface waters in the Levantine Basin using identical methodology (Rahav et al., 2013a). Two days prior to the experiment, N_2 fixation contributed 5.4 ± 1.7% to PP (**Table 2**), a slightly higher contribution than those estimated during the previous spring (~2%, Rahav et al., 2013a) and summer (~0.5–2%, Yogev et al., 2011; Rahav et al., 2013b) in the Eastern Mediterranean Sea. We postulate that this may have been due to the relatively high number of *nifH* gene copies observed from the non-filamentous photoautotrophic cyanobacteria *Trichodesmium* (>80,000 gene copies L^{-1}, **Table 2**) found in the Cretan water prior to the experiment. To date, only one sporadic bloom of *Trichodesmium* has been recorded in the EMS (Spatharis et al., 2012), and the reason for its rare occurrence in this warm, N-impoverished environment is unknown (Berman-Frank and Rahav, 2012). Our findings here combined with the published literature of N_2 in the Eastern Mediterranean Sea (e.g., Ibello et al., 2010; Bonnet et al., 2011; Yogev et al., 2011; Rahav et al., 2013a,b,c; Raveh et al., 2015; Rahav et al., 2016a) suggest patchy spatial and temporal occurrence of cyanobacterial (and other) diazotrophs with variable contribution to PP in the Cretan Sea.

The Response of Diazotrophy to Saharan Dust and Mixed Aerosol Amendments

The addition of Saharan dust (SD) triggered a rapid (30 h after enrichment) response, with a ~2-fold increase in N_2 fixation compared to the unamended controls (0.42 ± 0.08 and 0.24 ± 0.04 nmol N L^{-1} d^{-1}, respectively, one-way ANOVA, $P = 0.02$) (**Figure 1**). At T48, N_2 fixation rates declined in all mesocosms, yet remained higher in the SD and A mesocosms than in the controls (**Figure 1**). This decline in all mesocosms may suggest a weak, yet notable, bottle effect imposed by the mesocosm bags (Calvo-Díaz et al., 2011), low % enrichment of the enriched seawater used for the N_2 fixation measurements at this specific time point, or competition between the ambient surface microbial populations and diazotrophs that preclude diazotrophs from thriving. The marked and significant differences between the treatments throughout most samplings suggest that even if an experimental artifact occurred at T48, its impact on the measured

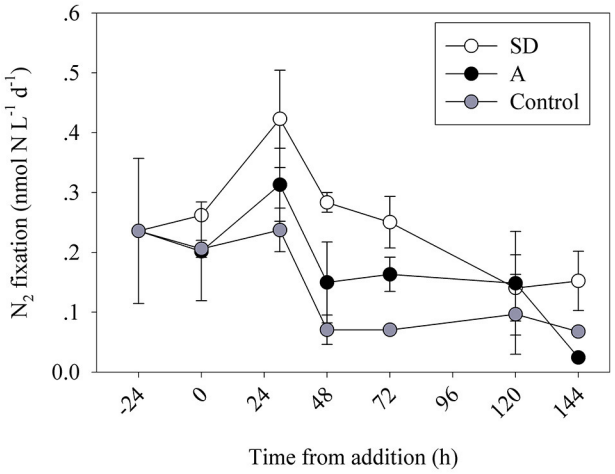

FIGURE 1 | Temporal changes in volumetric N_2 fixation rates during the mesocosm enrichment experiments. Data are averages of 3 replicate bottles per treatment of the control (gray), SD (white) and A (black) mesocosms during May 2012.

rates was weak overall. After 78 h, N_2 fixation declined in both SD treatments and control incubations. Yet, N_2 fixation remained 4 times higher in the SD treatments relative to the controls (∼0.25 ± 0.04 and ∼0.07 ± 0.01 nmol N L^{-1} d^{-1}, respectively, one-way ANOVA, $P = 0.004$). By day 5 (120 h), N_2 fixation rates in both SD treatments and control incubations were near the limit of analytical detection (∼0.10 nmol N L^{-1} d^{-1}, one-way ANOVA, $P > 0.05$, **Figure 1**). Similarly, the mixed aerosol (A) addition led to an overall increase in N_2 fixation rates in the short term (30 h post addition, **Figure 1**), although the responses were moderate (∼1.5–2-fold higher rates in treatment incubations relative to controls) and differences between treatments and controls were significant only at the 2 days time point. Similar to the SD treatments, N_2 fixation rates in the A treatments decreased to near the limits of analytical detection and were not significantly different from controls after 144 h (**Figure 1**). The observed changes in N_2 fixation following the SD or A addition can be explained by the enhanced concentrations of essential (and limiting in the unamended seawater) nutrients from the additives such as P (2–3 nmol P per mg dust/aerosol, Herut et al., this issue). It is also possible that leached Fe in the SD mesocosms (net change of ∼6 nM in dissolved Fe 3 h after SD addition), and the insignificant change in the A mesocosms (Herut et al., this issue) could explain the observed increase in N_2 fixation. Despite the increase in N_2 fixation rates in the 30–48 h following the SD or A additions, absolute N_2 fixation rates remained low overall throughout the experiment (**Figure 1**). This could be due to limited abundances of diazotrophs in the initial conditions so that overall rates remained low. Furthermore, after the initial enhanced response of the diazotrophs to the added dust- or aerosol-borne nutrients and/or trace elements, competition by more efficient non-diazotrophic phytoplankton or bacteria could have maintained low overall N_2 fixation rates.

The short-term enhancement of N_2 fixation rates measured after the addition of SD or A were similar to those observed previously in mesocosm experiments amended with a Saharan dust analog performed in the Western Mediterranean Sea (WMS) during the summer of 2008 and 2010 (2–5.3-fold and 4–6 days, Ridame et al., 2013). This may suggest common limiting factors for diazotrophy in these two contrasting systems. Elements leached off dust can introduce other nutrients and trace elements to the surface water in different quantities, chemical forms, concentrations and stoichiometry, depending on the dust/aerosol origin (Léon et al., 2015). In addition, atmospheric deposition can be a source of viable diazotrophic microbes as demonstrated from aerosols that originated in the Sahara desert, collected in Israel, and dissolved in seawater from the east Mediterranean Sea (Rahav et al., 2016b). N_2 fixation by these airborne diazotrophs delivered with atmospheric deposition comprised ∼10–15% (∼0.03 nmol N L^{-1} d^{-1}) of the "typical-average" rates measured in the EMS (0.10–0.20 nmol N L^{-1} d^{-1}), suggesting that atmospheric deposition can supply not only nutrients and trace metals to stimulate *in situ* N_2 fixation but may potentially deliver diazotrophs (Rahav et al., 2016b). Yet, the role of airborne diazotrophs should be extensively studied in the Mediterranean Sea as well as in other marine environments exposed to high atmospheric depositions such as the North Atlantic Ocean and the China Sea. In the present study, we did not determine the contribution of diazotrophs or other bacteria originating from our SD and A additions (i.e., measure N_2 fixation and BP, PP in SD or A added to sterile seawater). Other factors that regulating diazotrophs and N_2 fixation rates include top–down effects by grazing (Stukel et al., 2014), viral cell lysis (Hewson et al., 2009), competition with non-diazotrophic primary producers such as *Prochlorococcus* (Moisander et al., 2012) or bacterial heterotrophs (Thingstad et al., 2005), and other nutritional constraints such as carbon for heterotrophs (Rahav et al., 2016a) or vitamin B12 (Bonnet et al., 2010) may further limit production. Top–down grazing of diazotrophs probably did not greatly impact the diazotrophic populations in our experiments. Zooplankton abundance did not vary significantly between the mesocosms (M. Lou personal communication). Specifically, no known diazotroph grazers such as *Macrosetella gracilis* that feed on *Trichodesmium* cells were found in our mesocosms nor observed in the few surveys performed in the EMS (Kimor and Wood, 1975; Zakaria, 2015). In contrary, we hypothesize that airborne microbes or viruses can be important in regulating surface N_2 fixation in the Mediterranean Sea. Such interactions may occur especially in light of the high amount of aerosols deposited to the surface waters of Mediterranean Sea (Guerzoni et al., 1999), which potentially brings $\sim 10^7$ viruses per m^3 of air (Prospero et al., 2005; Womack et al., 2010; Polymenakou, 2012). Yet, examination of these factors was beyond the scope of the present study and warrants more research.

Both heterotrophic and cyanobacterial diazotrophs were present in this mesocosm study (**Figure 2**) with the Shannon diversity index ranging between 0.7 and 2.5 throughout the entire experiment (**Figure 2**). Based on the relative abundance of the *nifH* OTUs, most diazotrophs present in the original Cretan

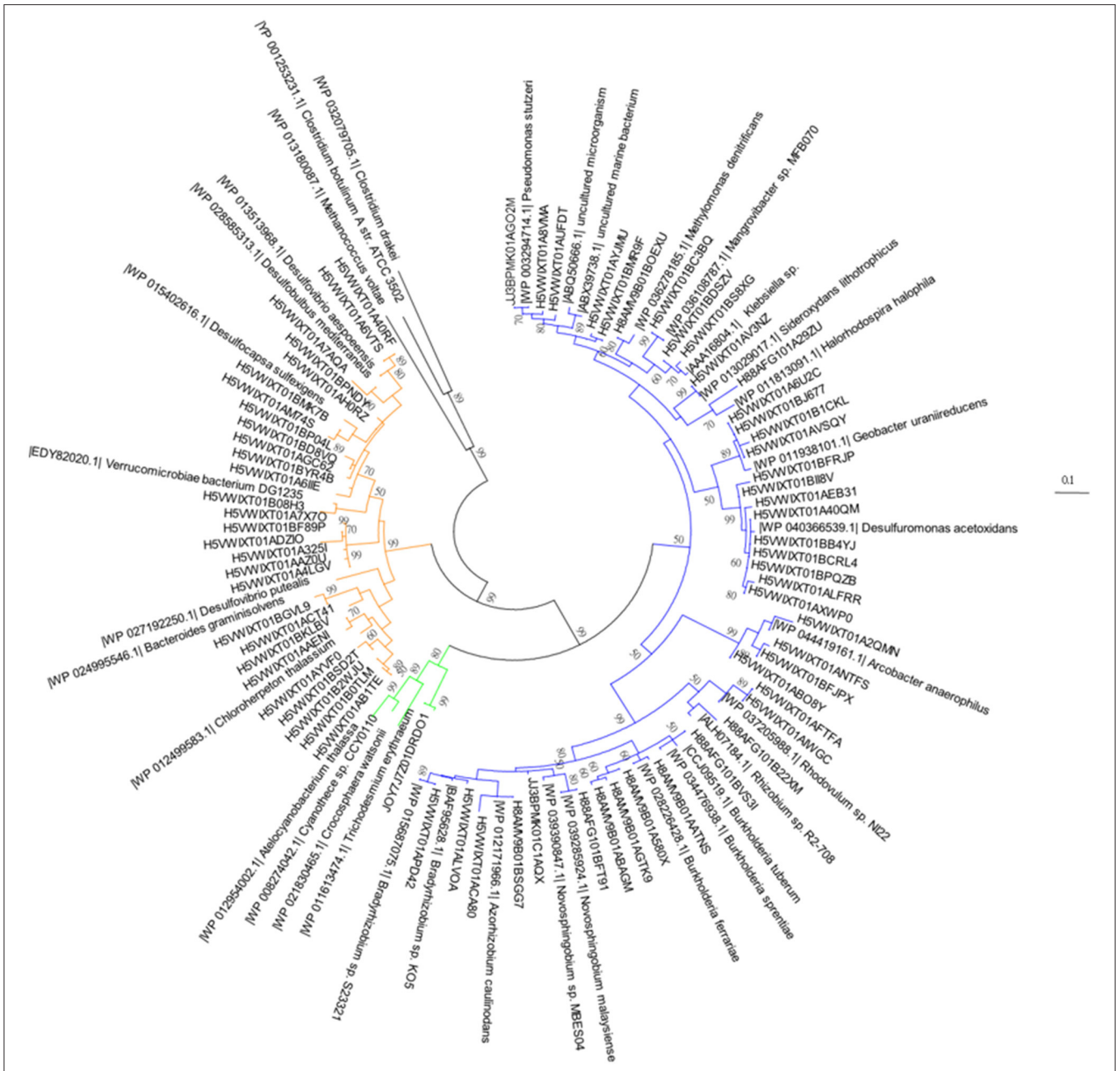

FIGURE 2 | A neighbor-joining phylogentic tree constructed with *nifH* gene amino acid sequences. Samples were taken 2 days prior to the addition of the SD or A addition. The differently-colored sequences are representative sequences of the OTUs revealed in this study. The sequences fall into Cluster I proteobacteria (blue), Cluster III (yellow), and cyanobacteria (green). The accession numbers of each reference sequence are shown in front of the sequence names.

Sea water samples grouped into known *nifH* clusters (**Figure 3**; Chien and Zinder, 1996; Zehr et al., 2003). After 2 days (48 h), the diazotroph community in the control treatments was dominated by *Sideroxydans* (30%) and *Acrobacter* (20%), whereas in the SD and A treatments *Trichodesmium* (68%) and *Pseudomonas* (41%) respectively dominated the diazotroph populations. At the conclusion of the experiment, the diazotrophic communities in the control mesocosms had shifted to *Azorhizobium* and *Novosphingobium*, *Azorhizobium* in the SD treatments, and *Burkholderia* in the A amended mesocosms (**Figure 3**). By the end of the experiment (144 h), the Shannon diversity dropped to 0.5–1.5. One explanation for this convergence in microbial populations is the potential of those OTUs to successfully utilize heavy metal concentrations as those found in the SD and A additions (see Table 4 in Herut et al., this issue).

While some cyanobacteria, including *Trichodesmium*, were present, most *nifH* OTUs retrieved in this experiment belonged to Proteobacteria. The overall predominance of non-cyanobacterial heterotrophic bacteria over autotrophic diazotrophs, highlights the importance of heterotrophic diazotrophy in the EMS waters as recorded in the Levantine Basin (Man-Aharonovich et al., 2007; Yogev et al., 2011; Rahav et al., 2013c) and also across the Mediterranean (Benavides et al., 2016). A greater contribution of heterotrophic diazotrophs is now recognized also from many other oceanic environments (reviewed in Riemann et al., 2010) including the Red Sea (Foster et al., 2009; Rahav et al., 2015), the western North Atlantic Ocean (Mulholland et al., 2012) and the English Channel (Rees et al., 2009, 2016).

To further estimate the role of heterotrophic diazotrophs in our system, we simultaneously incubated light and dark 4.6 L bottles (microcosms) from each treatment (**Table 3**). We assumed that dark incubations mainly reflect the activity of heterotrophic diazotrophs that do not require light energy for N_2 fixation, and estimated the heterotrophic contribution to N_2 fixation by comparing the dark incubations to light bottles incubated under the ambient surface irradiance. When we compared our light vs. dark bottle incubations, we found that the light:dark N_2 fixation ratio in the control mesocosms was usually ~1 (average 1.7 ± 1.6, **Table 3**), suggesting N_2 was fixed by both autotrophic and heterotrophic diazotrophs. Enrichment by SD or A caused the light:dark ratio to decline (an average of 0.8 ± 0.7 for SD and 0.8 ± 0.3 for A, **Table 3**), implying that the aerosol additions disproportionately stimulated heterotrophic N_2 fixation. Similar comparisons between ambient light and dark bottle N_2 fixation rates showed the same trend in the Mediterranean (also in the spring) and the Gulf of Aqaba/Northern Red Sea (in summertime), highlighting the important role of heterotrophs in fixing dinitrogen in

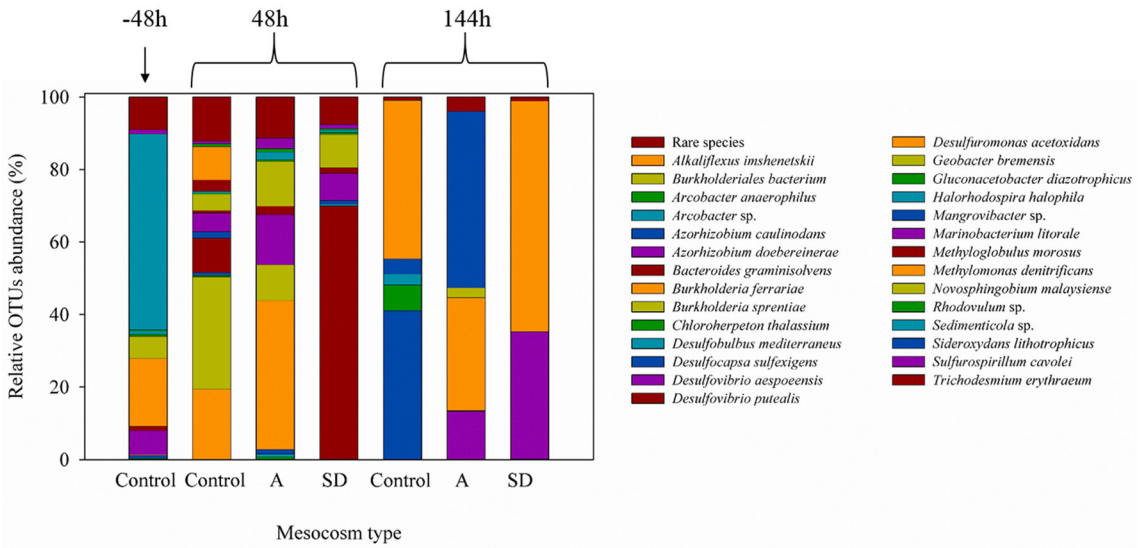

FIGURE 3 | The relative abundance (%) of the *nifH* DNA phyla during the mesocosm enrichment experiment of May 2012.

TABLE 3 | The N_2 fixation rates of Cretan sub-surface water in experimental mesocosms (controls, +SD, +A), for bottles incubated under ambient lighting (L) and in complete darkness (D) for 24 h.

Time after enrichment (h)	Incubation under ambient light			Incubation under complete dark			Light:dark N_2 fixation ratio		
	Control	SD	A	Control	SD	A	Control	SD	A
0	0.22 ± 0.01			0.05 ± 0.00			4.4		
30	0.24 ± 0.04	0.42 ± 0.08	0.31 ± 0.06	0.17 ± 0.09	0.22 ± 0.06	0.28 ± 0.02	1.4	1.9	1.1
48	0.07 ± 0.02	0.28 ± 0.02	0.15 ± 0.07	N.A	N.A	N.A	N.A	N.A	N.A
72	0.07 ± 0.01	0.25 ± 0.04	0.16 ± 0.03	0.05 ± 0.01	0.60 ± 0.02	0.34 ± 0.08	1.3	0.4	0.5
120	0.10 ± 0.07	0.14 ± 0.06	0.15 ± 0.09	0.44 ± 0.20	0.38 ± 0.01	0.18 ± 0.13	0.2	0.4	0.8
144	0.07 ± 0.00	0.15 ± 0.05	0.02 ± 0.00	0.07 ± 0.00	0.29 ± 0.03	0.05 ± 0.01	1.0	0.5	0.7
Average	0.14 ± 0.08	0.25 ± 0.09	0.18 ± 0.09	0.16 ± 0.16	0.37 ± 0.16	0.21 ± 0.13	1.7 ± 1.6	0.8 ± 0.7	0.8 ± 0.3

Values are averages of 3 independent replicates. The time 0 measurement is an average of 3 randomly picked mesocosms. N.A, not available.

ultra-oligotrophic systems (Bonnet et al., 2013; Rahav et al., 2013a, 2015).

The Contribution of N_2 Fixation to Primary Productivity in the Cretan Sea during Spring

To estimate the contribution of N_2 fixation to primary productivity, we calculated the contribution of the fixed N (as particulate organic nitrogen, PON) to the total particulate organic carbon (POC) from the mesocosms. An average POC:PON ratio of ~8 concurs with previous measurements from the open-waters of the Levantine basin (Yogev et al., 2011; Rahav et al., 2013b). We subsequently used this average to calculate the percent contribution of N_2 fixation to PP. Our results show that N_2 fixation contributed 2–4% ($P > 0.05$) of PP following the mixed aerosol additions and 3–8% ($P = 0.04$) after SD additions (**Figure 4**). These estimations (2–8%) are in line with other estimates from the Mediterranean Sea (Garcia et al., 2006; Bonnet et al., 2011; Yogev et al., 2011; Rahav et al., 2013b). However, this is not surprising as heterotrophic diazotrophs comprised the bulk of the retrieved *nifH* OTUs and the dark N_2 fixation was generally higher than the rates measured under ambient light (**Table 3** and discussion above). The positive coupling between N_2 fixation and bacterial abundance (BA) or bacterial production (BP), while no distinct pattern was observed with *Trichodesmium nifH* gene expression (**Figure 5**), further supports the importance of heterotrophic bacterial diazotrophs in this system (Rahav et al., 2013a, 2015).

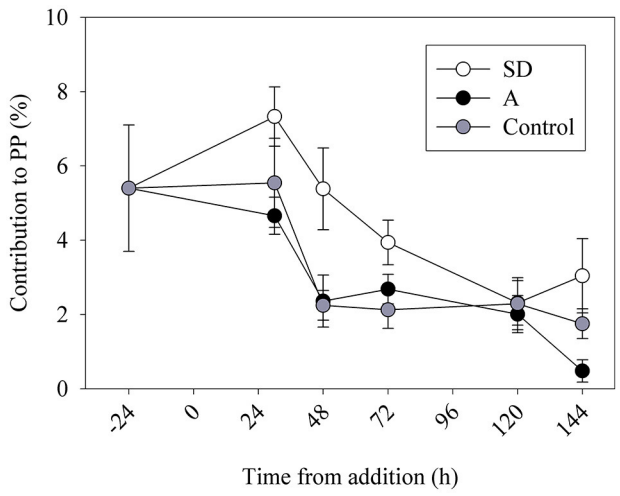

FIGURE 4 | The contribution of N_2 fixation to primary productivity (PP) in the control (gray), SD (white), and A (black) mesocosms.

Higher contributions of diazotrophs to primary productivity are typically found where filamentous cyanobacterial N_2-fixers predominate. For example, the contribution of *Trichodesmium* to PP was 11.6% in the outer Sanya Bay of the China Sea (Dong et al., 2008), 22 and 44% in the equatorial Atlantic and South Atlantic Gyre, respectively (Fernández et al., 2010), and 47% of the total depth-integrated PP in the North Atlantic Ocean (Carpenter et al., 2004).

In cases where EMS surface water receives Saharan dust inputs (as tested here), *Trichodesmium*-derived PP may be enhanced if there is a seed population that can respond to the addition. Yet, as previously observed, the diazotrophs that characterize the EMS are predominantly small-sized bacterial phylotypes (**Figure 3**; Man-Aharonovich et al., 2007; Yogev et al., 2011), and *Trichodesmium* is uncommon (Yogev et al., 2011; Spatharis et al., 2012).

Finally, our results demonstrate that intense dust and aerosol deposition events (as frequently occur in the Mediterranean Sea, Herut et al., 2002; Bonnet and Guieu, 2006) may potentially fuel diazotrophy and alter the composition of diazotrophic communities. Furthermore, these depositions to the Mediterranean Sea can also enrich surface waters with bioavailable N sources (Carbo et al., 2005; Herut et al., 2005; and see Table S1 in Rahav et al., 2016c). The higher N concentrations can stimulate new production and induce changes in community structure such as a shift from populations of picophytoplankton

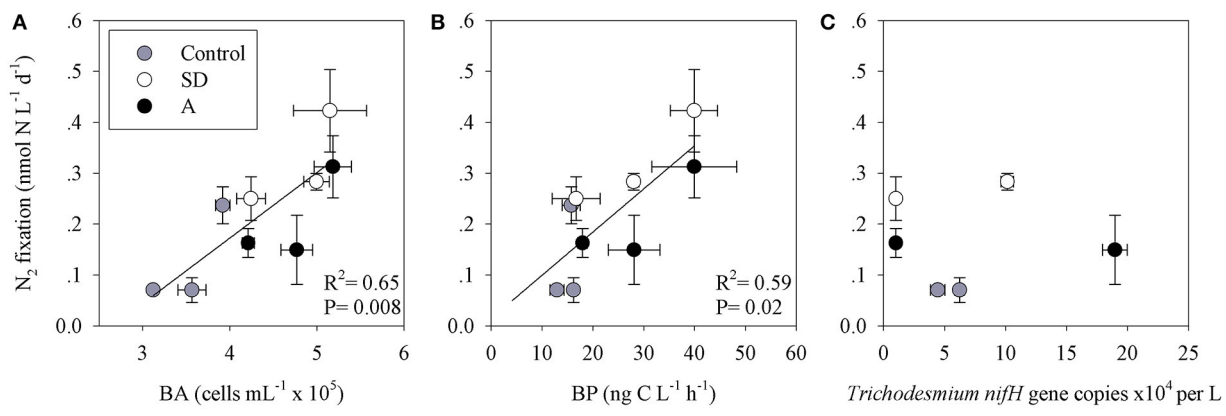

FIGURE 5 | The relationship between N_2 fixation and (A) bacterial abundance; BA, (B) bacterial production; BP, and (C) *Trichodesmium nifH* copies, in the first 144 h following the Saharan dust (SD) and mixed aerosol (A) enrichments.

to larger-size class microphytoplankton such as diatoms and dinoflagellates (Guieu et al., 2014), which, in turn, may enhance organic matter export and reduce the high recycling rates typical for the microbial food web of the EMS.

AUTHOR CONTRIBUTIONS

Conceived and designed the experiments: ER, BH, IB-F. Performed the experiments: ER, BH, IB-F, GC, HL, TT, AG, AT, SP, AL, MM, ES, PP. Analyzed the data: ER, BH, IB-F, CS. Contributed reagents/materials/analysis tools: BH, IB-F, MM, PP Wrote the paper: ER, BH, IB-F.

ACKNOWLEDGMENTS

The authors wish to thank Dr. P. Divanach for his valuable advice on technical matters, G. Piperakis for his inspired technical assistance, S. Zivanovic and E. Dafnomili for assisting with chemical analyses, A. Konstantinopoulou for assisting with bacterial production analyses, D. Podaras and S. Diliberto for assisting during the experiment, and N. Sekeris for his help with constructions and with ideas regarding technical solutions. The captain and the crew of the R/V Philia are also thanked for their assistance during the transportation of water from the sea to the mesocosms. This study was in partial fulfillment of a Ph.D. thesis for ER from Bar Ilan University. This work was financed by the European Union Seventh Framework Program (FP7/2007–2013) under grant agreement no. 228224, "MESOAQUA: Network of leading MESOcosm facilities to advance the studies of future AQUAtic ecosystems from the Arctic to the Mediterranean" through grants to ER, GC, HL, BH, and IB-F, by the EU and Greek-national-funded Program THALES-ADAMANT and the Israel Science Foundation grants (996/08) to IB-F and BH.

SUPPLEMENTARY MATERIAL

The Supplementary Material for this article can be found online at: http://journal.frontiersin.org/article/10.3389/fmars.2016.00180

REFERENCES

Benavides, M., Bonnet, S., Hernández, N., Martínez-Pérez, A. M., Nieto-Cid, M., Álvarez-Salgado, X. A., et al. (2016). Basin-wide N_2 fixation in the deep waters of the Mediterranean Sea. *Global Biogeochem. Cycles.* 30, 952–961. doi: 10.1002/2015GB005326

Berman-Frank, I., Cullen, J. T., Shaked, Y., Sherrell, R. M., and Falkowski, P. G. (2001). Iron availability, cellular iron quotas, and nitrogen fixation in *Trichodesmium*. *Limnol. Oceanogr.* 46, 1249–1260. doi: 10.4319/lo.2001.46.6.1249

Berman-Frank, I., Quigg, A., Finkel, Z. V., Irwin, A. J., and Haramaty, L. (2007). Nitrogen-fixation strategies and Fe requirements in cyanobacteria. *Limnol. Oceanogr.* 52, 2260–2269. doi: 10.4319/lo.2007.52.5.2260

Berman-Frank, I., and Rahav, E. (2012). "Nitrogen fixation as a source for new production in the Mediterranean Sea: a review," in *Life in the Mediterranean Sea: A Look at Habitat Changes*, ed N. E. Stambler (New York, NY: Nova Science Publishers), 199–226.

Bonnet, S., Dekaezemacker, J., Turk-Kubo, K. A, Moutin, T., Hamersley, R. M., Grosso, O., et al. (2013). Aphotic N_2 fixation in the Eastern Tropical South Pacific Ocean. *PLoS ONE* 8:e81265. doi: 10.1371/journal.pone.0081265

Bonnet, S., Grosso, O., and Moutin, T. (2011). Planktonic dinitrogen fixation along a longitudinal gradient across the Mediterranean Sea during the stratified period (BOUM cruise). *Biogeosciences* 8, 2257–2267. doi: 10.5194/bg-8-2257-2011

Bonnet, S., and Guieu, C. (2006). Atmospheric forcing on the annual iron cycle in the western Mediterranean Sea: a 1-year survey. *J. Geophys. Res. Oceans* 111, 1–13. doi: 10.1029/2005jc003213

Bonnet, S., Webb, E. A., Panzeca, C., Karl, D. M., Capone, D. G., and Sañudo-Wilhelmy, S. A. (2010). Vitamin B12 excretion by cultures of the marine cyanobacteria *Crocosphaera* and *Synechococcus*. *Limnol. Oceanogr.* 55, 1959–1964. doi: 10.4319/lo.2010.55.5.1959

Calvo-Díaz, A., Díaz-Pérez, L., Suárez, L. Á., Morán, X. A. G., Teira, E., and Marañón, E. (2011). Decrease in the autotrophic-to-heterotrophic biomass ratio of picoplankton in oligotrophic marine waters due to bottle enclosure. *Appl. Environ. Microbiol.* 77, 5739–5746. doi: 10.1128/AEM.00066-11

Campbell, J. W., and Yentsch, C. M. (1989). Variance within homogeneous phytoplankton populations, III: analysis of natural populations. *Cytometry* 10, 605–611. doi: 10.1002/cyto.990100516

Carbo, P., Krom, M. D., Homoky, W. B., Benning, L. G., and Herut, B. (2005). Impact of atmospheric deposition on N and P geochemistry in the southeastern Levantine basin. *Deep Sea Res. Part II Top. Stud. Oceanogr.* 52, 3041–3053. doi: 10.1016/j.dsr2.2005.08.014

Carpenter, E. J., Subramaniam, A., and Capone, D. G. (2004). Biomass and productivity of the cyanobacterium, *Trichodesmium* spp. in the tropical North Atlantic Ocean. *Deep Sea Res. I* 51, 173–203. doi: 10.1016/j.dsr.2003.10.006

Chien, Y. T., and Zinder, S. H. (1996). Cloning, functional organization, transcript studies, and phylogenetic analysis of the complete nitrogenase structural genes (*nifHDK2*) and associated genes in the archaeon *Methanosarcina barkeri* 227. *J. Bacteriol.* 178, 143–148.

Cho, B. C., and Azam, F. (1988). Major role of bacteria in biogeochemical fluxes in the ocean's interior. *Nature* 332, 441–443. doi: 10.1038/332441a0

Dong, J., Zhang, Y., Wang, Y., Zhang, S., and Wang, H. (2008). Spatial and seasonal variations of cyanobacteria and their nitrogen fixation rates in Sanya Bay, South China Sea. *Sci. Mar.* 72, 239–251. doi: 10.3989/scimar.2008.72n2239

Dyhrman, S. T., and Haley, S. T. (2006). Phosphorus scavenging in the unicellular marine diazotroph *Crocosphaera watsonii*. *Appl. Environ. Microbiol.* 72, 1452–1458. doi: 10.1128/AEM.72.2.1452-1458.2006

Falkowski, P. G. (1997). Evolution of the nitrogen cycle and its influence on the biological sequestration of CO_2 in the ocean. *Nature* 387, 272–275. doi: 10.1038/387272a0

Farnelid, H., Andersson, A. F., Bertilsson, S., Al-Soud, W. A., Hansen, L. H., Sørensen, S., et al. (2011). Nitrogenase gene amplicons from global marine surface waters are dominated by genes of non-cyanobacteria. *PLoS ONE* 6: e19223. doi: 10.1371/journal.pone.0019223

Farnelid, H., Bentzon-tilia, M., Andersson, A. F., and Bertilsson, S. (2013). Active nitrogen-fixing heterotrophic bacteria at and below the chemocline of the central Baltic Sea. *ISME J.* 7, 1413–1423. doi: 10.1038/ismej.2013.26

Fernández, A., Mouriño-Carballido, B., Bode, A., Varela, M., and Marañón, E. (2010). Latitudinal distribution of *Trichodesmium* spp. and N_2 fixation in the Atlantic Ocean. *Biogeosciences* 7, 2195–2225. doi: 10.5194/bgd-7-2195-2010

Foster, R. A., Paytan, A., and Zehr, J. P. (2009). Seasonality of N_2 fixation and *nifH* gene diversity in the Gulf of Aqaba (Red Sea). *Limnol. Oceanogr.* 54, 219–233. doi: 10.4319/lo.2009.54.1.0219

Garcia, N., Raimbault, P., Gouze, E., and Sandroni, V. (2006). Nitrogen fixation and primary production in Western Mediterranean. *C. R. Biol.* 329, 742–750. doi: 10.1016/j.crvi.2006.06.006

Gotsis-Skretas, O., Pagou, K., and Moraitou-Apostolopoulou, M. (1999). Seasonal horizontal and vertical variability in primary production and standing stocks of phytoplankton and zooplankton in the Cretan Sea and the Straits of the Cretan Arc (March 1994-Jannuary 1995). *Prog. Oceanogr.* 44, 625–649. doi: 10.1016/S0079-6611(99)00048-8

Gruber, N., and Galloway, J. N. (2008). An Earth-system perspective of the global nitrogen cycle. *Nature* 451, 293–296. doi: 10.1038/nature06592

Gruber, N., and Sarmiento, J. L. (1997). Global patterns of marine nitrogen fixation and denitrification. *Glob. Biogeochem. Cycles* 11, 235–266. doi: 10.1029/97GB00077

Guerzoni, S., Chester, R., Dulac, F., Measures, C., Migon, C., Molinaroli, E., et al. (1999). The role of atmospheric deposition in the biogeochemistry of the Mediterranean Sea. *Prog. Oceanogr.* 44, 147–190. doi: 10.1016/S0079-6611(99)00024-5

Guieu, C., Aumont, O., Paytan, A., Bopp, L., Law, C. S., Mahowald, N., et al. (2014). Global biogeochemical cycles deposition to low nutrient Low chlorophyll regions. *Global Biogeochem. Cycles* 28, 1179–1198. doi: 10.1002/2014GB004852

Herut, B., Collier, R., and Krom, M. D. (2002). The role of dust in supplying nitrogen and phosphorus to the Southeast Mediterranean. *Limnol. Oceanogr.* 47, 870–878. doi: 10.4319/lo.2002.47.3.0870

Herut, B., Krom, M. D., Pan, G., and Mortimer, R. (1999). Atmospheric input of nitrogen and phosphorus to the Southeast Mediterranean: sources, fluxes, and possible impact. *Limnol. Oceanogr.* 44, 1683–1692. doi: 10.4319/lo.1999.44.7.1683

Herut, B., Zohary, T., Krom, M. D., Mantoura, R. F. C., Pitta, P., Psarra, S., et al. (2005). Response of East Mediterranean surface water to Saharan dust: On-board microcosm experiment and field observations. *Deep Sea Res. Part II Top. Stud. Oceanogr.* 52, 3024–3040. doi: 10.1016/j.dsr2.2005.09.003

Hewson, I., Poretsky, R. S., Dyhrman, S. T., Zielinski, B., White, A. E., Tripp, H. J., et al. (2009). Microbial community gene expression within colonies of the diazotroph, *Trichodesmium*, from the Southwest Pacific Ocean. *ISME J.* 3, 1286–1300. doi: 10.1038/ismej.2009.75

Ibello, V., Cantoni, C., Cozzi, S., and Civitarese, G. (2010). First basin-wide experimental results on N_2 fixation in the open Mediterranean Sea. *Geophys. Res. Lett.* 37, 1–5. doi: 10.1029/2009GL041635

Ignatiades, L., Psarra, S., and Zervakis, V. (2002). Phytoplankton size-based dynamics in the Aegean Sea (Eastern Mediterranean). *J. Mar. Syst.* 36, 11–28. doi: 10.1016/S0924-7963(02)00132-X

Ivancic, I., and Deggobis, D. (1984). An optimal manual procedure for ammonia analysis in natural waters by indophenol blue method. *Water Res.* 18, 1143–1147. doi: 10.1016/0043-1354(84)90230-6

Kimor, B., and Wood, E. J. F. (1975). Plankton study in Eastern Mediterranean Sea. *Mar. Biol.* 29, 321–333. doi: 10.1007/BF00388852

Kitajima, S., Furuya, K., Hashihama, F., Takeda, S., and Kanda, J. (2009). Latitudinal distribution of diazotrophs and their nitrogen fixation in the tropical and subtropical western North Pacific. *Limnol. Oceanogr.* 54, 537–547. doi: 10.4319/lo.2009.54.2.0537

Kong, L., Jing, H., Kataoka, T., Buchwald, C., and Liu, H. (2013). Diversity and spatial distribution of hydrazine oxidoreductase (hzo) gene in the oxygen minimum zone off Costa Rica. *PLoS ONE* 8:e78275. doi: 10.1371/journal.pone.0078275

Lenes, J. M., Darrow, B. P., Cattrall, C., Heil, C. A., Callahan, M., Vargo, G. A., et al. (2001). Iron fertilization and the Trichodesmium response on the West Florida shelf. *Limnol. Oceanogr.* 46, 1261–1277. doi: 10.4319/lo.2001.46.6.1261

Léon, J.-F., Augustin, P., Mallet, M., Bourrianne, T., Pont, V., Dulac, F., et al. (2015). Aerosol vertical distribution, optical properties and transport over Corsica (western Mediterranean). *Atmos. Chem. Phys. Discuss.* 15, 9507–9540. doi: 10.5194/acpd-15-9507-2015

Man-Aharonovich, D., Kress, N., Zeev, E. B., Berman-Frank, I., and Béjà, O. (2007). Molecular ecology of nifH genes and transcripts in the eastern Mediterranean Sea. *Environ. Microbiol.* 9, 2354–2363. doi: 10.1111/j.1462-2920.2007.01353.x

Marañón, E., Fernández, A., Mouriño-Carballido, B., Martínez-García, S., Teira, E., Cermeño, P., et al. (2010). Degree of oligotrophy controls the response of microbial plankton to Saharan dust. *Limnol. Oceanogr.* 55, 2339–2352. doi: 10.4319/lo.2010.55.6.2339

Marie, D., Partensky, F., Jacquet, S., and Vaulot, D. (1997). Enumeration and cell cycle analysis of natural populations of marine picoplankton by flow cytometry using the nucleic acid stain SYBR I. *Appl. Environ. Microbiol.* 63, 186–193.

McGinnis, S., and Madden, T. L. (2004). BLAST: at the core of a powerful and diverse set of sequence analysis tools. *Nucleic Acids Res.* 32, 20–25. doi: 10.1093/nar/gkh435

Mills, M. M., Ridame, C., Davey, M., La Roche, J., and Geider, R. J. (2004). Iron and phosphorus co-limit nitrogen fixation in the eastern tropical North Atlantic. *Nature* 429, 292–294. doi: 10.1038/nature02550

Mohr, W., Großkopf, T., Wallace, D. W. R., and Laroche, J. (2010). Methodological underestimation of oceanic nitrogen fixation rates. *PLoS ONE* 49:e12583. doi: 10.1371/journal.pone.0012583

Moisander, P. H., Zhang, R., Boyle, E. A., Hewson, I., Montoya, J. P., and Zehr, J. P. (2012). Analogous nutrient limitations in unicellular diazotrophs and *Prochlorococcus* in the South Pacific Ocean. *ISME J.* 6, 733–744. doi: 10.1038/ismej.2011.152

Moore, M. C., Mills, M. M., Achterberg, E. P., Geider, R. J., LaRoche, J., Lucas, M. I., et al. (2009). Large-scale distribution of Atlantic nitrogen fixation controlled by iron availability. *Nat. Geosci.* 2, 867–871. doi: 10.1038/ngeo667

Mulholland, M. R., and Bernhardt, P. W. (2005). The effect of growth rate, phosphorus concentration, and temperature on N_2 fixation, carbon fixation, and nitrogen release in continuous cultures of *Trichodesmium* IMS101. *Limnol. Oceanog.* 50, 839–849. doi: 10.4319/lo.2005.50.3.0839

Mulholland, M. R., Bernhardt, P. W., Blanco-Garcia, J. L., Mannino, A., Hyde, K., Mondragon, E., et al. (2012). Rates of dinitrogen fixation and the abundance of diazotrophs in North American coastal waters between Cape Hatteras and Georges Bank. *Limnol. Oceanogr.* 57, 1067–1083. doi: 10.4319/lo.2012.57.4.1067

Nielsen, E. (1952). The use of radioactive carbon (^{14}C) for measuring organic production in the sea. *Conseil Permanent International pour l'Exploration de la Mer* 18, 117–140. doi: 10.1093/icesjms/18.2.117

Paerl, H. W., Crocker, K. M., and Prufert, L. E. (1987). Limitation of N2 fixation in coastal marine waters: relative importance of molybdenum, iron, phosphorus, and organic matter availability. *Limnol. Oceanogr.* 32, 525–536. doi: 10.4319/lo.1987.32.3.0525

Pitta, P., Nejstgaard, J. C., Tsagaraki, T. M., Zervoudaki, S., Egge, J. K., Frangoulis, C., et al. (2016). Confirming the "Rapid phosphorus transfer from microorganisms to mesozooplankton in the Eastern Mediterranean Sea" scenario through a mesocosm experiment. *J. Plankton Res.* 0, 1–20. doi: 10.1093/plankt/fbw010

Polymenakou, P. N. (2012). Atmosphere: a source of pathogenic or beneficial microbes? *Atmosphere (Basel)* 3, 87–102. doi: 10.3390/atmos3010087

Prospero, J. M., Blades, E., Mathison, G., and Naidu, R. (2005). Interhemispheric transport of viable fungi and bacteria from Africa to the Caribbean with soil dust. *Aerobiologia (Bologna)* 21, 1–19. doi: 10.1007/s10453-004-5872-7

Psarra, S., Tselepides, A., and Ignatiades, L. (2000). Primary productivity in the oligotrophic Cretan Sea (NE Mediterranean): seasonal and interannual variability. *Prog. Oceanogr.* 46, 187–204. doi: 10.1016/S0079-6611(00)00018-5

Rahav, E., Bar-Zeev, E., Ohayon, S., Elifantz, H., Belkin, N., Herut, B., et al. (2013c). Dinitrogen fixation in aphotic oxygenated marine environments. *Front. Microbiol.* 4:227. doi: 10.3389/fmicb.2013.00227

Rahav, E., Giannetto, J. M., and Bar-Zeev, E. (2016a). Contribution of mono and polysaccharides to heterotrophic N_2 fixation at the eastern Mediterranean coastline. *Sci. Rep.* 6:27858. doi: 10.1038/srep27858

Rahav, E., Herut, B., Levi, A., Mulholland, M. R., and Berman-Frank, I. (2013a). Springtime contribution of dinitrogen fixation to primary production across the Mediterranean Sea. *Ocean Sci.* 9, 489–498. doi: 10.5194/os-9-489-2013

Rahav, E., Herut, B., Mulholland, M., Belkin, N., Elifantz, H., and Berman-Frank, I. (2015). Heterotrophic and autotrophic contribution to dinitrogen fixation in the Gulf of Aqaba. *Mar. Ecol. Prog. Ser.* 522, 67–77. doi: 10.3354/meps11143

Rahav, E., Herut, B., Stambler, N., Bar-Zeev, E., Mulholland, M. R., and Berman-Frank, I. (2013b). Uncoupling between dinitrogen fixation and primary productivity in the eastern Mediterranean Sea. *J. Geophys. Res. Biogeosci.* 118, 195–202. doi: 10.1002/jgrg.20023

Rahav, E., Ovadia, G., Paytan, A., and Herut, B. (2016b). Contribution of airborne microbes to bacterial production and N2 fixation in seawater upon aerosol deposition. *Geophys. Res. Lett.* 43, 1–9. doi: 10.1002/2015GL066898

Rahav, E., Paytan, A., Chien, C.-T., Ovadia, G., Katz, T., and Herut, B. (2016c). The impact of atmospheric dry deposition associated microbes on the southeastern Mediterranean Sea surface water following an intense dust storm. *Front. Mar. Sci.* 3:127. doi: 10.3389/fmars.2016.00127

Raveh, O., David, N., Rilov, G., and Rahav, E. (2015). The temporal dynamics of coastal phytoplankton and bacterioplankton in the Eastern Mediterranean Sea. *PLoS ONE* 10:e0140690. doi: 10.1371/journal.pone.0140690

Rees, A. P., Gilbert, J. A., and Kelly-Gerreyn, B. A. (2009). Nitrogen fixation in the western English Channel (NE Atlantic Ocean). *Mar. Ecol. Prog. Ser.* 374, 7–12. doi: 10.3354/meps07771

Rees, A. P., Law, C. S., and Woodward, E. M. S. (2006). High rates of nitrogen fixation during an *in-situ* phosphate release experiment in the Eastern Mediterranean Sea. *Geophys. Res. Lett.* 33:L10607. doi: 10.1029/2006GL025791

Rees, A. P., Tait, K., Widdicombe, C. E., Quartly, G. D., McEvoy, A. J., and Al-Moosawi, L. (2016). Metabolically active, non-nitrogen fixing, *Trichodesmium* in UK coastal waters during winter. *J. Plankton Res.* 0:fbv123. doi: 10.1093/plankt/fbv123

Ridame, C., Guieu, C., and L'Helguen, S. (2013). Strong stimulation of N_2 fixation in oligotrophic Mediterranean Sea: Results from dust addition in large *in situ* mesocosms. *Biogeosciences* 10, 7333–7346. doi: 10.5194/bg-10-7333-2013

Ridame, C., Le Moal, M., Guieu, C., Ternon, E., Biegala, I. C., L'Helguen, S., et al. (2011). Nutrient control of N_2 fixation in the oligotrophic Mediterranean Sea and the impact of Saharan dust events. *Biogeosciences* 8, 2773–2783. doi: 10.5194/bg-8-2773-2011

Riemann, L., Farnelid, H., and Steward, G. (2010). Nitrogenase genes in non-cyanobacterial plankton: prevalence, diversity and regulation in marine waters. *Aquat. Microb. Ecol.* 61, 235–247. doi: 10.3354/ame01431

Rimmelin, P., and Moutin, T. (2005). Re-examination of the MAGIC method to determine low orthophosphate concentration in seawater. *Anal. Chim. Acta* 548, 174–182. doi: 10.1016/j.aca.2005.05.071

Sandroni, V., Raimbault, P., Migon, C., Garcia, N., and Gouze, E. (2007). Dry atmospheric deposition and diazotrophy as sources of new nitrogen to northwestern Mediterranean oligotrophic surface waters. *Deep Sea Res. Part I Oceanogr. Res. Pap.* 54, 1859–1870. doi: 10.1016/j.dsr.2007.08.004

Sañudo-Wilhelmy, S., Kustka, A. B., Gobler, C. J., San, S. A., Hutchins, D. A., Yang, M., et al. (2001). Phosphorus limitation of nitrogen fixation by *Trichodesmium* in the central Atlantic Ocean. *Nature* 411, 66–69. doi: 10.1038/35075041

Schloss, P. D., Westcott, S. L., Ryabin, T., Hall, J. R., Hartmann, M., Hollister, E. B., et al. (2009). Introducing mothur: open-source, platform-independent, community-supported software for describing and comparing microbial communities. *Appl. Environ. Microbiol.* 75, 7537–7541. doi: 10.1128/AEM.01541-09

Simon, M., Alldredge, A., and Azam, F. (1989). Protein-content and protein-synthesis rates of planktonic marine-bacteria. *Mar. Ecol. Prog. Ser.* 51, 201–213. doi: 10.3354/meps051201

Simon, M., Alldredge, A., and Azam, F. (1990). Bacterial carbon dynamics on marine snow. *Mar. Ecol. Prog. Ser.* 65, 205–211. doi: 10.3354/meps065205

Sohm, J. A., Webb, E. A., and Capone, D. G. (2011). Emerging patterns of marine nitrogen fixation. *Nat. Rev. Microbiol.* 9, 499–508. doi: 10.1038/nrmicro2594

Spatharis, S., Skliris, N., and Meziti, A. (2012). First record of a *Trichodesmium erythraeum* bloom in the Mediterranean Sea. *Can. J. Fish. Aquat. Sci.* 69, 1444–1455. doi: 10.1139/f2012-020

Strickland, J. D. H., and Parsons, T. R. (1972). *Bulletin of the Fisheries Research Board of Canada, Vol. 167, 2nd Edn.* Ottawa, ON: Fisheries Research Board of Canada.

Stukel, M. R., Coles, V. J., Brooks, M. T., and Hood, R. R. (2014). Top-down, bottom-up and physical controls on diatom-diazotroph assemblage growth in the Amazon River plume. *Biogeosciences* 11, 3259–3278. doi: 10.5194/bg-11-3259-2014

Tamura, K., Stecher, G., Peterson, D., Filipski, A., and Kumar, S. (2013). MEGA6: molecular evolutionary genetics analysis version 6.0. *Mol. Biol. Evol.* 30, 2725–2729. doi: 10.1093/molbev/mst197

Thingstad, T. F., Krom, M. D., Mantoura, R. F. C., Flaten, G. A. F., Groom, S., Herut, B., et al. (2005). Nature of phosphorus limitation in the ultraoligotrophic eastern Mediterranean. *Science* 309, 1068–1071. doi: 10.1126/science.1112632

Tsiola, A., Pitta, P., Fodelianakis, S., Pete, R., Magiopoulos, I., Mara, P., et al. (2016). Nutrient limitation in surface waters of the oligotrophic Eastern Mediterranean Sea: an Enrichment Microcosm Experiment. *Microb. Ecol.* 71, 575–588. doi: 10.1007/s00248-015-0713-5

Vaulot, D., and Marie, D. (1999). Diel variability of photosynthetic picoplankton in the equatorial Pacific. *Appl. Environ. Microbiol.* 104, 3297–3310. doi: 10.1029/98jc01333

Wang, Q., Iii, J. F. Q., and Fish, J.A. (2013). Ecological patterns of *nifH* genes in four terrestrial climatic zones. *MBio* 4, 1–9. doi: 10.1128/mBio.00592-13

Welschmeyer, N. A. (1994). Fluorometric analysis of chlorophyll a in the presence of chlorophyll b and pheopigments. *Limnol. Oceanogr.* 39, 1985–1992. doi: 10.4319/lo.1994.39.8.1985

Wilson, S. T., Böttjer, D., Church, M. J., and Karl, D. M. (2012). Comparative assessment of nitrogen fixation methodologies, conducted in the oligotrophic north pacific ocean. *Appl. Environ. Microbiol.* 78, 6516–6523. doi: 10.1128/AEM.01146-12

Womack, A. M., Bohannan, B. J. M., and Green, J. L. (2010). Biodiversity and biogeography of the atmosphere. *Philos. Trans. R. Soc. Lond. B. Biol. Sci.* 365, 3645–3653. doi: 10.1098/rstb.2010.0283

Wu, J., Sunda, W., Boyle, E. A., and Karl, D. M. (2000). Phosphate depletion in the Western North Atlantic Ocean. *Science* 289, 759–762. doi: 10.1126/science.289.5480.759

Yogev, T., Rahav, E., Bar-Zeev, E., Man-Aharonovich, D., Stambler, N., Kress, N., et al. (2011). Is dinitrogen fixation significant in the Levantine Basin, East Mediterranean Sea? *Environ. Microbiol.* 13, 854–871. doi: 10.1111/j.1462-2920.2010.02402.x

Zakaria, H. Y. (2015). Lessepsian migration of zooplankton through Suez Canal and its impact on ecological system. *Egypt. J. Aquat. Res.* 41, 129–144. doi: 10.1016/j.ejar.2015.04.001

Zehr, J. P., Jenkins, B. D., Short, S. M., and Steward, G. F. (2003). Minireview Nitrogenase gene diversity and microbial community structure: a cross-system comparison. *Environ. Microbiol.* 5, 539–554. doi: 10.1046/j.1462-2920.2003.00451.x

Zehr, J. P., and, Turner, P. J. (2001). "Nitrogen fixation: nitrogenase genes and gene expression," in *Methods in Marine Microbiology*, ed J. H. Paul (New York, NY: Academic Press), 271–286.

Zohary, T., Herut, B., Krom, M. D., Mantoura, R. F. C., Pitta, P., Psarra, S., et al. (2005). P-limited bacteria but N and P co-limited phytoplankton in the Eastern Mediterranean—a microcosm experiment. *Deep Sea Res. Part II Top. Stud. Oceanogr.* 52, 3011–3023. doi: 10.1016/j.dsr2.2005.08.011

Conflict of Interest Statement: The authors declare that the research was conducted in the absence of any commercial or financial relationships that could be construed as a potential conflict of interest.

frontiers in Marine Science

ORIGINAL RESEARCH
published: 14 September 2016
doi: 10.3389/fmars.2016.00170

Shifts in Microbial Community Structure and Activity in the Ultra-Oligotrophic Eastern Mediterranean Sea Driven by the Deposition of Saharan Dust and European Aerosols

*Cui Guo[1], Xiaomin Xia[1], Paraskevi Pitta[2], Barak Herut[3], Eyal Rahav[3], Ilana Berman-Frank[4], Antonia Giannakourou[5], Anastasia Tsiola[2], Tatiana M. Tsagaraki[2] and Hongbin Liu[1]**

[1] Division of Life Science, Hong Kong University of Science and Technology, Hong Kong, China, [2] Hellenic Centre for Marine Research, Institute of Oceanography, Heraklion, Greece, [3] Israel Oceanographic and Limnological Research, National Institute of Oceanography, Haifa, Israel, [4] Mina and Everard Goodman Faculty of Life Sciences, Bar-Ilan University, Ramat Gan, Israel, [5] Hellenic Centre for Marine Research, Institute of Oceanography, Anavyssos, Greece

OPEN ACCESS

Edited by:
Christos Dimitrios Arvanitidis, Hellenic Centre for Marine Research, Greece

Reviewed by:
Gordon T. Taylor, Stony Brook University, USA
Stephen Techtmann, Michigan Technological University, USA

***Correspondence:**
Hongbin Liu
liuhb@ust.hk

Specialty section:
This article was submitted to Marine Ecosystem Ecology, a section of the journal Frontiers in Marine Science

Received: 20 May 2016
Accepted: 30 August 2016
Published: 14 September 2016

Citation:
Guo C, Xia X, Pitta P, Herut B, Rahav E, Berman-Frank I, Giannakourou A, Tsiola A, Tsagaraki TM and Liu H (2016) Shifts in Microbial Community Structure and Activity in the Ultra-Oligotrophic Eastern Mediterranean Sea Driven by the Deposition of Saharan Dust and European Aerosols. Front. Mar. Sci. 3:170. doi: 10.3389/fmars.2016.00170

The atmospheric deposition of gases and particulates from the Sahara Desert and European landmass is an important source of nutrients for the Mediterranean Sea. In this study, we investigated how such atmospheric input might affect bacterial metabolic activities and community dynamics in the ultra-oligotrophic Eastern Mediterranean Sea. Thus, a mesocosm simulation experiment was conducted using "pure" Saharan dust (SD) and mixed aerosols (A, polluted and desert origin). The cell specific bacterial production (BP) was stimulated soon after the addition of SD and A, with a higher degree of stimulation being observed in the activity of *Alphaproteobacteria* than in *Gammaproteobacteria,* and this lead to significant increases in community BP. Subsequently, a shift between these two dominating classes was observed (such that the proportion of *Gammaproteobacteria* increased while that of *Alphaproteobacteria* decreased), along with significant increases in bacterial abundance and chlorophyll *a* concentration. After a few days, although the abundance of bacteria was still significantly higher in the SD- or A-treated groups, differences in the active community composition between the treatment and control groups were reduced. The altered activity of the two dominating *Proteobacteria* classes observed, might reflect their different strategies in responding to external nutrient input: with *Alphaproteobacteria* being more responsive to the direct dust input, whereas *Gammaproteobacteria* seemed to benefit more from the increase in phytoplankton biomass. In addition, the input of A had a stronger immediate effect and longer lasting influence on changing the active bacterial community

composition than did that of SD. Our findings show that episodic atmospheric deposition events might affect the microbial community with regards to their abundance, activity and composition over a short period of time, and thus regulate the function of the microbial community and carbon cycling in oligotrophic waters.

Keywords: 16s rRNA, pyrosequencing, saharan dust, atmospheric deposition, bacterial community structure, bacterial production

INTRODUCTION

The Mediterranean Sea (and particularly the eastern basin of the sea), is one of the most oligotrophic bodies of water in the world and is known as a low-nutrient-low-chlorophyll (LNLC) system with the biological production limited by phosphate (Krom et al., 1991; Pitta et al., 2005; Thingstad et al., 2005). However, the Mediterranean region receives a significant amount of aeolian material deposition, including both strong pulses of mineral dust and continuous deposition of anthropogenic aerosols (Guerzoni et al., 1999; Koçak et al., 2005). Each year, a high flux of dust from the Sahara, which is known to contain variable amounts of inorganic nutrients (especially phosphorus), is transported northeast to the adjacent Mediterranean Sea, with the highest loading being observed in the central and eastern basins during the spring (Moulin et al., 1997; Herut et al., 1999, 2002). The Mediterranean Sea also continually receives polluted air masses from populated areas of Europe; these contain high concentrations of nitrate and nitrite (NO_x) as well as NH_3 (Herut et al., 1999; Markaki et al., 2010). The ultra-oligotrophic conditions and high dust input make the Mediterranean Sea an ideal place to study the biogeochemical effects of atmospheric deposition.

Bacteria drive a wide range of biogeochemical processes that are important for the carbon and nutrient cycles in the ocean (Azam et al., 1983). They are an especially important component of oligotrophic ecosystems in which carbon flows mainly through the microbial food web. In ultra-oligotrophic systems, such as the Eastern Mediterranean Sea, bacterial growth is severely constrained by the bioavailable nutrients. Therefore, dust might be an important source of nutrients, which can strongly stimulate bacterial growth and significantly change bacterial assemblages. Indeed, in some cases, the bacterial community might be more responsive than large phytoplankton to dust due to their superior ability of taking up nutrients in oligotrophic waters (Pulido-Villena et al., 2008; Marañón et al., 2010). Several studies have been conducted to assess the effect of Saharan dust or European aerosols on the biogeochemical processes in the eastern Mediterranean (Herut et al., 2005), the western Mediterranean (Bonnet et al., 2005; Pulido-Villena et al., 2008; Lekunberri et al., 2010; Laghdass et al., 2011; Romero et al., 2011), and the Atlantic Ocean (Blain et al., 2004; Mills et al., 2004; Marañón et al., 2010). For example, previous dust addition experiments showed either increased (Herut et al., 2005; Pulido-Villena et al., 2008; Reche et al., 2009; Lekunberri et al., 2010), or unchanged bacterial abundance (Marañón et al., 2010; Laghdass et al., 2011) after the addition of Saharan dust. On the other hand, the stimulation of bacterial production (BP) was observed by almost all the studies that measured this parameter (Herut et al., 2005; Reche et al., 2009; Lekunberri et al., 2010; Marañón et al., 2010). Molecular techniques, such as denaturing gradient gel electrophoresis (DGGE) and fluorescence *in situ* hybridization (FISH), have been used to investigate the effect of Saharan dust on the composition of bacterial communities (Reche et al., 2009; Lekunberri et al., 2010; Marañón et al., 2010; Laghdass et al., 2011). The results to date, are inconclusive, as apparent changes in the bacterial assemblages were observed in some studies (Hill et al., 2010; Marañón et al., 2010; Laghdass et al., 2011), but in others, no direct effect of dust on bacterial community composition was demonstrated (Reche et al., 2009). However, there are several caveats and shortfalls in the above mentioned studies. First, few of the studies mimicked the scenario of a real natural dust deposition process from the perspective of the dust type (e.g., dust analog vs. "real" dust), the amendment concentration and the affecting season. Second, the response of active bacterial communities to atmospheric input was not well documented; for example, a time series investigation and high taxonomic resolution were lacking.

In this study, a mesocosm experiment was conducted by seeding natural Saharan dust (SD) and mixed aerosol (A) to investigate if the frequently occurring atmospheric deposition events might influence the activity and composition of microbes in the LNLC waters of the Eastern Mediterranean. In order to identify the composition of the active community alone, i.e., including the metabolically active and growing taxa, without interference from the senescent members of the community, we conducted phylogenetic profiling that was based solely on expressed 16S rRNA transcripts derived from cDNA, rather than on the more traditional 16S rRNA genes that may or may not be expressed. By evaluating the bacterial community at both the physiological and molecular levels, we aimed to answer the following questions: (1) Is there a fluctuation in the activities of different bacterial groups following input of SD or A? (2) Are there any differences between the effects induced by SD or A? (3) Is there any interaction between bacterial abundance, production, and active community composition in response to SD or A deposition? (4) Do heterotrophic bacteria respond directly to the addition of dust or do they respond to an increase in the activity of phytoplankton, (or do they respond to both)?

METHODS

Mesocosm Experiment Setup

Surface seawater was pumped from a depth of 10 m using a submersible centrifugal water pump into acid-cleaned high-density polyethylene (HDPE) containers at a station about 5 nautical miles north of Heraklion (Crete, Greece, 35° 24.957 N, 25° 14.441 E) in the Eastern Mediterranean Sea (EMS)

on May 9–10 2012. After seawater collection, the containers were immediately transported to the Hellenic Centre for Marine Research (HCMR) where the seawater was evenly distributed among nine 2.8–3 m^3 mesocosms immersed in a large pool with water at an *in situ* temperature (19.5°C). Air bubbled through an airlift pipe gently mixed the water in the mesocosms. A transparent lid was used to protect the mesocosms from atmospheric aerosols and a layer of mesh was attached on the lid to mimic the light conditions at a 10 m-depth.

SD were collected from Heraklion and Sambas (Crete) as well as Beit Yannay (Isreal) during Saharan dust events, and A, which contained a natural mixture of desert dust and polluted European particles, were collected in Heraklion (Crete) and Haifa (Israel). The two amendment sources (i.e., SD and A) were added each to triplicate mesocosms at final concentrations of ∼1.6 and ∼1 mg L^{-1}, respectively (**Table 1**). Triplicate mixtures of SD/A with 0.2 μm-filtered seawater were prepared in the acid-washed 100 mL polyethylene bottles before the experiment, and each of the concentrated mixture was then poured into the corresponding mesocosm bag at the beginning of the experiment. Three unamended mesocosms were kept as controls (C). The detailed dust collection and experimental setup protocols have been described in Herut et al. (this issue).

The mesocosm experiment lasted for 9 days. The time of the SD/A addition was considered to be the first time point. After the addition of SD or A, samples were taken at 3 h and then daily (i.e., at day 1–9) throughout the course of the experiment.

Leachable Inorganic Nutrients

Leaching experiments were performed by two different methodologies using sterile surface seawater from different origins, in the nutrient laboratories of the Israel Oceanographic and Limnological Research (Haifa) (Herut et al., this issue) and at the University of Leeds (Krom et al., 2016).

Bacterial Production

BP was estimated by the ^{3}H-leucine method (Kirchman, 1993). For each mesocosm, duplicate SD, A and control samples were incubated with a mixture of L-[4,5 ^{3}H]-leucine and non-radioactive leucine to a final concentration of 20 nM. Samples were incubated in the dark, at the *in situ* temperature, after which they were fixed and treated following the micro-centrifugation protocol (Smith and Azam, 1992), as described in detail by Van Wambeke et al. (2008). In brief, incubations were terminated after 2 h by the addition of trichloroacetic acid (TCA), samples were then centrifuged at 16 000 × g and the resulting cell pellet was washed twice with 5% TCA and twice with 80% ethanol. Incorporation of ^{3}H-leucine into the TCA-insoluble fraction was measured by liquid scintillation counting after resuspension of the cell pellet in scintillation cocktail. Duplicate incubations had an analytical error <10%. The optimal incubation time was determined with a time series experiment (i.e., from 1 to 8 h). Concentration kinetics optimization was also performed to ensure that the bacterial growth was not limited by the concentration of leucine.

TABLE 1 | The concentration of Sahara dust (SD) and mixed aerosol (A) added to the mesocosms, and leachable nutrient concentrations (nM) derived from these amendments.

Addition	Concentration (mg L^{-1})	NO_3+NO_2 (nM)	PO_4 (nM)	[NO_3+NO_2]/PO_4
SD	1.6	36.8	3.9	9
A	1	54	3.0	18

The leachable nutrient concentrations were calculated by conducting a leaching experiment (Section "Leachable Inorganic Nutrients" in the Methods).

Prokaryotic Abundance

The abundance of bacteria and autotrophic cyanobacteria (mainly *Synechococcus* spp.) was obtained by flow cytometric analysis using a FACSCalibur cell analyser, equipped with an air-cooled laser at 488 nm and standard filters (Becton Dickinson). Milli-Q water was used as the sheath fluid. For bacterial counts, samples were run at high speed for 1 min, whereas for autotrophic cyanobacterial counts, samples were run for 3 min. The exact flow rate of the high-speed FACS system was measured on a daily basis, and the abundance was calculated using the acquired cell counts and the respective flow rate. All flow cytometry data were acquired with the Cell Quest software and then processed with the Paint-A-Gate software.

To determine the abundance of bacteria, samples were fixed and processed according to Marie et al. (1999). Briefly, fixation was achieved with 0.2 μm pre-filtered 25% glutaraldehyde, to a final concentration of 0.5%. Samples were then kept at 4°C for ∼20 min, after which they were deep frozen in liquid nitrogen and then stored at −80°C until enumeration. For the total bacteria counts, samples were thawed at room temperature and incubated with SYBR Green I nucleic acid dye, to a final concentration of 0.0025, for 10 min in the dark. When needed, samples were then diluted in Tris-EDTA buffer (TE, 10mM Tris and 1 mM EDTA, pH = 8), in order to achieve a rate between 100 and 700 events s^{-1}. TE was autoclaved and 0.2 μm filtered immediately prior to dilution. Autotrophic cyanobacteria were identified by their autofluoresence and counted directly without fixation or staining. The abundance of heterotrophic bacteria was calculated by deducting the abundance of the autotrophic cyanobacteria from that of total bacteria.

RNA Collection, Extraction, and cDNA Synthesis

RNA samples were collected at 3 h, day 2 (D2) and day 6 (D6) in all mesocosms. Nine to ten liters of seawater were filtered over a period of 40 min through GF/D glass microfiber filters (2.7 μm, Whatman International Ltd.) and 0.2 μm pore-sized polyethersulfone membrane filters (Supor-200, Pall Corp.), using a peristaltic pump. Filters were immediately immersed in RNA*later* (Ambion) in a 2 mL RNase-free tube and stored at −80°C.

Total RNA was extracted from the bacterial biomass between the 0.2 and 2.7 μm size fraction with the TRIzol plus RNA purification kit (Invitrogen, Carlsbad, CA). Before extraction with TRIzol reagent, the RNA*later* was removed from the filters according to the procedure described by Xu et al. (2013). The

filters containing bacterial biomass were incubated in 1 mL TRIzol reagent for 5 min at room temperature. The bacterial lysate was then shaken thoroughly for 15 s after adding 200 μL chloroform and incubated for 3 min again at room temperature. The filters and the undissolved cell debris were removed by centrifugation at 12,000 *g* for 15 min at 4°C and the supernatant containing RNA was transferred to a new RNA-free tube. An equal volume of 70% ethanol was mixed with the supernatant and the RNA was then purified and washed with the purification column and finally eluted in 50 μL elution buffer (Invitrogen, Carlsbad, CA). The extracted RNA concentration was measured on a NanoDrop 1000 Spectrophotometer (Thermo Scientific).

The purified RNA was reverse transcribed to cDNA using the SuperScript III first strand cDNA synthesis kit (Invitrogen, Carlsbad, CA). Prior to cDNA synthesis, DNase I (RNase free) was used to digest any residual DNA present in the RNA extracts. RNA of 8 μL was mixed with 1 μL random hexamer (50 ng μl^{-1}), and 1 μL deoxynucleoside triphosphate (10 mM). The mixture was incubated at 65°C for 5 min and then placed on ice for at least 1 min, after which 10 μL cDNA synthesis mix [2 μL RT buffer (10 ×), 4 μL $MgCl_2$ (25 mM), 2 μL dithiothreitol (0.1 M), 1 μL RNaseOUT (40 U μL^{-1}) and 1 μL SuperScript III reverse transcriptase (RT, 200U/μL)], was added to the tube. The RT-PCR conditions were 25°C for 10 min, followed by 50°C for 50 min and finally 85°C for 5 min to terminate the reaction. Residual RNA was removed by the addition of 2 U RNase H at 37°C for 20 min. The transcribed cDNA from triplicate mesocosms were mixed together.

16S rRNA Gene Amplification and 454 Pyrosequencing

Fragments of bacterial 16S rRNA gene were amplified with 454 fusion primers of 16S-341F (5′- adaptor+MID+CCTACGGGAGGCAGCAG-3′) and 16S-787R (5′-adaptor+CCTATCCCCTGTGTGCCTTGGCAGTC-3′), which target the V3–V4 region of the 16S rRNA gene. The PCR reaction was carried out in 50 μL master mix including 5 μL of 10 × buffer, 2 μL of $MgCl_2$ (25 mM), 4 μL of dNTPs (2.5 mM), 0.2 μL of Taq polymerase (5 U, Invitrogen, Carlsbad, CA), 1 μL of each primer (10 μM), 1 μL of DNA template and 35.8 μL water. The PCR fragments from different samples were identified by the 10-bp multiplex identifier (MID) tags assigned in the forward primers. The PCR for each sample was carried out in triplicate with the following thermal cycles: 95°C for 5 min, followed by 30 cycles of 95°C for 30 s, 55°C for 30 s, and 72°C for 40 s, and a final extension of 72°C for 7 min. The non-template and non-RT controls were always used as PCR negative controls to confirm that there was no contamination in the DNA templates or PCR reagents.

Triplicate PCR products were pooled and then gel-cut purified using the Gel Band Purification kit (GE Healthcare), as described by the manufacturer. The purified PCR products were quantified with the Quant-iT picoGreen dsDNA Assay Kit (Invitrogen, USA). An equal amount of each amplicon was mixed to prepare the amplicon library, and emPCR was performed to produce millions of identical copies of the 16S rRNA amplicon linked to each bead, according to the 454 Pyrosequencing manual (Roche, 454 Life Science). The DNA beads were deposited onto the PicoTiterPlate and sequenced on a GS Junior system according to the manufacturer's instructions (Roche, 454 Life Sciences).

Data Analysis

Sequence processing was performed using MOTHUR (http://www.mothur.org/wiki/) following the standard operating procedure described by Schloss et al. (2009). Low quality sequences tags were first removed to minimize the effect of random sequencing errors. Sequence denoising was carried out using the shhh.seqs command, with a sigma value of 0.01. We eliminated sequences that: (1) contained more than one ambiguous nucleotide (N) or more than 8 homopolymers; (2) were shorter than 300 bp; (3) did not match the primer at the beginning of the read; (4) contained chimeras (Edgar et al., 2011); or (5) were chloroplast-derived sequences. Sequences were classified using the greengenes database (http://greengenes.secondgenome.com/downloads), with a minimum threshold of 60%.

Sequences were clustered into Operational Taxonomic Units (OTUs) at cut-off values of 0.03. Sample coverage was calculated based on OTU assignment. Cluster analysis (based on Bray-Curtis similarity with a cut-off value of 0.03) and SIMPER analysis were performed with PRIMER5 (PRIMER-E Ltd, Plymouth).

RESULTS

Hydrographical Background and Response of Bacterial Abundance and Production

The seawater used to fill the mesocosms exhibited ultra-oligotrophic characteristics, with a total dissolved inorganic nitrogen (DIN) concentration of 301 nM, a phosphate concentration of 9 nM (M. Tsapakis et al., unpubl.), and a chlorophyll *a* concentration of 0.06 μg L^{-1} (Herut et al., this issue). The nutrients released to the seawater from the SD and A amendments are shown in **Table 1**. Overall, 1.6 mg L^{-1} of SD released 36.8 nM NO_3+NO_2 and 3.9 nM PO_4, whereas 1 mg L^{-1} of A released 54 nM NO_3+NO_2 and 3 nM PO_4 (**Table 1**). These additions resulted in a lower leachable N/P ratio in the SD when compared to the A (i.e., 9 vs. 18, respectively; **Table 1**).

The abundance of the autotrophic cyanobacteria *Synechococcus* ranged from 1.8 × 10^4 to 4.1 × 10^4 cells mL^{-1}, with the maximum abundance in the control and treatments occurring on D2 (**Figure 1A**). The largest relative increase in the treatments when compared with the control (=[treatment-control]/control × 100%) was ∼40% on D2-D3. Overall, the abundance of *Synechococcus* showed a relative increase of ∼15–40% after the addition of SD or A over the entire incubation period, except on D5 when a smaller increase of ∼6% in the SD treatment group was observed (**Figure 1A**).

The abundance of bacteria ranged from 2 × 10^5 to 5 × 10^5 cells mL^{-1} throughout the experiment, with maximum and minimum values observed on D1 and D5, respectively. There were significant increases of 31–75% in the treatment groups when compared with the controls throughout the incubation period (**Figure 1B**). In addition, high nucleic acid (HNA)

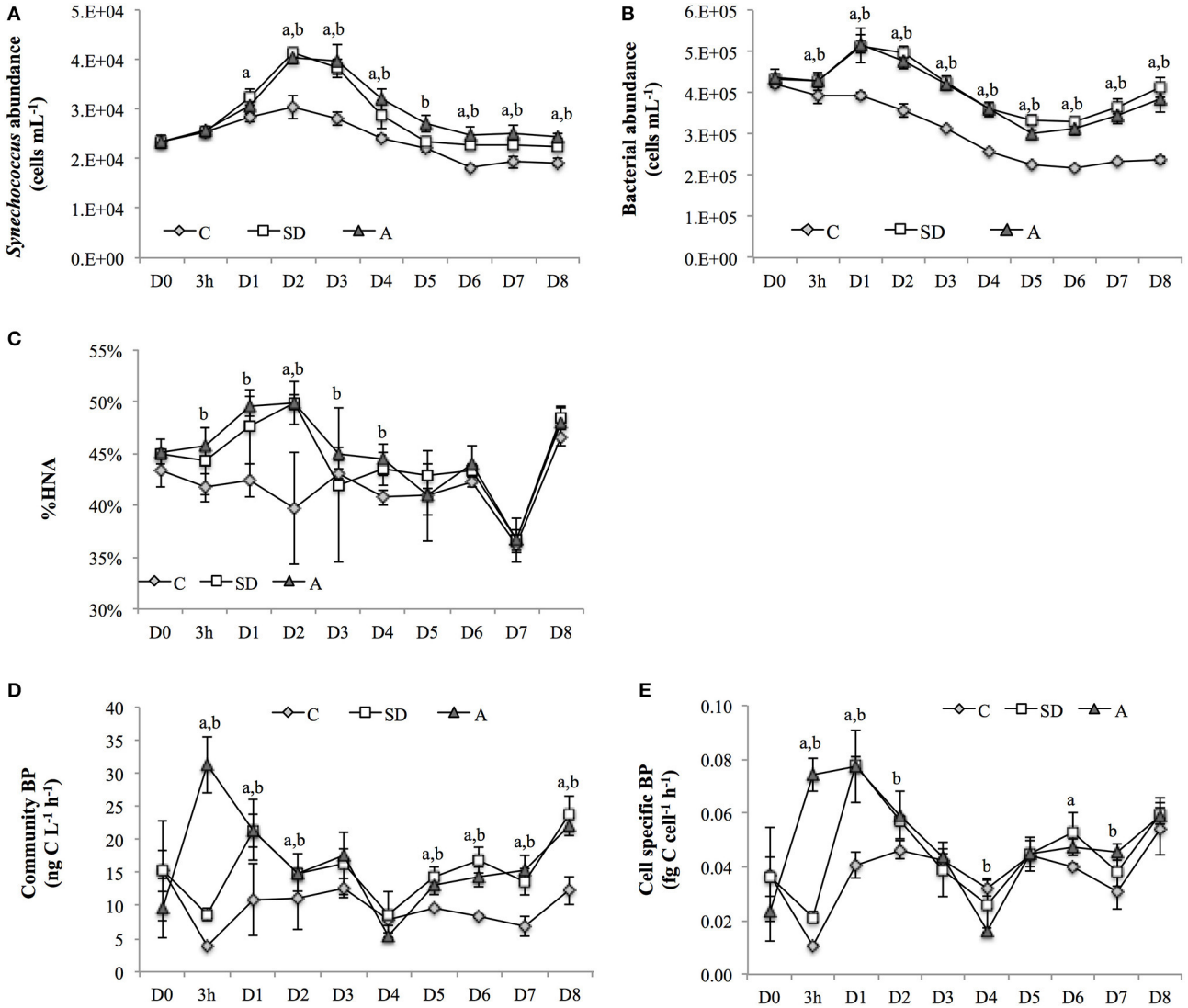

FIGURE 1 | (A) *Synechococcus* abundance, **(B)** bacterial abundance, **(C)** percentage of high nucleic acid bacteria in total bacterial community (HNA%), **(D)** community bacterial production (BP), and **(E)** cell specific BP in the control, and SD and A treated groups. Error bars represent the standard deviation of measurements. Letters "a" and "b" indicate statistically significant mean values ($p<0.05$) in the SD and A treatment groups, respectively, when compared with the corresponding controls (i.e., on the same day). It should be noted that the x-axis is not linearly scaled. SD, Sahara dust; A, mixed aerosol; C, control.

bacteria accounted for ∼45% of the total heterotrophic bacteria community on D0. The percentage of HNA bacteria then increased in both the SD and A mesocosms at 3h and reached the largest increase on D2 (**Figure 1C**).

The community BP was immediately stimulated at 3 h after SD and A addition, with relative increases of 154 and 663%, respectively being measured. The significant increases in community BP in the SD and A groups were observed from 3 h to D2 and from D5 to D8 (**Figure 1D**). A similar response was also observed for the cell specific BP (**Figure 1E**). The community BP was significantly and positively correlated with the total bacterial abundance, with a correlation coefficient of 0.671 ($p < 0.01$; **Table 2**). Moreover, the community BP showed a significant positive correlation with the HNA bacterial abundance, but exhibited no significant relationship with low nucleic acid (LNA) bacteria. Both community and cell specific BP were significantly and positively correlated with the percentage of HNA (**Table 2**).

Sequencing Statistics and Community Comparison

After removing the low-quality sequences, a total number of 113,204 high quality reads with an average length of ∼430 bp were generated for the nine samples. About 98–99% of the estimated richness was covered by the sequencing effort with a cutoff value set at 0.03.

According to the cluster analysis, the largest change in the active members of the bacterial community was observed at

3 h following SD and A amendment. The 3 h-SD and 3 h-A clustered together but were distant from the 3 h-C, which clustered with the D2-C. Similarities of 81.2% and 73.3% were calculated between each of the SD and A treatments and the control, respectively (**Figure 2**). On D2, the treatments were still distant from the control, with similarities of 79.7 and 81.9% being calculated between SD and the control, and A and control, respectively (**Figure 2**). On D6, the community differences between SD and control increased (88.5% similarity), whereas the similarity between A and the control remained at 80.9% (**Figure 2**).

Phylogenetic Identification and Key OTUs

The majority of the classified sequences were affiliated to bacterial phyla of *Proteobacteria*, *Cyanobacteria,* and *Bacteroidetes* (**Figure 3A**). 16S rRNA transcripts affiliated to *Proteobacteria* dominated all libraries, accounting for ∼80.3–91.8% of the total sequences, and the proportion only fluctuated slightly during the incubation, with a slight increase in the 3 h-SD group (88.7%) when compared with the 3 h-C group (83.7%); and a slight decrease in the D2-SD (82.2%) and D2-A (80.3%) groups when compared with the D2-C group (87.1%). The proportion of *Cyanobacteria* was ∼5.6–12.8% across the experiment, with higher values in the 3 h-A group (12.2%) than in the 3 h-C group (7.4%); and in the D2-SD (8.6%) and D2-A (12.8%) groups than in the D2-C group (5.8%).

TABLE 2 | Pearson correlations between the abundance of total bacteria, low nucleic acid (LNA) bacteria, high nucleic acid (HNA) bacteria, %HNA, and bacterial production (BP).

	Bacterial abundance	LNA abundance	HNA abundance	%HNA
Community BP	0.671**	0.539**	0.724**	0.561**
Cell specific BP		0.180	0.407**	0.437**

*N = 90; ** Correlation is significant at the 0.01 level.*

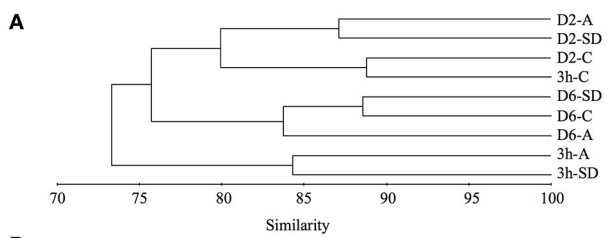

B

	3h		D2		D6	
	C	SD	C	SD	C	SD
SD	81.2%		79.7%		88.5%	
A	73.3%	84.3%	81.9%	87.1%	80.9%	86.6%

FIGURE 2 | (A) UPGMA trees generated by cluster analysis based on Bray-Curtis similarity with an OTU clustering cut-off value of 0.03, and **(B)** similarity shared between C, SD and A at each sampling time point. SD, Sahara dust; A, mixed aerosol; C, control.

16S rRNA transcripts belonging to *Bacteroidetes* accounted for 0.9–8.6% across the experiment. The percentage of these transcripts showed a decrease in both treatment groups at 3 h, but increases in the SD input group on D2 and increases in both treatment groups on D6. Within the *Proteobacteria* phylum, the *Alphaproteobacteria* and *Gammaproteobacteria* were the most abundant classes, representing respectively ∼28.8–51.3 and ∼18.9–42.7% of all the classified sequences (**Figure 3A**). Within the *Alphaproteobacteria*, families belonging to the *Rhodospirillales* (*Acetobacteraceae*, *Rhodospirillaceae*), *Rickettsiales* (*AEGEAN_112*, *Pelagibacteraceae*), *Rhizobiales* (*Cohaesibacteraceae*, *Hyphomicrobiaceae*, *Phyllobacteriaceae*), *Rhodobacterales* (*Rhodobacterales*), and *Kordiimonadales* (*Kordiimonadaceae*) orders comprised the major fractions (**Figure 3B**). *Gammaproteobacteria* were basically composed of 16S rRNA transcripts affiliated to the *Alteromonadales* and *Oceanospirillales* orders (**Figure 3C**).

Although the proportion of *Proteobacteria* did not show large changes in response to SD or A addition, the active members of the two dominant classes within the phylum exhibited clear shifts. At 3 h, the abundance of active *Alphaproteobacteria* exceeded that of *Gammaproteobacteria*. The percentage of 16S rRNA transcripts belonging to the *Alphaproteobacteria* was higher in the SD and A groups (with values of 47.0 and 51.4%, respectively) when compared with the control group (36.4%; **Figure 3A**). The proportion of active *Pelagibacteraceae* (the majority of which belonged to *Pelagibacter ubique*), as the most abundant family in the *Alphaproteobacteria* class, increased at 3 h in response to both SD and A when compared with the control (i.e., 11.4% in the control, 13.0% in SD, and 18.4% in A; **Figure 3B**). The share of another abundant family, *Rhodobacteraceae* (the majority of which belonged to *Phaeobacter*, *Roseovarius*, *Sediminimonas*, *Silicibacter,* and *Thalassococcus*), was also higher in the treatment groups at 3 h (i.e., 5.8% in the control, 7.7% in SD, and 8.0% in A; **Figure 3**B). In contrast, the relative abundance of 16S rRNA transcripts belonging to *Gammaproteobacteria* was lower in the treatment groups than in the control at 3 h (**Figure 3A**). *OM60,* which belongs to *Alteromonadales,* was the most abundant family of the *Gammaproteobacteria* and total *Proteobacteria*, and accounted for 11.3–32.8% of the total bacterial tags. At 3 h, the percentage of 16S rRNA transcripts of *OM60* decreased from 21.5% in the control group to 17.1 and 11.3% in the SD and A groups, respectively (**Figure 3C**). The changes in the percentages of the top 10 OTUs that contributed most to the community variation between samples were obtained by SIMPER analysis (**Figure 4**). The active community variations between the control and treatment groups at 3 h were mainly caused by a decreased expression of the 16S rRNA genes of *OM60* and *Flavobacteriaceae* and increased expression of the 16S rRNA genes of *Pelagibacteraceae, Synchococcaceae, HTCC2089,* and *Phaeobacter gallaeciensis* (**Figures 4A,B**). The difference between the active bacterial communities in the SD and A groups at 3 h was mainly due to different degrees of changes in *OM60*, *Synechococcaceae,* and *Pelagibacteraceae* (**Figure 4C**).

On D2, a reversal shift between the *Alpha-* and *Gamma-proteobacteria* was observed. The proportion of

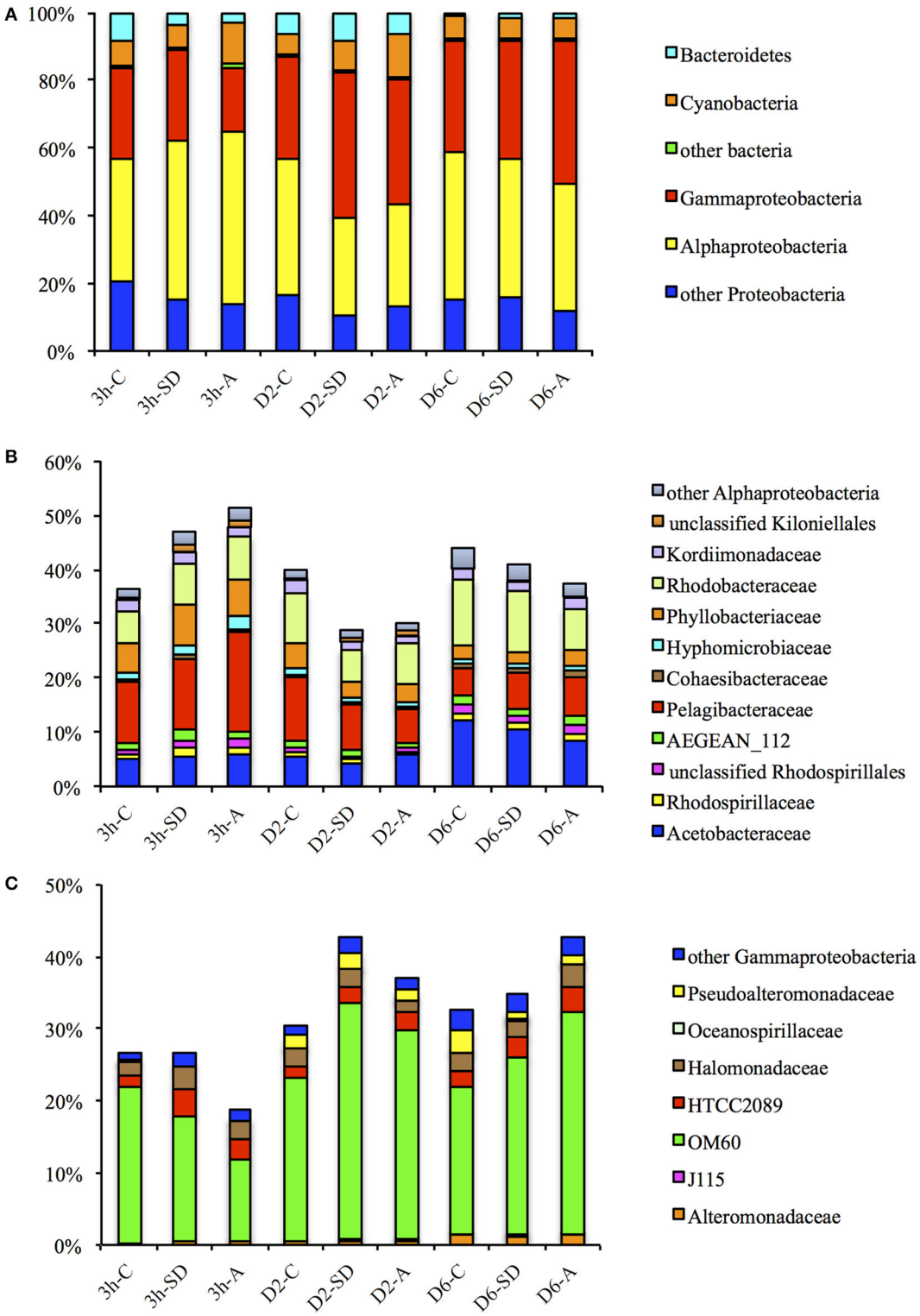

FIGURE 3 | Percentages of (A) bacterial phyla and proteobacterial classes, (B) Alpha- and (C) Gamma-proteobacterial families in total bacterial reads for different samples. SD: Sahara dust; A: mixed aerosol; C: control.

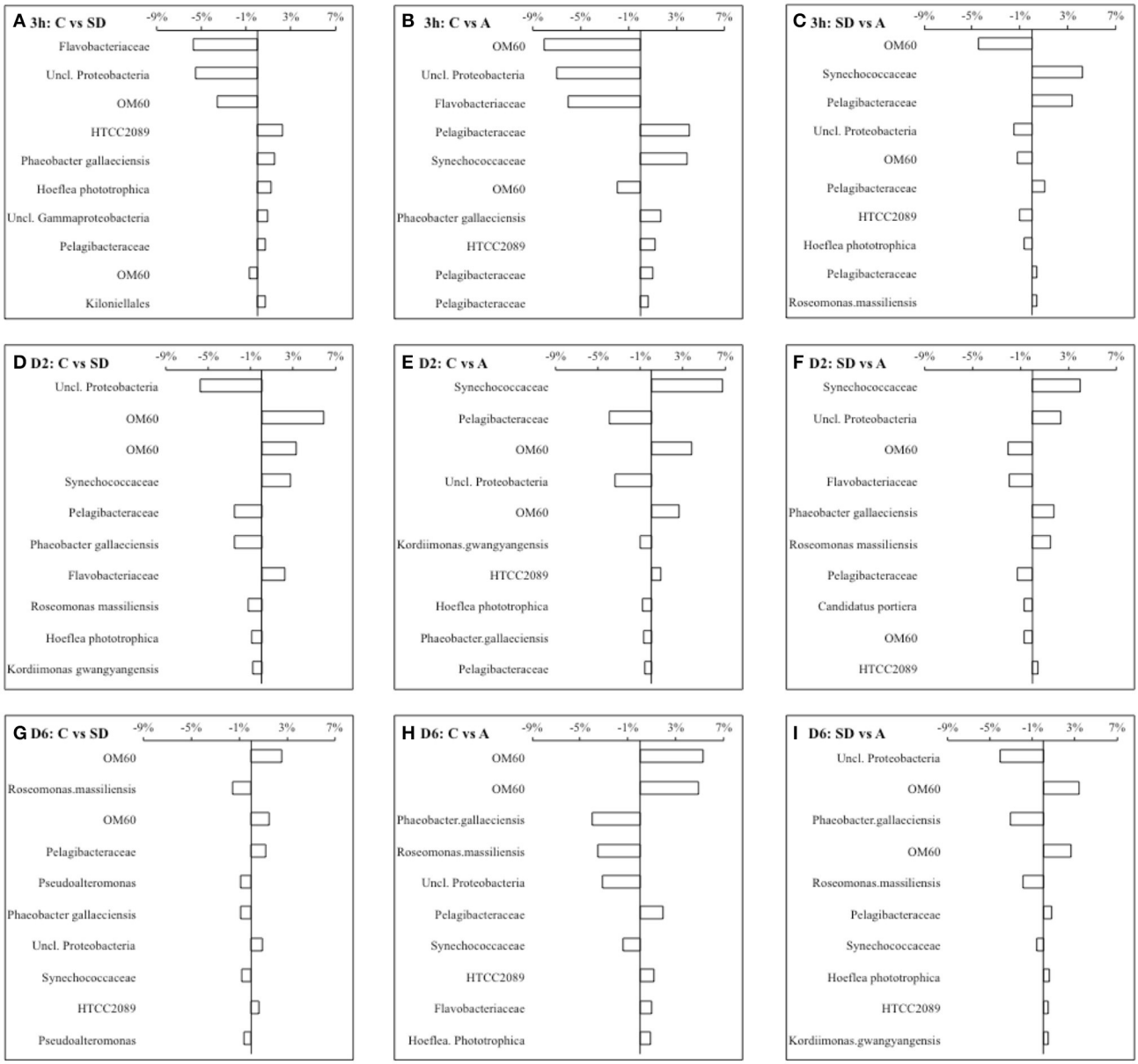

FIGURE 4 | Top-10 OTUs that contribute most to the variations among control, SD and A from SIMPER analysis. The columns are the relative changes (SD-C, A-C, and A-SD) in abundance (%) of each OTU at 3 h **(A–C)**, Day 2 **(D–F)** Day 2, and Day 6 **(G–I)**.

active *Alphaproteobacteria* was lower in both the treatment groups when compared with the control group (40.0% in control, 28.8% in SD and 30.1% in A; **Figure 3A**). Lower percentages of 16S rRNA transcripts in the treatment groups were also observed for both *Pelagibacteraceae* (10.9% in control, 7.5% in SD, 5.8% in A) and *Rhodobacteraceae* (8.9% in control, 6.0% in SD, 7.7% in A; **Figure 3B**). In contrast, the percentage of 16S rRNA transcripts belonging to the *Gammaproteobacteria* was higher in the SD and A groups (with values of 42.7 and 37.0%, respectively) when compared with the control group (30.6%), with most of the increase in transcripts being contributed by *OM60* (22.6% in control, 32.8% in SD, 29.2% in A; **Figure 3C**). In general, the increased 16S rRNA gene expression of *OM60* and *Synechococcaceae*, and decreased 16S rRNA gene expression of *Pelagibacteraceae*, contributed the most to the community change (**Figures 4D,E**). The difference between the bacterial communities in SD and A was mainly due to different degrees of changes in active *Synechococcaceae, OM60*, *Flavobacteriaceae, Phaeobacter gallaeciensis,* and *Roseomonas massiliensis* (**Figure 4F**).

On D6, the difference in the active communities between the treatments and control groups was smaller than that at 3h and D2. Shares of *Alphaproteobacteria* were lower in the treatment groups (41.0% in SD and 37.4% in A) than that

in the control (44.0%), whereas the opposite was observed for *Gammaproteobacteria* (32.5% in control, 35.0% in SD, 42.7% in A; **Figure 3A**). Increased 16S rRNA gene expression of *OM60* and *Pelagibacteraceae* and decreased 16S rRNA gene expression of *Phaeobacter gallaeciensis* and *Roseomonas massiliensis* contributed most to the community differences between the control and the treatment groups (**Figures 4G,H**), whereas the difference between bacterial communities in SD and A was mainly due to different degrees of changes in active *OM60, Phaeobacter gallaeciensis, Roseomonas massiliensis,* and *Pelagibacteraceae* (**Figure 4I**).

DISCUSSION

Only a small number of studies to date have addressed the effect of aerosol input on bacteria, and most of these describe the abundance and activity rather than the active community composition and the links between these various aspects. In addition, in these studies, traditional fingerprinting techniques were used to investigate changes in bacterial community composition, and thus the results obtained had relatively low taxonomic resolution (Reche et al., 2009; Lekunberri et al., 2010; Marañón et al., 2010; Laghdass et al., 2011; Guo et al., 2013). In contrast, the 454-pyrosequencing used in this study, allowed for more efficient and deep molecular sampling efforts of the microbial populations and with relatively high throughput (Sogin et al., 2006; Huse et al., 2008; Gilbert et al., 2009). Furthermore, we used the retrieved RNA samples as substitutes for metabolically active cells, and this allowed us to link the activity of different bacterial assemblages at molecular levels with actual bacterial metabolic rates at the community level. This gave us a better understanding of the physiological and ecological responses of bacteria to different atmospheric deposition events.

Quick and Active Response of Bacteria to Atmospheric Input

We observed very quick responses of bacteria to inputs of SD and A. An average N:P ratio of ∼34 was obtained in the ambient seawater used to fill the mesocosms; this was >2 times higher than the "typical" Redfield ratio of 16:1. The P turnover time at the beginning of our study was low (i.e., ∼1.9 h T. Tanaka et al. unpubl.), which further confirmed that the microbial community was initially P-starved. Under such nutrient-limited conditions, the bacterial community was likely to be strongly bottom-up regulated in the oligotrophic Mediterranean Sea (Pinhassi et al., 2006). Thus, any changes in the quantity or quality of external matter added will likely cause a significant change in the bacterial biomass, activity, and species composition, and consequently in carbon cycling throughout the microbial community. Moreover, in our study, microbes of <2 μm (including heterotrophic bacteria, autotrophic cyanobacteria, and picoeukaryotes), played a very active role in the P cycling in this area, accounting for >90% of the P uptake (T. Tanaka et al. unpubl.). Because of the smaller cell size and higher surface-to-volume ratios, bacteria can acquire inorganic nutrients more efficiently than phytoplankton when the ambient nutrient concentration is extremely low (Cotner and Biddanda, 2002; Joint et al., 2002). We showed that when compared with phytoplankton biomass (e.g., the concentration of total chlorophyll *a* and abundance of picophytoplankton), which started to increase from D1 in response to SD and A (Tsagaraki et al. this issue), bacteria responded more quickly in that their abundance started to increase at just 3 h following these two mesocosm amendments. At the same time, the BP increased significantly in the SD and A treatment groups, especially in the A group. This highlights the role of bacteria as active competitors and efficient utilizers for the limited amount of nutrients and dissolved organic matter available in this oligotrophic system. Furthermore, the fact that the shift in active bacterial community composition was immediate (i.e., observed as early as 3 h), which is before a significant increase in phytoplankton biomass occurred, also demonstrates the direct response of bacteria to SD and A input. Such increases in bacterial abundance and metabolic rates in response to dust from the Sahara have also been reported in the western Mediterranean Sea (Pulido-Villena et al., 2008), and in oligotrophic central Atlantic Ocean (Marañón et al., 2010).

The immediate response of bacterial activity to A was much stronger than it was to SD. This was indicated by the dramatically higher increase of BP (i.e., with a relative change of 661 and 118% in A and SD, respectively; **Figures 1C,D**), as well as the more substantial change of active bacterial community composition (i.e., exhibiting similarities of 73.3 and 81.2% in A and SD, respectively, when compared with the control; **Figures 2**, **3**). Furthermore, the addition of A seemed to have a longer lasting effect on shifting the microbial community composition, with similarities of 88.5 and 80.9% in the SD and A treatment groups, respectively, on D6 when compared with the control (**Figure 2B**). The different responses of the microbial communities to SD and A might be due to the different chemical compositions of the two atmospheric deposition sources, as the SD in general consisted of mineral particles, whereas A contained more anthropogenic components (such as pollution) and it might therefore contain a higher content of organic material. Indeed, several reports have described significantly different amounts of dissolved organic nitrogen and carbon associated with different sources of European atmospheric deposition and Sahara dust (Cornell et al., 1995; Pulido-Villena et al., 2008).

Changes in BP and HNA%

The BP might be directly stimulated by the nutrients released from the SD and A input. We observed a rapid increase in community BP, with relative increases of 118 and 663% following the addition SD and A, respectively, as quickly as 3 h following their addition. There was a similar level of increase in terms of cell specific BP (with relative increases of 100 and 598% in SD and A, respectively) but only a small increase in the bacterial abundance (with relative increases of 9% for both SD and A). Such decoupling between the BP and abundance suggests that the external dust and aerosol input directly stimulated the metabolic activity of bacterial cells, and that the degree of stimulation was different among the different bacterial groups. This was demonstrated by the strong increase in BP and the shift in active community composition at 3 h. On the other hand, on D2, the

relative increase in the community BP (i.e., 73% in SD and 74% in A), was much higher than that of the cell specific BP (with values of 24 and 28% for SD and A, respectively), when compared with those measured in the control mesocosms. At the same time, significant increases of bacterial abundance (with values of 40 and 34% increase in SD and A, respectively, as compared with that in control) were observed. Therefore, the stimulation of community BP on D2 appears to be largely due to the increase of bacterial abundance.

HNA bacteria might also play an important role in BP enhancement. The nucleic acid content of bacterial cells has been suggested to be a good indicator of bacterial metabolic activity, as HNA bacteria were observed to be responsible for the majority of the total BP (Lebaron et al., 2001). In general, the percentage of HNA cells relative to the total bacterial abundance (i.e., %HNA), is considered to be related to variables that track the productivity index of the ecosystem, such as chlorophyll stocks or bacterial production (Corzo et al., 2005; Morán X. A. G. et al., 2007). Interestingly, we observed a significant positive correlation between the %HNA and BP (**Table 2**). This, together with the significant positive correlation between cell specific BP and HNA bacterial abundance, and the lack of correlation between the abundance of LNA bacteria and the cell specific activity, indicate the importance of HNA bacteria in contributing to the community BP. However, the specific activities of HNA cells vary significantly among bacterial species (Lebaron et al., 2001). Therefore, detailed community composition data is still needed to explain the response of bacterial activity to nutrient input during a dust event.

The Different Responses of the Major Bacterial Groups to Atmospheric Input

Our data indicate that the major components of bacterial communities in the Eastern Mediterranean Sea respond differently to a nutrient pulse deposited via the atmosphere, resulting in clear shifts in the composition of the active bacteria community. Indeed, in response to SD or A, *Alphaproteobacteria* exhibited an initial more rapid expression of 16S rRNA genes, which was observed at 3 h, when compared to *Gammaproteobacteria*. At D2, however, the expression of the 16S rRNA genes in *Gammaproteobacteria* increased, whereas that of *Alphaproteobacteria* decreased. Such changes in the levels of the dominant bacterial groups in response to SD and A indicate the heterogeneity of nutrient acquisition abilities among the different bacterial taxa, which are likely due to their different cellular demands and metabolism strategies. Our data, which are based on quantifying 16S rRNA gene transcripts, are not consistent with those reported by Fodelianakis et al. (2014), who showed only a minimal effect on the structure of the bacterioplankton community following the addition of P, based on the 16S rRNA gene, although an increase in bacterial abundance and production was measured, at least during the first 72 h of a mesocosm experiment conducted in the same Eastern Mediterranean environment. The differences observed between our results and those reported previously (Fodelianakis et al., 2014), indicate that dust-associated nutrients other than P might play a more important role in regulating the bacterial composition. Our results also highlight the importance of using RNA-based methods rather than DNA-based approaches to study the effect of dust-associated nutrients on the active bacterial community. Indeed, to our knowledge, we are the first to test the immediate effect (i.e., within just a few hours) of adding dust-based nutrients on the composition of the active bacterial community based on expression of the 16S rRNA genes.

We showed that Alphaproteobacteria, dominated by Pelagibacteraceae (mostly Pelagibacter ubique, an abundant member of the SAR11 clade), Rhodobacteraceae (mainly Phaeobacter gallaeciensis, which belongs to the Roseobacter clade), Phyllobacteriaceae (mostly Hoeflea phototrophica), and Acetobacteriaceae, exhibited increased activity at 3 h, suggesting their ability to respond quickly to the SD- and A-derived inorganic and organic nutrients. It has been reported that SAR11 is the most abundant bacterial group in the ocean, and has the smallest "streamlined" genome known for a free-living microorganism, which enables it to survive in nutrient-limited waters (Morris et al., 2002; Giovannoni et al., 2005). As SAR11 bacteria have high-affinity nutrient acquisition systems, low ambient levels of substrates appear to represent a competitive advantage for them (Alonso and Pernthaler, 2006). Our data demonstrated that 3 h following the addition of A, there was a major increase in BP, and this was accompanied by an increased expression of the 16S rRNA gene of Pelagibacteraceae that accounted for ∼11.5% of the active composition difference when comparing the effect of the addition of SD and A (SIMPER analysis, **Figure 4**). We speculate that the increased proportion of SAR11 might make an important early contribution to the community BP enhancement. On D2, however, the proportion of SAR11 in the bacterial communities of SD or A amended mesocosms decreased. This is consistent with previous studies, which also showed that nutrient or dust enrichment had a negative effect on SAR11 after a 1-day incubation (Teira et al., 2008; Hill et al., 2010; Marañón et al., 2010). The cause for such a switch might be that opportunists, such as Gammaproteobacteria, with a larger cell size and higher growth rate, out-compete SAR11 bacteria and maybe other Alphaproteobacteria groups too, when the levels of phytoplankton begin to increase (Simu and Hagstrom, 2004; Teira et al., 2008).

The second most abundant *Alphaproteobacteria* we found was *Roseobacter,* which increased its expression of the 16S rRNA gene within the first 3 h of the mesocosm experiment. *Roseobacter* has been reported to respond positively to both organic and inorganic nutrients (Teira et al., 2010), and analysis of the genomes of this clade suggests that members of the group have multiple mechanisms for sensing and reacting to their environment while acquiring diverse substrates and nutrients for growth (Moran M. A. et al., 2007). Previous nutrient manipulation experiments have also demonstrated the high ability of *Roseobacter* to adapt to nutrient addition; for example, the proportion of this clade increased after aerosol addition in the South China Sea (Guo et al., 2013). However, in our current study, the clade did not seem to be a successful competitor in response to the addition of SD at D2 and D6, when compared with *Gammaproteobacteria*. Protist grazing and/or viral attack might contribute to a decrease in the proportion of *Roseobacter* (Sherr et al., 1992). In addition, different types of bacteria within this clade are known to have

diverse life strategies, and for the new species in the clade that are still being identified, the ecological niches and physiological traits are as yet to be characterized.

We showed that *Gammaproteobacteira* and *Bacteroidetes* have different responses than *Alphaproteobacteria*, due to their different life strategies. In contrast to the rapid response of *Alphaproteobacteria* at 3 h, the responses of both *Gammaproteobacteria* and *Bacteroidetes* were lagging at 3h, but exceeded that of *Alphaproteobacteria* on D2 and D6. The up-regulation of protein synthesis that occurred in *Gammaproteobacteria* and *Bacteroidetes* was accompanied by a large increase in both bacterial and phytoplankton abundance. This occurred after D1, which indicates the competitiveness and high growth potential of these groups as well as their possible association with phytoplankton. Several other studies have regarded opportunistic strategy as a conserved feature for some important lineages of *Gammaproteobacteria*, which showed extraordinarily high growth potential and efficient carbon utilization after nutrient addition (Lebaron et al., 1999; Eilers et al., 2000; Pinhassi and Berman, 2003; Buchan et al., 2005; Fuhrman and Hagström, 2008). Many *Gammaproteobacteria* species have been observed to actively and positively respond to disturbance events and to organic nutrient addition associated with phytoplankton blooms, and they tend to dominate in nutrient-enriched seawater incubations (Hutchins et al., 2001; Pinhassi and Berman, 2003; Teira et al., 2010; Nogales et al., 2011). Furthermore, it has been suggested that *Gammaproteobacteria* could highly express transporter genes linked to broad carbon uptake patterns during an *in situ* phytoplankton bloom (Teeling et al., 2012). The *OM60* clade, which account for ∼60–80% of *Gammaproteobacteria* tags and ∼11–33% of the total bacterial tags in our study, showed a relatively large increase on D2 and D6. This clade has been reported to coincide with a high chlorophyll *a* concentration (Yan et al., 2009), and associate with phytoplankton species such as diatoms (Eilers et al., 2001) and *Synechococcus* (Alonso-Sáez et al., 2007). There is also molecular evidence indicating an apparent increase in the genes involved in polysaccharide degradation and various other biosynthetic processes at the transcriptional level in *OM60,* in the latter stages of incubation following the addition of organic nutrients (Sharma et al., 2013). This clade is known to include representatives of aerobic anoxygenic phototrophic (AAnP) bacteria that use light as an energy source (Fuchs et al., 2007; Yan et al., 2009), and they play an important role in marine carbon cycling (Kolber et al., 2001).

Bacteroidetes (or CFB; *Cytophaga–Flavobacteria–Bacteroides*), have also been reported to be especially relevant in the cycling of organic matter during phytoplankton blooms, when they likely profit from complex DOC (Pinhassi et al., 2004; Alderkamp et al., 2006; Teira et al., 2008). In addition, it has been reported that OTUs belonging to *Flavobacteria* contribute substantially to the incorporation of a *Synechococcus* exudate (Nelson and Carlson, 2012).

CONCLUSIONS

In this study, we used a mesocosm experimental approach to investigate the impact of Saharan dust and mixed European aerosols on microbial biomass, production and active community composition in the Eastern Mediterranean Sea. The patterns we observed can be summarized as follows: (1) Active bacterial community composition shifts were observed in response to the addition of SD and A, with an immediate response being observed in *Alphaproteobacteria* and a slower but longer lasting response occurring in *Gammaproteobacteria*. (2) A had a stronger immediate effect and longer lasting influence than SD in changing the composition of the active bacterial community. (3) The SD and A input directly stimulated the bacterial cell specific metabolic activity, as shown by the immediate increase of cell specific BP. In addition, the degree of stimulation was different among the different bacterial groups, as shown by the shift in active bacterial community composition at 3 h, which was revealed by the expressed 16S rRNA genes.

DATA ACCESSIBILITY

All the raw sequences obtained from this study have been deposited in the National Center for Biotechnology Information (NCBI) Sequence Read Archive (SRA) under accession number of SAMN03323713-SAMN03323719.

AUTHOR CONTRIBUTIONS

CG designed and performed the experiments, analyzed data and wrote the paper; XX analyzed data and edited the paper; PP, BH, TT: designed the mesocosm experiment and edited the paper; ER, IB: helped during experimental sampling and edited the paper; AG, AT: performed flow cytometry and bacterial production analysis respectively and edited the paper; HL: designed the experiment, supervised the analysis and edited the paper.

ACKNOWLEDGMENTS

This study was funded by an EU project "MESOAQUA: Network of leading MESOcosm facilities to advance the studies of future AQUAtic ecosystems from the Arctic to the Mediterranean" through a grant to CG, BH, and HL. The authors wish to thank Dr. P. Divanach for his valuable advice on technical matters, Dr. M. Krom for his assistance in aerosol leaching experiments, G. Piperakis for his inspired technical assistance throughout the experiment, S. Zivanovic and E. Dafnomili for their assistance with the chemical analyses, D. Podaras and S. Diliberto for their assistance during the experiment and N. Sekeris for his help with constructions and ideas. The captain and the crew of the R/V Philia are also thanked for their assistance during the transportation of water from the sea to the mesocosms. Support from Hong Kong Research Grants Council via General Research Fund (GRF 661912 and 661813) is also acknowledged.

REFERENCES

Alderkamp, A.-C., Sintes, E., and Herndl, G. J. (2006). Abundance and activity of major groups of prokaryotic plankton in the coastal North Sea during spring and summer. *Aquat. Microb. Ecol.* 45, 237–246. doi: 10.3354/ame045237

Alonso, C., and Pernthaler, J. (2006). Roseobacter and SAR11 dominate microbial glucose uptake in coastal North Sea waters. *Environ. Microbiol.* 8, 2022–2030. doi: 10.1111/j.1462-2920.2006.01082.x

Alonso-Sáez, L., Balagué, V., Sà, E. L., Sánchez, O., González, J. M., Pinhassi, J., et al. (2007). Seasonality in bacterial diversity in north-west Mediterranean coastal waters: assessment through clone libraries, fingerprinting and FISH. *FEMS Microbiol. Ecol.* 60, 98–112. doi: 10.1111/j.1574-6941.2006.00276.x

Azam, F., Fenchel, T., Field, J. G., Gray, J. S., Meyer-Reil, L. A., and Thingstad, F. (1983). The ecological role of water-column microbes in the sea. *Mar. Ecol. Prog. Ser.* 1, 257–263. doi: 10.3354/meps010257

Blain, S., Guieu, C., Claustre, H., Leblanc, K., Moutin, T., Quéguiner, B., et al. (2004). Availability of iron and major nutrients for phytoplankton in the northeast Atlantic Ocean. *Limnol. Oceanogr.* 49, 2095–2104. doi: 10.4319/lo.2004.49.6.2095

Bonnet, S., Guieu, C., Chiaverini, J., Ras, J., and Stock, A. (2005). Effect of atmospheric nutrients on the autotrophic communities in a low nutrient, low chlorophyll system. *Limnol. Oceanogr.* 50, 1810–1819. doi: 10.4319/lo.2005.50.6.1810

Buchan, A., Gonzalez, J. M., and Moran, M. A. (2005). Overview of the Marine *Roseobacter* Lineage. *Appl. Environ. Microbiol.* 71, 5665–5677. doi: 10.1128/AEM.71.10.5665-5677.2005

Cornell, S., Rendell, A., and Jickells, T. (1995). Atmospheric inputs of dissolved organic nitrogen to the oceans. *Nature* 376, 243–246. doi: 10.1038/376243a0

Corzo, A., Rodríguez-Gálvez, S., Lubian, L., Sobrino, C., Sangrá, P., and Martínez, A. (2005). Antarctic marine bacterioplankton subpopulations discriminated by their apparent content of nucleic acids differ in their response to ecological factors. *Polar Biol.* 29, 27–39. doi: 10.1007/s00300-005-0032-2

Cotner, J. B., and Biddanda, B. A. (2002). Small players, large role: microbial influence on biogeochemical processes in pelagic aquatic ecosystems. *Ecosystems* 5, 105–121. doi: 10.1007/s10021-001-0059-3

Edgar, R. C., Haas, B. J., Clemente, J. C., Quince, C., and Knight, R. (2011). UCHIME improves sensitivity and speed of chimera detection. *Bioinformatics* 27, 2194–2200. doi: 10.1093/bioinformatics/btr381

Eilers, H., Pernthaler, J., and Amann, R. (2000). Succession of Pelagic Marine Bacteria during Enrichment: a Close Look at Cultivation-Induced Shifts. *Appl. Environ. Microbiol.* 66, 4634–4640. doi: 10.1128/AEM.66.11.4634-4640.2000

Eilers, H., Pernthaler, J., Peplies, J., Glockner, F. O., Gerdts, G., and Amann, R. (2001). Isolation of novel pelagic bacteria from the German Bight and their seasonal contributions to surface picoplankton. *Appl. Environ. Microbiol.* 67, 5134–5142. doi: 10.1128/AEM.67.11.5134-5142.2001

Fodelianakis, S., Pitta, P., Thingstad, T. F., Kasapidis, P., Karakassis, I., and Ladoukakis, E. D. (2014). Phosphate addition has minimal short-term effects on bacterioplankton community structure of the P-starved Eastern Mediterranean. *Aquat. Microb. Ecol.* 72, 98–104. doi: 10.3354/ame01693

Fuchs, B. M., Spring, S., Teeling, H., Quast, C., Wulf, J., Schattenhofer, M., et al. (2007). Characterization of a marine *gammaproteobacterium* capable of aerobic anoxygenic photosynthesis. *Proc. Natl. Acad. Sci. U.S.A.* 104, 2891–2896. doi: 10.1073/pnas.0608046104

Fuhrman, J. A., and Hagström, Å. (2008). "Bacterial and Archaeal Community Structure and its Patterns," in *Microbial Ecology of the Oceans, 2nd Edn*, ed D. L. Kirchman (Hoboken, NJ: John Wiley & Sons, Inc.). doi: 10.1002/9780470281840.ch3

Gilbert, J. A., Field, D., Swift, P., Newbold, L., Oliver, A., Smyth, T., et al. (2009). The seasonal structure of microbial communities in the Western English Channel. *Environ. Microbiol.* 11, 3132–3139. doi: 10.1111/j.1462-2920.2009.02017.x

Giovannoni, S. J., Tripp, H. J., Givan, S., Vergin, K. L., Baptista, D., Bibbs, L., et al. (2005). Genome streamlining in a Cosmopolitan Oceanic Bacterium. *Science* 309, 1242–1245. doi: 10.1126/science.1114057

Guerzoni, S., Chester, R., Dulac, F., Herut, B., Loÿe-Pilot, M.-D., Measures, C., et al. (1999). The role of atmospheric deposition in the biogeochemistry of the Mediterranean Sea. *Prog. Oceanogr.* 44, 147–190. doi: 10.1016/S0079-6611(99)00024-5

Guo, C., Jing, H., Kong, L., and Liu, H. (2013). Effect of East Asian aerosol enrichment on microbial community composition in the South China Sea. *J. Plankton Res.* 35, 485–503. doi: 10.1093/plankt/fbt002

Herut, B., Krom, M. D., Pan, G., and Mortimer, R. (1999). Atmospheric input of nitrogen and phosphorus to the Southeast Mediterranean Sources, fluxes, and possible impact. *Limnol. Oceanogr.* 44, 1683–1692. doi: 10.4319/lo.1999.44.7.1683

Herut, B., Collier, R., and Krom, M. D. (2002). The role of dust in supplying nitrogen and phosphorus to the Southeast Mediterranean. *Limnol. Oceanogr.* 47, 870–878. doi: 10.4319/lo.2002.47.3.0870

Herut, B., Zohary, T., Krom, M. D., Mantoura, R. F. C., Pitta, P., Psarra, S., et al. (2005). Response of East Mediterranean surface water to Saharan dust: On-board microcosm experiment and field observations. *Deep Sea Res. II* 52, 3024–3040. doi: 10.1016/j.dsr2.2005.09.003

Hill, P. G., Zubkov, M. V., and Purdie, D. A. (2010). Differential responses of *Prochlorococcus* and *SAR11*-dominated bacterioplankton groups to atmospheric dust inputs in the tropical Northeast Atlantic Ocean. *FEMS Microbiol. Lett.* 306, 82–89. doi: 10.1111/j.1574-6968.2010.01940.x

Huse, S. M., Dethlefsen, L., Huber, J. A., Welch, D. M., Relman, D. A., and Sogin, M. (2008). Exploring Microbial Diversity and Taxonomy Using SSU rRNA Hypervariable Tag Sequencing. *PLoS Genet.* 4:e1000255. doi: 10.1371/journal.pgen.1000255

Hutchins, D. A., Campbell, B. J., and Cottrell, M. T. (2001). Response of marine bacterial community composition to iron additions in three iron-limited regimes. *Limnol. Oceanogr.* 46, 1535–1545. doi: 10.4319/lo.2001.46.6.1535

Joint, I., Henriksen, P., Fonnes, G. A., Bourne, D., Thingstad, T. F., and Riemann, B. (2002). Competition for inorganic nutrients between phytoplankton and bacterioplankton in nutrient manipulated mesocosms. *Aquat. Microb. Ecol.* 29, 145–159. doi: 10.3354/ame029145

Koçak, M., Kubilay, N., Herut, B., and Nimmo, M. (2005). Dry atmospheric fluxes of trace metals (Al, Fe, Mn, Pb, Cd, Zn, Cu) over the Levantine Basin: a refined assessment. *Atmos. Environ.* 39, 7330–7341. doi: 10.1016/j.atmosenv.2005.09.010

Kolber, Z. S., Plumley, F. G., Lang, A. S., Beatty, J. T., Blankenship, R. E., VanDover, C. L., et al. (2001). Contribution of aerobic photoheterotrophic bacteria to the carbon cycle in the ocean. *Science* 292, 2492–2495. doi: 10.1126/science.1059707

Krom, M. D., Kress, N., Brenner, S., and Gordon, L. I. (1991). Phosphorus limitation of primary productivity in the eastern Mediterranean Sea. *Limnol. Oceanogr.* 36, 424–432. doi: 10.4319/lo.1991.36.3.0424

Krom, M. D., Shi, Z., Stockdale, A., Berman-Frank, I., Giannakourou, A., Herut, B., et al. (2016). Response of the Eastern Mediterranean microbial ecosystem to dust and dust affected by acid processing in the atmosphere. *Front. Mar. Sci.* 3:133. doi: 10.3389/fmars.2016.00133

Kirchman, D. L. (1993). "Leucine incorporation as a measure of biomass production by heterotrophic bacteria," in: *Handbook of Methods in Aquatic Microbial Ecology*, eds P. F. Kemp, J. J. Cole, B. F. Sherr, and E. B. Sherr (Lewis, IA: CRC Press), 509–512.

Laghdass, M., Blain, S., Besseling, M., Catala, P., Guieu, C., and Obernosterer, I. (2011). Effects of Saharan dust on the microbial community during a large in situ mesocosm experiment in the NW Mediterranean Sea. *Aquat. Microb. Ecol.* 62, 201–213. doi: 10.3354/ame01466

Lebaron, P., Servais, P., Agogue, H., Courties, C., and Joux, F. (2001). Does the high nucleic acid content of individual bacterial cells allow us to discriminate between active cells and inactive cells in aquatic systems? *Appl. Environ. Microbiol.* 67, 1775–1782. doi: 10.1128/AEM.67.4.1775-1782.2001

Lebaron, P., Servais, P., Troussellier, M., Courties, C., Vives-rego, J., Muyzer, G., et al. (1999). Chancres in bacterial community structure in seawater mesocosms differing in their nutrient status. *Aquat. Microbiol. Ecol.* 19, 255–267. doi: 10.3354/ame019255

Lekunberri, I., Lefort, T., Romero, E., Vazquez-Dominguez, E., Romera-Castillo, C., Marrase, C., et al. (2010). Effects of a dust deposition event on coastal marine microbial abundance and activity, bacterial community structure and ecosystem function. *J. Plankton Res.* 32, 381–396. doi: 10.1093/plankt/fbp137

Marañón, E., Fernández, A., Mouriño-Carballido, B., Martínez-García, S., Teira, E., Cermeño, P., et al. (2010). Degree of oligotrophy controls the response of microbial plankton to Saharan dust. *Limnol. Oceanogr.* 55, 2339–2352. doi: 10.4319/lo.2010.55.6.2339

Marie, D., Partensky, F., Vaulot, D., and Brussaard, C. (1999). Enumeration of phytoplankton, bacteria, and viruses in marine samples. *Curr. Protoc. Cytometry* Chapter 11:Unit 11.11. doi: 10.1002/0471142956.cy1111s10

Markaki, Z., Loÿe-Pilot, M. D., Violaki, K., Benyahya, L., and Mihalopoulos, N. (2010). Variability of atmospheric deposition of dissolved nitrogen and phosphorus in the Mediterranean and possible link to the anomalous seawater N/P ratio. *Mar. Chem.* 120, 187–194. doi: 10.1016/j.marchem.2008.10.005

Mills, M. M., Ridame, C., Davey, M., Roche, J. L., and Geider, R. J. (2004). Iron and phosphorus co-limit nitrogen fixation in the eastern tropical North Atlantic. *Nature* 429, 292–294. doi: 10.1038/nature02550

Moran, M. A., Belas, R., Schell, M. A., Gonzalez, J. M., Sun, F., Sun, S., et al. (2007). Ecological Genomics of Marine *Roseobacters. Appl. Environ. Microbiol.* 73, 4559–4569. doi: 10.1128/AEM.02580-06

Morán, X. A. G., Bode, A., Suárez, L. A., and Nogueira, E. (2007). Assessing the relevance of nucleic acid content as an indicator of marine bacterial activity. *Aquat. Microbiol. Ecol.* 46, 141–152. doi: 10.3354/ame046141

Morris, R. M., Rappe, M. S., Connon, S. A., Vergin, K. L., Siebold, W. A., Carlson, C. A., et al. (2002). SAR11 clade dominates ocean surface bacterioplankton communities. *Nature* 420, 806–810. doi: 10.1038/nature01240

Moulin, C., Lambert, C. E., Dulac, F., and Dayan, U. (1997). Control of atmospheric export of dust from North Africa by the North Atlantic Oscillation. *Nature* 387, 691–694. doi: 10.1038/42679

Nelson, C. E., and Carlson, C. A. (2012). Tracking differential incorporation of dissolved organic carbon types among diverse lineages of Sargasso Sea bacterioplankton. *Environ. Microbiol.* 14, 1500–1516. doi: 10.1111/j.1462-2920.2012.02738.x

Nogales, B., Lanfranconi, M. P., Piña-Villalonga, J. M., and Bosch, R. (2011). Anthropogenic perturbations in marine microbial communities. *FEMS Microbiol. Rev.* 35, 275–298. doi: 10.1111/j.1574-6976.2010.00248.x

Pinhassi, J., and Berman, T. (2003). Differential growth response of colony-forming α- and γ-*proteobacteria* in dilution culture and nutrient addition experiments from Lake Kinneret (Israel), the Eastern Mediterranean Sea, and the Gulf of Eilat. *Appl. Environ. Microbiol.* 69, 199–211. doi: 10.1128/AEM.69.1.199-211.2003

Pinhassi, J., Sala, M. M., Havskum, H., Peters, F., Guadayol, Ò., Malits, A., et al. (2004). Changes in bacterioplankton composition under different phytoplankton regimens. *Appl. Environ. Microbiol.* 70, 6753–6766. doi: 10.1128/AEM.70.11.6753-6766.2004

Pinhassi, J., Gómez-Consarnau, L., Alonso-Sáez, L., Sala, M. M., Vidal, M., Pedrós-Alió, C., et al. (2006). Seasonal changes in bacterioplankton nutrient imitation and their effects on bacterial community composition in the NW Mediterranean Sea. *Aquat. Microbiol. Ecol.* 44, 241–252. doi: 10.3354/ame044241

Pitta, P., Stambler, N., Tanaka, T., Zohary, T., Tselepides, A., and Rassoulzadegan, F. (2005). Biological response to P addition in the Eastern Mediterranean Sea. The microbial race against time. *Deep Sea Res. Part II: Top. Stud. in Oceanogr.* 52, 2961–2974. doi: 10.1016/j.dsr2.2005.08.012

Pulido-Villena, E., Wagener, T., and Guieu, C. (2008). Bacterial response to dust pulses in the western Mediterranean: Implications for carbon cycling in the oligotrophic ocean. *Global Biogeochem. Cycles* 22, GB1020. doi: 10.1029/2007gb003091

Reche, I., Ortega-Retuerta, E., Romera, O., Pulido-Villena, E., Morales-Baquero, R., and Casamayord, E. O. (2009). Effect of Saharan dust inputs on bacterial activity and community composition in Mediterranean lakes and reservoirs. *Limnol. Oceanogr.* 54, 869–879. doi: 10.4319/lo.2009.54.3.0869

Romero, E., Peters, F., Marrasé, C., Guadayol, Ò., Gasol, J. M., and Weinbauer, M. G. (2011). Coastal Mediterranean plankton stimulation dynamics through a dust storm event: an experimental simulation. *Estuar. Coast. Shelf Sci.* 93, 27–39. doi: 10.1016/j.ecss.2011.03.019

Schloss, P. D., Westcott, S. L., Ryabin, T., Hall, J. R., Hartmann, M., Hollister, E. B., et al. (2009). Introducing mothur: open-source, platform-independent, community-supported software for describing and comparing microbial communities. *Appl. Environ. Microbiol.* 75, 7537–7541. doi: 10.1128/AEM.01541-09

Sharma, A. K., Becker, J. W., Ottesen, E. A., Bryant, J. A., Duhamel, S., Karl, D. M., et al. (2013). Distinct dissolved organic matter sources induce rapid transcriptional responses in coexisting populations of *Prochlorococcus*, *Pelagibacter* and the *OM60* clade. *Environ. Microbiol.* 16, 2815–2830. doi: 10.1111/1462-2920.12254

Sherr, B. F., Sherr, E. B., and McDaniel, J. (1992). Effect of protistan grazing on the frequency of dividing cells in bacterioplankton assemblages. *Appl. Environ. Microbiol.* 58, 2381–2385.

Simu, K., and Hagstrom, A. (2004). Oligotrophic bacterioplankton with a novel single-cell life strategy. *Appl. Environ. Microbiol.* 70, 2445–2451. doi: 10.1128/AEM.70.4.2445-2451.2004

Smith, D. C., and Azam, F. (1992). A simple, economical method for measuring bacterial protein synthesis rates in seawater using 3H-leucine. *Mar. Microb. Food Webs* 6, 107–114.

Sogin, M. L., Morrison, H. G., Huber, J. A., Welch, D. M., Huse, S. M., Neal, P. R., et al. (2006). Microbial diversity in the deep sea and the underexplored "rare biosphere." *Proc. Natl. Acad. Sci. U.S.A.* 103, 12115–12120. doi: 10.1073/pnas.0605127103

Teeling, H., Fuchs, B. M., Becher, D., Klockow, C., Gardebrecht, A., Bennke, C. M., et al. (2012). Substrate-controlled succession of marine bacterioplankton populations induced by a phytoplankton bloom. *Science* 336, 608–611. doi: 10.1126/science.1218344

Teira, E., Gasol, J. M., Aranguren-Gassis, M., Fernández, A., González, J., Lekunberri, I., et al. (2008). Linkages between bacterioplankton community composition, heterotrophic carbon cycling and environmental conditions in a highly dynamic coastal ecosystem. *Environ. Microbiol.* 10, 906–917. doi: 10.1111/j.1462-2920.2007.01509.x

Teira, E., Martínez-García, S., Calvo-Díaz, A., and Morán, X. A. G. (2010). Effects of inorganic and organic nutrient inputs on bacterioplankton community composition along a latitudinal transect in the Atlantic Ocean. *Aquat. Microb. Ecol.* 60, 299–313. doi: 10.3354/ame01435

Thingstad, T. F., Krom, M. D., Mantoura, R. F. C., Flaten, G. A. F., Groom, S., Herut, B., et al. (2005). Nature of Phosphorus Limitation in the Ultraoligotrophic Eastern Mediterranean. *Science* 309, 1068–1071. doi: 10.1126/science.1112632

Wambeke, F. V., Obernosterer, I., Moutin, T., Duhamel, S., Ulloa, O., and Claustre, H. (2008). Heterotrophic bacterial production in the eastern South Pacific: longitudinal trends and coupling with primary production. *Biogeosciences* 5, 157–169. doi: 10.5194/bg-5-157-2008

Xu, J., Jing, H., Kong, L., Sun, M., Harrison, P. J., and Liu, H. (2013). Effect of seawater–sewage cross-transplants on bacterial metabolism and diversity. *Microb. Ecol.* 66, 60–72. doi: 10.1007/s00248-013-0207-2

Yan, S., Fuchs, B. M., Lenk, S., Harder, J., Wulf, J., Jiao, N. Z., et al. (2009). Biogeography and phylogeny of the *NOR5/OM60* clade of *Gammaproteobacteria*. *Syst. Appl. Microbiol.* 32, 124–139. doi: 10.1016/j.syapm.2008.12.001

Conflict of Interest Statement: The authors declare that the research was conducted in the absence of any commercial or financial relationships that could be construed as a potential conflict of interest.

The handling editor declared a shared affiliation, though no other collaboration, with several of the authors PP, AG, AT, TT and states that the process nevertheless met the standards of fair and objective review.

frontiers in Marine Science

ORIGINAL RESEARCH
published: 04 January 2017
doi: 10.3389/fmars.2016.00281

Bacterial Growth and Mortality after Deposition of Saharan Dust and Mixed Aerosols in the Eastern Mediterranean Sea: A Mesocosm Experiment

Anastasia Tsiola[1], Tatiana M. Tsagaraki[1†], Antonia Giannakourou[2], Nikolaos Nikolioudakis[3†], Nebil Yücel[4], Barak Herut[5] and Paraskevi Pitta[1]*

[1] Institute of Oceanography, Hellenic Centre for Marine Research, Heraklion, Greece, [2] Institute of Oceanography, Hellenic Centre for Marine Research, Anavyssos, Greece, [3] Institute of Marine Biological Resources and Inland Waters, Hellenic Centre for Marine Research, Heraklion, Greece, [4] Faculty of Marine Sciences and Technology, Iskenderun Technical University, Iskenderun, Hatay, Turkey, [5] Israel Oceanographic and Limnological Research Tel Shikmona, Haifa, Israel

OPEN ACCESS

Edited by:
Tilmann Harder, University of Bremen, Germany

Reviewed by:
Dolors Vaque, Spanish National Research Council, Spain
Toshi Nagata, University of Tokyo, Japan

***Correspondence:**
Anastasia Tsiola
atsiola@hcmr.gr

†Present Address:
Tatiana M. Tsagaraki, Department of Biology, University of Bergen, Bergen, Norway
Nikolaos Nikolioudakis, Institute of Marine Research, Bergen, Norway

Specialty section:
This article was submitted to Marine Ecosystem Ecology, a section of the journal Frontiers in Marine Science

Received: *22 September 2016*
Accepted: *13 December 2016*
Published: *04 January 2017*

Citation:
Tsiola A, Tsagaraki TM, Giannakourou A, Nikolioudakis N, Yücel N, Herut B and Pitta P (2017) Bacterial Growth and Mortality after Deposition of Saharan Dust and Mixed Aerosols in the Eastern Mediterranean Sea: A Mesocosm Experiment. Front. Mar. Sci. 3:281. doi: 10.3389/fmars.2016.00281

The impact of viral lysis and grazing by flagellates on bacterioplankton production was assessed during a mesocosm experiment in the Eastern Mediterranean Sea, in response to Saharan dust (SD) vs. mixed aerosols (A) addition. The results highlight a positive effect on bacterial abundance, production and growth rate (∼1.2, ∼2.4, and ∼1.9 –fold higher than the controls) in both SD and A, which was also confirmed by the increased portion of high DNA content bacteria (up to 48% of the bacterial community). Lytic viral production and the portion of bacterial production lost due to viral lysis were lower in SD and A after dust addition than in the controls ($0.33 \pm 0.17 \times 10^6$ virus-like particles mL^{-1} h^{-1} and $6 \pm 4\%$, respectively). Potential ingestion rate of bacteria by flagellates increased upon dust enrichment, but did not differ between mesocosms. Larger predators possibly down regulated flagellate abundance, and the calculated portion of bacterial production lost due to flagellate grazing was probably an artifact. Higher frequency of lysogenic cells in A compared to SD and the controls four days after dust addition may reflect faster phosphorus limitation in A, due to receiving less dissolved inorganic phosphorus and more dissolved inorganic nitrogen than SD.

Keywords: mesocosm experiment, East Mediterranean, dust, aerosols, lysis, lysogeny

INTRODUCTION

The Eastern Mediterranean Sea (EMS) is characterized by ultra—oligotrophic conditions, with low nutrient concentrations in surface layers (Krom et al., 1991) and low primary productivity and phytoplankton biomass (Siokou-Frangou et al., 2010). During the stratified period, EMS surface waters become nutrient-depleted. The high fluxes of atmospheric deposition during that period introduce material of Saharan desert and southern European origin into the marine system (Volpe et al., 2009). Aeolian dust events blow from the Saharan desert, frequently in the form of storms in spring and autumn, and as a consequence nutrients are leached from the dust particles (Carbo et al., 2005; Herut et al., 2005). The EMS is also constantly exposed to more polluted aerosols that are influenced by domestic and industrial activities (Lelieveld et al., 2016) and usually leach higher

amounts of nitrate relative to phosphorus when compared to desert dust (Herut et al., 2002; Bonnet et al., 2005). Atmospheric chemical processes, such as acidification, are mainly driven by human processes and air pollution (Seinfeld and Pandis, 1998) and significantly affect the final amount and chemical properties of the leaching procedure (Shi et al., 2015).

Research up to now has showed that bacteria are expected to quickly respond and grow during dust events (Herut et al., 2005; Guieu et al., 2014). A trigger of primary productivity was found across the Mediterranean in naturally occurring Saharan dust events and microcosm dust-addition experiments (Ternon et al., 2011). Heterotrophic metabolic rates also increased during a dust-addition mesocosm experiment in the northwestern basin (Pulido-Villena et al., 2014). In the same region, phosphorus released by dust was found to be one of the drivers of the bacterial community after dust addition (Laghdass et al., 2011). The response of the planktonic community to dust events largely depends on the solubility and elemental composition of aerosols and the degree of oligotrophy of the system at the time of deposition (Marañón et al., 2010), but is not necessarily linearly related to the intensity of the dust depositions.

Bacterioplankton standing stock is controlled by nutrient supply and the constant action of protists (mainly heterotrophic flagellates) and viruses (Thingstad, 2000) that leads to large biomass losses on a daily basis (Fuhrman and Noble, 1995). Acting simultaneously, grazers and viruses control the proportion of active and non-active bacteria, and, theoretically, the total bacterial abundance is mainly controlled by grazing, while the abundance of specific groups by viral lysis (Thingstad, 2000). Under certain circumstances one loss factor dominates over the other, but there is no general trend in this relationship, and it is difficult to separate them, both experimentally and conceptually. The proportion of viral lysis and grazing may vary even within hours (Winter et al., 2004), while grazing may have a negative effect on viral production due to preferential ingestion of lytically infected cells (Weinbauer and Peduzzi, 1994) or a positive effect on viral abundance due to induction of prophages or stimulation of new infections (Bonilla-Findji et al., 2009).

There is evidence that viruses-mediated bacterial mortality increases with the productivity of the environment (Weinbauer et al., 2003b) and it has been proposed that protistan grazing is the principal cause of bacterial mortality in highly oligotrophic systems (Pernthaler, 2005 and references therein). This proposition has been recently confirmed in the Northeastern Atlantic Ocean (Vaqué et al., 2014), and specific findings for the Northwestern Mediterranean Sea revealed that indeed grazing by heterotrophic flagellates dominated bacterial losses whereas losses due to viral lysis were more variable (Bettarel et al., 2002). The trophic status of a system was also found to drive the occurrence of lysogeny, which was prevalent under low inorganic nitrogen and phosphorus concentrations (Williamson et al., 2002) and under low bacterial abundance and productivity (Weinbauer et al., 2003a).

Bacterial abundance seems to be critical when trying to predict mortality by grazers and viruses. Based on a Lotka-Volterra type of mathematical model, Thingstad (2000) proposed that at high bacterial densities the contact probabilities between viruses and bacteria are increased, thus viral infection and lysis is more frequent. The same result is expected for the contact rates between protists and bacteria (Vaqué et al., 1994).

When dust events occur in the oligotrophic EMS, the proportion of bacterial losses due to grazing and viral lysis could be an indication of organic matter and nutrient cycling in the food web (channeled up or remineralized, respectively) with implications on total system's productivity. In this study we aimed to assess how bacterioplankton growth is affected by (1) dust of different origins and (2) the simultaneous impact of grazing by heterotrophic flagellates and viral lysis. For this reason, we performed viral production experiments and we applied a grazing model to predict ingestion rate of bacteria by flagellates, in order to estimate bacterial production losses after Saharan dust vs. mixed aerosols addition, simulating realistic storm events, during a mesocosm experiment in the EMS (Cretan Sea). We hypothesized that dust of either origin will have a positive effect on bacterial production and biomass. Based on this hypothesis, we tested whether bacterial losses would increase upon dust enrichment, as a consequence of their increased productivity.

MATERIALS AND METHODS

Experimental Setup

Seawater was collected from a site 5 nautical miles north of Heraklion port in the Cretan Sea (35° 24.975N, 25° 14.441E), transported to the CRETACOSMOS mesocosm facilities of the Hellenic Centre for Marine Research (HCMR) and then used to fill 9 food grade polyethylene mesocosm bags to a final volume of 3 m^3. The seawater was pumped on the 8 and 9th May 2012 from 10 m depth into 1 m^3 high density polypropylene containers which had been washed with acid (10% HCl) and rinsed with deionized water three times prior to filling. Within 2 h from collection, the seawater had been transported to HCMR and distributed evenly to the mesocosm bags by gravity siphoning with acid cleaned and deionized water rinsed plastic tubes. The bags were deployed in a large concrete tank (350 m^3) and incubated at *in situ* temperature, which was kept constant by a continuous flow system and was measured with HOBO data loggers (ONSET Corporation). An airlift system ensured a gentle mixing of the water column within the mesocosms to avoid stratification. A Plexiglas lid was used to protect mesocosms from atmospheric deposition and a mesh screen was also used to mimic the light conditions at the sampling depth.

Prior to any addition, a sampling was carried out on 10th May 2012 (T-1) in order to determine the initial conditions of several biotic and abiotic parameters (Herut et al., 2016, this SI; Tsagaraki et al., 2016). Immediately after T-1, three mesocosms were enriched with Saharan dust collected in Crete and Israel at a final concentration of 1.6 mg L^{-1} (treatment abbreviation hereafter: SD). Another three mesocosms were enriched with aerosol consisting of a mixture of Saharan desert dust and particles of European origin, also collected in Crete and Israel, at a final concentration of 1.0 mg L^{-1} (treatment abbreviation hereafter: A). The remaining three mesocosms served as control (abbreviation hereafter: C). The second sampling was performed

3 h after additions (T0), and then sampling was carried out daily for 8 days (T1–T8). Samples for the assessment of viral production rates (including lytic and lysogenic) were taken at T-1, T1, T4, and T8 from two control mesocosms (C1 and C2), two mesocosms enriched with Saharan dust (SD1 and SD2) and two mesocosms enriched with aerosol (A1 and A2). Samples from SD1 and SD2 at T-1 were lost during filtration.

Nutrients Released with Dust Addition

Leaching experiments were performed to estimate the amount of nutrients and trace metals released upon dust deposition. Results of these experiments are presented in Herut et al. (2016, this SI). **Table 1** summarizes the concentration of dust added in A and SD mesocosms and the amount of phosphate, nitrate and nitrite leached after deposition. Briefly, a mixture of aerosol of Saharan desert and European origin was added in A at 1 mg L^{-1} final concentration, leading to the release of 3.0 nM phosphate and 54 nM NOx per mg of dust, representing a relatively intense dust storm event (Herut et al., 2005). In SD, aerosols of pure Saharan desert origin were added at 1.6 mg L^{-1} final concentration, leading to the release of 2.4 nM phosphate and 23 nM NOx per mg of dust that represented an intense dust storm event (Herut et al., 2005).

Dissolved Nutrients and Dissolved Organic Carbon

The concentrations of dissolved nutrients and organic carbon are presented in details in Tsagaraki et al. (2016, this SI). Samples were collected daily for the estimation of dissolved phosphate concentration, with the use of the MAGIC method (Rimmelin and Moutin, 2005). The concentrations of dissolved silicate, nitrate and nitrite were also estimated daily, according to Strickland and Parsons (1972). The concentration of dissolved ammonium was assessed according to Ivančič and Deggobis (1984). The detection limits for phosphate, nitrate and ammonium were 0.8 nM, 0.017 and 0.019 μM, respectively.

Dissolved organic carbon was measured according to Sohrin and Sempéré (2005). Samples were transferred into dark glass bottles (pre-combusted at 330°C for 6 h) and then filtered through GF/F filters (pre-combusted at 450°C for 6 h). The filtrate was collected in 15-mL glass vials (pre-combusted at 450°C for 6 h) and acidified with 20 μL H_3PO_4 (85%). Samples were stored in the dark at 4°C pending laboratory analysis by high-temperature combustion on a Shimadzu TOC 5000 analyzer. A four-point calibration curve was constructed daily using standards, which were prepared by diluting a stock solution of potassium hydrogen phthalate in Milli-Q water. To avoid random errors associated with day-to-day instrument variability, all samples from a given day were analyzed in a single day. The procedural blanks (i.e., runs with Milli-Q water) ranged from 1–2 μM C whereas the analytical precision of the analysis was within 2%. Operational blanks related to transfer and storage of samples, filtration, and handling were 8.4 ± 2.5 μM C ($n = 7$).

Chlorophyll a

Chlorophyll a concentration was determined fluorometrically, according to Yentsch and Menzel (1963), using a Turner TD-700 fluorometer. Samples were collected daily and sequentially filtered through 2, 0.6 and 0.2 μm polycarbonate filters in low vacuum pressure.

Abundance of Bacteria and Viruses

Samples for the determination of bacterial and virus-like particles (VLP) abundance were collected every day. Samples were fixed with 25% 0.2 μm-filtered glutaraldehyde (0.5% final concentration), incubated at 4°C for approximately 45 min, flash frozen in liquid nitrogen and then transferred to −80°C until analysis. Frozen samples were thawed at room temperature and sub-samples were stained for viral and bacterial enumeration, according to Brussaard (2004) and Marie et al. (1997), respectively. Heterotrophic bacteria were stained with SYBR Green I (final dilution 4×10^{-4} of the stock solution in Tris-EDTA buffer, pH = 8) and incubated for 10 min in the dark. Heterotrophic bacteria were distinguished based on their fluorescence signal. According to that, bacterial DNA content was pooled in two categories: high DNA content (HDNA) and low DNA content (LDNA) bacterial cells. Samples for autotrophic bacterial abundance were not fixed and analyzed without prior staining, based on their auto-fluorescence signals. VLP were stained with SYBR Green I (final dilution 5×10^{-5} of the stock solution in Tris-EDTA buffer, pH=8) and incubated at 80°C for 10 min. Viral samples were diluted in Tris-EDTA buffer solution (1:80 or 1:100) prior to staining, in order to not exceed 1000 events second $^{-1}$ during counting. A FACSCalibur™ (Becton Dickinson) instrument was used, equipped with an air-cooled laser at 488 nm and standard filter set-up. Flow cytometry data were acquired and processed with the Cell Quest Pro software (Becton Dickinson). For the high-speed performance of the machine an estimated average flow rate was used (58 μL min^{-1}). Abundance of bacteria (cells mL^{-1}) was converted to carbon biomass using the conversion factor 20 fg C $cell^{-1}$ (Lee and Fuhrman, 1987).

Abundance of Heterotrophic Flagellates

Samples for heterotrophic flagellate (HF) counting were collected at T-1, T1, T4, and T8, fixed with glutaraldehyde (1% final concentration) and kept in the dark at 4°C. Flagellate cells were concentrated to approximately 10 mL, stained with 4′6-diamidino-2-phenylindole (DAPI at a final concentration of 1 μg mL^{-1}) for 10 min, and finally collected on a 25-mm diameter, 0.8 μm pore-sized black polycarbonate filter (Porter and Feig, 1980). The filters were mounted on slides and stored at −20°C. Flagellates were counted at 1000x magnification, using UV excitation under an Olympus BX60 epifluorescence microscope. All cells were measured and divided into four categories (1–3, 3–5, 5–10, and >10 μm) using an ocular micrometer.

Bacterial Production and Bacterial Growth Rate

Bacterial production (BP) was measured using the [^{3}H] leucine method, according to Kirchman et al. (1985) and modifications

TABLE 1 | Information regarding the dust added in the mesocosms; origin of dust, final concentration in the mesocosms, and the amounts of leached phosphate (PO_4) and nitrogen forms (NO_x) per mg of dust.

Mesocosm	Type of dust	Final concentration	Amount of PO_4 leached	Amount of NO_x leached
A	Mixture of aerosols of Saharan desert and European origin	1.0 mg L^{-1}	3.0 nM per mg dust (average of two leaching experiments)	54 nM per mg dust
SD	Aerosols of Saharan desert origin	1.6 mg L^{-1}	2.4 nM per mg dust (average of two leaching experiments)	23 nM per mg dust

A refers to the mesocosms that were enriched with aerosol and SD to the mesocosms that were enriched with Saharan dust. Data are mean ± standard deviation of triplicate mesocosms. Detailed information can be found in Herut et al. (2016, this SI).

by Smith and Azam (1992). Two replicated seawater samples (1.5 mL) and one trichloracetic acid (TCA)-killed control were incubated in 2 mL-tubes with a mixture of [4,5-^{3}H] leucine (Perkin Elmer, specific activity 115 Ci $mmol^{-1}$) and nonradioactive leucine at final concentrations of 16 and 7 nM, respectively. All samples, including controls, were incubated for 2 h in the dark at *in situ* temperature, based on daily temperature measurements. Incubation was terminated with the addition of 90 μL of 100% TCA. Samples were then stored at 4°C in the dark until further processing. Centrifugation was carried out at 16000 g for 10 min. After discarding the supernatant, 1.5 mL of 5% TCA was added, samples were vigorously shaken using a vortex and then centrifuged again at the same speed. After discarding the supernatant, 1.5 mL of 80% ethanol was added, samples were shaken and centrifuged again. The supernatant was then discarded and 1.5 mL of scintillation liquid was added. The radioactivity incorporated into the pellet was counted using a Packard LS 1600 Liquid Scintillation Counter. BP was calculated according to Kirchman (1993) in ng L^{-1} h^{-1}, from the ^{3}H-leucine incorporation rates, according to the following formula:

$$BP = Leu \times 131.2 \times (\%\,leu)^{-1} \times (C/protein) \times ID \times (hot + cold)/hot$$

where Leu = rate of leucine incorporation (mol L^{-1} h^{-1}), 131.2 = formula weight of leucine, % leu = fraction of leucine in protein (0.073), C/protein = ratio of cellular carbon to protein (0.86), "hot" and "cold" = respective concentrations of labeled and unlabelled leucine and ID = the isotope dilution. A time-series experiment was carried out in order to show that the incorporation of leucine was linear with time. Two concentration kinetic experiments were also performed in order to verify that the concentration of leucine added (20 nM) was sufficient to saturate incorporation (range of concentrations 3 to 50 nM). The results of the concentration kinetics showed that the degree of participation of 20 nM used for the BP production measurements was always >90%, thus the isotopic dilution was negligible.

Bacterial growth rate was calculated by dividing the bacterial carbon production to bacterial biomass.

Methods to Estimate BP Losses Due to Viral Lysis

For the estimation of BP losses due to viral lysis, the viral reduction approach was used, as described in Weinbauer et al. (2003a) and modified by Winter et al. (2004) and Winget et al. (2005). Details can be found in Appendix 1.

The frequency of lytically infected cells (FLIC) was estimated from the incubations that did not receive mitomycin C, based on the formula:

$$FLIC = 100 \times [VPlytic_1 + ... + VPlytic_n]/[BSxB0]$$

where BS is the burst size, B0 is the bacterial abundance at the beginning of the incubations and VPlytic (expressed as VLP mL^{-1} h^{-1}) refers to the lytic viral production and is calculated for the time intervals characterized by a net increase in viral abundance. Incubation lasted 24 h and sub-samples were taken at the beginning of the incubations and then after 1, 3, 6, 12, and 24 h. Hence,

$$VPlytic = [(Vmax_1 - Vmin_1)/(tmax_1 - tmin_1) + ... + (Vmax_n - Vmin_n)/(tmax_n - tmin_n)] \times [Boriginal/B0]$$

where Boriginal is the bacterial abundance measured in the original mesocosm sample. The correction factor (Boriginal/B0) was applied in order to correct for bacterial losses during filtration (Winget et al., 2005).

The frequency of lysogenic cells (FLC) was estimated from the difference in viral direct counts (VDCs) between mitomycin C-treated and control incubations, according to the formula:

$$FLC = 100 \times [VPlysogenic_1 + ... + VPlysogenic_n]/[BSxB0]$$

where BS is the burst size, B0 is the bacterial abundance at the beginning of the incubations and VPlysogenic refers to the lysogenic viral production, (expressed as VLP mL^{-1} h^{-1}) and is calculated as follows:

$$VPlysogenic = [(VDCmax_1 - VDCmin_1)/(tmax_1 - tmin_1) + ... + (VDCmax_n - VDCmin_n)/(tmax_n - tmin_n)]$$

Mean values of triplicate incubations were used for all estimations. A switch from the lysogenic to the lytic cycle (i.e., prophage induction) was assumed when we observed significantly higher viral abundance in the mitomycin C treatments relative to the controls (Cochran et al., 1998; Tapper and Hicks, 1998). Regarding burst size, we used the minimum published value (26) acquired from studies in surface waters of the Mediterranean Sea (Weinbauer et al., 2003a).

The % of bacterial production lost due to viral lysis (%BP-VIR) was then estimated, using the formula:

$$\%BP - VIR = [\text{lysis rate of bacteria}/BP]$$

where BP is the bacterial production measured in the original sample and lysis rate of bacteria is calculated in cells mL^{-1} h^{-1} using the formula:

$$\text{lysis rate of bacteria} = [VPlytic/BS].$$

Method to Estimate Ingestion Rate of Bacteria by Flagellates

A grazing model was applied in order to estimate the ingestion rate of bacteria by flagellates, and the subsequent grazing impact that flagellates had on bacteria (Peters, 1994). Equation 4 in Peters (1994) considers the weighted measured flagellate size in μm^3, bacterial and flagellate abundances in cells mL^{-1} and temperature, in order to estimate the ingestion rate (IR) according to the following formula:

$$\begin{aligned}\text{LogIR} = &-3.243 + 0.432\text{LogVPD} + 0.569\text{LogCPY} \\ &- 0.149\text{LogCPD} + 0.030\text{TEMP}\end{aligned}$$

where VPD refers to the volume of the predators, CPY refers to the concentration of the prey, CPD refers to the concentration of the predator and TEMP refers to the temperature. The obtained estimates of IR are given in number of prey cells per predator per hour.

For the calculation of average biovolume per cell in each size class we considered flagellate cells as spheroids and we used the average length and width in each size class. Cell volumes were calculated as $W^2*L*\pi/6$, where L and W are the measured length and width of the cells.

Statistical Analysis

Virus numbers in untreated and treated with mitomycin C samples were tested at each time point in the sampling sequence to test for prophage induction (considered to occur when virus numbers in treated samples were significantly higher than in untreated). Repeated measures analysis of variance (RM ANOVA) was used to test for differences in a given variable between different treatments (C, SD and A) throughout the experimental period, after checking the assumption of sphericity (Mauchly's test). One-way ANOVA was applied to test for differences of each variable between treatments at each time point (T-1, T1, T4, and T8). Significant differences between treatments at each time point were assessed by *post-hoc* Tukey tests (Tukey HSD). Homogeneity of variance for all one-way ANOVAs was checked using Levene's test. All statistical analyses were performed in IBM SPSS 24 software. All data presented here are the mean ± standard deviation (*s*) of triplicate measurements. When no *s* is given no replicated measurements were done.

RESULTS

Initial Water Conditions and Nutrients Released with Dust Addition

The seawater characteristics of the sampling site and of the mesocosm bags prior to additions are presented in details in Herut et al. (2016, this SI) and of the following days in Tsagaraki et al. (2016, this SI). In Herut et al. (2016, this SI) additional information on the amount of nutrients and trace metals that were released with dust deposition is given. In the present manuscript, data concern the concentrations of dissolved nutrients, dissolved organic carbon and chlorophyll a (1) at the sampling site, (2) at initial conditions (T-1, as the mean ± *s* of all mesocosm bags before dust addition) and (3) during the experimental days relevant to the current study (T1, T4, and T8, as the mean ± *s* of triplicate C, A, and SD mesocosms), and are summarized in **Table 2**.

Seawater temperature ranged between 19 and 20°C during the experiment and no stratification developed in the water column of the bags. The concentrations of dissolved phosphate and silicate at the sampling station were 12 and 972 nM, respectively. Significantly higher concentration of phosphate was found in A compared to the rest of the mesocosms at T-1 [one-way ANOVA, $F_{(2)} = 11.05$, $p < 0.05$], as well as at T1 and T4. Phosphate concentration decreased upon aerosol addition in both A and SD, while it remained stable in the controls. The concentration of dissolved nitrogen (as the sum of ammonium, nitrite and nitrate) was significantly higher in the controls and A than SD mesocosms before dust addition [one-way ANOVA, $F_{(2)} = 11.05$, $p < 0.05$]. Silicate concentration was not different between controls and treatments, except for T-1 that it was significantly higher in A [one-way ANOVA, $F_{(2)} = 19.08$, $p < 0.05$].

Dissolved organic carbon (DOC) was 153 (± 20) μM C before dust amendment. DOC concentration increased in all mesocosms toward T1 and then decreased until the end of the experiment.

Total chlorophyll a (calculated as the sum of 2, 0.6 and 0.2 μm size fractions) was 0.06 (±0.01) mg L^{-1} at T-1. Chlorophyll a concentration was higher at T1 in A and SD than the controls [one-way ANOVA, $F_{(2)} = 153.00$, $p < 0.05$], while at T8 it was in levels lower than the initial ones in all mesocosms.

Abundance of Bacteria, Viruses and Flagellates

Before enrichment (T-1), the abundance of total bacterial cells averaged $4.5 \times 10^5 \pm 6.9 \times 10^3$ cells mL^{-1} (Mean ± *s*). A significant difference in bacterial abundance was observed between the dust-added and control treatments [RM ANOVA, $F_{(2, 3)} = 151.56$, $p < 0.05$], with bacterial abundance being higher in A and SD (Tukey HSD test, $p < 0.05$). Total bacterial abundance increased 1.2–fold in the A and SD mesocosms from T-1 to T1, in contrast to the controls that did not fluctuate during that period (**Figure 1A**). Bacterial abundance dropped to almost initial values at T4 and remained stable until T8 in the A and SD mesocosms. In the controls, bacteria dropped from T1 until the end of the experiment. The contribution of HDNA bacteria in the different treatments at the experimental days is shown

TABLE 2 | Concentration of dissolved phosphate (PO_4), nitrite (NO_2), nitrate (NO_3), ammonium (NH_4), silicate [$Si(OH)_4$], organic carbon (DOC), and chlorophyll *a* at the ambient water collected between 7 and 8th May 2012 (*in situ*, 10 m depth), before dust deposition (T-1), and then at the experimental days when the viral reduction approach was performed (T1, T4, and T8).

Seawater sample	PO_4 nM	NO_2 nM	NO_3 nM	NH_4 nM	$Si(OH)_4$ nM	DOC μM	Chlorophyll a μg L^{-1}
in situ (10 m)	12.3	<DL	105	360	972	nm	nm
T-1	13.6 ± 4.4	<DL	146 ± 51	132 ± 56	1234 ± 350	153 ± 20	0.06 ± 0.01
T1 C	7.8 ± 1.1	<DL	134 ± 52	60 ± 8	1692 ± 122	177 ± 54	0.07 ± 0.00
T1 A	9.9 ± 2.3	<DL	204 ± 42	53 ± 0	1191 ± 169	174 ± 31	0.10 ± 0.00
T1 SD	9.1 ± 1.1	<DL	123 ± 21	51 ± 19	1770 ± 586	181 ± 23	0.10 ± 0.01
T4 C	5.6 ± 0.2	<DL	89 ± 52	32 ± 14	909 ± 9	121 ± 3	0.08 ± 0.01
T4 A	5.9 ± 0.1	<DL	140 ± 11	74 ± 35	939 ± 46	150 ± 17	0.10 ± 0.10
T4 SD	5.8 ± 0.6	<DL	143 ± 19	64 ± 14	978 ± 14	160 ± 14	0.11 ± 0.03
T8 C	4.3 ± 0.6	<DL	58 ± 6	14 ± 8	927 ± 18	96 ± 24	0.04 ± 0.01
T8 A	6.8 ± 0.7	<DL	56 ± 5	35 ± 17	960 ± 32	100 ± 18	0.05 ± 0.01
T8 SD	6.0 ± 1.0	<DL	44 ± 17	69 ± 14	957 ± 14	92 ± 15	0.04 ± 0.01

C refers to the control mesocosms, A to the mesocosms that were enriched with aerosol, and SD to the mesocosms that were enriched with Saharan dust. Data derive from the Mean ± standard deviation of triplicate mesocosms. "<DL" denotes measurements below the detection limit of the analytical method and "nm" denotes non-measured parameters.

in **Figure 1B**. Similarly to total bacterial abundance, significant differences between C and A, and C and SD mesocosms were observed [RM ANOVA, $F_{(2, 3)} = 465.94$, $p < 0.05$]; HDNA bacteria peaked at T1 (representing 46–48% of total bacteria) and then at T8 (representing 44–46% of total bacteria) in both A and SD treatments, contrary to the controls where HDNA bacterial abundance did not change throughout the experiment.

Initially, total virus-like particle abundances (VLP) ranged between 5.9 and 6.9 × 10^6 VLP mL^{-1}. VLP abundance showed a similar pattern between all tanks when considering all experimental days, characterized by a ∼1.2-fold decrease from T1 to T4, followed by an equivalent increase from T4 to T8 (**Figure 1C**). VLP abundance was significantly higher in A and SD than the controls at T1 [one-way ANOVA, $F_{(2)} = 7.60$, $p < 0.05$].

Heterotrophic flagellate abundance did not show a significantly different pattern between the controls and treatments over time and at any individual time point. Flagellate abundance continuously decreased in all mesocosms from T1 to T8 (**Figure 1D**) by 30–64% of their initial abundance (2933 ± 347 cells mL^{-1}, Mean ± *s*). The whole dataset of bacterial, viral and flagellate abundance of the experiment is presented in Appendix 2.

Bacterial Production and Bacterial Growth Rate

Bacterial production measurements for this study are shown in **Figure 2A**. At T-1, BP was 13.6 ± 1.8 ng C L^{-1} h^{-1} (Mean ± *s*). BP displayed a significantly different trend over time between controls and treatments [RM ANOVA, $F_{(2, 3)} = 94.23$, $p < 0.05$]. BP was significantly higher in A and SD than the controls at T1 [one-way ANOVA, $F_{(2)} = 42.88$, $p < 0.05$] and significantly higher in SD than the controls at T8 [one-way ANOVA, $F_{(2)} = 71.67$, $p < 0.05$]. The highest BP was measured at T1 in A (44.7 ± 1.9 ng C L^{-1} h^{-1}) and SD (38.2 ± 5.0 ng C L^{-1} h^{-1}).

Bacterial growth rate is presented in **Figure 2B**. At initial conditions bacterial growth rate was 0.0017 h^{-1} (± 0.0004) and it was significantly higher in A and SD than the controls at T1 [one-way ANOVA, $F_{(2)} = 30.40$, $p < 0.05$]. Bacterial growth rate reached minimum levels in A at T4 (0.0007–0.0008 h^{-1}), which were significantly different from the respective ones in the controls and SD [one-way ANOVA, $F_{(2)} = 29.73$, $p < 0.05$]. The whole dataset of bacterial production rates of the experiment is presented in Appendix 2.

Lytic and Lysogenic Viral Production Rates

Lytic viral production rate (VPlytic) is shown in **Figure 3** and lysis rate of bacteria in **Table 3**. Before dust addition, VPlytic was 0.33 ± 0.02 × 10^6 cells mL^{-1} h^{-1} and lysis rate of bacteria was 0.01 ± 0.0008 × 10^6 cells mL^{-1} h^{-1} (Mean ± *s*). Significant differences were detected in VPlytic and the lysis rate of bacteria between controls and treatments over time [RM ANOVA, $F_{(2, 15)} = 4.35$, $p < 0.05$]. At T1, both VPlytic and the lysis rate of bacteria were significantly higher in the controls than A and SD [one-way ANOVA, $F_{(2)} = 27.14$, $p < 0.05$], while at T8 significantly higher levels of both rates were found in SD compared to the controls [one-way ANOVA, $F_{(2)} = 14.92$, $p < 0.001$]. At T1 the highest values were measured for VPlytic and the lysis rate of bacteria in the controls (0.92 ± 0.34 × 10^6 cells mL^{-1} h^{-1} and 0.04 ± 0.001 cells mL^{-1} h^{-1}, respectively).

The frequency of lytically infected cells (FLIC) did not display significant differences between the controls and A and SD mesocosms throughout the experimental period. Only at T1, significantly lower FLIC levels were measured in A and SD than the controls [one-way ANOVA, $F_{(2)} = 26.36$, $p < 0.05$]. At T-1, FLIC was 5 ± 1% and ranged between 2 and 15% in the following days (**Figure 4A**).

Lysogenic viral production rates (expressed here as the frequency of lysogenic cells; FLC) represent the proportion of

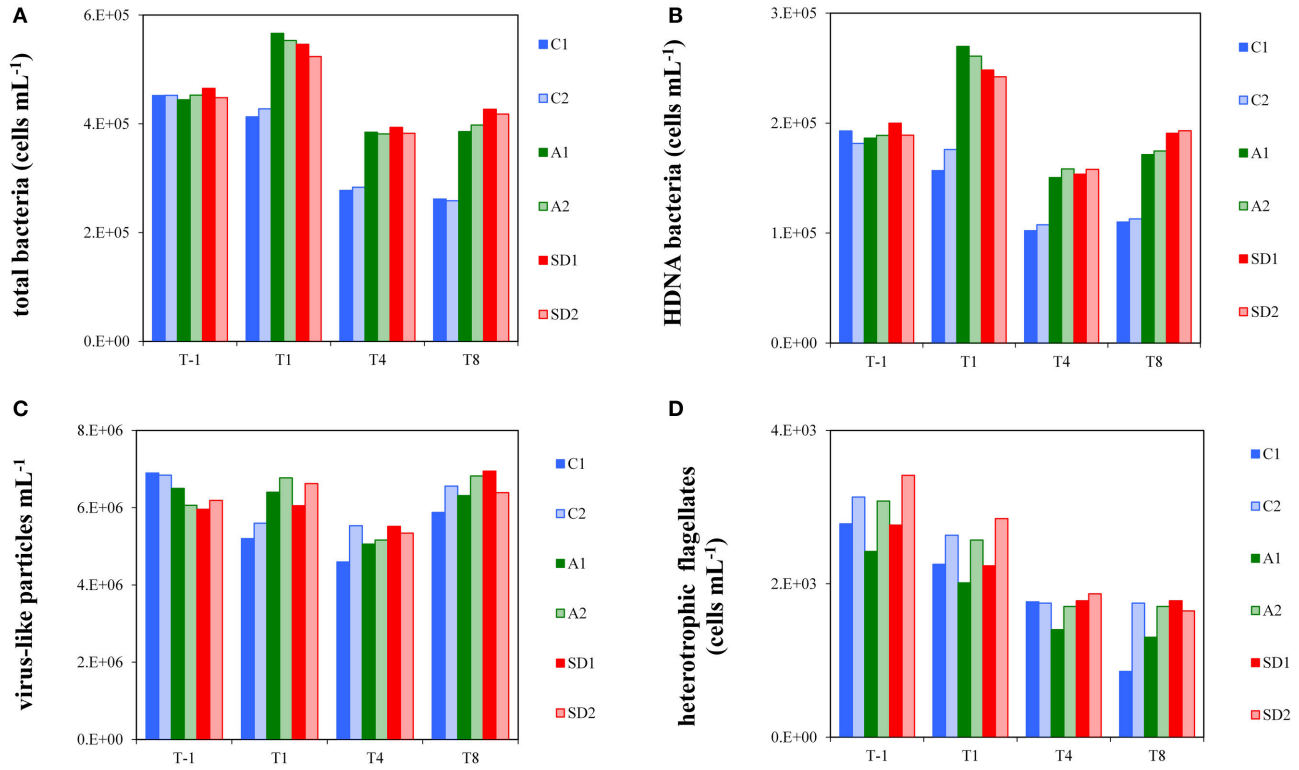

FIGURE 1 | Abundance of total bacteria (A), High DNA nucleic acid bacteria **(B)**, virus-like particles **(C)** and heterotrophic flagellates **(D)** in the different treatments at T-1, T1, T4, and T8. C1 and C2 refer to the control mesocosms, A1 and A2 to the mesocosms that were enriched with aerosol, and SD1 and SD2 to the mesocosms that were enriched with Saharan dust.

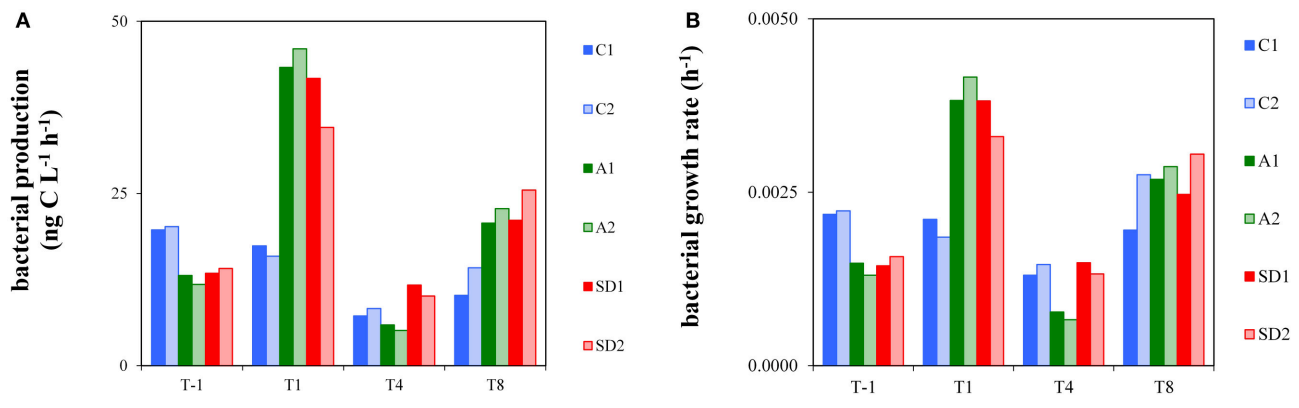

FIGURE 2 | Heterotrophic bacterial production (A) and bacterial growth rate **(B)** in the different treatments at T-1, T1, T4, and T8. C1 and C2 refer to the control mesocosms, A1 and A2 to the mesocosms that were enriched with aerosol, and SD1 and SD2 to the mesocosms that were enriched with Saharan dust.

lysogenic bacterial cells in a community, thus the bacterial cells that produce lysogenic viruses and are shown in **Figure 4B**. FLC levels displayed significant differences between controls and treatments [RM ANOVA, $F_{(2,\ 15)} = 6.72$, $p < 0.05$]. Compared to the controls (15 ± 11%), significantly higher FLC levels were found at T4 in the A mesocosms (44 ± 8%) [one-way ANOVA, $F_{(2)} = 24.70$, $p < 0.01$], while SD was significantly different from A at T4 too (12 ± 6%) [one-way ANOVA, $F_{(2)} = 24.70$, $p < 0.05$].

Bacterial Production Losses Due to Viral Lysis

The %BP-VIR fraction at initial conditions was 16 ± 4% (**Figure 5**). A significantly smaller fraction of %BP-VIRwas found at T1 in A and SD mesocosms compared to the controls [one-way ANOVA, $F_{(2)} = 26.82$, $p < 0.05$]. Between T-1 and T1%BP-VIR decreased to very low levels in A and SD (6 ± 4%), while it increased in the controls (maximum 45%) and remained in

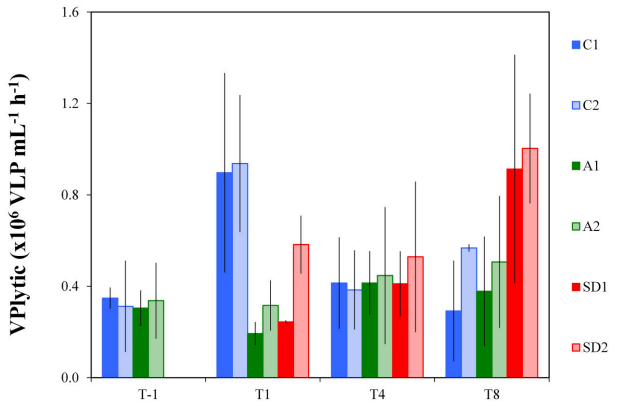

FIGURE 3 | Lytic viral production rate in the different treatments at T-1, T1, T4, and T8. C1 and C2 refer to the control mesocosms, A1 and A2 to the mesocosms that were enriched with aerosol, and SD1 and SD2 to the mesocosms that were enriched with Saharan dust. Values are Mean ± *s* of triplicate incubation experiments.

similar levels until T4. %BP-VIR in A mesocosms exceeded the levels of the controls at T4, but the difference was not significant.

Ingestion Rate of Bacteria by Flagellates

The potential ingestion rates of bacteria by heterotrophic flagellates at initial conditions were 3.4 (± 0.1) cells per predator per hour (**Table 3**). Ingestion rates peaked at T1 in A and SD (4.2 ± 0.2 cells per predator per hour) and were higher than in the controls also at T4 and T8, but the difference was not significant.

DISCUSSION

During the present study, we assessed bacterial growth after a sudden deposition of Saharan desert dust vs. mixed aerosols in the Eastern Mediterranean Sea, and the potential impact of lysis by viruses and grazing by flagellates on bacterial mortality. The EMS surface water used to fill the mesocosms was characterized by typically oligotrophic features; phosphate and chlorophyll a concentrations were 12.3 nM and 0.06 μg L^{-1}, and biological indexes, such as bacterial and primary production rates and phosphate turnover time, fell within the range of published levels for oligotrophic systems and particularly the EMS (reviewed by Herut et al., 2016, this SI). The sudden dust addition represented an intense (SD) and a relatively intense (A) dust event that caused the release of phosphorus (25–50% additional amount compared to the ambient levels) and nitrogen (higher amount in A than in SD) and had an immediate impact on bacterial growth.

Rapidly after deposition of both aerosol types, increased bacterioplankton production, growth rate and standing stock were measured. A positive effect on total and HDNA bacterial abundance was seen, suggesting that a community of more active cells (Lebaron et al., 2001) was dominant in the treated mesocosms compared to the controls. Morán et al. (2007) proposed that the HDNA fraction can be used as an index of bacterial activity if bacterial biomass is controlled by bottom-up factors. Increased bacterial growth rate was measured in experiments in other oceanic regions, also frequently affected by Saharan dust (Pulido-Villena et al., 2008, 2014; Marañón et al., 2010). In the current experiment, changes in bacterial diversity in the dust-treated mesocosms were also determined compared to the controls (Guo et al., 2016, this SI).

During the time of increased bacterial growth, low levels of %BP-VIR were measured in A and SD. Initial levels for VPlytic and %BP-VIR were in agreement with published data for the Mediterranean Sea (Bettarel et al., 2002; Boras et al., 2009) and other coastal systems (Winget and Wommack, 2009). At T1, VPlytic was particularly low in A and SD, and, while it still fell within the published range for the oligotrophic Northwestern Mediterranean (Boras et al., 2009), it was lower than anticipated

TABLE 3 | Viral reduction approach associated measurements [including B0 that refers to the bacterial abundance at the beginning of the incubation (Mean ± standard deviation of 6 replicates) and the lysis rate of bacteria (Mean ± standard deviation of triplicates)] and the potential ingestion rate of bacteria by flagellates, based on an empirical model described in Peters (1994), in the different treatments at T-1, T1, T4, and T8.

Experimental day	Mesocosm	B0 (×10^6 cells mL^{-1})	Lysis rate of bacteria (×10^6 cells mL^{-1} h^{-1})	Ingestion rate of bacteria (cells $predator^{-1}$ h^{-1})
T-1	C1	0.31 ± 0.005	0.01 ± 0.002	3.49
	C2	0.19 ± 0.01	0.01 ± 0.01	3.33
	A1	0.25 ± 0.01	0.01 ± 0.01	3.48
	A2	0.29 ± 0.01	0.01 ± 0.01	3.31
	SD1			3.66
	SD2			3.38
T1	C1	0.37 ± 0.004	0.03 ± 0.02	3.55
	C2	0.39 ± 0.004	0.04 ± 0.02	3.46
	A1	0.34 ± 0.02	0.01 ± 0.002	4.45
	A2	0.35 ± 0.09	0.01 ± 0.002	3.98
	SD1	0.46 ± 0.04	0.01 ± 0.001	4.35
	SD2	0.32 ± 0.004	0.02 ± 0.003	4.02
T4	C1	0.33 ± 0.01	0.02 ± 0.01	3.18
	C2	0.20 ± 0.01	0.02 ± 0.01	3.01
	A1	0.22 ± 0.01	0.02 ± 0.005	4.01
	A2	0.26 ± 0.005	0.02 ± 0.01	3.57
	SD1	0.29 ± 0.02	0.02 ± 0.01	3.97
	SD2	0.30 ± 0.01	0.02 ± 0.01	3.65
T8	C1	0.13 ± 0.005	0.01 ± 0.01	3.30
	C2	0.14 ± 0.003	0.02 ± 0.001	2.78
	A1	0.32 ± 0.02	0.02 ± 0.01	3.88
	A2	0.24 ± 0.02	0.02 ± 0.01	3.55
	SD1	0.27 ± 0.01	0.04 ± 0.02	4.04
	SD2	0.29 ± 0.01	0.04 ± 0.01	3.64

C1 and C2 refer to the control mesocosms, A1 and A2 to the mesocosms that were enriched with aerosol, and SD1 and SD2 to the mesocosms that were enriched with Saharan dust.

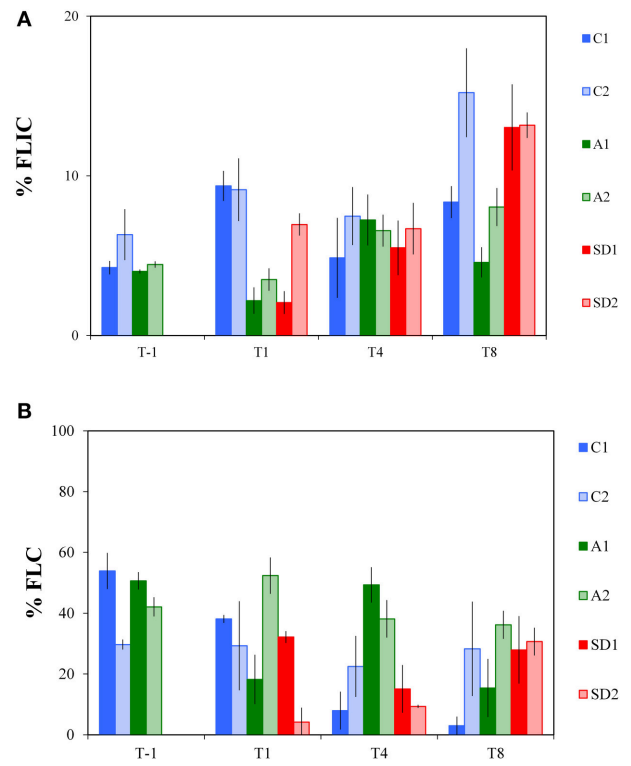

FIGURE 4 | Frequency of lytically infected cells (% FLIC, A) and lysogenic cells (% FLC, **B**) in the different treatments at T-1, T1, T4 and T8. C1 and C2 refer to the control mesocosms, A1 and A2 to the mesocosms that were enriched with aerosol, and SD1 and SD2 to the mesocosms that were enriched with Saharan dust. Values are Mean ± standard deviation of triplicate incubation experiments.

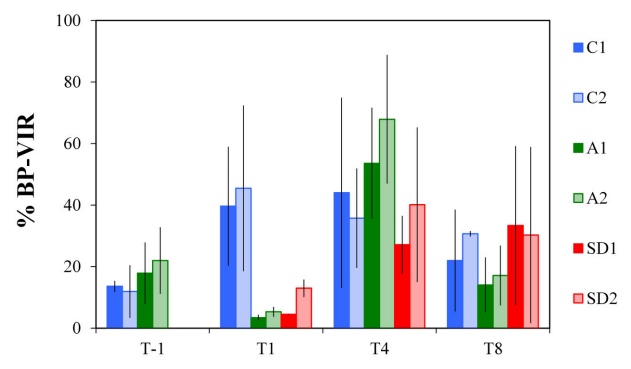

FIGURE 5 | Bacterial mortality expressed as the percentage of bacterial production (BP) lost due to viral lysis (%BP-VIR) in the different treatments at T-1, T1, T4, and T8. C1 and C2 refer to the control mesocosms, A1 and A2 to the mesocosms that were enriched with aerosol, and SD1 and SD2 to the mesocosms that were enriched with Saharan dust. Values are Mean ± standard deviation of triplicate incubation experiments.

and lower than in the controls. In support of the notion that viral production depends on host productivity and host-virus contact rates, we hypothesized that increased bacterial growth in A and SD would be followed by increased viral production (Motegi et al., 2009). The same hypothesis was drawn by Pulido-Villena et al. (2014) who proposed a shift from bottom up to moderate top down control of the bacterial biomass by viruses after dust addition, although they did not measure the viral production rates. In our study, the fact that VPlytic was lower in A and SD than in the controls prompted us to hypothesize the following scenarios for the dust-treated mesocosms after enrichment: (1) phage-bacteria dynamics were characterized by a time lag, (2) extensive and continuous lysis events obscured the detection of lytically infected bacterial cells and (3) lytically infected bacterial cells were preferentially grazed by predators due to their beneficial size and nutritional levels.

According to the first scenario, short-term dynamics in the dust-treated mesocosms (Needham et al., 2013) may have resulted in a time-lagged association of bacteria and viruses. Phages may have not been adequate (abundance) or in the appropriate range (composition) to affect bacteria that benefited from the sudden dust pulse in A and SD (Guo et al., 2016), leading to the low measurements of VPlytic. Bacterial resistance to viral infection was developed in experimental (Middelboe et al., 2001) as well as natural systems (Boras et al., 2009), ultimately leading to unaffected bacterial population size.

However, it is frequently seen that bacteria with high productivity support high viral infection and lysis rates, and elevated nutrient concentration favors the lytic cycle (Williamson et al., 2002). Moreover, lysis in nature is a temporally variable process and particularly variable in highly dynamic communities (Bettarel et al., 2002; Winter et al., 2004). Based on these observations, our second hypothesis was that continuous lysis events obscured the detection of lytically infected bacterial cells. In this scenario, the low levels of VPlytic are attributed to the viral reduction approach itself, which may have led to an "artifact" measurement. Zhang et al. (2014) proposed that lysis is constantly occurring in cultures, thus lytically infected cells cannot be measured, while Kimmance et al. (2007) and Winter et al. (2004) proposed that lysis cannot always be detected due to incubation drawbacks. For instance, the duration and time intervals of the incubation may conclude to misleading estimations. Viruses do not all have the same latent period and the possibility that lysis did not occur during the incubation or occurred during a long time interval (e.g., between 12 and 24 h) cannot be excluded. Winget and Wommack (2009) found that maximum VLP abundance was recorded at different times between spring and winter in coastal-system incubations. Cell death or inactivation due to intense light conditions at the sampling time and area may have also contributed to low VPlytic. We exclude the possibility to have induced viral inactivation during the viral reduction approach, as all incubations were done in the dark.

The significantly higher abundance of free viruses in A and SD than the controls at T1 may be a hint that lysis occurred prior to sampling. Similarly to this result, Bonilla-Findji et al. (2009) also measured higher abundance of low DNA content viruses in ambient waters and suggested that these viruses were responsible for lysing active bacterial cells. It is also important to notice that the highest VPlytic could have occurred even earlier in the experiment period, for instance, a few hours after

dust enrichment, as planktonic microbes were P-starved and responded extremely fast to the added phosphorus (Herut et al., 2016, this SI). The lack of viral production measurements in between T-1 and T1 does not allow us to test if VPlytic was higher immediately after dust enrichment. The approach we have used is the most commonly applied method for the estimation of viral production as it is assumed to be the most efficient and the least expensive and time-consuming one compared to others methods. A correction factor was applied in order to balance the bacterial losses due to filtration and manipulation during the experiment (Winget et al., 2005), but, still, activity parameters are highly dynamic (Winter et al., 2004) and make the study of viral production a challenging subject.

The high bacterial production in A and SD further led to the estimation of exceptionally low %BP-VIR, which is among the lowest published levels for coastal systems (Winget and Wommack, 2009). For the calculation of %BP-VIR we used an average burst size value for the Mediterranean Sea (Weinbauer et al., 2003a). However, the burst size may change when the trophic conditions and the activity of the host fluctuate (Parada et al., 2006).

The last scenario for explaining low VPlytic is that heterotrophic flagellates and larger predators preferentially grazed on lytically infected bacterial cells. Specific findings with natural assemblages support that viral infection and lysis depend on the host nutritional and activity characteristics; del Giorgio et al. (1996); Vaqué et al. (2001), and Corzo et al. (2005) found selective elimination of active bacteria by protists. Size and activity—dependent grazing have been also observed in a recent mesocosm experiment where a phytoplankton bloom developed (Baltar et al., 2016). In our study, the abundance of the most efficient bacteria in assimilating the released nutrients increased in response to dust deposition. These cells may have been preferentially infected by viruses and further grazed by bacterial predators. This proposition is supported by the fast increase in dinoflagellate abundance soon after the addition of dust (Tsagaraki et al., 2016, this SI). Dinoflagellates are known to be efficient removers of large amounts of bacterial biomass (Jeong et al., 2008; Dagenais-Bellefeuille and Morse, 2013).

Along with increased BP and decreased %BP-VIR at T1 in A and SD, higher ingestion rates, although not significant, were calculated compared to the controls, which persisted until T8. Ingestion rates were in comparable levels to the ones reported for the open oligotrophic Mediterranean Sea (reviewed by Siokou-Frangou et al., 2010). However, flagellates did not seem to benefit from grazing upon bacteria, as flagellate abundance decreased after dust deposition. The fast development of grazers of flagellates may have caused this, as in Herut et al. (2005) and Lekunberri et al. (2010) who indicated that flagellate grazing controlled bacterial biomass and that further grazing of flagellates by larger predators contributed to the subsequent decrease of the former cells.

Based on the ingestion rate, we tried to estimate the percentage of bacterial biomass removed by flagellates. The resulting percentage always exceeded 100%, indicating that the model was not applicable to our experimental system. The empirical model of Peters (1994) is based on a large dataset covering various ecosystems and it takes into account the size and concentration of predators and prey and temperature. A drawback of the use of this model in the current study may derive from the fact that mesocosms are a highly dynamic system; bacteria are grazed by flagellates, dinoflagellates and ciliates, and at the same time flagellates are consumed by dinoflagellates and ciliates. As a result, not all flagellates graze on bacteria at a given time and not all flagellate size fractions graze on bacteria with the same efficiency (Sato et al., 2007).

In this dynamic system, bacterial size and density change, thus the preference of predators also change, leading to predator-prey relationships, which may not be applicable for the grazing model (André et al., 1999; Böttjer and Morales, 2007). As a result, we assume that the calculated percentage of bacterial production removed by flagellate grazing was notional, and most probably bacteria were lysed before being grazed, while flagellates were also grazed themselves before grazing on bacteria. Even when applying other models (e.g., Vaqué et al., 1994) and when considering only flagellates $<5\,\mu m$ as bacterivorous (Jürgnes and Massana, 2008), which comprised approximately 70% of total flagellates, we obtained similar results.

The stoichiometry of added nutrients may have resulted in a more efficient and faster assimilation of the sudden pulse of nutrients by pico- and nano- sized cells, which led to larger prey availability for larger predators in SD. Apparently greater development of ciliates (including tintinnids) and dinoflagellates in SD took place (Tsagaraki et al., 2016, this SI). As shown before, addition of dust with high nitrogen content leads to faster phosphorus limitation of microbial growth (Christodoulaki et al., 2013; Ridame et al., 2014), and this was probably the case in A that received larger amount of nitrogen compared to SD. An indirect confirmation that at T4 bacteria in A were more P-limited compared to SD could be the higher frequency of lysogenic cells, along with the particularly low bacterial production and growth rate. A negative relationship between bacterial production and the fraction of lysogenic cells has been found in natural and experimental conditions (Jiang and Paul, 1996; Long et al., 2008); it has been suggested that lysogeny is a prevalent viral life cycle under conditions that do not favor the growth of the hosts (Williamson et al., 2002; Weinbauer et al., 2003a). In our experiment, more lysogenic cells were measured in A compared to SD and the controls 4 days after deposition, suggesting that conditions were less favorable for the growth of the hosts at that time. Lysogeny may have been underestimated to some extent, as mitomycin C may not induce nutrient-limited cells (Williamson et al., 2002). Thomas et al. (2011) pointed out that bacteria are differentially affected by mitomycin C and this inducing agent may also be toxic. Nevertheless, it is the most commonly used chemical agent for inducing lysis and it allows comparison with other studies.

CONCLUSIONS

Aeolian dust from the Saharan desert and southern Europe is deposited in the EMS, supplying the surface waters with

nutrients, trace metals and organic matter and influencing the structure and function of the planktonic food web. The results of our study confirm that bacteria were positively affected by dust in terms of biomass, production and growth rate (Pulido-Villena et al., 2008, 2014; Lekunberri et al., 2010; Marañón et al., 2010; Guieu et al., 2014). When bacterial growth rate peaked, bacterial losses due to viral lysis were low. Preferential ingestion of lytically infected cells by bacterivorous predators or continuous lysis events that were not synchronized to the sampling time and incubation intervals may have contributed to the low measurements of lytic viral production. The fast and continuous increase in the abundance of larger predators that grazed on flagellates may have down-regulated their abundance, possibly causing the calculation of misleading bacterial production losses with the use of a grazing model. Stoichiometric differences in the added nutrients through dust between A and SD may have resulted in faster phosphorus limitation in A than SD, which was also indirectly indicated by the higher frequency of lysogenic cells in A than SD. Aerosol deposition drives rapid community responses and the balance between remineralization processes and channeling of biomass further up in the food web is affected by this rapid response. Future research should be directed toward disentangling bacterial mortality due to viral lysis and grazing in order to be able to track the biomass transfer in the food web.

AUTHOR CONTRIBUTIONS

AT designed and conducted viral production experiments, performed flow cytometric and data analysis and wrote the paper. AG performed bacterial production analysis and edited the paper. NN determined flagellate abundance, performed data analysis and edited the paper. NY conducted viral production experiments and edited the paper. BH, TT, and PP obtained funding, designed the mesocosm experiment and edited the paper

ACKNOWLEDGMENTS

This study was funded by the European Union 7th Framework Program (FP7/2007-2013) under grant agreement no. 228224, "MESOAQUA: Network of leading MESOcosm facilities to advance the studies of future AQUAtic ecosystems from the Arctic to the Mediterranean" and by the project ADAMANT: Atmospheric deposition and Mediterranean sea water productivity (number code/MIS: 383551), co-financed by the European Union (European Social Fund–ESF) and Greek national funds through the Operational Program "Education and Lifelong Learning" of the National Strategic Reference Framework (NSRF) (Research Funding Program: THALES). The authors wish to thank the Captain and the crew of the R/V Philia for their assistance in transporting the water from the sea to the mesocosms. Thanks are also due to George Piperakis for his technical assistance throughout the experiment, Nafsika Papageorgiou for measuring chlorophyll *a* concentration, Manolis Tsapakis for measuring dissolved nutrient concentration, Christos Panagiotopoulos and Kalliopi Violaki for measuring dissolved organic carbon concentration, and Elisabet Laia Sá Lago for her valuable recommendations regarding the viral reduction approach. Nutrient leaching experiments were conducted in the Israel Oceanographic and Limnological Research (Haifa) and at the University of Leeds, and results are published in Herut et al. (2016). Finally, three reviewers are gratefully acknowledged for their valuable comments that largely improved the quality of the manuscript.

SUPPLEMENTARY MATERIAL

The Supplementary Material for this article can be found online at: http://journal.frontiersin.org/article/10.3389/fmars.2016.00281/full#supplementary-material

REFERENCES

André, J.-M., Navarette, C., Blanchot, J., and Radenac, M.-H. (1999). Picophytoplankton dynamics in the equatorial Pacific: growth and grazing rates from cytometic counts. *J. Geophys. Res.* 104, 3369–3380. doi: 10.1029/1998JC900005

Baltar, F., Palovaara, J., Unrein, F., Catala, P., Hornák, K., Simek, K., et al. (2016). Marine bacterial community structure resilience to changes in protist predation under phytoplankton bloom conditions. *ISME J.* 10, 568–581. doi: 10.1038/ismej.2015.135

Bettarel, Y., Dolan, J. R., Lemée, R., Masin, M., Pedrotti, M., Rochelle-newall, E., et al. (2002). Strong, weak, and missing links in a microbial community of. *FEMS Microbiol. Ecol.* 42, 451–462. doi: 10.1111/j.1574-6941.2002.tb01034.x

Bonilla-Findji, O., Herndl, G. J., Gattuso, J.-P., and Weinbauer, M. G. (2009). Viral and flagellate control of prokaryotic production and community structure in offshore Mediterranean waters. *Appl. Environ. Microb.* 75, 4801–4812. doi: 10.1128/AEM.01376-08

Bonnet, S., Chiaverini, J., Ras, J., and Stock, A. (2005). Effect of atmospheric nutrients on the autotrophic communities in a low nutrient, low chlorophyll system. *Limnol. Oceanogr.* 50, 1810–1819. doi: 10.4319/lo.2005.50.6.1810

Boras, J. A., Sala, M. M., Vázquez-Domínguez, E., Weinbauer, M. G., and Vaqué, D. (2009). Annual changes of bacterial mortality due to viruses and protists in an oligotrophic coastal environment (NW Mediterranean). *Environ. Microbiol.* 11, 1181–1193. doi: 10.1111/j.1462-2920.2008.01849.x

Böttjer, D., and Morales, C. E. (2007). Nanoplanktonic assemblages in the upwelling area off Concepción (36oS), central Chile: abundance, biomass, and grazing potential during the annual cycle. *Progr. Oceanogr.* 75, 415–434. doi: 10.1016/j.pocean.2007.08.024

Brussaard, C. P. (2004). Optimization of procedures for counting viruses by flow cytometry. *Appl. Environ. Microbiol.* 70, 1506–1513. doi: 10.1128/AEM.70.3.1506-1513.2004

Carbo, P., Krom, M. D., Homoky, W. B., Benning, L. G., and Herut, B. (2005). Impact of atmospheric deposition on N and P geochemistry in the southeastern Levantine basin. *Deep. Res. II Top. Stud. Oceanogr.* 52, 3041–3053. doi: 10.1016/j.dsr2.2005.08.014

Christodoulaki, S., Petihakis, G., Kanakidou, M., Mihalopoulos, N., Tsiaras, K., and Triantafyllou, G. (2013). Atmospheric deposition in the eastern mediterranean. A driving force for ecosystem dynamics. *J. Mar. Syst.* 109–110, 78–93. doi: 10.1016/j.jmarsys.2012.07.007

Cochran, P. K., Kellogg, C. A., and Paul, J. H. (1998). Prophage induction of indigenous marine lysogenic bacteria by environmental pollutants. *Mar. Ecol. Prog. Ser.* 164, 125–133. doi: 10.3354/meps164125

Corzo, A., Rodrıguez-Galvez, S., Lubian, L., Sobrino, C., Sangra, P., and Martinez, A. (2005). Antarctic marine bacterioplankton subpopulations discriminated by

their apparent content of nucleic acids differ in their response to ecological factors. *Polar Biol.* 29, 27–39. doi: 10.1007/s00300-005-0032-2

Dagenais-Bellefeuille, S., and Morse, D. (2013). Putting the N in dinoflagellates. *Front. Microbiol.* 4:369. doi: 10.3389/fmicb.2013.00369

del Giorgio, P. A., Gasol, J. M., Vaqub, D., Mura, P., Agustl, S., and Duarte, C. M. (1996). Bacterioplankton community structure: protists control net production and the proportion of active bacteria in a coastal marine community. *Limnol. Oceanogr.* 41, 1169–1179. doi: 10.4319/lo.1996.41.6.1169

Fuhrman, J. A., and Noble, R. T. (1995). Viruses and protists cause similar bacterial mortality in coastal seawater. *Limnol. Oceanogr.* 40, 1236–1242. doi: 10.4319/lo.1995.40.7.1236

Guieu, C., Ridame, C., Pulido-Villena, E., Bressac, M., Desboeufs, K., and Dulac, F. (2014). Impact of dust deposition on carbon budget: a tentative assessment from a mesocosm approach. *Biogeosciences* 11, 5621–5635. doi: 10.5194/bg-11-5621-2014

Guo, C., Xia, X., Pitta, P., Herut, B., Rahav, E., Berman-Frank, I., et al. (2016). Shifts in microbial community structure and activity in the ultra-oligotrophic eastern mediterranean sea driven by the deposition of saharan dust and European aerosols. *Front. Mar. Sci.* 3:170. doi: 10.3389/fmars.2016.00170

Herut, B., Collier, R., and Krom, M. D. (2002). The role of dust in supplying nitrogen and phosphorus to the South East Mediterranean. *Limnol. Oceanogr.* 47, 870–878. doi: 10.4319/lo.2002.47.3.0870

Herut, B., Rahav, E., Tsagaraki, T. M., Giannakourou, A., Tsiola, A., Psarra, S., et al. (2016). The potential impact of Saharan dust and polluted aerosols on microbial populations in the East Mediterranean Sea, an overview of a mesocosm experimental approach. *Front. Mar. Sci.* 3:226 doi: 10.3389/fmars.2016.00226

Herut, B., Zohary, T., Krom, M. D., and Mantoura, R. F. C. (2005). Response of East Mediterranean surface water to Saharan dust: on-board microcosm experiment and field observations. *Deep Sea Res. II Top. Stud. Oceanogr.* 52, 3024–3040. doi: 10.1016/j.dsr2.2005.09.003

Ivančič, I., and Deggobis, D. (1984). An optimal manual procedure for ammonia analysis in natural waters by the indophenol blue method. *Water Res.* 18, 1143–1147. doi: 10.1016/0043-1354(84)90230-6

Jeong, H. J., Seong, K. A., Yoo, Y. D., Kim, T. H., Kang, N. S., Kim, S., et al. (2008). Feeding and grazing impact by small marine heterotrophic dinoflagellates on heterotrophic bacteria. *J. Eukaryot. Microbiol.* 55, 271–288. doi: 10.1111/j.1550-7408.2008.00336.x

Jiang, S. C., and Paul, J. H. (1996). Occurrence of lysogenic bacteria in marine microbial communities as determined by prophage induction occurrence of lysogenic bacteria in marine microbial communities as determined by prophage induction. *Mar. Ecol. Prog. Ser.* 142, 27–38. doi: 10.3354/meps142027

Jürgnes, K., and Massana, R. (2008). "Protistan grazing on marine bacterioplankton," in *Microbial Ecology of the Oceans*, ed D. L. Kirchman (Hoboken, NJ: John Wiley and Sons, Inc), 383–441.

Kimmance, S. A., Wilson, W. H., and Archer, S. D. (2007). Modified dilution technique to estimate viral versus grazing mortality of phytoplankton: limitations associated with method sensitivity in natural waters. *Aquat. Microb. Ecol.* 49, 207–222. doi: 10.3354/ame01136

Kirchman, D. (1993). Measuring bacterial biomass production and growth rates from leucine incorporation in natural aquatic environments. *Methods Microbiol.* 30, 227–237. doi: 10.1016/S0580-9517(01)30047-8

Kirchman, D., K'nees, E., and Hodson, R. (1985). Leucine incorporation and its potential as a measure of protein synthesis by bacteria in natural aquatic systems. *Appl. Environ. Microbiol.* 49, 599–607.

Krom, M. D., Kress, N., Brenner, S., and Gordon, L. I. (1991). Phosphorus limitation of primary productivity in the eastern Mediterranean Sea. *Limnol. Oceanogr.* 36, 424–432. doi: 10.4319/lo.1991.36.3.0424

Laghdass, M., Blain, S., Besseling, M., Catala, P., Guieu, C., and Obernosterer, I. (2011). Effects of Saharan dust on the microbial community during a large *in situ* mesocosm experiment in the NW Mediterranean Sea. *Aquat. Microb. Ecol.* 62, 201–213. doi: 10.3354/ame01466

Lebaron, P., Servais, P., Agogué, H., Courties, C., and Joux, F. (2001). Does the high nucleic acid content of individual bacterial cells allow us to discriminate between active cells and inactive cells in aquatic systems? *Appl. Environ. Microbiol.* 67, 1775–1782. doi: 10.1128/AEM.67.4.1775-1782.2001

Lee, S., and Fuhrman, J. E. D. A. (1987). Relationships between biovolume and biomass of naturally derived marine bacterioplanktont. *Appl. Environ. Microbiol.* 53, 1298–1303.

Lekunberri, I., Lefort, T., Romero, E., Vazquez-Dominguez, E., Romera-Castillo, C., Marrase, C., et al. (2010). Effects of a dust deposition event on coastal marine microbial abundance and activity, bacterial community structure and ecosystem function. *J. Plankton Res.* 32, 381–396. doi: 10.1093/plankt/fbp137

Lelieveld, J., Proestos, Y., Hadjinicolaou, P., Tanarhte, M., Tyrlis, E., and Zittis, G. (2016). Strongly increasing heat extremes in the Middle East and North Africa (MENA) in the 21st century. *Clim. Change* 137, 245–260. doi: 10.1007/s10584-016-1665-6

Long, A., McDaniel, L. D., Mobberley, J., and Paul, J. H. (2008). Comparison of lysogeny (prophage induction) in heterotrophic bacterial and Synechococcus populations in the Gulf of Mexico and Mississippi River plume. *ISME J.* 2, 132–144. doi: 10.1038/ismej.2007.102

Marañón, E., Fernández, A., Mouriño-Carballido, B., Martínez-García, S., Teira, E., Cermeño, P., et al. (2010). Degree of oligotrophy controls the response of microbial plankton to Saharan dust. *Limnol. Oceanogr.* 55, 2339–2352. doi: 10.4319/lo.2010.55.6.2339

Marie, D., Partensky, F., Jacquet, S., and Vaulot, D. (1997). Enumeration and cell cycle analysis of natural populations of marine picoplankton by flow cytometry using the nucleic acid stain SYBR Green I. *Appl. Environ. Microbiol.* 63, 186–193.

Middelboe, M., Hagström, A., Blackburn, N., Sinn, B., Fischer, U., Borch, N. H., et al. (2001). Effects of bacteriophages on the population dynamics of four strains of pelagic marine bacteria. *Microb. Ecol.* 42, 395–406. doi: 10.1007/s00248-001-0012-1

Morán, X. A. G., Bode, A., Suárez, L. Á., and Nogueira, E. (2007). Assessing the relevance of nucleic acid content as an indicator of marine bacterial activity. *Aquat. Microb. Ecol.* 46, 141–152. doi: 10.3354/ame046141

Motegi, C., Nagata, T., Miki, T., Weinbauer, M. G., and Legendre, L. (2009). Viral control of bacterial growth efficiency in marine pelagic environments. *Limnol. Oceanogr.* 54, 1901–1910. doi: 10.4319/lo.2009.54.6.1901

Needham, D. M., Chow, C.-E., Cram, J. A., Sachdeva, R., Parada, A., and Fuhrman, J. A. (2013). Short-term observations of marine bacterial and viral communities: patterns, connections and resilience. *ISME J.* 7, 1274–1285. doi: 10.1038/ismej.2013.19

Parada, V., Herndl, G. J., and Weinbauer, M. G. (2006). Viral burst size of heterotrophic prokaryotes in aquatic systems. *J. Mar. Biol. Assoc. U.K.* 86, 613–621. doi: 10.1017/S002531540601352X

Pernthaler, J. (2005). Predation on prokaryotes in the water column and its ecological implications. *Nat. Rev. Microbiol.* 3, 537–546. doi: 10.1038/nrmicro1180

Peters, F. (1994). Prediction of planktonic protistan grazing rates. *Limnol. Oceanogr.* 39, 195–206. doi: 10.4319/lo.1994.39.1.0195

Porter, K. G., and Feig, Y. S. (1980). The use of DAPI for identifying aquatic microfloral. *Limnol. Oceanogr.* 25, 943–948. doi: 10.4319/lo.1980.25.5.0943

Pulido-Villena, E., Baudoux, A.-C., Obernosterer, I., Landa, M., Caparros, J., Catala, P., et al. (2014). Microbial food web dynamics in response to a Saharan dust event: results from a mesocosm study in the oligotrophic Mediterranean Sea. *Biogeosciences* 11, 5607–5619. doi: 10.5194/bg-11-5607-2014

Pulido-Villena, E., Wagener, T., and Guieu, C. (2008). Bacterial response to dust pulses in the western Mediterranean: implications for carbon cycling in the oligotropic ocean. *Glob. Biogeochem. Cycles* 22, 1–12. doi: 10.1029/2007GB003091

Ridame, C., Dekaezemacker, J., Guieu, C., Bonnet, S., L'Helguen, S., and Malien, F. (2014). Phytoplanktonic response to contrasted Saharan dust deposition events during mesocosm experiments in LNLC environment. *Biogeosciences* 11, 4783–4800. doi: 10.5194/bg-11-4783-2014

Rimmelin, P., and Moutin, T. (2005). Re-examination of the MAGIC method to determine low orthophosphate concentration in seawater. *Anal. Chim. Acta* 548, 174–182. doi: 10.1016/j.aca.2005.05.071

Sato, M., Yoshikawa, T., Takeda, S., and Furuya, K. (2007). Application of the size-franctionation method to simultaneous estimation of clearance rates by heterotrophic flagellates and ciliates of pico- and nanophytoplankton. *J. Exp. Mar. Ecol. Biol.* 349, 334–343. doi: 10.1016/j.jembe.2007.05.027

Seinfeld, J.H., and Pandis, S.N. (1998). *Atmospheric Chemistry and Physics*. New York, NY: Wiley.

Shi, Z., Krom, M. D., Bonneville, S., and Benning, L. G. (2015). Atmospheric processing outside clouds increases soluble iron in Mineral Dust. *Environ. Sci. Technol.* 49, 1472–1477. doi: 10.1021/es504623x

Siokou-Frangou, I., Christaki, U., Mazzocchi, M. G., Montresor, M., Ribera d' Alcalá, M., Vaqué, D., et al. (2010). Plankton in the open Mediterranean Sea: a review. *Biogeosciences* 7, 1543–1586. doi: 10.5194/bg-7-1543-2010

Smith, D. C., and Azam, F. (1992). A simple, economical method for measuring bacterial protein synthesis rates in seawater using 3H-leucine. *Mar. Microb. Food Webs* 6, 107–114.

Sohrin, R., and Sempéré, R. (2005). Seasonal variation in total organic carbon in the northeast Atlantic in 2000-2001. *J. Geophys. Res.* 110:C10S90, doi: 10.1029/2004jc002731

Strickland, J. D. H., and Parsons, T. R. (1972). "Determination of phosphorus," in *A Practical Handbook of Sea-Water Analysis, 2nd Edn., Bulletin No 167*, eds J. D. H. Strickland and T. R. Parsons (Ottawa: Fisheries Research Board of Canada), 123–124.

Tapper, M., and Hicks, R. (1998). Temperate viruses and lysogeny in lake superior bacterioplankton. *Limnol. Oceanogr.* 43, 95–103. doi: 10.4319/lo.1998.43.1.0095

Ternon, E., Guieu, C., Ridame, C., L'Helguen, S., and Catala, P. (2011). Longitudinal variability of the biogeochemical role of Mediterranean aerosols in the Mediterranean Sea. *Biogeosciences* 8, 1067–1080. doi: 10.5194/bg-8-1067-2011

Thingstad, T. F. (2000). Elements of a theory for the mechanisms controlling abundance, diversity, and biogeochemical role of lytic bacterial viruses in aquatic systems. *Limnol. Oceanogr.* 45, 1320–1328. doi: 10.4319/lo.2000.45.6.1320

Thomas, R., Berdjeb, L., Sime-Ngando, T., and Jacquet, S. (2011). Viral abundance, produciton, decay rates and life strategies (lysogeny versus lysis) in Lake Bourget (France). *Environ. Microbiol.* 13, 616–630. doi: 10.1111/j.1462-2920.2010.02364.x

Tsagaraki, M. T., Pitta, P., Herut, B., Rahav, E., Berman Frank, I., Tsiola, A., et al. (2016). Atmospheric deposition effects on plankton communities in the Eastern Mediterranean, a mesocosm experimental approach. *Front. Mar. Sci.* 3:226. doi: 10.3389/fmars.2016.00226

Vaqué, D., Alonso-Sáez, L., Arístegui, J., Agustí, S., Duarte, G. M., Sala, M. M., et al. (2014). Bacterial production and losses to predators along an open ocean productivity gradient in the subtropical North East Atlantic Ocean. *J. Plankton Res.* 36, 198–213. doi: 10.1093/plankt/fbt085

Vaqué, D., Casamayor, E. O., and Gasol, J. M. (2001). Dynamics of whole community bacterial production and grazing losses in seawater incubations as related to the changes in the proportions of bacteria with different DNA content. *Aquat. Microb. Ecol.* 25, 163–177. doi: 10.3354/ame025163

Vaqué, D., Gas, J. M., and Marrase, C. (1994). Grazing rates on bacteria: the significance of methodology and ecological factors. *Mar. Ecol. Prog. Ser.* 109, 263–274. doi: 10.3354/meps109263

Volpe, G., Banzon, V. F., Evans, R. H., Santoleri, R., Mariano, A. J., and Sciarra, R. (2009). Satellite observations of the impact of dust in a low-nutrient, low- chlorophyll region: fertilization or artifact? *Glob. Biochem. Cycles* 23, 1–14. doi: 10.1029/2008gb003216

Weinbauer, M. G., Brettar, I., and Höfle, M. G. (2003a). Lysogeny and virus-induced mortality of bacterioplankton in surface, deep, and anoxic marine waters. *Limnol. Oceanogr.* 48, 1457–1465. doi: 10.4319/lo.2003.48.4.1457

Weinbauer, M. G., Christaki, U., Nedoma, J., and Šimek, K. (2003b). Comparing the effects of resource enrichment and grazing on viral production in a meso-eutrophic reservoir. *Aquat. Microb. Ecol.* 31, 137–144. doi: 10.3354/ame031137

Weinbauer, M. G., and Peduzzi, P. (1994). Frequency, size and distribution of bacteriophages in different marine bacterial morphotypes. *Mar. Ecol. Prog. Ser.* 108, 11–20. doi: 10.3354/meps108011

Winget, D. M., Williamson, K. E., Helton, and Wommack, K. E. (2005). Tangential flow diafiltration: an improved technique for estimation of virioplankton production. *Aquat. Microb. Ecol.* 41, 221–232. doi: 10.3354/ame041221

Williamson, S. J., Houchin, L. A., Mcdaniel, L., and Paul, J. H. (2002). Seasonal variation in lysogeny as depicted by prophage induction in tampa bay, Florida. *Appl. Environ. Microbiol.* 68, 4307–4314. doi: 10.1128/AEM.68.9.4307

Winget, D. M., and Wommack, K. E. (2009). Diel and daily fluctuations in virioplankton production in coastal ecosystems. *Environ. Microbiol.* 11, 2904–2914. doi: 10.1111/j.1462-2920.2009.02038.x

Winter, C., Herndl, G. J., and Weinbauer, M. G. (2004). Diel cycles in viral infection of bacterioplankton in the North Sea. *Aquat. Microb. Ecol.* 35, 207–216. doi: 10.3354/ame035207

Yentsch, C. S., and Menzel, D. W. (1963). A method for the determination of phytoplankton chlorophyll and phaeophytin by fluorescence. *Deep Sea Res.* 10, 221–231. doi: 10.1016/0011-7471(63)90358-9

Zhang, J., Ormälä-Odegrip, A., Mappes, J., and Laakso, J. (2014). Top-down effects of a lytic bacteriophage and protozoa on bacteria in aqueous and biofilm phases. *Ecol. Evol.* 4, 4444–4453. doi: 10.1002/ece3.1302

Conflict of Interest Statement: The authors declare that the research was conducted in the absence of any commercial or financial relationships that could be construed as a potential conflict of interest.

frontiers in Marine Science

ORIGINAL RESEARCH
published: 27 April 2017
doi: 10.3389/fmars.2017.00113

Planktonic Lipidome Responses to Aeolian Dust Input in Low-Biomass Oligotrophic Marine Mesocosms

Travis B. Meador[1], Nadine I. Goldenstein[1], Alexandra Gogou[2], Barak Herut[3], Stella Psarra[4], Tatiana M. Tsagaraki[4] and Kai-Uwe Hinrichs[1]*

[1] Department of Geosciences, MARUM Center for Marine Environmental Sciences, University of Bremen, Bremen, Germany, [2] Institute of Oceanography, Hellenic Centre for Marine Research, Anavyssos, Greece, [3] National Institute of Oceanography, Israel Oceanographic and Limnological Research, Haifa, Israel, [4] Institute of Oceanography, Hellenic Centre for Marine Research, Heraklion, Greece

The effect and fate of dry atmospheric deposition on nutrient-starved plankton in the Eastern Mediterranean Sea (EMS; Crete, 2012) was tested by spiking oligotrophic surface seawater mesocosms (3 m^3) with Saharan dust (SD; 1.6 g L^{-1}; 23 nmol NO_x mg^{-1}; 2.4 nmol PO_4 mg^{-1}) or mixed aerosols (A; 1.0 g L^{-1}; 54 nmol NO_x mg^{-1}; 3.0 nmol PO_4 mg^{-1}) collected from natural and anthropogenic sources. Using high resolution liquid chromatography-mass spectrometry, the concentrations of over 350 individual lipids were measured in suspended particles to track variations in the lipidome associated with dust fertilization. Bacterial and eukaryotic intact polar lipid (IPL) biomarkers were categorized into 15 lipid classes based on headgroup identity, including four novel IPL headgroups. Bulk IPL concentrations and archaeal tetraether lipids were uncoupled with the doubling of chlorophyll concentrations that defined the stimulation response of oligotrophic plankton to SD or A amendment. However, molecular level analysis revealed the dynamics of the IPL pool, with significant additions or losses of specific IPLs following dust spikes that were consistent among treatment mesocosms. Multivariate redundancy analysis further demonstrated that the distribution of IPL headgroups and molecular modifications within their alkyl chains were strongly correlated with the temporal evolution of the plankton community and cycling of phosphate. IPLs with phosphatidylcholine, betaine, and an alkylamine-like headgroup increased in the post-stimulated period, when phosphate turnover time had decreased by an order of magnitude and phosphorus uptake was dominated by plankton >2 μm. For most IPL classes, spiking with SD or A yielded significant increases in the length and unsaturation of alkyl chains. A lack of corresponding shifts in the plankton community suggests that the biosynthesis of nitrogenous and phosphatidyl lipids may respond to physiological controls during episodic additions of dust to the EMS. Furthermore, alkyl chain distributions of IPLs containing N, P, and S invoked a bacterial source, suggesting that bacterioplankton are able to modulate these lipids in response to nutrient stress.

Keywords: diacylglycerol lipids, fatty acids, oligotrophic food web, dust fertilization, HPLC-MS/MS

OPEN ACCESS

Edited by:
Angel Borja, AZTI Pasaia, Spain

Reviewed by:
Jenan Kharbush, Harvard University, USA
Ana Marta Gonçalves, University of Coimbra, Portugal

****Correspondence:***
Travis B. Meador
travis.meador@uni-bremen.de

Specialty section:
This article was submitted to Marine Ecosystem Ecology, a section of the journal Frontiers in Marine Science

Received: *19 January 2017*
Accepted: *10 April 2017*
Published: *27 April 2017*

Citation:
Meador TB, Goldenstein NI, Gogou A, Herut B, Psarra S, Tsagaraki TM and Hinrichs K-U (2017) Planktonic Lipidome Responses to Aeolian Dust Input in Low-Biomass Oligotrophic Marine Mesocosms. Front. Mar. Sci. 4:113. doi: 10.3389/fmars.2017.00113

INTRODUCTION

In the ultra-oligotrophic Eastern Mediterranean Sea (EMS), biological production is (co)limited by both nitrogen (N) and phosphorus (P) (e.g., Krom et al., 1991; Thingstad et al., 2005a) and is primarily driven by picoplankton and recycling within the microbial loop. Atmospheric deposition of dust and aerosols has been acknowledged as a predominant source of nutrients and trace metals to the ultraoligotrophic surface waters of the EMS (e.g., Guerzoni et al., 1999; Herut et al., 1999; Guieu et al., 2002) that has basin-wide implications for the stoichiometric balance of N and P (Krom et al., 2004). The significant contribution of this nutrient source to biological production in the region has been invoked by both geochemical estimates of new production (Kouvarakis et al., 2001; Herut et al., 2002; Markaki et al., 2003) and biogeochemical responses to dust addition, including increases in primary and bacterial production and chlorophyll *a* (Chl-*a*) concentration (Herut et al., 2005; Laghdass et al., 2011; Guieu et al., 2014). The annual dust flux to Mediterranean surface waters can be controlled by just a few events that deliver up to 30% of the total flux (e.g., Guerzoni et al., 1999; Kubilay et al., 2000), and the number of these events are projected to increase with increasing temperatures and decreasing relative humidity associated with climate change (Klingmüller et al., 2016). As such, responses of the planktonic community to episodic dust pulses should play an increasing role in determining food web structure and the carbon budget of the oligotrophic ocean.

To further investigate this phenomenon, the MESOAQUA experiment (May 2012; Heraklion, Crete) simulated intense dry atmospheric deposition in the ultraoligotrophic EMS by spiking surface seawater mesocosms (Cretan Sea) with two different natural aerosols collected in the Levantine Basin: Saharan dust (SD) or mixed aerosols (A; Herut et al., 2016). Biogeochemical responses to the addition of SD or A, including plankton community composition and production, pigment concentration, and cycling of macro-nutrients and trace elements, were compared in triplicate to unamended control mesocosms over a period of 8 days (Guo et al., 2016; Herut et al., 2016; Rahav et al., 2016; Tsiola et al., 2016; Tsagaraki et al., under revision, this SI). In addition to these bulk biogeochemical measures of food web dynamics, the diversity of algal and bacterial cell membrane lipids provides a moderate level of taxonomic and physiological information (e.g., Sato, 1992; Guschina and Harwood, 2006; Sohlenkamp and Geiger, 2015) that can be applied to assess organic matter reactivity (Harvey and Macko, 1997; Wakeham et al., 1997), plankton communities in the ocean (e.g., Van Mooy and Fredricks, 2010), and carbon and nutrient fluxes in marine food webs (Dalsgaard et al., 2003; Sebastián et al., 2016). For example, phytoplankton populations are able to reduce their cellular P quota by substituting phospholipids with sulfolipids or betaine lipids when P is limiting (Van Mooy et al., 2009) and nutrient gradients across the Mediterranean appear to drive the lipid distribution of plankton communities (Popendorf et al., 2011b). Recent advances in lipid analysis via tandem ultra high pressure liquid chromatography mass spectrometry (UHPLC-MS) now allow rapid and enhanced detection of intact polar lipids (IPLs) as well as structural elucidation of their polar headgroups and alkyl chains (e.g., Wörmer et al., 2013). Sophisticated molecular networks have also been employed to facilitate the interpretation of the large data sets obtained by such analyses (Kharbush et al., 2016).

The goal of the current study was to track changes in lipid distributions associated with atmospheric deposition simulated during the MESOAQUA experiment. Parallel measurements of bulk biogeochemical parameters allowed for further assessment of lipid biomarkers as indicators of the taxonomic and physiological responses of marine plankton to dust fertilization in the oligotrophic ocean. Bacterial and eukaryotic IPLs were the most abundant and responsive biomarkers, and this study assesses the sources, cycling, and physiological adaptations of previously described and novel lipid classes.

MATERIALS AND METHODS

Mesocosm Experiment and Biomarker Sampling

Surface seawater was collected from 10 m depth on the 8th and 9th May 2012 aboard the R/V Philia from a site at 5 nautical miles off the north coast of Crete (35° 24.957′ N, 25° 14.441′ E) and pumped into nine mesocosm bags (3 m^3) located in the facilities of Hellenic Centre for Marine Research (HCMR, Crete, Greece). After filling, three mesocosms were inoculated with SD (1.6 g L^{-1}) collected during dust storms in Crete (Heraklion and Sambas) and Israel (Beit Yannay) or with a mixture of desert/mineral dust and polluted aerosols (A; 1.0 g L^{-1}) of European and desert origin; the final three mesocosms served as unamended control treatments (Herut et al., 2016). SD amendments corresponded to spikes of 37 nM NO_x (nitrate + nitrite), 3.9 nM PO_4 and increases in Mn and Fe by ∼6 and ∼4 nM, respectively (Herut et al., 2016). Amendments to A mesocosms corresponded to spikes of 54 nM NO_x and 2.0 nM P and an increase in Mn by ∼1 nM and no increase in Fe (Herut et al., 2016). Samples for biomarker analysis (20 L) were collected from each mesocosm before the dust addition (May 10th; day −1) and subsequently on days 3 and 6 following dust addition (May 13th and 16th; day 3 and day 6). Acid-washed *silicon* tubing was lowered to the middle of the mesocosm and seawater was pumped into 20 L acid-washed Nalgene carboys. Within 1 h, the samples were filtered via a vacuum manifold system onto glass fiber filters (GF/F, nominal pore size = 0.7 μm; Whatman) and stored at −20°C until extraction in the laboratory in Bremen, Germany.

Lipid Extraction and Analysis

GF/F samples were placed into 40 mL Teflon tubes containing 2–2.5 g combusted sand and a recovery standard (2 μg phosphatidylcholine C_{21} or C_{19} fatty acid; Avanti Polar Lipids Inc.). The samples were extracted twice with a solvent mixture (25 mL) containing methanol, methylene chloride, phosphate buffer (2/1/0.8 v/v) using a sonication probe (Bandelin Sonoplus Model HD2200; 5 min, 0.6 s pulses, 200 W). Following sonication, Teflon extraction tubes were centrifuged at 2,500 rpm for 10 min

and the supernatant was decanted into a combusted separation funnel. The extraction was repeated twice using a solvent mixture containing methanol, methylene chloride, and a trichloroacetic acid buffer (2/1/0.8 v/v; Sturt et al., 2004), and finally twice more using a solvent mixture containing methanol/methylene chloride (1/5, v/v). The supernatants were combined and partitioned into aqueous and apolar phases following the addition of methylene chloride and water to the separation funnel (30 mL each). The apolar phase was collected into an Erlenmeyer flask and the aqueous phase was re-extracted thrice with methylene chloride (30 mL). The aqueous phase was then discarded and the combined apolar phase was returned to the separation funnel and washed thrice with water.

The final total lipid extract (TLE) was dried under N_2 gas and biomarker analysis was performed using a Dionex Ultimate 3,000 ultra-high pressure liquid chromatography (UHPLC) system coupled to a Bruker maXis ultra-high resolution quadrupole time-of-flight (QTOF) mass spectrometer via electrospray ionization source. For IPL analysis, an aliquot containing 10% of the TLE was injected onto an Acquity BEH HILIC amide column (2.1 × 150 mm, 1.7 μm, Waters, Germany) following the protocol described by Wörmer et al. (2013). Lipids were identified according to their expected retention times, exact masses, and mass fragmentation patterns (**Table 1**; Figures S1–S6). IPL ions were quantified based on the recovery of the internal PC standard and their response relative to an injection standard (PAF, Avanti Polar Lipids Inc.). Response factors for the identified lipid classes were determined for representative diacylglycerol lipid standards (Table S1); the response factor data were acquired during the same week as IPL data. Only duplicate time point measurements are available for some experiments (i.e., day 3 for all treatments and day −1 for the A treatment) due to lack of an internal standard or available response factors.

Archaeal tetraether lipids were quantified following injection of 10% TLE onto an Agilent Eclipse XDB-C18 column (5 μm, 9.4 × 250 mm; after Zhu et al., 2013; Table S2). A C_{46} tetraether was used as the injection standard (Huguet et al., 2006) for quantification of archaeal tetraethers; no response factor was applied.

Ancillary Analyses of Environmental Parameters

Protocols for the determination of chlorophyll concentration, bacterio-and picoplankton cell abundances, primary and bacterial production, and phosphate concentration, uptake and turnover time in the mesocosms were reported by Herut et al. (2016) as well as Guo et al. (2016) and Tsiola et al. (2016). Tsagaraki et al. (under revision, this SI) additionally describe measurements of nutrient concentration, abundances of autotrophic picoplankton and zooplankton, and alkaline phosphatase activity.

Statistical Assessments

Hierarchical Clustering Analysis

The average relative abundance distribution of carbons and unsaturations in the alkyl chains attached to IPLs was compared via hierarchical clustering analysis. The similarity matrix was assembled using the unweighted average distance algorithm (UPGMA) and dissimilarity was measured as 1 min the Pearson correlation. The headgroups of some IPLs were attached to a limited number of diglyceride moieties (≤4; **Table 1**) and were not included in the hierarchical analysis, as their alkyl chain composition were relatively easily compared to that of other IPLs but skewed the dissimilarity matrix.

Redundancy Analysis (RDA)

Statistical modeling was conducted using R-3.0.2 and available package "vegan" (Oksanen et al., 2015). For the application of statistical methods, the dataset was reduced to an acceptable ratio of samples to variables of ≥1. To achieve this reduction, data were grouped based on structural similarities, such as headgroup commonalities, and investigated patterns within the chain distribution for each IPL class separately. An ordination method was used to explore the parametric relationships between abundance of lipid groups as well as distribution of core lipid composition and environmental parameters. Ordination creates linear combinations of variables represented by vectors that are called principal components, gradients, or axes. The multiplication factors are called loadings. The method applied here is based on constrained ordination, namely RDA, and it takes explanatory variables into account, which allows a direct modeling of the cause-effect relationship between species data (i.e., lipid groups) and environmental parameters (*ad-hoc*). RDA was performed to infer the influence of the different treatments on the distribution of IPL headgroups and on the alkyl chain distributions of the individual IPL groups (RDA_1). Thereafter, RDA was used to explore the impact of treatments compared to the day of sampling on variability of IPL headgroups and their alkyl chain composition (RDA_2). The significance of the individual models was evaluated by comparison of *p*-values (Tables S2, S3).

Because the time of sampling showed a high collinearity with several environmental parameters, the explanatory potential of these parameters was investigated in a separate analysis (Table S4). The control of environmental parameters on the IPL headgroup distribution was first tested for each parameter individually ($RDA_{3.1–3.31}$). Significant parameters were then chosen based on *p*-values, narrowing the environmental parameters to 13, which could then be included in a combined RDA analysis. Multi-collinearity between environmental variables was avoided by using variance inflation factors as a measure for insignificant results in ordination due to co-linearity. Monte Carlo permutation tests provide information on the general model performance and the significance of individual explanatory variables within the model, and were performed to test the significance of the combined RDA-derived model. Thereafter, variables were selected based on forward selection of explanatory variables using the function ordiR2step, available within "vegan," which uses R^2 adjusted and *p*-value as criteria for model reduction. A parsimonious RDA was calculated with the reduced set of selected explanatory variables and Monte Carlo permutation was again applied to gain information on the significance of the full reduced model and the individual terms within the reduced model.

TABLE 1 | IPLs detected in mesocosm incubations of surface seawater collected in the Eastern Mediterranean Sea.

Group	DAG Lipid	*n*	Relative Abundance (%)	Retention Time		(m/z)		Headgroup elemental formula[a]	MS^2 Characteristic
				Min	Max	Min	Max		
1	MGDG.1	38	29.4 ± 4.2	3.7	4.4	664.4994	802.6403	$C_{11}H_{20}NO_{10}$[b]	Neutral loss of 197
2	*MGDG.2*	30	6.4 ± 1.8	4.5	5.1	664.4994	856.6872	*ibid.*	*ibid.*
3	*MGDG.3*	12	1.1 ± 0.4	5.1	5.4	692.5307	794.5777	*ibid.*	*ibid.*
4	MGDG-OH	4	0.7 ± 0.4	4.5	5.9	732.5256	760.5569	*ibid.*	Neutral loss of 197, hydroxy fatty acid
5	*MGDG+H_2O*	4	0.6 ± 0.5	4.1	5.7	762.5726	790.6039	$C_{11}H_{22}NO_{11}$[b]	Neutral loss of 215
6	***AA-L.1***	3	2.1 ± 1.2	6.6	6.7	640.5875	696.6501	$C_{11}H_{20}$**N**O_5	Neutral loss of 199
7	***AA-L.2***	4	2.8 ± 0.8	7.3	7.5	642.5667	722.6293	$C_{12}H_{22}$**N**O_6	Neutral loss of 264, 238, or 210
8	**DGTS**	62	3.7 ± 0.4	7.3	7.7	626.4990	796.7025	$C_{12}H_{20}$**N**O_7	Neutral loss of 236
9	**DGTA**	53	3.2 ± 1.0	9.4	10.0	628.5147	796.7025	*ibid.*	Neutral loss of 236
10	***GSL-OH***	33	1.2 ± 0.7	8.6	9.1	710.5202	836.6610	$C_{10}H_{18}$**N**O_8	Neutral loss of 162
11	*GA-L*	24	5.0 ± 0.8	5.9	6.5	614.4626	742.6191	$C_8H_{16}NO_8$[b]	*ibid.*
12	SQ	7	4.4 ± 2.2	10.6	10.9	756.4926	868.6178	$C_{11}H_{17}O_{12}S$	285 fragment; loss of 261
13	MGA	22	8.3 ± 2.2	10.8	11.8	678.4787	844.6508	$C_{11}H_{20}NO_{11}$[b]	Neutral loss of 211
14	**PC**	40	2.0 ± 0.8	10.2	11.2	622.4440	840.6470	$C_{10}H_{19}$**N**O_8**P**	184 fragment
15	DGDG	20	3.0 ± 1.7	11.9	12.3	852.5679	938.6775	$C_{17}H_{30}NO_{15}$[b]	Neutral loss of 359

[a] *Ionized derivatives of IPL headgroups, including the glycerol moiety and carboxy terminus (as radical) of the alkyl chains (cf.* ***Figure 2****; Text S1).*
[b] *Ammonia adduct ion $[M+NH_4]^+$.*
Bold indicates IPLs that contain covalently linked N or P. Italics indicates the seven IPLs identified in the current study have been resolved and/or reported for the first time in surface seawater. See ***Figure 2*** *for abbreviations.*

Significance Tests

In support of the significant alterations of IPL distributions identified by RDA, the differences among specific IPLs between mesocosm treatments or time points were assessed via a two-tailed homoschedastic Student's *t*-test. Significant differences were denoted by $p < 0.05$.

RESULTS

Biological Responses to Dust Addition

Changes in the structure of the plankton community in response to SD or A addition were thoroughly assessed by companion studies (Guo et al., 2016; Herut et al., 2016; Tsiola et al., 2016; Tsagaraki et al., under revision, this SI) and can be summarized as follows. Chlorophyll a (Chl-*a*) concentrations had doubled in mesocosms on days 2 and 3 following the addition of SD or A, which were significantly higher compared to the control; this increase coincided with significant increases in *Synechococcus* and autotrophic picoeukaryotes (Guo et al., 2016). Concentrations of bacteria were also significantly higher in treatment mesocosms compared to the control (Guo et al., 2016). In contrast to significant increases in Chl-*a* on days 2 and 3, microzooplankton increased throughout the mesocosm experiment, with the major groups, including ciliates and tintinids, combining for up to ca. 2700 cells L^{-1} on average on the final sampling at day 8 (Tsagaraki et al., under revision, this SI). Collectively, the significant increases in both Chl-*a* and cell counts were indicative that dust and aerosol additions had positive effects on the plankton community, hereafter referred to as "stimulated plankton," even though Chl-*a* concentrations remained relatively low in these oligotrophic mesocosms in comparison to nutrient replete oceanographic regions (e.g., upwelling regimes).

In terms of the Chl-*a* response, biomarker sampling coincided with the pre-addition (day-1), stimulated (day 3), and post-stimulated (day 6) periods. By converting from Chl-*a*, bacteria, and zooplankton concentrations, IPLs associated with the stimulated plankton were predicted to reach maximum concentrations (ca. 1.5 μg IPL L^{-1}) within 1–3 days following amendment with SD or A (**Figure 1**).

Concentrations of Archaeal Lipids

Concentrations of archaeal glycerol dibiphytanyl glycerol tetraether (GDGT) ranged from 0.2 to 2.0 ng L^{-1} (**Figure 1D**). GDGTs decreased in concentration over the duration of each experimental treatment with the greatest losses observed in the SD treatment, which fell to roughly half of the initial values by day 6 (**Figure 1D**). The distribution of cyclopentane rings in the GDGT molecule did not vary significantly between treatments or time points, with caldarchaeol and crenarchaeol consistently dominating the lipid profile (28 ± 2.6% and 47 ± 2.5%, respectively; data not shown).

Intact Polar Lipids (IPLs)

IPL Headgroup Diversity

A total of 355 individual bacterial and eukaryotic IPL biomarkers were categorized into 15 lipid classes according to their headgroup composition (**Table 1**; **Figure 2**; Text S1). The mass spectral properties of four of these IPL classes (35

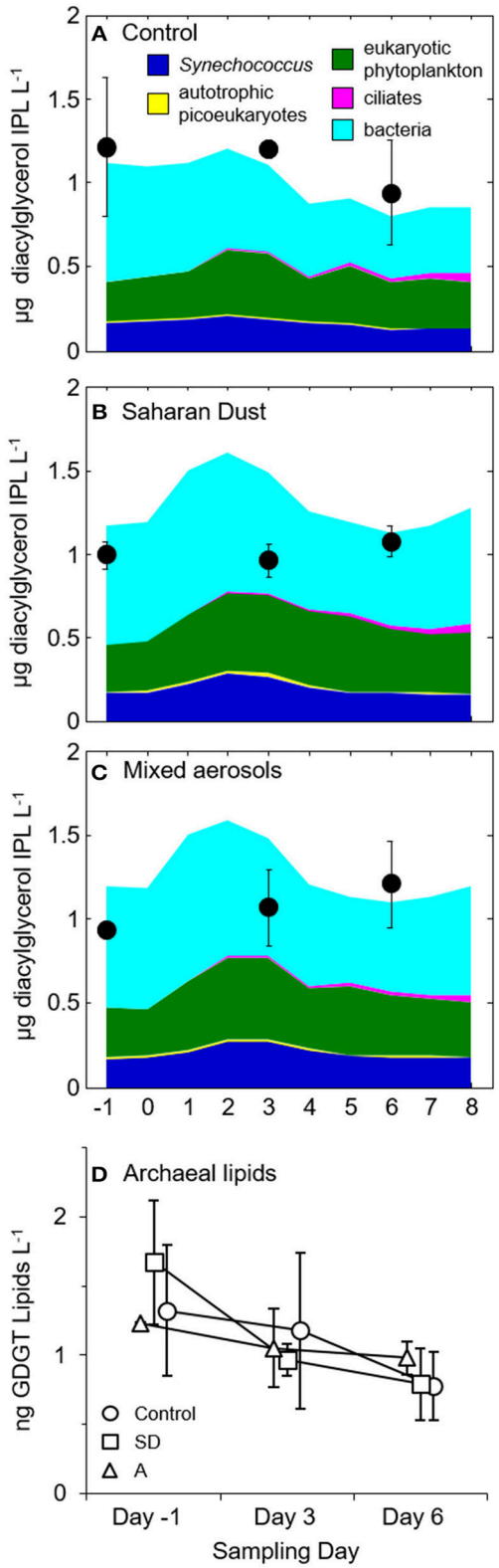

FIGURE 1 | Predicted (colored areas) and measured (black circles) IPL concentrations in (A) control, **(B)** Saharan dust, and **(C)** mixed aerosol mesocosms. Error bars represent the standard deviation of replicate

(Continued)

FIGURE 1 | Continued

mesocosms. The predicted concentrations of lipids belonging to bacteria (Bac), *Synechococcus* (Syn), and autotrophic picoeukaryotes (Pico) were estimated by converting from measurements of cell density and assuming cell diameter of 0.5 μm for bacteria (Simon and Azam, 1989), 1 μm for *Synechococcus* (Waterbury et al., 1979) and autotrophic picoeukaryotes (Palenik et al., 2007) and thus factors of 1.7, 6.8, and 6.8 fg lipid cell^{-1}, respectively (Lipp et al., 2008). Lipid concentrations of eukaryotic phytoplankton were converted from Chl-a concentrations of the large size class (>2 μm) via a Chl:C conversion factor of 0.03 (Geider et al., 1997) and assuming that C represents 50% of cell dry weight and lipids were 15% of the cell dry weight (e.g., Thompson, 1996). Lipids derived from ciliates were based on counts (cf. Section Biological Responses to Dust Addition) and assuming a conversion of 17.1 pg fatty acid ciliate^{-1} (Harvey and Macko, 1997). **(D)** Concentrations of archaeal tetraether lipids in control (circles), Saharan dust (SD; squares), and mixed aerosol mesocosms (A; triangles). Samples collected on the same day are offset on the x-axis to illustrate the association of each averaged value with its standard deviation, indicated by the error bars.

compounds) only allowed for tentative identification of headgroup and backbone linkages to alkyl chains. Multiple series of isobaric ions, i.e., with identical masses (±0.001 Da) eluting at different retention times, were identified for monoglycosides (MGDG; Figure S1) and the betaine lipids diacylglyceryl N,N,N-trimethylhomoserine (DGTS) and diacylglyceryl-hydroxymethyl-N,N,N-trimethyl-β-alanine (DGTA). Other IPLs comprised only single headgroup series, including sulfoquinovosyldiacylglycerol (SQ), diglycosides (DGDG), uronic acids (MGA; Figure S2), phosphatidyl choline (PC), and hydroxylated forms of MGDG (MGDG-OH; Figure S2) and glycosphingolipids (GSL-OH; Figure S3). Four novel lipid classes are described; they exhibited polarity, elemental formulae, and/or fragment ions consistent with IPLs, but their headgroups remain uncertain, including a hydrated MGDG (MGDG+H_2O; Figure S2), two alkylamine-like lipids (AA-L.1, AA-L.2; Figures S4, S5), and a glyceric acid-like lipid (GA-L; Figure S7). The most relatively abundant lipids were MGDG.1 (41 ± 6%), followed by MGA (12 ± 3%), MGDG.2 (9 ± 3%), and SQ (6 ± 3%; **Figure 3**). The average relative abundances of the remaining IPL classes were each <5%, but accounted for roughly 32 ± 4% of IPLs on average.

IPL Alkyl Chain Distributions

Lipid classes contained up to 62 individual IPLs that differed in the number of carbons and/or unsaturations in their alkyl chains (**Table 1**). In most cases, fatty acid chains are characterized by their summed number of carbons and unsaturations; therefore, odd vs. even-numbered fatty acids are not differentiated and odd sums refer to the attachment of both one even and one odd chain to the glycerol backbone. Based on the weighted average (wt. avg.) alkyl chain distributions, GSL-OH lipids exhibited the longest carbon chains and among the highest number of unsaturations (36.8 ± 1.0 and 2.3 ± 1.3, respectively; **Table 1**; **Figure 4A**), while the wt. avg. unsaturations of all other lipid classes were ≤1.6, with MGDG.3 and SQ classes containing the fewest unsaturations (wt. avg. unsaturations < 0.2; **Table 1**; **Figure 4B**). It is important to note that the backbone moiety of GSL-OH is a ceramide and not glycerol, and its alkyl chain

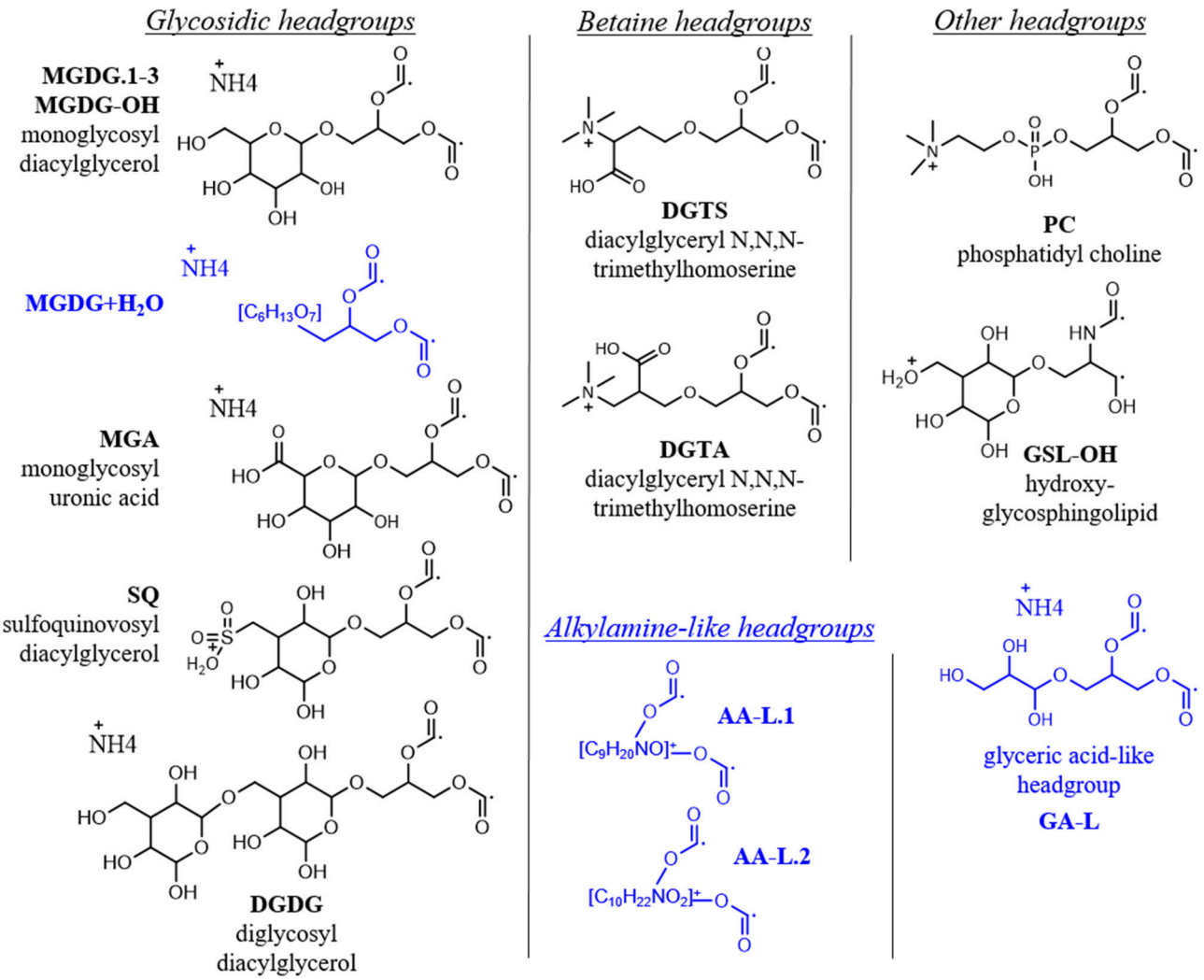

FIGURE 2 | IPL headgroups in oligotrophic ocean mesocosms. Depicted are the adducts of the headgroup and glycerol moieties with radical ions in place of alkyl chains, corresponding to their elemental formulae used for high resolution MS identification (i.e., CxHxNxOx; cf. **Table 1**). Putative structures of novel headgroups identified during this study are shown in blue. MS2 spectra for novel headgroups are provided in Figures S2–S6 and described in Text S1.

length described here refers to sum of the fatty acid and sphingoid base. Thus, the length of GSL-OH chains are three C atoms longer than other IPLs, as only the carbons in the headgroup have been excluded from this measure, whereas, for all other IPLs, both headgroup and glycerol carbons have been excluded. PCs spanned the largest range in molecular weight (m/z 622–840; **Table 1**), representing a difference of roughly 15 methylene groups, with a distribution that was weighted toward shorter alkyl chains (wt. avg. = 30.4 ± 0.7; **Figure 4A**). Other lipid classes exhibiting relatively short alkyl chains include MGDG.3 and SQ (wt. avg. < 30; **Table 1**; **Figure 4A**).

DGTS and DGTA, both betaine lipids, exhibited the highest diversity (i.e., Simpson diversity index) in terms of their alkyl chain composition (**Figure 4C**). Although the alkyl chain distributions of GA-L were highly diverse (**Figure 4C**), the number of C atoms and unsaturations in the diglyceride moiety cannot be further interpreted due to uncertainty in the headgroup composition (Figure S6). The IPL classes MGDG-OH, MGDG+H_2O, AA-L.1, and AA-L.2 each comprised ≤4 compounds, making them the least diverse among the IPLs detected in the mesocosms. The diversity in chain distribution for each lipid class was typically lowest in the control treatments (**Figure 4C**) but highly variable between replicate samples. A hierarchical clustering analysis of the diversity of IPL diglyceride moieties indicated that the alkyl chains of GSL-OH were the most unique, grouping independently of all other IPLs (**Figure 5**; Figure S7). This analysis further revealed two IPL subgroups according to the similarity/dissimilarity of their alkyl chain distributions (**Figure 5**), including a "glycosidic" group (i.e., MGDG.1, MGDG.2, MGA) and a "nutrient-availability" group (i.e., DGTA, DGTS, DGDG, PC, SQ, and MGDG.3;

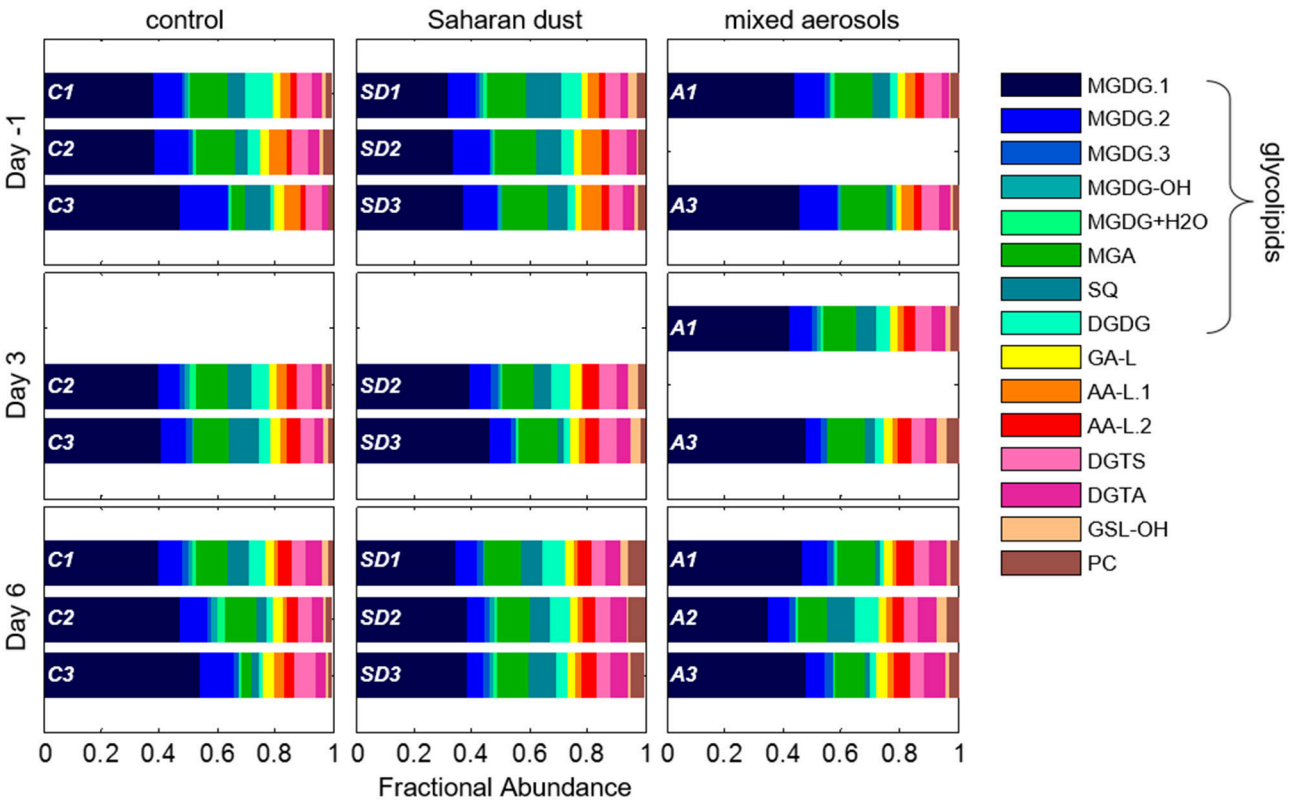

FIGURE 3 | Relative distribution of IPLs in replicate mesocosms of the control (C), Saharan dust (SD), and mixed aerosol (A) experiments on each sampling day. Data for each replicate mesocosm are shown as one barplot in each panel in consistent order.

cf. Section Hierarchical Clustering Analysis of IPL Alkyl Chains).

IPL Concentrations

While chlorophyll concentrations returned to pre-addition values by day 6 (Tsagaraki et al., under revision, this SI; Tsiola et al., 2016), total IPL concentration in all treatment mesocosms exhibited a net increase of 4–24% (40–220 ng L^{-1}). This is in contrast to control mesocosms, in which the chlorophyll response was lower than in treatment mesocosms and IPL concentrations fell by 12–35% by day 6 (140–530 ng L^{-1}; $p < 0.01$; **Figure 6**). Changes in IPL concentration between replicate mesocosms were more variable on day 3 (**Figure 6**).

IPL classes responded differently during the progression of the experiments. Increases in the concentration of the most abundant IPL (40–130 ng MGDG.1 L^{-1}) accounted for the majority of the gross increase in total IPL concentration on day 6 in treatment mesocosms (25–51%). Replicate mesocosms also exhibited consistent additions of some minor lipids, including DGTA (30–40 ng L^{-1}), PC (10–40 ng L^{-1}), and AA-L.2 (20–40 ng L^{-1}), together accounting for 38–51% of the gross increase in IPLs. In contrast, both control and treatment mesocosms exhibited consistent losses of MGDG.2 (10–90 ng L^{-1}) and AA-L.1 (20–80 ng L^{-1}) by day 6. The only IPL that paralleled changes in Chl-*a* concentration in both treatment mesocosms was GSL-OH, which increased by 10–30 ng L^{-1} (ca. 2–3 fold) on day 3 and returned to pre-addition values by day 6 (**Figure 6**). IPL classes among SD and A mesocosms exhibited the same general trends during the evolution of the plankton community, with few exceptions: (i) the increases in PC and DGDG on day 6 were significantly greater in response to SD additions ($p < 0.03$); (ii) day 3 losses of AA-L.1 were greater in the SD treatment (44 ± 6 vs. 15 ± 6 ng L^{-1}; $p < 0.05$); and (iii) SQ concentrations decreased in SD mesocosms on day 3 (32 ± 16 ng L^{-1}) but increased in A mesocosms (23 ± 12 ng L^{-1}; **Figure 6**). In terms of nutrient allocation, the net increases of AA-L.2, DGTA, GSL-OH, and PC in the treatment mesocosms represented, on average, 0.3 and 3.5% of the N and P added via SD, and 0.2 and 1.2% of the N and P added via A.

Redundancy Analysis (RDA) of IPL Distributions

The constrained ordination model based on RDA (Tables S2, S3) identified significant changes in IPL headgroup and alkyl chain relative abundance distributions in treatment vs. control samples (RDA_1). The significance of the model for explaining IPL headgroup and chain distributions increased with the addition of a temporal component that accounted for sampling day (RDA_2).

IPLs in SD or A Treatments vs. Control (RDA_1)

RDA revealed only slight differences in the SD or A treatments compared to the control (Table S2). For the SD treatment, the

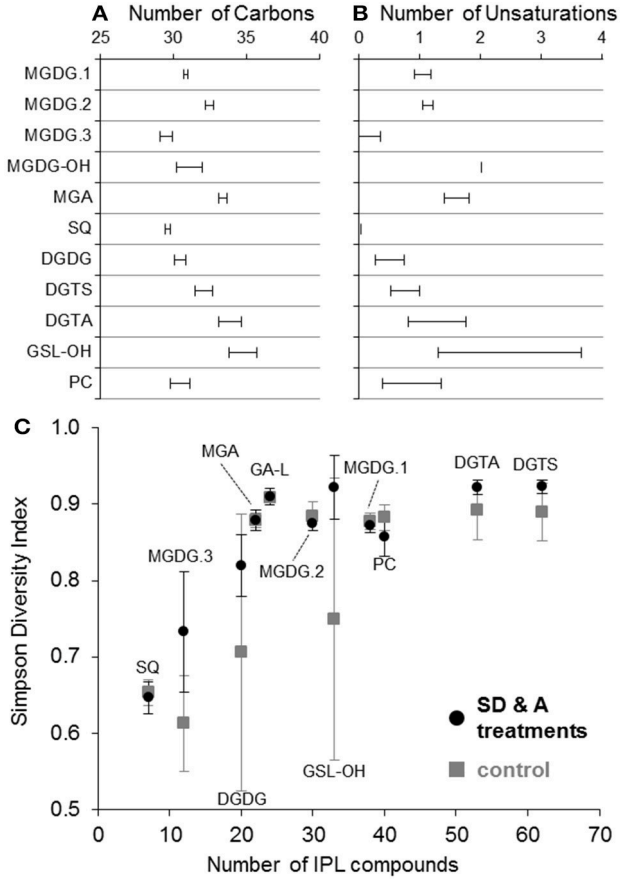

FIGURE 4 | Weighted average (±1 standard deviation) number of carbons (A) and unsaturations **(B)** in the alkyl chain of IPLs. The Simpson diversity index of each IPL class **(C)** was determined as: $1 - \sum_{i=1}^{N} (\text{fractional abundance})^2$, where f is the fractional abundance of lipid i, and N is the total number of lipids in each IPL class. The average Simpson index values for IPL classes in control ($n = 8$; gray squares) and treatment samples collected on days 3 and 6 ($n = 10$; black circles) are plotted against the total number of compounds identified for each IPL class. Error bars indicate one standard deviation.

average relative abundance (± standard deviation) of DGTA (4.4 ± 0.3%) and GSL-OH (2.9 ± 0.2%) were significantly higher than the control (3.0 ± 0.2% and 1.2 ± 0.1%, respectively; $p < 0.05$) on day 3 (**Figure 7**). PC relative abundance was significantly higher in the SD treatment at day 6 (4.8 ± 0.4%), compared to both the control (1.9 ± 0.4%; $p < 0.005$) and A treatments (3.0 ± 0.5%; $p < 0.01$). The A treatment exhibited significant enrichments in DGTA relative to the control on both day 3 (4.2 ± 0.1% vs. 3.0 ± 0.2%) and day 6 (6.2 ± 0.6% vs. 4.1 ± 0.7%; $p < 0.03$; **Figure 7**).

The RDA models comparing the alkyl chain distributions of individual headgroup classes between control and treatment mesocosms ($RDA_{1.1-1.13}$) identified significant differences for several lipid classes, including MGDG.1, MGDG.3, DGTS, and DGTA (Table S2). The relative abundance of longer alkyl chains ($>C_{34}$) and unsaturations generally increased in response to SD or A additions (**Table 2**). In particular, alkyl chains summing to C_{38} were relatively enriched for all of these IPLs, excluding MGDG.3, and consistent decreases in C_{30} alkyl chains were observed in A mesocosms (**Table 2**).

IPL Composition of Pre-addition, Stimulated, and Post-stimulated Samples (RDA_2)

To infer the influence of the day of sampling on the abundance of lipid classes and core lipid composition, a temporal term was added to the RDA model (RDA_2). By accounting for day of sampling, the model had a much higher potential for explaining the variability in IPL distributions ($p = 0.003$) and the core lipid composition of all but two lipid classes ($RDA_{2.1-2.11}$; $p < 0.05$; Table S3). The increased significance of the model containing a temporal component (RDA_2) is consistent with the stimulation of plankton on day 3 in all mesocosms and subsequent post-stimulated sampling on day 6. The significance of RDA_2 was further confirmed via Student's t-test comparisons of individual samples. In comparison to the headgroup distributions observed in SD or A mesocosms on day-1, the relative abundances of MGDG.2 and AA-L.1 significantly decreased, whereas DGTA, AA-L.1, and PC increased during the progression from pre- to post-stimulated conditions in the SD and A treatments (**Figure 7**). Control mesocosms also exhibited a significant decrease in AA-L.2 on day 6 (**Figure 7**). Only the SD treatment induced significant enrichments of GA-L ($p < 0.01$; **Figure 7**).

Similar patterns of alkyl chain distributions were observed in both treatments as well as the control mesocosms, including significant enrichments in MGDG.1 and DGTS lipids with alkyl chains comprising 28 and 31 carbons, respectively, and significant depletions of DGTS lipids comprising 28 carbons in the alkyl chain (**Table 2**). The relative increase in DGTA lipids observed for both the SD and A treatments (cf. **Figure 7**) was accompanied by more unsaturations as well as diglyceride moieties comprising 40 carbon atoms (**Tables 2, 3**). In general, for IPLs that were found to be significantly explained by the RDA_2 model (Table S3), the stimulation of plankton induced by either dust treatment resulted in elongation and increased unsaturation of the diglyceride moiety (**Tables 2, 3**).

Comparing IPL Distributions with Environmental Parameters (RDA_3)

Based on the evidence that alterations in IPL composition were synchronized with the evolution of the plankton community (RDA_2), another model was designed to further explore which environmental parameters were characteristic of the stimulation of plankton and may thus explain IPL variability ($n = 31$; RDA_3). Significant correlations between individual environmental parameters and IPL composition were assessed by the respective RDA models ($RDA_{3.1-31}$; cutoff value of $p < 0.1$; Table S4), thereby reducing the data set to 13 environmental parameters that potentially explained headgroup distribution. These 13 parameters were subjected to a forward selection procedure to reduce variance inflation, ultimately reducing the dataset to a single environmental parameter that best explained IPL distributions: phosphate turnover time (τ_{PO4}; $p < 0.001$). It is important to note that environmental variables that may have co-varied with τ_{PO4} (e.g., nutrient concentrations; cf. Table S4) were also significant for explaining IPL distributions. However,

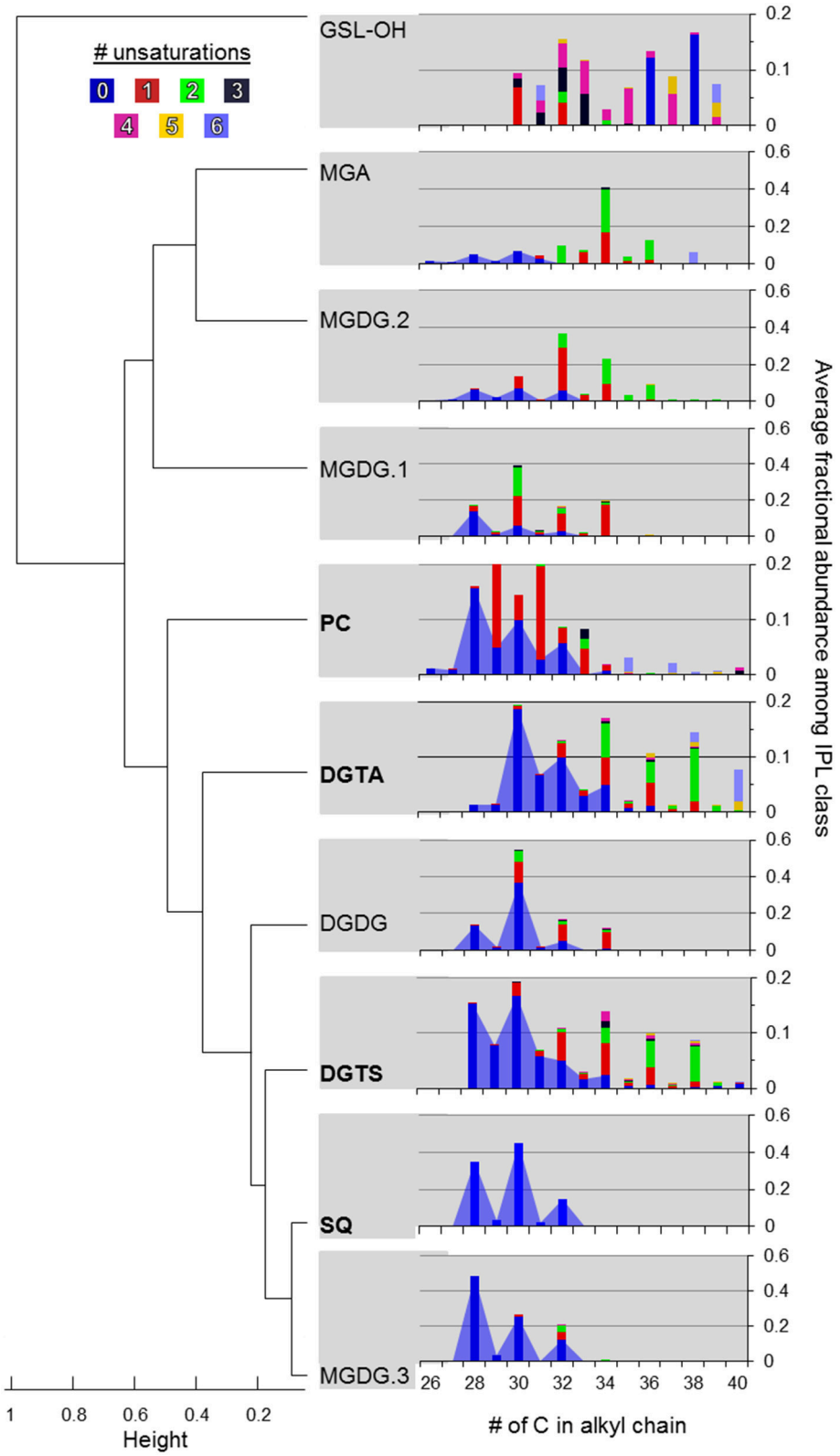

FIGURE 5 | Hierarchical clustering of IPL classes based on alkyl chain distributions in their diacylglycerol moiety. Agglomeration was determined via the unweighted average distance algorithm (UPGMA) and dissimilarity was measured as one minus the Pearson correlation. IPLs shown in bold are thought to be modulated by plankton in response to P-limitation (cf. Van Mooy et al., 2009). The color code refers to the number of unsaturations in the alkyl chains. The blue area shows the relative abundance of saturated alkyl chains summing to ≤34 carbons.

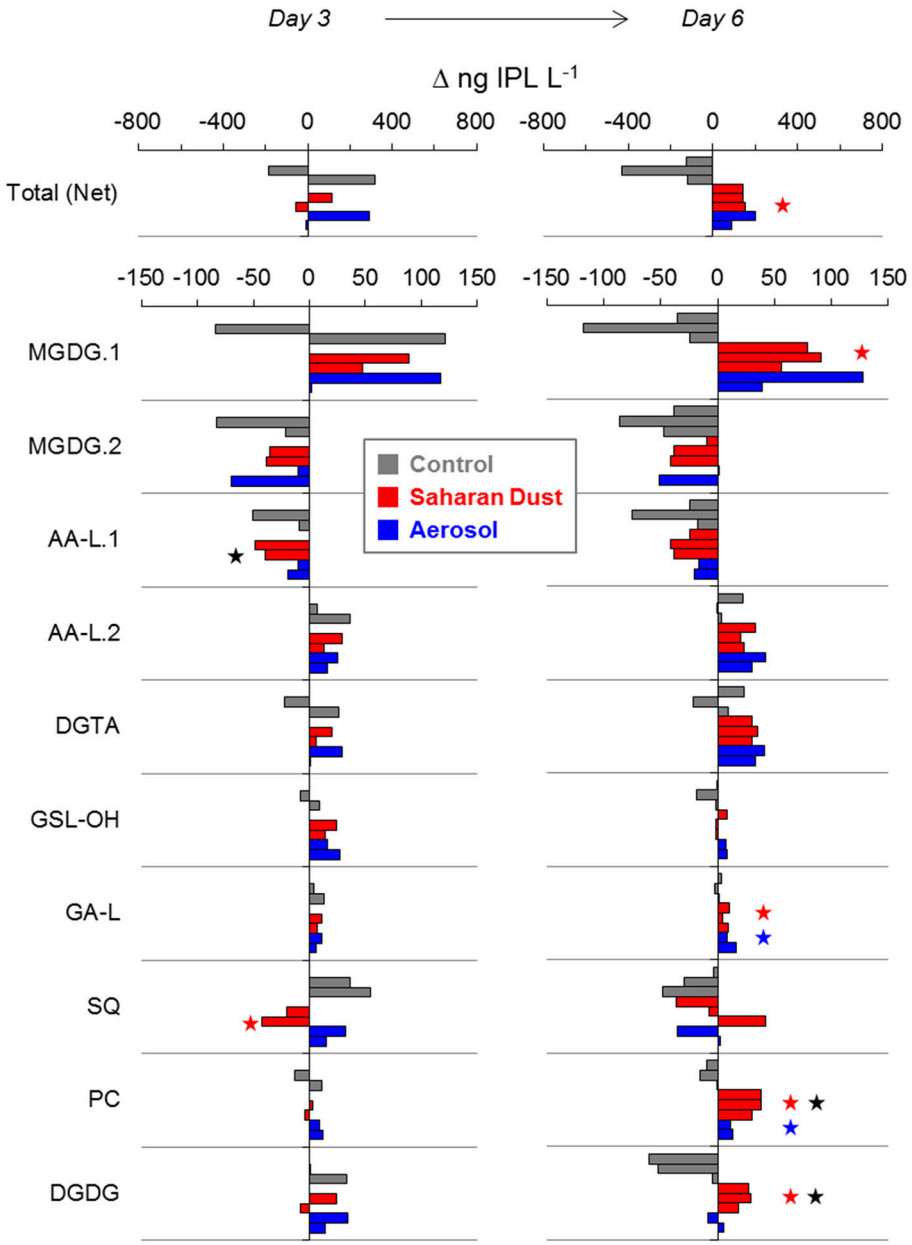

FIGURE 6 | Changes in IPL concentration relative to day −1 in each replicate mesocosm of control (gray), Saharan dust (red), and mixed aerosol (blue) treatments. Significant differences to the control mesocosms are indicated by a red or blue star. Black stars indicate significant differences between Saharan dust and mixed aerosol mesocosms. Each bar represents one replicate mesocosm of each treatment, shown in consistent order.

these additional environmental parameters were excluded from the parsimonious RDA because (i) the *p*-values derived from the Monte-Carlo simulation were not as significant as for τ_{PO4}, and (ii) as determined by the forward selection algorithm, their inclusion did not improve the significance of the parsimonious RDA model. Therefore, only τ_{PO4} was incorporated into a parsimonious RDA (**Figure 8**). Samples collected from control mesocosms and those collected prior to SD or A addition (i.e., on day −1) generally exhibited more negative values on the first RDA axis, whereas treatment samples collected on day 3 or 6 grouped with positive values. The negative loadings for τ_{PO4} along the first RDA axis correspond to increased τ_{PO4} in the control mesocosms and prior to day 3 sampling in the treatment mesocosms.

τ_{PO4} decreased from >60 min. at day −1 to <6 min. at day 6 in the treatment mesocosms (Herut et al., 2016; Tsagaraki et al., under revision, this SI) and was positively correlated to relative abundances of MGDG.2 and AA-L.1 ($p < 0.05$; **Figure 9**). DGTA, and PC, and AA-L.2 peaked at day 6 and were negatively correlated with τ_{PO4} ($p < 0.05$; **Figure 9**). The

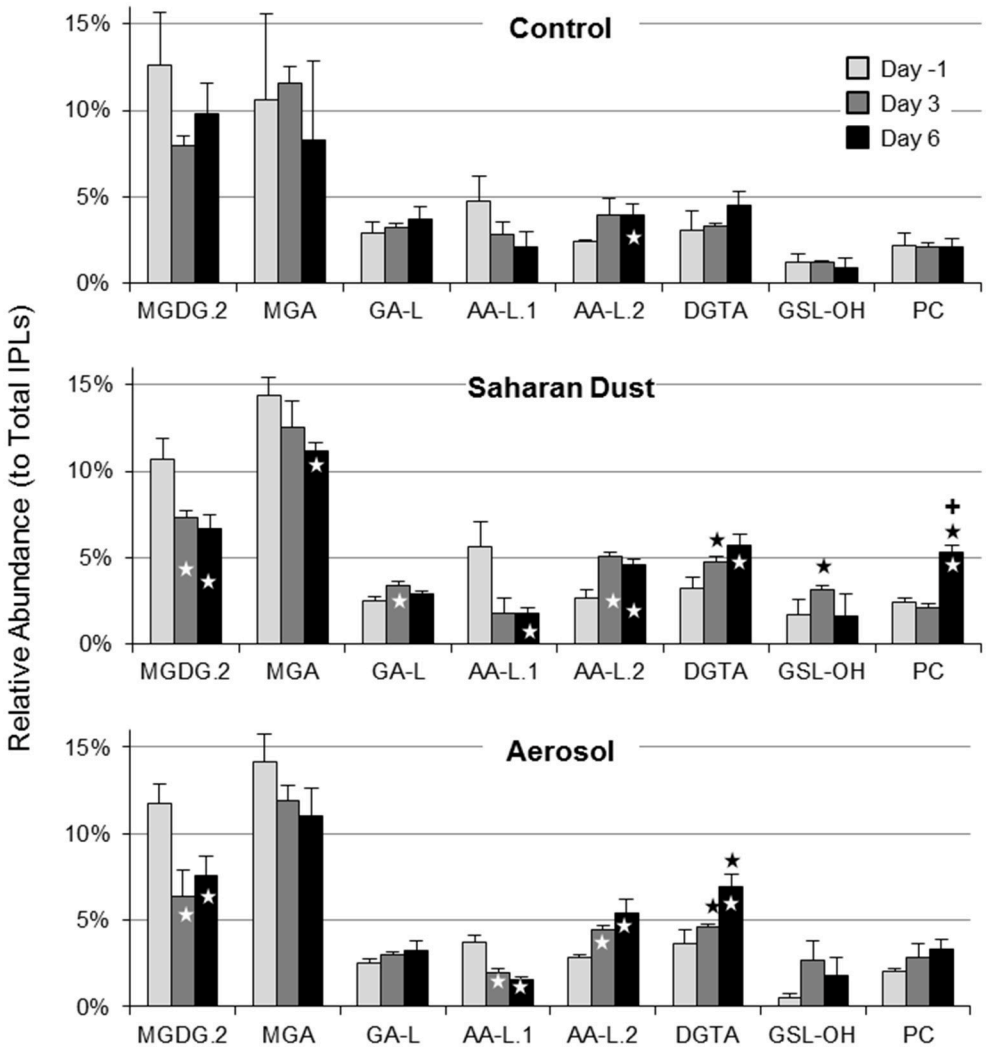

FIGURE 7 | Average relative abundance of selected IPLs in control, Saharan dust, and mixed aerosol mesocosms. Significant differences relative to the control or between Saharan dust and mixed aerosol treatments are indicated by black stars or plus symbols, respectively. Significant changes relative to the day −1 sample for each treatment are indicated by white stars. Error bars indicate one standard deviation.

size-fractionated distribution of P uptake (i.e., 0.2–0.6, 0.6–2, and >2 μm) also shifted during the evolution of the plankton community (Tsagaraki et al., under revision, this SI). P uptake by plankton > 2 μm increased to account for over one-third of total P uptake in the treatment mesocosms at day 6, coinciding with the significant increases in DGTA, PC, and AA-L.2 ($p < 0.01$). In contrast, the relative abundance of MGDG.2 and AA-L.1 were positively associated with percent uptake of P by the smallest size fraction of plankton (0.2–0.6 μm; $p < 0.01$), which was highest at day −1 in each mesocosm (>20%).

DISCUSSION

The additions of SD or A to oligotrophic surface seawater mesocosms were designed to mimic natural deposition events and triggered increases in Chl-*a* up to 0.15 μg L^{-1}, which is roughly 3- to 100-fold lower than the maximum concentrations encountered during previous IPL surveys (**Table 4**). The low range in Chl-*a* concentration underscores the oligotrophic setting of the EMS and thus the scope of this study, such that the stimulation of plankton and their associated lipid biomarkers recorded here were not as pronounced as in regions that span larger gradients in nutrient or Chl-*a* concentrations, thus complicating the assignment of IPLs to their source organisms. Archaeal GDGT lipid biomarkers were relatively low in abundance (corresponding to roughly 10^3 archaeal cells mL^{-1}; assuming 1.4 fg lipid $cell^{-1}$; Lipp et al., 2008) and the cycloalkyl distribution was similar between samples and consistent with previous reports in this region (Kim et al., 2015). Changes in GDGT concentration were similar in control and treatment mesocosms and are not further discussed.

TABLE 2 | Significant increases (+) or decreases (–) in the relative abundance distribution of C atoms in the alkyl chains of IPLs.

IPL	Treatment	26	27	28	29	30	31	32	33	34	35	36	37	38	39	40	41
TREATMENT vs. CONTROL MESOCOSMS																	
MGDG.1	SD						–										
	A					–								+			
MGDG.3	SD									+							
	A					–				+							
DGTS	SD										+			+		–	
	A					–								+			
DGTA	SD													+			
	A				–	–		–						+		+	
DAY –1 vs. DAY 3 | DAY 6																	
MGDG.1	C			|+													
	SD			|+		|–	|–	–|+		|+							
	A			|+													
MGDG.2	C		|–								|+			|–	|–		
	SD				|–												
	A	–|–	|–						|+					|–	|–		
MGDG.3	C				+|+												
	SD					–|–											
	A			–|–				+|+									
DGTS	C			|–			|+									+|+	
	SD			|–			|+	+|+	|+								
	A			|–			+|+					|+				+|+	
DGTA	C																
	SD															+|	
	A									|–			–|			|+	
GSL–OH	C																
	SD								+|+			+|	+|				
	A								|+	|–	|+	|+			|+	|–	
GA–L	C		|+														
	SD		|+	|–	|–			|+									
	A			|–			|+	+|+									
MGA	C								+|+			–|	+|				
	SD	|–							+|					+|			
	A	|–				|–								|+			
PC	C						|+			|–							
	SD			|+	|–		|–	|–			+|						
	A		–|					|–			|+					|–	
DGDG	C																
	SD				–|–	|–		|+		+|						
	A																

Comparisons refer to the average chain distributions in Saharan dust (SD) or mixed aerosol (A) vs. control (C) mesocosms or between days –1 and day 3 or 6 in the same treatment. The absence of an IPL class in the table is indicative of no significant change.

High resolution MS together with fragmentation patterns promoted identification and quantification of over 350 different IPLs and 15 IPL classes that were defined based on headgroup composition (**Table 1**; Text S1). The roster of IPLs identified in seawater was expanded to include chromatographically-resolved stereoisomers of previously known lipids (i.e., MGDG.1-3), molecular alterations of MGDG (i.e., MGDG-OH, MGDG+H_2O), lipids that have not previously been detected in the surface ocean (GSL-OH, GA-L), and additional novel, nutrient-bearing lipid headgroups (AA-L.1-2; **Table 1**; Text S1). 15 IPL headgroups (**Figure 2**; Text S1). Tentative assignment of shared vs. distinct sources of some IPL classes was gleaned from the composition of their alkyl chains (Section IPL Taxonomic Source Indications). IPLs delivered by dust has been acknowledged dust as a potentially important source of IPLs to the surface ocean (e.g., up to 0.43 mg g^{-1}; De Deckker et al., 2008) and, although the IPL concentration of SD or A material used to spike the mesocosms was not measured, this input is considered to explain differences and temporal evolution of the lipidome among SD, A, and control mesocosms. Based on the assumption that IPL concentrations scale linearly with the abundance of their source organisms, changes in lipid concentration were attributed to either allochthonous input, growth or removal processes (Section Turnover of the IPL Pool). RDA further identified the coupling of IPL relative abundance distributions with phosphate turnover time, which dropped to below 6 min in the post-stimulated period (Section Constrained Ordination Modeling of IPL Responses).

IPL Taxonomic Source Indications

Deciphering meaningful trends encoded by IPL composition is complicated by the multiple and often overlapping factors that determine the arrangement of polar headgroups and their linkage to fatty acids. Culture studies and oceanographic surveys of natural populations over broad physical and geochemical gradients have achieved some consensus on the association of lipid headgroups with plankton phylogeny (**Table 4**), with the caveat that several phylogenetic groups may produce the same IPL. The parallel changes in plankton abundance among treatment mesocosms (Guo et al., 2016; Tsagaraki et al., under revision, this SI; **Figure 1**) thus prohibit assignment of IPLs to their source organisms based solely on these data. However, from a taxonomic point of view, longer (C_{18}–C_{22}), even-numbered, and polyunsaturated fatty acids (PUFAs) are generally attributable to higher-level, eukaryotic plankton, whereas shorter (C_{10}–C_{20}), odd-numbered, and saturated or mono-unsaturated forms are characteristic features of bacterial fatty acids (e.g., Kaneda, 1991; Thompson, 1996; Bergé and Barnathan, 2005).

Most of the IPLs that have been described in other surface ocean environments (**Table 4**) were also detected in the mesocosms sampled during the current study, with the notable exception of phosphatidyl glycerol (PG) and phosphatidyl ethanolamine (PE). These IPLs are thought to derive from heterotrophic bacteria (**Table 4**), which may have passed through the GF/F filter (nominal pore size = 0.7 μm), but both PG and PE were detected by previous studies that have employed these

TABLE 3 | Significant increases (+) or decreases (–) in the relative abundance distribution of unsaturations in the alkyl chains of IPLs.

IPL	Treatment	0	1	2	3	4	5	6
TREATMENT vs. CONTROL MESOCOSMS								
MGDG.1	SD							
	A	–		+	+	+	+	
MGDG.3	SD	–						
	A	–	+					
DGTS	SD							
	A				+	+	+	+
DGTA	SD							
	A	–			+	+	+	+
GSL–L	SD		–		+	+	+	
	A	+	–				+	+
DAY –1 vs. DAY 3 | DAY 6								
MGDG.1	C							
	SD					+|		
	A						+|	
MGDG.2	C							
	SD							
	A							
MGDG.3	C							
	SD			|+				
	A	–|–	+|+	+|+				
DGTS	C							
	SD		|+			+|	+|	+|
	A					|+	|+	|+
DGTA	C							
	SD							
	A					|+	|+	|+
GSL–OH	C							
	SD					|+		
	A	+|+					+|	|+
GA–L	C							
	SD	|–						
	A							
MGA	C		|–					
	SD		|–	|+				+|
	A	|–	|–	|+				+|+
PC	C							
	SD	|+	–|–					
	A							|+
DGDG	C							
	SD	|–	|+					
	A	–|		|+	+|	+|		

Comparisons refer to the average chain distributions in Saharan dust (SD) or mixed aerosol (A) vs. control (C) mesocosms or between days –1 and day 3 or 6 in the same treatment. The absence of an IPL class in the table is indicative of no significant change.

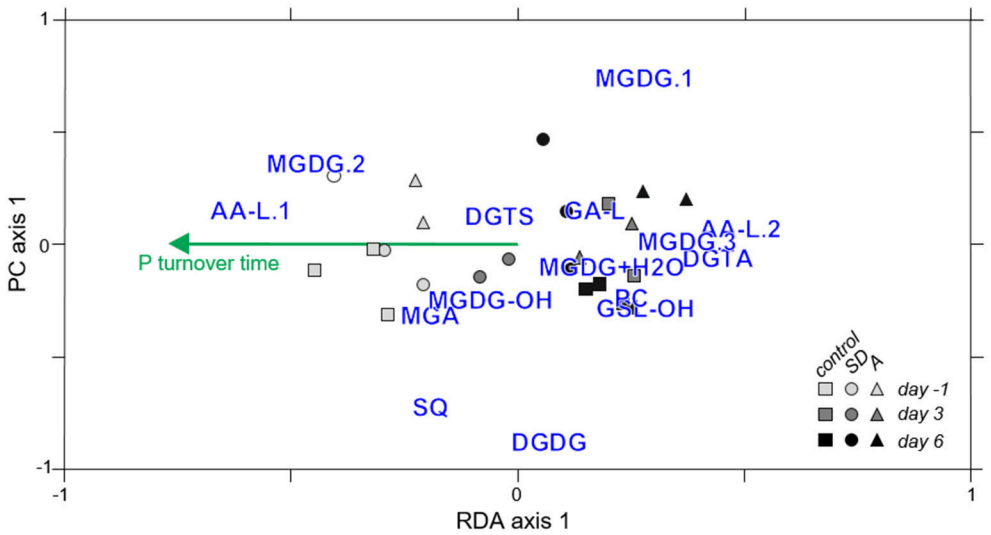

FIGURE 8 | Parsimonious RDA ($p = 0.001$) showing groupings of samples collected from control (circles), Saharan dust (squares), and mixed aerosol (triangles) mesocosms on days -1 (light gray symbols), day 3 (dark gray symbols), or day 6 (black symbols) with IPL relative abundance (blue text) and the weighting of the environmental parameter that best explained lipid headgroup distributions (P turnover time, τ_{PO4}, green).

same filters (Brandsma et al., 2012; Kharbush et al., 2016). The oligotrophic conditions and relatively lower amounts of biomass in the mesocosms investigated during the current study may thus explain why PG and PE were below the limit of detection. In contrast to PG and PE, PC lipids in the surface ocean are thought to be produced by eukaryotic phytoplankton (e.g., Kato et al., 1996) and are one of the few IPLs that cannot be attributed to a cyanobacterial source (**Table 4**). The alkyl chains of PC detected in the current study were relatively short (wt. avg. = 30.4 ± 0.7; **Figures 4A**, **5**) and saturated compared to those described in the surface equatorial N. Pacific (Van Mooy and Fredricks, 2010) or produced in algal cultures (Kato et al., 1996), including picoeukaryotes (Kharbush et al., 2016). The absence of the long chain $C_{22:6}$ fatty acid further discounts a eukaryotic source of PC (cf. Van Mooy and Fredricks, 2010). Dust additions could also represent a major source of PC, as observed in airborne particles in Australia, which were loaded with roughly 0.43 mg PC g^{-1} (De Deckker et al., 2008); however, the delayed increases in PC concentration on day 6 in treatment mesocosms (**Figures 6**, **7**) are not consistent with this interpretation. The most abundant alkyl chains of PC in the experimental mesocosms (i.e., $C_{28:0}$, $C_{29:1}$, and $C_{31:1}$) were composed of a mix of C_{14}, C_{15}, C_{16} fatty acids, and thus suggestive of a bacterial source, consistent with the assignment of PC to heterotrophic bacteria in the oligotrophic Sargasso Sea (Popendorf et al., 2011a; **Table 4**).

Hierarchical Clustering Analysis of IPL Alkyl Chains

Hierarchical clustering identified groups and outgroups of IPL classes based on their average alkyl chain distributions (**Figure 5**), which may be indicative of shared vs. unique source organisms, respectively. No clusters were exclusively defined according to IPL isomers (i.e., MGDG.1-3 or DGTS/DGTA; **Figure 7**), suggesting that the taxonomic or physiological factors that control headgroup stereochemistry may also yield larger dissimilarities in alkyl chain distributions. Therefore, chromatographic resolution may be of increasing importance for the investigation of samples with high biomass in order to distinguish the signals and thus contributions IPL stereoisomers from multiple phylogenetic groups.

GSL-OH lipids were distinguished from all other IPLs, which may be in part attributed to the nomenclature for assigning chain length (cf. Section IPL Alkyl Chain Distributions). However, the GSL-OH alkyl chain pattern also exhibited a distinctive bimodal distribution, with chains summing to C_{30}–C_{33} or C_{36}–C_{40} each accounting for roughly 45%, and a unique trend of increasing unsaturations in lipids with shorter alkyl chains (**Table 3**; **Figure 5**). GSLs are found in a variety of marine algae and phytoplankton (e.g., Muralidhar et al., 2003) as well as ciliates (15% of total lipids; Sul and Erwin, 1997), which were significantly enriched in the treatment mesocosms at the end of the incubation period (Tsagaraki et al., under revision, this SI). Sphingolipids could also derive from *Sphingobacterium* and some species of *Flavobacterium* (e.g., Yabuuchi and Moss, 1982; Yano et al., 1982; Yabuuchi et al., 1983; Dees et al., 1985). This notion is supported by (i) the relatively high abundance of their operational taxonomical units among 16S rRNA gene sequences identified during the Global Ocean Sampling survey of marine bacterioplankton metagenome (Yooseph et al., 2010), and (ii) 16S rDNA clone library analysis of dust rains in the Mediterranean, which can contribute roughly 20 µg DNA m^{-2} and may thus inoculate EMS surface waters with sphingobacteria and/or their characteristic lipids (Itani and Smith, 2016; Rahav et al., 2016).

While no GSL has been reported by previous IPL surveys of surface seawater (Van Mooy and Fredricks, 2010; Popendorf et al., 2011b; Brandsma et al., 2012; Kharbush et al., 2016), GSLs have been associated with anaerobic production in subsurface

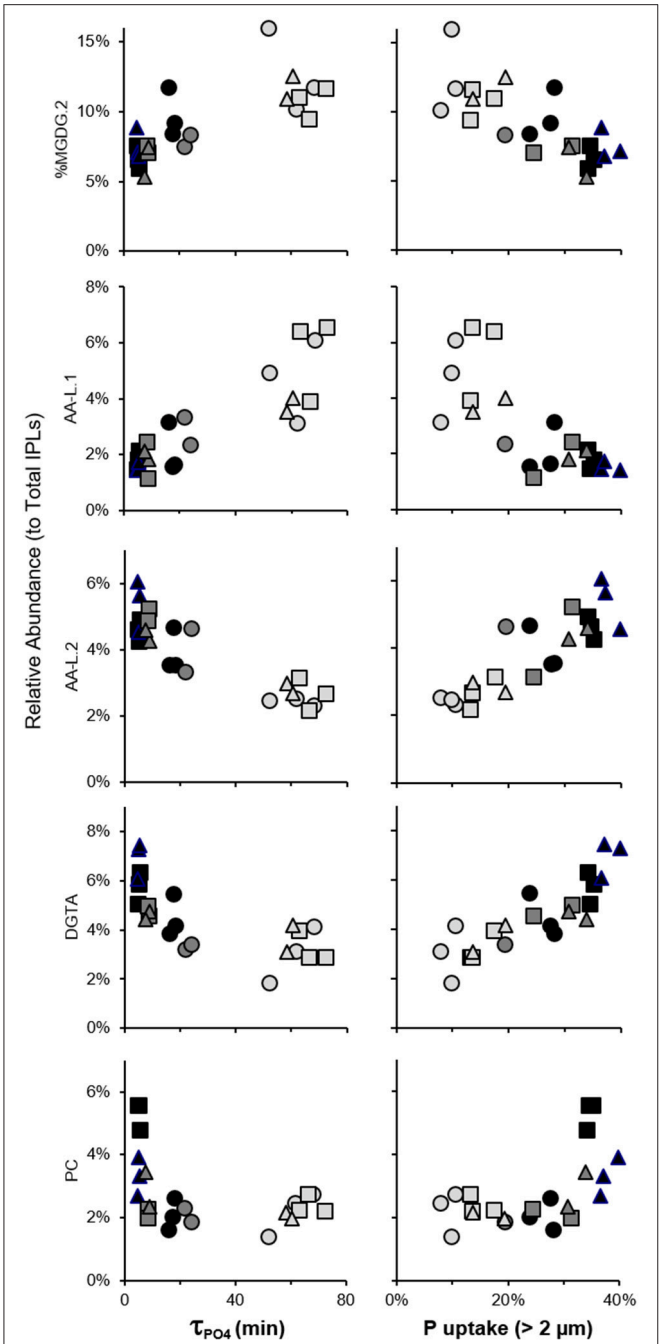

FIGURE 9 | Correlated changes in IPL relative abundance with τ_{PO4} and fractional phosphate uptake by plankton >2 µm in control mesocosms (circles) and those amended with Saharan dust (squares) or mixed aerosol (triangles) and collected on day −1 (light gray), day 3 (dark gray), or day 6 (black).

layers of the Black Sea (Schubotz et al., 2009). Also, multiple hydroxylated GSLs are known to be expressed during the infection of coccolithophores by marine viruses (Vardi et al., 2009). Constraining GSL sources based on the composition of GSL fatty acid and long-chain sphingoid base moieties is difficult because molecular modifications (e.g., unsaturations, hydroxylation, branching) are common across marine taxa (e.g., Muralidhar et al., 2003). The bimodal distribution of alkyl chains (**Figure 5**) may thus have resulted from the contribution of GSL-OH from multiple sources (e.g., shorter chains from heterotrophic bacteria and longer chains from eukarya); lipid assimilation and modification by secondary consumers (e.g., Ederington et al., 1995) could also explain these trends. The increases of GSL-OH following addition of SD or A (**Figures 6**, **7**) argue for further investigation of planktonic sources of GSLs in marine settings as potential biomarkers of both dust inputs and, as an N-containing lipid, portals for nutrient "tunneling" to ciliates and other mesozooplankton (cf. Thingstad et al., 2005a).

Most of the remaining IPLs considered in the clustering analysis have been attributed to a wide range of planktonic taxa (**Table 4**) and were categorized into two subgroups based on similarities and dissimilarities in their alkyl chain distributions (**Figure 5**). One subgroup comprised only glycolipids and the other comprised PC, DGTA, DGTS, and SQ, which are modulated by eukaryotes and cyanobacteria (Van Mooy et al., 2009) as well as heterotrophic bacteria (Sebastián et al., 2016) in response to nutrient availability.

In terms of alkyl chain distributions, SQ and MGDG.3 were the most similar, each with >95% of alkyl chains summing to C_{28}, C_{30}, or C_{32} (**Figure 5**). While this resemblance may be biased by the relatively few compounds and thus low diversity of each class (**Table 1**; **Figure 4C**), the similar alkyl chain distributions of MGDG.3 and SQ could be a signature of a shared source organism and/or biosynthetic pathway. These IPLs were nestled among a larger subgroup that is branded by PC, DGTS, and DGTA, the ratios of which vary via the replacement of PC with betaine lipids by P-limited eukaryotes (Van Mooy et al., 2009). Similarly, cyanobacteria were also proposed to substitute phospholipids with SQ when P is scarce, whereas heterotrophic bacteria maintained similar phospholipid cell quotas under P-replete and -deplete conditions (Van Mooy et al., 2009). However, in this study, IPLs that have been associated with nutrient-availability (i.e., PC, SQ, and betaine lipids; Van Mooy et al., 2009; **Table 4**) were relatively enriched in short (i.e., sum $\leq C_{34}$) and saturated alkyl chains (**Figure 5**), which is a feature that appears to distinguish this cluster from the major glycolipids and is generally attributed to heterotrophic bacteria (e.g., Kaneda, 1991; Thompson, 1996; Bergé and Barnathan, 2005). This finding is consistent with Sebastián et al. (2016), who suggested that heterotrophic bacteria remodel their cell membrane in response to nutrient availability, increasing levels of DGTS during P-deficiency and increasing levels of PC when P becomes available.

DGDG also sorted into this "nutrient availability" cluster, indicating that its alkyl chain distribution was distinct from that of the major glycolipids (i.e., MGDG.1, MGDG.2, and MGA), again, likely owing to the relatively high abundance of saturated alkyl chains summing up to C_{30}. This finding is in contrast to that of Van Mooy and Fredricks (2010), who noted similar diacylglyceride composition among glycolipids (i.e., MGDG, SQ, and DGDG) in the euphotic zone of the south Pacific, although the concentration profiles of DGDG were similar to phospholipids and betaine lipids. While heterotrophic bacteria are not known to produce DGDG or SQ (**Table 4**),

TABLE 4 | Association of IPL headgroups with phylogenetic groups in different oceanic environments.

Location (sampling depths)	Chl-*a* Range ($\mu g\ L^{-1}$)	MGDG	DGDG	SQ	MGA	DGTS	DGTA	DGCC	GSL-OH	PC	PG	PE	PDME
Black Sea[a] (≤ 60 m)	***no data***	eukaryotic phytoplankton, cyanobacteria	eukaryotic phytoplankton, cyanobacteria	eukaryotic phytoplankton, cyanobacteria	*n.d.*	eukaryotic phytoplankton	eukaryotic phytoplankton	*n.d.*	*n.d.*	eukaryotic phytoplankton, bacteria	eukaryotic phytoplankton, cyanobacteria	eukaryotic phytoplankton, bacteria	eukaryotic phytoplankton, bacteria
Mediterranean Sea[b] (≤ 300 m)	**ca. 0.1 to 0.5**	*Prochloro.*	*Synecho.*	—	*n.d.*	—	—	—	*n.d.*	—	—	—	*n.d.*
Sargasso Sea[c] (≤ 120 m)	**ca. 0.1 to 0.5**	phytoplankton, bacteria, *Prochloro., Synecho.*	*Synecho.*	phytoplankton, *Prochloro. Synecho.*	*n.d.*	phytoplankton	phytoplankton, heterotrophic bacteria	phytoplankton, heterotrophic bacteria	*n.d.*	heterotrophic bacteria	heterotrophic bacteria	heterotrophic bacteria	*n.d.*
North Sea[d] (10 m)	**0.22 to 9.24**	*n.d.*	*n.d.*	picoeukaryotes	*n.d.*	picoeukaryotes, nanoeukaryotes, cyanobacteria	cyanobacteria	cyanobacteria	*n.d.*	picoeukaryotes, nanoeukaryotes	picoeukaryotes	cyanobacteria, bacteria	*n.d.*
Equatorial Pacific[e] (≤ 250 m)	**ca. 0.1 to 2.0**	Prochlorophytes	—	Prochlorophytes	*n.d.*	eukaryotes	eukaryotes	eukaryotes	*n.d.*	eukaryotic phytoplankton	bacteria	bacteria	*n.d.*
South Pacific[f] (≤ 140 m)	**<0.05 to 0.4**	Dinoflagellates, *Pelagomonas, Prochloro.*	Dinoflagellates, *Pelagomonas, Prochloro.*	*Pelagomonas, Prochloro.*	*Prochloro.*	eukaryotic phytoplankton, *Pelagomonas*	eukaryotic phytoplankton, *Pelagomonas*	*n.d*	*n.d.*	eukaryotic phytoplankton	heterotrophic bacteria, *Prochloro.*	heterotrophic bacteria, *Prochloro.*	*n.d.*

[a]*Schubotz et al. (2009)*; [b]*Popendorf et al. (2011b)*; [c]*Popendorf et al. (2011a)*; [d]*Brandsma et al. (2012)*; [e]*Van Mooy and Fredricks (2010)*; [f]*Kharbush et al. (2016)*.
Chlorophyll-a (Chl-a) range refers to the maximum and minimum values corresponding to samples for which IPLs were also analyzed. IPLs listed in bold were also detected during the current study. Refer to text for abbreviations. Dashes indicated that the IPL was detected but not assigned to a phylogenetic group. Prochloro, Prochlorococcus; Synecho, Synechococcus; PG, phosphatidyl glycerol; PE, phosphatidyl ethylamine; PDME, phosphatidyl dimethylethylamine; n.d, not detected.

the shared feature of short and saturated alkyl chains is consistent with the production of PC, DGTS, DGTA, DGDG, SQ, and MGDG.3 by heterotrophic bacteria in the oligotrophic EMS, who may thus adjust these IPLs in response to nutrient availability via mechanisms previously described for eukaryotes and cyanobacteria (Van Mooy et al., 2009) and hetertrophic bacteria (Sebastián et al., 2016).

MGDG-OH, MGDG+H_2O, AA-L.1, and AA-L.2 lipids comprised ≤4 compounds and therefore were not included in the clustering analysis. Both MGDG-OH and the ambiguous MGDG-like lipid (MGDG+H_2O) were characterized by a combination of even-chain fatty acids (C_{14}, C_{16}, C_{18}) with zero or two unsaturations (Section IPL Taxonomic Source Indications), with the former also containing a hydroxyl group in the alkyl chain. This narrow distribution of alkyl chain length and unsaturation suggest that, rather than being products of diagenesis or non-selective transformation of a MGDG precursor, these modified MGDG lipids may be biomarkers of selective biosynthetic pathways. The MS2 fragments of AA-L.1 corresponded to odd-numbered, short-chain fatty acids (C_{17} and C_{15}; Section IPL Taxonomic Source Indications; Figure S4) and therefore likely derived from a bacterial source. As the fatty acids of AA-L.2 were also short (≤C_{18}), these putative alkylamine lipids may therefore represent a novel IPL biomarker to assess nutrient-stressed populations of heterotrophic bacteria. Although relatively high in diversity (**Table 1**; **Figure 4C**), the alkyl chain distribution of GA-L lipids (Figure S7) was not further interpreted via hierarchical cluster analysis as the headgroup and glycerol backbone linkages and thus the length of alkyl chains remains uncertain. However, based on the putative structure (**Figure 2**), the relatively high abundance of short and saturated alkyl chains featured by this lipid class is similar to that of IPLs in the "nutrient-availability" cluster (**Figure 5**).

Turnover of the IPL Pool

During the MESOAQUA experiment in 2012 (Heraklion, Greece), concentrations of bacteria, *Synechococcus*, and chlorophyll increased significantly in response to the addition of SD and A to oligotrophic seawater mesocosms (Herut et al., 2016; Tsiola et al., 2016; Tsagaraki et al., under revision, this SI). In parallel with the stimulation of picoplankton, Chl-*a* concentrations representative of larger phytoplankton (Chl>2 μm) had increased by >50% by day 3. However, the concentration of total suspended IPLs was surprisingly stable throughout the pre-addition, stimulated, and post-stimulated periods relative to the significant increases of both phytoplankton and bacteria (e.g., Guo et al., 2016; Herut et al., 2016). That is, based on the hypothesis that IPLs track plankton growth, one would have expected their summed concentrations to increase by >20% of the pre-addition concentrations on day 3 (**Figures 1B–C**); this value would rise to >60% if one assumes no heterotrophic bacteria were retained by the GF/F filter. The lack of a significant increase in total IPL concentration on day 3 (**Figures 1**, **6**) may be explained by the presence of a relatively refractory pool of IPLs that turnover more slowly (∼weeks; e.g., Logemann et al., 2011) than the biogenic lipid signal associated with the growth response of plankton that occurred 3 days after dust

addition. This interpretation is supported by the consistently higher measured concentrations of IPLs vs. that predicted based on increases in Chl-*a* (**Figure 1A**). Alternatively, the increases in cell abundance following dust amendments may have been accompanied by a reduction in IPL cell quota, thus resulting in a static IPL signal. This hypothesis is supported by the enhanced lipid content of chlorophytes under nutrient limited conditions (Griffiths and Harrison, 2009). For each treatment mesocosm, significant net increases in IPL concentration were not observed until day 6 ($p < 0.01$; **Figure 6**; cf. Section IPL Alkyl Chain Distributions), and could not be explained by growth of microzooplankton alone (cf. Section Biological Responses to Dust Addition). In summary, the net increases in total IPL concentration were uncoupled with pigment concentration and plankton biomass, representing a delayed response to the additions of SD and A that may be a hallmark of the episodic blooms occurring in this ultra-oligotrophic setting.

The experimental mesocosms were void of advective input or export fluxes; therefore, net changes in total suspended lipid concentration were presumably determined by the balance of plankton growth (i.e., IPL additions) vs. sinking and diagenesis (i.e., IPL removal). In terms of concentration, the only lipid class that appeared to track the stimulated plankton in SD or A mesocosms was GSL-OH, which increased from 11 ± 2 to 5 ± 2 ng L^{-1} on day-1, respectively, to maximum values of 30 ± 5 or 34 ± 13 ng L^{-1} on day 3, accounting for only a fraction of the expected IPL increase (cf. **Figure 1**). The consistent losses of MGDG.2 and AA-L.1 on days 3 and 6 in control and treatment mesocosms (**Figure 6**) suggest that these lipids, which accounted for 13–21% of IPLs at the onset of the experiment, were representative of the detrital pool that was removed from the system. In contrast, the additions of MGDG.1, AA-L.2, DGTA, GA-L, PC, and DGDG measured on day 6 among the treatment mesocosms (**Figure 6**) suggest that these biomarkers integrated biological production or otherwise may have accumulated during the post-stimulated phase in the mesocosm via nutrient stress responses by phytoplankton (e.g., Griffiths and Harrison, 2009) or lipid incorporation by secondary consumers (e.g., Ederington et al., 1995).

Constrained Ordination Modeling of IPL Responses

While changes in lipid concentration can be attributed to growth or removal processes in the context (i.e., time course) of this mesocosm experiment, fluxes of biomarkers in natural environments, such as lateral transport and dilution, are more difficult to constrain. Furthermore, concentrations of particles and thus biomarkers suspended in seawater often exhibit unidirectional trends over seasonal scales (e.g., increasing with production during bloom events; Christodoulou et al., 2009), spatial gradients (e.g., decreases with depth; Wakeham et al., 1997) or along estuarine transects (e.g., Canuel, 2001). These previous studies have therefore rather examined characteristic changes in biomarker *relative abundance* (as opposed to *concentration*), which, for our purposes, may better depict shifts in plankton community composition and physiological adaptations. In other words, because the variability overprinted by unilateral concentration change is removed, relative abundance comparisons may offer a more sensitive interpretation of biomarker reactivity.

The significant trends in IPL relative abundance distributions during the MESOAQUA experiment were gleaned via an RDA modeling approach that reduced the dimensionality of the data, which included measurements of 15 IPL classes and 31 environmental parameters for 23 different samples collected from control or treatment mesocosms during the progression of the plankton community (Tables S3, S4). The IPL composition that developed in SD or A mesocosms was distinct from that of the control (i.e., **Figure 7**; RDA_1) and that these differences were amplified during the post-stimulated period, such that adding a temporal component increased the explanatory value of the RDA [i.e., RDA_2, $p = 0.001$; Table S3; cf. Section IPLs in SD or A treatments vs. Control (RDA_1) and IPL Composition of Pre-Addition, Stimulated, and Post-Stimulated Samples (RDA_2)]. Although neither treatment nor day of sampling were included as discrete terms in the parsimonious RDA model, the combined effects of treatment and temporal development of the plankton community on IPL composition are evident by the grouping of control and day −1 samples (Quadrants III and IV) vs. treatment samples collected on day 3 or day 6 (Quadrants I and II; **Figure 8**).

Based on the sampling resolution, the largest change in environmental parameters was recorded by τ_{PO4} [cf. Section Comparing IPL Distributions with Environmental Parameters (RDA_3], which consequently best explained the changes among IPL lipids (**Figure 8**). Nevertheless, when considering the impact of the environmental parameters individually ($RDA_{3.1–31}$), other parameters could also significantly explain IPL distribution (Table S4), including alkaline phosphatase activity, concentrations of ammonia, phosphate, Chl-*a* and the pigment 19- butanoyloxyfucoxanthin, as well as and the fraction of Chl-*a* in particles >0.6 μm and the fraction of primary productivity in particles >2 μm. The explanatory potential for these parameters is much less than for τ_{PO4}, which resulted in the elimination of these parameters in the combined parsimonious RDA. This RDA modeling approach that employs a forward selection algorithm could be useful for assessing the potential controls of larger gradients in nutrient concentration and productivity on IPL composition.

IPL Signatures of Nutrient Turnover

Leaching of N and P from the SD treatment yielded a lower N:P ratio (ca. 10.1) compared to the A treatment (ca. 19.1; Herut et al., 2016). The relatively enhanced availability of phosphorus in SD mesocosms could thus explain the significantly higher additions of PC in on day 6 ($p < 0.04$; **Figures 6**, **7**). The delayed and significant increases in PC concentration in treatment mesocosms (**Figure 6**) is suggestive of autochthonous production rather than leaching from the amended dust (e.g., De Deckker et al., 2008). Given the capacity for SQ to substitute phospholipids (Van Mooy et al., 2009), the net removal of SQ on day 3 in the SD

treatments vs. net production in the A treatments (cf. Section IPL Concentrations; **Figure 6**) may be similarly explained. Further indication of surplus P in the SD treatment stems from the ratio of BL to PC, for which increased values have been interpreted as a signal of P-limitation (Van Mooy et al., 2009; Popendorf et al., 2011b). Conversely, the significantly lower BL:PC value in SD mesocosms on day 6 (2.0 ± 0.3) suggest that P was in excess, relative to control (5.2 ± 1.7) and A (3.7 ± 0.7) mesocosms as well as day −1 of the SD treatment (3.8 ± 0.6; $p < 0.04$).

Because there were only slight differences in the structure of plankton communities that developed in the treatment mesocosms (Guo et al., 2016; Herut et al., 2016; Tsagaraki et al., under revision, this SI), the significant additions of PC in SD mesocosms may be a signal of changes in plankton physiology rather than taxonomy. This conclusion is consistent with the interpretation of increased BL:PC ratios following N addition to oligotrophic seawater microcosms (Popendorf et al., 2011b), where nutrient additions were higher than the current study by one to two orders of magnitude and yielded in only small changes in community structure. In all treatment mesocosms ($n = 6$), phosphate concentrations dropped to below 8 nM, τ_{PO4} decreased to <6 min., and the balance of P uptake shifted toward larger organisms by day 6 (**Figure 9**); however, no significant increases in PC were observed in the A treatment. Additions of SD may have therefore initiated a mechanism by which larger plankton shuttled inorganic P into PC as a result of luxury N and P uptake (relative to A and control mesocosms), or a means of N and P storage, or both. In addition to PC, the significant correlations of DGTA and AA-L.2 relative abundances with τ_{PO4} and P uptake by plankton >2μm (**Figure 9**) implicate these IPLs as biomarkers of a physiological response to the conditions induced by SD and A deposition in surface oligotrophic seawater.

CONCLUSIONS

The enhanced UHPLC-MS protocols employed during this study allowed for identification of novel IPLs in seawater (**Table 1**) and resolution of their alternative fatty acid distributions (**Figure 5**, Figure S7), thereby serving to further constrain IPL sources, organic matter reactivity, and food web dynamics in the ocean. The total abundance of IPLs was uncoupled to the induced increases in Chl-*a*; however, their alkyl chains were typically elongated and more unsaturated in response to SD or A additions (**Tables 2, 3**). Elongation of fatty acid chains could be a mechanism associated with increases in cellular C storage and size, and accompanying increases in unsaturation would maintain membrane fluidity and thus solute transport (e.g., Chapman, 1975; Williams, 1998). These combined modifications may therefore represent a phenotypic feature of microbial "Winnie-the-Pooh strategists" in the oligotrophic ocean (Thingstad et al., 2005b). Increased desaturation of the fatty acid chain may also save reducing power via use of a polyketide synthase pathway (Ratledge, 2004).

While the stimulation of plankton was relatively low in biomass in comparison to other ocean regions, redundancy analysis indicated that significant changes in IPL headgroup and chain distributions were associated with sampling day and best explained by the large decreases in τ_{PO4} during the temporal evolution of the plankton community (**Figure 8**). IPLs containing N or N and P, including DGTA, PC, and AA-L.2 were (i) relatively enriched in alkyl chains thought to derive from heterotrophic bacteria, (ii) significantly enriched during the post-stimulated phase in treatment mesocosms (**Figure 7**), (iii) significantly correlated with decreases in τ_{PO4}, and (iv) significantly increased with fractional uptake of P by larger plankton (**Figure 9**). These IPLs may thus modulate with changes in plankton physiology and/or serve as a portal for nutrient shuttling in the oligotrophic food web.

AUTHOR CONTRIBUTIONS

TM contributed to the conception and design of this study, performed sampling, performed lipid analyses, interpreted the data, and drafted and revised the manuscript. NG contributed to data interpretation, multivariate analyses, preparation of tables and figures, and drafted and revised the manuscript. AG and SP contributed to the conception and design of this study, sampling, data interpretation and revision of the manuscript. BH and TT contributed to the conception and design of this study, data interpretation, and revision of the manuscript. KH contributed to lipid analysis, data interpretation, and revision of the manuscript for important intellectual content.

ACKNOWLEDGMENTS

This work was financed by the European Union Seventh Framework Program (FP7/2007–2013) under grant agreement no. 228224 "MESOAQUA: Network of leading MESOcosm facilities to advance the studies of future AQUAtic ecosystems from the Arctic to the Mediterranean." TM and KH were supported by the Deutsche Forschungsgemeinschaft (DFG) through Gottfried Wilhelm Leibniz Award awarded to KH (grant #HI 616-14); TM was additionally supported by DFG grant #ME 4594/2-1. Julius Lipp assisted with mass spectrometry protocols and interpretation of MS2 fragmentation patterns. Aerjen van den Akker assisted with sample collection from the mesocosms in Heraklion. All members of the MESOAQUA team are acknowledged for their invaluable contributions in support of the mesocosm experiment. We thank two reviewers for investing their time to improve this manuscript.

SUPPLEMENTARY MATERIAL

The Supplementary Material for this article can be found online at: http://journal.frontiersin.org/article/10.3389/fmars.2017.00113/full#supplementary-material

REFERENCES

Bergé, J.-P., and Barnathan, G. (2005). Fatty acids from lipids of marine organisms: molecular biodiversity, roles as biomarkers, biologically active compounds, and economical aspects. *Adv. Biochem. Eng. Biotechnol.* 96, 49–125. doi: 10.1007/b135782

Brandsma, J., Hopmans, E. C., Brussaard, C. P. D., Witte, H. J., Schouten, S., and Sinninghe Damsté, J. (2012). Spatial distribution of intact polar lipids in North Sea surface waters: relationship with environmental conditions and microbial community composition. *Limnol. Oceanogr.* 57, 959–973. doi: 10.4319/lo.2012.57.4.0959

Canuel, E. (2001). Relations between river flow, primary production and fatty acid composition of particulate organic matter in San Francisco and Chesapeake Bays: a multivariate approach. *Org. Geochem.* 32, 563–583. doi: 10.1016/S0146-6380(00)00195-9

Chapman, D. (1975). Phase transition and fluidity characteristics of lipids and cell membranes. *Quart. Rev. Biophys.* 8, 185–235. doi: 10.1017/S0033583500001797

Christodoulou, S., Marty, J.-C., Miquel, J.-C., Volkman, J. K., and Rontani, J.-F. (2009). Use of lipids and their degradation products as biomarkers for carbon cycling in the northwestern Mediterranean Sea. *Mar. Chem.* 113, 25–40. doi: 10.1016/j.marchem.2008.11.003

Dalsgaard, J., St. John, M., Kattner, G., Müller-Navarra, D., and Hagen, W. (2003). Fatty acid trophic markers in the pelagic marine environment. *Adv. Mar. Biol.* 46, 225–340. doi: 10.1016/S0065-2881(03)46005-7

De Deckker, P., Abed, R. M. M., de Beer, D., Hinrichs, K.-U., O'Loingsigh, T., Schefuß, E., et al. (2008). Geochemical and microbiological fingerprinting of airborne dust that fell in Canberra, Australia, in October 2002. *Geochem. Geophys. Geosyst.* 9:Q12QQ10. doi: 10.1029/2008GC002091

Dees, S. B., Carlone, G. M., Hollis, D., and, Moss, C. W. (1985). Chemical and phenotypic characteristics of *Flavobacterium* ialipophiljium compared with those of other *Flavobacterium* and *Sphingobacteriumn* species. *Int. J. Syst. Bacteriol.* 35, 16–22. doi: 10.1099/00207713-35-1-16

Ederington, M. E., McManus, G. B., and Harvey, H. R. (1995). Trophic transfer of fatty acids, sterols and a triterpenoid alcohol between bacteria, a ciliate, and the copepod Acartia tonsa. *Limnol. Oceanogr.* 40, 860–867. doi: 10.4319/lo.1995.40.5.0860

Geider, R. J., MacIntyre, H. L., and Kana, T. M. (1997). Dynamic model of phytoplankton growth and acclimation: responses of the balanced growth rate and the chlorophyll a: carbon ratio to light, nutrient-limitation and temperature. *Mar. Ecol. Prog. Ser.* 148, 187–200. doi: 10.3354/meps148187

Griffiths, M. J., and Harrison, S. T. L. (2009). Lipid productivity as a key characteristic for choosing algal species for biodiesel production. *J. Appl. Phycol.* 21, 493–507. doi: 10.1007/s10811-008-9392-7

Guerzoni, S., Chester, R., Dulac, F., Moulin, C., Herut, B., Loye-Pilot, M. D., et al. (1999). The role of atmospheric deposition in the biogeochemistry of the Mediterranean Sea. *Prog. Oceanogr.* 44, 147–190. doi: 10.,1016/S0079-6611(99)00024-5

Guieu, C., Loye-Pilot, M. D., Ridame, C., and Thomas, C. (2002). Chemical characterization of the Saharan dust end-member: some biogeochemical implications for the western Mediterranean Sea. *J. Geophys. Res. Atmos.* 107, 4250–4258. doi: 10.1029/2001JD000582

Guieu, C., Ridame, C., Pulido-Villena, E., Bressac, M., Desboeufs, K., and Dulac, F. (2014). Impact of dust deposition on carbon budget: a tentative assessment from a mesocosm approach. *Biogeosciences* 11, 5621–5635. doi: 10.5194/bg-11-5621-2014

Guo, C., Xia, X., Pitta, P., Herut, B., Rahav, E., Berman-Frank, I., et al. (2016). Shifts in microbial community structure and activity in the ultra-oligotrophic eastern Mediterranean Sea driven by the deposition of Saharan dust and European aerosols. *Front. Mar. Sci.* 3:170. doi: 10.3389/fmars.2016.00170

Guschina, I. A., and Harwood, J. L. (2006). Lipids and lipid metabolism in eukaryotic algae. *Prog. Lipid Res.* 45, 160–186. doi: 10.1016/j.plipres.2006.01.001

Harvey, R. H., and Macko, S. A. (1997). Catalysts or contributors? Tracking bacterial mediation of early diagenesis in the marine water column. *Org. Geochem.* 26, 531–544. doi: 10.1016/S0146-6380(97)00033-8

Herut, B., Collier, R., and Krom, M. D. (2002). The role of dust in supplying nitrogen and phosphorus to the Southeast Mediterranean. *Limnol. Oceanogr.* 47, 870–878. doi: 10.4319/lo.2002.47.3.0870

Herut, B., Krom, M. D., Pan, M. D., and Mortimer, R. (1999). Atmospheric input of nitrogen and phosphorus to the SE Mediterranean, sources, fluxes and possible impact. *Limnol. Oceanogr.* 44, 1683–1692. doi: 10.4319/lo.1999.44.7.1683

Herut, B., Rahav, E., Tsagaraki, T. M., Giannakourou, A., Tsiola, A., Psarra, S., et al. (2016). The potential impact of Saharan dust and polluted aerosols on microbial populations in the East Mediterranean Sea, an overview of a mesocosm experimental approach. *Front. Mar. Sci.* 3:226. doi: 10.3389/fmars.2016.00226

Herut, B., Zohary, T., Krom, M. D., Mantoura, R. F. C., Pitta, P., Psarra, S., et al. (2005). Response of East Mediterranean surface water to Saharan dust: on-board microcosm experiment and field observations. *Deep-Sea Res. II* 52, 3024–3040. doi: 10.1016/j.dsr2.2005.09.003

Huguet, C., Hopmans, E. C., Febo-Ayala, W., Thompson, D. H., Sinninghe Damsté, J. S., and Schouten, S. (2006). An improved method to determine the absolute abundance of glycerol dibiphytanyl tetraether lipids. *Org. Geochem.* 37, 1036–1041. doi: 10.1016/j.orggeochem.2006.05.008

Itani, G. N., and Smith, C. A. (2016). Dust rains deliver diverse assemblages of microorganisms to the Eastern Mediterranean. *Nature Sci. Rep.* 6:22657. doi: 10.1038/srep22657

Kaneda, T. (1991). Iso- and anteiso-fatty acids in bacteria: biosynthesis, function, and taxonomic significance. *Mirobiol. Rev.* 55, 288–302.

Kato, M., Sakai, M., Adachi, K., Ikemoto, H., and Sano, H. (1996). Distribution of betaine lipids in marine algae. *Phytochemistry* 42, 1341–1345. doi: 10.1016/0031-9422(96)00115-X

Kharbush, J. J., Allen, A. E., Moustafa, A., Dorrestein, P. C., and Aluwihare, L. I. (2016). Intact polar diacylglycerol biomarker lipids isolated from suspended particulate organic matter accumulating in an ultraoligotrophic water column. *Org. Geochem.* 100, 29–41. doi: 10.1016/j.orggeochem.2016.07.008

Kim, J.-H., Schouten, S., Rodrigo-Gámiz, M., Rampen, S., Marino, G., Huguet, C., et al. (2015). Influence of deep-water derived isoprenoid tetraether lipids on the TEX86 paleothermometer in the Mediterranean Sea. *Geochim. Cosmochim. Acta* 150, 125–141. doi: 10.1016/j.gca.2014.11.017

Klingmüller, K., Pozzer, A., Metzger, S., Stenchikov, G. L., and Lelieveld, J. (2016). Aerosol optical depth trend over the Middle East. *Atmos. Chem. Phys.* 16, 5063–5073. doi: 10.5194/acp-16-5063-2016

Kouvarakis, G., Mihalopoulos, N., Tselipides, A., and Stavrakakis, S. (2001). On the importance of atmospheric inputs of inorganic nitrogen species on the productivity of the Eastern Mediterranean Sea. *Glob. Biogeochem. Cycles* 15, 805–817. doi: 10.1029/2001GB001399

Krom, M. D., Brenner, S., Kress, N., and Gordon, L. I. (1991). Phosphorus limitation of primary productivity in the E. Mediterranean Sea. *Limnol. Oceanogr.* 36, 424–432. doi: 10.4319/lo.1991.36.3.0424

Krom, M. D., Herut, B., and Mantoura, F. (2004). Nutrient budget for the Eastern Mediterranean, implications for P limitation. *Limnol. Oceanogr.* 49, 1582–1592. doi: 10.4319/lo.2004.49.5.1582

Kubilay, N., Nickovic, S., Moulin, C., and Dulac, F. (2000). An illustration of the transport and deposition of mineral dust onto the eastern Mediterranean. *Atmos. Environ.* 34, 1293–1303. doi: 10.1016/S1352-2310(99)00179-X

Laghdass, M., Blain, S., Besseling, M., Catala, P., Guiue, C., and Obernosterer, I. (2011). Effects of Saharan dust on the microbial community during a large *in situ* mesocosm experiment in the NW Mediterranean Sea. *Aquat. Microb. Ecol.* 62, 201–213. doi: 10.3354/ame01466

Lipp, J. S., Morono, Y., Inagaki, F., and Hinrichs, K.-U. (2008). Significant contribution of Archaea to extant biomass in marine subsurface sediments. *Nature* 454, 991–994. doi: 10.1038/nature07174

Logemann, J., Graue, J., Köster, J., Engelen, B., Rullkötter, J., and Cypionka, H. (2011). A laboratory experiment of intact polar lipid degradation in sandy sediments. *Biogeosciences* 8, 2547–2560. doi: 10.5194/bg-8-2547-2011

Markaki, Z., Oikonomou, K., Kocak, M., Kouvarakis, G., Chaniotaki, A., Kubilay, N., et al. (2003). Atmospheric deposition of inorganic phosphorus in the Levantine Basin, eastern Mediterranean: spatial and temporal variability and its role in seawater productivity. *Limnol. Oceanogr.* 48, 1557–1568. doi: 10.4319/lo.2003.48.4.1557

Muralidhar, P., Radhika, P., Krishna, N., Venkata Rao, D., and Bheemasankara, R. C. (2003). Spingolipids from marine organisms: a review. *Nat. Prod. Sci.* 9, 117–142.

Oksanen, J., Blanchet, F. G., Kindt, R., Legendre, P., Minchin, P. R., O'Hara, R. B., et al. (2015). *Vegan: Community Ecology Package*. R package version 2.2-1. Available online at: http://CRAN.R-project.org/package=vegan

Palenik, B., Grimwood, J., Aerts, A., Rouzé, P., Salamov, A., Putnam, N., et al. (2007). The tiny eukaryote *Ostreococcus* provides genomic insights into the paradox of plankton speciation. *Proc. Nat. Acad. Sci. U.S.A.* 104, 7705–7710.

Popendorf, K. J., Lomas, M. W., and Van Mooy, B. S. (2011a). Microbial sources of intact polar diacyglycerolipids in the Western North Atlantic Ocean. *Org. Geochem.* 42, 803–811. doi: 10.1016/j.orggeochem.2011.05.003

Popendorf, K. J., Tanaka, T., Pujo-Pay, M., Lagaria, A., Courties, C., Conan, P., et al. (2011b). Gradients in intact polar diacylglycerolipids across the Mediterranean Sea are related to phosphate availability. *Biogeosciences* 8, 3733–3745. doi: 10.5194/bg-8-3733-2011

Rahav, E., Paytan, A., Chien, C.-T., Ovadia, G., Katz, T., and Herut, B. (2016). The impact of atmospheric dry deposition associated microbes on the southeastern Mediterranean Sea surface water following an intense dust storm. *Front. Mar. Sci.* 3:127. doi: 10.3389/fmars.2016.00127

Ratledge, C. (2004). Fatty acid biosynthesis in microorganisms being used for single cell oil production. *Biochimie* 86, 807–815. doi: 10.1016/j.biochi.2004.09.017

Sato, N. (1992). Betaine lipids. *Bot. Mag. Tokyo* 105, 185–197. doi: 10.1007/BF02489414

Schubotz, F., Wakeham, S. G., Lipp, J. S., Fredricks, H. F., and Hinrichs, K.-U. (2009). Detection of microbial biomass by intact membrane lipid analysis in the water column and surface sediments of the Black Sea. *Environ. Microbiol.* 11, 2720–2734. doi: 10.1111/j.1462-2920.2009.01999.x

Sebastián, M., Smith, A. F., González, J. M., Fredricks, H., Van Mooy, B., Koblízek, M., et al. (2016). Lipid remodeling is a widespread strategy in marine heterotrophic bacteria upon phosphorus deficiency. *ISME J.* 10, 968–978. doi: 10.1038/ismej.2015.172

Simon, M., and Azam, F. (1989). Protein content and protein synthesis rates of planktonic marine bacteria. *Mar. Ecol. Prog. Ser.* 51, 201–213.

Sohlenkamp, C., and Geiger, O. (2015). Bacterial membrane lipids: diversity in structures and pathways. *FEMS Microb. Rev.* 40, 133–159. doi: 10.1093/femsre/fuv008

Sturt, H. F., Summons, R. E., Smith, K., Elvert, M., and Hinrichs, K.-U. (2004). Intact polar membrane lipids in prokaryotes and sediments deciphered by high-performance liquid chromatography/electrospray ionization multistage mass spectrometry–new biomarkers for biogeochemistry and microbial ecology. *Rapid Commun. Mass Spectrom.* 18, 617–628. doi: 10.1002/rcm.1378

Sul, D., and Erwin, J. A. (1997). The membrane lipids of the marine ciliated protozoan *Parauronema acutum*. *Biochim. Biophys. Acta*. 1345, 162–171.

Thingstad, T. F., Krom, M. D., Mantoura, R. F. C., Flaten, G. A. F., Groom, S., Herut, B., et al. (2005a). Nature of phosphorus limitation in the ultraoligotrophic Eastern Mediterranean. *Science* 309, 1068–1071. doi: 10.1126/science.1112632

Thingstad, T. F., Øvreås, L., Egge, J. K., and Løvdal, T., Heldal, M. (2005b). Use of non-limiting substrates to increase size; a generic strategy to simultaneously optimize uptake and minimize predation in pelagic osmotrophs? *Ecol. Lett.* 8, 675–682. doi: 10.1111/j.1461-0248.2005.00768.x

Thompson, G. A. Jr. (1996). Lipids and membrane function in green algae. *Biochim. Biophys. Acta* 1302, 17–45. doi: 10.1016/0005-2760(96)00045-8

Tsiola, A., Tsagaraki, T. M., Giannakourou, A., Nikolioudakis, N., Yücel, N., Herut, B., et al. (2016). Bacterial growth and mortality after deposition of Saharan dust and mixed aerosols in the Eastern Mediterranean Sea: a mesocosm experiment. *Front. Mar. Sci.* 3:281. doi: 10.3389/fmars.2016.00281

Van Mooy, B. A. S., and Fredricks, H. F. (2010). Bacterial and eukaryotic intact polar lipids in the eastern subtropical South Pacific: water-column distribution, planktonic sources, and fatty acid composition. *Geochim. Cosmochim. Acta* 74, 6499–6516. doi: 10.1016/j.gca.2010.08.026

Van Mooy, B. A. S., Fredricks, H. F., Pedler, B. E., Dyhrman, S. T., Karl, D. M., Koblížek, M., et al. (2009). Phytoplankton in the ocean use non-phosphorus lipids in response to phosphorus scarcity. *Nature* 458, 69–72. doi: 10.1038/nature07659

Vardi, A., Van Mooy, B. A. S., Fredricks, H., Popendorf, K. J., Ossolinksi, J. E., Haramaty, L., et al. (2009). Viral glycosphingolipids induce lytic infection and cell death in marine phytoplankton. *Science* 326, 861–865. doi: 10.1126/science.1177322

Wakeham, S. G., Lee, C., Hedges, J. I., Hernes, P. J., and Peterson, M. L. (1997). Molecular indicators of diagenetic status in marine organic matter. *Geochim. Cosmochim. Acta* 61, 5363–5369. doi: 10.1016/S0016-7037(97)00312-8

Waterbury, J. B., Watson, S. W., Guillard, R. R. L., and Brand, L. E. (1979). Widespread occurrence of a unicellular, marine, planktonic, cyanobacterium. *Nature* 277, 293–294. doi: 10.1038/277293a0

Williams, W. P. (1998). "The physical properties of thylakoid membrane lipids and their relation to photosynthesis," in *Lipids in Photosynthesis: Structure, Function, and Genetics*, eds P.-A. Siegenthaler and N. Murata (Dordrecht: Kluwer Academic Publishers), 103–118.

Wörmer, L., Lipp,. J. S., Schröder, J. M., and Hinrichs, K.-U. (2013). Application of two new LC-ESI-MS methods for improved detection of intact polar lipids (IPLs) in environmental samples. *Org. Geochem.* 59, 10–21. doi: 10.1016/j.orggeochem.2013.03.004

Yabuuchi, E., Kaneko, T., Yano, I., Wayne Moss, C., and Miyoshi, N. (1983). Sphingobacterium gen. nov. *Sphingobacterium spiritivorum* comb. nov. *Sphingobacterium multivorum* comb. nov. *Sphingobacterium mizutae* sp. nov., and *Flavobacterium indologenes* sp. nov.: glucose-nonfermenting gram-negative rods in CDC groups IIK-2 and IIb. *Int. J. Syst. Bacteriol.* 33, 580–598. doi: 10.1099/00207713-33-3-580

Yabuuchi, E., and Moss, C. W. (1982). Cellular fatty acid composition of strains of three species of *Sphingobacterium* gen. and Cytophaga johnsonae. *FEMS Microbiol. Lett.* 13, 87–91. doi: 10.1111/j.1574-6968.1982.tb08233.x

Yano, I., Tomiyasu, I., and Yabuuchi, E. (1982). Long chain base composition of strains of three species of *Sphingobacterium* gen. nov. *FEMS Microbiol. Lett.* 15, 303–307. doi: 10.1111/j.1574-6968.1982.tb00239.x

Yooseph, S., Nealson, K. H., Rusch, D. B., McCrow, J. P., Dupont, C. L., Kim, M., et al. (2010). Genomic and functional adaptation in surface ocean planktonic prokaryotes. *Nature* 468, 60–67. doi: 10.1038/nature09530

Zhu, C., Lipp, J. S., Wörmer, L., Becker, K. W., Schröder, J., and Hinrichs, K.-U. (2013). Comprehensive glycerol ether lipid fingerprints through a novel reversed phase liquid chromatography-mass spectrometry protocol. *Org. Geochem.* 65, 53–62. doi: 10.1016/j.orggeochem.2013.09.012

Conflict of Interest Statement: The authors declare that the research was conducted in the absence of any commercial or financial relationships that could be construed as a potential conflict of interest.

frontiers in Marine Science

ORIGINAL RESEARCH
published: 14 February 2017
doi: 10.3389/fmars.2017.00035

Response of the Calanoid Copepod *Clausocalanus furcatus*, to Atmospheric Deposition Events: Outcomes from a Mesocosm Study

Epaminondas D. Christou[1]*, *Soultana Zervoudaki*[1], *Ma Luz Fernandez De Puelles*[2], *Maria Protopapa*[1], *Ioanna Varkitzi*[1], *Paraskevi Pitta*[3], *Tatiana M. Tsagaraki*[3] and *Barak Herut*[4]

[1] Hellenic Centre for Marine Research, Institute of Oceanography, Athens, Greece, [2] Centro de Baleares, Instituto Español de Oceanografia, Palma de Mallorca, Spain, [3] Hellenic Centre for Marine Research, Institute of Oceanography, Heraklion, Greece, [4] Israel Oceanographic and Limnological Research, National Institute of Oceanography, Haifa, Israel

Atmospheric deposition is assumed to stimulate heterotrophic processes in highly oligotrophic marine systems, controlling the dynamics and trophic efficiency of planktonic food webs, and is expected to be influenced by climate change. In the course of an 8-day mesocosm experiment, we examined the channeling, of the Saharan dust (SD) and mixed aerosols (A) effects on microplankton up to the copepod trophic level, in the highly oligotrophic Eastern Mediterranean Sea. Based on mesocosms with SD and A treatments, we evaluated the feeding response of the dominant copepod *Clausocalanus furcatus* every other day. We hypothesized that increased food availability under atmospheric deposition would result in increased copepod ingestion rates, selectivity and production. Overall, no robust pattern of food selection was documented, and daily rations on the prey assemblage of all mesocosms were very low indicating severe food limitation of *C. furcatus*. Although increased food availability was not true, after few days ingestion of ciliates was maximized, followed by egg production, in both the SD and A treatments, indicating their importance in the diet of this copepod as well as a response of *C. furcatus* feeding performance. Our results help in understanding the trophic efficiency of marine food webs in ultra-oligotrophic environments under atmospheric deposition. We suggest that future mesocosm research in oligotrophic waters should consider more than one copepod species.

Keywords: mesocosm experiments, dust, aerosols, copepods, feeding, *Clausocalanus furcatus*, Eastern Mediterranean

OPEN ACCESS

Edited by:
Xabier Irigoien, King Abdullah University of Science and Technology, Saudi Arabia

Reviewed by:
Dacha Atienza, Spanish National Research Council, Spain
Hans Uwe Dahms, Kaohsiung Medical University, Taiwan

***Correspondence:**
Epaminondas D. Christou
edc@hcmr.gr

Specialty section:
This article was submitted to Marine Ecosystem Ecology, a section of the journal Frontiers in Marine Science

Received: *30 September 2016*
Accepted: *27 January 2017*
Published: *14 February 2017*

Citation:
Christou ED, Zervoudaki S, Fernandez De Puelles ML, Protopapa M, Varkitzi I, Pitta P, Tsagaraki TM and Herut B (2017) Response of the Calanoid Copepod Clausocalanus furcatus, to Atmospheric Deposition Events: Outcomes from a Mesocosm Study. Front. Mar. Sci. 4:35. doi: 10.3389/fmars.2017.00035

INTRODUCTION

Inorganic nutrients are among the key abiotic factors regulating primary producers and, ultimately, the trophic status of marine ecosystems. Dust deposition is recognized as a significant source of macro- and micro-nutrients to the surface ocean (Jickells et al., 2005; Mahowald et al., 2008) and is particularly important in areas with little input from other external sources (e.g., Jickells et al., 2005; Duce et al., 2008), as in the Eastern Mediterranean Sea (Herut et al., 2002; Krom et al., 2004). Recent efforts to comprehend the action of these contributions on ocean biogeochemistry, has dedicated

on the influence on primary productivity, assumed their aptitude to generate new production (e.g., Ridame et al., 2014). However, recent studies, merging field and experimental work, indicated significant boost in heterotrophic bacterial abundance and respiration following up atmospheric deposition in oligotrophic systems (Lekunberri et al., 2010; Romero et al., 2011; Pulido-Villena et al., 2014). Additionally, heterotrophic processes were found to be further activated by dust pulses when compared to autotrophic processes with increasing degree of oligotrophy, the dominant response being controlled by the nutrients competition between bacteria and phytoplankton (Maranon et al., 2010).

Normally the dominance of copepods is a well-established pattern in extremely oligotrophic systems (Nuwer et al., 2008; Villar-Argaiz et al., 2012). Even if many factors have been identified to qualitatively affect zooplankton succession (temperature, predation rates, etc.), food availability has been identified as a key regulatory aspect of the zooplankton growth (Sterner and Elser, 2002). Marine copepods may reveal a considerable selective feeding response, selecting the most appropriate prey based on size (Mullin, 1963; Frost, 1972), motility (Atkinson, 1995; Broglio et al., 2001), and nutritional value (Cowles et al., 1988; Isari et al., 2013). Copepods usually choose microzooplankton prey over smaller phytoplankton (Calbet and Saiz, 2005; Saiz and Calbet, 2011), therefore microzooplankton may be an essential linkage between phytoplankton and metazoans (Stoecker and Capuzzo, 1990; Schmoker et al., 2013). Finally, in an increase of total food availability, feeding rates of copepods are expected to be increased and prey selection to be more intense (DeMott, 1989, 1995), ultimately leading to a positive influence of copepod production.

The present paper was aimed at elucidating how the impact of Saharan dust and mixed aerosols (polluted and desert origin) on microplankton may be channeled to marine copepods. The Mediterranean Sea might receive high amounts of atmospheric particles, of both natural (Saharan) and anthropogenic origin, over broad areas (e.g., Guerzoni et al., 1999; Pulido-Villena et al., 2014). These atmospheric depositions possibly represent the major input of external nutrients entering offshore surface waters (Herut et al., 2002; Bartoli et al., 2005; Guieu et al., 2010). A mesocosm experiment was designed to test the influence of atmospheric deposition on the plankton community of the Eastern Mediterranean. This extremely oligotrophic ecosystem, described as phosphorus limitated (Krom et al., 1991), or nitrogen and phosphorous co-limitated (Tanaka et al., 2011; Ternon et al., 2011), is ideal for testing the atmospheric deposition hypothesis. We hypothesized that increased food availability under atmospheric deposition would result in increased copepod ingestion rates, selectivity and production.

For the estimation of copepod vital rates three deposition treatments were used in parallel. Based on incubation experiments during the evolution of an initially triplicate plankton assemblage, we estimated the *Clausocalanus furcatus* response [based on feeding rates, prey preferences, daily ration (DR) and egg production], which dominated in the mesocosm plankton community. Although this copepod is known for its extensive distribution and biological importance, there is insufficient information on its feeding response under natural conditions (Paffenhofer et al., 2006; Cornils et al., 2007b). The present paper encompasses the first results on the *Clausocalanus furcatus* feeding ecology, triggered by atmospheric deposition events. This may help in explaining its response under specific nutrient regimes and in obtaining vision on the functioning of trophic webs in ultra-oligotrophic environments.

METHODS

Mesocosm Set up and experimental Design

The influence of atmospheric deposition on copepods was investigated as a part of the ATMOMED mesocosm experiment carried out from 10 to 18 May 2012 at the CRETACOSMOS facility of the Hellenic Centre for Marine Research in Crete, Greece (www.cretacosmos.eu). The facility consists of a 350 m^{-3} land-based concrete pond, 5 m deep, supplied with continuous seawater flow-through in order to maintain ambient surface water temperature. The experiment was carried out using surface (∼10 m depth) seawater that was collected using a rotary submersible pump placed on board the R/VPhilia from allocation 5 nautical miles north of Heraklion port in the Cretan Sea (35o 24.975N, 25o 14.441E). The collected seawater was equally distributed by gravity into nine food-grade polyethylene mesocosm bags to ensure the homogeneity of the collected seawater between bags. The mesocosms were mounted on aluminum frames (1.12 m diameter) attached to the pool's walls. Each mesocosm had a total volume of 3 m^{-3}. The mesocosms were gently mixed throughout the experiment, using an airlift pump to avoid stratification. They were covered with a two-layer lid in order to protect them from natural atmospheric aerosol depositions during the experiment and mimic the light conditions at a 10 m water depth.

The mesocosm set up involved two distinct deposition treatments [Sahara Dust (SD) and mixed aerosols (A)] and a control (C) all triplicated in the bags. A more detailed description of the mesocosm set up and experimental design is provided by Tsagaraki et al. (this issue) and Herut et al. (2016). For the copepod feeding and production experiments, we used all three treatments (C, SD, and A). The water was sampled by all three replicates of each treatment, which was then mixed to produce one water mass for each treatment.

Zooplankton Sampling/analysis

Zooplankton abundance (individuals m^{-3}) and copepod community composition were determined at the start (24 h before Day 0) and at the end (Day 18) of the mesocosm experiment. The initial zooplankton sampling was performed, when the water for the mesocosms was collected, using a modified WP2 45 μm net. Samples were preserved in 4% buffered formalin and then inspected under a stereoscopic microscope. At the end of the experiment, the water of each replicate treatment was filtered over a 45 μm net and zooplankton samples were treated as described above. A total of 12 samples were analyzed: three from the field and nine from the nine bags at the end of the experiment.

Clausocalanus furcatus Experiments

Copepod feeding and production were assessed on four dates (11, 12, 15, 17, May 2012), in each of the three mesocosm treatments. Four experiments were conducted, Exp1 on 11/5, Exp2 on 12/5, Exp3 on 15/5, and Exp4 on 17/5.

For the feeding experiments, adult females of the dominant copepod species *Clausocalanus furcatus* were used. The copepods were collected from the same area as the original water for the mesocosms, and pre-conditioned for 24 h in water from the corresponding treatment and under the respective ambient conditions. Water for the incubations was taken from each replicate enclosure early in the morning and mixed (three to one) according to the respective treatment. Then it was gently inversely filtered through a 100 mm mesh to exclude any zooplankton, while minimizing effects on delicate organisms such as ciliates (Broglio et al., 2004). For each mesocosm treatment, nine bottles (1.3 L polycarbonate) were prepared amended with 1 μM NH_4Cl, 0.07 μM Na_2HPO_4, and 0.5 μM Na_2SiO_3. This nutrient addition was used to ensure that nutrients were not limiting in any treatment (Calbet et al., 2012) and to avoid selectively increased phytoplankton growth in the copepod-amended bottles due to excretion. Adult copepods (ca. 10–12 females) were added to three of the nine bottles, whereas the other six served as initial (three) and control (three) bottles. The experimental bottles were incubated for ca. 24 h, hanged at 0.5 m depth from a floating wheel rotating at ca. 1 r.p.m and propelled by a submerged water pump. This approach assured that food conditions were homogeneous in all bottles (Calbet et al., 2012).

The content of the bottles was collected by reverse filtration over a 200 mm mesh, at the beginning for the initial ones and after 24 h for the rest ones. Then samples for chlorophyll a (Chl a) and microplankton analysis were taken. For the control and copepod bottles, the remaining content was carefully emptied over a 200 μm mesh, and the copepod number and condition was checked. Total mortality was almost 0. Aliquots of 500 mL were filtered onto 0.2, μm polycarbonate filters to estimate chlorophyll a concentration. We considered that microplankton included ciliates and dinoflagellates, assuming all dinoflagellates as potentially heterotrophic, as in Loder et al. (2011). Microplankton samples were preserved in 2% acidic Lugol, settled in sedimentation chambers (100 mL) and counted using an inverted microscope at 200–400 magnification. For each microplankton category considered, cell size was measured and then converted into biovolume using simple geometric formulae (Hillebrand et al., 1999). Biovolume conversion to carbon was done according to the equations given in Menden-Deuer and Lessard (Menden-Deuer and Lessard, 2000) for dinoflagellates. Separate conversion factors were applied to aloricate (Putt and Stoecker, 1989) and loricate (Verity and Langdon, 1984) ciliates. Chl a concentrations were converted to carbon biomass using a conversion factor of 50 (C:Chl a = 50).

For the estimation of the egg production 25–30 healthy-looking, actively swimming females without an egg-sac, were sorted using a stereomicroscope. Three to four females were placed in each of six 620 ml glass jars (replicates) containing well-mixed 60 μm filtered water collected from each treatment (for details see below). The females were incubated at the ambient sea temperature (20°C) and photoperiod for 24 h after which the spawned eggs were counted and female lengths and egg diameters were measured. Overall mortality was 0.

Feeding rates were determined according to the equations of Frost (Frost, 1972). The carbon content of *C. furcatus* was estimated from length measurements applying the length-body carbon regression equation for *Paracalanus* spp. by Uye (1991). Then daily rations (DRs) in % body carbon ingested per day were calculated. Copepod feeding preference of ciliates and dinoflagellates size fractions (small vs. large size cells) was assessed by the Chesson's selectivity index a (Chesson, 1983):

$$a = \frac{r_i/n_i}{\sum_{j=1}^{m} r_j/n_j}$$

where r_i is the frequency of the food type i in the diet, n_i is the frequency of the food type i in the available food and m is the number of food types. This index fluctuates between 0 and 1 and neutral selection corresponds to $a_i = 1/n$. Therefore, non-selective feeding is indicated by $a_i = 0.25$ in the case of a four-option choice (i.e., the taxonomic group, size). Higher values than these indicate positive preference for food type i, whereas lower values indicate avoidance for food type i.

RESULTS

Copepod Community

Copepods were the numerically dominant group both in the field at the onset of the experiment (87.6%) and in the three mesocosm treatments after the end of the experiment (C, SD, and A: 87.4–92.6), followed by pteropods (7–10.7%) and other zoolankton (0.2–4.1%). The composition of the copepod community is included in **Table 1**. Female *Clausocalanus furcatus* with the genus copepodites clearly dominated (field: 54%; C: 30%; SD: 35%, A: 32%), while copepodites of the cyclopoid Oithona spp., the copepod nauplii, and the harpacticoid *Microsetella* spp. followed in numbers. The copepod number in C at the end of the experiment (113 ind. m^{-3}) was higher than those of SD and A (96 and 98 ind. m^{-3}). The abundance of the genus Clausocalanus was almost triple in the field, when compared to the mesocosms (**Table 1**).

Clausocalanus furcatus Egg Production

Clausocalanus furcatus production (specific egg production, SEP) was extremely low, ranging from 0 to 0.67% body C day^{-1} in the C treatment, from 0 to 6.32% body C day^{-1} in the SD treatment and from 0 to 7.53% body C day^{-1} in the A treatment. The two maxima 6.32 and 7.53% body C day^{-1}, corresponding to 5.6 and 6.7 eggs ind^{-1} day^{-1} respectively, were recorded in Exp3.

Potential Prey of *C. furcatus*

The evolution of the Chl a values in the 3 mesocosms during the experiment is presented in **Figure 1A**. The SD and A treatments revealed a gradual decrease from the first to the last day. In general Chl a showed very low values in all treatments due to the oligotrophy of the area. The Chl a concentrations in SD

TABLE 1 | Copepods identified at the beginning of the experiment (in the field) and at the end of the experiment (in the mesocosm treatments C, SD, and A).

Order	Copepod taxa	Abundance (ind. m^{-3})				Relative abundance (%)			
		Field	C	SD	A	Field	C	SD	A
Calanoida	*Acartia* spp.	0.0	0.1	0.0	0.0	0.0	0.1	0.0	0.0
	Acartia cop.	0.0	1.0	0.4	0.5	0.0	0.9	0.4	0.5
	Calocalanus spp.	0.0	0.0	0.0	0.4	0.0	0.0	0.0	0.4
	Clausocalanus spp.	0.0	3.7	5.4	2.9	0.0	3.3	5.7	2.9
	Clausocalanus furcatus fem	5.7	6.7	6.9	8.6	3.4	5.9	7.3	8.7
	Clausocalanus males	0.3	5.2	4.6	5.7	0.2	4.6	4.8	5.8
	Clausocalanus cop.	82.3	26.7	26.3	22.7	50.1	23.6	27.7	23.1
	Paracalanus cop.	0.0	2.0	3.0	0.1	0.0	1.8	3.1	0.1
	Temora stylifera cop.	0.0	0.3	0.2	0.0	0.0	0.2	0.2	0.0
	Unknown cop.	0.3	2.5	2.4	1.2	0.2	2.2	2.5	1.2
	Nauplii	47.0	17.1	9.6	17.1	28.6	15.1	10.1	17.3
Cyclopoida	*Corycaeus* spp.	0.0	0.0	0.1	0.0	0.0	0.0	0.1	0.0
	Corycaeus cop.	0.0	1.1	1.0	2.2	0.0	1.0	1.1	2.2
	Farranula rostrata fem	1.0	0.1	0.0	0.0	0.6	0.1	0.0	0.0
	Farranula rostrata cop.	0.3	0.0	0.0	0.0	0.2	0.0	0.0	0.0
	Mormonilla minor	0.0	0.0	0.2	0.0	0.0	0.0	0.2	0.0
	Oithona spp.	0.3	0.5	0.0	0.8	0.2	0.5	0.0	0.8
	Oithona similis	1.0	0.1	0.2	0.3	0.6	0.1	0.2	0.3
	Oithona cop.	16.0	21.9	21.3	22.4	9.7	19.4	22.4	22.7
	Oithona males	0.0	0.4	0.3	0.0	0.0	0.3	0.3	0.0
	Oncaea spp.	0.0	2.1	2.3	1.7	0.0	1.9	2.4	1.7
	Oncaea males	0.7	3.2	1.4	1.2	0.4	2.8	1.5	1.2
	Oncaea cop.	2.3	4.1	1.5	2.4	1.4	3.6	1.6	2.4
Harpacticoida	*Microsetella* spp.	7.0	14.2	7.9	8.5	4.3	12.5	8.3	8.7
	Total copepod abundance	164.3	113.1	95.1	98.5				

Abundance data (ind. m^{-3}) and relative copepod abundance (%) are included (cop: copepodites, fem: females).

and A were, on average across all samplings, higher than in C mesocosm. Dinoflagellates (DF) showed a gradual decrease from Exp1 to Exp3 in both SD and A treatments. Ciliates (CIL) exhibited an increase from Exp1 to Exp3 in C and A treatments, and an overall increase after Exp1 in SD mesocosm (**Figure 1A**). Two-way ANOVA tests showed no significant differences among the treatments comparing with the initial prey concentrations

Total available carbon exhibited a gradual decrease from Exp1 to Exp4 in both SD and A treatments (**Figure 2A**). However, this decrease in control was interrupted by a maximum in Exp3. DF was the major food component contributing from 47 to 95% (**Figure 2A**). The carbon development pattern was comparable in SD and A treatments, with decreasing DF and increasing CIL. In almost all cases, but one, DF had the higher contribution to the total available carbon. However, DF/CIL equaled in Exp3 in the SD and A treatments, comprising 50.5/49.5 and 50.7/49.3 respectively.

Clausocalanus furcatus Feeding Response

Vital feeding was found in all cases on DF and CIL, whereas clearance rates on Chl a were lower (**Figure 3**). Clearance rates on both DF and CIL were more or less similar (DF: 22–97 ml cop^{-1} d^{-1}; CIL: 14–152 ml cop^{-1} d^{-1}). Clearance rates on CIL attained some higher values, with the highest ones to be detected in Exp3 in the A and SD treatments. In contrast, in SD mesocosms DF were cleared at significantly lower rate than the other two treatments ($p < 0.05$). Finally, Chl a was cleared at much lower rates (2–54 ml cop^{-1} d^{-1}).

An increasing trend was evident concerning Chl a ingestion rates in the C incubations, opposing to the decreasing trend in the SD ones (**Figure 1B**). DF ingestion rates did not exhibit any distinct pattern and the highest values were observed in the C and A treatments in Exp2 and Exp1, respectively. However, CIL ingestion rates showed an increasing trend from Exp1 to Exp3 in all treatments, with the highest values for both DF and CIL to be detected in Exp3 (**Figure 1B**). No statistically significant differences were found.

Taking into account the total consumed carbon (**Figure 2B**), no clear pattern was identified among treatments, but an increase from Exp1 to Exp3 in the SD treatment and from Exp2 to Exp4 in the A treatment. Average consumed carbon was 4.6, 3.8, and

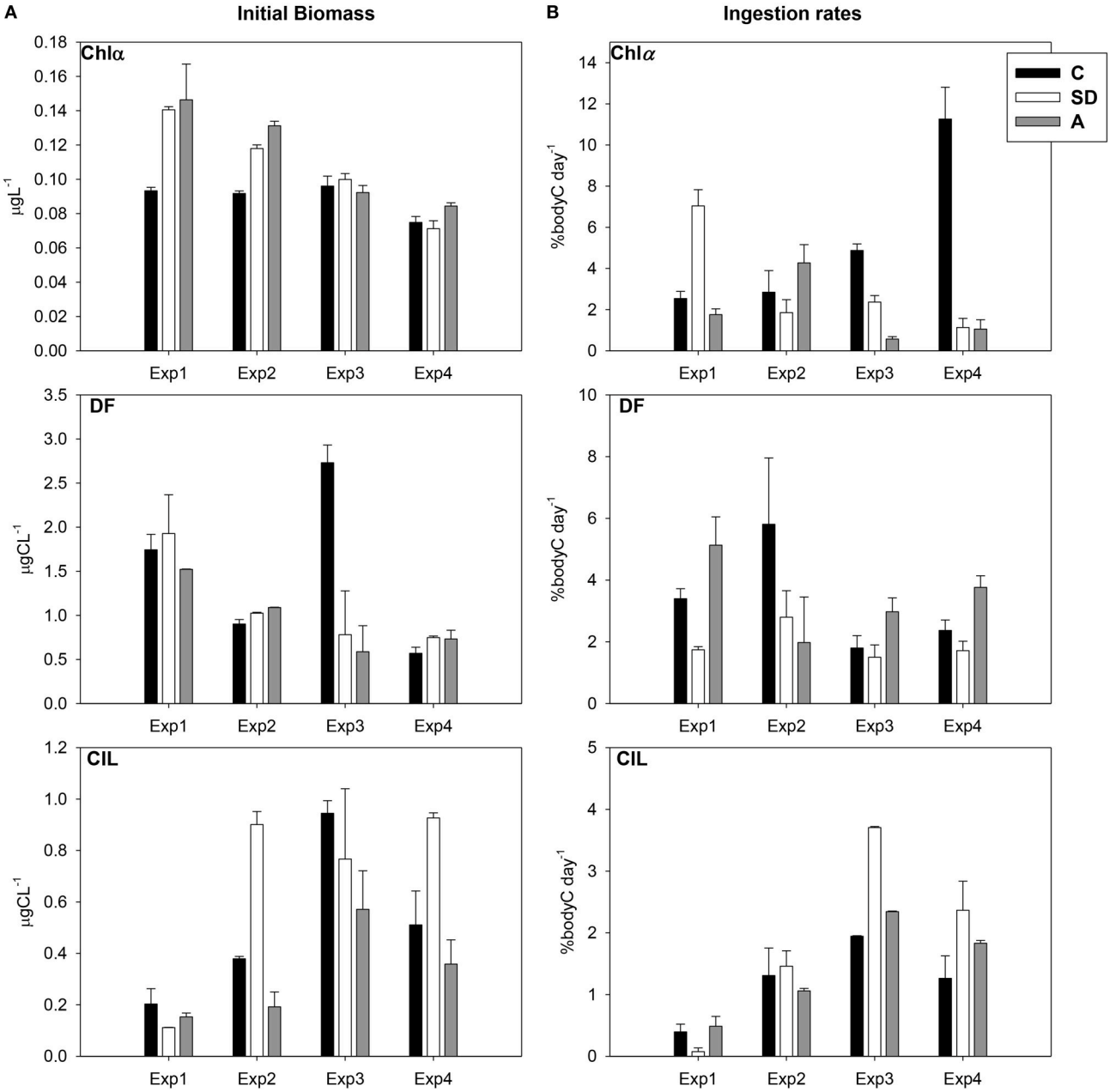

FIGURE 1 | (A) Temporal variation of chlorophyll a (Chl a, µg l^{-1}), dinoflagellates (DF, µg C l^{-1}), and ciliates (CIL, µg C l^{-1}) in the mesocosm treatments for the days of the feeding experiments (values represent initial samples of the feeding experiments) **(B)** Temporal variation of ingestion rates (% body C d^{-1}) on Chl a, DF and CIL.

4.9 % body C d^{-1} in the C, SD, and A mesocosms respectively, ranging in total from 1.2 to 7.1% body C d^{-1}. No positive relation was observed between DR and prey availability. The highest ingestion rate in the C mesocosm was recorded in Exp2, Concerning SD and A treatments, total ingestion rates were very low (<6% body C d^{-1}). However, regarding CIL contribution to the total DR, an increase was evident from Exp1 to Exp3 in both the SD and A treatments (**Figure 2B**). No statistically significant differences were found.

The results of Chesson's selectivity index (Chesson, 1983) are presented in **Figure 4**. In the C treatment, *C. furcatus* exhibited the highest selectivity for DF, mostly for those <20 µm. Under SD and A conditions, selectivity patterns confirmed the DF preference. However, in the SD treatment, the overall preference was stronger for the >20 µm DF, opposing to the <20 µm DF selectivity which was stronger in the A treatment. The highest selectivity, for <20 µm DF, was observed on the third day.

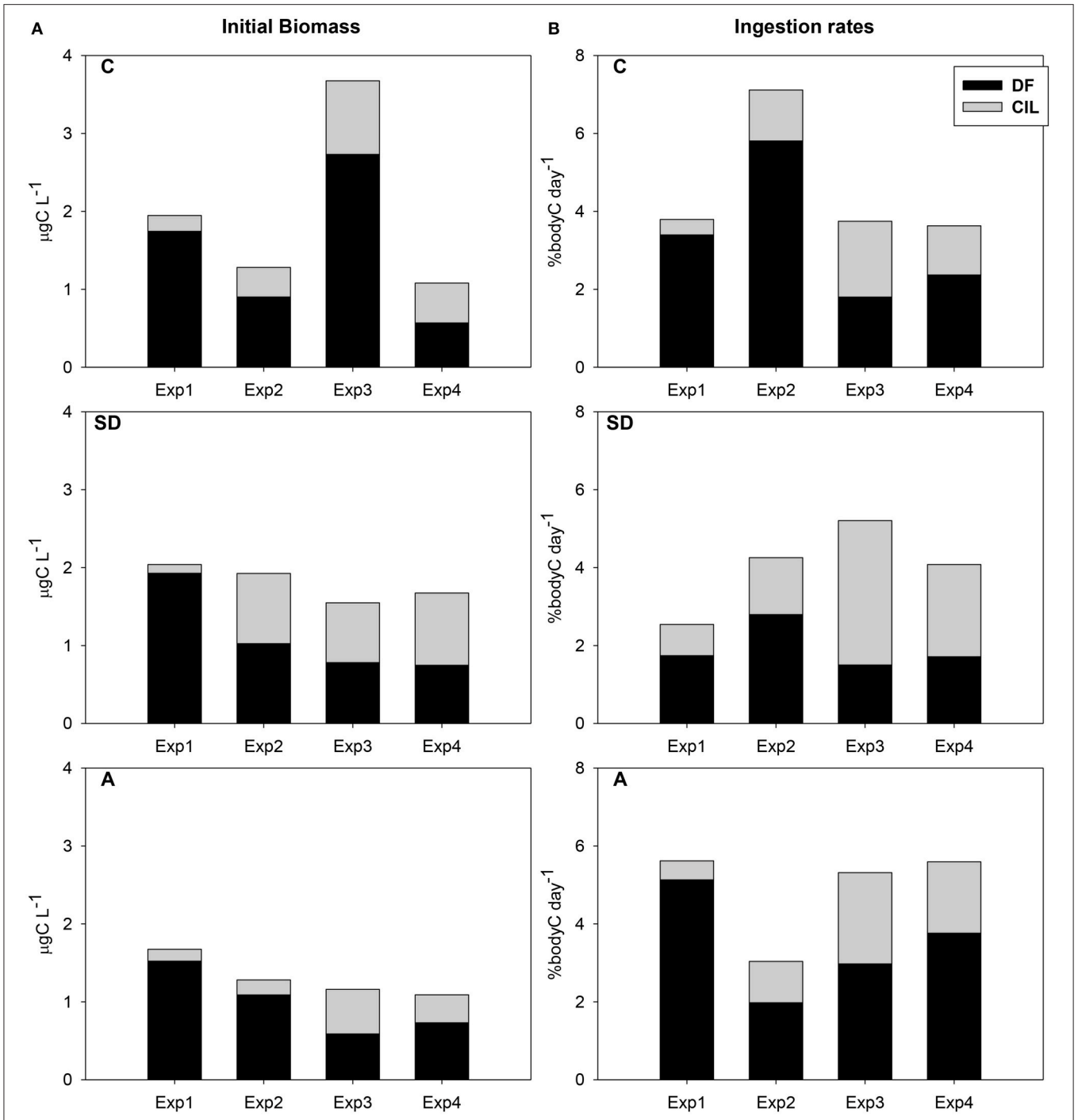

FIGURE 2 | (A) Temporal variation of the contribution to the available heterotroph carbon (DF and CIL) in the mesocosm treatments during the experiments (values represent initial samples of the feeding experiments) **(B)** Contribution of DF and CIL to the DR of *C. furcatus* in the mesocosm treatments.

DISCUSSION

Clausocalanus furcatus, a small clausocalanid, is one of the dominant calanoid copepods in warm waters globally (e.g., Mazzocchi and Ribera d'Alcalà, 1995; Cornils et al., 2007a; Miyashita et al., 2009; Schnack-Schiel et al., 2010; Siokou-Frangou et al., 2010). This copepod occurs in the epipelagic zone all over the world (Frost and Fleminger, 1968), also in the Mediterranean region (e.g., Siokou-Frangou et al., 2010), and usually dominates zooplankton communities in oligotrophic environments (Schulz, 1986; Mazzocchi and Ribera d'Alcalà, 1995; Webber and Roff, 1995; Cornils et al., 2007a). In a

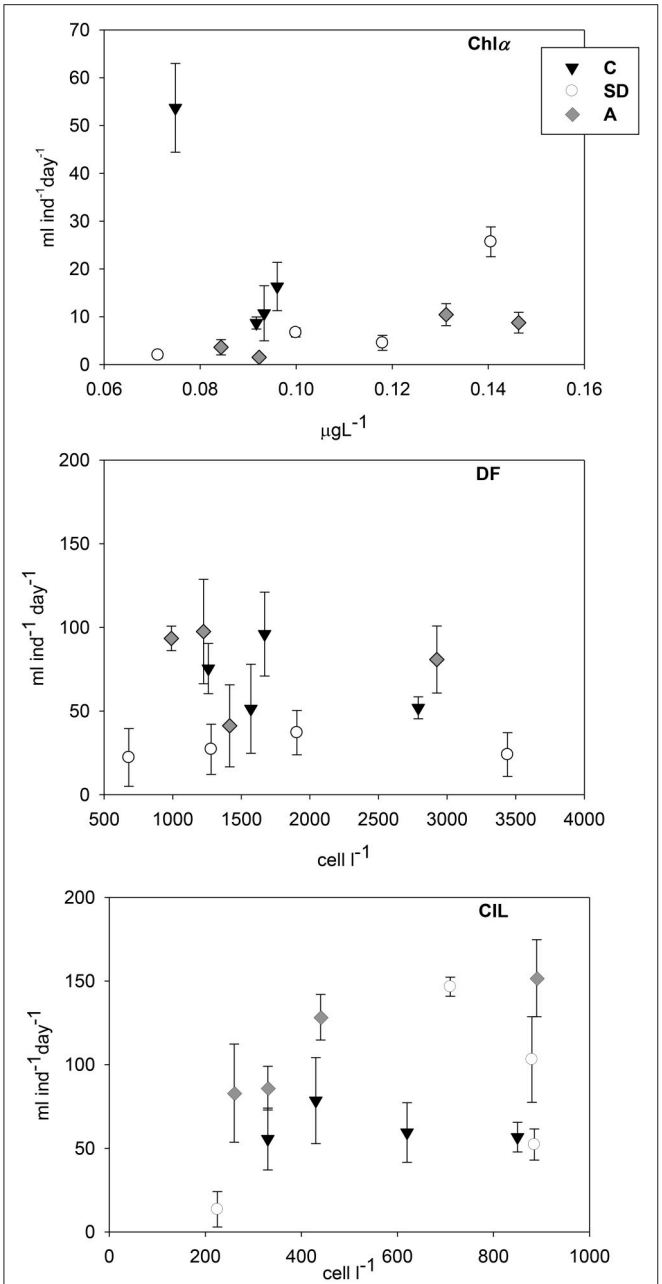

FIGURE 3 | Copepod clearance rates (ml cop^{-1} d^{-1}) on chlorophyll a (Chl a), dinoflagellates (DF), and ciliates (CIL) in the three mesocosm treatments. Error bars indicate the standard error.

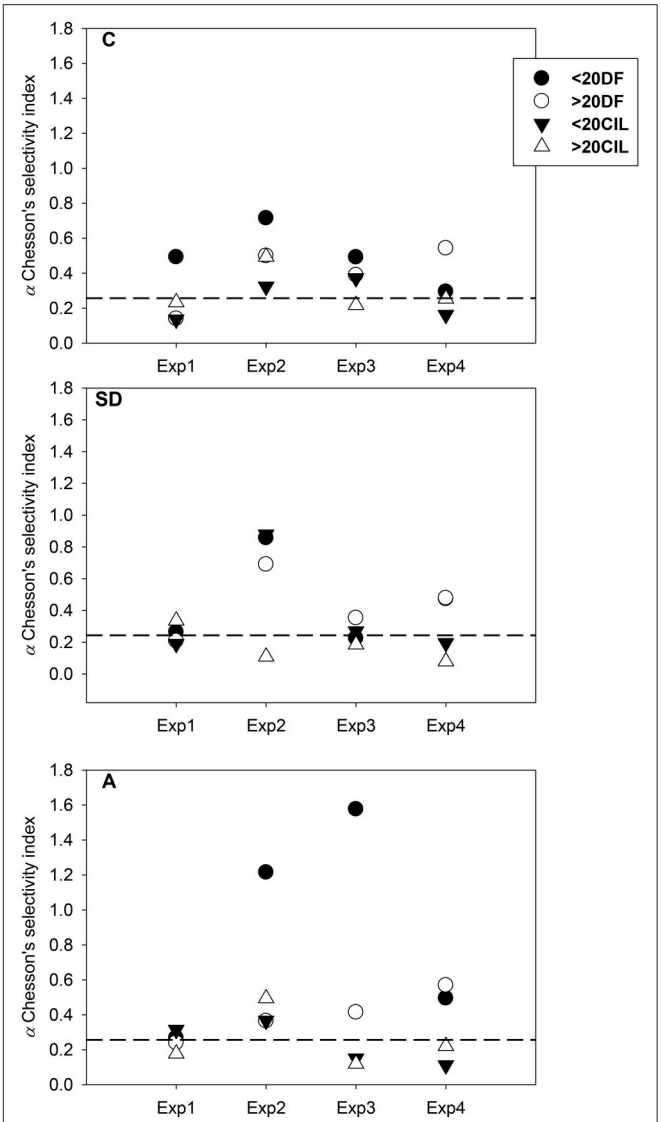

FIGURE 4 | Chesson's selectivity index values calculated for (circles) dinoflagellates >20 μm over <20 μm, (triangles) ciliates >20 μm over <20 μm. The dashed horizontal line represents a level of a, where no selectivity is detected (a: 0.25). SD, Saharan dust; A, mixed aerosols; C, control.

recent paper, investigating the niche separation of *Clausocalanus* species in the Atlantic Ocean, it was found that *C. furcatus* had a narrow thermal and salinity niche and its optimal conditions were warm, saline and very oligotrophic waters (Peralba et al., in press).

The maximum egg production of *C. furcatus* found in our work was almost half to that reported for the same species in the Gulf of Mexico (Bi and Benfield, 2006) and fall in the range reported for *C. furcatus* in the Gulf of Aqaba (Cornils et al., 2007a). In the Atlantic Ocean, the shortest interclutch period of *C. furcatus* was recorded in mesotrophic sites (around the NW African upwelling), where the potential food availability would be favorable for egg production (Peralba et al., in press). On the other hand, it has been observed that *C. furcatus* production rate in laboratory conditions, was higher at low food concentrations (Mazzocchi and Paffenhofer, 1998). Peralba et al. (in press), commenting on this issue, explained that the high diversity of a natural diet may be more profitable for the metabolic needs and would enhance higher egg production rates.

In the present work *C. furcatus* appeared to produce eggs at low available food, although in most cases could not. It has been reported that clausocalanoids are able to produce eggs at low food availability (Mazzocchi and Paffenhofer, 1998,

1999; Bi and Benfield, 2006; Cornils et al., 2007a). Indeed, Mazzocchi and Paffenhofer (1998) showed that in the lab, *C. furcatus* egg production was higher when food (dinoflagellates and diatoms) concentrations were low than when provided with high food concentrations, hence proposing an adaptive strategy of this copepod to oligotrophic environments. In general egg production of clausocalanids, especially those producing egg sacs, appears to be low when compared to other calanoids (Cornils et al., 2007a; review in Mauchline, 1998).

Comparisons with data available on *C. furcatus* feeding rates revealed that the ingestion rates of the present work stand within the lower part of the range reported for experiments with natural prey assemblage or with cultured monospecific diets. The low ciliate and dinoflagellate ingestion rates in our study are comparable to the laboratory findings of Mazzocchi and Paffenhofer (1998) with dinoflagellates as food. However, the latter rates enhanced with increasing cell concentrations (Cornils et al., 2007b). Mazzocchi and Paffenhofer (1999) found low ratios in spite of their observations of increased swimming movement, suggesting that nonstop movement might be energetically superior to discontinuing movement. In the NW Mediterranean ingestion rates for *Clausocalanus* spp. (10–40% body C d^{-1}, Broglio et al., 2004) were 3 to 4 times higher than those of the present study. In general, under natural conditions, the ingestion rates can fluctuate within a broad range, as it has been reported for other medium to small sized copepods (e.g., *Centropages typicus*, 4–70%; Dagg and Grill, 1980).

In our work, clearance rates of *C. furcatus* on the different food types fall in the range reported for this copepod in other oligotrophic areas (Paffenhofer et al., 2006; Isari et al., 2014). Daily rations (DRs) on the available food of all treatments were low, either taking into account only ciliate or dinoflagellate food (maxima of 3.7% in SD and 5.8% in A, respectively) or as a total (maximum of 7.1% in C). These values are lower than DRs (10–34%) based on feeding rates of this copepod on monospecific dinoflagellate diets (Mazzocchi and Paffenhofer, 1998), and are either much lower or slightly higher than results for other clausocalanids fed on natural diets in subtropical oligotrophic waters (Paffenhofer et al., 2006: 38%; Cornils et al., 2007b: 2%). DRs of this study are, also, a bit lower than those of *C. furcatus* from an earlier mesocosm experiment, at the same area but not same season (Isari et al., 2014). Evaluating the adequacy of the DRs taking into account the daily metabolic requirements, we found that the daily basal metabolic demands at 20°C would account for 23.4% of its body weight, which would need a DR of 26% using an assimilation efficiency of 90% (Paffenhofer, 2006). This value is more than duplicated the DRs achieved in our feeding experiments, indicating serious food limitation of *C. furcatus* in the mesocosm experiments. It has been suggested that the basal metabolic demands of *C. furcatus* may be satisfied even under the mostly limited food availability in the subtropical open seas (Paffenhofer et al., 2006). Nevertheless, the strategy developed by this copepod to deal with the scarcity of food in the marine environment is not clear (Paffenhofer et al., 2006; Cornils et al., 2007b), and it is worth questioning in what way an ingestion hardly sufficient to meet the energy requirements in our experiment would sustain the egg production of this copepod in the mesocosms. Information about nanoplankton availability as potential food is lacking from our work. Nanoplankton has been found to be important in the diet of *C. furcatus* from an earlier mesocosm experiment, at the same area (Isari et al., 2014). Copepods, depending on the species and the feeding strategy, may fulfill their metabolic requirements by foraging on other non-living material as well (e.g., detrital material; Roman, 1984) or even utilizing prey patchiness (Tiselius, 1992; Saiz et al., 1993). However, it is impossible that such procedures may be triggered inside mesocosms.

Food availability has been considered as a major importance issue in determining copepod feeding strategy in the marine environment (Saiz and Calbet, 2007, 2011). Overall, in the present work, no robust pattern of food selection was observed, in agreement with the prediction of the optimal foraging theory, demonstrating that copepods may feed selectively when food is plentiful and non-selectively when food is limited (DeMott, 1989, 1995). In the oligotrophic Gulf of Aqaba, *C. furcatus* ingested preferably ciliates and dinoflagellates, whereas no preference was detected for diatoms and flagellates (Cornils et al., 2007b); nevertheless, selectivity indices, calculated according to Chesson (1983), revealed no preference of any food type. Therefore, it was assumed that the *C. furcatus* diet in the Gulf of Aqaba was diverse and depended mainly on food abundance rather than food type (Cornils et al., 2007b).

Selective predation on CIL is well documented in copepod feeding behavior (Calbet and Saiz, 2005; Saiz and Calbet, 2011), related with their high nutritional quality (Stoecker and Capuzzo, 1990), their optimal size range, and their motility pattern (Tiselius and Jonsson, 1990; Atkinson, 1995; Saiz and Kiørboe, 1995; Kiørboe et al., 1996). Preference for CIL has been pointed out for *Clausocalanus* spp. in NW Mediterranean (Batten et al., 2001; Broglio et al., 2004) and a selection for both CIL and DF, was indicated for *C. furcatus* in the Gulf of Aqaba (Cornils et al., 2007b). In addition to CIL, DF also comprise a substantial amount of the carbon consumed by copepods in oligotrophic seas and in many cases are positively selected, even though to a lower degree when compared to CIL (Saiz and Calbet, 2011). In this work, according to Chesson (1983), *C. furcatus* revealed preference for DF <20 μm and in a lesser degree for CIL. However, CIL ingestion was maximized in Exp3, in both the SD and A treatments, and concurred with the highest copepod spawning, indicating that CIL consumption might enhance copepod production. This can be likely explained not only by the conventional size-dependent selective feeding strategy but also by a selectivity based on nutritional criteria. It was found that *C. furcatus* retains an array of mechanical, chemical and dual-function sensors over its antenna (A_1), by which the copepod can identify surroundings stimuli (Uttieri et al., 2008), thus improving its feeding success.

In general, the food types tested in all related studies involved only a small variation in the food concentration, which remained mostly in the ranges of oligotrophy (Isari and Saiz, 2011). Therefore, there is a lack of comprehensive information on the ability of *C. furcatus* for energy exploitation in environments without food limitation (Isari and Saiz, 2011), where they can also populate (e.g., Valdes et al., 2007).

Concluding on *C. furcatus* feeding response in the present study, based on (a) the lack of robust food selection patterns (b) the lack of statistically significant differences, (c) the DF <20 μm preference according to Chesson (1983), and (d) the maximum CIL ingestion along with the maximum egg production, in Exp3; it appears that *C. furcatus* "touches the threshold" between feeding selectively and feeding non-selectively, switching continuously, very efficiently, from one mode to the other. This flexibility can be the *C. furcatus* setup, for the optimum exploitation of all available food (including food patchiness events) in oligotrophic environments.

CONCLUSIONS

Our data showed that, although increased food availability was not true, the feeding performance of the dominant copepod *C. furcatus* did have a response to the atmospheric deposition, through the changes mediated in the microbial food web (Tsagaraki et al., this issue; Herut et al., 2016). This is of great importance for the coupling between lower and higher trophic levels, through a more efficient transfer of food toward top consumers. However, the impact of atmospheric deposition, on the allocation of matter and energy through the planktonic food wed, is critically dependent on the copepod community composition; even if *Clausocalanus furcatus* is the dominant copepod, definitely does not represent the complete copepod diversity concerning trophic pathways. Different copepods and copepod stages display variable behaviorally driven feeding activities and preferences (Castellani et al., 2008), and daily feeding behaviors (Calbet et al., 1999). Future mesocosm research of the impact of atmospheric depositions on marine system performance should consider, if not the whole copepod community, more copepod species, especially regarding ultra-oligotrophic waters, and when necessary, deploy technologically highly developed experimental set-ups (Riebesell et al., 2013), closely imitating the actual characteristics of natural environment.

AUTHOR CONTRIBUTIONS

EC participation in experimental work, work planning, writing the ms. SZ participation in the field and experimental work, work planning, sample analysis, data processing. MF participation in the field and experimental work. MP sample analysis. IV sample analysis. PP work planning. TT participation in experimental work. BH work planning.

FUNDING

Hellenic Centre for Marine Research.

ACKNOWLEDGMENTS

This work was financed by the EU-FP7 project (grant agreement no. 228224) "MESOAQUA: Network of leading MESOcosm facilities to advance the studies of future AQUAtic ecosystems from the Arctic to the Mediterranean" and by the project ADAMANT: Atmospheric deposition and Mediterranean sea water productivity (nr code/MIS: 383551), co-financed by the European Union (European Social Fund –ESF) and Greek national funds through the Operational Program "Education and Lifelong Learning" of the National Strategic Reference Framework (NSRF) (Research Funding Program: THALES).

REFERENCES

Atkinson, A. (1995). Onmivory and feeding selectivity in five copepod species during spring in the Bellingshausen Sea, Antarctica. *ICES J. Mar. Sci.* 52, 385–396. doi: 10.1016/1054-3139(95)80054-9

Bartoli, G., Migon, C., and Losno, R. (2005). Atmospheric input of dissolved inorganic phosphorus and silicon to the coastal northwestern Mediterranean Sea: fluxes, variability and possible impact on phytoplankton dynamics. *Deep Sea Res. I* 52, 2005–2016. doi: 10.1016/j.dsr.2005.06.006

Batten, S. D., Fileman, E. S., and Halvorsen, E. (2001). The contribution of microzooplankton to the diet of mesozooplankton in an upwelling filament off the north west coast of Spain. *Prog. Oceanogr.* 51, 385–398. doi: 10.1016/S0079-6611(01)00076-3

Bi, H., and Benfield, M. (2006). Egg production rates and stage-specific development times of *Clausocalanus furcatus* (Copepoda, Calanoida) in the northern Gulf of Mexico. *J. Plankton Res.* 28, 1199–1216. doi: 10.1093/plankt/fbl050

Broglio, E., Johansson, M., and Jonsson, P. R. (2001). Trophic interaction between copepods and ciliates: effects of prey swimming behavior on predation risk. *Mar. Ecol. Prog. Ser.* 220, 179–186. doi: 10.3354/meps220179

Broglio, E., Saiz, E., Calbet, A., Trepat, I., and Alcaraz, M. (2004). Trophic impact and prey selection by crustacean zooplankton on the microbial communities of an oligotrophic coastal area (NW Mediterranean Sea). *Aquat. Microb. Ecol.* 35, 65–78. doi: 10.3354/ame035065

Calbet, A., Martınez, R. A., Isari, S., Zervoudaki, S., Nejstgaardc, J. C., Pitta, P., et al. (2012). Effects of light availability on mixotrophy and microzooplankton grazing in an oligotrophic plankton food web: evidences from a mesocosm study in Eastern Mediterranean waters. *J. Exp. Mar. Biol. Ecol.* 424–425, 66–77. doi: 10.1016/j.jembe.2012.05.005

Calbet, A., and Saiz, E. (2005). The ciliate-copepod link in marine ecosystems. *Aquat. Microb. Ecol.*, 38, 157–167. doi: 10.3354/ame038157

Calbet, A., Saiz, E., Irigoien, X., Alcaraz, M., and Trepat, I. (1999). Food availability and diel feeding rhythms in the marine copepods *Acartia grani* and *Centropages typicus*. *J. Plankton Res.*, 21, 1009–1015. doi: 10.1093/plankt/21.5.1009

Castellani, C., Irigoien, X., Mayor, D. J., Harris, R. P. and Wilson, D. (2008). Feeding of Calanus finmarchicus and Oithona similis on the microplankton assemblage in the Irminger Sea, North Atlantic. *J. Plankton Res.* 30, 1095–1116. doi: 10.1093/plankt/fbn074

Chesson, J. (1983). The estimation and analysis of preference and its relationhip to foraging models. *Ecology*, 64, 1297–1304. doi: 10.2307/1937838

Cornils, A., Niehoff, B., Richter, C., Al-Najjar, T., and Schnack-Schiel, S. B. (2007a). Seasonal abundance and reproduction of clausocalanid copepods in the northern Gulf of Aqaba (Red Sea). *J. Plankton Res.* 29, 57–70. doi: 10.1093/plankt/fbl057

Cornils, A., Schnack-Schiel, S. B., Boer, M., Graeve, M., Struck, U., Al-Najjar, T., et al. (2007b). Feeding of Clausocalanids (Calanoida, Copepoda) on naturally occurring particles in the northern Gulf of Aqaba (Red Sea). *Mar. Biol.*, 151, 1261–1274. doi: 10.1007/s00227-006-0569-9

Cowles, T. J., Olson, R. J., and Chisholm, S. W. (1988). Food selection by copepods: discrimination on the basis of food quality. *Mar. Biol.* 100, 41–49. doi: 10.1007/BF00392953

Dagg, M. J., and Grill, D. W. (1980). Natural feeding rates of *Centropages typicus* females in the New York Bight. *Limnol. Oceanogr.* 25, 597–609. doi: 10.4319/lo.1980.25.4.0597

DeMott, W. R. (1989). Optimal foraging theory as a predictor of chemically mediated food selection by suspension-feeding copepods. *Limnol. Oceanogr.* 34, 140–154. doi: 10.4319/lo.1989.34.1.0140

DeMott, W. R. (1995). Optimal foraging by a suspension-feeding copepod: responses to short-term and seasonal variation in food resources. *Oecologia* 103, 230–240. doi: 10.1007/BF00329085

Duce, R. A., LaRoche, J., Altieri, K., Arrigo, K. R., Baker, A. R., Capone, D. G., et al. (2008). Impacts of atmospheric anthropogenic nitrogen on the open ocean. *Science* 320, 893–897. doi: 10.1126/science.1150369

Frost, B., and Fleminger, A. (1968). A revision of the genus Clausocalanus (Copepoda: Calanoida) with remarks on distributional patterns in diagnostic characters. *Bull. Scripps Inst. Oceanogr.* 12, 1–235.

Frost, B. W. (1972). Effects of size and concentration of food particles on the feeding behavior of the marine planktonic copepod Calanus pacificus. *Limnol. Oceanogr.* 17, 805–815. doi: 10.4319/lo.1972.17.6.0805

Guerzoni, S., Chester, R., Dulac, F., Herut, B., Loye-Pilot, M. D., Measures, C., et al. (1999). The role of atmospheric deposition in the biogeochemistry of the Mediterranean Sea. *Prog. Oceanogr.* 44, 147–190. doi: 10.1016/S0079-6611(99)00024-5

Guieu, C., Loye-Pilot, M. D., Benyaya, L., and Dufour, A. (2010). Spatial variability of atmospheric fluxes of metals (Al, Fe, Cd, Zn and Pb) and phosphorus over the whole Mediterranean from a one year monitoring experiment: biogeochemical implications. *Mar. Chem.* 120, 164–178. doi: 10.1016/j.marchem.2009.02.004

Herut, B., Collier, R., and Krom, M. D. (2002). The role of dust in supplying nitrogen and phosphorus to the Southeast Mediterranean. *Limnol. Oceanogr.* 47, 870–878. doi: 10.4319/lo.2002.47.3.0870

Herut, B., Rahav, E., Tsagaraki, T. M., Giannakourou, A., Tsiola, A., Psarra, S., et al. (2016). The impact of Saharan dust and polluted aerosols on biogeochemical processes in the East Mediterranean Sea, an overview of a mesocosm experimental approach. *Front. Mar.Sci.* 3:226. doi: 10.3389/fmars.2016.00226

Hillebrand, H., Durselen, C. D., Kirschtel, D., Pollingher, U., and Zohary, T. (1999). Biovolume calculation for pelagic and benthic microalgae. *J. Phycol.* 35, 403–424. doi: 10.1046/j.1529-8817.1999.3520403.x

Isari, S., Anto, M., and Saiz, E. (2013). Copepod foraging on the basis of food nutritional quality: can copepods really choose? *PLoS ONE* 8:e84742. doi: 10.1371/journal.pone.0084742

Isari, S., and Saiz, E. (2011). Feeding performance of the copepod Clausocalanus lividus (Frost and Fleminger, 1968). *J. Plankton Res.* 33, 715–728. doi: 10.1093/plankt/fbq149

Isari, S., Zervoudaki, S., Calbet, A., Saiz, E., Ptacnikova, R., Nejstgaard, J. C., et al. (2014). Light-induced changes on the feeding behaviour of the calanoid copepod *Clausocalanus furcatus* (Brady, 1883): evidence from a mesocosm study. *J. Plankton Res.* 36, 1233–1246. doi: 10.1093/plankt/fbu054

Jickells, T. D., An, Z. S., Andersen, K. K., Baker, A. R., Bergametti, G., Brooks, N., et al. (2005). Global iron connections between desert dust, ocean biogeochemistry, and climate. *Science* 308, 67–71. doi: 10.1126/science.1105959

Kiørboe, T., Saiz, E., and Viitasalo, M. (1996). Prey switching behaviour in the planktonic copepod Acartia tonsa. *Mar. Ecol. Prog. Ser.* 143, 65–75. doi: 10.3354/meps143065

Krom, M. D., Herut, B., and Mantoura, R. F. C. (2004). Nutrient budget for the Eastern Mediterranean: implications for phosphorus limitation. *Limnol. Oceanogr.* 49, 1582–1592. doi: 10.4319/lo.2004.49.5.1582

Krom, M. D., Kress, N., Brenner, S., and Gordon, L. I. (1991). Phosphorus limitation of primary productivity in the eastern Mediterranean Sea. *Limnol. Oceanogr.* 36, 424–432. doi: 10.4319/lo.1991.36.3.0424

Lekunberri, I., Lefort, T., Romero, E., Vazquez-Dominguez, E., Romera-Castillo, C., Marrase, C., et al. (2010). Effects of a dust deposition event on coastal marine microbial abundance and activity, bacterial community structure and ecosystem function. *J. Plank. Res.* 32, 381–396. doi: 10.1093/plankt/fbp137

Loder, M. G. J., Meunier, C., Wiltshire, K. H., Boersma, M., and Aberle, N. (2011).The role of ciliates, heterotrophic dinoflagellates and copepods in structuring spring plankton communities at Helgoland Roads, North Sea. *Mar. Biol.* 158, 1551–1580. doi: 10.1007/s00227-011-1670-2

Mahowald, N., Jickells, T. D., Baker, A. R., Artaxo, P., Benitez- Nelson, C. R., et al. (2008). Global distribution of atmospheric phosphorus sources, concentrations and deposition rates, and anthropogenic impacts. *Global Biogeochem. Cy.* 22, GB4026. doi: 10.1029/2008GB003240

Maranon, E., Fernandez, A., Mourino-Carballido, B., Martinez-Garcia, S., Teira, E., Cermeno, P., et al. (2010). Degree of oligotrophy controls the response of microbial plankton to Saharan dust. *Limnol. Oceanogr.* 55, 2339–2352. doi: 10.4319/lo.2010.55.6.2339

Mauchline, J. (1998). The biology of calanoid copepods. *Adv. Mar. Biol.* 33, 1–710.

Mazzocchi, M. G., and Paffenhofer, G. A. (1998). First observations on the biology of *Clausocalanus furcatus* (Copepoda, Calanoida). *J. Plankton Res.* 20, 331–342. doi: 10.1093/plankt/20.2.331

Mazzocchi, M. G., and Paffenhofer, G. A. (1999). Swimming and feeding behaviour of the planktonic copepod *Clausocalanus furcatus*. *J. Plankton Res.* 21, 1501–1518. doi: 10.1093/plankt/21.8.1501

Mazzocchi, M. G., and Ribera d'Alcalà, M. (1995). Recurrent patterns in zooplankton structure and succession in a variable coastal environment. *ICES J. Mar. Sci.* 52, 679–691. doi: 10.1016/1054-3139(95)80081-6

Menden-Deuer, S., and Lessard, E. J. (2000). Carbon to volume relationships for dinoflagellates, diatoms, and other protist plankton. *Limnol. Oceanogr.* 45, 569–579. doi: 10.4319/lo.2000.45.3.0569

Miyashita, L. K., de Melo, J. M., and Lopes, R.M. (2009). Estuarine and oceanic influences on copepod abundance and production of a subtropical coastal area. *J. Plankton Res.* 31, 815–826. doi: 10.1093/plankt/fbp039

Mullin, M. M. (1963). Some factors affecting the feeding of marine copepods of the genus Calanus. *Limnol. Oceanogr.* 8, 239–250. doi: 10.4319/lo.1963.8.2.0239

Nuwer, M. L., Frost, B. W., and Armbrust, E. V. (2008). Population structure of the planktonic copepod *Calanus pacificus* in the North Pacific Ocean. *Mar. Biol.* 156, 107–115. doi: 10.1007/s00227-008-1068-y

Paffenhofer, G. A. (2006). Oxygen consumption in relation to motion of marine planktonic copepods. *Mar. Ecol. Prog. Ser.* 317, 187–192. doi: 10.3354/meps317187

Paffenhofer, G. A., Mazzocchi, M. G., and Tzeng, M. W. (2006). Living on the edge: feeding of subtropical open ocean copepods. *Mar. Ecol.* 27, 99–108. doi: 10.1111/j.1439-0485.2006.00086.x

Peralba, À., Mazzocchi, M. G., and Harris, R. P. (in press). Niche separation and reproduction of *Clausocalanus* species (Copepoda, Calanoida) in the Atlantic Ocean. *Prog. Oceanogr.* doi: 10.1016/j.pocean.2016.08.002

Pulido-Villena, E., Baudoux, A. C., Obernosterer, I., Landa, M., Caparros, J., Catala, P., et al. (2014). Microbial food web dynamics in response to a Saharan dust event: results from a mesocosm study in the oligotrophic Mediterranean Sea. *Biogeosciences* 11, 5607–5619. doi: 10.5194/bg-11-5607-2014

Putt, M., and Stoecker, D. K. (1989). An experimentally determined carbon: volume ratio for marine oligotrichous ciliates from estuarine and coastal waters. *Limnol. Oceanogr.* 34, 1097–1103 doi: 10.4319/lo.1989.34.6.1097

Ridame, C., Dekaezemacker, J., Guieu, C., Bonnet, S., L'Helguen, S., and Malien, F. (2014). Phytoplanktonic response to contrasted Saharan dust deposition events during mesocosm experiments in LNLC environment, Biogeosciences Discuss. 11, 753–796, doi: 10.5194/bgd-11-753-2014.

Riebesell, U., Czerny, J., Von Brockel, K., Boxhammer, T., Budenbender, J., Deckelnick, M., et al. (2013). Technical Note: a mobile sea-going mesocosm system—new opportunities for ocean change research. *Biogeosciences* 10, 1835–1847. doi: 10.5194/bg-10-1835-2013

Roman, M. R. (1984). Utilization of detritus by the copepod, *Acartia tonsa*. *Limnol. Oceanogr.* 29, 949–959. doi: 10.4319/lo.1984.29.5.0949

Romero, E., Peters, F., Marrasé, C., Guadayol, O., Gasol, J. M., and Weinbauer, M. (2011). Coastal Mediterranean plankton stimulation dynamics through a dust storm event: an experimental simulation. *Estuar. Coast. Shelf Sci.* 93, 27–39. doi: 10.1016/j.ecss.2011.03.019

Saiz, E., and Calbet, A. (2007). Scaling of feeding in marine calanoid copepods. *Limnol. Oceanogr.* 52, 668–675. doi: 10.4319/lo.2007.52.2.0668

Saiz, E., and Calbet, A. (2011). Copepod feeding in the ocean: scaling patterns, composition of their diet and the bias of estimates due to microzooplankton grazing during incubations. *Hydrobiologia* 666, 181–196. doi: 10.1007/s10750-010-0421-6

Saiz, E., and Kiørboe, T. (1995). Predatory and suspension feeding of the copepod Acartia tonsa in turbulent environments. *Mar. Ecol. Prog. Ser.* 122, 147–158. doi: 10.3354/meps122147

Saiz, E., Tiselius, P., Jonsson, P. R., Verity, P., and Paffenhofer, G. A. (1993). Experimental records of the effects of food patchiness and predation on egg production of *Acartia tonsa*. *Limnol. Oceanogr.* 38, 280–289. doi: 10.4319/lo.1993.38.2.0280

Schmoker, C., Hernandez-Leon, S., and Calbet, A. (2013). Microzooplankton grazing in the oceans: impacts, data variability, knowledge gaps and future directions. *J. Plankton Res.* 35, 691–706. doi: 10.1093/plankt/fbt023

Schnack-Schiel, S. B., Mizdalski, E., and Cornils, A. (2010). Copepod abundance and species composition in the Eastern subtropical/tropical Atlantic. *Deep Sea Res. II Topic. Stud. Oceanogr.* 57, 2064–2075. doi: 10.1016/j.dsr2.2010.09.010

Schulz, K. (1986). Aspects of calanoid copepod distribution in the upper 200 m of the central and southern Sargasso Sea in spring 1979. *Syllogeus* 58, 459–466.

Siokou-Frangou, I., Christaki, U., Mazzocchi, M. G., Montresor, M., Ribera d'Alcalà, M., Vaqué, D., et al. (2010). Plankton in the open Mediterranean Sea: a review. *Biogeosciences* 7, 1–44. doi: 10.5194/bg-7-1543-2010

Sterner, R. W., and Elser, J. J. (2002). *Ecological Stoichiometry: The Biology of Elements from Molecules to the Biosphere*. Princeton, NJ: Princeton University Press.

Stoecker, D. K., and Capuzzo, J. M. (1990). Predation on protozoa: its importance to zooplankton. *J. Plankton Res.* 12, 891–908. doi: 10.1093/plankt/12.5.891

Tanaka, T., Thingstad, T. F., Christaki, U., Colombet, J., Cornet-Barthaux, V., Courties, C., et al. (2011). Lack of P-limitation of phytoplankton and heterotrophic prokaryotes in surface waters of three anticyclonic eddies in the stratified Mediterranean Sea. *Biogeosciences* 8, 525–538. doi: 10.5194/bg-8-525-2011

Ternon, E., Guieu, C., Ridame, C., L'Helguen, S., and Catala, P. (2011). Longitudinal variability of the biogeochemical role of Mediterranean aerosols in the Mediterranean Sea. *Biogeosciences* 8, 1067–1080 doi: 10.5194/bg-8-1067-2011

Tiselius, P. (1992). Behavior of Acartia tonsa in patchy food environments. *Limnol. Oceanogr.* 37, 1640–1651. doi: 10.4319/lo.1992.37.8.1640

Tiselius, P., and Jonsson, P. R. (1990). Foraging behaviour of six calanoid copepods: observations and hydrodynamic analysis. *Mar. Ecol. Prog. Ser.* 66, 23–33. doi: 10.3354/meps066023

Uttieri, M., Brown, E. R., Boxshall, G. A., and Mazzocchi, M. G. (2008). Morphology of antennular sensors in *Clausocalanus furcatus* (Copepoda: Calanoida). *J. mar. biol. Ass. UK*, 88, 535–541 doi: 10.1017/s0025315408000854

Uye, S. (1991). Length-weight relationships of important zooplankton from the Inland Sea of Japan. *J. Oceanogr. Soc. Jpn.* 38, 149–158. doi: 10.1007/BF02110286

Valdes, L., Lopez-Urrutia, A., Cabal, J., Alvarez-Ossorio, M., Bode, A., Miranda, A., et al. (2007). A decade of sampling in the Bay of Biscay: what are the zooplankton time series telling us? *Prog. Oceanogr.* 74, 98–114. doi: 10.1016/j.pocean.2007.04.016

Verity, P., and Langdon, C. (1984). Relationships between lorica volume, carbon, nitrogen and ATP content of tintinnids in Narragansett Bay. *J. Plankton Res.* 6, 859–868. doi: 10.1093/plankt/6.5.859

Villar-Argaiz, M., Bullejos, F. J., Medina-Sanchez, J. M., Ramos-Rodriguez, E., Delgado-Molina, J. A., and Carrillo, P. (2012). Disentangling food quantity and quality effects in zooplankton response to P-enrichment and UV radiation. *Limnol.Oceanogr.* 57, 235–250. doi: 10.4319/lo.2012.57.1.0235

Webber, M. K., and Roff, J. C. (1995). Annual biomass and production of the oceanic copepod community of Discovery Bay, Jamaica. *Mar. Biol.* 123, 481–495. doi: 10.1007/BF00349227

Conflict of Interest Statement: The authors declare that the research was conducted in the absence of any commercial or financial relationships that could be construed as a potential conflict of interest.

frontiers in Marine Science

ORIGINAL RESEARCH
published: 17 August 2016
doi: 10.3389/fmars.2016.00133

Response of the Eastern Mediterranean Microbial Ecosystem to Dust and Dust Affected by Acid Processing in the Atmosphere

Michael D. Krom[1,2], Zongbo Shi[3], Anthony Stockdale[2], Ilana Berman-Frank[4], Antonia Giannakourou[5], Barak Herut[6], Anna Lagaria[7], Nafsika Papageorgiou[7], Paraskevi Pitta[7], Stella Psarra[7], Eyal Rahav[4,6], Michael Scoullos[8], Eleni Stathopoulou[8], Anastasia Tsiola[7,9] and Tatiana M. Tsagaraki[7,10]*

[1] Department of Marine Biology, Charney School of Marine Sciences, Haifa University, Haifa, Israel, [2] School of Earth and Environment, University of Leeds, Leeds, UK, [3] School of Geography, Earth and Environmental Sciences, University of Birmingham, Birmingham, UK, [4] Mina and Everard Goodman Faculty of Life Sciences, Bar-Ilan University, Ramat Gan, Israel, [5] Hellenic Centre for Marine Research, Attiki, Greece, [6] National Institute of Oceanography, Israel Oceanographic and Limnological Research, Haifa, Israel, [7] Hellenic Centre for Marine Research, Heraklion, Greece, [8] Laboratory of Environmental Chemistry, University of Athens, Athens, Greece, [9] Department of Biology, University of Crete, Heraklion, Greece, [10] Department of Biology, University of Bergen, Bergen, Norway

OPEN ACCESS

Edited by:
Javier Arístegui, University of Las Palmas de Gran Canaria, Spain

Reviewed by:
Elvira Pulido-Villena, Mediterranean Institute of Oceanography, France
Nazli Olgun, Istanbul Technical University, Turkey

***Correspondence:**
Michael D. Krom
m.d.krom@leeds.ac.uk

Specialty section:
This article was submitted to Marine Ecosystem Ecology, a section of the journal Frontiers in Marine Science

Received: *07 June 2016*
Accepted: *19 July 2016*
Published: *17 August 2016*

Citation:
Krom MD, Shi Z, Stockdale A, Berman-Frank I, Giannakourou A, Herut B, Lagaria A, Papageorgiou N, Pitta P, Psarra S, Rahav E, Scoullos M, Stathopoulou E, Tsiola A and Tsagaraki TM (2016) Response of the Eastern Mediterranean Microbial Ecosystem to Dust and Dust Affected by Acid Processing in the Atmosphere. Front. Mar. Sci. 3:133. doi: 10.3389/fmars.2016.00133

Acid processes in the atmosphere, particularly those caused by anthropogenic acid gases, increase the amount of bioavailable P in dust and hence are predicted to increase microbial biomass and primary productivity when supplied to oceanic surface waters. This is likely to be particularly important in the Eastern Mediterranean Sea (EMS), which is P limited during the winter bloom and N&P co-limited for phytoplankton in summer. However, it is not clear how the acid processes acting on Saharan dust will affect the microbial biomass and primary productivity in the EMS. Here, we carried out bioassay manipulations on EMS surface water on which Saharan dust was added as dust (Z), acid treated dust (ZA), dust plus excess N (ZN), and acid treated dust with excess N (ZNA) during springtime (May 2012) and measured bacterioplankton biomass, metabolic, and other relevant chemical and biological parameters. We show that acid treatment of Saharan dust increased the amount of bioavailable P supplied by a factor of ~40 compared to non-acidified dust (18.4 vs. 0.45 nmoles P mg^{-1} dust, respectively). The increase in chlorophyll, primary, and bacterial productivity for treatments Z and ZA were controlled by the amount of N added with the dust while those for treatments ZN and ZNA (in which excessive N was added) were controlled by the amount of P added. These results confirm that the surface waters were N&P co-limited for phytoplankton during springtime. However, total chlorophyll and primary productivity in the acid treated dust additions (ZA and ZNA) were less than predicted from that calculated from the amount of the potentially limiting nutrient added. This biological inhibition was interpreted as being due to labile trace metals being added with the acidified dust. A probable cause for this biological inhibition was the addition of dissolved Al, which forms potentially toxic Al

nanoparticles when added to seawater. Thus, the effect of anthropogenic acid processes in the atmosphere, while increasing the flux of bioavailable P from dust to the surface ocean, may also add toxic trace metals such as Al, which moderate the fertilizing effect of the added nutrients.

Keywords: microcosm experiment, Eastern Mediterranean, dust, atmospheric acid processes, phosphorus, nitrogen, trace metals aluminum

INTRODUCTION

Atmospheric dust and aerosols represent an important source of dissolved nutrients to the offshore global ocean and can increase primary and bacterial productivity and thus carbon uptake (reviewed in Guieu et al., 2014). This is particularly important in regions of the ocean that are strongly impacted by desert dust such as the Central N. Atlantic, the NW Pacific Ocean and the Mediterranean Sea (Mahowald et al., 2005, 2008). The most important nutrient elements controlling primary productivity in the Eastern Mediterranean are phosphorus (P) and nitrogen (N). Previous studies have demonstrated that the system is P limited in winter during the annual phytoplankton bloom (Krom et al., 1991) and N&P co-limited for phytoplankton during the spring/summer (Thingstad et al., 2005; Zohary et al., 2005; Pitta et al., 2016; Rahav et al., 2016; Tsiola et al., 2016). All of the inorganic N supplied from the atmosphere is bioavailable, since it is present as water-soluble ammonium or nitrate. By contrast, most of the P in Saharan dust is supplied as apatite, and to a lesser extent P bound to iron minerals (Eijsink et al., 2000; Singer et al., 2004; Nenes et al., 2011; Stockdale et al., 2015). These minerals are only poorly soluble in seawater (Atlas and Pytkowicz, 1977). Since dust sediments relatively rapidly through the surface layers of the ocean where phytoplankton grow, only the soluble fraction of P in dust is immediately bioavailable with some additional P dissolving on a timescale of hours to days (Mackey et al., 2012). Mahowald et al. (2008) estimate that, globally, about 17% of total atmospheric P deposited at the sea surface is water-soluble. The soluble fraction, however, is highly variable, with values ranging between 7 and 100% (Mahowald et al., 2008).

Dust in the atmosphere is known to cycle between clouds, where it is frequently the nucleus of cloud droplets, and wet aerosols where the water has evaporated, leaving a thin film of water that can have a much higher pH than the original cloud water (Shi et al., 2015). Nenes et al. (2011) found that acidic atmospheric processes increased the amount of leachable P and suggested that there is a direct feedback mechanism between additional acid gases including NO_x and SO_x in the atmosphere and the amount of leachable P in the depositing aerosols. Although acid gases in the atmosphere can be formed naturally, e.g., NO_x from lightning and SO_x from the oxidation of dimethyl sulfide—a gas emitted by phytoplankton, the majority of such gases at present are the result of anthropogenic inputs (Seinfeld and Pandis, 2006). The Eastern Mediterranean Sea (EMS) is a particularly important location for the interaction between mineral dust and anthropogenic gases as dust-laden air masses from the Sahara desert interact with polluted air masses from southern Europe. Stockdale et al. (2015) showed that the amount of P released from dust is a linear function of the amount of H^+ ions present in the atmosphere over a wide range of H^+ ion addition. When the buffer capacity of atmospheric dust, due mainly to $CaCO_3$ present in the dust, is exceeded, excess acid remains and all of the acid-soluble P bearing minerals are converted to bioavailable labile P.

The fertilizing effect of nutrient input by dust can be moderated by the trace metals that are added simultaneously with the aerosol (Paytan et al., 2009). They particularly identified Cu as being a potent algicide, which may be the cause of reduced phytoplankton biomass, though they noted that other metals, such as Al, may play a role (Paytan et al., 2009). As with P, much of the potentially toxic trace metals in dust are present initially as insoluble minerals. However, it is probable that acid processes in the atmosphere may also increase the amount of dissolved toxic minerals in the atmospheric aerosol at the same time as increasing the amount of leachable P.

The EMS is the largest body of water in the ocean that is known to be P limited (Krom et al., 1991). The atmospheric input of nutrients is particularly important in the ultra-oligotrophic Eastern Mediterranean where ∼60% of the externally supplied N and ∼30% of the leachable P are supplied via atmospheric deposition (Markaki et al., 2003; Krom et al., 2004). The fertilizing effect of atmospheric dust on the EMS microbial ecosystem has been examined previously (Herut et al., 2005; Ternon et al., 2011). They suggested that the major control on the amount of phytoplankton biomass and primary productivity is the amount of the labile limiting nutrient, which is added via the dust/aerosol. During spring/summer, the surface waters of the EMS are co-limited by N and P (Thingstad et al., 2005), while there is abundant Fe derived mainly from atmospheric input (Statham and Hart, 2005). Thus, it is the amount of leachable N&P and its sources, which are important factors in controlling microbial processes including primary productivity in the EMS.

To determine the amount of labile N&P added to a microcosm/mesocosm experiment, it is usual to carry out separate dust leaching experiments in abiotic seawater (e.g., Guerzoni et al., 1999; Herut et al., 2002; Carbo et al., 2005). Mackey et al. (2012) have shown that for a series of dust samples collected on filters and exposed to seawater, while there was a rapid release of phosphate initially, the amount continued to increase over a period of up to 72 h.

In this study, we added to triplicate microcosms, an untreated mineral aerosol, and the same aerosol that had been treated with acid (pH = 2) to simulate acidic atmospheric processing. The experimental design involved untreated dust, acid treated dust, and both with sufficient ammonium added to relieve the

N co-limitation found in EMS surface waters at the time of the experiment. The amount of dissolved inorganic nutrients and trace metals added with dust samples were quantified. Measurements were made to determine the biological response to the modified Saharan dust, including determining the changes in phytoplankton and bacterial biomass and productivity as well as other relevant microbial parameters. The experiment was designed to investigate the net effect of simulated atmospheric acidic processes on the microbial ecosystem and provided initial results of the relative importance of acidic processes on stimulating and inhibiting biological processes in this vulnerable ecosystem. These experiments were carried out simultaneously to a mesocosm experiment in which Saharan dust and Polluted aerosol were added and the biological responses determined (Tsagaraki et al.—this issue).

MATERIALS AND METHODS

Dust Leaching Experiments

Prior to the leaching of phosphate and ammonia, 120 ml plastic containers were coated with iodine by adding a crystal or two of elemental iodine and placed in oven at 40°C for 10 min. The containers were cooled to room temperature (22°C) and swilled with Milli-Q water to remove all the excess I_2. For the nitrate leaching, uncoated 250 ml plastic containers were used. For the phosphate/ammonia leaching experiment, 50 mL of sterile seawater was added to each container in a biological safety cabinet. 0.16 ml of 6 N HCl was added to three of the sample containers to simulate acid conditions in the atmosphere. ∼6 mg of accurately weighed dust was then added and the containers were placed on a shaking table for 30 min, 2, 6, 24, and 48 h situated in a light proof box. The duration of the leaching experiment was based on the study of Mackey et al. (2012), which found an increasing amount of leached P after 24–48 h. This was also the period of our microcosm experiment, chosen in that case for practical reasons as the experiment was carried out in parallel to the labor intensive mesocosm experiment. At each sampling, ∼7 mL of sample was removed by syringe, filtered through 0.45 μm polycarbonate filters and stored at 4°C for subsequent analysis. For the nitrate leaching experiment, 100 ml of sterile seawater was used and was sampled in the same way as for the other determinants, after 30 min leaching. The length of time used for nutrient leaching was determined by preliminary experiments on samples of dust collected in Rosh Pina, Israel (see Supplementary Information **Figures S1A,B**, **S2A,B**). The analysis of all the nitrate and phosphate samples was carried out after the 48 h sample was collected. The ammonium samples were frozen and analyzed subsequently. A series of six blank samples were run through the sampling procedure and the average value subtracted for each sample analyzed (mean blank values were P 3 ± 4 nmol L^{-1} and nitrate 48 ± 50 nmol L^{-1}. Nutrient content was determined by standard SEAL AA-3 automated methods for phosphate (using the molybdate blue method), nitrate (as nitrite after Cd column reduction) and ammonium (using a fluorescence method). The precision of replicate analysis was 1.8 $\pm$ 0.01 μM for phosphate, 6.0 $\pm$ 0.05 μM for nitrate and 5.75 $\pm$ 0.05 μM for ammonium.

Microcosm Experiment

A dust-enrichment microcosm experiment was carried out using surface (∼10 m depth) seawater pumped into holding tanks on-board the R/V *Philia* from a location 5 nautical miles north of Heraklion (Crete, Greece, 35.4159 N, 25.2407 E) on May 10th, 2012. The experiment was carried out at the CRETACOSMOS facility of the Hellenic Centre for Marine Research (cretacosmos.eu), in 15 translucent 8 L polyethylene (PE) bottles/microcosms, that were washed with 10% hydrochloric acid, rinsed three times with Milli-Q water and finally three times with seawater from the sampling site before filling them.

The 15 microcosms were separated into five sets of triplicates, dependant on the experimental amendments made: (1) Control—original seawater, no addition (C); (2) Original seawater + Saharan dust precursor (Z); (3) Original seawater + Saharan dust precursor + 200 nM NH_4 mg^{-1} dust (ZN); (4) Original seawater + acid treated Saharan dust precursor (ZA); and (5) Original seawater + acid treated Saharan dust precursor + 2000 nM NH_4 mg^{-1} dust (ZNA).

Saharan Dust Proxy Treatment

In order to have enough particulate material of known composition, size fractionated surface soil taken from Northern Libya (32.29237N 22.30437S) was used as proxy for Saharan dust. As in previous experiments (Shi et al., 2011), only the fine-grained fraction (PM10, <10 μm), which corresponds to the material that is transported for long distances, was used. The proxy dust was resuspended using a custom-made resuspension chamber and the PM10 was separated for subsequent use. Previous studies have used similar procedures for experimental work with Saharan dust (Lafon et al., 2006; Guieu et al., 2010; Shi et al., 2011). Within the text we use the term PM10 dust or simply dust for this size fractionated proxy.

To mimic the effect of atmospheric acid processes on dust (Nenes et al., 2011), 200 mg of PM10 were added to 50 ml of milli-Q water, acidified to pH 2, in a plastic vial. They were mixed and shaken for 5 min and then 8 ml of the dust suspension were added to each acidified PM10 treatment microcosm (ZA and ZNA). This gave a final dust concentration of 4 mg L^{-1} seawater in the microcosm. Similarly, 200 mg of PM10 were added to 50 ml of milli-Q water in a plastic vial and 8 ml of dust suspension were added to each non-acidified PM10 treatment microcosm (Z and ZN). Ammonium Chloride was added to the ammonium-amended treatments (ZN, ZNA) to give final concentrations of the values given in **Table 1**.

The bottles were incubated for 48 h in a large pond of seawater under flow-through conditions to maintain ambient temperature and were covered with a layer of neutral density net mimicking light intensity at the depth layer (10 m) from which water was collected. The ambient seawater was also tested/characterized for most biomass and activity variables prior to the seawater being added to the microcosms. All microcosm treatments were sampled once, immediately after material additions (T_0), and then daily, at 08:30 a.m. for a period of 2 days after material addition (T_{24} and T_{48}).

TABLE 1 | Concentration of leachable nutrients (inorganic P and inorganic N) added to each one of triplicate sets of microcosms (treatments).

Treatment	Total conc. of PM10 added (mg L^{-1})	Leachable P added with the dust (nM L^{-1})	Leachable inorganic N added with the dust (nM L^{-1})	Conc. of extra N added to relieve N limitation (nM L^{-1})	Total inorganic N in bottles (nM L^{-1})	Molecular N:P ratio of added nutrients
Control	0	0	0	0	0	
Z	4	1.8	8.0	0	8.0	4.4:1
ZN	4	1.8	8.0	200	208	118:1
ZA	4	80.8	8.0	0	8	0.1:1
ZNA	4	80.8	8.0	2000	2008	25:1

Z, ZN, non acidified treatments; ZA, ZNA, acidified treatments; ZN, ZNA, treatments with artificially added N; C, Controls, no addition. The values are given in nanomoles per liter of seawater to enable easy comparison with the biological response measurements.

Measurement of Chlorophyll a Concentration

Water samples (500 ml) were filtered through 47 mm diameter polycarbonate membranes of 0.2 μm pore size, using low vacuum pressure (<200 mm Hg). The filters were immediately extracted in 90% acetone at 4°C in the dark overnight (for 14–20 h); Chl-*a* concentrations were determined using a Turner TD-700 fluorometer (Yentsch and Menzel, 1963).

Primary Production

Primary production (PP) was measured using the ^{14}C incorporation method (Steeman-Nielsen, 1952). Three light and one dark 170 ml polycarbonate bottles were filled with sample water from each microcosm in the morning, inoculated with 20 μCi of $NaH^{14}CO_3$ tracer each, and incubated in the large concrete tank for 3 h around midday. After the incubation, samples were filtered through 0.2 μm polycarbonate filters under low vacuum pressure (<200 mm Hg) and filters were put in scintillation vials where 1 ml of 1% HCl solution was immediately added in order to remove excess ^{14}C-bicarbonate overnight. Then, 4 ml scintillation fluor (BSF, Packard) was added to the vials, and samples were counted in a scintillation counter (Packard Tri-Carb 4000TR). PP (mg C m^{-3} h^{-1}) was then calculated from the radioactivity (disintegrations per minute, dpm) measured in the light and dark samples, as shown in the following formula:

$$PP = \frac{[(\text{dpm light} - \text{dpm dark}) \times \text{DIC} \times 1.05]}{\text{dpm total} \times \text{h}}.$$

Where DIC (Dissolved Inorganic Carbon) = 26.400 mg C m^{-3}, 1.05 = correction factor for the lower uptake of ^{14}C as compared to ^{12}C and h = duration of the incubation (hours).

Bacterial Production

Bacterial production (BP) was measured daily in all microcosms, using the ^{3}H-leucine incorporation method modified by Smith and Azam (1992). Water samples (1.5 ml) were collected, in triplicate, in 2 ml Eppedorf tubes and 50 μl of [4,5-^{3}H]-l-leucine (Amersham TRK 636, specific activity 165 Ci $mmol^{-1}$) was added at 20 nM final concentration. Controls received 90 μl of 100% trichloroacetic acid (TCA) before injection of tritiated leucine. All samples, including controls, were incubated for 2 h in the dark, at *in situ* temperature. Incubations were stopped with 90 μl of 100% TCA and the samples were stored at 4°C. BP was calculated according to Kirchman (1993), from ^{3}H-leucine incorporation rates. Concentration kinetic experiments were performed in order to verify that the concentration of leucine added (20 nM) was sufficient to saturate incorporation (Van Wambeke et al., 2002).

Measurement of Abundance and Biomass of Heterotrophic Bacteria and Cyanobacteria *Synechococcus* Spp.

Abundance of heterotrophic bacteria and cyanobacteria *Synechococcus* spp. was obtained by flow cytometric analyses. A FACS Calibur instrument was used (Becton Dickinson), equipped with an air-cooled laser at 488 nm and standard filters. Milli-Q water was used as sheath fluid. Samples were run at high speed (58 μl min^{-1}) for 1 min for heterotrophic bacteria counts and for 3 min for cyanobacterial counts. Abundance was then calculated using the acquired cell counts and the flow rate. All flow cytometry data were acquired with the CellQuest and analyzed with the Paint-A-Gate software packages (Becton Dickinson).

Samples for heterotrophic bacterial counts were fixed and processed according to Marie et al. (1999). Briefly, fixation was achieved with 0.2 μm pre-filtered 25% glutaraldehyde at 0.5% final concentration. Samples were then kept at 4°C for ∼20 min, deep frozen in liquid nitrogen and finally stored at −80°C until enumeration. For heterotrophic bacteria, samples were thawed at room temperature and stained with SYBR Green I nucleic acid dye at a final dilution 4×10^{-4} of the stock solution. The stained samples were incubated for 10 min in the dark. Heterotrophic bacteria were grouped in two groups according to their SYBR Green I fluorescence intensity (low and high DNA content). Cyanobacteria *Synechococcus* spp. were counted fresh, without fixation and staining steps, using their characteristic auto-fluorescence chlorophyll/phycoerythrin signals. Multi-fluorescence beads (0.93 μm, Polysciences) were used as an internal standard of fluorescence at all runs.

Abundance data were converted into C biomass using 20 fg C $cell^{-1}$ for heterotrophic bacteria (Lee and Fuhrman, 1987) and 250 fg C $cell^{-1}$ for *Synechococcus* (Kana and Glibert, 1987).

Alkaline Phosphatase Activity (APA)

Samples of APA were collected in triplicate prior the experiment (Ambient), at T_0 and T_{24} and analyzed according to Thingstad and Mantoura (2005). One milliliter of seawater sample was added to the substrate MUF-P. The alkaline phosphatase (AP) hydrolyses the fluorogenic substrate MUF-P and yields a highly fluorescent product (methyllumbelliferon: MUF) and a phosphate group in equimolar concentrations (i.e., Luna et al., 2012). The MUF produced was detected as increase in fluorescence with spectrofluorometer (Hithachi F-2000, excitation-364 nm and emission-448 nm). A standard curve with MUF (Sigma Co.) was used to quantify the amount of MUF produced by APA, so the phosphate liberated in the reaction could be estimated.

Trace Metal Analysis

The samples for the analysis of trace metals (volume of 1 L each), were collected in PTFE bottles (pre-treated overnight with 2N HNO_3 and rinsed afterwards with ultrapure Milli-Q water) and within 12 h from their collection, the samples were filtered through pre-weighted nitrocellulose membrane filters (Millipore 0.45 μm pore size) under a clean laminar hood (class 100) in order to separate the particulate from the dissolved form of metals.

The dissolved metals in the filtered samples were determined immediately after filtration through a process of pre-concentration by passing the sample through Chelex-100 resin columns for retaining the metals and elution of them by the use of 10 ml nitric acid 2N s.p. under the clean laminar hood (pre-concentration factor = 100). The pre-concentration procedure is a slight modification (Scoullos et al., 2007) of that proposed by Riley and Taylor (1968) and Kingston et al. (1978).

Trace metals concentrations (Cu, Pb, Zn, Mn, Al, Fe) in the eluates were determined by employing for Zn, Al, Fe, a Varian SpectrAA 200 Flame Atomic Absorption Spectrophotometer (FAAS) and for Cu, Pb, Mn, a Varian SpectrAA-640Z Graphite Furnace Atomic Absorption Spectrophotometer (GFAAS) with Zeeman background correction. The relative standard deviation [$Sr = (S/\chi) \times 100$] of the measurements resulting from replicate (3–4) determinations and standard addition experiments was <5%. The details for these methods are given in **Table 2**.

Statistical Analyses

Test of statistical significance was carried out using a one-way analysis of variance (ANOVA) followed by Tukey's *post-hoc* test. This test was used to compare between the controls and the different treatments ($P < 0.01$) at the conclusion of the microcosm experiment. All tests were performed using the XLSTAT.

RESULTS

The amount of P leached from untreated PM10 dust was 0.45 nmoles P mg dust^{-1} (averaging the values for 24 and 48 h leaching excluding PM10_2 48 h; **Figure 1A**) and 2 nmoles N mg dust^{-1} as nitrate (using the measured value after 30 min; **Table S1**). It is noted that the phosphate added is a minimum because there may have been some readsorption of phosphate onto the PM10 dust particles during the leaching experiment. The amount of P leached from the acidified dust (0.01 N) was 18.4 nmoles P mg dust^{-1} also averaged for 24 and 48 h; **Figure 1B**) and it was assumed that there was also 2 nmoles N mg dust^{-1} leached from the acid treatment. The concentration of ammonia leached from the dust was 0.08 ± 0.3 nmoles N mg dust^{-1} (**Table S1**). This average value is considered below the practical detection limit and assumed to be zero for all subsequent calculation. These values were used to calculate the amount of N & P added to the microcosms shown in **Table 1**. The pH change caused by the addition of 8 mls of pH = 2 water to 4 L of seawater was −0.02 pH units.

The 10 m deep seawater used in this experiment, which is labeled ambient (Amb.), exhibited typical oligotrophic characteristics, with 0.074 μg Chl.a L^{-1} and 0.22 ± 0.01 μg C L^{-1} h^{-1} primary productivity (PP). The bacterial abundance was 2.8×10^5 cells ml^{-1}, resulting in a calculated biomass of 5.57 μg C L^{-1}. Alkaline Phosphatase Activity (APA) was 4.69 ± 0.12

TABLE 2 | Summary table of the methods used to determine biogeochemical changes in the microcosms during this experiment.

Parameter	Unit of measurement	Method of measurement
Primary productivity (PP)	μg C L^{-1} h^{-1}	^{14}C incorporation method (Steeman-Nielsen, 1952)
Chlorophyll-*a* (Chl.*a*)	μg L^{-1}	Acetone extraction method (Yentsch and Menzel, 1963)
Synechococcus biomass	μg C L^{-1}	C biomass converted from abundance using 250 fg C cell^{-1} (Kana and Glibert, 1987)
Synechococcus abundance	Cells ml^{-1}	Flow cytometry (Kana and Glibert, 1987)
Heterotrophic bacterial biomass	μg C L^{-1}	C biomass converted from abundance using 20 fg C cell^{-1} (Lee and Fuhrman, 1987)
Heterotrophic bacterial abundance	Cells ml^{-1}	Flow cytometry (Marie et al., 1999)
Bacterial productivity	μg C L^{-1} h^{-1}	^{3}H leucine incorporation technique (Smith and Azam, 1992; Kirchman, 1993)
Alkaline phosphatase activity	nM MUF h^{-1}	Maximum hydrolysis rate of a fluorogenic substrate, methyllumbelliferone phosphate (Thingstad and Mantoura, 2005)
Trace metals (Zn, Fe, Mn, Cu, Pb, Cd, Al) of seawater and seawater leached PM-10	nM L^{-1}	Extraction into Chelex 100 resin, leaching by 10 ml 2N nitric acid and measurement by ICP-MS
Trace metals (Zn, Fe, Mn, Cu, Pb, Cd, Al) of acid leached PM-10 samples	nM L^{-1}	Extracted into pH = 2 MQ and analysed by ICP-MS

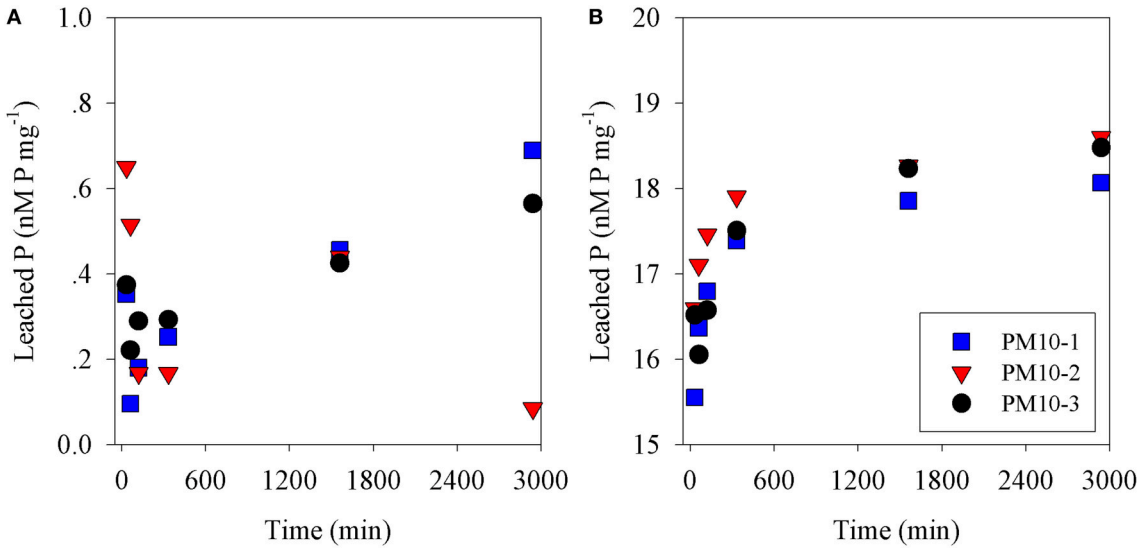

FIGURE 1 | Phosphate leached from (A) PM10 (three replicates) vs. time into seawater and (B) PM10 leached into seawater acidified to pH = 2 (three replicates) expressed as nM phosphate mg dust^{-1}.

nmoles MUF h^{-1} (all data from the microcosms are presented in **Table S2**). The dissolved nutrients (phosphate and nitrate) were below analytical detection limits.

The pattern of observed changes in the microcosms was broadly similar for Chl-a, primary and bacterial productivity (**Figures 2–4A**). Thus, for Chl-a, the measured concentration in the microcosms at T_0 was 0.05 μg chl.a L^{-1}, slightly less than that of ambient values (0.07 μg chl.a L^{-1}; **Figure 2**). After 48 h, the ZA microcosms showed no measurable increase in Chl.a (0.09 ± 0.01 μg chl.a L^{-1}) compared with the control microcosms (0.09 ± 0.01 μg chl.a L^{-1}; **Figure 2**). Chl.a in ZN additions was slightly higher than Z additions after 48 h (0.12 ± 0.02 vs. 0.11 ± 0.02 μg chl.a L^{-1}). The greatest increase was in the acidified ZNA treatments, which ended up with a value of 0.30 ± 0.07 μg chl.a L^{-1} after 48 h which was significantly higher than all other treatments ($p < 0.01$; **Table S3**).

The primary productivity measured at the ZA microcosms after 48 h was the same as for the control microcosms; 0.23 ± 0.03 μg C L^{-1} h^{-1} (**Figure 3**). Both untreated dust additions (Z and ZN) caused an increase in primary productivity by ca. 50% to 0.37 ± 0.13 and 0.39 ± 0.04 μg C L^{-1} h^{-1}, respectively, while ZNA, by ca. 500% to 1.16 ± 0.30 μg C L^{-1} h^{-1} (**Figure 3**), significantly greater than all other treatments ($p < 0.01$; **Table S3**).

Bacterial biomass in the control increased from 6 μg C L^{-1} at T_0 to 7.6 μg C L^{-1} after 48 h (**Figure 4B**). As with bacterial activity, the only treatment that showed a decrease compared with the control was ZA. All the other treatments showed an increase, although the largest one was at Z (11.1 μg C L^{-1}) while ZN (8.3 μg C L^{-1}) and ZNA (9.8 μg C L^{-1}) were somewhat lower. Bacterial productivity showed the largest increase over 48 h at ZNA which, in this case, reached 273 ng C L^{-1} h^{-1} compared with 21 ng C L^{-1} h^{-1} for the control (**Figure 4A**) and was significantly greater than all other treatments ($p < 0.01$; **Table S3**). For this parameter, ZN was greater (82 ng C L^{-1} h^{-1}) than Z (53 ng C L^{-1} h^{-1}) and ZA increased to 58 ng C L^{-1} h^{-1} compared with Z.

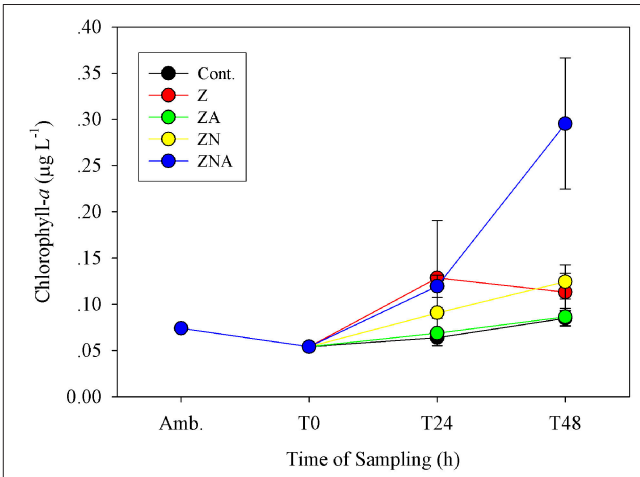

FIGURE 2 | Measured changes in chlorophyll-*a* concentration in the microcosm treatments compared with the initial ambient values of the water used to inoculate the microcosm bottles.

Synechococcus cell numbers in the controls increased from 20260 to 32 ± 4 cells × 10^3 ml^{-1} (**Figure 5**). Compared to the controls, both non-acidified treatments (Z and ZN) showed an increase in *Synechococcus* cell numbers after 48 h, to 43 ± 7 cells × 10^3 ml^{-1} for Z and to 34 ± 1 cells x10^3 ml^{-1} for ZN. By contrast, both acid treated microcosms (ZA and ZNA) resulted in a decrease in *Synechococcus* cell numbers, to values of 27 ± 3 and 27 ± 3 cells × 10^3 ml^{-1}, respectively.

APA continuously decreased within 24 h of dust addition, from 4.69 nM MUF h^{-1} to values at or below 1 nM MUF h^{-1} (**Figure 6**). This decrease occurred in the treatments where phosphate was added in relatively large amounts (ZA and ZNA), in the Z treatment where P was added with a small deficit of N, and also in the controls. The only treatment where APA first decreased (T_0) and then increased to 4 nM MUF h^{-1} (T_{24}) was ZN where there had been a small increase in P and a relatively large increase in N.

Trace metal concentrations increased considerably, particularly those of Al, Mn, and Fe in the acid treated PM10 sample, which represents the dust sample after being affected by acid processes in the atmosphere compared with the untreated PM10 sample (**Table 3**). The ambient and experimental trace metals were measured after filtration through 0.2 μm filters followed by pre-concentration through ion exchange resins. Thus, the concentrations of trace metals in the experimental microcosms represent dissolved inorganic trace metals in the ambient solution that the organisms are present in. The amount that has been lost from solution has also been calculated in **Table 3**. This was calculated by assuming that without any PM10 the concentration in solution would be the same as the control. The missing trace metal is then the measured value (the control value plus the added metal from the PM10). Positive numbers

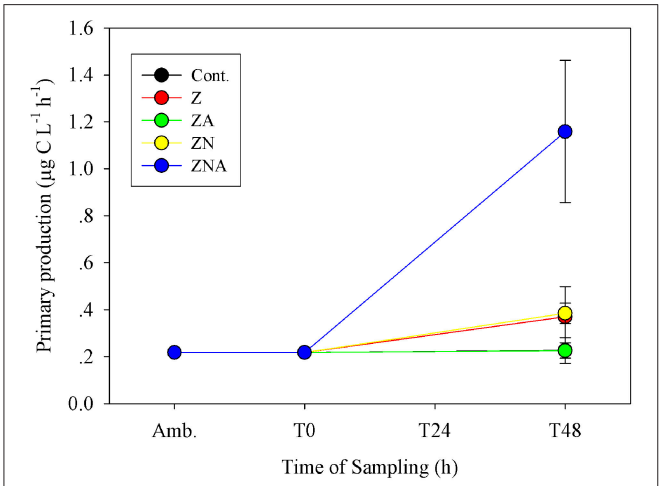

FIGURE 3 | Measured changes in primary productivity rate in the microcosm treatments compared with the initial ambient values of the water used to inoculate the microcosm bottles.

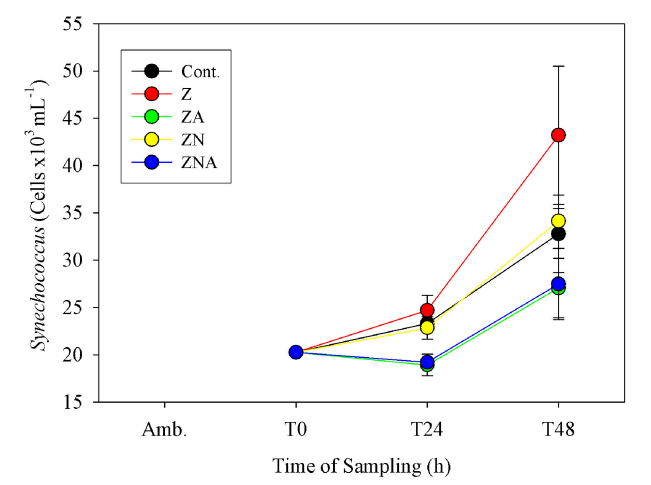

FIGURE 5 | Measured changes in calculated *Synechococcus* biomass determined by flow cytometry in the microcosm treatments compared with the initial values at the beginning of the experiment.

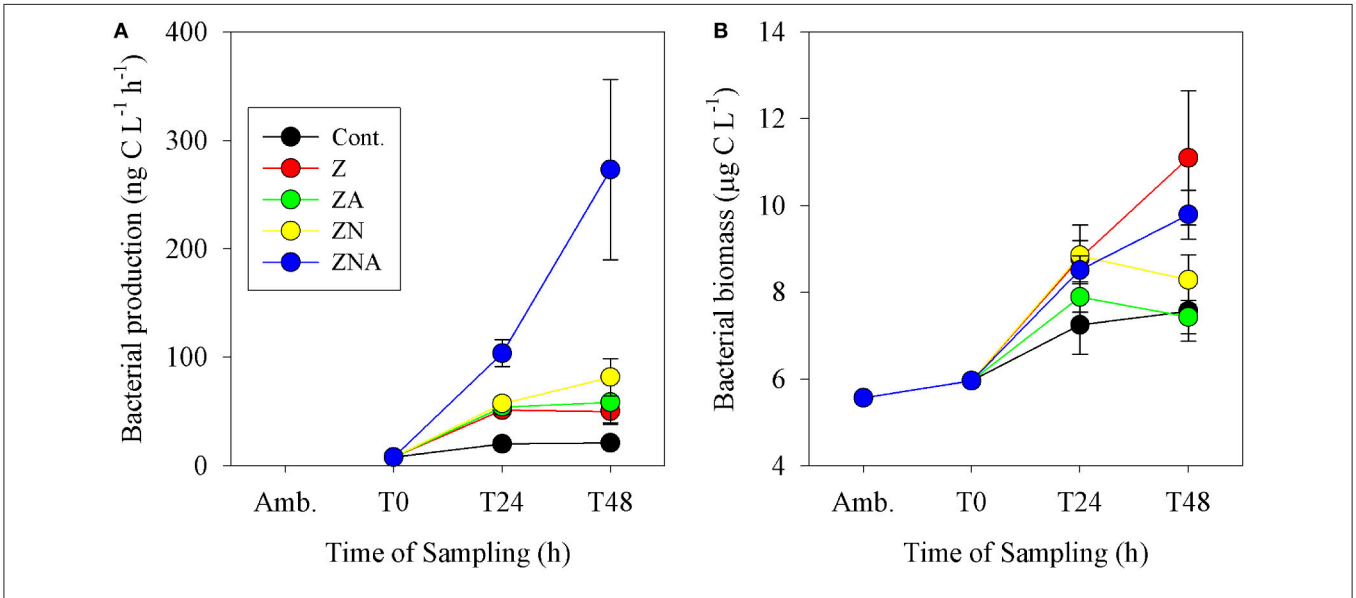

FIGURE 4 | Measured changes in (A) bacterial activity rate and (B) calculated bacterial biomass in the microcosm treatments compared with the initial ambient values of the water used to inoculate the microcosm bottles.

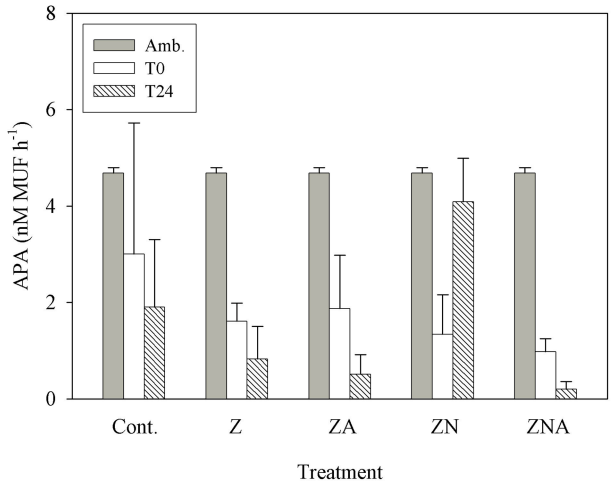

FIGURE 6 | Measured changes in alkaline phosphatase activity between T_0 and T_{24} (hours) for the control and all treatments (Z, ZA, ZN, and ZNA).

represent additional trace metal in solution, while negative numbers represent trace metals missing from solution. It is likely that this missing metal have been taken up by the organisms, or converted into a form that is not determined by the extraction system employed to pre-concentrate the samples. It cannot be entirely excluded that trace metals are adsorbed onto the walls of the container, however this seems unlikely since the control sample was carried out in the same vessels. While the analytical variability is ∼5%, the total variability including sampling was higher. Here, we use the measured variability of the control samples (2 × *SD*) as an estimate of the values above which it is reasonable to interpret the changes as meaningful. These data are marked in bold in **Table 3**.

In all cases, the amount of trace metals added to the experimental microcosms, when the untreated PM10 dust was added, had no measurable effect on the concentrations observed in the microcosms (**Table 3**).

The major change in trace metals was for treatments with acidified dust added (ZA and ZNA microcosms). In those treatments, [Al] increased by more than ∼180 nM while the Al content in the Z and ZN microcosms decreased by a factor of almost 50% compared to the control. [Mn] also increased as a result of the addition of acidified dust, from 1.9 nM in the ambient to 14.4–15.8 nM in the acidified PM10 additions (ZA and ZNA, respectively). This was approximately half of the added Mn from the PM10 (36.5 nM). Fifty-one nM of dissolved Fe was added to the microcosms with the acid PM10 and yet, the final measured concentrations were only slightly higher in the acidified microcosms (13.7 and 11.1 nM in ZA and ZNA, respectively) compared with the control (10 nM) and the non-acidified microcosms Z and ZN (10.2 and 10.0 nM, respectively). This is likely to be because dissolved Fe is very insoluble at ambient seawater pH's (7.8–8.3) and tends to precipitate rapidly as ferrihydrite. This solid also is a known substrate for trace metal (and phosphate) adsorption. The trace metal most commonly

TABLE 3 | Concentration of trace metals in the ambient seawater before the start of the experiment, calculated concentration of trace metals added with the acidified (pH = 2) PM10 and the non-acidified PM10, measured concentration of trace metals in the microcosms after 48 h, and calculated concentrations of trace metals missing from solution (calculated from the final concentration minus the control plus the added trace metals from the PM-10).

Treatment	Fe	Mn	Cu	Zn	Pb	Al
Ambient	8.8	1.9	1.35	33.8	0.76	35.3
PM-10	0.04	0.008	0.02	0.01	0.002	2.5
Acid PM10	51	36.5	0.29	6	0.2	751
MEASURED CONCENTRATION IN MICROCOSM AFTER 48 H						
C	10.0	2.32	0.60	15.8	3.24	78.2
Z	10.2	3.95	0.47	14.1	6.34	15.2
ZA	13.7	14.4	0.73	9.4	4.76	262
ZN	10.0	4.4	0.67	12.0	8.40	27.8
ZNA	11.1	15.8	0.55	8.1	4.61	258
CALCULATED CONCENTRATION OF TRACE METALS MISSING FROM SOLUTION AFTER 48 H						
Z	1.6	0.1	−0.1	−1.7	3.1	−65.2
ZA	2.1	0	0.1	−3.9	5.2	−52.6
ZN	−24.4	−24.4	−0.2	−12.4	1.3	−457
ZNA	−23	−23	−0.3	−13.7	1.2	−461
MEASURED VARIABILITY IN THE CONTROL SAMPLES EXPRESSED AS 2 *SD* OF THE MEAN						
	0.3	5.0	0.4	20	3.4	130

All concentrations are given in nmoles L^{-1}.

associated with the inhibition of phytoplankton activity is Cu (Paytan et al., 2009; Jordi et al., 2012). In this experiment, the Cu measured in the microcosms was ∼half the value measured in the ambient waters. In addition, although 0.29 nM of Cu was added to the acid microcosms ZA and ZNA, the concentration remaining in the microcosms after 48 h (0.73 and 0.55 nM for ZA and ZNA, respectively) was similar to the control (0.60 nM) and the other non-acidified microcosms (0.47 and 0.67 nM for Z and ZN, respectively). All the observed changes in Cu were within the variability found in the replicate control samples (±0.6 nM) and are thus not considered significant. The Zn content in the acidified microcosms ZA and ZNA (9.4 and 8.1 nM, respectively) was less than that in the control (15.8 nM) and the non-acid PM10 additions (14.1 and 12.0 nM in Z and ZN, respectively).

The missing trace metals, showed a similar pattern, with the largest missing amount of trace metal being ∼460 nM Al from the acid PM10 samples. There was ∼50 nM Fe, and ∼24 nM Mn missing from solution in the acidified PM10 samples while the missing Cu, Zn, and Pb (in both acidified and non-acidified samples), and the Al and Fe in the non-acidified samples were within the variability of the control samples. The missing Mn in the non-acidified samples was only ∼2 nM.

DISCUSSION

In this study, PM10 samples were leached into surface Eastern Mediterranean seawater to determine how fast N&P were released from untreated dust samples. Our results showed that

while nitrate was leached essentially completely within 30 min (**Figure S1**), phosphate continued to increase from 6 h (0.28 nmoles P mg^{-1}) to 24 h (0.44 nmoles P mg^{-1}) and to 0.45 nmoles P mg^{-1} after 48 h. This pattern was similar to that observed in our preliminary experiments using Rosh Pina dust (**Figures S1A,B**). This is similar but not identical to the results obtained by Mackey et al. (2012), who observed that an increasing amount of P was leached from dust samples over the first 24 h followed by a smaller increase over the next 2 days. A similar pattern was obtained from the dust samples used in the mesocosm experiments (Herut et al., submitted—this issue), as well as in experiments using dust collected during a dust storm from Rosh Pina, Israel (Stockdale and Krom; unpublished data). These experiments, all performed with different samples of untreated dust, show small differences in the rate of increase in P leached with time. A possible explanation for these differences is that natural apatite, the major P containing mineral in Saharan dust (Stockdale et al., 2015) exists in several subtly different mineral forms. It is likely that these dissolve at different rates when placed in an excess of seawater. We also note that lower concentrations of dissolved minerals appear to drive faster dissolution of phosphate although this possible effect requires further investigation (**Figure S1**).

In our microcosm experiment, Chl.a and PP values were characteristic of an ultraoligotrophic environment in early summer (Siokou-Frangou et al., 2010). The Chl.a values were similar to those measured in EMS offshore waters (Psarra et al., 2005; Ignatiades et al., 2009; Rahav et al., 2013), to those in coastal waters off Crete (Psarra et al., 2000; Pitta et al., 2016; Tsiola et al., 2016), and off Israel (Kress et al., 2005; Raveh et al., 2015). PP was somewhat higher than offshore waters and somewhat lower than observations off the Israeli coastal waters recorded at the same season.

It has been suggested that acid processes in the atmosphere result in an increased supply of leachable inorganic P (LIP) resulting from the dissolution of P minerals (apatite and Fe-Bound minerals; Nenes et al., 2011; Stockdale et al., 2015). We chose in this study to dissolve the PM10 dust precursor at pH = 2 with a high water to dust ratio. This pH represents that in wet aerosols that have been in contact with polluted air masses (Meskhidze et al., 2003; Nenes et al., 2011). The LIP of the acidified PM10 dust was 18.4 nM mg $dust^{-1}$, which was ∼40 times higher that of non-acidified samples (0.45 nM mg $dust^{-1}$, **Figure 1**). Since it is known that the surface waters of the EMS are N&P co-limited for phytoplankton in May (Thingstad et al., 2005; Zohary et al., 2005), with inorganic nutrients below analytical detection limits, it is possible to predict the effective limiting nutrient in each treatment from the amount of dissolved nutrients added. The amount of N in the PM10 added microcosms (Z and ZA; 2 nM mg $dust^{-1}$, **Table 1**) was relatively low, in part because the PM10 soil precursor sample had not been exposed to the hydrophilic N gases in the atmosphere. This low N in the untreated PM10 treatment (Z) meant that after addition to the microcosms, the treatment became N limited with an added N:P ratio of 7.0. The acidified PM10 treatment (ZA) added a similarly low N, while the P concentration was ∼40 times higher. This treatment was similarly N limited. By contrast, in those treatments where N was added (ZN and ZNA), the systems became P limited (N:P ratio = 118:1 and 25:1, respectively). The primary response of the treatments reflected these nutrient additions and the resulting limiting nutrient with large and significant increases in Chl.*a*, PP and BP in the ZNA microcosms (**Figures 2–4**) reflecting the much higher amount of phosphate added and greater availability of phosphate for primary and bacterial metabolism.

The sequence and approximate magnitude of changes in phytoplankton, as measured by Chl.*a*, and PP was controlled by the relative amount of the limiting nutrient added. Thus, the response of the Z treatment (N limited) after 48 h as somewhat lower than ZN (P limited) for both variables and was significantly lower than the response of the ZNA treatment where the added limiting nutrient P concentration was 40 times higher than Z and ZN (**Figures 2**, **3**). This confirms that the dust provided a bioavailable (leachable) source of N and P as found in other studies (Herut et al., 1999, 2000, 2002; Migon et al., 2001; Ridame and Guieu, 2002) and relieved the phytoplankton community of N and P co-limitation (Kress et al., 2005; Krom et al., 2005; Pitta et al., 2005; Tanaka et al., 2011).

Ambient levels of APA were found to be high, as is typically found in the EMS (Thingstad and Mantoura, 2005) since the system is strongly P starved (Krom et al., 2005). In all of the treatments where P was added by PM10 addition, the APA decreased as the P deficiency was alleviated (**Figure 6**). The exception to this was ZN where a small amount of P and a large amount of N were added. In this case, it is suggested that the microbial community increased the APA to try to obtain new P to balance the extra N added externally.

Other microbial responses to the dust addition included bacterial productivity that increased substantially more after ZNA addition compared to other treatments (**Figure 4A**). It is suggested that greater phytoplankton production in ZNA microcosms (**Figure 3**) may have produced an increased concentration of labile organic carbon to fuel heterotrophic bacterial respiration (Siokou-Frangou et al., 2010). However, this increase was not matched by an increase in bacterial biomass (**Figure 4B**). This suggests that although the addition of the highest amount of N and P allowed for an increase in BP, the standing crop of bacteria was controlled by grazers such as heterotrophic nanoflagellates and ciliates (Kress et al., 2005; Pitta et al., 2005; Romero et al., 2011) or that the cell specific BP changed.

The magnitude of the increases in Chl.*a* and PP were not, however, simply related to the concentration of the added limiting nutrient. Thus, although treatments Z and ZA, both had the same amount of the limiting nutrient (N) added, the response was different. The final Chl.*a* and PP of the ZA treatment was lower than for the Z treatment, and almost exactly the same as the control (**Figures 2**, **3**). The Chl.*a*/limiting nutrient ratio for Z, which is only PM10, was 16.6 ng chl.a/nM PO_4 (**Table 4**)—similar to that measured for the ratios for previous dust addition experiments to the EMS, carried out in early summer [9.7–15.7 ng chl-*a* L^{-1} nM PO_4^{-1}, **Table 4**, (Herut et al., 2005)]. It is unlikely that the lower response of ZA was due to higher grazing rates since there is no reason why there should be higher grazing in this treatment compared with the others. It is also unlikely to be

TABLE 4 | Table showing the ratio of Chlorophyll-a increase relative to the controls/concentration of the limiting nutrient added for a series of micro- and mesocosm-experiments carried out in the EMS during May.

P added (nM)	N added (nM)	Limiting nutrient (nM)	Increase in Chl.*a* (ng l^{-1})	Type of sample added	Chl.a/limiting nutrient (ng nM^{-1})	References
18	570	18	175	Dissolved nutrient	9.7	Zohary et al., 2005
16	750	16	180	Dust	11.3	Herut et al., 2005
16	750	16	180	Dust	11.3	Herut et al., 2005
7	307	7	110	Dust	15.7	Herut et al., 2005
1.8	8	1.8	30	Dust (Z)	16.6	This study
80.8	8	8 = 0.5 nM P	1	Acidified dust (ZA)	2	This study
1.8	208	1.8	40	Dust & N (ZN)	22.2	This study
80.8	2008	80.8	220	Acidified dust & N (ZNA)	2.7	This study
2.8	18.9	18.9 = 1.2 nMP	26	Dust	22	Mesocosm, Herut et al., submitted; Tsagaraki et al., in preparation, both in this issue
3.7	55.1	55.1 = 3.4 nMP	33	Mixed aerosol	9.7	Mesocosm, Herut et al., submitted; Tsagaraki et al., in preparation, both in this issue

The waters at this time are N&P co-limited and the concentration of limiting nutrient is calculated from the smaller value of the actual P added or N added, divided by 16 expressed as P.

due to the "acid" added since the pH change was only a decrease of 0.02 pH units. The probable reason for this partial suppression of both PP and phytoplankton biomass is the trace metals added with the nutrients (Paytan et al., 2009).

Additional evidence suggesting that it is the trace metals released by the acid treatment that caused measurable biological suppression comes from the ZNA treatment in which the Chl.*a*/limiting nutrient ratio was 2.7 μg chl.a L^{-1}/nM PO_4^{-1} which was similar to that of ZA (2 ng chl-a/nM PO_4^{-1}) even though the actual chl.a change was much larger 220 ng chl.a L^{-1} vs. 1 ng chl.a L^{-1}. These two samples had much higher trace metals added compared with the Z and ZN treatments (**Table 3**). It is also noted that the unpolluted Saharan dust addition to the main mesocosm experiment (see Herut et al., submitted; Tsagaraki et al., in preparation—both in this issue for more details) had a ratio of 22 ng chl.a L^{-1}/nM PO_4^{-1} compared with a ratio of 9.7 ng chl.a L^{-1}/nM PO_4^{-1} for the polluted aerosol addition (**Table 4**).

One of the characteristics of aerosols from polluted air masses is that they contain higher amounts of potentially bioavailable trace metals. These are derived both from anthropogenic sources and from trace metals being mobilized by atmospheric acids (e.g., Herut et al., 2001; Wuttig et al., 2013; Shi et al., 2015). Our "polluted" analog aerosols in this experiment (ZA and ZNA) had contained much higher amounts of labile trace metals particularly Al, Fe, and Mn compared with non-acidified samples (**Table 3**). This is similar to the previous results of Spokes and Jickells (1995) who showed that these metals are particularly soluble at the low pH observed in clouds.

Previous studies have shown that phytoplankton activity is inhibited by the addition of trace metals from dust (Paytan et al., 2009; Jordi et al., 2012). In this experiment, Al was the element added in the largest amount (750 nM) and which remained in solution to the highest concentration (∼250 nM). Al is a major element in almost all aerosols and is likely to dissolve under the low pH conditions generated in the atmosphere, especially when somewhat polluted cloud droplets evaporate into wet aerosols (Shi et al., 2015). Although Al has been recognized as a phytoplankton toxin, it has mainly been studied in freshwater systems (Gensemer and Playle, 1999); it does not seem to have been considered as potentially toxic in marine systems possibly because the typical concentration of dissolved Al in seawater is relatively low (Hydes, 1983). However, it is likely that when atmospherically supplied dissolved Al reaches seawater, it will first precipitate as nanoparticles in a similar way to dissolved Fe. Recent studies have shown that such Al nanoparticles are more toxic to microalgae than simple dissolved Al (Sadiq et al., 2011). Although Paytan et al. (2009) suggested that Cu is the element most likely to cause phytoplankton inhibition, they mentioned the possibility that Al (or other trace metals) might be a contributory element to phytoplankton toxicity by dust addition. All of the changes in Cu concentration in this study were within sampling and analytical error and thus it is unlikely that Cu toxicity was important in this study. Similarly, it is considered unlikely that Mn or Fe, the two other elements that were leached in large amounts with acidified PM10, caused major phytoplankton inhibition because Mn is generally not considered a plant toxin and Fe is an essential micronutrient.

In addition to inhibiting total chl.*a*, primary and bacterial activity, the acid treatments also resulted in a smaller increase in *Synechococcus* biomass compared with both the control and the non-acidified PM10 additions (**Figure 5**). Paytan et al. (2009) also found that the abundance of *Synechococcus* was greater in the controls and in European aerosol treatment which had lower trace metal content added compared with their Saharan dust treatment which had increased trace metal supply. It is therefore considered likely that acid mobilization of toxic trace metals in dust particles may have disrupted *Synechococcus* metabolism.

CONCLUSIONS

Overall, the primary control of phytoplankton biomass and productivity was controlled by the amount of limiting nutrient added. When the amount of P was increased by a factor of ∼40 as a result of simulated atmospheric acidic processes (suggested by Nenes et al., 2011) converting solid P minerals into labile phosphate, and N limitation was relieved, there was a considerable increase in the phytoplankton growth. Recent results have suggested that atmospheric control is more complex than previously thought and depends on the amount of hydrogen ions present in the water film around aerosol particles and on whether the particles are internally or externally mixed (Stockdale et al., 2015). Here, it was shown that there was also an inhibitory effect of acid treatment on phytoplankton biomass, primary, and bacterial activity (though not bacterial biomass). Our results indicate that this inhibition was caused by the trace metals mobilized by the similar acid processes to those, which caused the P minerals to dissolve. Here, we suggest that Al, and not Cu (Paytan et al., 2009; Jordi et al., 2012), may be a key element in this inhibition, possibly in the form of nanoparticles.

Our acid treatments were designed as analogs for acidic atmospheric processes, particularly where polluted air masses interact with Saharan Dust. Such air masses have higher NO_x/SO_x, which will increase the amount of LIP formed but will also increase the amount of dissolved trace metals. In addition, such air masses are likely to contain aerosol particles which themselves have high original labile trace metals. The results presented here suggest that although overall acid processes in the atmosphere will increase the amount of labile P added to the photic zone and subsequently the phytoplankton biomass and PP, this is likely to be moderated by increased input of toxic trace metals. Further, research is required to understand and predict the overall balance of effects of these two conflicting processes on the microbial ecosystem.

AUTHOR CONTRIBUTIONS

Planning of the original experimental design and carrying out of experiment and sampling in the field (MK and ZS). Leaching rate of nutrients from dust (MK and AS). Chlorophyll a concentration (NP). Primary production (AL, SP). Synochococcus abundance and biomass (AT). Bacterial abundance, biomass and rate (AT, AG). Alkaline phosphatase activity (ER, IB, and BH). Trace metals (ES, MS). Organizing the data sets and calculating simple statistics (ER). Organizing the operation of microcosms and obtaining funding (PP, TT). Writing up manuscript (MK, ZS, AS, PP, IB, ER).

ACKNOWLEDGMENTS

This work was financed by the European Union Seventh Framework Program (FP7/2007–2013) under grant agreement no. 228224, "MESOAQUA: Network of leading MESOcosm facilities to advance the studies of future AQUAtic ecosystems from the Arctic to the Mediterranean" through grants to MK, ZS, IB, BH, and ER. The authors wish to thank G. Piperakis for his inspired technical assistance, A. Konstantinopoulou for assistance with bacterial production analyses, D. Podaras, and S. Diliberto for assistance during the experiment and N. Sekeris for his help with constructions and ideas on technical solutions. The captain and the crew of the R/V Philia are also thanked for their assistance during the transportation of water from the sea to the CRETACOSMOS facility. Funding was also provided by Leverhulme Trust entitled "Understanding the delivery of phosphorus nutrient to the oceans" Grant Number RPG 406. MDK would like to acknowledge the input from Yasmin Spain, Hannah deFrond and Emily Buckley who did their senior projects at Leeds University and whose input helped me clarify my thoughts on these experiments. Funding allowing the participation of ER, IB, and BH was also provided by the Israel Science Foundation grants (996/08) to IB, BH and ZS by NERC (NE/I021616/1).

SUPPLEMENTARY MATERIAL

The Supplementary Material for this article can be found online at: http://journal.frontiersin.org/article/10.3389/fmars.2016.00133

Figure S1 | (A,B) Phosphate leached from dust collected after two different dust storms in Rosh Pina, Israel into seawater. RPA was sampled in April 2014 and RPS was in September 2015. Note, the difference *Y*-axis.

Figure S2 | (A,B) Nitrate leached from dust collected after two different dust storms in Rosh Pina, Israel into seawater. RPA was sampled in April 2014 and RPS was in September 2015. Note, that the Nitrate concentration remained essentially constant after 30 min leaching. Note the difference *Y*-axis.

Table S1 | Ammonia and nitrate leached from 3 PM10 dust samples (PM10_1, PM10_2, PM10_3). Results are shown in nM N mg dust^{-1}.

Table S2 | Table showing the values of all the biological parameters used in this study as well as the calculated average values and standard deviations.

Table S3 | Summary of the statistical comparison (one-way ANOVA followed by Tukey's *post-hoc* test) between the different treatments (C, Z, ZN, and ZNA) at the conclusion of the microcosm experiment (2 days). Significant differences are in bold ($P < 0.05$).

REFERENCES

Atlas, E., and Pytkowicz, R. M. (1977). Solubility behaviour of apatites in sea water. *Limnol. Oceanogr.* 22, 290–300. doi: 10.4319/lo.1977.22.2.0290

Carbo, P., Krom, M. D., Homoky, W. B., Benning, L. G., and Herut, B. (2005). Impact of atmospheric deposition on N and P geochemistry in the southeastern Levantine basin. *Deep Sea Res. II Top. Stud. Oceanogr.* 52, 3041–3053. doi: 10.1016/j.dsr2.2005.08.014

Eijsink, L. M., Krom, M. D., and Herut, B. (2000). Speciation and burial flux of phosphorus in surface sediments of the Eastern Mediterranean. *Am. J. Sci.* 300, 483–503. doi: 10.2475/ajs.300.6.483

Gensemer, R. W., and Playle, R. C. (1999). The bioavailability and toxicity of aluminum in aquatic environments. *Crit. Rev. Environ. Sci. Technol.* 29, 315–450. doi: 10.1080/10643389991259245

Guerzoni, S., Chester, R., Dulac, F., Herut, B., Loÿe-Pilot, M.-D., Measures, C., et al. (1999). The role of atmospheric deposition in the biogeochemistry of the Mediterranean Sea. *Prog. Oceanogr.* 44, 147–190. doi: 10.1016/S0079-6611(99)00024-5

Guieu, C., Aumont, O., Paytan, A., Bopp, L., Law, C. S., Mahowald, N., et al. (2014). The significance of the episodic nature of atmospheric deposition to low nutrient low chlorophyll regions. *Glob. Biogeochem. Cycles* 28, 1179–1198. doi: 10.1002/2014GB004852

Guieu, C., Dulac, F., Desboeufs, K., Wagener, T., Pulido-Villena, E., Grisoni, J. M., et al. (2010). Large clean mesocosms and simulated dust deposition: a new methodology to investigate responses of marine oligotrophic ecosystems to atmospheric inputs. *Biogeosciences* 7, 2765–2784. doi: 10.5194/bg-7-2765-2010

Herut, B., Almogi-Labin, A., Jannink, N., and Gertman, I. (2000). The seasonal dynamics of nutrient and chlorophyll a concentrations on the SE Mediterranean shelf-slope. *Oceanol. Acta* 23, 771–782. doi: 10.1016/S0399-1784(00)01118-X

Herut, B., Kress, N., and Tibor, G. (2002). The use of hyper-spectral remote sensing in compliance monitoring of water quality (phytoplankton and suspended particles) at "hot spot" areas (Mediterranean coast of Israel). *Fresenius Environ. Bull.* 11, 782–787.

Herut, B., Krom, M. D., Pan, G., and Mortimer, R. (1999). Atmospheric input of nitrogen and phosphorus to the Southeast Mediterranean: sources, fluxes, and possible impact. *Limnol. Oceanogr.* 44, 1683–1692. doi: 10.4319/lo.1999.44.7.1683

Herut, B., Nimmo, M., Medway, A., Chester, R., and Krom, M. D. (2001). Dry atmospheric inputs of trace metals at the Mediterranean coast of Israel (SE Mediterranean): sources and fluxes. *Atmos. Environ.* 35, 803–813. doi: 10.1016/S1352-2310(00)00216-8

Herut, B., Zohary, T., Krom, M. D., Mantoura, R. F. C., Pitta, P., Psarra, S., et al. (2005). Response of East Mediterranean surface water to Saharan dust: on-board microcosm experiment and field observations. *Deep Sea Res. II Top. Stud. Oceanogr.* 52, 3024–3040. doi: 10.1016/j.dsr2.2005.09.003

Hydes, D. (1983). Distribution of aluminium in waters of the North East Atlantic 25 N to 35 N. *Geochim. Cosmochim. Acta* 47, 967–973. doi: 10.1016/0016-7037(83)90164-3

Ignatiades, L., Gotsis-Skretas, O., Pagou, K., and Krasakopoulou, E. (2009). Diversification of phytoplankton community structure and related parameters along a large-scale longitudinal east-west transect of the Mediterranean Sea. *J. Plankton Res.* 31, 411–428. doi: 10.1093/plankt/fbn124

Jordi, A., Basterretxea, G., Tovar-Sɑnchez, A., Alastuey, A., and Querol, X. (2012). Copper aerosols inhibit phytoplankton growth in the Mediterranean Sea. *Proc. Natl. Acad. Sci. U.S.A.* 109, 21246–21249. doi: 10.1073/pnas.1207567110

Kana, T., and Glibert, P. M. (1987). Effect of irradiances up to 2000 μE m-2 s-1 on marine Synechococcus WH 7803-I. *Growth pigmentation and cell composition. Deep Sea Res. I* 34, 479–516. doi: 10.1016/0198-0149(87)90001-X

Kingston, H. M., Barnes, I. L., Brady, T. J., Rains, T. C., and Champ, M. A. (1978). Separation of eight transition elements from alkali and alkaline earth elements in estuarine and seawater with chelating resin and their determination by graphite furnace atomic absorption spectrometry. *Anal. Chem.* 50, 2064–2070. doi: 10.1021/ac50036a031

Kirchman, D. L. (1993). "Leucine incorporation as a measure of biomass production by heterotrophic bacteria," in *Handbook of Methods in Aquatic Microbial Ecology,* eds P. F. Kemp, B. F. Sherr, E. B. Sherr, and J. J. Cole (Boca Raton, FL: Lewis Publishers), 509–512.

Kress, N., Thingstad, F., Pitta, P., Psarra, S., Tanaka, T., Zohary, T., et al. (2005). Effect of P and N addition to oligotrophic Eastern Mediterranean waters influenced by near-shore waters: a microcosm experiment. *Deep Sea Res. II Top. Stud. Oceanogr.* 52, 3054–3073. doi: 10.1016/j.dsr2.2005.08.013

Krom, M. D., Herut, B., and Mantoura, R. F. C. (2004). Nutrient budget for the Eastern Mediterranean: implications for phosphorus limitation. *Limnol. Oceanogr.* 49, 1582–1592. doi: 10.4319/lo.2004.49.5.1582

Krom, M. D., Kress, N., Brenner, S., and Gordon, L. I. (1991). Phosphorus limitation of primary productivity in the eastern Mediterranean Sea. *Limnol. Oceanogr.* 36, 424–432. doi: 10.4319/lo.1991.36.3.0424

Krom, M. D., Thingstad, T. F., Brenner, S., Carbo, P., Drakopoulos, P., Fileman, T. W., et al. (2005). Summary and overview of the CYCLOPS P addition Lagrangian experiment in the Eastern Mediterranean. *Deep Sea Res. II Top. Stud. Oceanogr.* 52, 3090–3108. doi: 10.1016/j.dsr2.2005.08.018

Lafon, S., Sokolik, I. N., Rajot, J. L., Caquincau, S., and Gaudichet, A. (2006). Characterization of iron oxides in mineral dust aerosols: implications for light absorption. *J. Geophys. Res. Atmos.* 111, 1–19. doi: 10.1029/2005jd007016

Lee, S., and Fuhrman, J. A. (1987). Relationships between biovolume and biomass of naturally derived marine bacterioplankton. *Appl. Environ. Microbiol.* 53, 1298–1303.

Luna, G. M., Bianchelli, S., Decembrini, F., De Domenico, E., Danovaro, R., and Dell'Anno A. (2012). The dark portion of the Mediterranean Sea is a bioreactor of organic matter cycling. *Glob. Biogeochem. Cycles* 26:GB2017. doi: 10.1029/2011GB004168

Mackey, K. R. M., Roberts, K., Lomas, M. W., Saito, M. A., Post, A. F., and Paytan, A. (2012). Enhanced solubility and ecological impact of atmospheric phosphorus deposition upon extended seawater exposure. *Environ. Sci. Technol.* 46, 10438–10446. doi: 10.1021/es3007996

Mahowald, N., Jickells, T. D., Baker, A. R., Artaxo, P., Benitez-Nelson, C. R., Bertgametti, G., et al. (2008). Global distribution of atmospheric phosphorus sources, concentrations and deposition rates, and anthropogenic impacts. *Glob. Biogeochem. Cycles* 22, GB24026. doi: 10.1029/2008GB003240

Mahowald, N. M., Baker, A. R., Bergametti, G., Brooks, N., Duce, R. A., Jickells, T. D., et al. (2005). Atmospheric global dust cycle and iron inputs to the ocean. *Glob. Biogeochem. Cycles* 19, GB4025. doi: 10.1029/2004GB002402

Marie, D., Brussaard, C. P. D., Thyrhaug, R., Bratbak, G., and Vaulot, D. (1999). Enumerating of marine viruses in culture and natural samples by flow cytometry. *Appl. Environ. Microbiol.* 65, 45–52.

Markaki, Z., Oikonomou, K., Kocak, M., Kouvarakis, G., Chaniotaki, A., Kubilay, N., et al. (2003). Atmospheric deposition of inorganic phosphorus in the Levatine Basin, eastern Mediterranean: spatial and temporal variability and its role in seawater productivity. *Limnol. Oceanogr.* 48, 1557–1568. doi: 10.4319/lo.2003.48.4.1557

Meskhidze, N., Chameides, W. L., Nenes, A., and Chen, G. (2003). Iron mobilization in mineral dust: can anthropogenic SO_2 emissions affect ocean productivity? *Geophys. Res. Lett.* 30:2085. doi: 10.1029/2003GL018035

Migon, C., Sandroni, V., and Béthoux, J. P. (2001). Atmospheric input of anthropogenic phosphorus to the northwest Mediterranean under oligotrophic conditions. *Mar. Environ. Res.* 52, 413–426. doi: 10.1016/S0141-1136(01)00095-2

Nenes, A., Krom, M. D., Mihalopoulos, N., Van Cappellen, P., Shi, Z., Bougiatioti, A., et al. (2011). Atmospheric acidification of mineral aerosols: a source of bioavailable phosphorus for the oceans. *Atmos. Chem. Phys.* 11, 6265–6272. doi: 10.5194/acp-11-6265-2011

Paytan, A., Mackey, K. R. M., Chen, Y., Lima, I. D., Doney, S. C., Mahowald, N., et al. (2009). Toxicity of atmospheric aerosols on marine phytoplankton. *Proc. Natl. Acad. Sci. U.S.A.* 106, 4601–4605. doi: 10.1073/pnas.0811486106

Pitta, P., Nejstgaard, J. C., Tsagaraki, T. M., Zervoudaki, S., Egge, J. K., Frangoulis, C., et al. (2016). Confirming the "Rapid phosphorus transfer from microorganisms to mesozooplankton in the Eastern Mediterranean Sea" scenario through a mesocosm experiment. *J. Plankton Res.* 38, 502–521. doi: 10.1093/plankt/fbw010

Pitta, P., Stambler, N., and Tanaka, T. (2005). Biological response to P addition in the Eastern Mediterranean Sea. *The microbial race against time. Deep Sea Res. II Top. Stud. Oceanogr.* 52, 2961–2974. doi: 10.1016/j.dsr2.2005.08.012

Psarra, P., Tselepides, A., and Ignatiades, L. (2000). Primary productivity in the oligotrophic Cretan Sea (NE Mediterranean) seasonal and interannual variability. *Prog. Oceanogr.* 46, 187–204. doi: 10.1016/S0079-6611(00)00018-5

Psarra, S., Zohary, T., Krom, M. D., Mantoura, R. F. C., Polychronaki, T., Stambler, N., et al. (2005). Phytoplankton response to a Lagrangian phosphate addition in the Levantine Sea (Eastern Mediterranean). *Deep Sea Res. II* 52, 2944–2960. doi: 10.1016/j.dsr2.2005.08.015

Rahav, E., Giannetto, M. J., and Bar-Zeev, E. (2016). Contribution of mono and polysaccharides to heterotrophic N_2 fixation at the eastern Mediterranean coastline. *Sci. Rep.* 6:27858. doi: 10.1038/srep27858

Rahav, E., Herut, B., Stambler, N., Bar-Zeev, E., Mulholland, M. R., and Berman-Frank, I. (2013). Uncoupling between dinitrogen fixation and primary

productivity in the eastern Mediterranean Sea. *J. Geophys. Res. Biogeosci.* 118, 195–202. doi: 10.1002/jgrg.20023

Raveh, O., David, N., Rilov, G., and Rahav, E. (2015). The temporal dynamics of coastal phytoplankton and bacterioplankton in the Eastern Mediterranean Sea. *PLoS ONE* 10:e0140690. doi: 10.1371/journal.pone.0140690

Ridame, C., and Guieu, C. (2002). Saharan input of phosphate to the oligotrophic water of the open western Mediterranean Sea. *Limnol. Oceanogr.* 47, 856–869. doi: 10.4319/lo.2002.47.3.0856

Riley, J. P., and Taylor, D. (1968). Chelating resins for the concentration of trace elements from sea water and their analytical use in conjunction with atomic absorption spectrophotometry. *Anal. Chim. Acta* 40, 479–485. doi: 10.1016/S0003-2670(00)86764-1

Romero, E., Peters, F., Marrasé, C., Guadayol, S., Gasol, J. M., and Weinbauer, M. G. (2011). Coastal Mediterranean plankton stimulation dynamics through a dust storm event: an experimental simulation. *Estuar. Coast. Shelf Sci.* 93, 27–39. doi: 10.1016/j.ecss.2011.03.019

Sadiq, I. M., Pakrashi, S., Chandrasekaran, N., and Mukherjee, A. (2011). Studies on toxicity of aluminum oxide (Al2O3) nanoparticles to microalgae species: Scenedesmus sp. *and Chlorella sp. J. Nanopart. Res.* 13, 3287–3299. doi: 10.1007/s11051-011-0243-0

Scoullos, M. J., Sakellari, A., Giannopoulou, K., Paraskevopoulou, V., and Dassenakis, M. (2007). Dissolved and particulate trace metal levels in the Saronikos Gulf, Greece, in 2004. *The impact of the primary Wastewater Treatment Plant of Psittalia. Desalination* 210, 98–109. doi: 10.1016/j.desal.2006.05.036

Seinfeld, J. H., and Pandis, S. N. (2006). *Atmospheric Chemistry and Physics from Air Pollution to Climate Change*, *2nd Edn*. New York, NY: John Wiley & sons Inc.

Shi, Z., Krom, M. D., Bonneville, S., Baker, A. R., Bristow, C., Drake, N., et al. (2011). Influence of chemical weathering and aging of iron oxides on the potential iron solubility of Saharan dust during simulated atmospheric processing. *Glob. Biogeochem. Cycles* 25:GB2010. doi: 10.1029/2010GB003837

Shi, Z., Krom, M. D., Bonneville, S., and Benning, L. G. (2015). Atmospheric processing outside clouds increases soluble iron in mineral dust. *Environ. Sci. Technol.* 49, 1472–1477. doi: 10.1021/es504623x

Singer, A., Dultz, S., and Argaman, E. (2004). Properties of the non-soluble fractions of suspended dust over the Dead Sea. *Atmos. Environ.* 38, 1745–1753. doi: 10.1016/j.atmosenv.2003.12.026

Siokou-Frangou, I., Christaki, U., Mazzocchi, M. G., Montresor, M., Ribera d'Alcalα, M., Vaqué, D., et al. (2010). Plankton in the open Mediterranean Sea: a review. *Biogeosciences* 7, 1543–1586. doi: 10.5194/bg-7-1543-2010

Smith, D. C., and Azam, F. (1992). A simple, economical method for measuring bacterial protein synthesis rates in seawater using ^{3}H-leucine. *Mar. Microb. Food Webs* 6, 107–114.

Spokes, L. J., and Jickells, T. D. (1995). Factors controlling the solubility of aerosol trace metals in the atmosphere and on mixing into seawater. *Aquat. Geochem.* 1, 355–374. doi: 10.1007/BF00702739

Statham, P. J., and Hart, V. (2005). Dissolved iron in the Cretan Sea (eastern Mediterranean). *Limnol. Oceanogr.* 50, 1142–1148. doi: 10.4319/lo.2005.50.4.1142

Steeman-Nielsen, E. (1952). The use of radioactive carbon (C14) for measuring organic production in the sea. *J. Cons.* 18, 117–140. doi: 10.1093/icesjms/18.2.117

Stockdale, A., Krom, M. D., Mortimer, R. J. M., Benning, L. G., Carslaw, K., and Shi, Z. (2015). "Controls of acid dissolution of P in Mineral Dust during Atmospheric Processing," in *Abstract Presented at Goldschmidt Conference of the European Association of Geochemists, August 16th-21st 2015* (Prague).

Tanaka, T., Thingstad, T. F., Christaki, U., Colombet, J., Cornet-Barthaux, V., Courties, C., et al. (2011). Lack of P-limitation of phytoplankton and heterotrophic prokaryotes in surface waters of three anticyclonic eddies in the stratified Mediterranean Sea. *Biogeosciences* 8, 525–538. doi: 10.5194/bg-8-525-2011

Ternon, E., Guieu, C., Ridame, C., L'Helguen, S., and Catala, P. (2011). Longitudinal variability of the biogeochemical role of Mediterranean aerosols in the Mediterranean Sea. *Biogeosciences* 8, 1067–1080. doi: 10.5194/bg-8-1067-2011

Thingstad, T. F., Krom, M. D., Mantoura, R. F. C., Flaten, G. A. F., Groom, S., Herut, B., et al. (2005). Nature of phosphorus limitation in the ultraoligotrophic eastern Mediterranean. *Science* 309, 1068–1071. doi: 10.1126/science.1112632

Thingstad, T., and Mantoura, R. (2005). Titrating excess nitrogen content of phosphorous-deficient eastern Mediterranean surface water using alkaline phosphatase activity as a bio-indicator. *Limnol. Oceanogr. Methods* 3, 94–100. doi: 10.4319/lom.2005.3.94

Tsiola, A., Pitta, P., Fodelianakis, S., Pete, R., Magiopoulos, I., Mara, P., et al. (2016). Nutrient limitation in surface waters of the oligotrophic Eastern Mediterranean Sea: an Enrichment Microcosm Experiment. *Microb. Ecol.* 71, 575–588. doi: 10.1007/s00248-015-0713-5

Van Wambeke, F., Christaki, U., Giannakourou, A., Moutin, T., and Souvermezoglou, E. (2002). Longitudinal and vertical trends of bacterial limitation by phosphorus and carbon in the Mediterranean Sea. *Microb. Ecol.* 43, 119–133. doi: 10.1007/s00248-001-0038-4

Wuttig, K., Wagener, T., Bressac, M., Dammshäuser, A., Streu, P., Guieu, C., et al. (2013). Impacts of dust deposition on dissolved trace metal concentrations (Mn, Al and Fe) during a mesocosm experiment. *Biogeosciences* 10, 2583–2600. doi: 10.5194/bg-10-2583-2013

Yentsch, C. S., and Menzel, D. W. (1963). A method for the determination of phytoplankton chlorophyll and phaeophytin by fluorescence. *Deep Sea Res. Oceanogr. Abstr.* 10, 221–231. doi: 10.1016/0011-7471(63)90358-9

Zohary, T., Herut, B., Krom, M. D., Fauzi, C., Mantoura, R., Pitta, P., et al. (2005). P-limited bacteria but N and P co-limited phytoplankton in the Eastern Mediterranean—a microcosm experiment. *Deep Sea Res. II Top. Stud. Oceanogr.* 52, 3011–3023. doi: 10.1016/j.dsr2.2005.08.011

Conflict of Interest Statement: The authors declare that the research was conducted in the absence of any commercial or financial relationships that could be construed as a potential conflict of interest.

frontiers in Marine Science

ORIGINAL RESEARCH
published: 02 May 2017
doi: 10.3389/fmars.2017.00117

Saharan Dust Deposition Effects on the Microbial Food Web in the Eastern Mediterranean: A Study Based on a Mesocosm Experiment

Paraskevi Pitta[1], Maria Kanakidou[2], Nikolaos Mihalopoulos[2,3], Sylvia Christodoulaki[1,2], Panagiotis D. Dimitriou[1,4], Constantin Frangoulis[1], Antonia Giannakourou[5], Margarita Kagiorgi[1], Anna Lagaria[1], Panagiota Nikolaou[2], Nafsika Papageorgiou[1], Stella Psarra[1], Ioulia Santi[1,4], Manolis Tsapakis[1], Anastasia Tsiola[1,4], Kalliopi Violaki[2] and George Petihakis[1]*

[1] Hellenic Centre for Marine Research, Institute of Oceanography, Heraklion, Greece, [2] Chemistry Department, University of Crete, Heraklion, Greece, [3] Institute for Environment and Sustainable Development, National Observatory of Athens, Athens, Greece, [4] Biology Department, University of Crete, Heraklion, Greece, [5] Hellenic Centre for Marine Research, Institute of Oceanography, Athens, Greece

OPEN ACCESS

Edited by:
Christian Grenz, Mediterranean Institute of Oceanography, France

Reviewed by:
E. Elena Garcia-Martin, University of East Anglia, UK
Suzanne Jane Painting, Centre for Environment, Fisheries and Aquaculture Science, UK

***Correspondence:**
Paraskevi Pitta
vpitta@hcmr.gr

Specialty section:
This article was submitted to Marine Ecosystem Ecology, a section of the journal Frontiers in Marine Science

Received: *19 December 2016*
Accepted: *11 April 2017*
Published: *02 May 2017*

Citation:
Pitta P, Kanakidou M, Mihalopoulos N, Christodoulaki S, Dimitriou PD, Frangoulis C, Giannakourou A, Kagiorgi M, Lagaria A, Nikolaou P, Papageorgiou N, Psarra S, Santi I, Tsapakis M, Tsiola A, Violaki K and Petihakis G (2017) Saharan Dust Deposition Effects on the Microbial Food Web in the Eastern Mediterranean: A Study Based on a Mesocosm Experiment. Front. Mar. Sci. 4:117. doi: 10.3389/fmars.2017.00117

The effect of episodicity of Saharan dust deposition on the pelagic microbial food web was studied in the oligotrophic Eastern Mediterranean by means of a mesocosm experiment in May 2014. Two different treatments in triplicates (addition of natural Saharan dust in a single-strong pulse or in three smaller consecutive doses of the same total quantity), and three unamended controls were employed; chemical and biological parameters were measured during a 10-day experiment. Temporal changes in primary (PP) and bacterial (BP) production, chlorophyll *a* (Chl *a*) concentration and heterotrophic bacteria, *Synechococcus* and mesozooplankton abundance were studied. The results suggested that the auto- and hetero-trophic components of the food web (at least the prokaryotes) were enhanced by the dust addition (and by the nitrogen and phosphorus added through dust). Furthermore, a 1-day delay was observed for PP, BP, and Chl *a* increases when dust was added in three daily doses; however, the maximal values attained were similar in the two treatments. Although, the effect was evident in the first osmotrophic level (phytoplankton and bacteria), it was lost further up the food web, masked under the impact of grazing exerted by predators such as heterotrophic flagellates, ciliates and dinoflagellates. This was partly proved by two dilution experiments. This study demonstrates the important role of atmospheric deposition and protist grazing when evaluating the effect on oligotrophic systems characterized by increased numbers of trophic levels.

Keywords: natural Saharan dust, Eastern Mediterranean, mesocosm, plankton food web, grazing

INTRODUCTION

Atmospheric deposition is an important source of macro-nutrients and micro-trace metals to the ocean (Jickells et al., 2005; Mahowald et al., 2008). In high-nutrient low-chlorophyll (HNLC) areas, dust deposition provides iron to the ocean surface and therefore stimulates phytoplankton growth rate and ocean productivity (Martin, 1990; Jickells et al., 2005; Boyd et al., 2007). In low-nutrient

low-chlorophyll (LNLC) areas, dust deposition also affects the productivity and function of the ecosystem through the simultaneous input of phosphate and iron (Blain et al., 2004; Mills et al., 2004; Marañón et al., 2010).

The Eastern Mediterranean is a typical LNLC environment. The low nutrient concentrations, caused by the lack of large rivers in the eastern basin and deteriorated by the Mediterranean anti-estuarine circulation, together with the nitrate:phosphate (N:P) ratio in the deep layers of ca. 28:1, far in excess of the Redfield ratio of 16:1, result in a P-limited system (Krom et al., 1991, 2005a; Kress and Herut, 2001). After the winter-spring bloom period and during the summer (warm) stratification period, inorganic nutrient concentrations are extremely low in the surface layers. A Lagrangian experiment in the Levantine Sea suggested bacterioplankton limitation by phosphorus (P) and phytoplankton co-limitation by nitrogen (N) & P in the summer (Krom et al., 2005b; Pitta et al., 2005; Thingstad et al., 2005; Zohary et al., 2005). A mesocosm experiment, conducted in the Cretan Sea during late summer, using a comparable, in terms of nutrient content, but different water mass, supported these findings (Pitta et al., 2016). However, N-limitation of primary production (Lagaria et al., 2011) and N & P co-limitation of heterotrophic prokaryote growth (Tanaka et al., 2011) have also been found during summer time in the Levantine Basin during microcosm experiments, although the ratio N:P in both dissolved and particulate organic fractions suggested P starvation.

The Mediterranean Sea receives one of the highest inputs of atmospheric dust in the contemporary ocean throughout the year, mainly from the Sahara Desert ($20–50 \times 10^6$ tons yr^{-1}, Guerzoni et al., 1999). Therefore, during the warm stratification period of limited nutrient availability, Saharan dust is not only a significant but the dominant supplier of inorganic nutrients and trace metals to the surface layers of the Eastern Mediterranean. A lot is known about the mineralogical composition, the transformation during Aeolian transportation and the chemical fate of the Saharan dust in the surface layers of the Mediterranean Sea (Guerzoni et al., 1999; Desboeufs et al., 2014). However, the effect of dust deposition on the biological productivity and function of the surface pelagic ecosystem have been much less studied. To fill this knowledge gap, both microcosm and mesocosm experiments were performed.

Microcosm experiments, conducted at both the Western and the Eastern Mediterranean, have provided a lot of information on biological processes and biomass; however, the results of these experiments are very fragmented. For instance, a microcosm experiment conducted in Blanes Bay, Spain, in May 2006, resulted in an increased bacterial abundance and production and in altered bacterial diversity (Lekunberri et al., 2010; Romero et al., 2011) but, in terms of phytoplankton, it produced increases only in autotrophic nanoflagellates (Romero et al., 2011). Two microcosm experiments conducted in August 2003 and 2006, using water from the DYFAMED station, reported increases in primary production (Bonnet et al., 2005) and bacterial abundance and respiration (Pulido-Villena et al., 2008). Only one microcosm experiment, conducted earlier (May 2002) in the Eastern Mediterranean, provides information on both biomass and rates of the auto- and hetero-trophic components of the food web as well as on P uptake and, at the same time, on larger grazers such as pelagic ciliates (Herut et al., 2005).

Although, providing valuable information in many aspects, all microcosm experiments suffer from a main drawback, which is the experimental volume; microcosms are usually small-volume (<10 or a few tens of liters) bottles. For this reason, only the lower trophic food web can be studied; no results can be obtained on zooplankton because the natural zooplankton density is too low. Furthermore, the duration of microcosm experiments cannot easily exceed 2–3 days so only the short-scale effects may be studied. Finally, modern molecular techniques requiring large sampling volumes cannot be used.

One way to overcome these difficulties is to perform mesocosm experiments, i.e., large-volume experimental set ups which allow hypothesis testing under replicated, controlled, and repeatable conditions as close as possible to the natural environment. Two large-scale *in situ* mesocosm experiments took place in the Western Mediterranean, in 2008 and 2010, in order to study the effect of Saharan dust on the pelagic environment. The available information on the biological processes from these two experiments comes from four publications that focus on either the autotrophic (Giovagnetti et al., 2013; Ridame et al., 2014) or the heterotrophic (Laghdass et al., 2011; Pulido-Villena et al., 2014) component of the food web. During the 2008 experiment, a single-dose dust addition resulted in a 2-fold increase in the Chl *a* concentration (Laghdass et al., 2011) but the heterotrophic bacterial abundance was not affected; total and active bacterial community clustered according to the sampling time points but independently of treatment. During the 2010 experiment, during which dust was added in two doses, the results were more or less similar regarding the heterotrophic component (Pulido-Villena et al., 2014). As far as the autotrophic component is concerned, Giovagnetti et al. (2013) showed differential responses of different size fractions to the dust addition, with picophytoplankton increasing mainly after the first seeding while the second addition led to an increase in both pico- and nano/microphytoplankton.

However, there is very scarce or no information published on biological productivity, either primary (in only Ridame et al., 2014) or bacterial production. In addition, the impact of grazing was only studied as far as heterotrophic flagellates are concerned; the effect of larger grazers such as pelagic ciliates is missing, even though ciliates constitute one of the major grazing groups in the oligotrophic Mediterranean (Pitta et al., 2001). The effect of dust addition on meso-zooplankton is also missing. Finally, often phytoplankton is examined only in relation to nutrient availability and heterotrophs only in relation to grazing although it is well-known that very complex trophic relationships characterize the microbial food web, especially in oligotrophic environments with resource scarcity.

In order to study the effect of Saharan dust on the oligotrophic Eastern Mediterranean, two mesocosm experiments were performed in Crete, in 2012 and 2014. To our knowledge, these are the first experiments that studied the biological response of the entire pelagic food web while, at the same time, a lot of attention was given to the chemical changes occurring after the dust addition. During the 2012 experiment, the addition of either

natural pure Saharan dust or mixed aerosol (desert dust and polluted particles) into the ultra-oligotrophic environment of the Eastern Mediterranean in a single pulse resulted in a net response of both the auto- and the hetero-trophic components (Tsagaraki et al., in review).

The 2014 mesocosm experiment, presented here, studied the effect of dust deposition on the entire pelagic microbial food web of the Eastern Mediterranean when added in multiple, successive dust pulses. It is widely recognized that dust deposition is highly episodic, generally occurring in either single, strong events during which a large quantity of dust is added to the ocean surface within a very short time-scale of hours, or in repetitive, smaller events during which small quantities of dust are added into the sea repetitively, over a number of days (Vincent et al., 2016 and references therein). The 2012 mesocosm experiment was a simulation of the former case while the 2014 experiment was a comparison of both cases. To our knowledge, these two experiments are the first mesocosm studies in which naturally collected aerosols, not dust analogs, were used in the Mediterranean.

In May 2014, during a 10-day experiment, daily sampling allowed the disclosure of the rapid biological processes of a highly oligotrophic environment when nutrients are offered via dust. All groups, from viruses through bacteria, phytoplankton, and protozoa to zooplankton were examined in terms of abundance, production, and/or community composition.

The goals of this experiment were (1) to estimate the influence of dust addition on the microbial food web of the Eastern Mediterranean, (2) to investigate whether the quantity and episodicity of dust addition influence the dynamics of different components of the food web in terms of abundance and/or production, and (3) to examine the role of grazing of microzooplankton on different fractions of phytoplankton and also on the way the impact of dust addition on the lower food web is finally perceived.

MATERIALS AND METHODS

Mesocosm Experimental Design and Sampling

A mesocosm experiment took place in May 2014 at the mesocosm facility of HCMR CRETACOSMOS (http://cretacosmos.eu) in Crete, Greece, in the framework of the project ADAMANT. To fill the mesocosms, 27 m^3 of water were collected on the 8th and 9th of May aboard the R/V Philia from a site five nautical miles off the north coast of Crete (35° 24.957 N, 25° 14.441 E). Sub-surface water from 10 m depth was pumped into several 1 m^3 high-density polyethylene (HDPE) barrels by means of a submersible water pump. All equipment had been previously aged for at least 1 week with tap water; subsequently, in order to avoid contamination in the highly oligotrophic conditions prevailing in this environment, all equipment used, including the HDPE barrels, were washed with HCl (10%) and rinsed three times with de-ionized water. After filling, the 1 m^3 barrels were shipped to the Heraklion harbor and then transported by truck to the mesocosm facility on the north coast of Crete, 15 km east of Heraklion. From the filling of the barrels on board to their final arrival at HCMR, on average, transport took 2 h; during this time, the water temperature inside the barrels was kept unchanged by constantly pouring sea water on the barrels. Upon arrival at the mesocosm facility, the water was gravity-poured into nine mesocosms (polyethylene bags, 1.32 m diameter) of 3 m^3 each. Special care was taken to divide the water equally from each of the 1 m^3 barrels among all nine mesocosms in order to ensure homogeneity of initial conditions. The mesocosms were submerged in a 150 m^3 concrete tank, with running surface sea water that kept the temperature stable throughout the experiment, at the levels prevailing at the site and depth from which water was collected (20 ± 0.5°C). Each mesocosm was covered by a two-layered lid which protected it from atmospheric deposition and also mimicked the light conditions at 10 m depth from where the water was pumped. Once the filling of mesocosms was completed, the water was left overnight.

The experiment started on the day after (May 10th, Day 0). Two different dust treatments were tested in triplicate mesocosms. In the first treatment (hereafter referred to as SA: single addition), Saharan dust was added only once, on the first day of the experiment (May 10th, Day 0). Four grams of natural Saharan dust collected in Crete and Cyprus (see below) were added in each of the three SA mesocosms, this quantity representing a concentration of 1.3 mg L^{-1}. In the second treatment (hereafter referred to as RA: repetitive addition), the same total quantity as for SA but divided into three doses, was added to each of the three RA mesocosms, on the first 3 days of the experiment (May 10th, 11th, and 12th, Days 0, 1, and 2, respectively); details on the quantities of dust added are shown in **Table 1**. Three more mesocosms were used as the Control, where no addition was performed (hereafter referred to as Cnt). The dust addition by weight (in both treatments) is considered representative of a realistic dust deposition event of 0.7 g m^{-2} day^{-1} (Gerasopoulos et al., 2006; Ternon et al., 2010).

Mixing in the mesocosms was achieved by light bubbling using a PVC tube of diameter 4 cm, creating an airlift from just above the bottom of the mesocosms and releasing the water and bubbles under the surface to avoid damaging the delicate planktonic organisms. All mesocosms were sampled daily throughout the 10-day experiment. Samples were taken by means of silicon tubes, permanently placed in all nine mesocosms, which directed the water to sampling carboys by creating a light suction using a large-volume syringe. All nine silicon tubes and sampling carboys were previously aged, washed with HCl (10%) and rinsed three times with de-ionized water. They were also washed and rinsed three times with de-ionized water before every daily sampling.

Dilution Experiment

The growth rate of different phytoplankton groups and the grazing mortality exerted by microzooplankton in the Cnt and the SA treatment were measured on Days 2 and 4 by the dilution technique (Landry and Hassett, 1982), following the protocols of Landry et al. (2003). The dilution series was prepared using unfiltered seawater at 25, 50, 75, and 100%. The particle-free

TABLE 1 | Quantity and concentration of dust added to mesocosms, in SA (Day 0) and RA (Days 0, 1, 2).

Dust added	Quantity added (g)	Concentration (mg L^{-1})
Cnt1	0	0
Cnt2	0	0
Cnt3	0	0
SA1 (Day 0)	4.02	1.34
SA2 (Day 0)	4.01	1.33
SA3 (Day 0)	4.00	1.33
RA1 (Day 0, Day 1, Day 2)	4.04 (1.00; 2.01; 1.03)	1.35
RA2 (Day 0, Day 1, Day 2)	4.02 (1.01; 2.01; 1.01)	1.34
RA3 (Day 0, Day 1, Day 2)	4.11 (1.04; 2.01; 1.07)	1.37

In parentheses, quantities added on three consecutive days, 0, 1, and 2. Cnt = Control mesocosms (no addition), SA = single addition, mesocosms where dust was added once, on the first day of the experiment, RA = repetitive addition, mesocosms where the same quantity of dust was added, divided into three doses, on the first 3 days of the experiment, Days 0, 1, and 2.

seawater was prepared from 10 L of water collected from the three Cnt replicates, which was then mixed and filtered by gravity through 0.2 μm capsules (Pall Corporation). The filtered water was put into 2 L polycarbonate bottles, which were then gently filled with unfiltered water (collected from the Cnt or the SA mesocosms) and incubated in the large concrete tank under the same conditions as the mesocosms for 24 h. All bottles and tubes used in the experiment were washed with 10% HCl and deionized water and rinsed with the incubated seawater. Samples for measuring *Synechococcus,* pico-eukaryote and autotrophic flagellate abundance were taken at T0, from the unfiltered water, and at the termination of the experiment.

The apparent prey growth rate (AGR) was estimated using the equation: AGR (day^{-1}) = ln (C_t/C_0)/t, where C_t and C_0 are the final and initial concentrations of the prey organisms, respectively, and t is the time of incubation [day]. AGR was estimated for both pico- and nano-size fractions. The rates of growth and grazing mortality were calculated by the linear regression of AGR vs. the dilution factor. The absolute value of the slope of the regression is the grazing rate m (day^{-1}) and ordinal intercept (y-intercept) of the regression is the growth rate μ in the absence of grazing (day^{-1}; Landry and Hassett, 1982; Landry et al., 2003).

Dust Collection

The dust samples used for the mesocosm experiment were collected weekly or on a dust-event basis over a period of more than a year (October 2012–March 2014) from the East Mediterranean (Crete and Cyprus). **Figure 1A** presents the temporal distribution of the collected dust dry deposition. Overall, 83% of the total dust mass added was collected in Heraklion, Crete (35% was collected during an intensive dust event period from 1 to 9 June 2013), and the remaining 17% was collected in Larnaca, Cyprus. These dry deposition samples were mixed, homogenized by stirring and chemically characterized for nutrients and metals before being added in the mesocosms.

Chemical Analyses of Dust

Anions/Cations

A Dionex AS4A-SC column with ASRS-300 4 mm suppressor in auto-suppression mode of operation was used for the analysis of anions (Cl^-, Br^-, NO_3^-, SO_4^{2-}, HPO_4^{2-}, $C_2O_4^{2-}$) in aerosol extractions. All the anions were determined with isocratic elution at 1.5 mL min^{-1} of Na_2CO_3/$NaHCO_3$ eluent. For the cations (Na^+, NH_4^+, K^+, Mg^{2+}, and Ca^{2+}), a CS12-SC column was used with a CSRS-300 4 mm suppressor. Separation was achieved under isocratic conditions with MSA (20 mM) eluent at a flow rate of 1.0 mL min^{-1}. The reproducibility of the measurements was >2% and the detection limit was about 1 ppb for both anions and cations. Mean blank values were 5–10 ppb for Na^+; Ca^{2+} and <3 ppb for the rest of the main anions and cations. Details on the chromatographic conditions are reported in Bardouki et al. (2003).

Metals (Al, V, Cr, Mn, Fe, Co, Ni, Cu, Zn, As, Sb, Pb) and Total Phosphorus (TP)

Metals and TP in the dust were measured by acid digestion with concentrated nitric acid (puriss. p.a., Fluka Prod. No. 84380) under controlled conditions [Berghof Microwave System-2, Teflon vessels (DAP—60 K, 60 mL/40 bar)]. After cooling at room temperature, the digested solution was transferred to an acid-cleaned polyethylene container and stored in the freezer. The obtained solutions were analyzed by an Inductively Coupled Argon Plasma Optical Emission Spectrometer (ICP-OES), which uses an Echelle optical design and a Charge Injection Device (CID) solid-state detector (iCAP 6000 spectrometer by Thermo). Recoveries obtained with the use of certified reference materials (MESS-3) ranged from 90.0 to 104.1% (Paraskevopoulou et al., 2015).

Water Soluble Organic Carbon (WSOC) and Total Dissolved Nitrogen (TDN)

A total organic carbon (TOC)/total nitrogen (TN) analyser (Model TOC-$V_{CSH/CSN}$ Analyser, Shimadzu) was used to determine the WSOC and TDN in the dust. A portion of the dust was extracted with ultra-pure Milli-Q water using an ultrasonic bath (15 min × 3 times). The extracts were filtered with a disc filter [polyethersulfone membrane (PES) filters, 0.45 μm pore size diameter] to remove suspended particles and injected into the analyser, according to the protocol described in Miyazaki et al. (2011).

Water-Soluble Organic Nitrogen (WSON)

WSON was determined by subtracting Inorganic Nitrogen (NO_3^- and NH_4^+) from the Total Dissolved Nitrogen (TDN).

Chemical Analyses in Sea Water Samples

Total Organic Carbon (TOC) Analysis

TOC concentration was measured by the high-temperature catalytic oxidation method with a total organic carbon (TOC) analyser (Model TOC-$V_{CSH/CSN}$ Analyser, Shimadzu), according to protocol described in Sempéré et al. (2002). Prior to analysis, sea water samples (20 mL) were transferred in glass vials

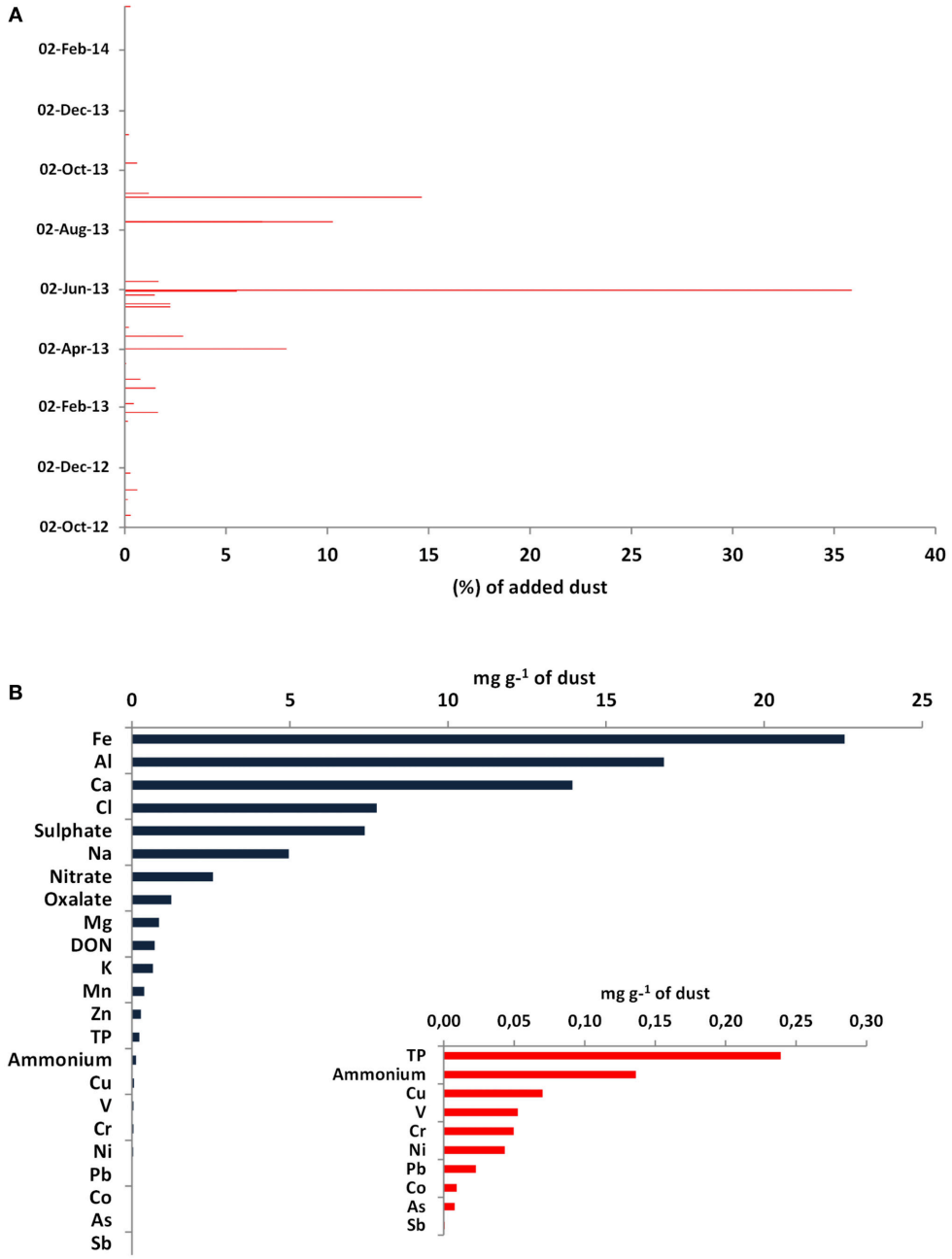

FIGURE 1 | (A) Temporal distribution of the collected dust deposition samples in Crete and Cyprus during a 1-year period (October 2012–November 2013). The dates correspond to the end of the dust collections, while the x axis represents the percentage contribution of each dust sample (in mass) to the total mass of the added dust, **(B)** Chemical characterization of the dust used in the mesocosm experiment. Only 8% of the dust mass was characterized.

(pre-combusted at 450°C for 6 h) and acidified with 20 μL H_3PO_4 (85%).

Particulate Metals (Fe, V, Cr, Ni) and Particulate Total Phosphorus (TP-Particulate)

Particulate metals (Fe, V, Cr, Ni), including TP-particulate, in sea water samples were measured by acid digestion of GFF filters (pre-combusted at 450°C for 6 h) with concentrated nitric acid (puriss. p.a., Fluka Prod. No. 84380) following the protocol described above for metal analysis.

Total Dissolved Nitrogen (TDN) and Dissolved Organic Nitrogen (DON)

A total nitrogen (TN) analyser (Model TOC-$V_{CSH/CSN}$ Analyser, Shimadzu) was used to determine the total dissolved nitrogen (TDN) in sea water samples, according to Miyazaki et al. (2011).

Prior to analysis, sea water samples (1,000 mL) were filtered with a GFF filter (pre-combusted at 450°C for 6 h) and the extracts were injected into the analyser. The concentration of DON was determined by subtracting inorganic nitrogen (NO_3^- and NH_4^+) from the total dissolved nitrogen (TDN).

Total Dissolved Phosphorus (TDP)

Total dissolved phosphorus (TDP) concentrations were measured by autoclave-assisted persulfate oxidation followed by the standard phosphomolybdenum blue method by using a10-cm quartz cell, according to the protocol described in Lin et al. (2012). Prior to analysis, 1,000 mL of each sea water sample were filtered with a GFF filter (pre-combusted at 450°C for 6 h).

Inorganic Nutrients, Particulate Organic C and N

Water samples were analyzed daily for phosphate according to the MAGIC method (Rimmelin and Moutin, 2005), for silicate, nitrite, and nitrate according to Strickland and Parsons (1972), and for ammonium according to Ivancic and Degobbis (1984). The detection limits were 0.8 nM for phosphate, 0.017 μM for nitrate, 0.019 μM for ammonium, and 0.025 μM for silicate.

Particulate organic carbon (POC) and nitrogen (PON) were determined using a Perkin Elmer 2,400 CHN Elemental Analyser according to the procedure described by Hedges and Stern (1984).

Chlorophyll *a*

Concentration of size-fractionated chlorophyll *a* (Chl *a*) was measured daily in all mesocosms according to Holm-Hansen et al. (1965). In the present study, only total Chl *a* concentrations are presented. For methodology and details on size-fractionation values, see Lagaria et al. (2017, this SI).

Primary and Bacterial Production

Primary production (PP) was measured daily in all mesocosms, using the ^{14}C incorporation method of Steemann-Nielsen (1952). In the present study, only total PP values are presented. For methodology and details on size-fractionation values, see Lagaria et al. (2017, this SI).

Bacterial production (BP) was estimated by the ^3H-leucine method (Kirchman et al., 1986) as modified by Smith and Azam (1992). For each mesocosm, SA, RA, and Cnt samples (1.5 mL) in duplicate were incubated with a mixture of L-[4,5 3H]-leucine (Perkin Elmer, 115 Ci $msol^{-1}$) and non-radioactive leucine to a final concentration of 20 nM. Samples were incubated for 2 h in the dark at *in-situ* temperature, after which they were fixed and treated following the micro-centrifugation protocol (Smith and Azam, 1992), as described in detail by Van Wambeke et al. (2008). In brief, incubations were terminated after 2 h by the addition of trichloroacetic acid (TCA). Samples were then centrifuged at 16,000 × g and the resulting cell pellet was washed twice with 5% TCA and with 80% ethanol. Incorporation of ^3H- leucine into the TCA-insoluble fraction was measured by liquid scintillation counting (Packard Tri-Carb 4000TR) after resuspension of the cell pellet in a scintillation cocktail (Ultima-Gold). Bacterial production was calculated according to Kirchman (1993), from ^3H-leucine incorporation rates. Duplicate incubations had an analytical error of <10%. Concentration kinetics optimization was also performed to ensure that the bacterial growth was not limited by the concentration of leucine.

Chlorophyll-normalized production was calculated for phytoplankton (by dividing primary production by Chl *a*) and Specific Growth Rate (SGR) for bacteria (by dividing bacterial production by bacterial biomass).

Plankton Abundances

Viruses, Heterotrophic Bacteria, Cyanobacteria, Autotrophic Pico-Eukaryotes

The abundance of viruses, heterotrophic bacteria, cyanobacteria *Synechococcus* spp. and autotrophic pico-eukaryotes was obtained by flow cytometric analyses on a daily basis. A FACSCalibur™ was used (Becton Dickinson), equipped with an air-cooled laser at 488 nm and standard filters. Milli-Q water was used as sheath fluid. Samples were run at high speed for 1 min for viral and heterotrophic bacteria counts and for 3 min for cyanobacterial counts and pico-eukaryotes. Multifluorescence beads (1 μm, Polysciences) were used as an internal standard of fluorescence at all runs. The exact flow rate of high speed performance was measured on a daily basis. Abundance was then calculated using the acquired cell counts and the respective flow rate. All flow cytometry data were acquired with the CellQuest Pro package (Becton Dickinson).

Samples (2 mL) for viral and heterotrophic bacteria counts were fixed and processed according to Brussaard (2004) and Marie et al. (1999), respectively. Briefly, fixation was achieved with 0.2 μm pre-filtered 25% glutaraldehyde at 0.5% final concentration. Samples were then kept at 4°C for ∼20 min, deep frozen in liquid nitrogen and finally stored at −80°C until enumeration. For viral counts, samples were thawed at room temperature and then diluted in Tris-EDTA buffer (TE, 10 mM Tris and 1 mM EDTA, pH = 8) in order to achieve a flow rate of between 100 and 700 events s^{-1}. Freshly-made TE was autoclaved and 0.2 μm filtered immediately prior to dilution. Staining was conducted with SYBR Green I nucleic acid dye (Molecular Probes) at a final dilution 5×10^{-5} of the stock solution and then incubated for 10 min at 80°C. Viruses were grouped into three groups according to their SYBR Green I fluorescence intensity (low, medium, and high DNA content). For heterotrophic bacteria counts, samples were thawed at room temperature and stained with SYBR Green I nucleic acid dye at a final dilution 4×10^{-4} of the stock solution. The stained samples were incubated for 10 min in the dark. Heterotrophic bacteria were grouped into two groups according to their SYBR Green I fluorescence intensity (low and high DNA content).

Cyanobacteria *Synechococcus* spp. and autotrophic pico-eukaryotes were counted fresh, without fixation and staining steps, using their characteristic autofluorescence chlorophyll/phycoerythrin signals.

Abundance data were converted into C biomass using 20 fg C $cell^{-1}$ for heterotrophic bacteria (Lee and Fuhrman, 1987) and 250 fg C $cell^{-1}$ for *Synechococcus* (Kana and Glibert, 1987). The biovolume of autotrophic pico-eukaryotes was calculated assuming they are spherical with diameter 1.7 μm. Biovolumes

were then converted into C biomass using 183 fg C μm^{-3} (Caron et al., 1995).

Auto- and Hetero-Trophic Flagellates

Samples (20 mL) for flagellate counting were collected daily until Day 3 and every other day afterwards, fixed with glutaraldehyde (final concentration, 1%), and kept in the dark at 4°C. Flagellate cells were concentrated to ca. 10 mL on a 25 mm diameter, 0.8 μm pore-sized black polycarbonate filter, stained with 4′6-diamidino-2-phenylindole (DAPI: 1 μg mL^{-1}) for 10 min, and finally collected on the filter (Porter and Feig, 1980). The filters were mounted on slides and stored frozen (−20°C). Autotrophic and heterotrophic flagellates (AF, HF) were examined on at least 50 fields at 1,000×, using UV and blue excitations under an Olympus BX60 epifluorescence microscope. All cells were sized and divided into five categories (2–3, 3–5, 5–7, 7–10, >10 μm) using an ocular micrometer in at least 50 fields.

Formulas of approximate geometric shapes were used to calculate the biovolume of heterotrophic flagellates (W^2 L π/6 where L and W are the measured length and width of the cell, respectively). Biovolumes were converted into C biomass using 183 fg C μm^{-3} (Caron et al., 1995).

Microplankton (Diatoms, Coccolithophores, Dinoflagellates, and Ciliates)

Samples for diatom, coccolithophore, and dinoflagellate enumeration were collected on Days 0, 2, 4, 6, and 9, fixed with alkaline Lugol's solution (2% final concentration), and stored at 4°C until counting. For the analysis, 100 mL samples were left to sediment for 24 h (Utermöhl, 1958) and then observed under an Olympus IX70 inverted microscope. Organisms larger than 10 μm were distinguished into diatoms, dinoflagellates, coccolithophores, and other flagellates, and identified down to genus or species level where possible.

Samples for ciliate enumeration were collected daily until Day 3, and every other day afterwards, fixed with acid Lugol's solution (2% final concentration), and stored at 4°C until counting. For the analysis, 100 mL samples were left for 24 h sedimentation and examined using an Olympus IX70 inverted microscope, equipped for phase contrast, at 150× magnification. Ciliates were distinguished into loricate species (hereafter referred to as tintinnids, order Tintinnida) and aloricate ones (hereafter referred to as aloricates, further distinguished into size-classes, orders Oligotrichida, and Choreotrichida) and identified down to genus or species level where possible. Ciliate cell sizes were measured by means of image analysis and converted into biovolumes by approximation to the nearest geometric shape from measurements of cell length and width. Biovolumes were converted into C biomass using 190 fg C μm^{-3} (Putt and Stoecker, 1989).

Mesozooplankton

The total abundance (ind m^{-3}) and biomass (mg C m^{-3}) of metazoans were determined at the start and termination of the mesocosm experiment. The initial stock of metazoans was measured by filtering, through a 45 μm net, water pumped from 10 m depth (collected as described above, to fill the barrels for the mesocosms). At the end of the experiment, the content of each of the mesocosms was also filtered through the 45 μm net. All samples were preserved with a 4% buffered-formaldehyde seawater solution (Postel et al., 2000). A known fraction of each sample was scanned on a flatbed scanner at 4,800 dpi then image analysis was completed using the software Image-pro plus, processing similarly to Frangoulis et al. (2016). In each fraction, 1,000–2,000 organisms were identified and measured. Organisms <100 μm were not identifiable when looking at the images, therefore in the following text, "mesozooplankton" corresponds to the captured metazoans >100 μm. The sizes of metazoans were converted to carbon based on literature size-carbon relationships (Alcaraz and Calbet, 2003).

Statistical Analysis

The quality of the mesocosm replication during the experiment was evaluated based on the coefficient of variation (CV = Standard deviation/average) of several variables (Chl *a*, primary, and bacterial production, etc.).

A repeated measures ANOVA (RM-ANOVA) was used to compare the values of the variables between the Cnt, SA, and RA mesocosms. The grouping factor was the Cnt vs. SA, RA mesocosms, and "experimental day" (Day 0–9) was treated as a repeated measure, i.e., treatment was considered the between-subjects factor and "experimental day" the within-subjects factor. Subsequently, the *post-hoc* Tukey test was employed for comparison of each variable between different dust additions.

On individual experimental days, one-way analysis of variance (1Way-ANOVA) was used to compare variables between the Cnt, SA and RA. Following the 1Way-ANOVA, significance of differences was checked by means of Tukey's HSD test.

RESULTS

Characterization of Dust Particles Used in the Mesocosm Experiment

Only a small fraction (about 8%) of the dust sample was characterized chemically, with a prevalence of Fe, Al, and Ca with percentage contributions of 2, 2, and 1%, respectively, and minor contributions by Co, As, and Sb (**Figure 1B**). As shown in **Table 2**, dust presented a high N:P ratio of ca. 29.

SA (Single Addition) represented a strong dust deposition event of 3 g m^{-2} day^{-1} while in terms of nutrient content, TDN and TP, it corresponds to daily deposition fluxes of 294.9 μmol N m^{-2} d^{-1} and 22.7 μmol P m^{-2} day^{-1}, respectively, which are typical for an intense single-day dust event. The deposition fluxes of inorganic nutrients (DIN and PO_4^{3-}) were estimated at 143.5 μmol N m^{-2} $day^{-1}$and 5.0 μmol P m^{-2} day^{-1}, respectively, with a DIN/DIP atomic ratio 28.7, which is higher than the Redfield N:P analogy of 16.

RA (Repetitive Addition) was equivalent to three sequential dust events with deposition fluxes of 0.7, 1.5, and 0.8 g m^{-2} day^{-1}. The additions corresponded to deposition fluxes for TDN of 74.7, 147.6, and 76.0 μmol N m^{-2}, respectively, and for TP of 5.7, 11.3, and 5.8 μmol P m^{-2}, respectively. The additions corresponded to per-event deposition fluxes of DIN equal to

TABLE 2 | Concentrations and speciation of Phosphorus and Nitrogen added with dust.

Nutrients added (nM)	NH_4^+	NO_3^-	PO_4^{3-}	TDN	DON	TP	DIN/DIP
Nutrient speciation of dust (μmol g^{-1})	7.6	41.4	1.7	100.6	51.7	7.7	28.3
SA -Day 0*	10.1	55.2	2.3	134.1	68.9	10.3	28.3
RA -Day 0	2.5	13.8	0.6	33.6	17.3	2.6	28.3
RA -Day 1	5.0	27.3	1.1	66.4	34.1	5.1	28.3
RA -Day 2	2.6	14.1	0.6	34.2	17.6	2.6	28.3

**Nutrients added were calculated according to the amount of the dust inputs divided by mesocosm volume (3,000 L). SA = single addition, mesocosms where dust was added once, on the first day of the experiment, RA = repetitive addition, mesocosms where the same quantity of dust was added, divided into three doses, on the first 3 days of the experiment, Days 0, 1 and 2.*

36.3, 71.8, and 37.0 μmol N m^{-2} and of PO_4^{3-}, equal to 1.3, 2.5, 1.3 μmol P m^{-2}, respectively.

Results from the Mesocosm Experiment

Throughout the experiment, replication between the mesocosms of each treatment (within treatment replication) was good. The coefficient of variation (CV = standard deviation/average) between the replicate mesocosms ranged, on average, between 3 and 22% for Chl *a*, 3 and 22% for primary production, 1 and 31% for bacterial production, 1 and 9% for heterotrophic bacteria counts, and 2 and 15% for *Synechococcus* counts.

All results are presented as average values followed by the standard deviation (SD) of three replicates.

Inorganic Nutrients

The initial concentration of inorganic nutrients in the water used to fill the mesocosms was 62 ± 22 nM DIN (dissolved inorganic nitrogen) and 6 ± 0.9 nM DIP (dissolved inorganic phosphorus). The content of the natural dust added was 65.4 nM DIN and 2.3 nM DIP; in other words, by adding dust into the treated mesocosms (SA and RA), the initial DIN and DIP concentration increased 2- and 1.3-fold, respectively, while the N:P ratio changed from ca. 10:1 to ca. 16:1.

During the first 2 days of the experiment, DIN concentration ranged from 44 to 82 nM in the Cnt and 47–87 nM in the RA treatment, while it slightly increased from 21 to 116 nM in the SA treatment (**Figure 2A**). After Day 2, DIN concentration increased 2.2-fold in both SA and RA until they reached the highest values (135 ± 19 nM) on Day 7 and 4, respectively, after which concentration decreased in all mesocosms.

Phosphates presented a different pattern (**Figure 2B**). From Day 0 to Day 1, PO_4 concentration increased by 1.2-fold in SA and by 1.8-fold in RA (highest values reached in RA, 9.5 ± 1.61 nM PO4), then it sharply decreased until Day 2, after which it remained stable at low levels. In the Cnt, PO_4 concentration decreased 2.7-fold on the first 2 days, after which it remained steadily low (<4 nM) throughout the experiment.

Starting from a N:P ratio of ca. 10:1 in the water used to fill the mesocosms, (**Figure 2C**) N:P increased to reach values close to the Redfield ratio on Day 1, then it attained maximum values,

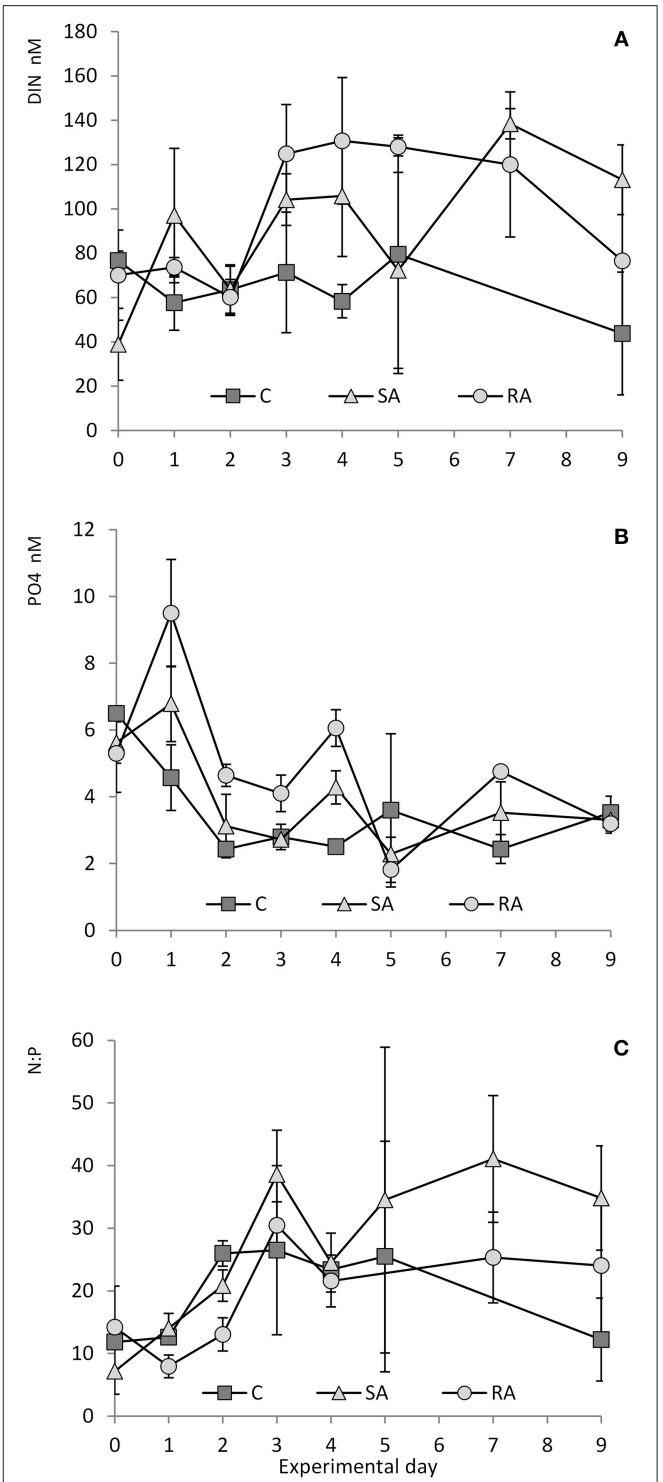

FIGURE 2 | (A) Concentration of DIN (dissolved inorganic nitrogen), **(B)** concentration of PO_4, and **(C)** N:P ratio throughout the mesocosm experiment. Cnt = Control mesocosms (no addition), SA = single addition, mesocosms where dust was added once, on the first day of the experiment, RA = repetitive addition, mesocosms where the same quantity of dust was added, divided into three doses, on the first 3 days of the experiment, Days 0, 1, and 2. Data are mean ± SD of 3 replicates. **(A,B)** are from Lagaria et al. (2017), this SI, mod.

much higher than Redfield, on Day 3 (39:1 in SA, 30:1 in RA, and 27:1 in Cnt). Then it decreased but remained at levels higher than Redfield until the end of the experiment (34:1 in SA, 24:1 in RA, and 20:1 in Cnt).

Silicate concentration did not vary throughout the experiment [0.81 ± 0.03 μM $Si(OH)_4$, data not shown].

Particulate Organic Nitrogen, Phosphorus, and Carbon

The concentration of particulate organic nitrogen (PON) increased by 1.5 times from Day 0 (0.29 ± 0.04 μM) to Day 9 (0.45 ± 0.3 μM) in both treatments and the Cnt. No significant differences were found between SA, RA, and Cnt (RM-ANOVA, $P > 0.05$; **Figure 3A**).

Starting from 0.014 ± 0.002 μM on Day 0, particulate organic phosphorus (POP) concentration decreased to 0.009 ± 0.002 μM on Day 9 in the Cnt, SA, and RA (**Figure 3B**). On Day 4, it reached maximum values in RA (0.018 ± 0.004 μM) and SA (0.016 ± 0.005 μM). No significant differences were found between the two treatments and the Cnt nor between the treatments (RM-ANOVA, $P > 0.05$) due to high variability of values.

From 2.2 ± 0.27 μM on Day 0, particulate organic carbon (POC) reached maximum values on Day 2 in SA (5.8 ± 3.89 μM), Day 3 in RA (4.0 ± 0.24 μM), and Day 4 in Cnt (4.2 ± 0.69 μM; **Figure 3C**). No significant differences were found between the two treatments and the Cnt, nor between the treatments (RM-ANOVA, $P > 0.05$).

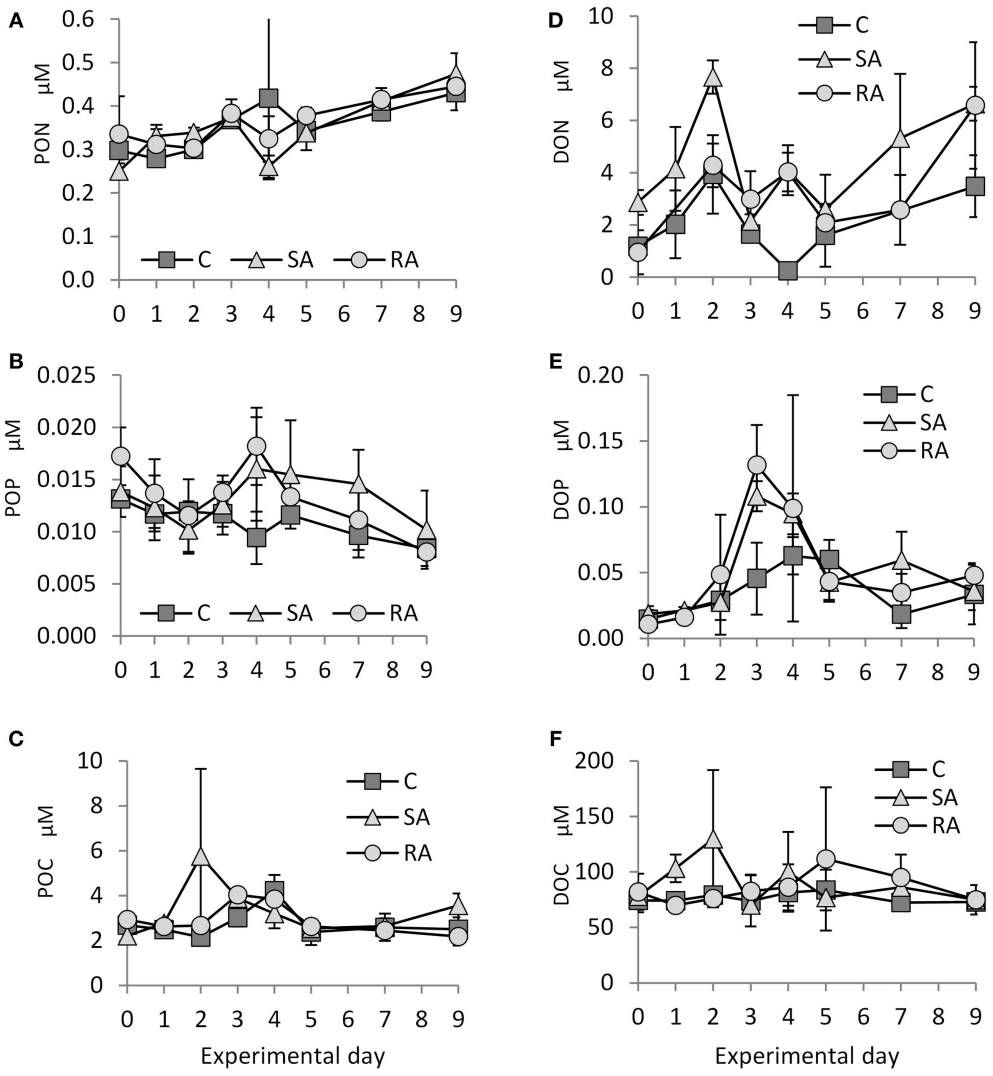

FIGURE 3 | Concentration of (A) PON (particulate organic nitrogen), **(B)** POP (particulate organic phosphorus), **(C)** POC (particulate organic carbon), **(D)** DON (dissolved organic nitrogen), **(E)** DOP (dissolved organic phosphorus), and **(F)** DOC (dissolved organic carbon) throughout the mesocosm experiment. Cnt = Control mesocosms (no addition), SA = single addition, mesocosms where dust was added once, on the first day of the experiment, RA = repetitive addition, mesocosms where the same quantity of dust was added, divided into three doses, on the first 3 days of the experiment, Days 0, 1, and 2. Data are mean ± SD of three replicates.

Dissolved Organic Nitrogen, Phosphorus, and Carbon

Dissolved organic nitrogen (DON) concentration varied a lot during the experiment (**Figure 3D**). Starting from a value of 1.7 ± 1.25 μM, DON concentration initially peaked on Day 2 in SA (7.7 ± 0.64 μM) and RA (4.9 ± 0.86 μM), then it fluctuated until the end of the experiment. In the Cnt, there was also a peak on Day 2 (3.9 ± 1.51 μM), followed by a decrease until Day 4 and a second, smaller increase until Day 9. Due to the high variability of values, significantly higher DON concentration was found only on Day 2 between SA and the rest of the mesocosms (1Way-ANOVA, $P < 0.01$).

Dissolved organic phosphorus (DOP) concentration showed an important increase until Day 3 in both SA and RA treatments (**Figure 3E**, 0.11 ± 0.01 μM in SA and 0.13 ± 0.03 μM in RA compared to 0.015 ± 0.006 μM on Day 0), then it decreased until Day 5 and remained at this level (0.04 ± 0.01 μM) until the end of the experiment. DOP concentration was significantly higher in SA and RA compared to Cnt on Day 3 (1Way-ANOVA, $P < 0.01$); however, SA and RA did not differ between them (1Way-ANOVA, $P > 0.05$). The Cnt mesocosms also presented an increase in DOP concentration, although much smaller; DOP peaked on Day 4 (0.06 ± 0.01 μM) and then it dropped to the same levels as the amended mesocosms.

Only in the SA treatment did dissolved organic carbon (DOC) concentration present an important increase on Day 2 (129.9 ± 61.9 μM) compared to Day 0 (78.04 ± 6.04 μM), then it returned to initial levels; in contrast, it remained stable in the Cnt and RA throughout the experiment (**Figure 3F**); RA showed an increase in DOC concentration only on Day 5 compared to the rest of mesocosms. However, variability was high in many cases and treatments did not differ significantly between them (1Way-ANOVA, $P > 0.05$).

Primary Production and Bacterial Production

Soon after the addition of dust, there was a 2-fold increase in primary production (PP) in both treatments compared to the Cnt, in which PP did not change throughout the experiment (**Figure 4A**). PP reached the same maximum levels at both treatments. For details on PP, see Lagaria et al. (2017, this SI).

Throughout the experiment, bacterial production was significantly higher in both treatments compared to the Cnt (RM-ANOVA, $P < 0.01$), which remained unchanged (**Figure 4B**). In the SA mesocosms, BP peaked on Day 2 (31.03 ± 6.72 ng C L^{-1} h^{-1}), reaching a 2-fold increase, then it declined continuously to reach minimum values by Day 6 (but higher than Cnt). In RA, similar maximum BP values were attained but with a time lag of 1 day. They were then followed by a decrease until Day 7.

Chlorophyll a

From a low value on Day 0 (0.04 ± 0.004 μg L^{-1}), total Chl *a* concentration significantly increased after the addition of dust in SA and RA compared to Cnt (RM-ANOVA, $P < 0.01$), by 1.7 times in the SA on Day 2 and by 1.6 times in the RA mesocosms on Day 4 (**Figure 5**). Chl *a* increased first in SA while RA followed with a time lag of 1 day; however, the maximum values attained were similar. For details on Chl *a*, see Lagaria et al. (2017, this SI).

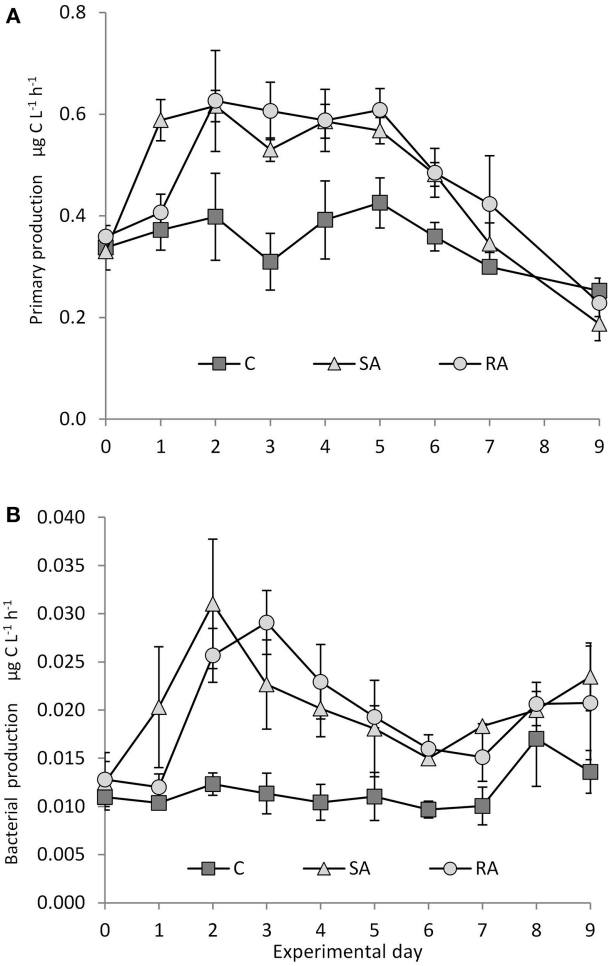

FIGURE 4 | (A) Primary and **(B)** bacterial production during the mesocosm experiment. Cnt = Control mesocosms (no addition), SA = single addition, mesocosms where dust was added once, on the first day of the experiment, RA = repetitive addition, mesocosms where the same quantity of dust was added, divided into three doses, on the first 3 days of the experiment, Days 0, 1, and 2. Data are mean ± SD of 3 replicates. **(A)** is from Lagaria et al. (2017), this SI, mod.

Autotrophs

Synechococcus spp. (Syn) density doubled on Day 3 in SA (2.18 × 10^4 ± 1.02 × 10^3 cells mL^{-1}) and on day 4 in RA (2.24 × 10^4 ± 2.5 × 10^3 cells mL^{-1}) and was significantly higher in both dust treatments than in the Cnt until the end of the experiment (RM-ANOVA, $P < 0.01$, **Figure 6A**). No significant difference was found between the two treatments (RM-ANOVA, $P > 0.05$). *Synechococcus* abundance did not change in the Cnt mesocosms throughout the experiment.

Pico-eukaryote (Peuk) density presented a 2-fold increase in SA and RA until Days 3 and 4, respectively (time lag of 1 day between SA and RA), and then it declined until the end of the experiment (**Figure 6B**). No differences were found between the treatments and the Cnt (RM-ANOVA, $P > 0.05$).

Autotrophic flagellate (AF) abundance, starting from initial values of 599 ± 105 cells mL^{-1}, decreased in RA and the Cnt

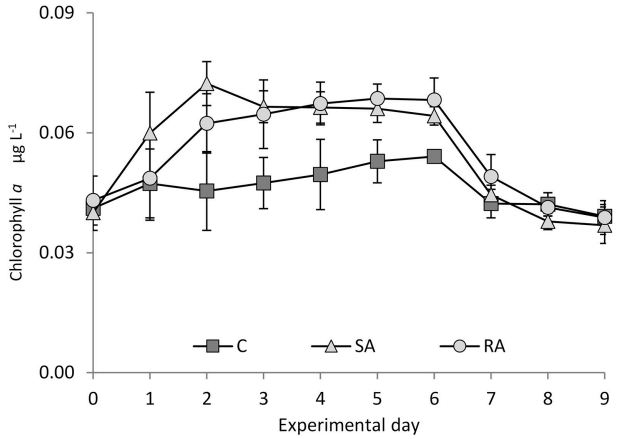

FIGURE 5 | Chlorophyll *a* concentration during the mesocosm experiment. Cnt = Control mesocosms (no addition), SA = single addition, mesocosms where dust was added once, on the first day of the experiment, RA = repetitive addition, mesocosms where the same quantity of dust was added, divided into three doses, on the first 3 days of the experiment, Days 0, 1, and 2. Data are mean ± SD of three replicates. This Figure is from Lagaria et al. (2017), this SI, mod.

until the end of the experiment, whereas in SA it remained stable during the first 4 days, after which it declined (**Figure 6C**). No differences were found between the treatments and the Cnt (RM-ANOVA, $P > 0.05$). Autotrophic flagellates were dominated by the 3–5 µm fraction (53 ± 14%) while the 2–3 µm fraction contributed 17 ± 12% to total abundance. For more details on autotrophs, see Lagaria et al. (2017, this SI).

Diatoms and coccolithophores were found only sporadically throughout the experiment; their abundances averaged 40 ± 38 cells L^{-1} for diatoms and 31 ± 17 cells L^{-1} for coccolithophores (data not shown).

Heterotrophs

Virus density declined 1.2-fold from Day 0 to Day 3 in Cnt, SA, and RA (**Figure 7A).** After Day 3, it reached maximal values on Day 4 in RA ($5.0 \times 10^6 \pm 1.8 \times 10^5$ viruses mL^{-1}) and on Day 7 in SA ($5.0 \times 10^6 \pm 4.7 \times 10^5$ viruses mL^{-1}) while it remained unchanged in the Cnt. There were significant differences only between SA and the Cnt (RM-ANOVA, $P < 0.05$).

Heterotrophic bacteria density was significantly higher in both treatments compared to the Cnt throughout the experiment (RM-ANOVA, $P < 0.01$). Starting from an initial density of $2.3 \times 10^5 \pm 0.03 \times 10^5$ cells mL^{-1}, heterotrophic bacteria reached a peak (1.4 times higher than in the Cnt) on Days 2 and 3 in the SA and RA treatments, respectively, then they declined until Day 5, after which they remained constant at initial levels until Day 7 and then increased again (**Figure 7B**). No significant difference was found between the two treatments (RM-ANOVA, $P > 0.05$). Density in the Cnt decreased all along the experiment and on Day 9 it was 1.6-fold lower than on Day 0.

In Cnt, starting from 20 ± 1, VBR (Viruses to Bacteria Ratio, a measure of the viruses' relative significance compared to bacteria) showed similar values until Day 3 (**Figure 7C**) and

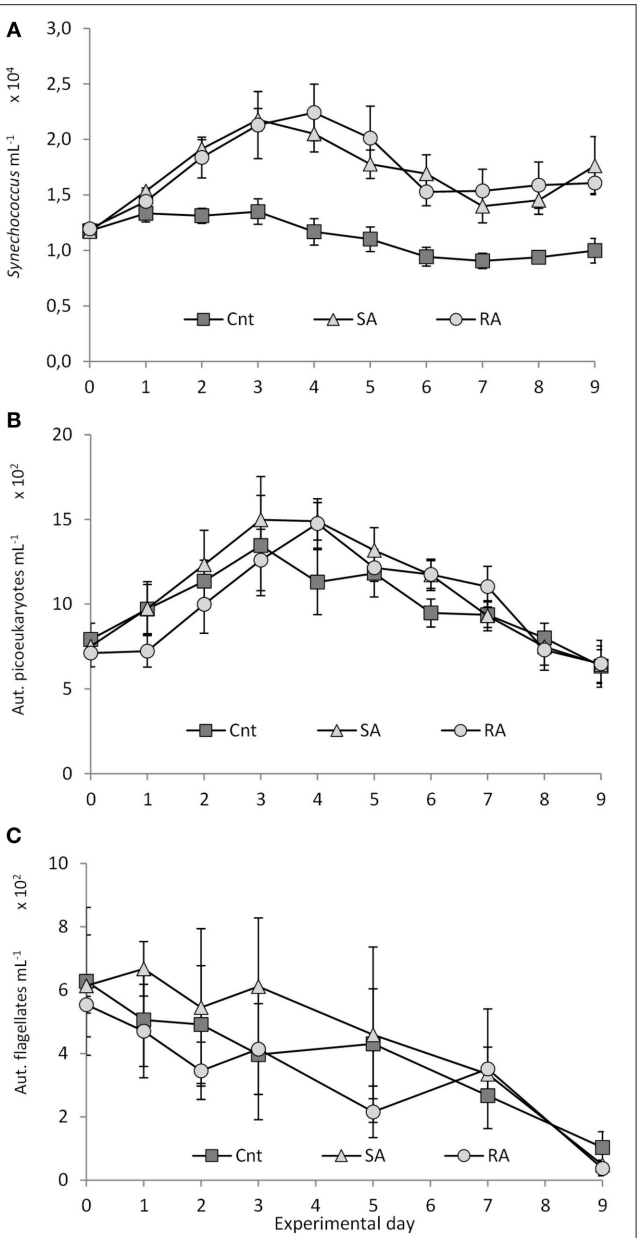

FIGURE 6 | (A) *Synechococcus*, **(B)** pico-eukaryote, and **(C)** autotrophic flagellate abundances during the mesocosm experiment. Cnt = Control mesocosms (no addition), SA = single addition, mesocosms where dust was added once, on the first day of the experiment, RA = repetitive addition, mesocosms where the same quantity of dust was added, divided into three doses, on the first 3 days of the experiment, Days 0, 1, and 2. Data are mean ± SD of three replicates. This Figure is from Lagaria et al. (2017), this SI, mod.

then a continuous increase until the end of the experiment (28 ± 2 on Day 9). In contrast, in SA and RA, VBR declined to 13 ± 2 until Day 3 and then returned to initial values, oscillating around 19 ± 3 until Day 9. VBR did not differ between SA and RA treatments (RM-ANOVA, $P > 0.05$); however, values in the Cnt were significantly higher than both treatments (RM-ANOVA, $P < 0.01$).

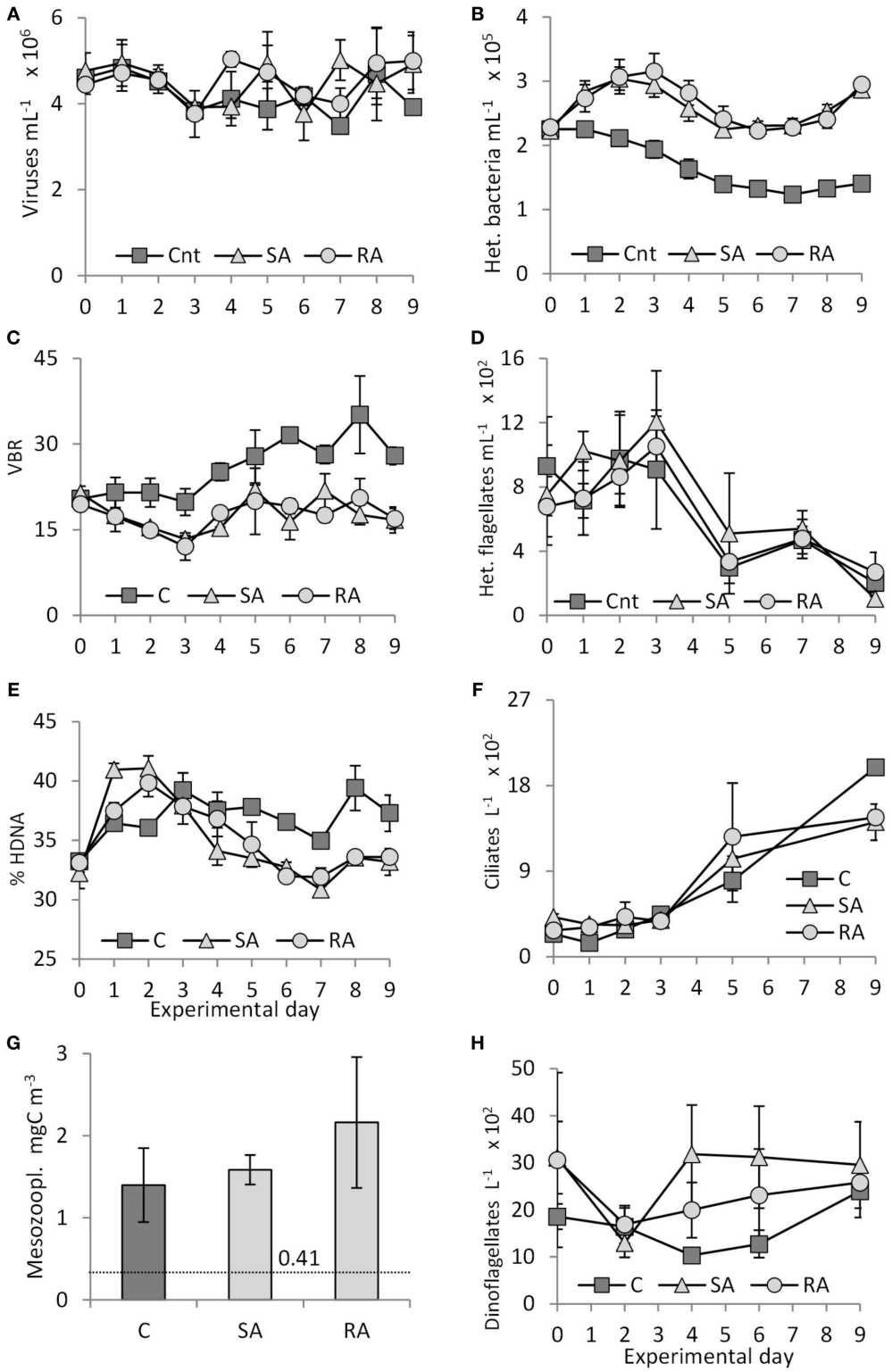

FIGURE 7 | (A) Virus abundance, **(B)** heterotrophic bacterial abundance, **(C)** Virus to bacteria ratio (VBR), **(D)** heterotrophic flagellate abundance, **(E)** percentage of High DNA bacteria (HDNA), **(F)** ciliate abundance, **(G)** mesozooplankton biomass on the last day of the experiment (dashed line indicates mesozooplankton biomass (0.41 mgC m^{-3}) in the field, at the start of the experiment), and **(H)** dinoflagellate abundance during the mesocosm experiment. Cnt = Control mesocosms (no addition), SA = single addition, mesocosms where dust was added once, on the first day of the experiment, RA = repetitive addition, mesocosms where the same quantity of dust was added, divided into three doses, on the first 3 days of the experiment, Days 0, 1, and 2. Data are mean ± SD of three replicates.

Until Day 2 for SA and RA and Day 3 for Cnt, there was an increase in the % contribution of High DNA content (HDNA) bacteria, but the increase was steeper in both treatments compared to Cnt (41% in SA, 40% in RA, 36% in Cnt, starting from 33%, **Figure 7E**). After Day 3, the % of HDNA bacteria stabilized in Cnt whereas, in SA and RA, it sharply declined to values lower than Cnt, at least until Day 7, after which it increased again.

From 785 ± 130 cells mL^{-1} on Day 0, heterotrophic flagellate (HF) density increased 1.6-fold in both treatments until Day 3, after which it declined to values lower than the initial ones until the end of the experiment (**Figure 7D**). No significant differences were found between the treatments (RM-ANOVA, $P > 0.05$); however, the increase in RA followed the one in SA. In the Cnt, HF density remained unchanged until Day 3, after which it declined. In both treatments and the Cnt, heterotrophic flagellates were dominated by the pico-fraction (44 ± 13%), and the 2–3 μm fraction contributed 19 ± 9% to total abundance.

Starting from a low density at the beginning of the experiment (310 ± 86 cells L^{-1}), ciliate abundance showed an increasing pattern in both treatments and the Cnt (**Figure 7F**); especially after Day 3, the increase was sharper. Finally, after 9 days of the experiment, higher densities were reached in the Cnt mesocosms (1,990 ± 71 cells L^{-1}) than in the SA (1,415 ± 191 cells L^{-1}) and the RA (1,465 ± 78 cells L^{-1}) mesocosms (1Way-ANOVA, $P < 0.01$). Only on Days 1 and 5 was ciliate abundance higher in both treatments compared to the Cnt.

Dinoflagellate abundance varied a lot (around 2,200 ± 550 cells L^{-1}) in the treatments and the Cnt (**Figure 7H**). Both treatments started from a higher density compared to the Cnt. Interestingly, in both treatments, density showed a remarkable decrease on Day 2, after which it increased to reach maximum values on Day 4 and Day 9 for the SA and RA treatments, respectively.

Mesozooplankton biomass had increased in all mesocosms by the end of the experiment compared to the field-initial values (**Figure 7G**), by 3.4, 3.9, and 5.3 times in the Cnt, SA, and RA, respectively. When comparing between treatments, RA showed significantly higher biomass compared to the Cnt (1Way-ANOVA, $P < 0.05$) by 1.5 times. The mean size of the animals, 20% of which were nauplii and the remainder small-sized juvenile copepods, was around 400 μm. There were no carnivorous species so the mortality can be considered as non-predatory.

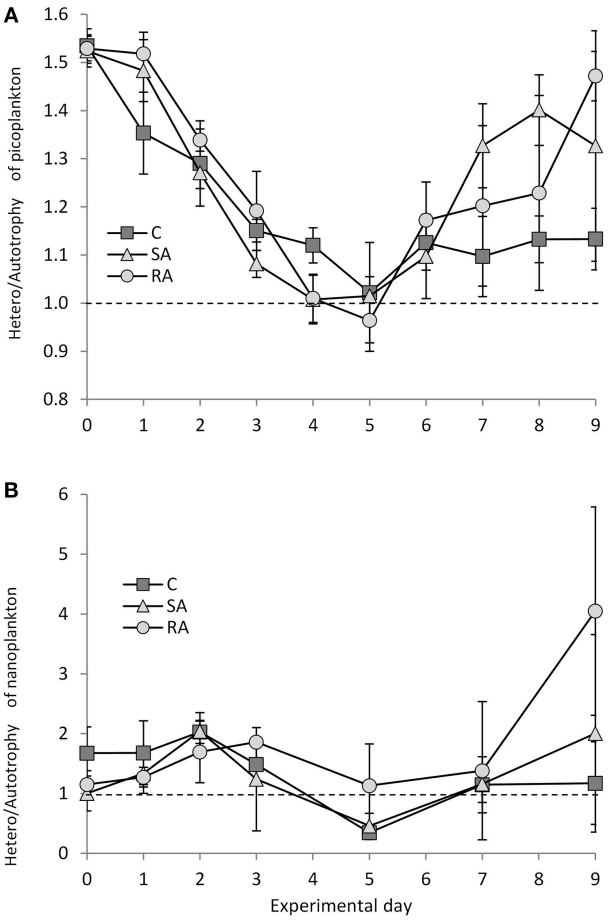

FIGURE 8 | Ratio of heterotrophic to autotrophic biomass for (A) pico-plankton and **(B)** nano-plankton during the mesocosm experiment. Cnt = Control mesocosms (no addition), SA = single addition, mesocosms where dust was added once, on the first day of the experiment, RA = repetitive addition, mesocosms where the same quantity of dust was added, divided in three doses, on the first 3 days of the experiment, Days 0, 1, and 2. Data are mean ± SD of three replicates. Dashed line indicates balance between autotrophic and heterotrophic biomass.

Heterotrophy vs. Autotrophy (H/A)

The picoplankton fraction of the food web (heterotrophic bacteria, cyanobacteria *Synechococcus,* and pico-eukaryotes) was heterotrophic at the beginning of the experiment (**Figure 8A**). The heterotrophic-to-autotrophic biomass ratio was 1.53 ± 0.028 on Day 0 and progressively decreased to reach equilibrium between auto- and heterotrophs (1.02 ± 0.07) on Days 4 and 5 in SA and RA, respectively. Then it increased again toward heterotrophy until the end of the experiment. Although, no differences were found between the Cnt and the treatments, or between the treatments (RM-ANOVA, $P > 0.05$), SA and RA mesocosms were characterized by a relatively faster relaxation of heterotrophy to approach balanced conditions compared to the Cnt, and then a sharper increase of the ratio and return toward heterotrophy.

The nanoplankton fraction behaved differently compared to picoplankton (**Figure 8B**); starting from equilibrium between auto- and heterotrophs on Day 0, increasing heterotrophy was observed until Days 2 (2.04 ± 0.31) and 3 (1.86 ± 0.002) in SA and RA, respectively, after which the ratio H/A decreased until autotrophy was reached in SA and the Cnt on Day 5. Then, equilibrium was reached in Cnt while SA returned to heterotrophy by Day 9. In RA, the ratio turned around equilibrium after Day 3 and reached a high degree of heterotrophy on Day 9; however, the variability was high.

Chlorophyll-Normalized Production and Bacteria Specific Growth Rate

Chlorophyll-normalized production showed a decreasing trend throughout the experiment (**Figure 9A**) whereas an increasing trend was observed for the specific bacterial growth rate (**Figure 9B**). No significant difference was found between all treatments for phytoplankton (RM-ANOVA, $P > 0.05$), whereas some variation (not significant though) was found for bacteria during the first 2 days of the experiment; bacteria seemed to grow faster in SA compared to RA and Cnt.

Growth Rate (μ) and Grazing Mortality (m)

The response of net growth rate of pico- and nano-autotrophs to dust addition (SA), calculated as μ, was variable on Day 2 (**Figure 10A**): only picoplankton cells (Syn and Peuk) showed a positive growth (0.61 and 0.18 day^{-1}, respectively) compared to the Cnt. Grazing rates, calculated as m, increased by 2-fold for AF and Syn after dust addition (0.59 and 0.3 day^{-1}, respectively, **Figure 10B**) and decreased 2-fold for Peuk (0.13 day^{-1}). On Day 4, only Peuk continued to show positive growth, similarly in all treatments and higher than on Day 2 (1.2 day^{-1}), whereas their grazing rates were 2-fold lower in the dust treatment compared to the Cnt (0.23 day^{-1}). On the contrary, the AF grazing rate was more or less similar to Day 2 in all treatments although slightly increased by 1.3-fold in the dust-treated mesocosms (0.48 day^{-1}).

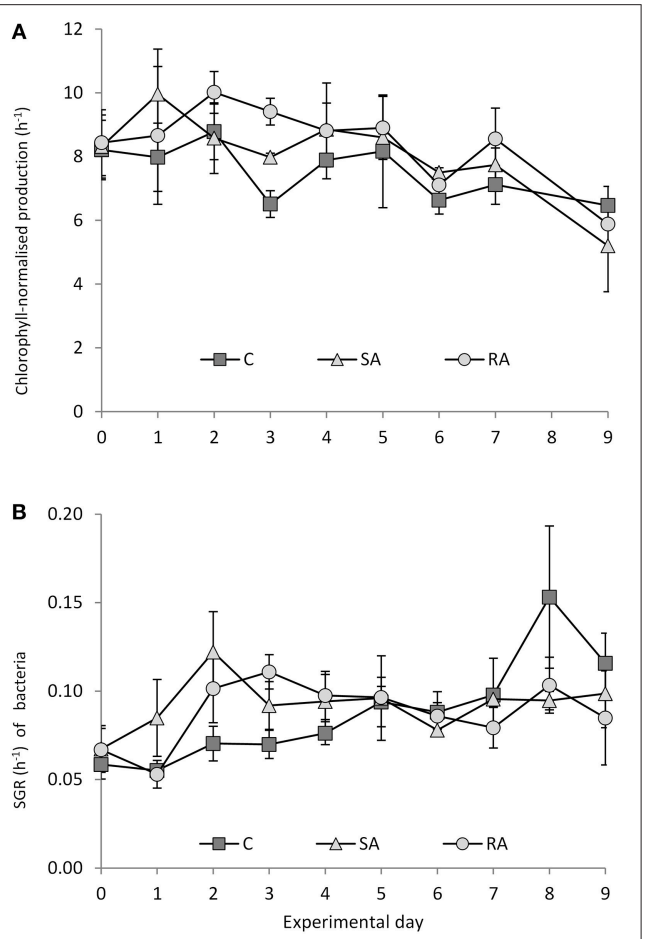

FIGURE 9 | (A) Chlorophyll-normalized production and **(B)** specific growth rate of bacteria during the mesocosm experiment. Cnt = Control mesocosms (no addition), SA = single addition, mesocosms where dust was added once, on the first day of the experiment, RA = repetitive addition, mesocosms where the same quantity of dust was added, divided into three doses, on the first 3 days of the experiment, Days 0, 1 and 2. Data are mean ± SD of 3 replicates. **(A)** is from Lagaria et al. (2017), this SI, mod.

DISCUSSION

Impact of Dust Addition on Biological Productivity and Biomass

The impact of Saharan dust deposition on the pelagic food web was studied in the Eastern Mediterranean. The effect of the episodicity of the phenomenon was studied in a mesocosm experiment by simulating two patterns of dust deposition events, both encountered in nature: (1) a single, strong event, or "dust storm," during which a large quantity of dust is added once into the surface layers of the sea vs. (2) repetitive events during which smaller quantities of dust are added to the sea over a longer time period. The dust addition was representative of a realistic dust deposition event in the area according to Gerasopoulos et al. (2006) and Ternon et al. (2010).

Just 1–2 days after the addition of dust to the amended mesocosms, both the autotrophic and heterotrophic components of the microbial food web presented a positive response compared to the Cnt mesocosms. Independently of the way dust was added, i.e., either in a single strong pulse (SA) or in three repetitive smaller pulses (RA), primary and bacterial productions significantly increased and so did the Chl *a* concentration, the densities of heterotrophic bacteria, and autotrophic cyanobacteria, the mesozooplankton biomass at the end of the experiment and the concentration of dissolved organic N and P on specific days. Phytoplankton production responded first, followed by bacterial production. The quantitative response to the dust addition did not differ between the two treatments; in other words, it was independent of the way dust was added.

Although, the quantity of nutrients added through the dust was very low (66 nM N and 2 nM P), it resulted in a considerable % increase of the initial nutrient concentration (2-fold increase for N and 1.3-fold for P) due to the oligotrophic conditions prevailing in the area. As a result, the food web replied with an increase of 2-fold for PP and BP, 1.6-fold for Chl *a* concentration, 1.4-fold for heterotrophic bacteria and 1.9-fold for cyanobacterial abundance.

This response is an indication that phytoplankton and heterotrophic bacteria were N or N and P co-limited prior to dust addition. With an initial N:P ratio of ca. 10, the system seemed to be N-limited. At the same time, the N:P ratio of dust added was ca. 29; in other words, dust transported a disproportionately high load of N relative to P in the amended mesocosms. Thus, during the first 2 days of the experiment and due to the N-deficit, the DIN added with the dust was directly taken up, so there was not a considerable increase in the DIN pool; in contrast, the added

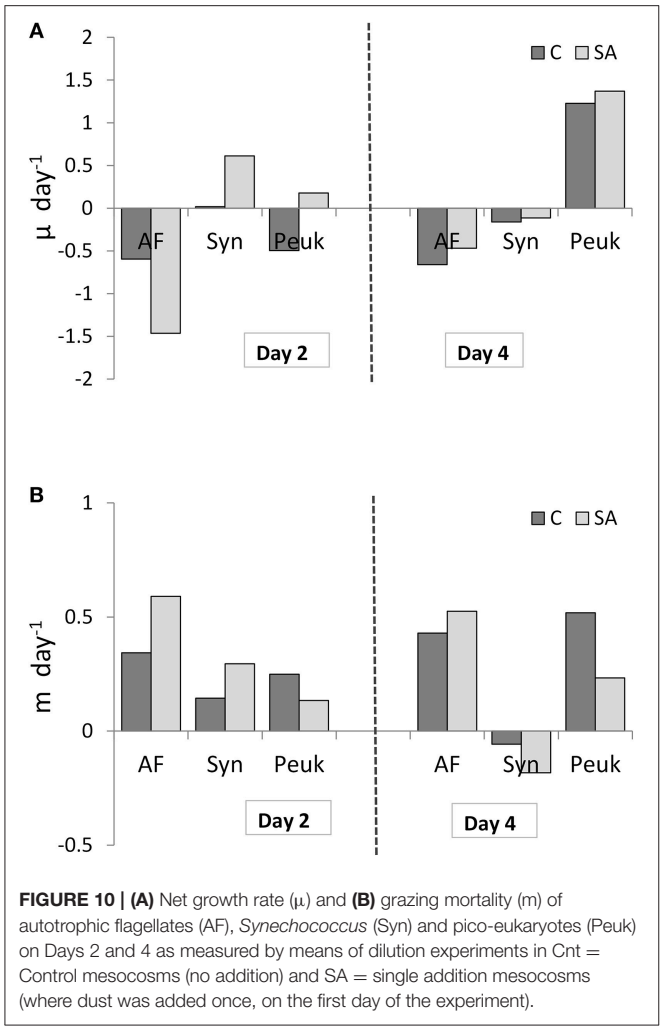

FIGURE 10 | (A) Net growth rate (μ) and **(B)** grazing mortality (m) of autotrophic flagellates (AF), *Synechococcus* (Syn) and pico-eukaryotes (Peuk) on Days 2 and 4 as measured by means of dilution experiments in Cnt = Control mesocosms (no addition) and SA = single addition mesocosms (where dust was added once, on the first day of the experiment).

phosphate was not instantly taken up. It presented elevated values 2 day after the additions then was totally taken up within 3 days in all mesocosms. Excess N added to the system was released again after Day 3 in the form of recycled DIN, presenting significant increases in both SA and RA mesocosms, presumably resulting in P-limited conditions, as also seen by the N:P ratio during the experiment.

The increase in heterotrophic bacterial production and abundance may be explained by the addition of P through the added dust. The response of bacteria to P-addition in the Eastern Mediterranean has been seen during a Lagrangian experiment (Krom et al., 2005b; Pitta et al., 2005; Thingstad et al., 2005) and verified during a mesocosm experiment (Pitta et al., 2016). On the other hand, the increase in the autotrophic production and biomass may be attributed to the simultaneous addition of N and P through the added dust since phytoplankton has been found to be N and P-co-limited in the area (Zohary et al., 2005; Pitta et al., 2016).

The clear and significant response of both auto- and heterotrophs to dust addition, observed during the present mesocosm experiment, was also evident during the first dust-addition mesocosm experiment conducted in Crete in May, 2012 (Tsagaraki et al., in review). In that experiment, the same quantity of dust was added, and resulted in similar increases in phytoplankton and heterotrophic bacteria to our experiment. The results of these two experiments may be considered a solid indication of the influence of Saharan dust on the microbial food web of the oligotrophic Eastern Mediterranean.

However, these results partly differ from the findings of the DUNE mesocosm experiments conducted in the Western Mediterranean (Laghdass et al., 2011; Giovagnetti et al., 2013; Guieu et al., 2014; Pulido-Villena et al., 2014; Ridame et al., 2014) and from some of the results of the microcosm experiments performed in the Mediterranean (Bonnet et al., 2005; Herut et al., 2005; Pulido-Villena et al., 2008; Lekunberri et al., 2010; Romero et al., 2011), the Atlantic (Marañón et al., 2010) and the South China Sea (Guo et al., 2012, 2013).

During the DUNE experiments, bacterial abundance was not affected by dust addition (Laghdass et al., 2011; Pulido-Villena et al., 2014). As far as phytoplankton is concerned, pico- vs. nano- and micro-size fractions behaved differently after two consecutive wet dust additions (Giovagnetti et al., 2013). Interestingly, Ridame et al. (2014) reported a significant stimulation of PP and Chl *a* after wet dust deposition but no changes after dry deposition; they explained these results by the lack of nitrate in the dry deposition events. In contrast, in the two mesocosm experiments conducted in Crete (the present one, and the one reported in Tsagaraki et al., in review), dry dust addition resulted in a net and important increase in both PP and Chl *a* although, indeed, nitrate concentration was low in the dust added (**Figure 1B**). Our results agree more with several microcosm experiments conducted in Blanes Bay, Spain (Lekunberri et al., 2010; Romero et al., 2011), at the DYFAMED station (Bonnet et al., 2005; Pulido-Villena et al., 2008), at the Cyprus Gyre (Herut et al., 2005), and in the Atlantic (Marañón et al., 2010), where, in most of the cases, both auto- and hetero-trophs were favored after dust addition.

Effect of the Episodicity of Dust Deposition or "How Dust is Added"

Despite the similarities of the system's response to the two dust treatments, some differences were also observed.

In SA, which received the strong dust pulse, PP, BP, and to a lesser extent Chl *a,* started to increase from the first day and presented maxima on Day 2. In RA, however, which received the three smaller dust pulses, a delay of 1 day was observed in the increase of PP and BP and of 2 days in the case of Chl *a*. Nevertheless, the maximal values of these parameters were similar to SA.

In contrast to the production rates, there was not any time lag between SA and RA regarding bacterial and cyanobacterial abundances. Both bacterial and cyanobacterial abundances peaked and then decreased in the same time period in both treatments. However, bacteria presented a significant increase on Day 1 while cyanobacteria on Day 2. This was also observed by Tsagaraki et al. (in review) and is an indication that bacteria out-competed cyanobacteria for nutrients.

Interestingly, in both dust treatments, the values of PP and Chl *a* concentration remained at high levels, at least until Days 5 and 6, respectively, whereas BP sharply decreased immediately after its peak on Days 2 and 3. In fact, phytoplankton biomass was characterized by different fractions in different periods of the experiment; *Synechococcus* (picoplankton) peaked first and larger-than-2 μm cells (nanoplankton) followed. According to Lagaria et al. (2017, this SI), *Synechococcus* were related to P, which was taken up until Day 3, whereas larger cells to N, which remained at a higher concentration after P exhaustion.

Impact of Dust Addition on Larger Organisms and Food Web Interactions

While the response to dust addition was clearly reflected on PP, BP, Chl *a* concentration and cyanobacterial and heterotrophic bacterial densities, there was not any effect on the trophic levels further up the food web; the dynamics of autotrophic flagellates and also of the grazers such as heterotrophic flagellates, ciliates, dinoflagellates, even of viruses, did not follow an obvious pattern and the difference between treatments and Cnt was lost. These results indicate that nutrient addition fueled primary and bacterial production at the beginning. The size class that significantly responded first was picoplankton, both auto- and hetero-trophic. Subsequently, grazing processes played a role in the regulation of the populations recently built up.

The initial increase in % of HDNA bacteria in both SA and RA could indicate a change in bacterial community composition toward more active cells in the dust-treated mesocosms. This shift in bacterial community composition has also been reported in Guo et al. (2016, this SI) during the 2012 dust-addition experiment conducted in the same area. The increase in % of HDNA bacteria was followed by an increase in bacteria grazers, the heterotrophic flagellates which seem to have been the main factor causing the reduction of bacterioplankton abundance after Day 3; in fact, the decline of HDNA bacterial abundance was sharper in the treated mesocosms compared to Cnt. HF have been shown to graze selectively on active HDNA bacteria (Baltar et al., 2015). On the other hand, it seems that during the present study, viral infection was not important for bacteria mortality, since total virus abundance did not increase in the dust-treated mesocosms at any time during the experiment, not even when bacterial activity was at its highest; neither total nor LDNA viruses, assumed to be mostly bacteriophages, increased in abundance. In the 2012 Crete experiment, Tsiola et al. (2017, this SI) found that viral production rate did not increase when dust was added in the Eastern Mediterranean but, surprisingly, it was decreased. The authors attributed this finding to processes not synchronized to the viral production experiments, such as extensive lysis events occurred prior to sampling. During the DUNE-R experiment, Pulido-Villena et al. (2014) attributed the lack of increase in heterotrophic bacteria and HF abundance after dust addition to viral infection; however, viral rates were not measured. In the present experiment, although the increase of HF abundance followed that of their prey, heterotrophic bacteria, no difference was found between treatments and Cnt; at this point, our results agree with those of the DUNE-R experiment during which Pulido-Villena et al. (2014) reported no differences in terms of HF between dust-amended mesocosms and Cnt.

The increase in HF numbers was followed by a decline under the pressure of their own grazers, ciliates and dinoflagellates, which progressively increased after Day 2 and 3, respectively, until the end of the experiment. It is interesting to note that on the last day of the experiment, the ciliate abundance was higher in the Cnt than in the treatments; this could perhaps be attributed to a relaxation of grazing exerted on ciliates by mesozooplankton. Indeed, the mesozooplankton biomass, measured on the last day, was higher in the amended mesocosms compared to the Cnt. This biomass increase is not particularly big considering the size-developmental stage of the animals, the temperature and the absence of predatory mortality. The growth rate, estimated from the difference of biomass between the start and end of the 10-day long experiment, was normal. Even for the treatment with the highest biomass increase (RA), the growth rate was within the range of values at 20°C, under *in situ* food conditions, for small copepods constituted mostly by juvenile stages (Hirst and Bunker, 2003). This is valid even when considering the maximum non-predatory mortality reported in the Mediterranean (0.05 day^{-1}, Frangoulis et al., 2011).

The results of this study allow us to conclude that on the very first days of the experiment, the osmotrophic populations were clearly favored by the N and P added through dust and built their populations; after that period, grazing pressures, exerted on multiple levels of the complex food web, masked the difference between the treated mesocosms and the Cnt. This masking of the impact of nutrient addition when moving away from the osmotrophic part of the food web has been observed in mesocosm experiments with nutrient additions (Pitta et al., 2016; Tsagaraki et al., in review). It may be related to the complex trophic relationships prevailing in the microbial food web, which become even more complex because of the occurrence of mixotrophic species in almost all functional groups.

The role of grazing in masking the effect of nutrient addition on parts of the food web, which was mainly assumed in previous experiments, was partly verified during the present study by the means of two dilution experiments. Grazing on AF and *Synechococcus* was found to be stimulated by dust addition compared to the Cnt (whereas this was not verified in the case of picoeukaryotes). This may have been the reason why no difference was found between SA and Cnt in terms of AF density. We may assume that similar masking effects have also taken place between other predators and prey, finally resulting in the impact of dust addition being visible again as the difference between amended mesocosms and Cnt, much further up the food web, on mesozooplankton, perhaps simply because grazers of mesozooplankton were absent from this particular experimental set-up.

CONCLUSIONS

Our data showed that independently of the way dust was added to the surface of the oligotrophic marine environment of the Eastern Mediterranean, either in a single strong pulse (SA) or

in three repetitive smaller pulses (RA), both the autotrophic and heterotrophic components of the microbial food web presented a significant response. Both primary and bacterial productions showed a clear effect (2-fold increase), fuelled by nutrients (N and P) added via dust. Phytoplankton biomass as well as heterotrophic bacteria and cyanobacteria abundances also showed an important increase. Phytoplankton responded first, followed by bacterioplankton. When dust was added in three repetitive doses, the response presented a delay of 1 day; however, maximum values attained were similar in both treatments. The effect of dust addition was later lost in the intermediate trophic levels, masked by multiple grazing processes taking place in this complex multitrophic food web; until it was again visible in mesozooplankton, which presented a higher density in the dust-amended mesocosms.

AUTHOR CONTRIBUTIONS

Planning of the original experimental design: PP, GP, SC, MKan, NM. Carrying out of experiment and sampling in the field: PP, IS, AT. Characterization of dust: KV, PN, MKan. Sea water chemical analyses: MT, KV, PN. Chlorophyll a concentration: NP, PD. Primary production: AL, SP. Bacterial production: AG. Virus, heterotrophic bacteria and Synochococcus abundance and biomass: AT. Flagellate and ciliate counts: MKag. Mesozooplankton abundance and biomass: CF. Dilution experiment: PP, AG, NP, IS, AT, PD. Organizing the data set and calculating simple statistics: PP, AT. Organizing the operation of mesocosms and obtaining funding: PP, GP. Writing up manuscript: PP, AG, AL, SP, KV, MT.

ACKNOWLEDGMENTS

This study was funded by the project ADAMANT—"Atmospheric deposition and Mediterranean sea water productivity" project (nr code/MIS: 383551), co-financed by the European Union (European Social Fund–ESF) and Greek national funds (Operational Program "Education and Lifelong Learning" of the National Strategic Reference Framework—NSRF, Research Funding Program: THALES). We wish to thank G. Piperakis for his inspired technical assistance throughout the experiment, D. Amanatidis for assistance during the mesocosm filling, S. Zivanovic and E. Dafnomili for assistance with chemical analyses, A. Konstantinopoulou, S. Diliberto, and D. Podaras for assistance during the experiment, S. Batziakas for support with zooplankton counting and N. Sekeris for his help with constructions and ideas for technical solutions. The captain and the crew of the R/V Philia are also thanked for their assistance during the transportation of water from the sea to the mesocosms. Finally, the two reviewers are thanked for their important contributions to the improvement of this manuscript.

REFERENCES

Alcaraz, M., and Calbet, A. (2003). "Zooplankton ecology," in *Marine Ecology. Encyclopedia of Life Support Systems (EOLSS)*, eds C. Duarte and A. Lott Helgueras (Oxford: Developed under the Auspices of the UNESCO, Eolss Publishers), 295–318.

Baltar, F., Palovaara, J., Unrein, F., Catala, P., and Horňák, K., Šimek, K., et al. (2015). Marine bacterial community structure resilience to changes in protist predation under phytoplankton bloom conditions. *ISME J.* 10, 568–581. doi: 10.1038/ismej.2015.135

Bardouki, H., Liakakou, H., Economou, C., Sciare, J., Smolík, J., Ždímal, V., et al. (2003). Chemical composition of size resolved atmospheric aerosols in the Eastern Mediterranean during summer and winter. *Atmos. Environ.* 37, 195–208. doi: 10.1016/S1352-2310(02)00859-2

Blain, S., Guieu, C., Claustre, H., Leblanc, K., Moutin, T., Quéguiner, B., et al. (2004). Availability of iron and major nutrients for phytoplankton in the northeast Atlantic Ocean. *Limnol. Oceanogr.* 49, 2095–2104. doi: 10.4319/lo.2004.49.6.2095

Bonnet, S., Guieu, C., Chiaverini, J., Ras, J., and Stock, A. (2005). Effect of atmospheric nutrients on the autotrophic communities in a low nutrient, low chlorophyll system. *Limnol. Oceanogr.* 50, 1810–1819. doi: 10.4319/lo.2005.50.6.1810

Boyd, P. W., Jickells, T. D., Law, C. S., Blain, S., Boyle, E. A., Buesseler, K. O., et al. (2007). Mesoscale iron enrichment experiments 1993-2005: synthesis and future directions. *Science* 315, 612–617. doi: 10.1126/science.1131669

Brussaard, C. P. D. (2004). Optimization of procedures for counting viruses by flow cytometry. *Appl. Environ. Microbiol.* 70, 1506–1513. doi: 10.1128/AEM.70.3.1506-1513.2004

Caron, D. A., Dam, H. G., Kremer, P., Lessard, E. J., Madin, L. P., Malone, T. C., et al. (1995). The contribution of microorganisms to particulate carbon and nitrogen in surface waters of the Sargasso Sea near Bermuda. *Deep-Sea Res. I* 42, 943–972. doi: 10.1016/0967-0637(95)00027-4

Desboeufs, K., Leblond, N., Wagener, T., Bon Nguyen, E, and Guieu, C. (2014). Chemical fate and settling of mineral dust in surface seawater after atmospheric deposition observed from dust seeding experiments in large mesocosms. *Biogeosciences* 11, 5581–5594. doi: 10.5194/bg-11-5581-2014

Frangoulis, C., Grigoratou, M., Zoulias, T., Hannides, C. C. S., Pantazi, M., Psarra, S., et al. (2016). Expanding zooplankton standing stock estimation from meso- to metazooplankton: a case study in the N. Aegean Sea (Mediterranean Sea). *Cont. Shelf Res.* doi: 10.1016/j.csr.2016.10.004

Frangoulis, C., Skliris, N., Lepoint, G., Elkalay, K., Goffart, A., Pinnegar, J. K., et al. (2011). Importance of copepod carcasses versus faecal pellets in the upper water column of an oligotrophic area. *Estuar. Coast. Shelf Sci.* 92, 456–463. doi: 10.1016/j.ecss.2011.02.005

Gerasopoulos, E., Kouvarakis, G., Babasakalis, P., Vrekoussis, M., Putaud, J.-P., and Mihalopoulos, N. (2006). Origin and variability of particulate matter (PM10) mass concentrations over the Eastern Mediterranean. *Atmos. Environ.* 40, 4679–4690. doi: 10.1016/j.atmosenv.2006.04.020

Giovagnetti, V., Brunet, C., Conversano, F., Tramontano, F., Obernosterer, I., Ridame, C., et al. (2013). Assessing the role of dust deposition on phytoplankton ecophysiology and succession in a low-nutrient low-chlorophyll ecosystem: a mesocosm experiment in the Mediterranean Sea. *Biogeosciences* 10, 2973–2991. doi: 10.5194/bg-10-2973-2013

Guerzoni, S., Chester, R., Dulac, F., Herut, B., Loÿe-Pilot, M. D., Measures, C., et al. (1999). The role of atmospheric deposition in the biogeochemistry of the Mediterranean Sea. *Prog. Oceanogr.* 44, 147–190. doi: 10.1016/S0079-6611(99)00024-5

Guieu, C., Ridame, C., Pulido-Villena, E., Bressac, M., Desboeufs, K., and Dulac, F. (2014). Impact of dust deposition on carbon budget: a tentative assessment from a mesocosm approach. *Biogeosciences* 11, 5621–5635. doi: 10.5194/bg-11-5621-2014

Guo, C., Jing, H., Kong, L., and Liu, H. (2013). Effect of East Asian aerosol enrichment on microbial community composition in the South China Sea. *J. Plankton Res.* 35, 485–503. doi: 10.1093/plankt/fbt002

Guo, C., Xia, X., Pitta, P., Herut, B., Rahav, E., Berman-Frank, I., et al. (2016). Shifts in microbial community structure and activity in the ultra-oligotrophic Eastern Mediterranean Sea driven by Saharan Dust and European aerosol deposition. *Front. Mar. Sci.* 3:170. doi: 10.3389/fmars.2016.00170

Guo, C., Yu, J., Ho, T.-Y., Wang, L., Song, S., Kong, L., et al. (2012). Dynamics of phytoplankton community structure in the South China Sea in response to the East Asian aerosol input. *Biogeosciences* 9, 1519–1536. doi: 10.5194/bg-9-1519-2012

Hedges, J. I., and Stern, J. H. (1984). Carbon and Nitrogen determination of carbonate-containing solids. *Limnol. Oceanogr.* 29, 657–663. doi: 10.4319/lo.1984.29.3.0657

Herut, B., Zohary, T., Krom, M. D., Mantoura, R. F. C., Pitta, P., Psarra, S, et al. (2005). Response of East Mediterranean surface water to Saharan dust: on-board microcosm experiment and field observations. *Deep Sea Res.* 52, 3024–3040. doi: 10.1016/j.dsr2.2005.09.003

Hirst, A. G., and Bunker, A. J. (2003). Growth of marine planktonic copepods: global rates and patterns in relation to chlorophyll a, temperature, and body weight. *Limnol. Oceanogr.* 48, 1988–2010. doi: 10.4319/lo.2003.48.5.1988

Holm-Hansen, O., Lorenzen, C. J., Holmes, R. W., and Strickland, J. D. H. (1965). Fluorometric determination of chlorophyll. *ICES J. Mar. Sci.* 30, 3–15. doi: 10.1093/icesjms/30.1.3

Ivancic, I., and Degobbis, D. (1984). An optimal manual procedure for ammonia analysis in natural waters by the indophenol blue method. *Water Res.* 18, 1143–1147. doi: 10.1016/0043-1354(84)90230-6

Jickells, T. D., An, Z. S., Andersen, K. K., Baker, A. R., Bergametti, G., Brooks, N., et al. (2005). Global iron connections between desert dust, ocean biogeochemistry, and climate. *Science* 308, 67–71. doi: 10.1126/science.1105959

Kana, T., and Glibert, P. M. (1987). Effect of irradiances up to 2000 μE m-2 s-1 on marine Synechococcus WH 7803-I. Growth, pigmentation and cell composition. *Deep Sea Res.* 34, 479–516. doi: 10.1016/0198-0149(87)90001-X

Kirchman, D. L. (1993). "Leucine incorporation as a measure of biomass production by heterotrophic bacteria," in *Handbook of Methods in Aquatic Microbial Ecology*, eds P. F. Kemp, B. F. Sherr, E. B. Sherr, and J. J. Cole (Lewis, IA: Lewis Publishers) 509–512.

Kirchman, D. L., Newell, S. Y., and Hodson, R. E. (1986). Incorporation versus biosynthesis of leucine: implications for measuring rates of protein syntheis and biomass production by bacteria in marine systems. *Mar. Ecol. Prog. Ser.* 32, 47–59. doi: 10.3354/meps032047

Kress, N., and Herut, B. (2001). Spatial and seasonal evolution of dissolved oxygen and nutrients in the Southern Levantine Basin (Eastern Mediterranean Sea): chemical characterization of the water masses and inferences on the N: P ratios. *Deep Sea Res. I* 48, 2347–2372. doi: 10.1016/S0967-0637(01)00022-X

Krom, M. D., Kress, N., Brenner, S., and Gordon, L. I. (1991). Phosphorus limitation of primary productivity in the eastern Mediterranean Sea. *Limnol. Oceanogr.* 36, 424–432. doi: 10.4319/lo.1991.36.3.0424

Krom, M. D, Thingstad, T. F., Brenner, S., Carbo, P., Drakopoulos, P., Fileman, T. W., et al. (2005b). Summary and overview of the CYCLOPS P addition Lagrangian experiment in the Eastern Mediterranean. *Deep Sea Res. II* 52, 3090–3108. doi: 10.1016/j.dsr2.2005.08.018

Krom, M. D., Woodward, E. M. S., Herut, B., Kress, N., Carbo, P., Mantoura, R. F. C., et al. (2005a). Nutrient cycling in the south east Levantine basin of the eastern Mediterranean: results from a phosphorus starved system. *Deep Sea Res. II* 52, 2879–2896. doi: 10.1016/j.dsr2.2005.08.009

Lagaria, A., Mandalakis, M., Mara, P., Papageorgiou, N., Pitta, P., Tsiola, A., et al. (2017). Phytoplankton response to Saharan dust depositions in the eastern Mediterranean Sea: a mesocosm study. *Front. Mar. Sci.* 3:287. doi: 10.3389/fmars.2016.00287

Lagaria, A., Psarra, S., Lefèvre, D., Van Wambeke, F., Courties, C., Pujo-Pay, M., et al. (2011). The effects of nutrient additions on particulate and dissolved primary production and metabolic state in surface waters of three Mediterranean eddies. *Biogeosciences* 8, 2595–2607. doi: 10.5194/bg-8-2595-2011

Laghdass, M., Blain, S., Besseling, M., Catala, P., Guieu, C., and Obernosterer, I. (2011). Effects of Saharan dust on the microbial community during a large *in situ* mesocosm experiment in the NW Mediterranean Sea. *Aquat. Microb. Ecol.* 62, 201–213. doi: 10.3354/ame01466

Landry, M. R., Brown, S. L., Neveux, J., Dupouy, C., Blanchot, J., Christensen, S., et al. (2003). Phytoplankton growth and microzooplankton grazing in high-nutrient, low-chlorophyll waters of the equatorial Pacific: community and taxon-specific rate assessment from pigment and flow cytometric analyses. *J. Geophys. Res.* 108:8142. doi: 10.1029/2000jc000744

Landry, M. R., and Hassett, R. P. (1982). Estimating the grazing impact of marine micro-zooplankton. *Mar. Biol.* 67, 283–288. doi: 10.1007/BF00397668

Lee, S., and Fuhrman, J. A. (1987). Relationships between biovolume and biomass of naturally derived marine bacterioplankton. *Appl. Environ. Microbiol.* 53, 1298–1303.

Lekunberri, I., Lefort, T., Romero, E., Vázquez-Domínguez, E., Romera-Castillo, C., Marrasé, C., et al. (2010). Effects of a dust deposition event on coastal marine microbial abundance and activity, bacterial community structure and ecosystem function. *J. Plankton Res.* 32, 381–396. doi: 10.1093/plankt/fbp137

Lin, P., Chen, M., and Guo, L. (2012). Speciation and transformation of phosphorus and its mixing behavior in the Bay of St. Louis estuary in the northern Gulf of Mexico. *Geochim. Cosmochim. Acta* 87, 283–298. doi: 10.1016/j.gca.2012.03.040

Mahowald, N. M., Baker, A. R., Bergametti, G., Brooks, N., Duce, R. A., Jickells, T. D., et al. (2008). Atmospheric global dust cycle and iron inputs to the ocean. *Glob. Biogeochem. Cycles* 19: GB4025. doi: 10.1029/2004GB002402

Marañón, E., Fernández, A., Mouri-o-Carballido, B., Martinez-Garcia, S., Teira, E., Cerme-o, P., et al. (2010). Degree of oligotrophy controls the response of microbial plankton to Saharan dust. *Limnol. Oceanogr.* 55, 2339–2352. doi: 10.4319/lo.2010.55.6.2339

Marie, D., Brussaard, C. P. D., Thyrhaug, R., Bratbak, G., and Vaulot, D. (1999). Enumerating of marine viruses in culture and natural samples by flow cytometry. *Appl. Environ. Microbiol.* 65, 45–52.

Martin, J. H. (1990). Glacial-interglacial CO2 change: the iron hypothesis. *Paleoceanography* 31, 1–13. doi: 10.1029/PA005i001p00001

Mills, M. M., Ridame, C., Davey, M., LaRoche, J., and Geider, R. J. (2004). Iron and phosphorus co-limit nitrogen fixation in the eastern tropical North Atlantic. *Nature* 429, 292–294. doi: 10.1038/nature02550

Miyazaki, Y., Kawamura, K., Jung, J., Furutani, H., and Uematsu, M. (2011). Latitudinal distributions of organic nitrogen and organic carbon in marine aerosols over the western North Pacific. *Atmos. Chem. Phys.* 11, 3037–3049. doi: 10.5194/acp-11-3037-2011

Paraskevopoulou, D., Liakakou, E., Gerasopoulos, E., and Mihalopoulos, N. (2015). Sources of atmospheric aerosol from long-term measurements (5 years) of chemical composition in Athens, Greece. *Sci. Tot. Environ.* 527–528, 165–178. doi: 10.1016/j.scitotenv.2015.04.022

Pitta, P., Giannakourou, A., and Christaki, U. (2001). Planktonic ciliates in the oligotrophic Mediterranean Sea: longitudinal trends of standing stocks, distributions and analysis of food vacuole contents. *Aquat. Microb. Ecol.* 24, 297–311. doi: 10.3354/ame024297

Pitta, P., Nejstgaard, J. C., Tsagaraki, T. M., Zervoudaki, S., Egge, J. K., Frangoulis, C., et al. (2016). Confirming the "Rapid phosphorus transfer from microorganisms to mesozooplankton in the Eastern Mediterranean Sea" scenario through a mesocosm experiment. *J. Plankton Res.* 38, 502–521. doi: 10.1093/plankt/fbw010

Pitta, P., Stambler, N., Tanaka, T., Zohary, T., Tselepides, A., and Rassoulzadegan, F. (2005). Biological response to P addition in the Eastern Mediterranean Sea. The microbial race against time. *Deep Sea Res. II* 52, 2961–2974. doi: 10.1016/j.dsr2.2005.08.012

Porter, K. G., and Feig, Y. S. (1980). The use of DAPI for identifying and counting of aquatic microflora. *Limnol. Oceanogr.* 25, 943–948. doi: 10.4319/lo.1980.25.5.0943

Postel, L., Fock, H., and Hagen, W. (2000). "Biomass and abundance," in *Zooplankton Methodology Manual*, eds R. P. Harris, P. H. Wiebe, J. Lenz, H. R. Skjoldal, and M. Huntley (London: Academic Press), 83–192.

Pulido-Villena, E., Baudoux, A.-C., Obernosterer, I., Landa, M., Caparros, J., Catala, P., et al. (2014). Microbial food web dynamics in response to a Saharan dust event: results from a mesocosm study in the oligotrophic Mediterranean Sea. *Biogeosciences* 11, 5607–5619. doi: 10.5194/bg-11-5607-2014

Pulido-Villena, E., Wagener, T., and Guieu, C. (2008). Bacterial response to dust pulses in the western Mediterranean: implications for carbon cycling in the oligotrophic ocean. *Glob. Biogeochem. Cycles* 22:GB1020. doi: 10.1029/2007gb003091

Putt, M., and Stoecker, D. K. (1989). An experimentally determined carbon: volume ratio for marine "oligotrichous" ciliates from estuarine and coastal waters. *Limnol. Oceanogr.* 34, 1097–1103. doi: 10.4319/lo.1989.34.6.1097

Ridame, C., Dekaezemacker, J., Guieu, C., Bonnet, S., L'Helguen, S., and Malien, F. (2014). Contrasted Saharan dust events in LNLC environments: impact on nutrient dynamics and primary production. *Biogeosciences* 11, 4783–4800. doi: 10.5194/bg-11-4783-2014

Rimmelin, P., and Moutin, T. (2005). Re-examination of the MAGIC method to determine low orthophosphate concentration in seawater. *Anal. Chim. Acta* 548, 174–182. doi: 10.1016/j.aca.2005.05.071

Romero, E., Peters, F., Marrasé, C., Guadayol, O., Gasol, J. M., and Weinbauer, M. G. (2011). Coastal Mediterranean plankton stimulation dynamics through a dust storm event: an experimental simulation. *Estuar. Coast. Shelf Sci.* 93, 27–39. doi: 10.1016/j.ecss.2011.03.019

Sempéré, R., Panagiotopoulos, C., Lafont, R., Marroni, B., and Van Wambeke, F. (2002). Total organic carbon dynamics in the Aegean Sea. *J. Mar. Syst.* 33–34, 355–364. doi: 10.1016/S0924-7963(02)00066-0

Smith, D. C., and Azam, F. (1992). A simple, economical method for measuring bacterial protein synthesis rates in seawater using 3H-leucine. *Mar. Microb. Food Webs* 6, 107–114.

Steemann-Nielsen, E. (1952). The use of radio-active carbon (C14) for measuring organic production in the sea. *J. Cons. Explor. Mer.* 18, 117–140. doi: 10.1093/icesjms/18.2.117

Strickland, J. D., and Parsons, T. R. (1972). A practical handbook of seawater analysis. *J. Fish. Res. Board Can.* 167, 71–76.

Tanaka, T., Thingstad, T. F., Christaki, U., Colombet, J., Cornet-Barthaux, V., Courties, C., et al. (2011). Lack of P-limitation of phytoplankton and heterotrophic prokaryotes in surface waters of three anticyclonic eddies in the stratified Mediterranean Sea. *Biogeosciences* 8, 525–538. doi: 10.5194/bg-8-525-2011

Ternon, E., Guieu, C., Loÿe-Pilot, M.-D., Leblond, N., Bosc, E., Gasser, B., et al. (2010). The impact of Saharan dust on the particulate export in the water column of the NorthWestern Mediterranean Sea. *Biogeosciences* 7, 809–826. doi: 10.5194/bg-7-809-2010

Thingstad, T. F., Krom, M. D., Mantoura, R. F. C., Flaten, G. A. F., Groom, S., Herut, B., et al. (2005). Nature of phosphorus limitation in the ultraoligotrophic eastern Mediterranean. *Science* 309, 1068–1071. doi: 10.1126/science.1112632

Tsiola, A., Tsagaraki, M.T., Giannakourou, A., Nikolioudakis, N., Yucel, N., Herut, B., et al. (2017). Viruses and flagellates impact upon bacteria in the Eastern Mediterranean Sea after Saharan dust and polluted aerosol enrichment. *Front. Mar. Sci.* 3:281. doi: 10.3389/fmars.2016.00281

Utermöhl, H. (1958). Zur Vervollkommung der quantitativen Phytoplankton-methodik. *Mitt. Int. Ver. Theor. Angew Limnol.* 9, 1–38.

Van Wambeke, F., Obernosterer, I., Moutin, T., Duhamel, S., Ulloa, O., and Claustre, H. (2008). Heterotrophic bacterial production in the eastern South Pacific: longitudinal trends and coupling with primary production. *Biogeosciences* 5, 157–169. doi: 10.5194/bg-5-157-2008

Vincent, J., Laurent, B., Losno, R., Bon Nguyen, E., Roullet, P., Sauvage, S., et al. (2016). Variability of mineral dust deposition in the western Mediterranean basin and south-east of France. *Atmos. Chem. Phys.* 16, 8749–8766. doi: 10.5194/acp-16-8749-2016

Zohary, T., Herut, B., Krom, M. D., Mantoura, R. F. C., Pitta, P., Psarra, S., et al. (2005). P-limited bacteria but N and P co-limited phytoplankton in the Eastern Mediterranean – A microcosm experiment. *Deep Sea Res. II* 52, 3011–3023. doi: 10.1016/j.dsr2.2005.08.011

Conflict of Interest Statement: The authors declare that the research was conducted in the absence of any commercial or financial relationships that could be construed as a potential conflict of interest.

frontiers in Marine Science

ORIGINAL RESEARCH
published: 09 January 2017
doi: 10.3389/fmars.2016.00287

Phytoplankton Response to Saharan Dust Depositions in the Eastern Mediterranean Sea: A Mesocosm Study

Anna Lagaria[1], Manolis Mandalakis[2], Paraskevi Mara[3], Nafsika Papageorgiou[1], Paraskevi Pitta[1], Anastasia Tsiola[1,4], Margarita Kagiorgi[1] and Stella Psarra[1]*

[1] Institute of Oceanography, Hellenic Centre for Marine Research, Heraklion, Greece, [2] Institute of Marine Biology, Biotechnology and Aquaculture, Hellenic Centre for Marine Research, Heraklion, Greece, [3] Department of Chemistry, University of Crete, Heraklion, Greece, [4] Department of Biology, University of Crete, Heraklion, Greece

The response of phytoplankton populations from surface ultra-oligotrophic waters of the Eastern Mediterranean Sea to Saharan dust additions was studied during a 10-day mesocosm experiment in May 2014. A set of triplicate mesocosms entitled "Single Addition" treatment (SA) was amended with Saharan dust once, while another triplicate set entitled "Repetitive Addition" treatment (RA) received the same amount of dust divided into three consecutive daily doses administered within the first three experimental days, both simulating patterns of dust deposition events taking place in the field. In both treatments, dust particles released small amounts of dissolved inorganic nitrogen and phosphorus which stimulated by 2-fold both chlorophyll-*a* concentration and primary production for a time period of 6 days, as compared to a set of control mesocosms carried out without dust addition. Phytoplankton response was similar in both treatments, regardless of the dust addition pattern, and it evolved through two distinct phases in both cases. The first phase (i.e., 1–2 days after initial addition) was characterized by enhancement of picoplankton chlorophyll-normalized production rates as a result of elevated orthophosphate concentrations while the second phase (i.e., 3–4 days after initial dust addition), was characterized by elevated chlorophyll-normalized production rates corresponding to larger cells (>5 μm) as a result of increased mineral nitrogen concentrations. The stimulated primary production of larger cells was not accompanied by a respective increase in carbon biomass suggesting important top-down control. The major phytoplankton taxa detected during the experiment were *Synechococcus*, Pelagophytes, and Prymnesiophytes. Estimations of cellular pigment concentrations and carbon-to-chlorophyll ratios of identified groups and differences between prokaryotic and eukaryotic cells are discussed.

Keywords: atmospheric deposition, ultra-oligotrophic conditions, phytoplankton pigments, productivity, carbon-to-chlorophyll ratio

OPEN ACCESS

Edited by:
Angel Borja, AZTI, Spain

Reviewed by:
Gianluca Volpe, Istituto di Scienze dell'Atmosfera e del Clima—CNR, Italy
Marcos Mateus, Universidade de Lisboa, Portugal
Savvas Genitsaris, Aristotle University of Thessaloniki, Greece

****Correspondence:***
Anna Lagaria
lagaria@hcmr.gr

Specialty section:
This article was submitted to Marine Ecosystem Ecology, a section of the journal Frontiers in Marine Science

Received: *20 September 2016*
Accepted: *21 December 2016*
Published: *09 January 2017*

Citation:
Lagaria A, Mandalakis M, Mara P, Papageorgiou N, Pitta P, Tsiola A, Kagiorgi M and Psarra S (2017) Phytoplankton Response to Saharan Dust Depositions in the Eastern Mediterranean Sea: A Mesocosm Study. Front. Mar. Sci. 3:287. doi: 10.3389/fmars.2016.00287

INTRODUCTION

The Mediterranean Sea is one of the most oligotrophic marine regions worldwide, characterized by a west-east gradient of increasing oligotrophy in terms of macronutrients (nitrogen and phosphorus), biomass and production (Krom et al., 1991; Moutin and Raimbault, 2002; Ignatiades et al., 2009). The depletion of nutrients in the eastern Mediterranean basin, especially in the upper

water layer is the main limiting factor of osmotrophs growth (Thingstad and Rassoulzadegan, 1995; Thingstad and Mantoura, 2005; Tanaka et al., 2011). Recent studies have highlighted the impact of atmospheric deposition on the productivity of such oligotrophic systems. It has been suggested that the frequent Saharan and Middle East dust deposition events taking place in the eastern basin (Engelstaedter et al., 2006) may serve as important external sources of bioavailable macro- and trace-nutrients in the surface mixed layer, promoting osmotrophs growth (Marañón et al., 2010; Ternon et al., 2010; Christodoulaki et al., 2013; Giovagnetti et al., 2013; Gallisai et al., 2014).

Microcosm and mesocosm experimental studies performed mostly in NW Mediterranean and the Atlantic Ocean demonstrated that inputs of dust and aerosols enhanced primary production (Ridame and Guieu, 2002; Bonnet et al., 2005; Marañón et al., 2010) and phytoplankton biomass (Guo et al., 2012; Giovagnetti et al., 2013), as well as bacterial abundance (Herut et al., 2005; Marañón et al., 2010) and/or bacterial respiration (Pulido-Villena et al., 2014). However, phytoplankton and heterotrophic prokaryotes did not show a consistently positive response, in terms of biomass and production, to dust additions nor presented similar patterns among all experiments. The biological responses mediated through the release of nutrients from dust particles depended on the environmental conditions (e.g., nutrient regime), the quantity/quality of the dust added and the initial composition and physiological state of the various osmotroph groups present in the sampled seawater. For example, concerning phytoplankton, input of small amounts of dust particles in oligotrophic seawaters of South China Sea did not result in biomass accumulation or community structure changes, while large amounts of dust resulted in the increase of both biomass and photosynthetic efficiency (Guo et al., 2012). During a bioassays experiment performed in the Atlantic Ocean, where a certain amount of dust was added to microcosms representing different degrees of oligotrophy, it was found that primary production was stimulated only in the least oligotrophic waters (Marañón et al., 2010). Moreover, successive dust deposition events may induce different biogeochemical responses (Ternon et al., 2010; Wagener et al., 2010). For example, a mesocosm experiment performed in the NW Mediterranean demonstrated that a first dust addition favored picoplankton while a second addition a few days later induced a response of larger phytoplankton cells (Giovagnetti et al., 2013).

Overall, dust deposition is deemed to serve as a source of nutrients and it is believed to impact the productivity of oligotrophic systems. However, the response of phytoplankton assemblages to dust inputs, in terms of biomass and activity, is still unpredictable. Furthermore, the significance of phytoplankton response over ecological timescales or broad spatial scales is also under question (Volpe et al., 2009; Spivak et al., 2011; Gallisai et al., 2014). In the field, intense dust deposition fluxes may result from either a single strong or several smaller consecutive dust deposition events (Vincent et al., 2016 and references therein). The majority of previous mesocosm experiments have studied the response of plankton community to single dust additions. In our study, we performed both single and consecutive dust additions in well-controlled mesocosms in order to investigate how the magnitude and time intervals between consecutive Saharan dust deposition events affect phytoplankton activity and community structure in an ultra-oligotrophic site of the east Mediterranean Sea. Moreover, we investigated which, if any, phytoplankton groups were particularly favored by the supply of new nutrients resulting from the dissolution of dust particles. Finally, we examined whether dust additions could stimulate significant physiological changes in phytoplankton cells (e.g., cellular pigment content, C:Chl*a* ratio). To accomplish these objectives, we monitored the response of autotrophic community, through size fractionated chlorophyll and production measurements as well as single cell counts and pigment analysis.

MATERIALS AND METHODS

Experimental Set Up and Sampling

The experiment, undertaken within the ADAMANT project, was performed in May 2014 in the mesocosm facilities of the Hellenic Centre for Marine Research in Crete, Greece. A detailed description of the mesocosms' setup and experimental design is presented in Pitta et al., (in review). Briefly, 27 m^3 of pelagic seawater were collected from 10 m depth at a shelf site aboard the R/V FILIA and were transferred to mesocosm installations using acid-clean tanks (1 m^3 each). Three sets of three mesocosms (a total of nine polyethylene containers up to 3 m^3 each) were filled with the collected seawater. The mesocosms were deployed in a large, land-based tank with running surface sea water allowing temperature control and were covered with a screen mesh in order to reduce light intensity by approximately 30%. Three mesocosms were amended with 4 g Saharan dust each, on day zero ("Single Addition" treatment, SA), another set of three mesocosms received three consecutive dust additions of 1, 2, and 1 g on days 0, 1, and 2, respectively ('Repetitive Addition' treatment, RA), while three mesocosms were run without dust addition and used as controls (CNT). The total quantity of dust added (4 g) to the mesocosms corresponded to a final concentration of ca. 1.3 mg L^{-1} and was selected to represent realistic atmospheric deposition events in the east Mediterranean Sea (Pitta et al., in review).

The experiment lasted 10 days in total (D0–D9) and sampling for the analysis of mineral nutrients, size fractionated chlorophyll *a* and primary production, phytoplankton pigments, and picoplankton (<2 μm) cell counts took place every day before any dust addition. Sampling for cell counting of autotrophic nanoplankton (2–20 μm) and microplankton (>20 μm), by microscopy methods, took place every second day due to their long analysis time. Nevertheless, the specific sampling strategy was considered adequate for the detection of potential changes in community structure.

Mineral Nutrients

Nitrate (NO_3^-), nitrite (NO_2^-), and ammonium (NH_4^+) were measured according to Strickland and Parsons (1972) while orthophosphate (PO_4^{3-}) was measured according to Rimmelin

and Moutin (2005). Total dissolved inorganic nitrogen (DIN) is estimated by the sum of NO_3^-, NO_2^-, and NH_4^+.

Chlorophyll-*a* per Size Class

The amount of chlorophyll-*a* corresponding to picoplankton (<2 μm, pChl*a*), small nanoplankton (2–5 μm, snChl*a*), and larger nano- and microplankton (>5 μm, nμChl*a*) was determined according to the fluorometric acidification method (Holm-Hansen et al., 1965). Water samples of 1 L were collected from each mesocosm and sequentially filtered through 5, 2, and 0.2 μm polycarbonate filters (47 mm diameter) under low vacuum pressure. Filters were kept frozen at −20°C until analysis. Extraction was performed in 90% acetone solution overnight and the measurements were performed with a TURNER TD700 fluorometer. Total chlorophyll-*a* (Chl*a*) was derived by summing up the concentrations of chlorophyll-*a* in all three size classes.

Phytoplankton Pigments

Phytoplankton pigments were determined by High Performance Liquid Chromatography analysis (HPLC). 2L seawater were filtered through GF/F filters (25 mm) under low vacuum pressure (<150 mmHg). The filters were immediately placed in liquid nitrogen and stored at −80°C until analysis. The filters were immersed in 3 mL of acetone, disrupted in an ice-bath using a sonication probe for 1.5 min (50% amplitude, 0.5 cycle) and incubated at −20°C overnight. Prior to extraction, each filter was spiked with 20 μL of an internal standard solution (β-apo-8′-carotenal 3 ng μL^{-1}). All sample extracts were clarified by centrifugation (10000 rpm for 10 min), as well as by filtration through a 0.2 μm syringe filter (Whatman ReZist, PTFE, 0.2 μm pore size, 13 mm diameter). The filter extracts were analyzed using an Agilent 1260 Infinity Binary Pump HPLC system (Agilent Technologies) equipped with a Poroshell 120 column (EC-C18, 150 × 3 mm, 2.7 μm particles; Agilent Technologies). A detailed description of the applied chromatographic conditions is provided in Lagaria et al. (2016). The abbreviations of detected pigments and calculated sums of pigments are presented in **Table 1**.

Pigment data were further processed with the CHEMTAX software (Mackey et al., 1996) in order to calculate the relative contribution of the different functional phytoplankton groups to total phytoplankton biomass (in chlorophyll units). Although several pigments are known to be present in multiple phytoplankton groups, CHEMTAX algorithm is able to break down phytoplankton composition by considering a large suite of pigments simultaneously. The selection of the chemotaxonomic groups to be included in CHEMTAX analysis was based on the main pigment markers detected by HPLC, in conjunction with observations made by flow-cytometry and optical microscopy about phytoplankton composition. To avoid potentially unreliable initial pigment:Chl*a* ratios, sixty ratio matrices were generated by adjusting each of the pigment ratios according to a random function described in Wright et al. (2009). The best 10% of the outputs, based on lower Root Mean Square (RMS) errors, were selected as starting matrices to determine the contribution of each class to TChl*a* concentration.

TABLE 1 | Abbreviations of detected pigments and calculated pigment sums.

Pigments	Abbreviation
Chlorophyll-*a*	Chl*a*
Chlorophyll c_2	Chlc_2
Chlorophyll c_3	Chlc_3
Chlorophyll *b*	Chl*b*
Zeaxanthin	Zea
19′-butanoyloxyfucoxanthin	But
19′-hexanoyloxyfucoxanthin	Hex
Peridinin	Peri
Fucoxanthin	Fuco
ββ-carotene + βε-carotene	Caro
Diadinoxanthin	Diadino
Diatoxanthin	Diato
Violaxanthin	Viola
Auxiliary photosynthetic pigments (PSC)	Chlc_2 + Chlc_3 + Chl*b* + But + Fuco + Hex + Peri
Photoprotective pigments (PPT)	Caro + Diadino + Diato + Viola + Zea
Total pigments (TP)	PSC + PPT + Chl*a*

Primary Production

Three light and one dark 320 mL polycarbonate bottles filled with seawater sample from each mesocosm bag were spiked with 5 μCi of $NaH^{14}CO_3$ tracer each and incubated in the land-based tank, under natural temperature, and daylight conditions for approximately 3 h around midday (Steemann-Nielsen, 1952). After incubation, water samples were filtered through 5, 2, and 0.2 μm polycarbonate filters (47 mm diameter) under low vacuum pressure (<50–150 mmHg). The filters were acidified in order to remove excess $NaH^{14}CO_3$ and their radioactivity (disintegrations per minute, dpm) was measured in a scintillation counter after the addition of 4 mL scintillation cocktail. Primary production rate (PP) was calculated by subtracting the dpm of the dark bottles from the respective light ones. A value of 26400 mg C m^{-3} was used for the concentration of dissolved inorganic carbon and a value of 1.05 was applied for the isotopic discrimination factor. PP corresponding to picoplankton (0.2–2 μm, pPP), small nanoplankton (2–5 μm, snPP) and larger nano- and microplankton (>5 μm, nμPP) was assessed by subtraction of the respective filters.

Phytoplankton Abundance and Carbon Biomass Estimations

For counts of cyanobacteria and autotrophic eukaryotic cells of size <2 μm that usually belong to various phytoplankton groups (Marie et al., 2006), herein called "pico-eukaryotes," 2 mL duplicate water samples were fixed with glutaraldehyde (0.5% final concentration), deep-frozen in liquid nitrogen and kept at −80°C until analysis. Analysis was performed in thawed samples without prior staining and cells were distinguished based on their autofluorescence signals in a FACSCalibur flow cytometer according to Marie et al. (1997). Carbon biomass was calculated from cell counts assuming a carbon content of 151 fg C $cell^{-1}$ for

Synechococcus sp. (mean values obtained from Bertilsson et al., 2003; Worden et al., 2004; Marañón et al., 2013) and 471 fg C cell^{-1} for pico-eukaryotes, value derived assuming a biovolume of 2.6 μm^3 cell^{-1} and the conversion factor 183 fg C μm^{-3} (Caron et al., 1995).

Counts of autotrophic nanoflagellates (ANF) were performed on 30 mL samples by applying cell fixation with borax-buffered formalin (final concentration 2% formaldehyde), filtration on black polycarbonate (Poretics) filters with 0.6 μm pore-size, staining with DAPI (Porter and Feig, 1980) and enumeration using epifluorescence microscopy. The specific cells were distinguished using UV excitation, and categorized into five size-classes (2–3 μm, 3–5 μm, 5–7 μm, 7–10 μm, and >10 μm) using an ocular micrometer. Formulas of approximate geometric shapes were used to calculate cell biovolume using the measurements of cell length and width. Then, biovolumes were converted into carbon biomass using 183 fg C μm^{-3} (Caron et al., 1995).

Counting of larger phytoplankton cells, i.e., coccolithophores, diatoms and dinoflagellates (approx. >7 mm cell size) was performed with inverted microscopy on 100 mL water samples preserved in alkaline Lugol's solution (2% final concentration; Utermöhl, 1958). They were identified down to genus or species level and the mean cell biovolume for each species/taxon was calculated using its size measures (e.g., length, width) and appropriate simulations of its geometric shape according to Hillebrand et al. (1999). Then, cell volumes were converted to carbon biomass applying appropriate conversion factors per genus or species (Verity et al., 1992; Montagnes et al., 1994).

Statistics

For comparison of the various variables among the CNT, SA, and RA treatments during the entire experimental period (D0–D9) a repeated measurements ANOVA (RM-ANOVA) was performed. For this analysis, data were log-transformed in order to meet homogeneity of variance. In addition, a principal component analysis (PCA) was performed with standardized data in order to reduce the dimensionality of variables and detect response phases of phytoplankton community to dust inputs. Selected phytoplankton parameters (e.g., chlorophyll-*a*, primary production, and chlorophyll-normalized production per size fraction, phytoplankton groups derived by CHEMTAX) were used as independent variables in PCA. Moreover, concentrations of mineral and organic nutrients (presented in Pitta et al., in review) were added as supplementary variables in order to see how they were correlated with the selected variables used to build the PCA.

RESULTS

Initial Characteristics of Sampled Seawater and Dust Additions

The surface water sampled from the Cretan Sea displayed particularly low inorganic nutrient concentrations. NO_2^- and NO_3^- were close to or in certain samples below the detection limit of the applied methods and together represented 26% of DIN. The initial DIN: PO_4^{3-} (N:P) ratio was approximately 10. Chl*a* and PP presented low values (**Table 2**) typical of surface oligotrophic waters. Cyanobacteria were only comprised by *Synechococcus* sp. populations while *Prochlorococcus* sp. were absent. *Synechococcus* sp. was the most abundant phytoplankton group, followed by pico-eukaryotes (**Table 2**). Autotrophic nanoflagellates (ANF) were mostly comprised from cells in the 2–5 μm size range, which accounted 84% of the initial ANF abundance. Dinoflagellates were mostly comprised by <20 μm cells and presented quite low abundance (**Table 2**). Very few diatoms and coccolithophores (<30 cells L^{-1}) were detected in the sampled water.

Detailed results of dust composition and nutrient analysis are presented in Pitta et al., (in review). Briefly, the amendment of each 3 m^3 mesocosm with 4 g dust resulted in adding 10 nM NH_4^+, 55 nM NO_3^-, 2 nM PO_4^{3-}, and 69 nM dissolved organic nitrogen (DON). This addition resulted in 100 and 30% enrichment of DIN and PO_4^{3-}, respectively. The temporal pattern of mineral nutrients concentrations during the experiment is presented in **Figure 1**. The concentration of DIN (**Figure 1A**) was significantly affected by dust additions (RM-ANOVA, $p < 0.001$). PO_4^{3-} concentration was slightly higher in the dust treatments, especially in the RA, than in the CNT during the first four experimental days after initial dust addition (**Figure 1B**). Nevertheless, PO_4^{3-} concentration was not found to be significantly different among treatments and CNT over the whole experimental period (RM-ANOVA, $p > 0.05$).

Response of Phytoplankton Photosynthetic Parameters

Chlorophyll-*a*

Both SA and RA dust additions caused a significant positive effect on Chl*a* concentrations as compared to CNT (RM-ANOVA, $p < 0.001$). In the SA treatment, Chl*a* presented the highest increase (by 1.8-fold) 2 days after dust addition (D2) and remained higher than CNT until Day 6, after which it decreased to CNT levels (**Figure 2A**). In the RA treatment, Chl*a* presented the highest

TABLE 2 | Initial characteristics of seawater collected for mesocosm experiments (Day 0, prior to any dust additions).

Parameter	Value
PO_4^{3-} (nM)	5.8 (±0.8)
DIN (nM)	62 (±22)
Chl*a* (μg L^{-1})	0.04 (±0.01)
PP (mg C m^{-3} h^{-1})	0.34 (±0.02)
PP^B (mg C [mg Chl*a*] h^{-1})	8.23 (±0.86)
Synechococcus sp. (cells mL^{-1})	11805 (±279)
Pico-eukaryotes (cells mL^{-1})	751 (±74)
Autotrophic nanoflagellates (cells mL^{-1})	493 (±120)
Coccolithophores (cells L^{-1})	30 (±12)
Diatoms (cells L^{-1})	30 (±12)
Dinoflagellates (cells L^{-1})	2673 (±1186)

Data represent the average values (±standard deviation) obtained from all nine mesocosm containers.

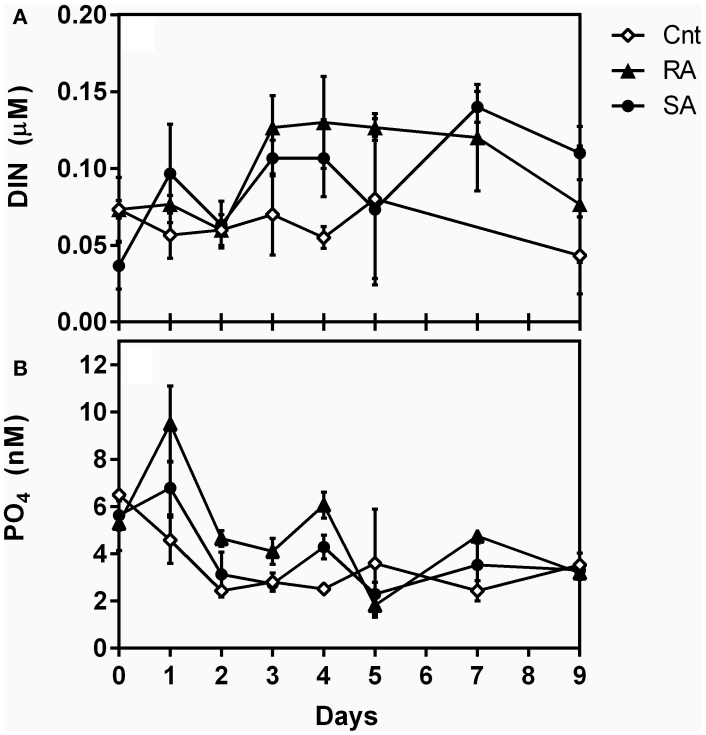

FIGURE 1 | Concentrations of (A) Dissolved inorganic nitrogen (DIN, μM) and **(B)** orthophosphate (PO_4^{3-}, nM) during the experiment. CNT, Control; RA, Repetitive Addition treatment; SA, Single Addition treatment.

increase (by 1.6-fold) on D4 and decreased to CNT level after D6 (**Figure 2A**).

The amount of chlorophyll-*a* corresponding to picoplankton (pChl*a*) was also significantly affected by dust additions (RM-ANOVA, $p < 0.01$) and presented a similar pattern to total Chl*a* (**Figure 2B**). The highest increase of pChl*a* was 2-fold on D2 in SA and 1.5-fold on D4 in RA. The amount of chlorophyll-*a* corresponding to cells >2 μm (**Figure 2C**) presented a 1.5-fold increase on D2 in both SA and RA and remained higher than CNT levels until D6 but this response was not found to be significant compared to CNT (RM-ANOVA, $p > 0.05$). However, when considering the 2–5 μm size fraction alone (data not shown), dust additions had a significant positive effect on the respective Chl*a* amount (RM-ANOVA, $p = 0.04$). On average, during the experimental period, picoplankton (0.2–2 μm) contributed 59–60% to total chlorophyll-*a*, while the contribution of 2–5 μm and >5 μm cell sizes were 19–20% and 20–21%, respectively.

Primary Production

Besides Chl*a*, primary production was also stimulated by dust additions (RM-ANOVA, $p < 0.001$). PP increased by 1.8-fold on D2 both in SA and RA and remained high until D6 after which it decreased to CNT levels (**Figure 2D**). The production rates that corresponded to picoplankton (0.2–2 μm) and to >2 μm cells were both positively affected by dust additions as compared to CNT (RM-ANOVA, $p < 0.05$ and $p < 0.01$, respectively). pPP rate increased by 1.8-fold during D1–D2 in SA and by 1.5-fold during D2–D3 in RA (**Figure 2E**) while production rate of cells >2.0 μm increased by 2.5-fold on D4 in both treatments (**Figure 2F**). On average, during the experimental period, picoplankton was responsible for 38–41% of total primary production, while phytoplankton cells of size 2–5 μm and >5 μm were responsible for 20–25% and 38–39%, respectively.

The chlorophyll-normalized production (PP^B) indicates the efficiency of producing organic carbon per unit of chlorophyll *a*. PP^B of the entire phytoplankton assemblage (**Figure 2G**) and of picoplankton (**Figure 2H**) were not affected by dust additions (RM-ANOVA, $p > 0.05$). Generally, PP^B decreased at the end of the experiment. The chlorophyll-normalized production of cells >2 μm presented higher values than picoplankton, and was significantly affected by dust additions (RM-ANOVA, $p < 0.01$). It presented a 1.7-fold increase on D4 in both treatments (**Figure 2I**).

Phytoplankton Pigments

Generally, a limited number of pigments were detected throughout the mesocosm experiment. The most abundant diagnostic pigments were Hex, Zea, But and Fuco (**Table 1**) which are typically found in Prymnesiophytes, Cyanobacteria, Pelagophytes, and Prymnesiophytes/Diatoms, respectively. Moreover, traces (< 5 ng L^{-1}) of Chl*b* (typical of Prasinophytes, Chlorophytes) and Peri (typical of Dinoflagellates) were occasionally detected. Hex increased significantly in both

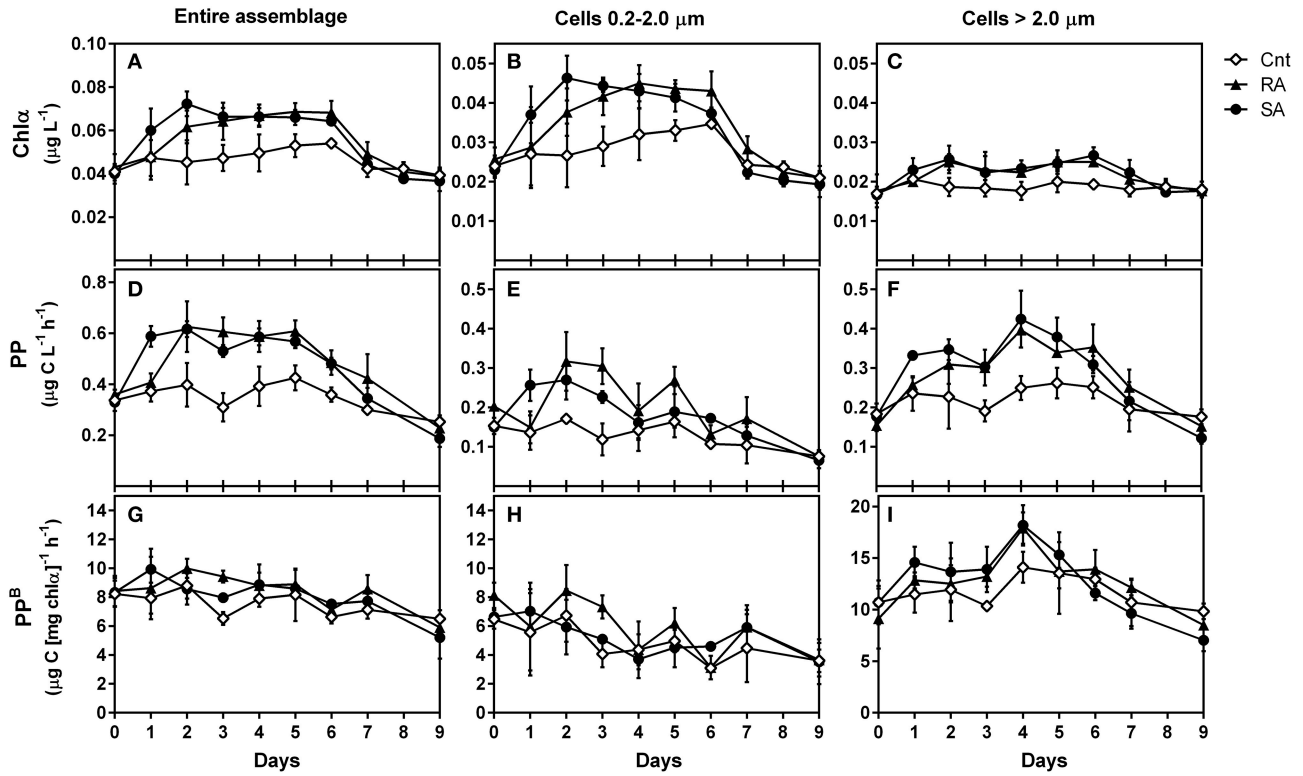

FIGURE 2 | Chlorophyll *a* (Chl*a*, μg L^{-1}), primary production (PP, μg C L^{-1} h^{-1}), and normalized-to-chlorophyll production (PP^B, μg C [μg chla]$^{-1}$ h^{-1}) for the entire phytoplankton assemblage (**A**, **D**, **G**, respectively), as well as for the 0.2–2 μm (**B**, **E**, **H**, respectively) and >2 μm (**C**, **F**, **I**, respectively) size classes during the experiment. CNT, Control; RA, Repetitive Addition; SA, Single Addition.

SA and RA as compared to CNT (RM-ANOVA, $p < 0.001$), presenting the highest concentrations on D2 and D3, respectively (**Figure 3A**). Similarly, an almost 2-fold increase was observed for But and Fuco 4 days after the initial addition of dust in both treatments (**Figures 3C,D**). Nevertheless, only the response of Fuco proved to be significantly different between CNT and dust treatments (RM-ANOVA, $p < 0.001$). Zea (**Figure 3B**) was also shown to be significantly influenced by dust additions as compared to CNT (RM-ANOVA, $p < 0.001$), but it presented a different temporal pattern compared to the other pigments; its concentration increased by 1.7-fold in both treatments on D2 and remained high during the entire experimental period.

With regard to phytoplankton pigment indices (**Table 1**), the ratio of auxiliary photosynthetic pigments to total pigments (PSC:TP) increased from 0.32 to 0.38 during the experimental days D2–D5 (**Figure 4B**). In particular, the ratio of chlorophylls *b* and *c* over TP presented slightly higher value than the CNT in the SA on D1–2 and in both SA and RA on D5 (**Figure 4A**). On the other hand, the respective ratio of photoprotective pigments (**Table 1**) showed a gradual increase after D6 followed by a sharp decrease on the last day of the experiment (**Figure 4C**). These variations were significant on the time scale (RM-ANOVA, $p < 0.01$) although no significant difference was detected among CNT and dust treatments (RM-ANOVA, $p > 0.05$).

Phytoplankton Community

Cell Abundance and Carbon Biomass

Among all identified phytoplankton groups, only picoplankton cell numbers were significantly affected by dust (RM-ANOVA, $p < 0.01$). *Synechococcus* abundance progressively increased after D1 in both treatments presenting an almost 2-fold increase on D3–D4 and remained high until the end of the experiments (**Figure 5A**). Pico-eukaryotes were also significantly affected by dust additions as compared to CNT (RM-ANOVA, $p < 0.05$); presenting higher abundances on D4 in both SA and RA compared to the CNT (**Figure 5B**). In general, the least abundant autotrophic nanoflagellates and dinoflagellates presented higher cell numbers in the SA treatment, but it was not possible to identify any statistical significant differences against the control conditions, most likely as a result of the large variance (CV = 0.3–0.6) accompanying those measurements (**Figures 5C,D**). Generally, large sized cells were not detected throughout the experimental period. Microphytoplankton cells (>20 μm), such as diatoms and large dinoflagellates, as well as larger nanoflagellates (>10 μm), were practically absent.

The carbon biomass of individual phytoplankton groups, derived from cell counts and biovolume/carbon conversion factors (see methods), followed the temporal patterns of the respective abundances, as shown in **Figure 5**. Total

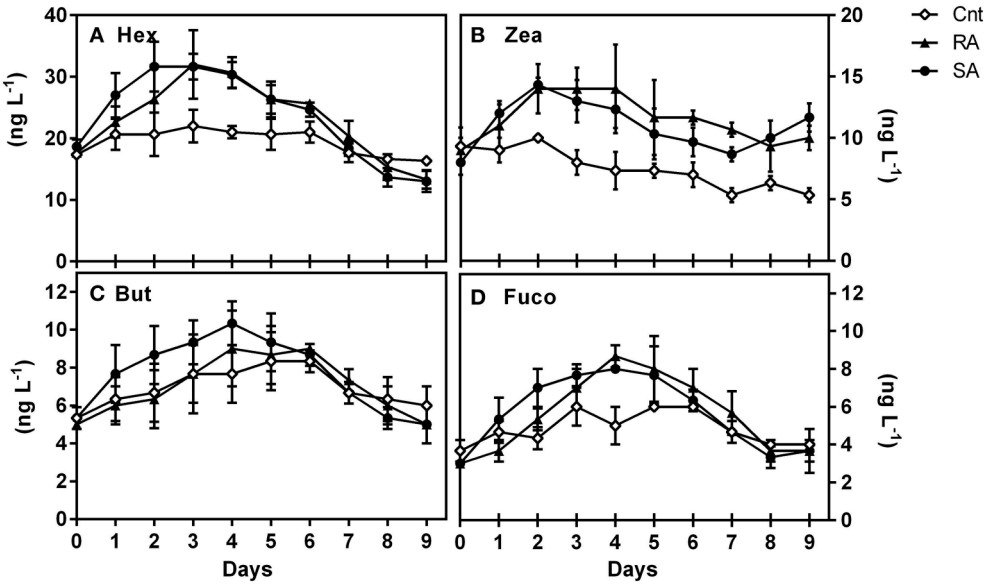

FIGURE 3 | Concentrations (ng L^{-1}) of major diagnostic pigments during the experiment, (A) 19′ hexanoyloxyfucoxanthin (Hex), **(B)** Zeaxanthin (Zea), **(C)** Fucoxanthin (Fuco), and **(D)** 19′-butanoyloxyfucoxanthin (But). CNT, Control; RA, Repetitive Addition; SA: Single Addition.

phytoplankton carbon biomass was significantly affected by dust additions (RM-ANOVA, $p < 0.01$), presenting 1.5- and 1.3-fold increase in SA and RA, respectively, on D3 (**Figure 6**). Generally, phytoplankton carbon biomass in SA was significantly higher than in RA. When considering both dust treatments, *Synechococcus* carbon biomass ranged from 1.8 to 3.3 μg C L^{-1} throughout the experimental period. It represented 45–77% of phytoplankton carbon biomass in RA and 42–77% in SA, with the highest relative contribution recorded at the end of the experiment. ANF carbon biomass ranged from 0.1 to 2.0 μg C L^{-1}, representing 4–41 and 5–44% of phytoplankton carbon biomass in the RA and SA treatment, respectively, with the minimum relative contribution recorded at the end of the experiment. In the untreated CNT, *Synechococcus* biomass ranged from 1.4 to 2.0 μg C L^{-1} while ANF biomass ranged from to 0.4 1.8 μg L^{-1}. The respective contributions were 43–63% for *Synechococcus* and 15–44% for ANF. ANF during the experimental period were mostly comprised from cells in the 2–5 μm size range (**Figure 6**) which accounted on average 64% of ANF carbon biomass. Carbon biomass of autotrophic dinoflagellates ranged from 0.10 to 0.23 μg C L^{-1} in CNT, from 0.14 to 0.29 μg C L^{-1} in RA and from 0.10 to 0.30 μg C L^{-1} in SA, constantly representing <10% of phytoplankton carbon biomass throughout the experiment (data not shown).

The carbon-to-chlorophyll (C:Chl*a*) ratio of the entire phytoplankton community, derived by total carbon biomass estimates and total chlorophyll measurements, was not significantly affected by dust additions (RM-ANOVA, $p > 0.05$). C:Chl*a* ranged on average from 62 (±10) to 101 (±2) in the CNT and from 71 (±9) to 101 (±15) in the dust treatments (RA and SA). In all cases, the highest value was recorded at D0, prior to dust additions (data not shown).

CHEMTAX Analysis of Phytoplankton Functional Groups

CHEMTAX analysis was run with the entire pigment dataset. Three phytoplankton functional groups (Prymnesiophytes, Pelagophytes, and Cyanobacteria-type 2 (for *Synechococcus* sp., Higgins et al., 2011) were selected for CHEMTAX analysis, based on the major diagnostic pigments detected (Hex, But, Fuco, Zea) and phytoplankton cells indentified by light/epifluorescence microscopy and flow-cytometry. Since diatoms were not present, fucoxanthin was attributed to Prymnesiophytes and Pelagophytes. Moreover, Zeaxanthin was entirely attributed to Cyanobacteria-type 2 (*Synechococcus* sp.), as *Prochlorococcus* sp. cells were not detected throughout the experiment. It should also be stressed that peridinin, a typical biomarker of dinoflagellates was almost undetectable in our study and thus the specific chemotaxonomic group was not included in the CHEMTAX analysis. The final pigment:Chl*a* ratios derived by CHEMTAX for the three functional groups under investigation are shown in **Table 3**.

CHEMTAX results for Cyanobacteria (**Figure 7A**) reproduced the abundance and carbon biomass pattern of *Synechococcus* (**Figure 5A**). Indeed, the levels of Cyanobacteria (in chlorophyll units) showed a strong correlation with *Synechococcus* carbon biomass ($r = 0.84$, $n = 90$, $p < 0.0001$). Moreover, prymnesiophytes (**Figure 7C**) presented a similar pattern with total Chl*a* concentrations (**Figure 2A**) while the pattern of Pelagophytes (**Figure 7B**) was similar to that of pico-eukaryotes (**Figure 5B**). The levels of prymnesiophytes and pelagophytes (in chlorophyll units) derived by CHEMTAX were compared with the carbon biomass of different size classes of flagellates (nanoflagellates and pico-eukaryotes). Prymnesiophytes presented significant correlations with all size

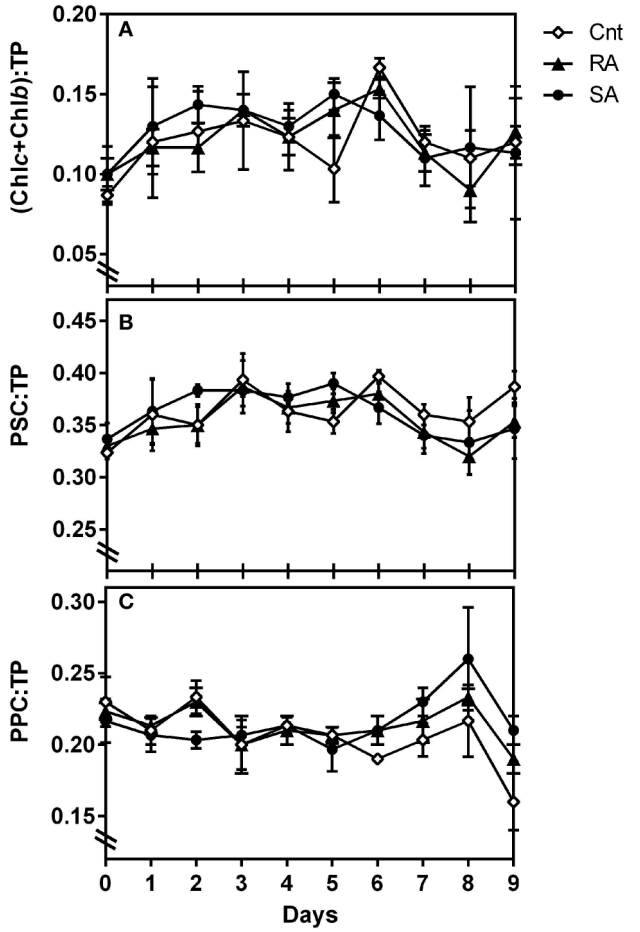

FIGURE 4 | Pigment indices (ratios) during the experiment. Chl*b*, Chlorophyll *b*; Chl*c*, Chlorophyll c_2 and c_3; PSC, Photosynthetic pigments; PPC, Protoprotective pigments; TP, Total pigments. CNT, Control; RA, Repetitive Addition; SA, Single Addition.

classes, while Pelagophytes were strongly associated only with pico-eukaryotes (**Table 4**).

Specific Characteristics of Phytoplankton Groups

The fluorometric measurements of chlorophyll-*a* per size fractions were used in conjunction with the CHEMTAX results. The amount of chlorophyll-*a* that corresponds to pico-eukaryotes ($Chla_{pEu}$) would be:

$$Chla_{pEu} = pChla - Chla_{cyano} \quad (1)$$

where pChl*a* is the amount of chlorophyll-*a* corresponding to picoplankton (<2 μm), as measured by fluorometry, and $Chla_{cyano}$ is the amount of chlorophyll-*a* corresponding to Cyanobacteria (*Synechococcus* sp.), as derived by CHEMTAX. As revealed in the previous section, pelagophytes belonged entirely to the picoplankton size class. Consequently, the fluorometrically measured chlorophyll-*a* in cells >2 μm ($Chla_{>2}$) may be attributed only to Prymnesiophytes that fall within the nanoplankton size fraction ($Chla_{prymne>2}$). Thus:

$$Chla_{>2} = Chla_{prymne>2} \quad (2)$$

Meanwhile, the amount of chlorophyll-*a* that corresponds to pico-eukaryotes ($Chla_{pEu}$) estimated from Equation (1) may be attributed to both pelagophytes ($Chla_{pelago}$) and prymnesiophytes that fall within the picoplankton size fraction ($Chla_{prymne<2}$). Therefore:

$$Chla_{pEu} = Chla_{pelago} + Chla_{prymne<2} \quad (3)$$

Using these equations, pico-eukaryotes in the CNT mesocosms were calculated to consist of 42% prymnesiophytes and 58% pelagophytes. Assuming that this composition is also applicable to cell counts and carbon biomass of pico-eukaryotes, we estimated the cellular pigment amount of each group (**Table 5**). We here present values only from the CNT mesocosms. The respective values from SA and RA did not exhibit any significant differences from CNT.

Phytoplankton Response to Dust Additions through PCA

To further evaluate the response of phytoplankton community among the different samples (sampling days of CNT, SA, and RA) principal component analysis (PCA) was applied. The phytoplankton parameters used as independent variables in this analysis included chlorophyll-*a*, primary production and chlorophyll-normalized production per size fraction, as well as biomass of cyanobacteria, pelagophytes and prymnesiophytes (in chlorophyll units as derived from CHEMTAX analysis), while the concentrations of mineral and organic nutrients were used as supplementary variables. The first two principal components (PCs) explained 61.3 and 16.2%, respectively, of the total variance of phytoplankton data. The score plot of PC1 versus PC2 describes the relationships among samples (**Figure 8A**), while the relationships among variables are displayed in the loading plot of PC1, PC2 (**Figure 8B**). According to the score plot (**Figure 8A**), two clusters of samples were spotted in the lower left and upper left quadrant, indicating significant differences in phytoplankton community. Both clusters were well separated from the other samples along the first principal component while they segregated from each other along the second principal component (**Figure 8A**). The samples on the right side of PCA plot included all sampling days of CNT and the last sampling days (D7–D9) of RA and SA treatments, representing the untreated mesocosm conditions and the end of treatment status. The cluster in the lower left side of the plot included D1–D2 of SA and D2–D3 of RA, representing a first response phase of the phytoplankton community while the cluster in the upper left side of the panel included D3–D5 of SA and D4–D5 of RA, representing a second phase of response. According to the loadings plot (**Figure 8B**), the first cluster of samples (lower left quadrant) was mostly characterized by higher normalized-production rates of picoplankton (pPP^B) which were correlated with PO_4^{3-} and DON, as shown by their position on PC2. The second cluster (upper, left quadrant) was characterized by relatively higher concentration of Pelagophytes and higher chlorophyll normalized-production rate of cells >5.0 μm ($n\mu PP^B$), which were correlated with DIN concentration.

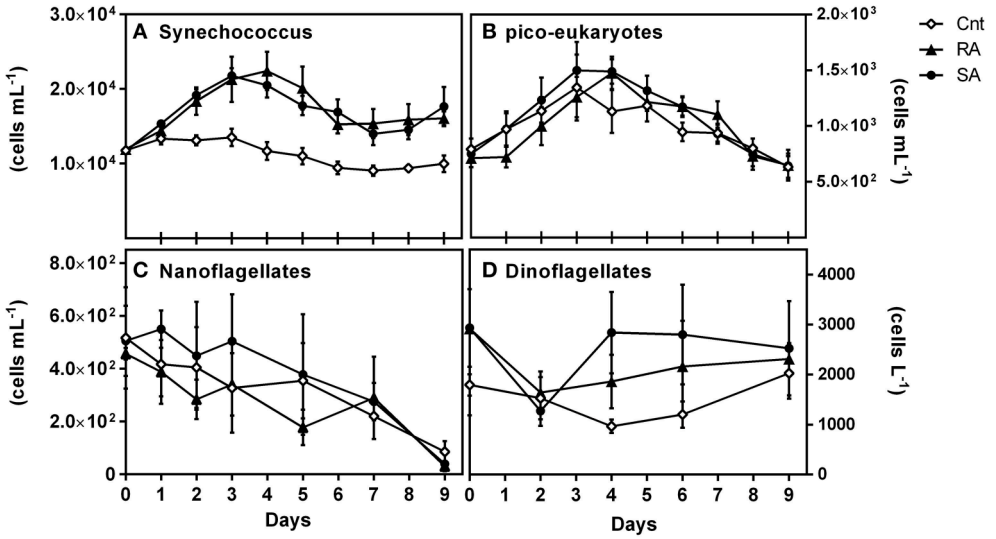

FIGURE 5 | Abundances of (A) *Synechococcus* sp. (cells mL^{-1}), **(B)** pico-eukaryotes (cells mL^{-1}), **(C)** Nanoflagellates (cells mL^{-1}) and **(D)** Dinoflagellates (cells L^{-1}) during the experiment. CNT, Control; RA, Repetitive Addition; SA, Single Addition.

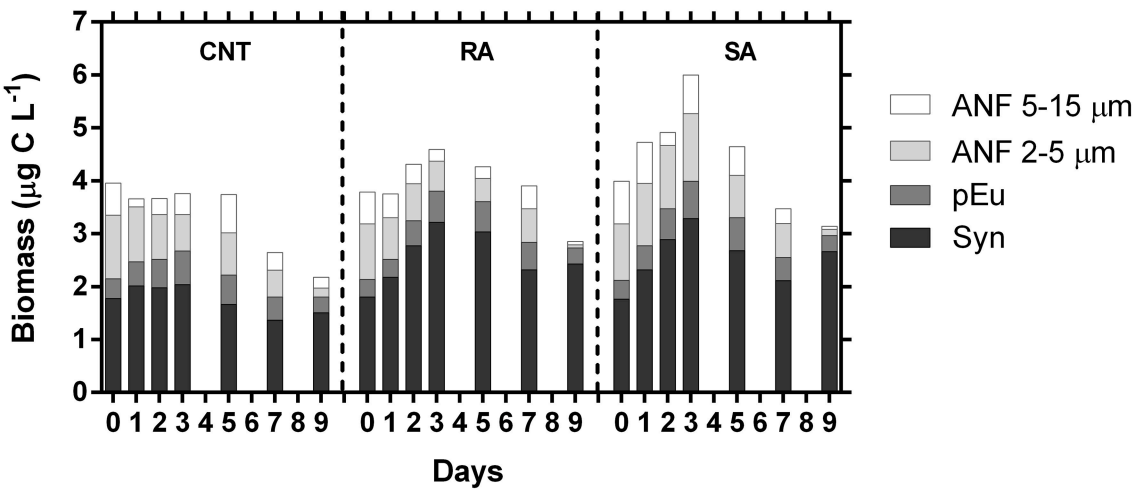

FIGURE 6 | Estimated carbon biomass ($\mu g\ C\ L^{-1}$) of major phytoplankton groups during the experiment. ANF, Autotrophic nanoflagellates; pEu, pico-Eukaryotes; Syn, *Synechococcus* sp. CNT, Control; RA, Repetitive Addition; SA, Single Addition.

DISCUSSION

The Effect of Dust Addition Treatments on Phytoplankton Activity and Structure

In the present study, mesocosm experiments were performed using ultra-oligotrophic surface waters from the east Mediterranean basin (Cretan Sea) in order to investigate the short-term response of phytoplankton community to Saharan dust deposition. It is known that phytoplankton community in the surface waters of the east Mediterranean Sea presents N and P co-limitation during the spring/summer period (Psarra et al., 2005; Thingstad et al., 2005; Zohary et al., 2005; Pitta et al., 2016; Tsiola et al., 2016). Initial conditions revealed the oligotrophic status of the collected seawater presenting particularly low concentrations of nutrients and chlorophyll as well as an apparent N-deficiency (N:P = 10). However, this N:P ratio includes certain elements of uncertainty, since concentrations of NO_3^- and NO_2^- were close to the detection limit of the applied method. A single addition of ca. 1.3 $\mu g\ L^{-1}$ Saharan dust in mesocosms seawater (SA treatment), representing natural deposition events in the east Mediterranean, caused the enrichment of initial DIN and PO_4^{3-} concentrations by 100 and 30%, respectively. This enrichment, in turn, resulted in stimulating total chlorophyll-*a* concentration and primary production by almost 2-folds for a time period of 6 days. An increase of the overall phytoplankton carbon biomass was also

TABLE 3 | Final optimized pigment ratios of the three phytoplankton functional groups under investigation, as determined by CHEMTAX analysis.

Class/Pigment	Chlc_2:Chl*a*	Chlc_3:Chl*a*	But:Chl*a*	Fuco:Chl*a*	Hex:Chl*a*	Zea:Chl*a*
Prymnesiophytes	0.23	0.12	0.01	0.08	0.66	
Pelagophytes	0.58	0.07	0.64	0.27	0.01	
Cyanobacteria						0.66

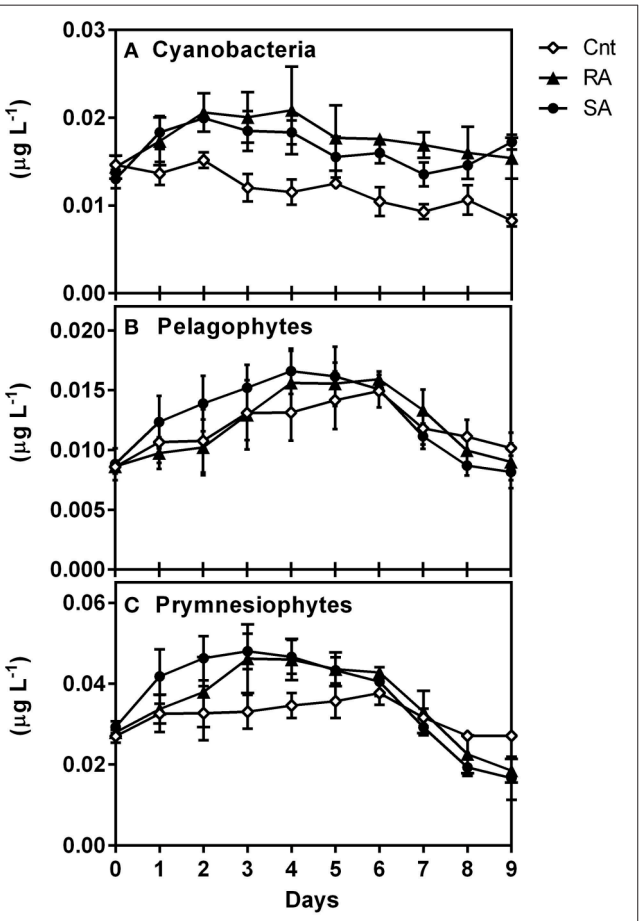

FIGURE 7 | Response of phytoplankton groups to dust additions as determined by pigment/Chemtax analysis (in chlorophyll units, µg L^{-1}), (A) Cyanobacteria, **(B)** Pelagophytes and **(C)** Prymnesiophytes. CNT, Control; RA, Repetitive Addition; SA, Single Addition.

TABLE 4 | Pearson's correlation matrix of Pelagophytes and Prymnesiophytes (in chlorophyll units, µg L^{-1}) determined by CHEMTAX analysis with carbon biomass (µg C L^{-1}) of different size classes of flagellates.

	PEu	ANF (2–5 µm)	ANF (>5 µm)
Pelagophytes	0.78** ($n = 89$)	ns	ns
Prymnesiophytes	0.52** ($n = 89$)	0.53** ($n = 61$)	0.29 ($n = 59$)*

*ANF, autotrophic nanoflagellates; pEu, pico-eukaryotes; **$p < 0.0001$, *$p < 0.05$, ns, non significant; n, number of samples.*

observed, but this effect was less pronounced (1.5-fold). The positive response of phytoplankton to dust addition is largely in accordance with many previous microcosm and mesocosm experiments performed in oligotrophic low nutrients low chlorophyll (LNLC) sites, such as in the east ((Herut et al., 2005); Tsagaraki et al., in review) and west Mediterranean basins (Bonnet et al., 2005; Lekunberri et al., 2010; Romero et al., 2011; Ridame et al., 2014), in the Atlantic Ocean (Marañón et al., 2010) and in South China Sea (Guo et al., 2012).

Besides the single-addition experiment, additional mesocosm containers were subjected to three consecutive inoculations with smaller amounts of Saharan dust (RA treatment) in order to better simulate the recurrent pattern of Saharan dust events in the eastern Mediterranean, where continuing dust deposition events may occur over a period of several days (Meloni et al., 2008; Gaetani and Pasqui, 2014; Vincent et al., 2016). The sum of the three dust additions equaled the amount of dust added in the SA treatment. Interestingly, the combination of the three successive inoculations of Saharan dust resulted in a similar response of the phytoplankton assemblage to the single addition, both quantitatively and qualitatively. However, the response of the system in the RA treatment showed a 1-day delay, as compared to the SA treatment. In particular, the first addition of dust did not exert any discernible effect either on total chlorophyll-*a* or on primary production rate, but both parameters increased significantly after the second dust addition. These results indicate that small consecutive dust events may trigger ecosystem productivity in a similar way to single larger deposition events, at least when they are of an overall equivalent level and exceed a certain threshold. In our study, this threshold was reached after the second dust addition in RA (3 g dust in total) which corresponded to a final concentration of 1 µg L^{-1}. To our knowledge, there are no previous studies investigating the impact of successive dust additions in ultra-oligotrophic systems, while only one mesocosm study has been conducted in the west Mediterranean (DUNE experiment) where a secondary addition was performed 6 days after the initial one (Guieu et al., 2014). In that study, the first addition of dust caused an increase of the NO_3^- concentration and the consequent enhancement of both chlorophyll-*a* and primary production for a time period of 6 days (Ridame et al., 2014), which was similar to that experienced in our study. The second addition, 6 days later, caused the increase of both NO_3^- and PO_4^{3-} concentrations for several days and resulted in even larger increases of phytoplankton biomass and production (Ridame et al., 2014).

It is of particular interest that in our study chlorophyll-*a* and primary production rates presented maxima 1–2 days after initial dust addition and remained higher than those in the untreated controls for 6 days. This temporal pattern is different

TABLE 5 | Cellular pigments' concentration (fg cell^{-1}) and carbon-to-chlorophyll ratio of the three major phytoplankton functional groups.

	Cyanobacteria	Pelagophytes	Prymnesiophytes <2 μm	Prymnesiophytes 2–7 μm
Zea (fg cell^{-1})	0.67 ± 0.10			
Fuco (fg cell^{-1})		6 ± 2	0.18 ± 0.05	0.58 ± 0.22
But (fg cell^{-1})		14 ± 4	0.02 ± 0.01	0.07 ± 0.03
Hex (fg cell^{-1})		0.22 ± 0.06	1.45 ± 0.38	4.76 ± 1.84
Chl*a* (fg cell^{-1})	1.06 ± 0.15	22 ± 6	22 ± 6	72 ± 28
Carbon (fg cell^{-1})*	151	471	471	2164–3721
C:Chl*a*	143	21	21	30–51

**Assumed or estimated from biovolume measurements, see methods.*

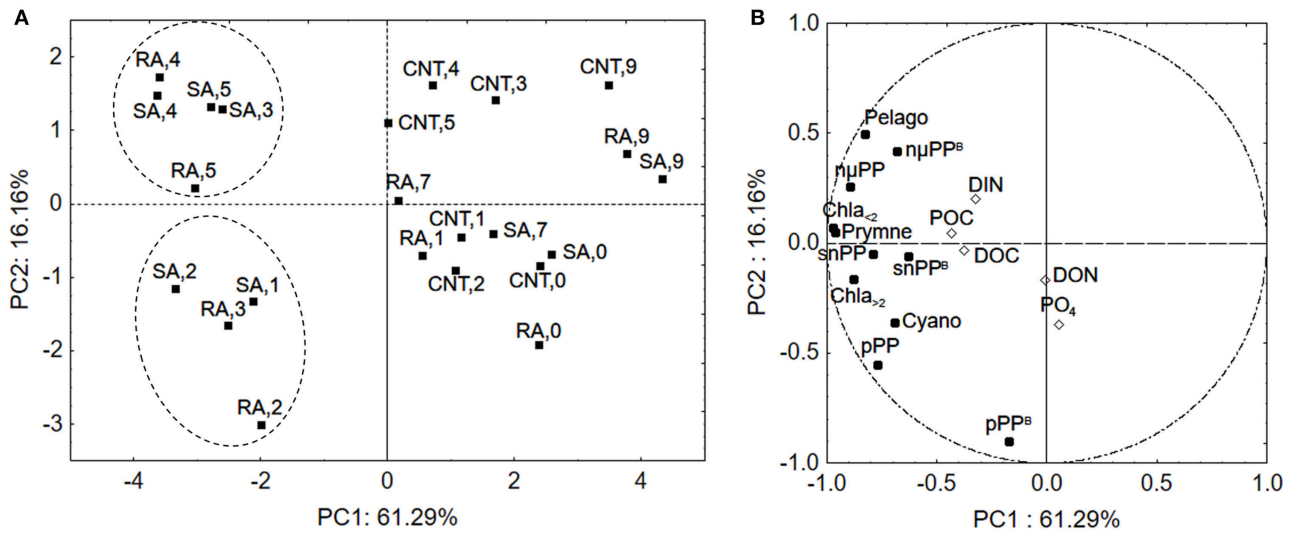

FIGURE 8 | Principal Component Analysis (A) score plot and **(B)** loading plot for phytoplankton community in samples. The numbers represent the experimental days for CNT, Control; RA, Repetitive Addition; SA, Single Addition. DIN, Dissolved inorganic nitrogen; PO_4, Orthophosphate; DOC, Dissolved organic carbon; DON, Dissolved organic nitrogen; POC, Particulate organic carbon; $Chla_{<2}$, $Chla_{>2}$: Chlorophyll-*a* of cells <2 μm and >2 μm, respectively, pPP, snPP, nmPP: Production rates of cells <2 μm, 2–5μm, >5μm, respectively, pPP^B, $snPP^B$, $nmPP^B$: Chlorophyll-*a* normalized production rates of cells <2 μm, 2–5μm, >5μm, respectively, Cyano, Cyanobacteria; Pelago, Pelagophytes; Prymne, Prymnesiophytes.

than what has been observed in previous mesocosm experiments investigating the response of Cretan Sea surface waters to the addition of inorganic nutrients (N and/or P) during summer, where chlorophyll-*a* and production reached maxima at the fourth experimental day and decreased thereafter (Pitta et al., 2016). A basic difference is the level of nutrients concentrations in the two studies. The study of Pitta et al. (2016) was conducted during late summer (September) and concentrations of mineral nutrients were steadily close to or below detection limits, while concentrations were comparatively higher in our study. However, the relatively elongated period of phytoplankton response could also be attributed to dissimilarities in the response of the various phytoplankton size groups. By using PCA, we were able to distinguish two phases of phytoplankton response. The first phase, 1–2 days after first additions, was characterized by higher normalized-to-chlorophyll production rates of picoplankton while the second one, three to 4 days after initial dust additions, was mostly associated with higher normalized-to-chlorophyll production rate of the larger cells (>5 μm). In the DUNE experiment, it was also found that primarily picoplankton responded to first dust input while the second addition led to increases of nano- and microplankton (Giovagnetti et al., 2013).

Picoplankton is known to prevail under oligotrophic conditions and surface seawaters in particular, characterized by an extreme depletion of nutrients and high irradiances, as they are believed to have an ecological advantage over bigger phytoplankton cells in these environments (Magazzù and Decembrini, 1995; Raven et al., 2005; Veldhuis et al., 2005; Siokou-Frangou et al., 2010), due to their competent capacity to acquire nutrients (Agawin et al., 2000). This competitive advantage of small cells is generally attributed to their higher surface area to volume ratios, which facilitate the diffusion of nutrients through cell membranes (Moore et al., 2013). Another factor that governs nutrient uptake by phytoplankton cells is the binding affinity of nutrients with the transport proteins embedded in the cell's membrane. For example, high affinity transporters operate most efficiently at low substrate concentrations (Lin et al., 2016). In a study performed in the

Mediterranean Sea, it was shown that *Synechococcus* cells, have a high affinity for orthophosphate and higher uptake rates than eukaryotic autotrophs (Moutin et al., 2002). In our study, *Synechococcus* represented the largest part of picoplankton assemblage both in terms of abundance and carbon biomass while PCA showed that the higher normalized production rate of picoplankton was correlated with PO_4^{3-} concentration indicating that picoplankton was most probably, quickly favored by bioavailable phosphorus released from dust particles. Additionally, as shown by PCA analysis, it is possible that DON released from dust particles played an auxiliary role in stimulating cyanobacteria, in the first response phase. This is not suprising since there is evidence that cyanobacteria can assimilate some small labile components of DON (Zubkov et al., 2003; Wawrik et al., 2009). DIN seemed to accumulate after the first two experimental days (**Figure 1**) mostly influencing the larger phytoplankton cells in the second response phase as shown by PCA analysis.

The effect of dust additions on carbon biomass *o*f phytoplankton groups was less evident than the response of chlorophyll-*a* and primary production. Partly, this may be due to the large standard variations of cell counts. However, the difference in the response between the photosynthetic parameters and carbon biomass may be also explained by intracellular cycling of newly fixed carbon (Marra, 2009; Halsey et al., 2010). It has been proposed that newly fixed carbon may be catabolized for ATP and reductant generation within the period of a cell cycle (Halsey et al., 2010, 2013). The increase of phytoplankton carbon biomass was mostly attributed to the accumulation of *Synechococcus* sp., which was found to represent >70% of phytoplankton carbon biomass at the end of the experiment. A slight effect was also observed for picoeukaryotes, the cell numbers and carbon biomass of which presented a modest increase at the fourth experimental day. With the exception of picoplankton groups, no significant effect of dust was found on the carbon biomass of any other group. To note that, microscope analysis showed that particularly large cells such as microplanktonic diatoms or dinoflagellates were practically absent. Abundance and carbon biomass of nanoflagellates significantly decreased during the experiment, although production of cells >2.0 μm showed a positive response to dust addition. This implies that there was a strong grazing pressure on them. It was found that ciliates which are their main predators presented an increase at the end of the experiment (Pitta et al., in review). Furthermore, recent studies have shown that many small flagellates may be mixotrophic, grazing on cyanobacteria and heterotrophic bacteria (Frias-Lopez et al., 2009; Unrein et al., 2014). The decline of populations of mixotrophic nanoflagellates would extenuate their grazing pressure on cyanobacteria, resulting in the accumulation of the latter as was observed in our study.

The Effect of Dust Additions on Physiological Characteristics of Phytoplankton Cells

In both RA and SA, primary production rates reached maximum values quicker than the respective chlorophyll-*a* or carbon biomass, indicating that the phytoplankton assemblage quickly became metabolically active by assimilating the new nutrients released from dust particles, but without resulting in the built up of new biomass. An increase of the auxiliary photosynthetic pigments (**Table 1**) would promote the efficiency of the photosynthetic rate, since their role is to extend the range of light that can be absorbed and used for photosynthesis (Brunet et al., 2011). Indeed, pigment analysis showed that the relative importance of accessory photosynthetic pigments (e.g., Chl*c* in particular), over total pigments increased after dust additions (**Figure 4**). Although this increase was not found to be statistically significant among treatments, it may still represent a meaningful finding. It has been shown that pigment ratios generally present small variations due to co-variations of pigments and chlorophyll-*a* (Trees et al., 2000; Rodríguez et al., 2006). In the DUNE experiment, a similar chlorophyll-*a* and production response pattern was observed, with primary production presenting 2-fold increase 24 h after dust addition while chlorophyll increased rather gradually (Ridame et al., 2014). In that study, it was found that cellular pigment concentrations increased after dust additions (Giovagnetti et al., 2013).

The normalized-to-chlorophyll production of larger cells was estimated to be much higher than that of picoplanktonic cells, implying that larger cells were more efficient in producing organic carbon per unit of chlorophyll *a*. In particular, picoplankton was found to account for approximately 60% of the total chlorophyll and 40% of the total primary production, while the respective contributions of the >2 μm cells were 40 and 60%. Such a disproportionate contribution of picoplankton cells to phytoplankton biomass and production has been also reported in previous studies (Marañón et al., 2001; Fernández et al., 2003), and it has been suggested to result from the higher light utilization efficiency of larger phytoplankton cells.

Pigment/CHEMTAX analysis (**Figure 7**) generally reproduced the response patterns observed by cell counts (**Figure 5**) and enabled the identification of the major phytoplankton taxa present in our experiment (*Synechococcus*, Pelagophytes, and Prymnesiophytes). In combination with cell counts, pigment/CHEMTAX analysis showed that Prymnesiophytes belonged both to picoplankton and nanoplankton size class while Pelagophytes belonged entirely to picoplankton (**Table 4**). The combination of all methods (pigment/CHEMTAX analysis, cell counts and fluorometric chlorophyll-*a* measurements per size fraction) enabled also the determination of some characteristics of the three groups, such as cellular pigment concentrations and C:Chl*a* ratios (**Table 5**). For example, the cellular zeaxanthin content of *Synechococcus* was found to be 0.67 fg cell^{-1} on average. This value is lower than values reported from cultures under nutrient replete conditions (Kana et al., 1988), but within the range of values reported from the DUNE experiment with natural surface populations (Giovagnetti et al., 2013). Studies have shown that nutrients regime may influence the cellular content of pigments and that under nutrient-depletion conditions, as is the case of Mediterranean surface waters, the pigment

content may be reduced (Kana and Glibert, 1987; Morel et al., 1993; Henriksen et al., 2002). In the DUNE experiment, for example, where the concentrations of mineral nutrients after dust additions increased by several-folds, much more than in our experiment (e.g., >20-fold for NO_3^- reaching concentrations >3 μM), it was found that cellular zeaxanthin content increased (Giovagnetti et al., 2013; Ridame et al., 2014). In our study, the estimated cellular pigment concentrations and C:Chl*a* ratios of specific phytoplankton groups in our experiments, were not found to be significantly affected by dust additions. This may be attributed to the relatively smaller amounts of mineral nutrients released from dust particles (e.g., <60 nM for NO_3^-).

It is worth mentioning that, while such specific phytoplankton parameters are of great importance for both experimental and modeling studies, it is particularly difficult to assess their actual values when dealing with complex datasets from natural populations. The present mesocosm experiments offer valuable estimates for those parameters and specific results are here summarized for the CNT mesocosms. Our estimates of the cellular chlorophyll-*a* content (**Table 4**) are generally within the range of values reported so far for picoplankton which are derived considering together prokaryotic and eukaryotic cells of size <2 μm (Brunet et al., 2006, 2008; Giovagnetti et al., 2013). In our study, due to the absence of large sized cells and the few phytoplankton taxa present, we were able to provide separate values for prokaryotic and eukaryotic cells. Our results showed that *Synechococcus* presented much lower cellular chlorophyll-*a* concentrations than pico-eukaryotes (**Table 4**), while they presented the highest C:Chl*a* ratios (∼140). All these estimates should be generally used with caution since they are strongly affected by both the pigment:Chl*a* ratios used and the chosen carbon conversion factors. In particular, CHEMTAX optimizes pigment:Chl*a* ratios for each specific data set (Mackey et al., 1998), which in our case concerns populations in surface ultra-oligotrophic waters collected in early summer and consequently may not be relevant in other areas, depth layers or seasons. Moreover, a higher cellular carbon concentration for *Synechococcus*, e.g., 250 fg C $cell^{-1}$ (Kana and Glibert, 1987), would result in a C:Chl*a* ratio around 235, while higher cellular carbon concentrations for pico-eukaryotes, such as 530 fg C $cell^{-1}$ (Worden et al., 2004) and 836 fg C $cell^{-1}$ (Verity et al., 1992) would result in a C:Chl*a* around 24 and 38, respectively. In spite of the variability of estimates, our results showed that there were differences in the intrinsic properties between *Synechococcus* and pico-eukaryotes populations which may be indicative of their different response patterns to dust additions.

Moreover, the estimated C:Chl*a* of the entire phytoplankton assemblage which ranged between 62 and 101, as derived from phytoplankton carbon biomass and total chlorophyll measurements, seems as a rough mean value of the cellular C:Chl*a* ratios of the major phytoplankton groups reported above. This highlights the fact that C:Chl*a* ratio, a parameter often requested in modeling studies and used as a constant (Tsiaras et al., in review), varies in function of both carbon biomass and cellular chlorophyll as well as in function of community composition. Nevertheless, the estimated range of C:Chl*a* in our study is in accordance with values reported from surface oligotrophic waters in the Aegean Sea (Lagaria et al., 2016), the Sargasso Sea (Malone et al., 1993), and the Atlantic Ocean (Marañón, 2005).

In summary, Saharan dust additions representing two different patterns of natural atmospheric deposition events in ultra-oligotrophic seawater of the eastern Mediterranean Sea during early summer, resulted in stimulating phytoplankton production and to a lesser degree carbon biomass for a time period of 6 days. The two patterns of dust deposition events (SA and RA) tested in our study were found to have similar impact on the system. Our results showed that picoplankton was quickly favored by the small amounts of new nutrients released from dust particles, especially from bioavailable phosphorus, to be followed by nanoplankton cells, 2 days later, mostly favored by increased mineral nitrogen levels. Additionally, our findings highlighted differences in the intrinsic properties (cellular pigment amounts, C:Chl*a* ratios) of prokaryotic and eukaryotic cells. Our study indicates that Saharan dust deposition events taking place in the east Mediterranean Sea may be significant over the ecological timescales of some days to 1 week and further highlights the importance of atmospheric deposition on the productivity and functioning of LNLC ecosystems.

AUTHOR CONTRIBUTIONS

Planning of the original experimental design and carrying out of experiment and sampling: AL, PP, AT, and SP. Pigment analysis: AL and MM. Chlorophyll a fluorometric analysis: NP. Flow cytometry cell counting: AT. Light microscopy cell counting: PM. Epifluorescence microscopy cell counting: MK. Writing up manuscript and critical reading/revision: AL, MM, PP, AT, and SP.

ACKNOWLEDGMENTS

The ADAMANT project—"Atmospheric deposition and Mediterranean sea water productivity" (project code nr/MIS:383551) was implemented through the Operational Program "Education and Lifelong Learning 2007–2013" (CCI:2007GRO5UPO002) of the National Strategic Reference Framework (NSRF), more specifically through the Research Funding Program: "THALES" and has been co–financed by the European Union (European Social Fund— ESF) and Greek national funds. Funding was also provided by the AegeanMarTech project ("THALES" project code nr/MIS:383548) through grants to AL and PM. We wish to thank E. Dafnomili and S. Zivanovic for support with nutrients analysis.

REFERENCES

Agawin, N. S. R., Duarte, C. M., and Agustí, S. (2000). Nutrient and temperature control of the contribution of picoplankton to phytoplankton biomass and production. *Limnol. Oceanogr.* 45, 591–600. doi: 10.4319/lo.2000.45.3.0591

Bertilsson, S., Berglund, O., Karl, D. M., and Chisholm, S. W. (2003). Elemental composition of marine *Prochlorococcus* and *Synechococcus:* implications for the ecological stoichiometry of the sea. *Limnol. Oceanogr.* 48, 1721–1731. doi: 10.4319/lo.2003.48.5.1721

Bonnet, S., Guieu, C., Chiaverini, J., Ras, J., and Stock, A. (2005). Effect of atmospheric nutrients on the autotrophic communities in a low nutrient, low chlorophyll system. *Limnol. Oceanogr.* 50, 1810–1819. doi: 10.4319/lo.2005.50.6.1810

Brunet, C., Casotti, R., and Vantrepotte, V. (2008). Phytoplankton diel and vertical variability in photobiological responses at a coastal station in the Mediterranean Sea. *J. Plankton Res.* 30, 645–654. doi: 10.1093/plankt/fbn028

Brunet, C., Johnsen, G., Lavaud, J., and Roy, S. (2011). "Pigments and photoacclimation processes," in *Phytoplankton Pigments,* eds Z. Roy, C. Llwellyn, E. S. Egeland, and G. Johnsen (New York, NY: Cambridge University Press), 445–471.

Brunet, C., Gasotti, R., Vantrepotte, V., Corato, F., and Conversano, F. (2006). Picophytoplankton diversity and photoacclimation in the Strait of Sicily (Mediterranean Sea) in summer. I. Mesoscale variations. *Aquat. Microb. Ecol.* 44, 127–141. doi: 10.3354/ame044127

Caron, D., Dam, H. G., Kremer, P., Lessard, E. J., Madin, L. P., Malone, T. C., et al. (1995). The contribution of microorganisms to particulate carbon and nitrogen in surface waters of the Sargasso Sea near Bermuda. *Deep Sea Res. I* 42, 943–972. doi: 10.1016/0967-0637(95)00027-4

Christodoulaki, S., Petihakis, G., Kanakidou, M., Mihalopoulos, N., Tsiaras, K., and Triantafyllou, G. (2013). Atmospheric deposition in the Eastern Mediterranean. A driving force for ecosystem dynamics. *J. Mar. Syst.* 109–110, 78–93. doi: 10.1016/j.jmarsys.2012.07.007

Engelstaedter, S., Tegen, I., and Washington, R. (2006). North African dust emissions and transport. *Earth Sci. Rev.* 79, 73–100. doi: 10.1016/j.earscirev.2006.06.004

Fernández, E., Maranón, E., Morán, X. A. G., and Serret, P. (2003). Potential causes for the unequal contribution of picophytoplankton to total biomass and productivity in oligotrophic waters. *Mar. Ecol. Prog. Ser.* 254, 101–109. doi: 10.3354/meps254101

Frias-Lopez, J., Thompson, E., Waldbauer, J., and Chiisholm, S. W. (2009). Use of stable isotope-labelled cells to identify active grazers of picocyanobacteria in ocean surface waters. *Environ. Microbiol.* 11, 512–525. doi: 10.1111/j.1462-2920.2008.01793.x

Gaetani, M., and Pasqui, M. (2014). Synoptic patterns associated with extreme dust events in the Mediterranean Basin. *Reg. Environ. Change* 14, 1847–1860. doi: 10.1007/s10113-012-0386-2

Gallisai, R., Peters, F., Volpe, G., Basart, S., and Baldasano, J., M (2014). Saharann dust deposition may affect phytoplankton growth in the Mediterranean Sea at ecological time scales. *PLoS ONE* 9:e110762. doi: 10.1371/journal.pone.0110762

Giovagnetti, V., Brunet, C., Conversano, F., Tramontano, F., Obernosterer, I., Ridame, C., et al. (2013). Assessing the role of dust deposition on phytoplankton ecophysiology and succession in a low-nutrient low-chlorophyll ecosystem: a mesocosm experiment in the mediterranean sea. *Biogeosciences* 10, 2973–2991. doi: 10.5194/bg-10-2973-2013

Guieu, C., Dulan, G., Rodame, C., and Pondaven, P. (2014). Introduction to project DUNE, a DUst experiment in a low nutrient, low chlorophyll ecosystem. *Biogeosciences* 11, 425–442. doi: 10.5194/bg-11-425-2014

Guo, C., Yu, J., HO, Y.-T., Wang, L., Song, S., Kong, L., et al. (2012). Dynamics of phytoplankton community structure in the South China Sea in response to the East Asian aerosol input. *Biogeosciences* 9, 1519–1536. doi: 10.5194/bg-9-1519-2012

Halsey, K. H., Milligan, A. J., and Behrenfeld, M. J. (2010). Physiological optimization underlies growth rate-independent chlorophyll-specific gross and net primary production. *Photosynth. Res.* 103, 125–137. doi: 10.1007/s11120-009-9526-z

Halsey, K. H., O'Malley, R. T., Graff, J. R., Milligan, A. J., and Behrenfeld, M. J. (2013). A common partitioning strategy for photosynthetic products in evolutionarily distinct phytoplankton species. *New Phytol.* 198, 1030–1038. doi: 10.1111/nph.12209

Henriksen, P., Riemann, B., Kaas, H., Sørensen, H. M., and Sørensen, H. L. (2002). Effects of nutrient-limitation and irradiance on marine phytoplankton pigments. *J. Plankton Res.* 24, 835–858. doi: 10.1093/plankt/24.9.835

Herut, B., Zohary, T., Krom, M. D., Mantoura, R. F. C., Piita, P., Psarra, S., et al. (2005). Response of East Mediterranean surface water to Saharann dust: on-board microcosm experiment and field observations. *Deep Sea Res. II* 52, 3024–3040. doi: 10.1016/j.dsr2.2005.09.003

Higgins, H. W., Wright, S. W., and Schlüter, L. (2011). "Quantitative interpretation of chemotaxonomic pigment data," in *Phytoplankton Pigments,* eds Z. Roy, C. Llwellyn, E. S. Egeland, and G. Johnsen (New York, NY: Cambridge University Press), 257–313.

Hillebrand, H., Dürselen, C. D., Kirschtel, D., Pollingher, U., and Zohary, T. (1999). Biovolume calculation for pelagic and benthic microalgae. *J. Phycol.* 35, 403–424. doi: 10.1046/j.1529-8817.1999.3520403.x

Holm-Hansen, O., Lorenzen, C. J., Holmes, R. W., and Strickland, J. D. H. (1965). Fluorometric determination of chlorophyll. *J. Cons. Perm. Int. Explor. Mer.* 30, 3–15.

Ignatiades, L., Gotsis-Skretas, O., Pagou, K., and Krasakopoulou, E. (2009). Diversification of phytoplankton community structure and related parameters along a large-scale longitudinal east-west transect of the Mediterranean Sea. *J. Plankton Res.* 31, 411–428. doi: 10.1093/plankt/fbn124

Kana, T. M., and Glibert, P. M. (1987). Effect of irradiance up to 2000 E m^{-2} s^{-1} on marine Synechococcus WH7803-I. Growth, pigmentation, and cell composition. *Deep Sea Res.* 34, 479–495. doi: 10.1016/0198-0149(87)90001-X

Kana, T. M., Glibert, P. M., Goericke, R., and Welschmeyer, N. (1988). Zeaxanthin and β-carotene in Synechococcus WH7803 respond differently to irradiance. *Limnol. Oceanogr.* 33, 1623–1627.

Krom, M. D., Kress, N., Brenner, S., and Gordon, L. I. (1991). Phosphorus limitation of primary productivity in the Eastern Mediterranean Sea. *Limnol. Oceanogr.* 36, 424–432. doi: 10.4319/lo.1991.36.3.0424

Lagaria, A., Mandalakis, M., Mara, P., Frangoulis, F., Karatsolis, B. Th., Pitta, P., et al. (2016). Phytoplankton variability and community structure in relation to hydrographic conditions in the NE Aegean frontal area (NE Mediterranean Sea). *Cont. Shelf Res.* doi: 10.1016/j.csr.2016.07.014

Lekunberri, I., Lefort, T., Romero, E., Vázquez-Domíngue, E., Romera-Castillo, C., Marrasé, C., et al. (2010). Effects of a dust deposition event on coastal marine microbial abundance and activity, bacterial community structure and ecosystem function. *J. Plankton Res.* 32, 381–396. doi: 10.1093/plankt/fbp137

Lin, S., Litaker, R. W., and Sunda, W. G. (2016). Phosphorus physiological ecology and molecular mechanisms in marine phytoplankton. *J. Phycol.* 52, 10–36. doi: 10.1111/jpy.12365

Mackey, D. J., Higgins, H. W., Mackey, M. D., and Holdsworth, D. (1998). Algal class abundances in the western equatorial Pacific: estimation from HPLC measurements of chloroplast pigments using CHEMTAX. *Deep Sea Res. I* 45, 1441–1468. doi: 10.1016/S0967-0637(98)00025-9

Mackey, M. D., Mackey, D. J., Higgins, H. W., and Wright, S. W. (1996). CHEMTAX - A program for estimating class abundances from chemical marker: application to HPLC measurements of phytoplankton pigments. *Mar. Ecol. Prog. Ser.* 144, 265–283.

Magazzù, G., and Decembrini, F. (1995). Primary production, biomass and abundance of phototrophic picoplankton in the Mediterranean Sea: a review. *Aquat. Microb. Ecol.* 9, 97–104. doi: 10.3354/ame009097

Malone, T. C., Pike, S. E., and Conley, D. J. (1993). Transient variations in phytoplankton productivity at the JGOFS Bermuda time series station. *Deep Sea Res. I* 40, 903–924.

Marañón, E. (2005). Phytoplankton growth rates in the Atlantic subtropical gyres. *Limnol. Oceanogr.* 50, 299–310. doi: 10.4319/lo.2005.50.1.0299

Marañón, E., Cermeño, P., López-Sandoval, C., Rodríguez-Ramos, T., Sobrino, C., Huerte-Ortiga, M., et al. (2013). Unimodal size scaling of phytoplankton growth and the size dependence of nutrient uptake and use. *Ecol. Lett.* 16, 371–379. doi: 10.1111/ele.12052

Marañón, E., Fernández, A., Mouri-o-Carballido, B., Martínez-García, S., Teira, E., Cermeño, P., et al. (2010). Degree of oligotrophy controls the response of microbial plankton to Saharann dust. *Limnol. Oceanogr.* 55, 2339–2352. doi: 10.4319/lo.2010.55.6.2339

Marañón, E., Holligan, P. M., Barciela, R., González, N., Mouri-o, B., Pazó, V., et al. (2001). Patterns of phytoplankton size structure and productivity in contrasting open-ocean environments. *Mar. Ecol. Prog. Ser.* 216, 43–56. doi: 10.3354/meps216043

Marie, D., Partensky, F., Jacquet, S., and Vaulot, D. (1997). Enumeration and cell cycle analysis of natural populations of marine picoplankton by flow cytometry using the nucleic acid stain SYBR Green, I. *Appl. Environ. Microbiol.* 63, 186–193.

Marie, D., Zhu, F., Balagué, V., Ras, J., and Vaulot, D. (2006). Eukaryotic picoplankton communities of the Mediterranean Sea in summer assessed bymolecular approaches (DGGE, TTGE, QPCR). *FEMS Microbiol. Ecol.* 55, 403–415. doi: 10.1111/j.1574-6941.2005.00058.x

Marra, J. (2009). Net and gross productivity: weighing in with 14C. *Aquat. Microb. Ecol.* 56, 123–131. doi: 10.3354/ame01306

Meloni, D., Di Sarra, A., Monteleone, F., Pace, G., Piacentino, S., and Sferlazzo, D. M. (2008). Seasonal transport patterns of intense Saharann dust events at the Mediterranean island of Lampedusa. *Atmos. Res.* 88, 134–148. doi: 10.1016/j.atmosres.2007.10.007

Montagnes, S. J. D., Berges, A. J., Harrison, J. P., and Taylor, F. J. R. (1994). Estimating carbon, nitrogen, protein, and chlorophyll a from volume in marine phytoplankton. *Limnol. Oceanogr.* 39, 1044–1060.

Moore, C. M., Mills, M. M., Arrido, K. R., Berman-Frank, I., Bopp, L., Boyd, P. W., et al. (2013). Processes and patterns of oceanic nutrient limitation. *Nat. Geosci.* 6, 701–710. doi: 10.1038/ngeo1765

Morel, A., Ahn, Y.-H., Partensky, F., Vaulot, D., and Claustre, H. (1993). Prochlorococcus and Synechococcus: a comparative study of their optical properties in relation to their size and pigmentation. *J. Mar. Syst.* 51, 617–649. doi: 10.1357/0022240933223963

Moutin, T., and Raimbault, P. (2002). Primary production, carbon export and nutrients availability in western and eastern Mediterranean Sea in early summer 1996 (MINOS cruise). *J. Mar. Syst.* 33–34, 273–288. doi: 10.1016/S0924-7963(02)00062-3

Moutin, T., Thingstad, T. F., Van Wambeke, F., Marie, D., Slawyk, G., Raimbault, P., et al. (2002). Does competition for nanomolar phosphate supply explain the predominance of the cyanobacterium *Synechococcus? Limnol. Oceanogr.* 47, 1562–1567. doi: 10.4319/lo.2002.47.5.1562

Pitta, P., Nejstgaard, J. C., Tsagaraki, T. M., Zervoudaki, S., Egge, J. K., Frangoulis, C., et al. (2016). Confirming the "Rapid phosphorus transfer from microorganisms to mesozooplankton in the Eastern Mediterranean Sea" scenario through a mesocosm experiment. *J. Plankton Res.* 38, 502–521. doi: 10.1093/plankt/fbw010

Porter, K. G., and Feig, Y. S. (1980). The use of DAPI for identifying and counting of aquatic microflora. *Limnol. Oceanogr.* 25, 943–948.

Psarra, S., Zohary, T., Krom, M. D., Mantoura, R. F. C., Polychronaki, T., Stambler, N., et al. (2005). Phytoplankton response to a Lagrangian phosphate addition in the Levantine Sea (Eastern Mediterranean). *Deep Sea Res. II* 52, 2944–2960. doi: 10.1016/j.dsr2.2005.08.015

Pulido-Villena, E., Baudoux, A.-C., Obernosterer, I., Landa, M., Caparros, J., Catala, P., et al. (2014). Microbial food web dynamics in response to a Saharann dust event: results from a mesocosm study in the oligotrophic Mediterranean Sea. *Biogeosciences* 11, 337–371. doi: 10.5194/bgd-11-337-2014

Raven, J. A., Finkel, Z. V., and Irwin, A. J. (2005). Phytoplankton: bottom-up and top-down controls on ecology and evolution. *Vie Milieu* 55, 209–215. doi: 10.3410/f.1015747.389046

Ridame, C., Dekaezemacker, J., Guieu, C., Bonnet, S., L'Helguen, S., and Malieu, F. (2014). Contrasted Saharann dust events in LNLC environments: impact on nutrient dynamics and primary production. *Biogeosciences* 11, 4783–4800. doi: 10.5194/bg-11-4783-2014

Ridame, C., and Guieu, C. (2002). Saharan input of phosphate to the oligotrophic water of the open western Mediterranean Sea. *Limnol. Oceanogr.* 47, 856–869. doi: 10.4319/lo.2002.47.3.0856

Rimmelin, P., and Moutin, T. (2005). Re-examination of the MAGIC Method to determine low orthophosphate concentration in seawater. *Anal. Chim. Acta* 548, 174–182. doi: 10.1016/j.aca.2005.05.071

Rodríguez, F., Chauton, M., Johnsen, G., Andresen, K., Olsen, I. M., and Zapata, M. (2006). Photoacclimation in phytoplankton: implications for biomass estimates, pigment functionality and chemotaxonomy. *Mar. Biol.* 148, 963–971. doi: 10.1007/s00227-005-0138-7

Romero, E., Peters, F., Marrasé, C., Guadayol, O., Gasol, J. M., and Weinbauer, M. G. (2011). Coastal Mediterranean plankton stimulation dynamics through a dust storm event: an experimental simulation. *Estuar. Coast. Shelf Sci.* 93, 27–39. doi: 10.1016/j.ecss.2011.03.019

Siokou-Frangou, I., Christaki, U., Mazzocchi, M. G., Montresor, M., Ribera d'Alcalá, M., et al. (2010). Plankton in the open mediterranean Sea: a review. *Biogeosciences* 7, 1543–1586. doi: 10.5194/bg-7-1543-2010

Spivak, A. C., Vanni, M. J., and Mette, E. M. (2011). Moving on up: can results from simple aquatic mesocosm experiments be applied across broad spatial scales? *Freshw. Biol.* 56, 279–291. doi: 10.1111/j.1365-2427.2010.02495.x

Steemann-Nielsen, E. (1952). The use of radioactive carbon (^{14}C) for measuring organic production in the sea. *J. Cons. Int. Explor. Mer.* 18, 117–140.

Strickland, J. D., and Parsons, T. R. (1972). A practical handbook of seawater analysis. *J. Fish. Res. Board Can.* 167, 71–76.

Tanaka, T., Thingstad, T. F., Christaki, U., Colombet, J., Cornet-Barthaux, V., Courties, C., et al. (2011). Lack of P-limitation of phytoplankton and heterotrophic prokaryotes in surface waters of three anticyclonic eddies in the stratified Mediterranean Sea. *Biogeosciences* 8, 525–538. doi: 10.5194/bg-8-525-2011

Ternon, E., Guieu, C., Loÿe-Pilot, M.-D., Leblond, N., Bosc, E., Gasser, B., et al. (2010). The impact of Saharann dust on the particulate export in the water column of the North Western Mediterranean Sea. *Biogeosciences* 7, 809–826. doi: 10.5194/bg-7-809-2010

Thingstad, T. F., Krom, M. D., Mantoura, R. F. C., Flaten, G. A. F., Groom, S., Herut, B., et al. (2005). Nature of phosphorus limitation in the ultraoligotrophic Eastern Mediterranean. *Science* 309, 1068–1071. doi: 10.1126/science.1112632

Thingstad, T. F., and Mantoura, R. F. C. (2005). Titrating excess nitrogen content of phosphorous-deficient eastern Mediterranean surface water using alkaline phosphatase activity as a bio-indicator. *Limnol. Oceanogr. Meth.* 3, 94–100. doi: 10.4319/lom.2005.3.94

Thingstad, T. F., and Rassoulzadegan, F. (1995). Nutrient limitations, microbial food webs, and 'biological C-pumps': suggested interactions in a P-limited Mediterranean. *Mar. Ecol. Prog. Ser.* 117, 299–306. doi: 10.3354/meps117299

Trees, C. C., Clark, D. K., Bidigare, R. R., Ondrusek, M. E., and Mueller, J. L. (2000). Accessory pigments versus chlorophyll a concentrations within the euphotic zone: a ubiquitous relationship. *Limnol. Oceanogr.* 45, 1130–1143. doi: 10.4319/lo.2000.45.5.1130

Tsiola, A., Pitta, P., Fodelianakis, S., Pete, R., Magiopoulos, I., Mara, P., Psarra, S., et al. (2016). Nutrient limitation in surface waters of the oligotrophic eastern Mediterranean Sea: an enrichment microcosm experiment. *Microb. Ecol.* 71, 575–588. doi: 10.1007/s00248-015-0713-5

Unrein, F., Gasol, J. M., Not, F., Forn, I., and Massana, R. (2014). Mixotrophic haptophytes are key bacterial grazers in oligotrophic coastal waters. *ISME J.* 8, 164–176. doi: 10.1038/ismej.2013.132

Utermöhl, H. (1958). Zur vervollkommnung der quantitativen Phytoplankton Methodik. *Mitt. Int. Ver. Theor. Angew. Limnol.* 9, 1–38.

Veldhuis, M. J. W., Timmermans, K. R., Croot, P., and van der Wagt, B. (2005). Picophytoplankton; a comparative study of their biochemical composition and photosynthetic properties. *J. Plankton Res.* 53, 7–24. doi: 10.1016/j.seares.2004.01.006

Verity, P. G., Robertson, C. Y., Tronzo, C. R., Andrews, M. G., Nelson, J. R., and Sieraki, M. E. (1992). Relationships between cell volume and the carbon and nitrogen content of marine photosynthetic nanoplankton. *Limnol. Oceanogr.* 37, 1434–1446.

Vincent, J., Laurent, B., Losno, R., Bon Nguyen, E., Roullet, P., Sauvage, S., et al. (2016). Variability of mineral dust deposition in the western Mediterranean basin and south-east of France. *Atmos. Chem. Phys.* 16, 8749–8766. doi: 10.5194/acp-16-8749-2016

Volpe, G., Banzon, V. F., Evans, R. H., Santoleri, R., Mariano, A. J., and Sciarra, R. (2009). Satellite observations of the impact of dust in a low-nutrient, low chlorophyll region: fertilization or artifact? *Global Biogeochem. Cycle* 23:GB3007. doi: 10.1029/2008GB003216

Wagener, T., Guieu, C., and Leblond, N. (2010). Effects of dust deposition on iron cycle in the surface Mediterranean Sea: results from a mesocosm seeding experiment. *Biogeosciences* 7, 3769–3781. doi: 10.5194/bg-7-3769-2010

Wawrik, B., Callaghan, A. V., and Bronk, D. A. (2009). Use of inorganic and organic nitrogen by *Synechococcus* spp. and diatoms on the west florida

shelf as measured using stable isotope probing. *Appl. Environ. Microbiol.* 75, 6662–6670. doi: 10.1128/AEM.01002-09

Worden, A. Z., Nolan, J. K., and Palenik, B. (2004). Assessing the dynamics and ecology of marine picophytoplankton: the importance of the eukaryotic component. *Limnol. Oceanogr.* 49, 168–179. doi: 10.4319/lo.2004.49.1.0168

Wright, S. W., Ishikawa, A., Marchant, H. J., Davidson, A. T., van den Enden, R. L., and Nash, G. V. (2009). Composition and significance of picophytoplankton in Antarctic waters. *Polar Biol.* 32, 797–808. doi: 10.1007/s00300-009-0582-9

Zohary, T., Herut, B., Krom, M. D., Mantoura, R. F. C., Pitta, P., Psarra, S., et al. (2005). P-limited bacteria but N and P co-limited phytoplankton in the Eastern Mediterranean—a microcosm experiment. *Deep Sea Res. I* 52, 3011–3023. doi: 10.1016/j.dsr2.2005.08.011

Zubkov, M. V., Fuchs, B. M., Tarran, G. A., Burkill, P. H., and Amann, R. (2003). High rate of uptake of organic nitrogen compounds by *Prochlorococcus cyanobacteria* as a key to their dominance in oligotrophic oceanic waters. *Appl. Environ. Microbiol.* 69, 1299–12304. doi: 10.1128/AEM.69.2.1299-1304.2003

Conflict of Interest Statement: The authors declare that the research was conducted in the absence of any commercial or financial relationships that could be construed as a potential conflict of interest.

frontiers in Marine Science

ORIGINAL RESEARCH
published: 04 May 2017
doi: 10.3389/fmars.2017.00120

Model Simulations of a Mesocosm Experiment Investigating the Response of a Low Nutrient Low Chlorophyll (LNLC) Marine Ecosystem to Atmospheric Deposition Events

Kostas P. Tsiaras[1], Sylvia Christodoulaki[2,3], George Petihakis[2], Constantin Frangoulis[2] and George Triantafyllou[1]*

[1] Institute of Oceanography, Hellenic Centre for Marine Research, Anavyssos, Greece, [2] Institute of Oceanography, Hellenic Centre for Marine Research, Heraklion, Greece, [3] Department of Chemistry, University of Crete, Heraklion, Greece

OPEN ACCESS

Edited by:
Tatiana Margo Tsagaraki, University of Bergen, Norway

Reviewed by:
Rodrigo Riera, Centro de Investigaciones Medioambientales del Atlántico (CIMA, S.L.), Spain
Christopher Kenneth Algar, Marine Biological Laboratory, USA

***Correspondence:**
Kostas P. Tsiaras
ktsiaras@hcmr.gr

Specialty section:
This article was submitted to Marine Ecosystem Ecology, a section of the journal Frontiers in Marine Science

Received: *30 September 2016*
Accepted: *13 April 2017*
Published: *04 May 2017*

Citation:
Tsiaras KP, Christodoulaki S, Petihakis G, Frangoulis C and Triantafyllou G (2017) Model Simulations of a Mesocosm Experiment Investigating the Response of a Low Nutrient Low Chlorophyll (LNLC) Marine Ecosystem to Atmospheric Deposition Events. Front. Mar. Sci. 4:120. doi: 10.3389/fmars.2017.00120

Atmospheric deposition of nitrogen and phosphorus represents an important source of nutrients, enhancing the marine productivity in oligotrophic areas, e.g., the Mediterranean. A comprehensive biogeochemical model (ERSEM) was setup and customized to simulate a mesocosm experiment, where dissolved inorganic nitrogen and phosphorus by means of atmospheric dust (single addition/SA and repetitive addition/RA in three successive doses) was added in controlled tanks and compared with a control (blank), all with Cretan Sea (Eastern Mediterranean) water. Observations on almost all components of the pelagic ecosystem in a ten-day period allowed investigating the effect of atmospheric deposition and the pathways of the added nutrients. The model was able to reasonably capture the observed variability of different ecosystem components and reproduce the main features of the experiment. An enhancement of primary production and phytoplankton biomass with added nutrients was simulated, in agreement with observations. A significant increase of bacterial production was also reproduced, while the model underestimated the observed increase and variability in bacterial biomass, but this deviation could be partly removed considering a lower carbon conversion factor from cell abundance data. A slightly stronger overall response was simulated with the single dust addition, compared to the repetitive that showed a few days delay. The simulated carbon pathways indicated that nutrient additions did not modify the microbial food web structure, but just increased its trophic status. Changes in model assumptions and parameter set that were necessary to reproduce the observed variability in the mesocosm experiment were discussed through a series of sensitivity simulations. Bacterial production was assumed to be mostly affected by the *in situ* produced labile organic matter, while it was further stimulated by the addition of inorganic nutrients, adopting a function of external nutrient concentrations for bacteria nutrient limitation. The effective increase in phytoplankton nutrient uptake rate was

necessary, in order to reproduce the observed primary production, under such low nutrient concentrations, as also the increase of the grazers growth rate. The model was thus tuned to better work under very low nutrient concentrations, such as those found in the Eastern Mediterranean.

Keywords: model, mesocosm, atmospheric deposition, marine ecosystem, Mediterranean

INTRODUCTION

The atmospheric deposition of trace elements in the marine environment plays a major role in low-nutrient low-chlorophyll (LNLC) regions, such as the Mediterranean Sea (Jickells et al., 2005; Krom et al., 2010). Particularly the deposition of nitrogen (mainly nitrate and ammonium) and phosphorus (phosphate) represents an important source of essential nutrients for the growth of phytoplankton and bacteria, enhancing the marine productivity in these oligotrophic areas (Christodoulaki et al., 2013). The Mediterranean Sea is of particular interest for both its marine and atmospheric environment. Especially the Eastern Mediterranean sub-basin is characterized by very low nutrient levels and is globally one of the least productive seas (Azov, 1991; Krom et al., 1991, 2004; Thingstad and Rassoulzadegan, 1995; Bethoux et al., 1998; Crise et al., 1999; Van Wambeke et al., 2002). Moreover, the Mediterranean atmosphere, characterized by high photochemical activity, is a crossroad for air masses of distinct origin, affected by both natural and anthropogenic emissions that interact chemically, leading to the formation of nutrients, such as nitrogen compounds (Vrekoussis et al., 2006; Finlayson-Pitts, 2009). Dust aerosols, transported from the African continent in the form of non-continuous dust pulses over the Mediterranean atmosphere, are also affecting the area as carriers of nutrients, such as iron (Fe) and phosphorus (P) (Gallisai et al., 2014). Interaction of these aerosols with acid gasses from anthropogenic sources causes reduced pH and increases the fraction of bioavailable Fe and P in the dust laden air masses (Nenes et al., 2011).

There are very few studies investigating the effect of dust additions in the Mediterranean Sea experimentally. Previous efforts based on mesoscale field studies in the frame of ADIOS European Program (Heussner et al., 2003), as well as microcosms experiments (e.g., Herut et al., 2005) in the Eastern Mediterranean, have examined the biogeochemical response of Mediterranean waters to atmospheric deposition and its fate in different ecosystem compartments, but an accurate understanding of the ecosystem dynamics and the underlying biogeochemical processes is still lacking. Recently, a holistic approach was attempted for the Western Mediterranean oligotrophic marine waters, through two mesocosm experiments (DUNE 2008 and 2010, Guieu et al., 2014), with no explicit description of the fate and impact of dust constituents onto surface seawater biochemistry, with some exceptions (Laghdass et al., 2011; Giovagnetti et al., 2013; Pulido-Villena et al., 2014; Ridame et al., 2014).

In May 2014, a mesocosm experiment was carried out at the HCMR facilities to understand the complex ecosystem functioning in the Eastern Mediterranean Sea and the effect of atmospheric aerosol deposition. Ambient atmospheric dust samples were added in a number of controlled tanks previously filled with subsurface water from the Cretan Sea. These treatments with additions of primary limiting nutrients (phosphate, nitrate), in the form of environmental dust, were compared with a control (blank), allowing to investigate the effect of the atmosphere on the Mediterranean marine system and the pathways of these added nutrients in the pelagic ecosystem. This experiment is a holistic studying approach of atmosphere-ocean as a single system, for the Eastern Mediterranean Sea.

Biogeochemical processes and interactions between living and non-living components of the ecosystem are difficult to describe and understand using observations alone, as these provide static distributions of the ecosystem components, but cannot capture the dynamics lying underneath the rates and processes controlling these distributions (e.g., Fennel and Neumann, 2004). Biogeochemical models are particularly useful in providing a better understanding of these dynamics and complete missing data in a dynamically consistent way. Moreover, models can be used to test and efficiently analyze the relative importance of different factors and processes of the ecosystem.

Mesocosm experiments are of particular significance, as they may offer frequent observations of various ecosystem components from sea water samples, under controlled environmental conditions, providing adequate information to increase our understanding of the marine ecosystem functioning. These observations can also be used to test thoroughly and validate biogeochemical models. Implementing ecological models to study the dynamics of mesocosms has been successful in many instances (Watts and Bigg, 2001, and references therein).

In the present study, for the first time to our knowledge, a mesocosm experiment is combined with a marine biogeochemical model to investigate the effect of atmospheric aerosol deposition, as source of inorganic nutrients (nitrogen and phosphorus), on the Cretan Sea (Eastern Mediterranean) marine productivity, and ecosystem functioning. The results from the mesocosm experiment are used to analyze the marine ecosystem processes, triggered by the atmospheric aerosol deposition, enabling the integration and parameterization of these processes into the marine biogeochemical model. After the necessary tuning and validation, the model is used to improve our understanding of the ecosystem response to nutrient additions, describing the nutrient uptake by organisms, the triggered food web interactions and how these are translated regarding carbon and nutrient fluxes.

In section Materials and methods, a brief description of the biogeochemical model and the mesocosm experimental setup is provided. In section Reference simulation, the model

results, simulating the mesocosm experiment, are presented in conjunction with the observations, investigating the effect of atmospheric deposition on productivity and ecosystem dynamics. In section Model sensitivity simulations, model modifications, necessary in order to reproduce the observed variability in the mesocosm treatments and the model sensitivity to different parameters are discussed, through a series of sensitivity simulations.

MATERIALS AND METHODS

Model Description/Setup

A 0-D biogeochemical model was developed to simulate the evolution and dynamics of the pelagic marine ecosystem, as this was observed in the mesocosm experiment within a 10-day period. The model is based on the European Regional Seas Ecosystem Model (ERSEM, Baretta et al., 1995), a generic comprehensive model that has been successfully implemented across a wide range of coastal and open ocean ecosystems, including the Mediterranean (Allen et al., 2002; Petihakis et al., 2002, 2015; Tsiaras et al., 2014). ERSEM follows a functional group approach, describing the marine ecosystem with different groups based on their functional role and size classes. The pelagic plankton food web (see **Figure 1**) is described by four phytoplankton groups (diatoms, nanophytoplankton, picophytoplankton, dinoflagellates), bacteria and three zooplankton groups (heterotrophic nanoflagellates/HNAN, microzooplankton, and mesozooplankton). A schematic diagram of the model trophic interactions among different groups is shown in **Figure 1**. The pelagic model also includes particulate and dissolved organic matter (produced by the mortality, excretion and lysis of primary and secondary producers, and utilized by bacteria), along with dissolved inorganic nutrients (nitrate, ammonia, phosphate, silicate). Each plankton group has dynamically varying C/N/P pools and carbon dynamics are loosely coupled to the dynamics of nitrogen and phosphorus. The uptake of dissolved inorganic nutrients by phytoplankton is regulated based on the difference between external and internal nutrient pools, following a Droop kinetics formulation (Droop, 1974). The model configuration and parameter set have been adopted from Petihakis et al. (2002). The initial food web matrix and plankton maximum growth rates were slightly modified by Tsiaras et al. (2014), while the bacteria sub-model has also been revised (Petihakis et al., 2015) from the one in Petihakis et al. (2002), allowing for a more realistic representation of the dissolved organic matter (DOM) pool. In the present study, a few additional changes in the model parameter set and formulations were needed, as further hereafter described, to achieve a better fit of the model simulations with *in situ* measurements from the mesocosm experiment. The model parameter values are given in Supplementary Material (Tables A1–A3 in Supplementary Material), while the attributes of sensitivity model simulations are shown in **Table 1**.

A constant temperature (20°C) was adopted in the model, equal to the one measured on the mesocosm tanks. Light conditions were assumed to be those of the ambient water

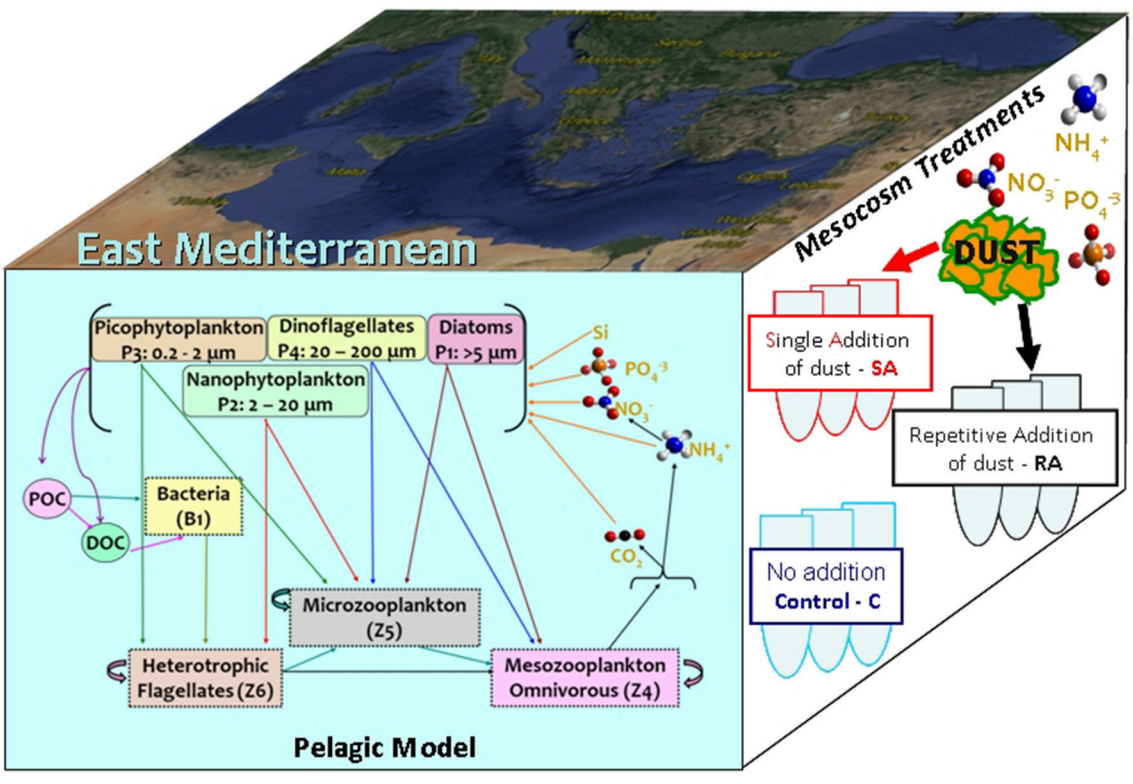

FIGURE 1 | Model schematic indicating the plankton food web interactions. A schematic of the mesocosm treatments and the study area are also shown.

TABLE 1 | Attributes of model simulations.

Simulation	Run1 (REF)	Run2	Run3	Run4	Run5	Run6	Run7	Run8	Run9
Phytoplankton nutrient uptake half-saturation K_P/K_N (mmol/m^3)	0.025/0.85	–	–	*	*	*	*	*	*
Phytoplankton affinity *qurP* (mgC/m^3)$^{-1}$day^{-1}	–	0.0025	0.05	–	–	–	–	–	–
Z4 half-saturation K_{Z4} (mgC/m^3)	3	*	*	14	*	*	*	*	*
Z5 half-saturation K_{Z5} (mgC/m^3)	10	*	*	24	24	*	*	*	*
Z6 half-saturation K_{Z6} (mgC/m^3)	16	*	*	49	49	49	*	*	*
Initial DOC/POC (mgC/m^3)	4/4.6	*	*	*	*	*	400/32	*	*
Bacteria nutrient limitation	**	*	*	*	*	*	***	*	***
Bacterial assimilation efficiency (*puB*)	****	*	*	*	*	*	0.15	0.15	0.15

The model parameter set is given in the appendix (Tables A1–A3 in Supplementary Material).
**as in Run1 (Reference simulation).*
***Bacterial nutrient limitation is a function of external nutrient concentrations (Equation 12).*
****Bacterial nutrient limitation is a function of the internal bacteria nutrient quotas (Equation 11).*
*****Bacterial assimilation efficiency is assumed to depend on nutrient limitation (Equation 14).*

in the area of the collected samples, while settling velocity for particulate organic matter was assumed close to zero, as continuous stirring was applied in the mesocosm tanks. Dissolved inorganic nutrients and biomasses of different plankton groups were initialized taking the average of three replicate measurements of the mesocosm water samples prior to the addition of dust. Initial dissolved (DOM) and particulate (POM) organic matter constituents (carbon, nitrogen, phosphorus) were also based on the measurements, but adopting much lower initial DOM/POM concentrations, representing the most labile fraction of organic matter, resulted in a significantly better agreement of the simulated bacteria variability with observations, as discussed below. Three simulations were performed, mimicking the mesocosm treatments (for mesocosm setup and experimental design see below section Model sensitivity simulations and Pitta et al., 2017): (a) Control, without any addition of dust, (b) Single Addition (SA), adding the amount of phosphate and nitrate corresponding to the total amount of dust (4 g), added in the beginning of the experiment, and (c) Repetitive Addition (RA), where the total amount of phosphate and nitrate was portioned (1+2+1 = 4 g dust) and added in the first 3 days of the experiment. The initial phosphate and nitrate of the control experiment were practically increased by 30 and 100% respectively in the SA and RA (in three portions) experiments.

Mesocosm Experiment Data

The experiment was performed between the 10 and 19th May 2014, using 9 mesocosms of 3 m^3, filled with subsurface seawater (10 m depth) collected ∼5 nm north of Heraklion, Greece. Details of water collection and transfer, as well as of mesocosm's filling can be found in Pitta et al. (2017). The mesocosms were submerged in a 150 m^3 concrete tank, with running sea surface water that kept the mesocosms at 20.2 ± 0.3°C throughout the experiment. Three mesocosms received 4 g of Saharan dust as a single addition (SA), three others received three consecutive additions (1, 2, 1 g of Saharan dust) on the first 3 days (repetitive addition, RA) and finally, three mesocosms were kept without any addition as control (C). The repetitive addition was found a reasonable practical choice within the limited time frame of the experiment in order to mimic the recurrence pattern of Saharan dust events in the Eastern Mediterranean, where successive dust deposition events may occur over a period of several days (Gaetani and Pasqui, 2014; Lagaria et al., 2017). SA and RA treatments had a final dust concentration of 1.3 mg L^{-1}. Water sampling from the mesocosms was made in order to determine: (a) inorganic nutrients, dissolved organic nitrogen, particulate and total organic carbon, size fractionated Chl-a, viruses, bacteria, *Prochlorococcus*, *Synechococcus*, picoeukaryotes (autotrophic and heterotrophic), bacterial production, primary production (approximately daily), (b) nanoflagellates (autotrophic and heterotrophic), dinoflagellates (autotrophic and mixotrophic), ciliates (heterotrophic and mixotrophic), diatoms, coccolithophores (approximately every other day), and (c) metazoans (at the start and end of the experiment). Details on sampling and analysis protocols of these parameters, as well as the literature carbon conversion factors used to convert raw biological data to carbon can be found in Pitta et al. (2017) and Lagaria et al. (2017). Most of the measured plankton variables mentioned above (except bacteria and diatoms) did not have a direct correspondence with the model's state variables (see **Figure 1**). To create a correspondence, some variables had to be split into subgroups based on their size (e.g., dinoflagellates >20 μm and dinoflagellates <20 μm) and/or trophic functioning (e.g., autotrophic and heterotrophic nanoflagellates). These size and trophic sub-divisions were made by the scientists that provided the data. In the measured plankton samples, some mixotrophic organisms were identified. Larger size (>20 μm) mixotrophs biomass was very small, while smaller size (<20 μm) mixotrophs biomass was comparable to autotrophic nanophytoplankton (∼40% on average) and much lower (∼20% on average) than picophytoplankton. Model simulations showed that including mixotrophs as part of nanophytoplankton did not have a noticeable effect on dissolved inorganic nutrients and other plankton groups simulated evolution. Therefore, it was decided to exclude mixotrophs in the model-data correspondence to avoid unnecessary complexity in the model analysis, since this particular type of

organism is currently not represented in the model's functional groups.

RESULTS

Reference Simulation

Comparison with Data/Effect of Dust Addition

In **Figure 2**, the model simulated results are shown against the observations for the three mesocosm treatments (control without any addition of dust, single addition/SA and repetitive addition/RA). These include dissolved inorganic nutrients, Chlorophyll-a (Chl-a), net primary production, biomass of picophytoplankton and nanophytoplankton that represents more than 93% of the total phytoplankton, bacterial production and biomass, as well as the biomass of heterotrophic nanoflagellates (HNAN), microzooplankton and mesozooplankton.

As expected, the dust addition in SA and RA treatments provoked an increase in both dissolved inorganic nitrogen (DIN = nitrate + ammonium) and phosphorus (phosphate, PO_4) observed concentrations (**Figures 2A,B**), as compared to the control experiment. This difference was larger for DIN, as the amount of nitrogen added with the dust is much higher (+100% of the initial DIN concentration) compared to phosphorus (+30% of the initial PO_4 concentration). A decreasing trend can be seen for the observed DIN concentration of the control treatment and particularly for PO_4 (all treatments), which is related to the nutrient uptake by phytoplankton and bacteria. Interestingly, the measured DIN concentration in the addition treatments shows an increasing trend, suggesting a potential nitrogen excess due to a stronger phosphorus limitation. The model captured the observed decreasing trend of PO_4 and control DIN concentration, but with slightly lower concentrations by day-10 (**Figures 2A,B**). The higher increase in DIN (as compared to PO_4) in the addition treatments (SA/RA) was also simulated. However, the observed increasing trend of DIN in SA/RA was not simulated, even though an increasing DIN/DIP ratio from ~13 on day-1, indicative of nitrogen and phosphorus co-limitation, to ~35 on day-10, suggesting

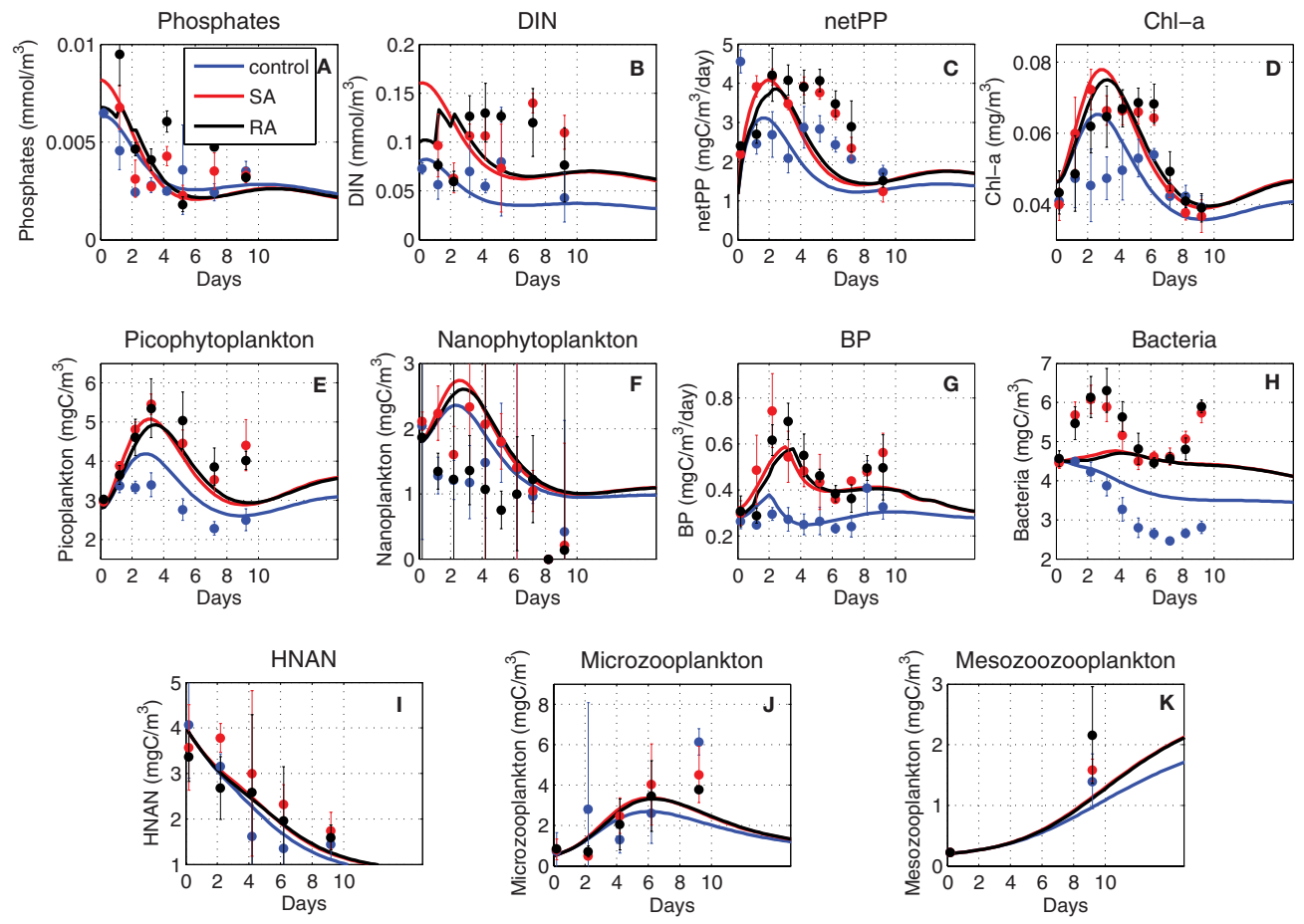

FIGURE 2 | Model simulated (A) phosphate (mmol/m^3), **(B)** dissolved inorganic nitrogen (DIN, mmol/m^3), **(C)** net primary production (netPP, mgC/m^3/day), **(D)** Chl-a (mg/m^3), **(E)** picophytoplankton biomass (mgC/m^3), **(F)** nanophytoplankton biomass (mgC/m^3), **(G)** bacterial production (BP, mgC/m^3/day), **(H)** bacteria biomass (mgC/m^3), and **(I)** HNAN biomass (mgC/m^3), **(J)** microzooplankton biomass (mgC/m^3), **(K)** mesozooplankton biomass (mgC/m^3), for the three (Control = blue line, Single Addition/SA = red line and Repetitive Addition/RA = black line) treatments, against observations. The standard deviation of measurements from three replicates is indicated.

a stronger phosphorus limitation, was simulated (not shown) in agreement with the observations. One can also notice that the model PO_4 in the addition treatments presented a slightly stronger decrease after day-5, as compared to the control, which can be explained by the larger nutrient uptake from the increased phytoplankton biomass (**Figures 2E,F**), resulted from the nutrient enrichment by the dust additions. This stronger simulated decrease in PO_4 led to a slightly lower mean PO_4 in SA/RA over the 10-day period (**Figure 3**), in contrast with the observations that show an overall PO_4 increase in the addition treatments. We should note, however, that the observed PO_4 in the control treatment appears occasionally (day-5, -9) higher than SA/RA after day-4, which is in agreement with the model results.

Following the enrichment with dissolved inorganic nutrients, the simulated net primary production (netPP) appears enhanced in the dust addition treatments (**Figure 2C**), in agreement with the observations, even though their simulated decline starts a bit sooner (∼day-3) compared to the observed (∼day-6). The overall 10-day simulated increase in netPP in SA/RA (∼ +25%) is slightly smaller than the observed one (**Figure 3**). The SA netPP presents a slightly higher increase, as compared to RA, in the model simulation. This result seems reasonable, considering that in SA, added nutrients are available to phytoplankton from the start of the experiment, giving more time to stimulate the production of biomass, as compared to RA, where the same added amount is portioned on a 3-day period. Interestingly, the observations show the opposite, with RA showing a slightly higher overall increase of primary production, as compared to SA. The observed difference between SA and RA, however, might be considered relatively small (<10%, **Figure 3**), considering their standard deviation (from the three replicates), making it difficult to conclude safely that RA presents a higher production.

The simulated evolution of picophytoplankton biomass, showing a peak at ∼day-3 and a secondary increase after day-8 that is mostly related to the decrease of its predator, HNAN (**Figure 2I**), is in good agreement with the observations, except a slight overestimation in the control treatment (**Figure 2E**). Both observations and model results show a higher picophytoplankton biomass in SA/RA treatments. The simulated nanophytoplankton biomass appears slightly overestimated (**Figure 2F**), showing a similar pattern to picophytoplankton, but with a slightly steeper decline after day-3, which may be attributed to the predation pressure exerted by increasing microzooplankton (**Figure 2J**). The same pattern is depicted from observations in the SA experiment. The observed evolution of nanophytoplankton biomass appears less clear in the control and RA experiments, with the latter showing the lowest biomass values. The observed Chl-a, dominated by picophytoplankton (Lagaria et al., 2017), is reasonably well-reproduced by the model, except an overestimation in the control treatment and a slight time-lag of its peak (**Figure 2D**). This deviation might be related to the observed time variability of phytoplankton Chl-a:C ratio, showing higher values between day-4 and -8, in the control treatment (Lagaria et al., 2017), which explains the measured Chl-a increase during this period. This observed variability cannot be captured by the model, which adopts a fixed Chl-a:C ratio.

The observed bacterial production (BP) presented a significant increase in the addition treatments, showing peaks between day-2 (SA) and day-3 (RA), a decline on day-6 and an increasing trend afterward (**Figure 2G**). The same growing trend at the end could also be seen in the control BP that was otherwise relatively constant until day-7. A similar pattern was followed by the observed bacterial biomass, except for an initial decrease in the control, until day-7 (**Figure 2H**). Therefore,

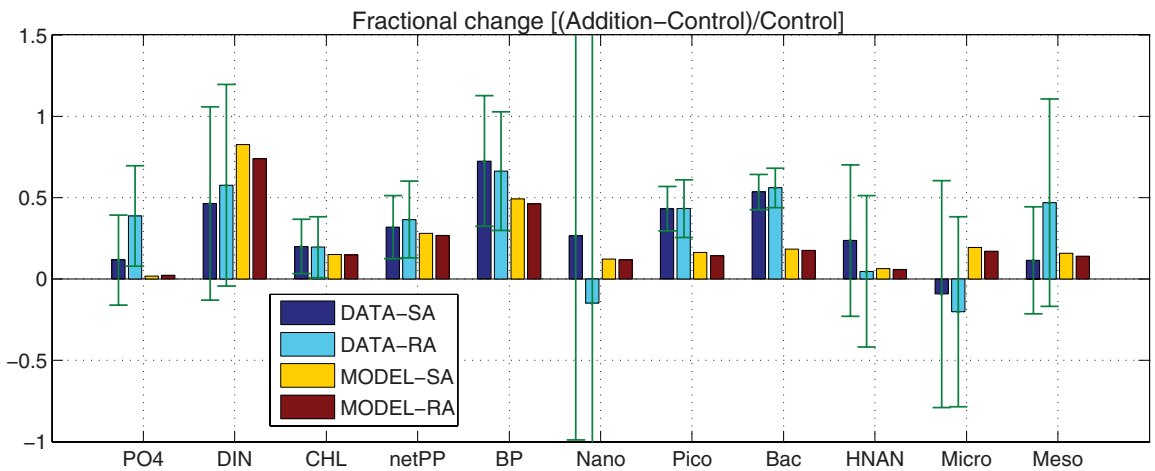

FIGURE 3 | Model simulated (MODEL-SA, MODEL-RA) and observed (DATA-SA, DATA-RA) mean fractional change [(Addition − Control)/Control] for phosphate, DIN, Chl-a, net primary production (netPP), bacterial production (BP), biomass of nanophytoplankton (Nano), picophytoplankton (Pico), bacteria (Bac), HNAN, microzooplankton (Micro), and mesozooplankton (Meso). The standard deviation in the observed fractional change is indicated. This was computed using the 10-day average of the mean (μ) and standard deviation (σ) from the three replicate measurements of the Addition (A) and Control (C) treatments as: $\sigma(A/C-1) \sim \sqrt{[\mu_A^2/\mu_C^{2*}(\sigma_A^2/\mu_A^2+\sigma_C^2/\mu_C^{2)}]}$ (Stuart and Ord, 1998).

bacterial production and biomass appeared closely coupled to phytoplankton biomass, particularly picophytoplankton that showed a very similar evolution. This was to a point expected, as both picophytoplankton and bacteria are prey for HNAN. As the latter decreased throughout the 10-day period (**Figure 2I**), its predation on picophytoplankton and bacteria was relaxed, allowing for their biomass increase at the end of the experiment. This top-down control, however, cannot explain the significant stimulation of BP in SA/RA that appeared to drive also the bacterial biomass increase. Another strong coupling mechanism is the production of dissolved organic carbon by phytoplankton that bacteria rely on for their growth. As later discussed in the model sensitivity section, on the short time scale (∼days) of the experiment, one may assume that bacterial production is mostly affected by the labile organic matter *in situ* produced/excreted by plankton, rather than the semi-labile organic carbon that is decomposed on a longer time-scale. The increase in phytoplankton due to the nutrient enrichment with dust additions may thus explain the observed increase in BP. Under the assumption of bacteria utilizing mainly *in situ* produced dissolved organic carbon (see later discussion in section Bacterial dynamics), the model was able to reproduce the observed BP variability and particularly its increase in SA/RA experiments (**Figure 2G**). An overall BP increase of about +40% was simulated in SA/RA relative to the control, which was slightly smaller, as compared to the observed increase (+65%) in BP (**Figure 3**). The simulated bacterial biomass has a similar pattern with the observed, but shows a much weaker variability (**Figure 2H**). We should note however that the observed bacterial biomass initial increase (∼1 mgC/m^3/day) would probably require about twice the observed BP (∼0.5 mgC/m^3/day), even ignoring bacteria mortality and predation losses. This suggests that the conversion factor (20 mgC/cell, Lee and Fuhrman, 1987) used to calculate carbon biomass from bacteria cell abundance might be a bit overestimated. Indeed, the bacteria variability was much better reproduced by the model (not shown), when the observed bacteria biomass (and its initial value used in the model simulations) was decreased by some factor.

The model reasonably captured the evolution of other heterotrophs (HNAN, microzooplankton, mesozooplankton). A continuous decrease in HNAN with time was simulated in agreement with the observations (**Figure 2I**). The model HNAN was slightly higher in SA/RA, as compared to the control, while observations suggested a stronger HNAN overall increase in SA (**Figure 3**). The observed increase in both microzooplankton and mesozooplankton was well-reproduced by the model that also simulated a decrease of microzooplankton mainly after the end of the experiment, related to the predation by mesozooplankton (**Figure 2J**). Again, as in most cases, the model simulated an overall higher biomass in SA, followed by RA, for both microzooplankton and mesozooplankton (**Figure 3**).

In order to investigate the overall effect of the dust addition in the two different treatments, both in terms of observations (DATA-SA & DATA-RA) and model simulations (MODEL-SA & MODEL-RA), the fractional change of the Addition with respect to the Control treatment [(Addition − Control)/Control] was computed (**Figure 3**). Considering the standard deviation from the three replicates, overall there are no significant differences in the observations between the single (SA) and repetitive (RA) addition treatments, both showing a positive change, with the exception of nanophytoplankton, where the repetitive addition results in a negative fractional change in contrast to the single addition, which is positive and microzooplankton that shows a negative change in both SA/RA. In contrast with the observations, the model results show a positive change in all cases. The model produces a smaller positive change for autotrophs, bacteria and grazers, compared to the observations, with the exception of HNAN in RA, showing a slightly higher positive change than the observed.

The model skill in reproducing the observed variability (**Figure 2**) for different variables may be graphically summarized in a quantitative way using taylor (Taylor, 2001) and target (Jolliff et al., 2009) diagrams (**Figure 4**). In the taylor diagram,

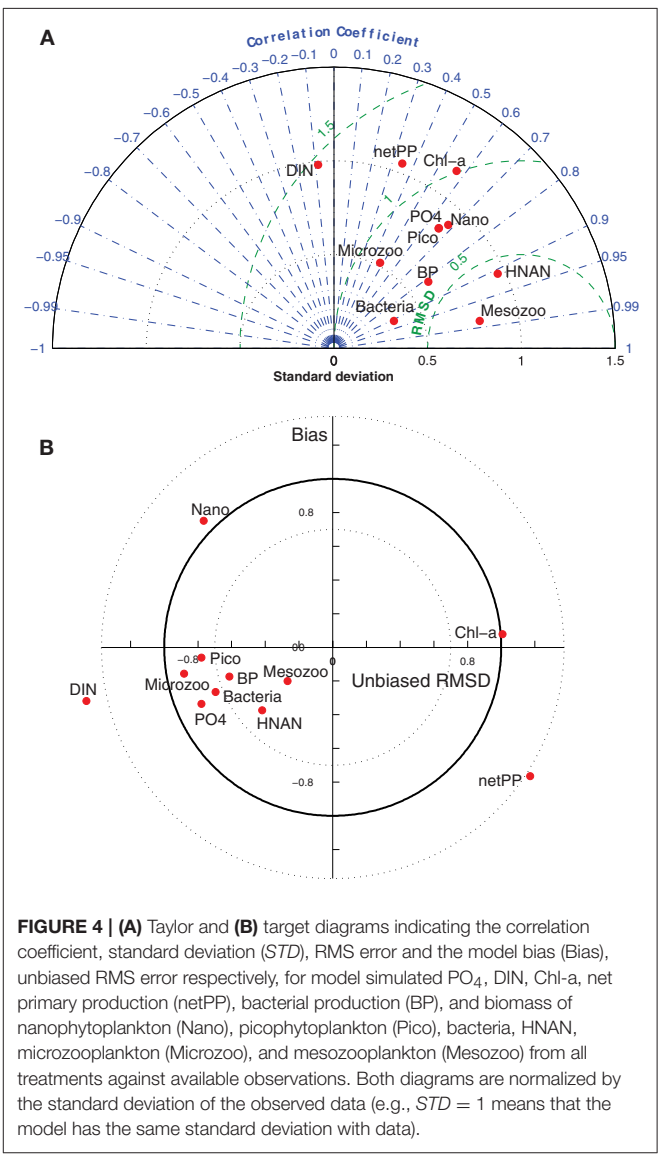

FIGURE 4 | (A) Taylor and **(B)** target diagrams indicating the correlation coefficient, standard deviation (*STD*), RMS error and the model bias (Bias), unbiased RMS error respectively, for model simulated PO_4, DIN, Chl-a, net primary production (netPP), bacterial production (BP), and biomass of nanophytoplankton (Nano), picophytoplankton (Pico), bacteria, HNAN, microzooplankton (Microzoo), and mesozooplankton (Mesozoo) from all treatments against available observations. Both diagrams are normalized by the standard deviation of the observed data (e.g., *STD* = 1 means that the model has the same standard deviation with data).

one can see the model skill for different variables regarding correlation, standard deviation (as an index of variability) and RMS error against the observations, while the target diagram also indicates the model bias and unbiased RMS error. From the two diagrams, one can identify some model variables (mesozooplankton, PO_4, Chl-a) presenting relatively good scores in all skill indexes (correlation $r > 0.6$, $STD \sim 1$, BIAS < 0.5). Nanophytoplankton presents a good correlation ($r \sim 0.7$) and the correct variability ($STD \sim 0.8$), but is slightly biased, as indicated in the target diagram. Picophytoplankton, bacterial production and biomass show good correlation and bias scores, but have relatively small variability, particularly the bacterial biomass. Net primary production is a bit out of phase with the observed one (**Figure 2C**), which results in its poor correlation and RMS error. DIN appears with a slightly negative correlation, as the model fails to capture the observed increasing trend at the end of the experiments (**Figure 2B**).

Carbon Fluxes/Fate of Added Nitrogen and Phosphorus

Models are excellent tools in exploring processes which are difficult or impossible to monitor and measure in the field. To investigate the impact of nutrient additions in terms of carbon flows within the food web and the possible differences between the two addition treatments, the corresponding carbon fluxes and their fractional change [(Addition − Control)/Control] were computed (**Figure 5**). In most cases, there was an initial increase in the carbon fluxes, followed by a gentler decrease. Slightly different from the dominant evolution, is the continuously decreasing flux from bacteria to heterotrophic nanoflagellates (B1Z6), related to the decreasing biomass of both Z6 and bacteria (**Figure 2**), while the flux from microzooplankton to the higher predator of the food web, mesozooplankton (Z5Z4) followed an increasing trend. Overall, in both treatments, there was an increase in the carbon flux from prey to predator but depending on the time scale of the process, this increase settled back to normal (in this case the control run) toward the end of the period. Smaller heterotrophs reacted faster to the dust addition, taking advantage of their relatively higher growth rates and the increasing abundance of their prey (P2Z6, P3Z6), followed by bigger animals such as microzooplankton (P2Z5, P3Z5, Z6Z5), while the 10 days experimental period did not seem to be enough for the biggest ones (mesozooplankton) to converge to the control. In all cases, the single addition treatment resulted in a small but visible initially higher carbon flux, converging after day 4 or 5 with the repeated addition treatment, which seemed to have a couple of days delay. The same dominant trend (initial increase, more gradual decrease) was visible in the fractional change of fluxes from phytoplankton to heterotrophs (P2Z5, P2Z6, P3Z5, P3Z6). This was maximized before day-5 at around +50%, with a small time-lag between SA and RA, before these started settling back to the control. This was not the case for bacteria (B1Z6) and mesozooplankton (Z5Z4), where SA/RA did not appear to converge back to the control.

From the mean food web fluxes (**Figure 6**), model results showed that most of the carbon flowed from small phytoplankton and in particular from picophytoplankton (P3) to the smaller heterotrophs (Z6 & Z5). Although mean fluxes in the addition treatments were higher compared to the control run, there was no change in the pattern. This supports the argument that the dust addition has not modified the food web structure i.e., causing a shift from a microbial food web to a more classical food web, dominated by large phytoplankton-zooplankton, but just increased the trophic status (less oligotrophic), with more carbon circulating in the entire food web. Thus, the increase of different fluxes (SA/RA-Control, **Figure 6**) appears proportional to each flux magnitude. The two major pathways of carbon, further stimulated by the dust additions, were those from the photosynthetic P3 and bacteria to the smallest heterotrophic nanoflagellates (P3Z6, BZ6), and the second and greater channel from the small phytoplankton to microzooplankton (P2Z5 & P3Z5). Besides these two main channels, smaller pathways were the predation processes within the zooplankton groups (Z6Z5, Z6Z4, Z5Z4).

To investigate the fate of the added nitrogen and phosphorus, the evolution of the (Addition − Control) difference in different nitrogen and phosphorus pools (dissolved inorganic, particulate and dissolved organic, phytoplankton, bacteria, and zooplankton) was computed (**Figure 7**). This nicely illustrates the transfer of added nitrogen/phosphorus as this passed from one pool to the other. Initially the difference was zero in all pools except for the dissolved inorganic (PO_4, DIN). These were quickly reduced, taken up by phytoplankton, which was the first to increase, showing a peak on day-3 and decreasing afterward due to nutrient limitation and predation by zooplankton. Nitrogen and phosphorus were then directed to zooplankton that followed phytoplankton with a time-lag ($\sim$4 days). Bacteria, stimulated by the organic matter produced by phytoplankton/zooplankton, also took a major part of nitrogen and phosphorus pools, consuming dissolved organic nitrogen and phosphorus that appear to decrease. Particulate organic pools were initially reduced, being smaller in the addition treatments, as phytoplankton mortality is a function of nutrient limitation. After day-3 they gradually built up from mortality losses of all plankton groups. At the end of the 20-day period, some of the phosphorus pools (PO_4, phytoplankton-P DOP, bacteria) appeared to be settling back to the control (Addition − Control = 0), with the added phosphorus remaining mostly in the form of POP and zooplankton-P. For nitrogen, the largest pool remained in the form of DIN, given its excess over DIP (DIN/DIP $\sim$35), with the increase of phytoplankton-N pool being related to luxury uptake. The other pools (bacteria, PON, zooplankton-N) followed a similar pattern as in phosphorus.

Model Sensitivity Simulations

A few changes in the model parameter set and formulations were needed, before this could capture the observed variability in the mesocosm experiment. These changes in the model are discussed below through a series of sensitivity experiments related to three main model components: (a) phytoplankton (nutrient uptake rates and formulation), (b) zooplankton (grazing half-saturation parameter values), and (c) bacteria (initial DOM pool, bacteria nutrient limitation, bacterial efficiency).

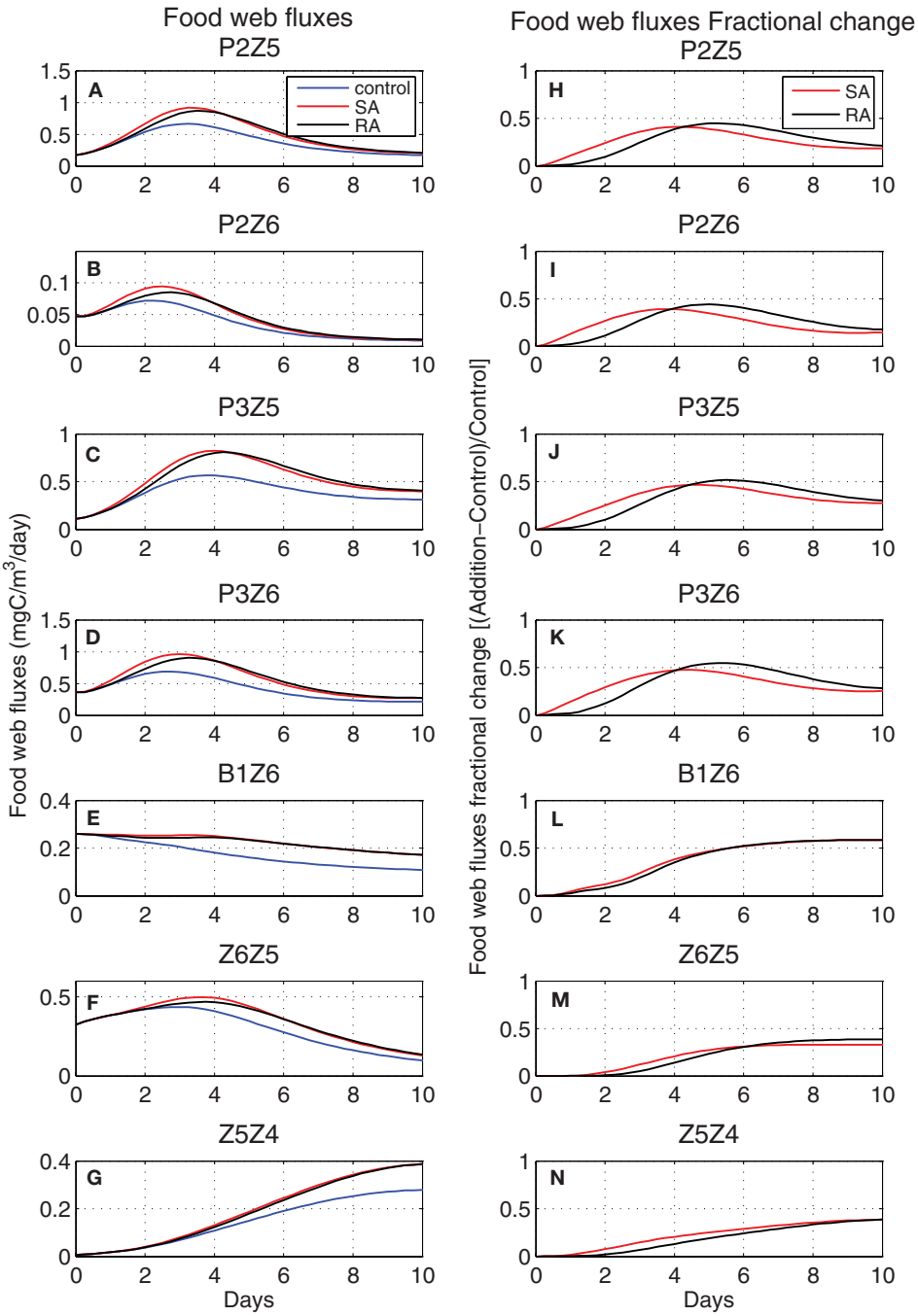

FIGURE 5 | Evolution of food web carbon fluxes (left, mgC/m^3/day) for (A) P2Z5, **(B)** P2Z6, **(C)** P3Z5, **(D)** P3Z6, **(E)** B1Z6, **(F)** Z6Z5, **(G)** Z5Z4 in Control (blue line) and Addition (SA red line, RA black line) treatments and respectively their fractional change [(Addition − Control)/Control] (right) **(H–N)**. P2, nanophytoplankton; P3, picophytoplankton; B1, bacteria; Z6, HNAN; Z5, microzooplankton; Z4, mesozooplankton (see **Figure 1**).

Phytoplankton/Nutrient Uptake

In ERSEM, the nutrient uptake is constrained by a maximum uptake rate (V_0) that depends on the dissolved inorganic nutrients external concentration and phytoplankton affinity. In the case of phosphorus uptake (PO_4) this is:

$$V_0 = qurP \cdot PO_4 \cdot PhytoC, \quad (1)$$

with $qurP$ being the specific affinity for phosphorus uptake (Table A1 in Supplementary Material), while this is regulated by the amount of nutrient that is necessary for the cell to address its needs for growth and intracellular storage:

$$V_{needed} = runP \cdot qpP_{\max} + (qpP_{\max} \cdot PhytoC - PhytoP), \quad (2)$$

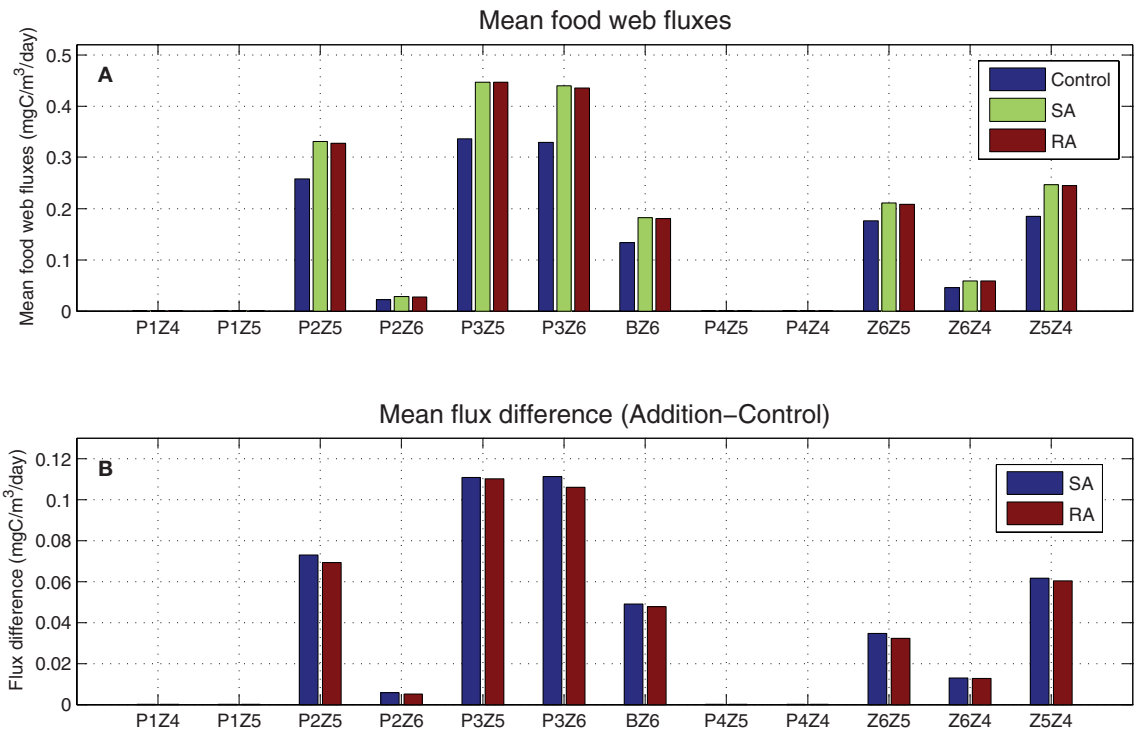

FIGURE 6 | (A) Simulated mean food web carbon fluxes for addition (SA/RA) and control treatments (mgC/m^3/day) and **(B)** their difference (SA/RA-Control). P1, diatoms; P2, nanophytoplankton; P3, picophytoplankton; P4, dinoflagellates; B, bacteria; Z6, HNAN; Z5, microzooplankton; Z4, mesozooplankton (see **Figure 1**).

where *runP* is the phytoplankton net production (photosynthesis-excretion-respiration), $qpP_{\max}$ is the maximum phosphorus internal quota ($qpP_{\max}$ = 2 × Redfield ratio, Table A1 in Supplementary Material) and *PhytoC*, *PhytoP* are the carbon and phosphorus phytoplankton pools respectively. The actual nutrient rate is then taken as:

$$V = \min(V_0, V_{needed}), \tag{3}$$

With this formulation and the adopted specific affinity parameter values [$qurP$ = 0.0025 (mgC/m^3)$^{-1}$ day^{-1}], the simulated phytoplankton nutrient uptake was quite low, as V_0 (Equation 1) was constrained by the very low initial nutrient concentrations of the mesocosms (∼0.005 mmol/m^3 PO_4, ∼0.1 mmol/m^3 DIN). This reduced nutrient uptake resulted in a close to zero primary production (**Figure 8**, Run2), as it quickly leads to a sub-optimal phytoplankton internal stoichiometry that triggered an increased carbon excretion and cell lysis, as adopted in ERSEM formulation (Baretta-Bekker et al., 1997):

$$Excretion = sumP \cdot (1 - Q\lim) \cdot seoP_{\max}, \tag{4}$$

$$Lysis = 1/(Q\lim + 0.1) \cdot sdoP, \tag{5}$$

where *sumP* is the carbon uptake, $seoP_{\max}$ is the maximum fraction excreted, *sdoP* is the lysis rate and Qlim is the Droop nutrient limitation function of internal cell quotas (*qpP*, *qnP*), which in the case of phosphorus is:

$$Q\lim = (qpP - qpP_{\min})/(qpP_{\max} - qpP_{\min}), \tag{6}$$

with $qpP_{\max}/qpP_{\min}$ being the maximum/minimum phosphorus internal quotas.

In order for simulated net primary production and phytoplankton biomass to approach the observed values in the mesocosm experiment, much higher affinity parameters [$qurP$ × 20 ∼0.05 (mgC/m^3)$^{-1}$day^{-1}] were necessary (**Figure 8**, Run3). An even better agreement of simulated results, particularly in terms of dissolved inorganic nutrients that were slightly reduced toward observations, was found when nutrient uptake rates were assumed to follow the classic Michaelis-Menten kinetics as in Geider et al. (1998):

$$\begin{aligned} V &= V_{\max} \cdot PO_4/(PO_4 + K_P) \\ &= sumP \cdot qpP_{red} \cdot PO_4/(PO_4 + K_P) \cdot Q_{\max} \cdot PhytoC, \end{aligned} \tag{7}$$

where *sumP* is the carbon specific maximum growth rate, qpP_{red} is the Redfield phosphorus quota, K_p is the half-saturation (fitted parameter) for phosphorus uptake and *Qmax* = $(qpP_{\max} - qpP)/(qpP_{\max} - qpP_{\min})$, with $qpP_{\max}/qpP_{\min}$ being the maximum/minimum phosphorus internal quotas (see Table A1 in Supplementary Material). *Qmax* approaches zero when the phytoplankton internal phosphorus quota *Q* is maximum (=$qpP_{\max}$), resulting in the decline of nutrient

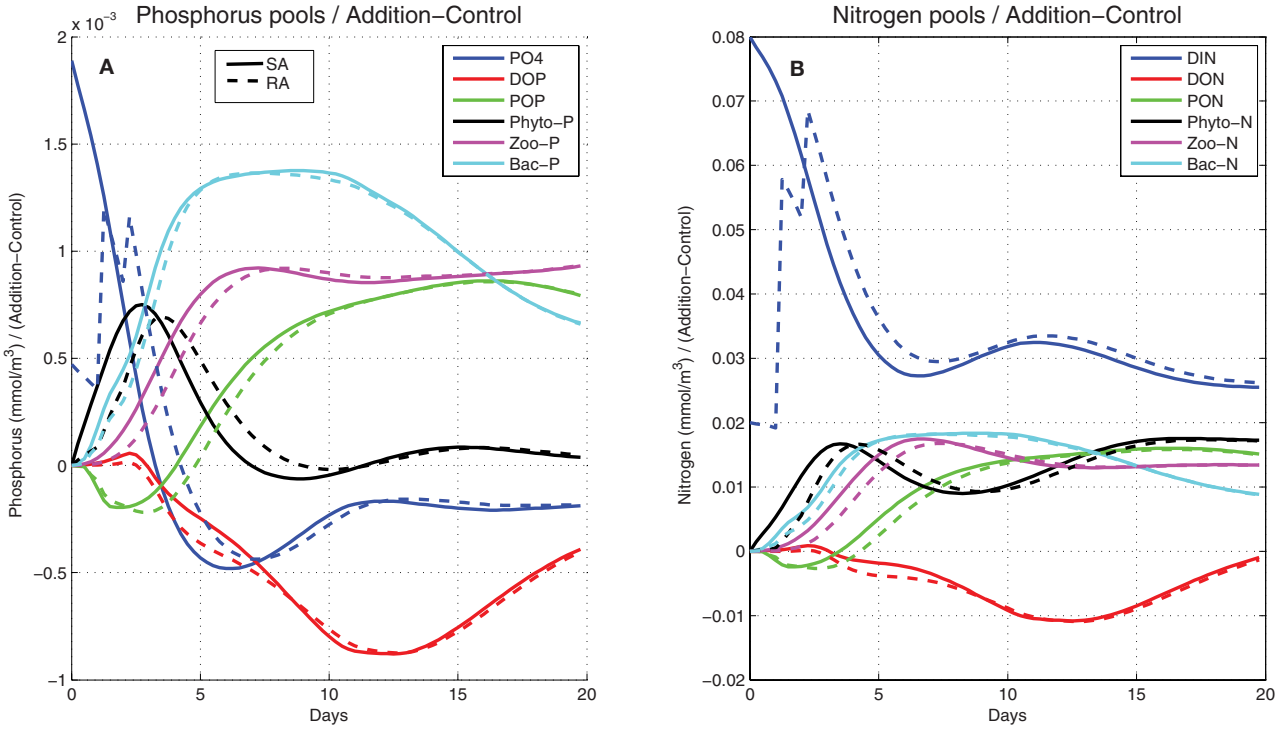

FIGURE 7 | Simulated difference between the addition (SA, continuous line; RA dashed line) and control treatments in (A) phosphorus and **(B)** nitrogen pools (mmol/m^3) in the form of dissolved inorganic (blue line), dissolved organic (red line), particulate organic (green line), phytoplankton (black line), zooplankton (magenta line), and bacteria (cyan line).

uptake. When Equation (7) was used for nutrient uptake instead of Equation (3), the simulated net primary production better reproduced the observed evolution, showing a slightly more extended peak (**Figure 8**, Run1), while simulated inorganic nutrients got closer to the slightly lower observed values, particularly for phosphate. This is related to the use of the Michaelis-Menten sigmoid function in Equation (7) that results in a more gradual decrease of nutrient uptake and the steepest decrease of nutrients, as compared to those simulated when the linear function Equation (1) is used.

The phytoplankton affinity, defined as the initial slope of nutrient uptake at very low nutrient concentrations ($PO_4 + K_p \sim K_p$) can be calculated from Equation (7) as $qurP \sim V_{\max}/K_p$, which gives 0.11 and 0.13 $(\text{mgC/m}^3)^{-1}\text{day}^{-1}$ for nanophytoplankton and picophytoplankton, respectively. These are slightly higher than the fitted affinity parameters [0.05–0.0625 $(\text{mgC/m}^3)^{-1}\text{day}^{-1}$] using the original ERSEM formulation and much higher than the previously adopted affinity parameters [0.0025 $(\text{mgC/m}^3)^{-1}\text{day}^{-1}$].

Zooplankton (Grazing Half-Saturation Parameter)

The prey uptake by *Zi* zooplankton heterotrophic groups (Z4 = mesozooplankton, Z5 = microzooplankton, Z6 = heterotrophic nanoflagellates, see **Figure 1**) in ERSEM is described by a Holling-II type function:

$$U^{Zi} = {F_{tot}}^{Zi}/({F_{tot}}^{Zi} + K_{Zi}), \tag{8}$$

where K_{Zi} is a half-saturation constant (where the uptake rate is half its maximum value) and F_{tot}^{Zi} is the total available amount of food from different sources:

$${F_{tot}}^{Zi} = \sum_j su_{ij} \cdot F_j \cdot F_j/(F_j + \min food_{Zi}), \tag{9}$$

with su_{ij} being the preference of *Zi* group on different preys F_j and min $food_{Zi}$ another half-saturation constant used to prevent from exhausting a prey food source when this is scarce, as compared to some minimum food requirement (see Tables A2, A3). The total amount of food is thus calculated from Equation (8), based on the preference and the relative availability of different preys. In order to correctly simulate the observed biomass of zooplankton groups, the half-saturation constant (K_{Zi}) parameters were decreased from their initial values ($K_{Z4} = 14$, $K_{Z5} = 24$, $K_{Z6} = 49$ mgC/m^3, see **Table 1**). As shown in **Figure 9U**, mesozooplankton was initially significantly underestimated (Run4, see **Table 1**). Adopting a lower half-saturation ($K_{Z4} = 3$ mgC/m^3), the simulated mesozooplankton biomass in Run5 approached the observations (**Figure 9V**) but the biomass of its prey, microzooplankton, was decreased (**Figure 9R**). Decreasing also the microzooplankton half-saturation constant ($K_{Z5} = 10$ mgC/m^3) in Run6, the microzooplankton underestimation was removed (**Figure 9S**), mesozooplankton was further increased (**Figure 9W**), but an underestimation was now found for heterotrophic nanoflagellates (**Figure 9O**). This was finally removed (**Figure 9P**) in Run1 when the respective half-saturation

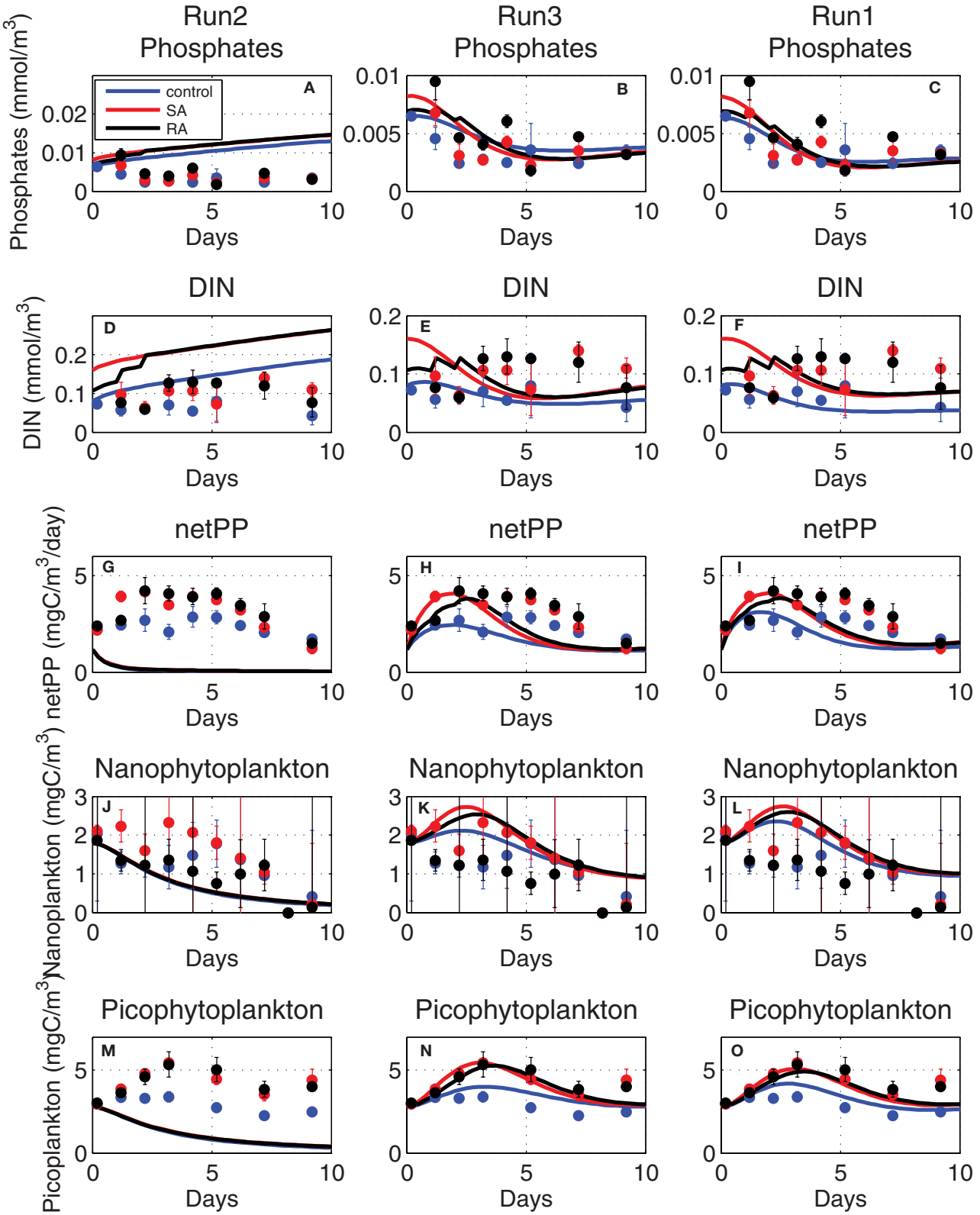

FIGURE 8 | Evolution of (A–C) phosphate (mmol/m^3), **(D–F)** dissolved inorganic nitrogen (DIN, mmol/m^3), **(G–I)** net primary production (netPP, mgC/m^3/day), biomass of **(J–L)** nanophytoplankton (mgC/m^3) and **(M–O)** picophytoplankton (mgC/m^3), simulated adopting old phytoplankton affinity (Equation 1, Run2), higher (fitted) affinity (Equation 1, Run3), and with the Michaelis-Menten kinetics (Equation 7, Run1) adopted formulation (see **Table 1** for simulations attributes).

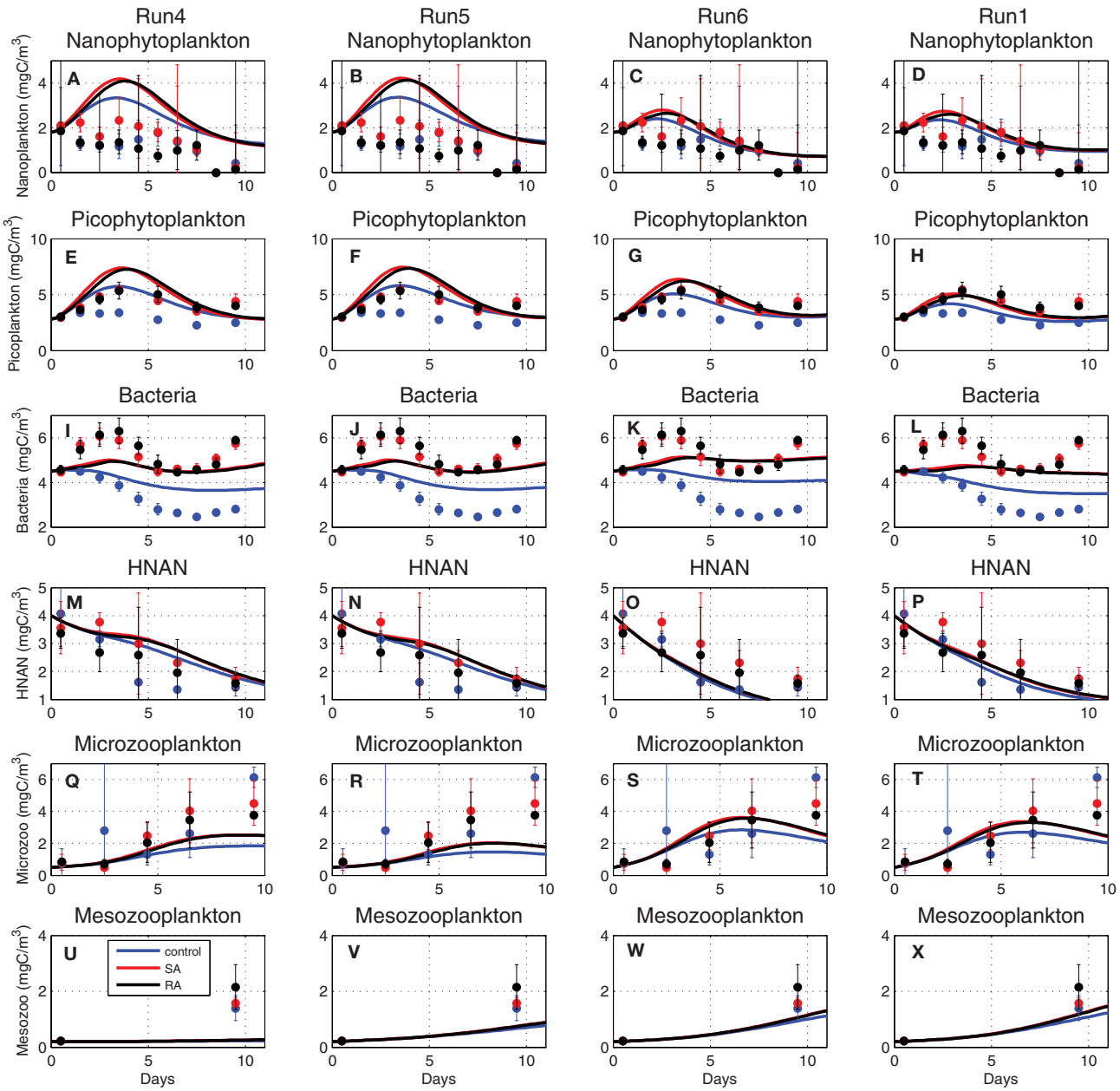

FIGURE 9 | Evolution of (A–D) nanophytoplankton, **(E–H)** picophytoplankton, **(I–L)** bacteria, **(M–P)** HNAN, **(Q–T)** microzooplankton, and **(U–X)** mesozooplankton biomass (mgC/m^3) simulated by Run4, Run5, Run6, and Run1, adopting different half-saturation constants for zooplankton uptake (see **Table 1** for simulations attributes).

constant was also decreased (K_{Z6} = 16 mgC/m^3), showing also a slightly better agreement for microzooplankton and mesozooplankton (**Figures 9T,X**). This series of sensitivity experiments illustrates the prey-predator trophic relations. One may notice, for example, the increase in bacteria in Run6 (**Figures 9I–L**), following the decrease of their predator, HNAN (**Figures 9M–P**), or the increase in nanophytoplankton (**Figures 9A–D**) and picophytoplankton (**Figures 9E–H**) in Run4/Run5 due the relatively low microzooplankton biomass (**Figures 9Q–T**).

Bacterial Dynamics

The observed variability in the mesocosm experiment was characterized by a significant enhancement of bacterial production and biomass in the two addition treatments (SA, RA), as compared to the control mesocosms. This increased bacterial productivity, triggered by dust additions, appeared to be closely coupled to the phytoplankton productivity increase. The ERSEM bacteria sub-model in Petihakis et al. (2002) has been revised by Petihakis et al. (2015), following Anderson and Williams (1998) and Petihakis et al. (2009), allowing for a

better representation of the DOM pool, which was particularly important in the presence of significant lateral inputs (e.g., rivers, Black Sea Water) of DOM. The uptake of DOM by bacteria is described by:

$$U_B = sumB \cdot f(T) \cdot f(O2) \cdot \min(\min(N_{Lim}, P_{Lim}), C_{Lim}), \quad (10)$$

where *sumB* is the maximum bacterial growth rate, *f(T)* is the growth temperature dependence, *f(O2)* the oxygen limitation, (N_{Lim}, P_{Lim}) is the nutrient limitation on nitrogen/phosphorus and C_{Lim} the limitation on available DOC. The bacteria nutrient limitation (N_{Lim}, P_{Lim}) is assumed to depend on the intracellular nitrogen (N/C) and phosphorus (P/C) bacteria quotas (*qnB*, *qpB*), compared to the maximum internal quotas ($qnB_{\max}$, $qpB_{\max}$):

$$\begin{aligned} N_{Lim} &= \min(1, \max(0, qnB/qnB_{\max})) \\ P_{Lim} &= \min(1, \max(0, qpB/qpB_{\max})), \end{aligned} \quad (11)$$

Alternatively, the bacteria nutrient limitation may be assumed to be a function of external nutrient concentrations, as adopted by Blackford et al. (2004):

$$\begin{aligned} N_{Lim} &= (DON + DIN)/(DON + DIN + K_{NBac}) \\ P_{Lim} &= (DOP + PO_4)/(DOP + PO_4 + K_{PBac}), \end{aligned} \quad (12)$$

Where *DON/DOP* is dissolved organic phosphorus/nitrogen and $K_{N/PBac}$ is a half-saturation constant.

The carbon limitation (Clim) is described by:

$$C_{Lim} = DOC/(DOC + K_{DOC}) \quad (13)$$

where *DOC* represents labile and semi-labile *DOC* and K_{DOC} is a half-saturation constant (Table A2).

When the DOC pool was initialized from the mesocosm measurements (~400 mgC/m^3 **Figure 10E**, Run7), the simulated bacterial production/biomass overall mean was consistent with the measured values, but the model was not able to reproduce the observed variability and particularly the strong differentiation of the addition treatments in relation to the control (**Figures 10A,I**, Run7). DOC is produced by mortality, excretion and lysis of primary and secondary producers and is mostly labile that is

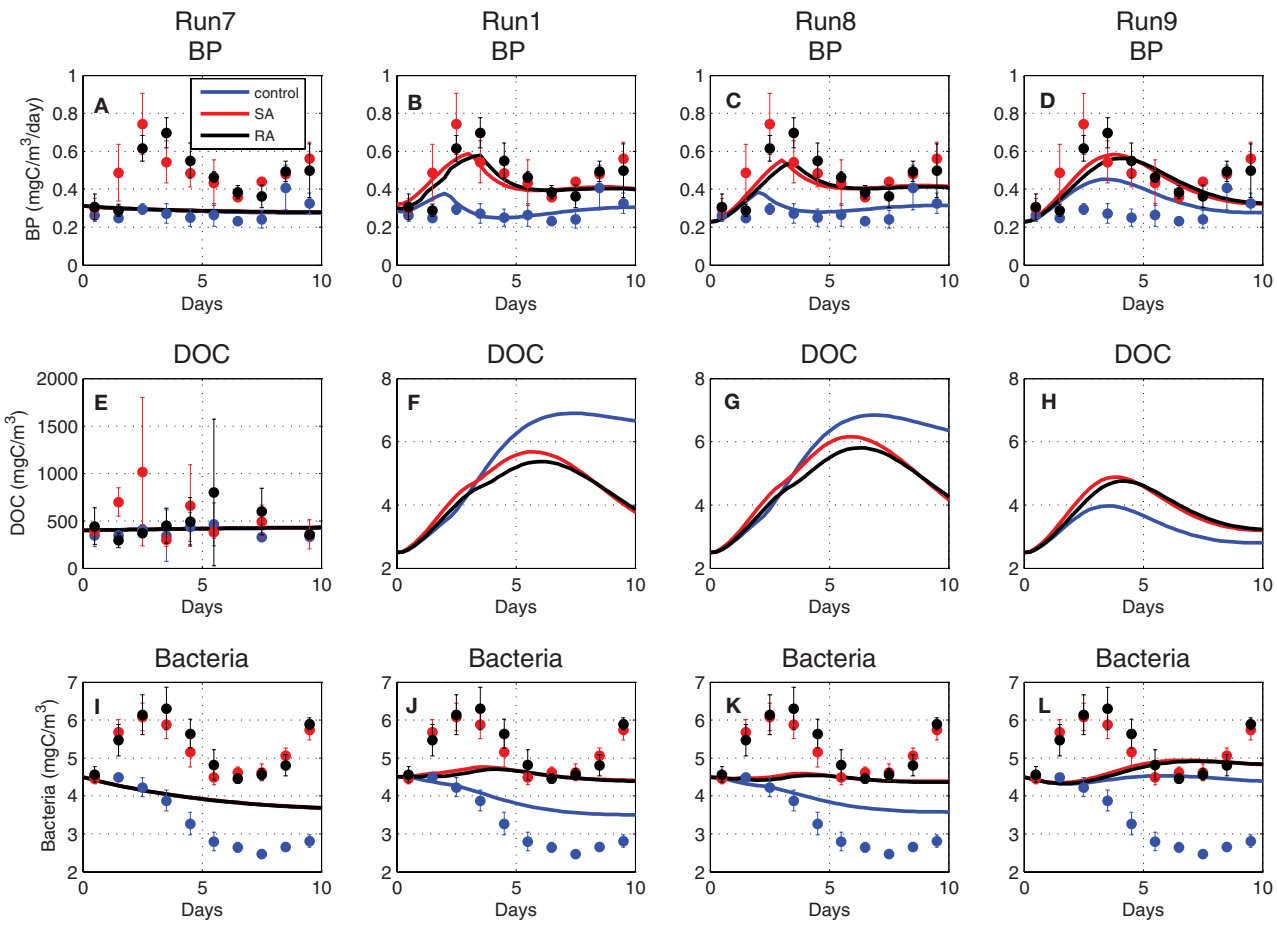

FIGURE 10 | Evolution of (A–D) bacterial production (BP, mgC/m^3/day), **(E–H)** dissolved organic carbon (DOC, mgC/m^3), and **(I–L)** bacterial biomass (mgC/m^3) simulated in Run7, Run1, Run8, and Run9 (see **Table 1** for simulation attributes).

readily available for bacteria. Semi-labile DOC takes longer to decompose by bacteria and can accumulate with time. One can assume that the initial measured DOC pool was mostly semi-labile, while bacterial production on the short (∼days) time scale of the experiment was primarily affected by labile organic matter, as the one produced/excreted by plankton biomass. To test this hypothesis, the initial DOC pool was significantly decreased (∼3 mgC/m^3 **Figures 10F–H**), considering only its labile component, as also the half-saturation for DOC uptake ($K_{DOC} = 4$ mgC/m^3). Indeed, in this case, bacterial production presented an increase in the addition treatments (**Figure 10D**, Run9), being closely coupled to the enhanced plankton biomass that released additional DOC. The simulated bacterial production presented a slightly weaker variability, as compared to the observed that showed a stronger and slightly earlier peak in the addition treatments, as well as a higher increasing trend at the end of the 10-day period. Moreover, the model failed to reproduce the observed early peak of bacterial biomass in the addition treatments (**Figure 10L**, Run9). The simulated bacterial production and biomass were further improved (**Figures 10C,K**, Run8) when bacterial nutrient limitation was assumed to be a function of external nutrient concentrations (Equation 12), rather than the bacteria internal quotas (Equation 11). In this case, bacterial production appeared to be directly stimulated by the addition of inorganic nutrients, showing an earlier peak on day-3, in agreement with observations, as well as a stronger differentiation between the addition and control treatments. The simulated bacterial biomass, despite the weaker variability, now showed a similar pattern with observations, initially increasing in SA/RA and decreasing in the control (**Figure 10K**). The simulated bacterial production was still slightly underestimated in the SA/RA treatments. Given its strong sensitivity to the bacterial assimilation efficiency parameter (see next section Model parameter sensitivity), a final model improvement was explored, adopting a variable bacterial assimilation efficiency, depending on nutrient limitation. Specifically, a function of nutrient limitation (*NP*lim, Equation 12) was introduced in the computation of bacterial respiration as:

$$R_B = U_B \cdot [1 - (puB \cdot eO2 - puBo \cdot (1 - eO2)) \cdot f(NP\,\mathrm{lim})] + R_{Bb}, \quad (14)$$

where U_B is the bacterial growth rate (Equation 10), *puB*/*puBo* is the bacteria assimilation efficiency parameter at sufficient/low oxygen (Table A2), *eO2* is the relative oxygen saturation, R_{Bb} is the temperature dependent basal respiration ($R_{Bb} = srsB^{*}f(T)$, Table A2) and

$$f(NP\,\mathrm{lim}) = 2 \cdot \min(P\,\mathrm{lim}, N\,\mathrm{lim}) / [\min(P\,\mathrm{lim}, N\,\mathrm{lim}) + 0.1], \quad (15)$$

The introduced function of nutrient limitation varied between 0.91 and 1.14 in the control and between 0.95 and 1.24 in SA/RA treatments and effectively resulted in a slightly stronger variability of Bacterial Growth Efficiency (BGE∼($U_B - R_B$)/U_B), depending on nutrient limitation. This model modification lead to a higher bacterial production and biomass in the addition treatments (**Figures 10B,J**) that were characterized by a relaxed nutrient limitation, improving the model fit with observations.

Model Parameter Sensitivity

A minimum set of parameters/formulations of the existing model were carefully revised, as discussed in the previous section in order to obtain an optimum fit with the observations. The rest of model parameters and formulations were kept fixed to their old values, as their modification did not show any significant improvement. To test the model sensitivity to different parameters, a series of sensitivity experiments were performed, adopting a 10% increase in the value of chosen parameters (see Tables A1, A2 in Supplementary Material for their definition and reference value). The output from these sensitivity simulations with modified parameter values was then compared to the reference simulation, computing the fractional change [(sensitivity − reference)/reference] for different variables. As shown in **Figure 11**, dissolved inorganic nutrients were mostly affected by phytoplankton maximum growth rate (*sumP*) and half-saturation coefficients for nutrient uptake (K_P, K_N). An increase in *sumP* results in the increase of phytoplankton growth rate and thus, to the decrease of nutrients, while an increase in K_P/K_N results in a reduction of nutrient uptake rate (see Equation 7). Phytoplankton biomass (p2c, p3c) is mostly sensitive to *sumP*, as well as to the lysis rate (*sdoP*) and particularly to the grazing half-saturation constants (K_{Z5}, K_{Z6}) that affect their predation by zooplankton (z5c, z6c, see Equation 8). An increase in K_{Z5} results in the increase in nanophytoplankton (p2c) and heterotrophic nanoflagellates (z6c), the main preys of microzooplankton (z5c), while increasing K_{Z6} mainly affects picophytoplankton (p3c). Finally, increasing K_{Z4} mainly affects mesozooplankton and to a lesser degree its preys z5c and z6c. Bacterial production is among the most sensitive model variables, particularly affected by bacterial assimilation efficiency (*puB*), growth rate (*sumB*) and basal respiration (*srsB*), as well as to the half-saturation for DOC uptake (K_{DOC}). It is also sensitive to the first order breakdown rate from POC to DOC (*fr6r1*, Petihakis et al., 2015) and the maximum DOC phytoplankton excretion rate under nutrient limitation ($seoP_{\max}$), both related to the supply of DOC that is necessary for bacteria to grow. Bacterial biomass depends on the same parameters but appears much less sensitive.

DISCUSSION AND CONCLUDING REMARKS

Among the primary goals of the present study was to thoroughly test and improve the biogeochemical model parameterizations, given the significant amount of available observations on most components of the modeled system that presented a rare opportunity. Often one attempts to validate a model using *in situ* data collected from a few stations in the area of interest. However, hydrodynamic processes, such as advection and mixing, normally confound the temporal change related to biogeochemical processes with spatial changes, in a manner that is difficult to discern. Therefore, the degree of mismatch between a calculation and a field observation cannot be safely assigned to a

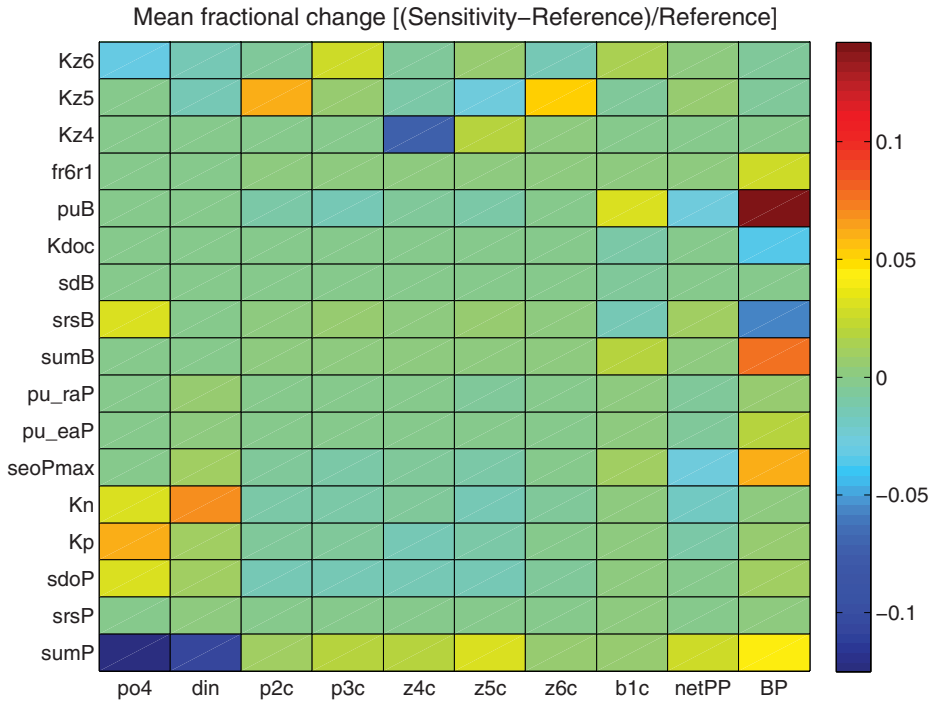

FIGURE 11 | Mean fractional change [(Sensitivity − Reference)/Reference) of model simulated PO_4, DIN, nanophytoplankton (p2c), picophytoplankton (p3c), mesozooplankton (z4c), microzooplankton (z5c), HNAN (z6c), bacteria (b1c), net primary production (netPP), and bacterial production (BP) adopting a 10% increase of different model parameters (see Tables A1, A2 in Supplementary Material for their definition and reference values).

failure of the theory, as formulated by the model or to inadequate field observations. Mesocosm experiments include most of the marine environmental factors (light, temperature etc), providing a realistic description of the ecosystem, while they remove the effect of hydrodynamics, random fluctuations and patchiness, offering a way to test the biogeochemical model formulations and its ability to reproduce the ecosystem dynamics. On the other hand, biogeochemical models are usually designed to be generic in order to describe the ecosystem functioning across a wide range of environmental conditions from coastal to open sea and/or from more productive to oligotrophic conditions, found in the area of interest. Mesocosms represent a more local part of the ecosystem. Given the great diversity of plankton organisms, the mesocosm plankton communities enclosed from the field may still be too complicated for testing biological models, except in respect to their most general features (e.g., Steele and Frost, 1977). Biogeochemical models are therefore not intended to provide a perfect fit with mesocosm observations, but the description of the ecosystem main features, while maintaining their generic nature.

Atmospheric deposition of nitrogen and phosphorus represents an important source of nutrients, enhancing the marine productivity in oligotrophic areas, such as the Mediterranean. Within ADAMANT project, a mesocosm experiment was carried out (Lagaria et al., 2017; Pitta et al., 2017), adding dissolved inorganic nitrogen and phosphorus by means of atmospheric dust (single addition and repetitive addition in three successive doses) in controlled tanks with Cretan Sea water and compared with control (blank) tanks. Observations on almost all components of the pelagic ecosystem on a 10-day period allowed investigating the effect of atmospheric deposition and the pathways of the added nutrients in the marine ecosystem. In the present study, a comprehensive biogeochemical model was setup and customized to simulate the mesocosm experiment. After certain modifications and the necessary tuning, the model was able to reasonably capture the observed variability of different ecosystem components and reproduce the main features of the experiment. In agreement with the observations, model results indicated an enhancement of primary production and phytoplankton biomass with added nutrients. A significant increase was also simulated for bacterial production. Its stimulation was found to be mainly related to the *in situ* produced dissolved organic matter, as well as to the relaxed nutrient limitation in the addition treatments. The model was less successful with bacterial biomass, underestimating its observed increase and variability. However, this model deviation could be partly removed if the measured biomass was decreased by some factor i.e., considering a smaller conversion factor from cell abundance that might be more appropriate in oligotrophic seas, such as the Mediterranean. The model also reasonably captured the evolution of other heterotrophs, characterized by the decrease of heterotrophic nanoflagellates and the increase of microzooplankton and mesozooplankton. The model results indicated that the impact of the single dust addition event in the

marine system was slightly stronger than three successive smaller ones, which is consistent with the general ecosystem stable state theory (Scheffer et al., 2001; Collie et al., 2004). However, this difference was relatively small, not being able to be verified by observations, considering the standard deviation of replicate measurements.

Model results were used to identify the main carbon pathways and to investigate the impact of nutrient additions in terms of carbon flows within the food web. The dust addition did not modify the food web structure that was dominated by fluxes from picophytoplankton/bacteria to heterotrophic nanoflagellates and particularly from nanophytoplankton/picophytoplankton to microzooplankton, but just increased its trophic status, with more carbon circulating in the entire food web. Model results were also used to track the fate of the added nitrogen/phosphorus. These were initially channelled from the dissolved inorganic pools to phytoplankton, followed by zooplankton with a time-lag, with bacteria consuming the produced dissolved organic nitrogen/phosphorus and all contributing to the build-up of particulate organic pool through mortality losses.

In the Cretan Sea, primary production is increased during winter and early spring (Siokou-Frangou et al., 2002) due to intense winter mixing that supplies the euphotic zone with nutrients from the deeper layers. The mesocosm experiments were carried out during the stratification period (May), when inorganic nutrient concentrations at the Cretan Sea surface layer are extremely low and dust atmospheric deposition is the only source of nutrients sustaining primary production, along with nutrient recycling (Christodoulaki et al., 2013). The plankton response to atmospheric dust additions, captured by the mesocosm experiments and model simulations, may thus be considered representative of this period, when the effect of atmospheric deposition is mostly demonstrated. In the near future (2030), nutrient inputs with atmospheric deposition in the Eastern Mediterranean are expected to increase for nitrogen and remain similar for phosphorus, as estimated by Duce et al. (2008) and Mahowald et al. (2008), based on global chemistry-transport model calculations. Given the P-limited characteristics of the Eastern Mediterranean marine ecosystem, such changes are expected to have a limited effect on plankton biomass stocks, but may contribute to a further increase of N:P ratio and a stronger P-limitation (Christodoulaki et al., 2016).

In order to correctly reproduce the observed variability in the mesocosm experiment, certain model assumptions, along with few changes in the model parameter set and formulations were necessary. These were discussed through a series of sensitivity simulations. Noticing the strong coupling of the observed bacterial production to phytoplankton biomass, it was assumed that on the short (∼days) time scale of the experiment, bacteria were primarily affected by labile organic matter as the one *in situ* produced/excreted by plankton biomass, rather than semi-labile that is decomposed on a longer time-scale. The simulated variability of bacteria was further improved adopting a function of external nutrient concentrations for nutrient limitation of their growth, rather than their internal stoichiometry. In this way, bacterial production was directly stimulated by the addition of inorganic nutrients, showing a similar to phytoplankton early peak, in agreement with observations. A final model improvement was explored, adopting variable bacterial assimilation efficiency (BGE), depending on nutrient limitation. Such dependence is consistent with field data studies, suggesting that BGE varies according to the trophic richness of the ecosystem (del Giorgio and Cole, 1998). The simulated bacterial biomass reproduced the observed pattern in the addition and control treatments, but showed a much weaker variability. This model deviation could be partly removed if the measured biomass (and its initial value used in the model simulations) was decreased by some factor. Bacteria carbon biomass was converted from cell abundance using a conversion factor of 20 mgC/cell based on Lee and Fuhrman (1987), which, although widely used, is known to lead in overestimations (as much as 330%) in oligotrophic seas, such as the Mediterranean, where values of 12.4 ± 6.3 mgC/cell have been suggested (Fukuda et al., 1998). Another source of uncertainty in the simulated bacteria biomass was the effect of viral lysis that is not explicitly represented in the model.

Another important change in the model that was found necessary in order to reproduce the observed primary production, was the effective increase of phytoplankton nutrient uptake rate, either by increasing phytoplankton affinity parameter ($\times$ 20) or by adopting Michaelis-Menten kinetics with properly tuned half-saturation constants. The higher adopted phytoplankton affinity values are closer to those reported in recent reviews of experimental data (e.g., Tambi et al., 2009), also showing an inverse relationship with size (e.g., Edwards et al., 2012). Particularly for the Mediterranean, Tanaka et al. (2004) estimates for affinity were ∼0.8–2 $(\mathrm{mgC/m^3})^{-1}\mathrm{day}^{-1}$ for picophytoplankton and ∼0.06–0.24 $(\mathrm{mgC/m^3})^{-1}\mathrm{day}^{-1}$ for autotrophic flagellates, while Moutin et al. (2002) has reported a dependence of phytoplankton affinity on nutrient limitation conditions, showing an increasing trend in the Eastern oligotrophic conditions. Phytoplankton affinity reflects its efficiency to grow in oligotrophic environments, such as the Eastern Mediterranean. In less nutrient-limiting conditions, such as the North Sea, where ERSEM was initially tested, the model sensitivity to the phytoplankton affinity parameters is expected to be much weaker. Furthermore, given the limitations measuring very low nutrient concentrations, particularly with older methods characterized by relatively high detection limits, it was difficult to validate correctly the model simulated productivity under nutrient-depleted conditions, when using old *in situ* data. Therefore, the simulated integrated primary production might be in reasonable agreement with *in situ* data, but a model underestimation in near-surface nutrient depleted waters might be unnoticed. Indeed, in previous implementations with a 3-D ERSEM model version in the Mediterranean (e.g., Petihakis et al., 2002, 2015; Tsiaras et al., 2014) the simulated integrated primary production was in reasonable agreement with observations, while near-surface nutrients/production during stratified periods might be overestimated/underestimated.

Finally, the growth rate of heterotrophic nanoflagellates, microzooplankton and mesozooplankton was effectively

increased by decreasing their feeding half-saturation constants, as their biomass was initially underestimated. This model modification, combined with the increased phytoplankton nutrient uptake has implications mainly on dissolved inorganic nutrients that are now relaxed to lower concentrations. With the new model configuration (higher nutrient uptake/higher grazing pressure), simulated phytoplankton with the 3-D biogeochemical model might be similar, at least on a seasonal scale, but nutrient concentrations are expected to be lower and probably closer to observations in nutrient depleted waters. We should note however that in the present study the model was tuned to the oligotrophic Cretan Sea conditions. Therefore, changes in the model formulation/parameterization for its 3-D Mediterranean implementation will require careful testing to ensure that this maintains its generic character, describing the ecosystem functioning across a wide range of environmental conditions. The model simulated heterotrophs should also be further validated, as available field data has been very scarce, particularly on microzooplankton and heterotrophic nanoflagellates and collected mostly from more productive areas, such as the N. Aegean.

AUTHOR CONTRIBUTIONS

KT designed the study and model simulations, made the figures, and wrote the manuscript. SC contributed in the discussions of the study, figures preparation, and writing of the manuscript. GP contributed in the design and discussions of the study and writing of the manuscript. CF collated observational data and contributed in the discussions of the study and writing of the manuscript. GT contributed in the discussions of the study and writing of the manuscript.

ACKNOWLEDGMENTS

This research has been co-financed by the European Union (European Social Fund–ESF) and Greek national funds through the Operational Program "Education and Lifelong Learning" of the National Strategic Reference Framework (NSRF) Research Funding Program: THALES (ADAMANT–Atmospheric Deposition And MediterraneAN sea water producTivity), Investing in knowledge society through the European Social Fund. We would like to thank Dr. P. Pitta (HCMR) for the helpful comments on the manuscript. We also thank all scientists from HCMR that analyzed and provided data from the mesocosm experiment: S. Zivanovic, E. Dafnomili, and M. Tsapakis (inorganic nutrients), K. Violaki (dissolved organic carbon), A. Lagaria and S. Psarra (primary production and phytoplankton abundance), N. Papageorgiou and P.D. Dimitriou (Chl-a), A. Giannakourou (bacterial production), A. Tsiola (heterotrophic bacteria and cyanobacteria abundance), M. Kagiorgi (nanoflagellates and microzooplankton counts), S. Mpatziakas (mesozooplankton counts), and P. Pitta for organizing the mesocosm experiment and dataset.

SUPPLEMENTARY MATERIAL

The Supplementary Material for this article can be found online at: http://journal.frontiersin.org/article/10.3389/fmars.2017.00120/full#supplementary-material

REFERENCES

Allen, J. I., Somerfield, P. J., and Siddorn, J. (2002). Primary and bacterial production in the Mediterranean Sea: a modelling study. *J. Mar. Syst.* 33–34, 473–495. doi: 10.1016/S0924-7963(02)00072-6

Anderson, T. R., and Williams, P. J. I. B. (1998). Modelling the seasonal cycle of dissolved organic carbon at Station E_1 in the English Channel. *Estuar. Coast. Shelf Sci.* 46, 93–109. doi: 10.1006/ecss.1997.0257

Azov, Y. (1991). Desert. *Mar. Pollut. Bull.* 23, 225–232. doi: 10.1016/0025-326X(91)90679-M

Baretta, J. W., Ebenhoh, W., and Ruardij, P. (1995). The European regional seas ecosystem model, a complex marine ecosystem model. *Netherlands J. Sea Res.* 33, 233–246. doi: 10.1016/0077-7579(95)90047-0

Baretta-Bekker, J. G., Baretta, J. W., and Ebenhoh, W. (1997). Microbial dynamics in the marine ecosystem model ERSEM II with decoupled carbon assimilation and nutrient uptake. *J. Sea Res.* 38, 195–211. doi: 10.1016/S1385-1101(97)00052-X

Bethoux, J. P., Morin, P., Chaumery, C., Connan, O., Gentili, B., and Ruiz-Pino, D. (1998). Nutrients in the Mediterranean Sea, mass balance and statistical analysis of concentrations with respect to environmental change. *Mar. Chem.* 63, 155–169. doi: 10.1016/S0304-4203(98)00059-0

Blackford, J. C., Allen, J. I., and Gilbert, F. J. (2004). Ecosystem dynamics at six contrasting sites: a generic modelling study. *J. Mar. Syst.* 52, 191–215. doi: 10.1016/j.jmarsys.2004.02.004

Christodoulaki, S., Petihakis, G., Kanakidou, M., Mihalopoulos, N., Tsiaras, K., and Triantafyllou, G. (2013). Atmospheric deposition in the Eastern Mediterranean, A driving force for ecosystem dynamics. *J. Mar. Syst.* 109–110, 78–93. doi: 10.1016/j.jmarsys.2012.07.007

Christodoulaki, S., Petihakis, G., Mihalopoulos, N., Tsiaras, K.,Triantafyllou, G., and Kanakidou, M. (2016). Human-driven atmospheric deposition of N and P controls on the East Mediterranean marine ecosystem. *J. Atmos. Sci.* 73, 1611–1619. doi: 10.1175/JAS-D-15-0241.1

Collie, J. S., Richardson, K., and Steele, J. H. (2004). Regime shifts: can ecological theory illuminate the mechanisms? *Prog. Oceanogr.* 60, 281–302. doi: 10.1016/j.pocean.2004.02.013

Crise, A., Allen, J. I., Baretta, J., Crispi, G., Mosetti, R., and Solidoro, C. (1999). The Mediterranean pelagic ecosystem response to physical forcing. *Prog. Oceanogr.* 44, 219–243. doi: 10.1016/S0079-6611(99)00027-0

del Giorgio, P. A., and Cole, J. (1998). Bacterial growth efficiency in natural aquatic systems. *Annu. Rev. Ecol. Syst.* 28, 503–541. doi: 10.1146/annurev.ecolsys.29.1.503

Droop, M. R. (1974). The nutrient status of algal cells in continuous culture. *J. Mar. Biol. Assoc. UK.* 54, 825–855. doi: 10.1017/S002531540005760X

Duce, R. A., LaRoche, J., Altieri, K., Arrigo, K. R., Baker, A. R., Capone, D. G. et al. (2008). Impacts of atmospheric anthropogenic nitrogen on the open ocean. *Science* 320, 893–897. doi: 10.1126/science.1150369

Edwards, K. F., Thomas, M. K., Klausmeier, C. A., and Litchman, E. (2012). Allometric scaling and taxonomic variation in nutrient utilization traits and maximum growth rate of phytoplankton. *Limnol. Oceanogr.* 57, 554–566. doi: 10.4319/lo.2012.57.2.0554

Fennel, W., and Neumann, T. (2004). *Introduction to the Modelling of Marine Ecosystems*. Amsterdam: Elsevier (Oceanographic Series).

Finlayson-Pitts, B. J. (2009). Reactions at surfaces in the atmosphere: integration of experiments and theory as necessary (but not necessarily sufficient) for predicting the physical chemistry of aerosols. *Phys. Chem. Chem. Phys.* 11, 7760–7779. doi: 10.1039/b906540g

Fukuda, R., Ogawa, H., Nagata, T., and Koike, I. (1998). Direct determination of carbon and nitrogen contents of natural bacterial assemblages in marine environments. *Appl. Environ. Microbiol.* 64, 3352–3358.

Gaetani, M., and Pasqui, M. (2014). Synoptic patterns associated with extreme dust events in the Mediterranean Basin. *Reg. Environ. Change* 14, 1847–1860. doi: 10.1007/s10113-012-0386-2

Gallisai, R., Peters, F., Volpe, G., Basart, S., and Baldasano, J. M. (2014). Saharan dust deposition may affect phytoplankton growth in the Mediterranean Sea at ecological time scales. *PLoS ONE* 9:e110762. doi: 10.1371/journal.pone.0110762

Geider, R. J., MacIntyre, H. L., and Kana, T. M. (1998). A dynamic regulatory model of phytoplankton acclimation to light, nutrients and temperature. *Limnol. Oceanogr.* 43, 679–694. doi: 10.4319/lo.1998.43.4.0679

Giovagnetti, V., Brunet, C., Conversano, F., Tramontano, F., Obernosterer, I., Ridame, C., et al. (2013). Assessing the role of dust deposition on phytoplankton ecophysiology and succession in a low-nutrient low-chlorophyll ecosystem: a mesocosm experiment in the Mediterranean Sea. *Biogeosciences* 10, 2973–2991. doi: 10.5194/bg-10-2973-2013

Guieu, C., Dulac, F., Ridame, C., and Pondaven, P. (2014). Introduction to project DUNE, a DUst experiment in a low Nutrient, low chlorophyll Ecosystem. *Biogeosciences* 11, 425–442. doi: 10.5194/bg-11-425-2014

Herut, B., Zohary, T., Krom, M., Mantoura, R. F. C., Pitta, P., Psarra, S., et al. (2005). Response of east Mediterranean surface water to Saharan dust: on-board microcosm experiment and field observations. *Deep Sea Res. II* 52, 3024–3040. doi: 10.1016/j.dsr2.2005.09.003

Heussner, S., Charrière, B., and ADIOS Consortium (2003). "A basin-wide survey of the impact of atmospheric deposition of pollutants and nutrients on the open Mediterranean Sea (ADIOS)," in *The Impact of Human Activities on the Marine Environment Quality and Health: the EC Impacts Cluster: Proceedings of the First Workshop*, eds P. Caumette, C. Eccles, P. Garrigues, M. Krom, and P. Lebaron (Pau), 31–47.

Jickells, T. D., An, Z. S., Andersen, K. K., Baker, A. R., Bergametti, G., Brooks, N., et al. (2005). Global iron connections between desert dust, ocean biogeochemistry, and climate. *Science* 308, 67–71. doi: 10.1126/science.1105959

Jolliff, J., Kindle, J., and Shulman, I. (2009). Summary diagrams for coupled hydrodynamic-ecosystem model skill assessment. *J. Mar. Syst.* 76, 64–82. doi: 10.1016/j.jmarsys.2008.05.014

Krom, M. D., Emeis, K. C., and Van Cappellen, P. (2010). Why is the Eastern Mediterranean phosphorus limited? *Prog. Oceanogr.* 85, 236–244. doi: 10.1016/j.pocean.2010.03.003

Krom, M. D., Kress, N., and Brenner, S. (1991). Phosphorus limitation of primary productivity in the eastern Mediterranean Sea. *Limnol. Oceanogr.* 36, 424–432. doi: 10.4319/lo.1991.36.3.0424

Krom, M., Herut, B., and Mantoura, C. F. R. (2004). Nutrient budget for the Eastern Mediterranean: implications for phosphorus limitation. *Limnol. Oceanogr.* 49, 1582–1592. doi: 10.4319/lo.2004.49.5.1582

Lagaria, A., Mandalakis, M., Mara, P., Papageorgiou, N., Pitta, P., Tsiola, A., et al. (2017). Phytoplankton response to Saharan dust depositions in the Eastern Mediterranean Sea: a mesocosm study. *Front. Mar. Sci.* 3:287. doi: 10.3389/fmars.2016.00287

Laghdass, M., Blain, S., Besseling, M., Catala, P., Guieu, C., and Obernosterer, I. (2011). Effects of Saharan dust on the microbial community during a large *in situ* mesocosm experiment in the NW Mediterranean Sea. *Aquat. Microb. Ecol.* 62, 201–213. doi: 10.3354/ame01466

Lee, S., and Fuhrman, J. A. (1987). Relationships between biovolume and biomass of naturally derived marine bacterioplankton. *Appl. Environ. Microbiol.* 53, 1298–1303.

Mahowald, M. N., Jickells, T. D., Baker, A. R., Artaxo, P., Benitez-Nelson, C. R., Bergametti, G., et al. (2008). Global distribution of atmospheric phosphorus sources, concentrations and deposition rates, and anthropogenic impacts. *Global Biogeochem. Cycles*. 22:GB4026. doi: 10.1029/2008GB003240

Moutin, T., Thingstad, T. F., Van Wanbeke, F., Marie, D., Slawyk, G., Raimbault, P., et al. (2002). Does competition for nanomolar phosphate supply explain the predominance of the cyanobacterium Synechococcus? *Limnol. Oceanogr.* 47, 1562–1567. doi: 10.4319/lo.2002.47.5.1562

Nenes, A., Krom, M. D., Mihalopoulos, N., Van Cappellen, P., Shi, Z., Bougiatioti, A., et al. (2011). Atmospheric acidification of mineral aerosols: a source of bioavailable phosphorus for the oceans. *Atmos. Chem. Phys.* 11, 6265–6272. doi: 10.5194/acp-11-6265-2011

Petihakis, G., Triantafyllou, G., Allen, I. J., Hoteit, I., and Dounas, C. (2002). Modelling the spatial and temporal variability of the Cretan Sea ecosystem. *J. Mar. Syst.* 36, 173–196. doi: 10.1016/S0924-7963(02)00186-0

Petihakis, G., Triantafyllou, G., Tsiaras, K., Korres, G., Pollani, A., and Hoteit, I. (2009). Eastern Mediterranean biogeochemical flux model–Simulations of the pelagic ecosystem. *Ocean Sci.* 5, 29–46. doi: 10.5194/os-5-29-2009

Petihakis, G., Tsiaras, K., Triantafyllou, G., Kalaroni, S., and Pollani, A. (2015). Sensitivity of the N. Aegean Sea ecosystem to Black Sea Water inputs. *Mediterr. Mar. Sci.* 15, 790–804. doi: 10.12681/mms.955

Pitta, P., Kanakidou, M., Mihalopoulos, N., Christodoulaki, S., Dimitriou, P. D., Frangoulis, C., et al. (2017). Saharan dust deposition effects on the microbial food web in the Eastern Mediterranean: a study based on a mesocosm experiment. *Front. Mar. Sci.* 4:117. doi: 10.3389/fmars.2017.00117

Pulido-Villena, E., Baudoux, A.-C., Obernosterer, I., Landa, M., Caparros, J., Catala, P., et al. (2014). Microbial food web dynamics in response to a Saharan dust event: results from a mesocosm study in the oligotrophic Mediterranean Sea. *Biogeosciences* 11, 5607–5619. doi: 10.5194/bg-11-5607-2014

Ridame, C., Dekaezemacker, J., Guieu, C., Bonnet, S., L'Helguen, S., and Malien, F. (2014). Contrasted Saharan dust events in LNLC environments: impact on nutrient dynamics and primary production. *Biogeosciences* 11, 4783–4800. doi: 10.5194/bg-11-4783-2014

Scheffer, M., Carpenter, S., Foley, J. A., Folke, C., and Walker, B. (2001). Catastrophic shifts in ecosystems. *Nature* 413, 591–596. doi: 10.1038/35098000

Siokou-Frangou, I., Bianchi, M., Christaki, U., Christou, E. D., Giannakourou, A., Gotsis, O., et al. (2002). Carbon flow in the planktonic food web along a gradient of oligotrophy in the Aegean Sea (Mediterranean Sea). *J. Mar. Syst.* 33–34, 335–353. doi: 10.1016/S0924-7963(02)00065-9

Steele, J. H., and Frost, B. W. (1977). The structure of plankton communities. *Philos. Trans. R. Soc. Lond. Sci.* 280, 485–534. doi: 10.1098/rstb.1977.0119

Stuart, A., and Ord, J. K. (1998). *Kendall's Advanced Theory of Statistics, Vol. 1: Distribution Theory, 6th Edn.* London: Arnold.

Tambi, H., Flaten, G. A. F., Egge, J. K., Bodtker, G., Jacobsen, A., and Thingstad, T. F. (2009). Relationships between phosphate affinities and cell size and shape in various bacteria and phytoplankton. *Aquat. Microb. Ecol.* 57, 311–320. doi: 10.3354/ame01369

Tanaka, T., Rassoulzadegan, F., and Thingstad, T. F. (2004). Orthophosphate uptake by heterotrophic bacteria, cyanobacteria, and autotrophic nanoflagellates in Villefranche Bay, northwestern Mediterranean: vertical,seasonal, and short-term variations of the competitive relationship for phosphorus. *Limnol. Oceanogr.* 49, 1063–1072. doi: 10.4319/lo.2004.49.4.1063

Taylor, K. K. E. (2001). Summarizing multiple aspects of model performance in a single diagram. *J. Geophys. Res. Atmos.* 106, 7183–7192. doi: 10.1029/2000JD900719

Thingstad, T. F., and Rassoulzadegan, F. (1995). Nutrient limitations, microbial food webs, and 'biological C-pumps': suggested interactions in a P-limited Mediterranean. *Mar. Ecol. Prog. Ser.* 117, 299–306. doi: 10.3354/meps117299

Tsiaras, K., Petihakis, G., Kourafalou, V., and Triantafyllou, G. (2014). Impact of the river nutrient load variability on the N. Aegean ecosystem functioning over the last decades. *J. Sea Res.* 86, 97–109. doi: 10.1016/j.seares.2013.11.007

Van Wambeke, F., Christaki, U., Giannakourou, A., Moutin, T., and Souvermezoglou, E. (2002). Longitudinal and vertical trends of bacterial limitation by phosphorus and carbon in the Mediterranean Sea. *Microb. Ecol.* 43, 119–133. doi: 10.1007/s00248-001-0038-4

Vrekoussis, M., Liakakou, E., Mihalopoulos, N., Kanakidou, M., Ctutzen, P. J., and Lelieveld, J. (2006). Formation of HNO3 and $NO3^{-}$ in the anthropogenically-influenced eastern Mediterranean marine boundary layer. *Geophys. Res. Lett.* 33, L05811. doi: 10.1029/ 2005GL025069

Watts, M. C., and Bigg, G. R. (2001). Modelling and the monitoring of mesocosm experiments: two case studies. *J. Plankton Res.* 23, 1081–1093. doi: 10.1093/plankt/23.10.1081

Conflict of Interest Statement: The authors declare that the research was conducted in the absence of any commercial or financial relationships that could be construed as a potential conflict of interest.

frontiers in Marine Science

ORIGINAL RESEARCH
published: 21 July 2016
doi: 10.3389/fmars.2016.00127

The Impact of Atmospheric Dry Deposition Associated Microbes on the Southeastern Mediterranean Sea Surface Water following an Intense Dust Storm

Eyal Rahav[1]*, *Adina Paytan*[2], *Chia-Te Chien*[2], *Galit Ovadia*[1], *Timor Katz*[1] and *Barak Herut*[1]

[1] Israel Oceanographic and Limnological Research, National Institute of Oceanography, Haifa, Israel, [2] Institute of Marine Science, University of California Santa Cruz, Santa Cruz, CA, USA

OPEN ACCESS

Edited by:
Christos Dimitrios Arvanitidis, Hellenic Centre for Marine Research, Greece

Reviewed by:
Christina Pavloudi, Hellenic Centre for Marine Research, Greece; University of Bremen, Germany; University of Ghent, Belgium
Elena Tamburini, University of Cagliari, Italy
William J. Broughton, Bundesanstalt für Materialforschung und - prüfung (BAM), Germany

***Correspondence:**
Eyal Rahav
eyal.rahav@ocean.org.il

Specialty section:
This article was submitted to Marine Ecosystem Ecology, a section of the journal Frontiers in Marine Science

Received: 27 March 2016
Accepted: 07 July 2016
Published: 21 July 2016

Citation:
Rahav E, Paytan A, Chien C-T, Ovadia G, Katz T and Herut B (2016) The Impact of Atmospheric Dry Deposition Associated Microbes on the Southeastern Mediterranean Sea Surface Water following an Intense Dust Storm. Front. Mar. Sci. 3:127. doi: 10.3389/fmars.2016.00127

This study explores the potential impacts of microbes deposited into the surface seawater of the southeastern Mediterranean Sea (SEMS) along with atmospheric particles on marine autotrophic and heterotrophic production. We compared *in situ* changes in autotrophic and heterotrophic microbial abundance and production rates before and during an intense dust storm event in early September 2015. Additionally, we measured the activity of microbes associated with atmospheric dry deposition (also referred to as airborne microbes) in sterile SEMS water using the same particles collected during the dust storm. A high diversity of prokaryotes and a low diversity of autotrophic eukaryotic algae were delivered to surface SEMS waters by the storm. Autotrophic airborne microbial abundance and activity were low, contributing ~1% of natural abundance in SEMS water and accounting for 1–4% to primary production. Airborne heterotrophic bacteria comprised 30–50% of the cells and accounted for 13–42% of bacterial production. Our results demonstrate that atmospheric dry deposition may supply not only chemical constitutes but also microbes that can affect ambient microbial populations and their activity in the surface ocean. Airborne microbes may play a greater role in ocean biogeochemistry in the future in light of the expected enhancement of dust storm durations and frequencies due to climate change and desertification processes.

Keywords: dust storm, southeastern Mediterranean Sea, atmospheric dry deposition associated microbes, primary production, bacterial production

INTRODUCTION

Aerosols, including mineral-dust, are regularly transported across marine systems, supplying nutrients and trace metals to the surface water (Prospero et al., 2005). Aerosols may also contain a wide array of microorganisms (reviewed in Griffin, 2007; Després et al., 2012; Polymenakou, 2012), which can be transported thousands of kilometers from their place of origin within a few days (Prospero et al., 2005; Kellogg and Griffin, 2006). These aerosol-associated (airborne) microbes may include heterotrophic bacteria (e.g., Seifried et al., 2015), fungi (e.g., Dannemiller et al., 2014), cyanobacteria, chemolitoptophic bacteria, and other autotrophic algae

(e.g., Marshall and Chalmers, 1997; Lang-Yona et al., 2014; Gat et al., 2016), as well as viruses (e.g., Chow and Suttle, 2015). The diversity and viability of airborne microbes depends on the aerosol's route prior deposition (Rahav et al., 2016a).

Several studies have examined the effect desert dust and aerosols have on ocean productivity and microbial biomass, via on-board microcosm or mesocosm experiments that simulated atmospheric nutrient addition (e.g., Mills et al., 2004; Herut et al., 2005; Mackey et al., 2007; Pulido-Villena et al., 2008; Christaki et al., 2011). Overall, the impacts observed following desert dust or aerosol additions are diverse and cannot all be explained by the inducement of a "fertilization response" (Guieu et al., 2014). Although variability in aerosol composition and changes in ocean hydrography and ecosystem structure at the time of deposition have been invoked in order to explain the diverse responses (Paytan et al., 2009), another possible explanation is the impact of the airborne microbes delivered with the added dust/dry aerosol deposition. Such microbes, if viable, may interact with ambient microbial populations in the receiving environment. A recent study conducted across the North Atlantic Ocean measured the abundance of microbes in the lower atmosphere and estimated that airborne microbes cross over 10,000 Km in several days and that millions of microbes are being exchanged on a daily basis between the atmosphere and the ocean's surface layer (Mayol et al., 2014). Further, studies performed in freshwater (Reche et al., 2009; Peter et al., 2014) and marine (Rahav et al., 2016a) environments suggest that airborne microorganisms may remain viable after deposition and thus may play an important role in the receiving aquatic system. For example, Peter et al. (2014) reported viable airborne bacteria following dust deposition into sterile lake water, and Rahav et al. (2016a) showed activity of heterotrophic airborne bacteria in sterile seawater and measured both carbon and nitrogen fixation by these microbes. Airborne microbes can remain viable for decades (Gorbushina et al., 2007), and yet, the full extent of this "biological" addition and the ecological importance of airborne microbes in natural environments are unclear (Hervas et al., 2009; Rahav et al., 2016a). This is because our knowledge about the viability and functionality of airborne microorganisms upon deposition in the ocean is scant (Polymenakou et al., 2008).

The southeastern Mediterranean Sea (SEMS) is an ideal marine environment for studying the role of aerosols and associated microbes on surface ocean microbial production for multiple reasons. First, it is subjected to relatively high aerosol deposition throughout the year (Guerzoni et al., 1999; Ganor et al., 2010). Secondly, it is an oligotrophic environment with low inorganic nutrients (Herut et al., 2000; Kress and Herut, 2001; Kress et al., 2014) and low autotrophic and heterotrophic activity (Raveh et al., 2015). Thus, any external input of micro/macronutrients, along with aerosols-associate microbiota, can have a substantial effect upon interaction with the ambient microbial populations.

In this study, we followed the *in situ* temporal dynamics of autotrophic and heterotrophic microbial abundances and production rates in the SEMS surface waters during an intense natural dust storm event that lasted a few days. Specifically, we evaluated the role that the autotrophic and heterotrophic microbial communities associated with atmospheric dry deposition particles play in the SEMS surface water following this event.

MATERIALS AND METHODS

Sampling Strategy

Surface SEMS water (∼1 m depth) was sampled every 12 h at a coastal station near the National Institute of Oceanography (Haifa, Israel, Lat. 32.28N, Lon. 34.95E), from the 8th to the 13th of September 2015, during an intense storm event (**Figures 1A,B**). Seawater temperatures were measured using an *in situ* HOBO Pendant Temperature data logger (model UA-002-64, Onset Computer Corporation) mounted on the rocky bottom at a depth of ∼4 m. Salinity was measured using a Yellow Spring Instruments YSI-6000. In order to quantify dry deposition during the dust storm event, atmospheric suspended particles were collected on a Whatman 41 filter (125 mm, ∼20 μm pore size) using a high volume total suspended particles (TSP) sampler (located on a headland pointing into the sea, 22 m above sea level) at a flow rate of 60 m^3 h^{-1} for 24 h (**Figure 1**), as described in Herut et al. (2002). Dry deposition rates were calculated based on Al concentration in the collected aerosol (measured by XRF, 7.6% dry wt. Table S1), a settling velocity of 1.8 cm s^{-1} (Kocak et al., 2005), and the particles weight collected on the filter for the volume pumped during the collection time (1.77 mg m^{-3} air). This yielded a deposition of 1.05 mg of dry deposition L^{-1} in seawater when integrated over the upper 5 m mixed layer, similar to values reported for other intense dust storm events in this area (Herut et al., 2005). Seawater was sampled twice a day for chlorophyll-*a* (acetone extraction), cyanobacterial abundance, pico-eukaryotic abundance and heterotrophic bacterial abundance (flow-cytometry), primary production ($NaH^{14}CO_3$ incorporation), and bacterial production (^{3}H-Leucine incorporation) measurements.

Aerosol Collection and Bioassay Experiment

Dry deposited material was collected on September 8th 2015 during a major dust storm event using a pre-cleaned glass deposition plate. The deposited particles were collected from the plate using a clean plastic knife, transferred into prewashed (10% hydrochloric acid) sterile 2 ml plastic tubes and stored at −20°C until further analyses. Three-day back trajectories arriving at 500 and 1000 m altitude levels were calculated, commencing at 10.00 UTC using the HYSPLIT model from the Air-Resources Laboratory, NOAA (**Figure 1C**). A few days after the aerosol deposition event (between the 16th and 20th of September 2015), an aerosol-enrichment microcosm bioassay experiment was carried out in triplicate using 4.6-L acid-washed polycarbonate Nalgene bottles and sterile (0.2 μm filtered and autoclaved-killed) surface SEMS water. The collected aerosol was added to each of the bottles (∼1.5 mg dust L^{-1} of sterile surface seawater), and the bottles were incubated in an outdoor pool with seawater flow-through in order to maintain ambient temperatures. The pool was covered with a neutral density screening mesh to simulate ambient light and the experiment

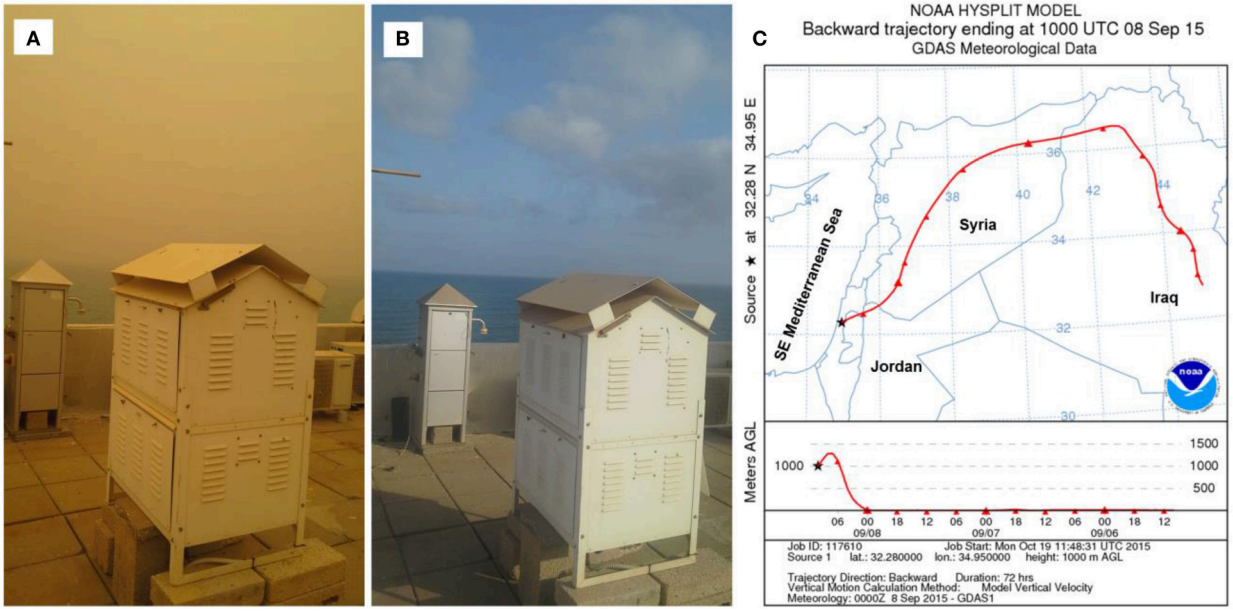

FIGURE 1 | Dusty (A) and clear (B) skies off the SE Mediterranean coast between the 8th (A) and 13th (B) of September 2015. Air mass back trajectory analysis shows the dust's origin **(C)**.

lasted for 4 days. Blank treatments of sterile SEMS water without added aerosol were carried out in parallel and sampled at the beginning (0.5 h) and at the end of the experiment (96 h). Subsamples of seawater from each incubation bottle were collected for chlorophyll-*a*, cyanobacterial abundance, pico-eukaryote abundance, heterotrophic bacteria abundance, primary production, and bacterial production measurements, at 0.5, 9, 24, 48, 57, 72, and 96 h after aerosol addition. The differences between *in situ* values (measured during September 8–13, 2015, and representing the ambient community's response to the dust storm event) and those measured during the enrichment experiments (September 16–20, 2015) performed in sterile seawater using the same particles that were collected during the dust storm, were used to estimate the potential contribution of the autotrophic and heterotrophic microbes associated with the event (hereafter airborne microbes) to the overall *in situ* microbial abundance and production rates following aerosol deposition during the storm.

Inorganic Nutrients and Trace Metals Leached from the Aerosol

These micro- and macro-nutrients from the aerosol particles were extracted according to Buck et al. (2012) and analyzed using a flow injection autoanalyzer (FIA, Lachat Instruments model QuickChem 8000) as describe in Chen et al. (2006). A detailed description of the method can be found in the supporting information.

X-Ray Fluorescence (XRF)

An elemental analysis of the collected aerosol particles was carried out using an ED-XRF spectrometer (SPECTROSCOUT) in a vacuum chamber. A detailed description of this method can be found in the supporting information.

DNA Extractions and High-Throughput Phylogenetic and Sequence Analyses

DNA was extracted from the aerosol particles that were collected on the clean glass deposition plates during the atmospheric deposition event. The DNA was extracted using the phenol–chloroform method, modified from Massana et al. (1997). A detailed description of this method can be found in the supporting information.

Chlorophyll-*a* Extraction

Autotrophic biomass was determined using the non-acidification method (Welschmeyer, 1994). A detailed description of this method can be found in the supporting information.

Pico-Phytoplankton and Bacterial Abundance

Water samples (1.8 mL) were analyzed using an Attune® Acoustic Focusing Flow Cytometer (Applied Biosystems) equipped with a syringe-based fluidic system and 488 and 405 nm lasers (Vaulot and Marie, 1999). A detailed description of this method can be found in the supporting information.

Primary Production

Photosynthetic carbon fixation rates were estimated using the ^{14}C incorporation method (Steemann-Nielsen, 1952). A detailed description of this method can be found in the supporting information.

Bacterial Production

Rates were estimated using the ^{3}H-leucine (Amersham, specific activity: 160 Ci mmol^{-1}) incorporation method (Simon et al., 1990). A detailed description of this method can be found in the supporting information.

Statistical Analyses

The different variables presented in the figures and tables are averages and standard deviation (biological replicates, $n = 3$). Changes in chl-*a*, production rates, and abundance of cyanobacteria, pico-eukaryotes, and bacteria throughout each of the experiments (4–5 days) were evaluated using a one-way analysis of variance (ANOVA), followed by a Fisher LSD multiple comparison *post-hoc* test with a confidence level of 95% ($\alpha = 0.05$). The difference between samples collected *in situ* at the SEMS during the dust storm event (8–13 September 2015) and those from the sterile seawater bioassay experiments (16–20 September 2015) were evaluated using a student *t*-test with a confidence level of 95% ($\alpha = 0.05$). These statistical analyses were carried out using the XLSTAT software. The Shannon-Weiner diversity index (Margalef, 1958) was calculated using the primer software.

RESULTS

The initial pre-storm physiochemical characteristics of the surface SEMS are shown in **Table 1**. The ambient surface seawater depicts a high temperature (∼30°C) and high salinity (39.8). The algal biomass, derived from chl-*a* levels, was low overall (0.17 ± 0.02 mg m^{-3}), as were the cyanobacterial and picophytoplankton abundances (1.9×10^4 and 8.0×10^2 cells mL^{-1}, respectively). Concurrently, the primary production rates were low (1.99 ± 0.41 μg C L^{-1} d^{-1}). In contrary to the low autotrophic biomass, bacterial heterotrophs were more abundant (8.5×10^5 cells mL^{-1}), and active (5.18 ± 1.51 μg C L^{-1} d^{-1}).

The aerosols collected during early September 2015 had a very high fraction of Ca (20%) and were rich in Mg (4.3%), Fe (6.3%), Mn (945 ppm), Sr (450 ppm), Al (∼67 ng mg^{-1}), and Cu (∼25 ng mg^{-1}; **Table 2**, Table S1). They also had significant amounts of soluble $NO_3^- + NO_2^-$ (∼176 nmol mg^{-1}) and relatively less NH_4^+ (∼5.4 nmol mg^{-1}) and PO_4^{3-} (∼1.5 nmol mg^{-1}), resulting in a high N:P ratio of ∼120:1 (**Table 2**, Table S1).

Aerosol-derived autotrophic and heterotrophic microorganisms were also transported with the atmospheric particles (**Figure 2**). These included a wide array of prokaryotes (>100 families in 23 different phylum, ∼650 species, Shannon-Weiner diversity index = 3.88) and a small number of autotrophic eukaryotic microbes (4 families in 2 phyla, 4 species, Shannon-Weiner diversity index = 1.03). Among the prokaryotes, the most dominant families (as relative operational taxonomic units, OTUs) were Cytophagaceae (10.3%), Chloroflexaceae (7.8%), Frankiales and Rhodobacteraceae (6.4% each), and Bacillaceae (4.3%), as well as other bacteria (**Figure 2A**). The autotrophic eukaryotic microorganisms contained within the aerosol particles belonged to Tracheophyta (61.5%), Chlorodendraceae (23.1%), Bryophyta (8.9%), and Pedinomonadaceae (6.5%) taxa (**Figure 2B**). Despite the low number of the different eukaryotic-autotrophic families, ∼30% were of marine or freshwater origin (i.e., green algae).

TABLE 1 | The initial characteristics of the SE Mediterranean seawater 3 days prior to the dust storm event (5th September 2015).

Variable	Unit	Value
Temperature	°C	30.1
Salinity	–	39.8
Chl-*a*	mg m^{-3}	0.17 ± 0.02
Cyanobacteria	Cells mL^{-1}	1.9×10^4
Picoeukaryotes	Cells mL^{-1}	8.0×10^2
Heterotrophic bacteria	Cells mL^{-1}	8.5×10^5
Primary production	μg C L^{-1} d^{-1}	1.99 ± 0.41
Bacterial production	μg C L^{-1} d^{-1}	5.18 ± 1.51

TABLE 2 | The trace metals derived from the aerosols collected in September 8, 2015 and the subsequent values following the dust storm in the SEMS water.

Variable	Leached element conc. (ng mg^{-1})[a]	Element conc. (ng mg^{-1})[b]	Leachable fraction (%)	Amount deposited (nM)[c]	Amount added in bioassay (nM)[d]
Pb	0.34	34	1.0	0.36	0.51
Al	66.8	76000	0.09	70.14	100.20
Mn	83.4	945	8.8	87.57	125.10
Fe	20.6	63000	0.03	21.63	30.90
Ni	2.69	250	1.1	2.82	4.04
Zn	1.40	377	0.4	1.47	2.10
Mg	NA	43000	NA	NA	NA
Ca	NA	200000	NA	NA	NA
Sr	NA	4.5×10^{-4}	NA	NA	NA
Cu	25.4	105	24.2	26.67	38.10

[a] *Leaching experiments were performed as described in Chen et al. (2006, 2007).*
[b] *Measured by XRF.*
[c] *Assuming a 1.05 mg L^{-1} dust deposition in the upper mixed layer (5 m).*
[d] *Addition of 1.5 mg L^{-1} dust.*
NA, not available.

The *In situ* Temporal Dynamics of Autotrophic and Heterotrophic Microbial Communities during the Dust Storm Event

The *in situ* chl-*a* concentrations gradually increased from its background pre-storm levels (**Table 1**) to 0.24 mg m^{-3} within 55 h, corresponding to ∼40% change, and decreased back to background levels at day 5 following the dust storm (0.19 mg m^{-3}, **Figure 3A**, Figure S1). Contrary to the chl-*a* levels, cyanobacterial abundance exhibited a different yet insignificant temporal trend ($P > 0.05$), with an immediate 20% decrease in cell numbers (∼1.3×10^4 cells mL^{-1}), an increase back to the initial levels after 48 h (∼1.7×10^4 cells mL^{-1}), which was followed by another decrease (∼1.3×10^4 cells mL^{-1}; **Figure 3B**, Figure S1). The picoeukaryotes remained unchanged (∼8.2×10^2 cells mL^{-1}, $P > 0.05$; **Figure 3C**, Figure S1). Heterotrophic bacterial abundance increased by 30% within 10 h (8.7×10^5 cells mL^{-1}, $P = 0.05$), an increase that lasted for 3 days (**Figure 3D**,

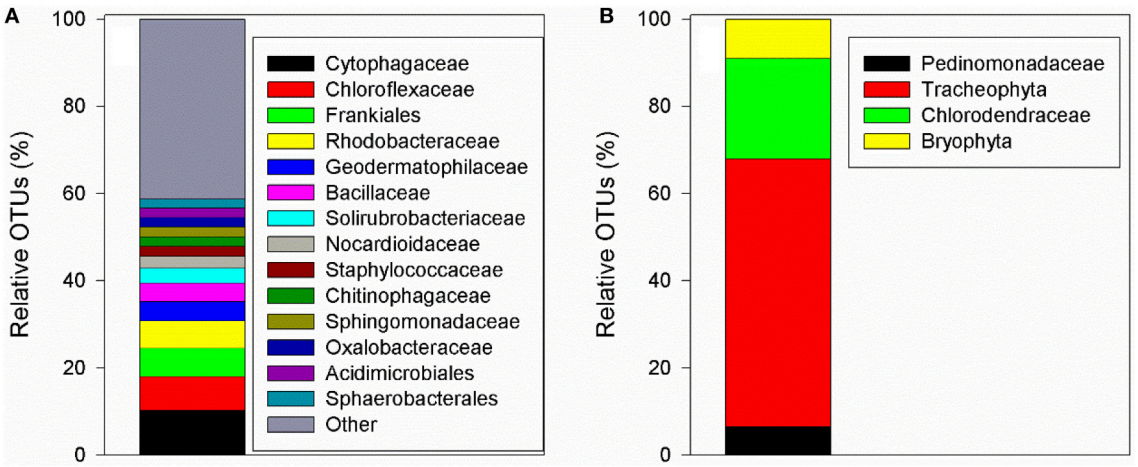

FIGURE 2 | Distributions of bacterial 16S rRNA (A) and 18S rRNA (B) gene reads at a family level, retrieved from a dry deposition particles sample collected on September 8th 2015 off the SE Mediterranean Sea coast.

Figure S1, $P < 0.05$). *In situ* primary production rates reached maximal values 48 h after deposition (a 25% increase, $P > 0.05$) and then decreased to background levels over the course of 5 days (**Figure 4A**, Figure S2). Bacterial production increased slightly (∼15%, $P > 0.05$), however this increase lasted for only 48 h (**Figure 4B**, Figure S2).

The Impact of Airborne Autotrophic and Heterotrophic Microorganisms

Airborne autotroph abundance (measured in the sterile seawater after aerosol addition) constituted only a small fraction of the overall photosynthetic biomass observed *in situ* (**Figures 3A–C**). Airborne cyanobacteria and picoeukaryotes comprised <1% of the autotrophic microbial abundance (**Figures 3B,C**, Figure S1). Airborne heterotrophic bacteria were more significant (Figure S1), comprising 30–50% (abundance per gram of aerosol added) of the total heterotrophic bacteria in the SEMS water during the dust storm (**Figure 3D**).

Concurrent with the low airborne contribution to autotrophic biomass, the airborne primary production was low (Figure S2), comprising 1–4% of the rates measured *in situ* (activity per gram aerosol added) during the dust storm event (**Figure 4A**). The airborne bacterial production rates were higher (Figure S2), corresponding to 13–42% of the rates measured *in situ* during the dust storm event (**Figure 4B**). Taken together, the airborne heterotrophic cell specific activity (bacterial production per cell) was not different from the activity measured in the seawater during the dust storm event (∼0.01 fg C d^{-1} $cell^{-1}$, $n = 6$, $P = 0.67$). The airborne autotrophic cell specific activity (primary production per cell) was three-fold lower than in seawater (∼19 vs. 6 μg C μg chl-a^{-1} d^{-1}, $n = 6$, $P < 0.001$).

DISCUSSION

The SEMS is constantly exposed to high levels of atmospheric deposition derived primarily from surrounding deserts and land sources (Herut et al., 2002; Lawrence and Neff, 2009). These atmospheric inputs provide a variety of nutrients and trace metals (Table S1 and reviewed in Guieu et al., 2014), which are required for microbial cellular metabolism, enzymatic activity and growth (e.g., Cvetkovic et al., 2010; Huertas et al., 2014). In addition to nutrients and trace metals, atmospheric deposition may also introduce a wide array of airborne microorganisms to surface seawater (reviewed in Griffin, 2007; Polymenakou, 2012). Some of these microbes can remain viable and fix carbon (C) and dinitrogen (N_2) upon deposition in seawater (Rahav et al., 2016a).

The aerosol deposition event into the SEMS water in early September 2015 was an exceptional regional event. Previous works linked dust fallout over the Levantine Basin to Saharan origins (Ganor and Mamane, 1982; Herut et al., 1999, 2005), whereas the studied event originated from drylands in Eastern Syria (**Figure 1C**). This difference in origin is evident in the chemical composition of the Syrian aerosol particles when compared to the reported composition of Saharan dust particles (**Table 2**, Table S1). The most prominent difference was in Ca, which was much higher than the reported fraction in Saharan aerosols (Krom et al., 1999; Goudie and Middleton, 2001; Herut et al., 2001). This high Ca content in the Syrian aerosols likely reflects a source origin of calciorthid soils, which covers large areas in Syria (Ilaiwi, 1985). The Syrian aerosol was also richer in Mg, Fe, Mn, and Sr (normalized to Al) when compared to the reported concentrations in Saharan samples (Table S1, Krom et al., 1999; Goudie and Middleton, 2001; Herut et al., 2001). When calculating the soluble fraction of trace metals that were leached from the aerosols and added to seawater during this event (**Table 2**) concentrations were below the threshold for toxicity for phytoplankton in seawater (e.g., Sunda, 2012). In fact, some of the added trace metals, such as Fe or Zn, are key cofactors for many enzymatic reactions in the marine environment, including photosynthesis and N_2 fixation (Falkowski, 1997; Sohm et al., 2011), and may contribute to enhancing production.

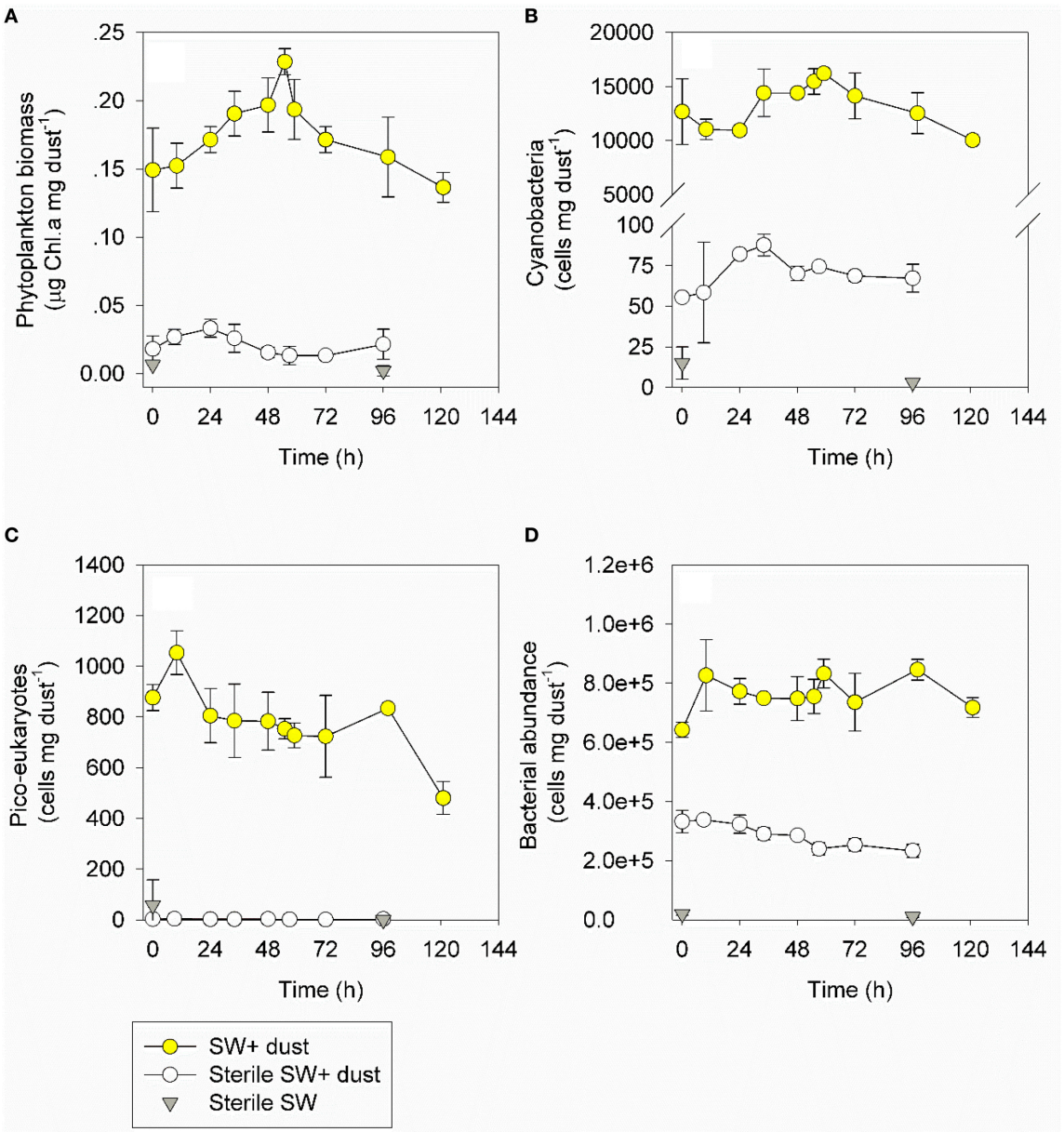

FIGURE 3 | The temporal dynamics of chl-*a* (A), cyanobacterial abundance (B), pico-eukaryotes abundance (C), and heterotrophic bacterial abundance (D) during a dust storm event (*in situ* measurements, 1.05 mg L^{-1}, yellow) off the SEMS between the 8th and 13th of September 2015. The contribution of airborne microbes was tested between the 16th and 20th of September 2015 in sterile seawater, either supplemented with 1.5 mg L^{-1} of the same atmospheric particles deposited the previous week (white) or without any addition (gray). Values (as averages and standard deviations, $n = 3$) are normalized to the amount of dust added. The un-normalized values are presented in Figure S1.

The studied Syrian aerosol particles released soluble $NO_3^- + NO_2^-$ and PO_4^{3-} (**Table 3**, Table S1), which may relieve nutrient stress for autotrophic and heterotrophic microbial biomass and activity in the surface SEMS (i.e., Kress et al., 2005; Zohary et al., 2005; Pitta et al., 2016). Assuming 1.05 mg L^{-1} of dust deposition into the upper SEMS 5 m mixed layer (see Materials and Methods), ~185 nM of $NO_3^- + NO_2^-$ and ~1.5 nM PO_4^{3-} were actually added into this water layer (**Table 3**), which constitutes ~50 and 5–10% of the nutrient concentration typically reported for this system during summer, respectively (Kress et al., 2014; Raveh et al., 2015). Due to the extremely oligotrophic nature of the SEMS, any amendment might prove to be important and may alter microbial dynamics via the release of scarce, key-limiting nutrients. For example, several authors showed that inorganic nitrogen (N) and phosphorus (P) may enhance algae biomass and growth rates in the SEMS water (Kress et al., 2005; Lagaria et al., 2011; Pitta et al., 2016), whereas P (Thingstad et al., 2005; Zohary et al., 2005) or dissolved organic

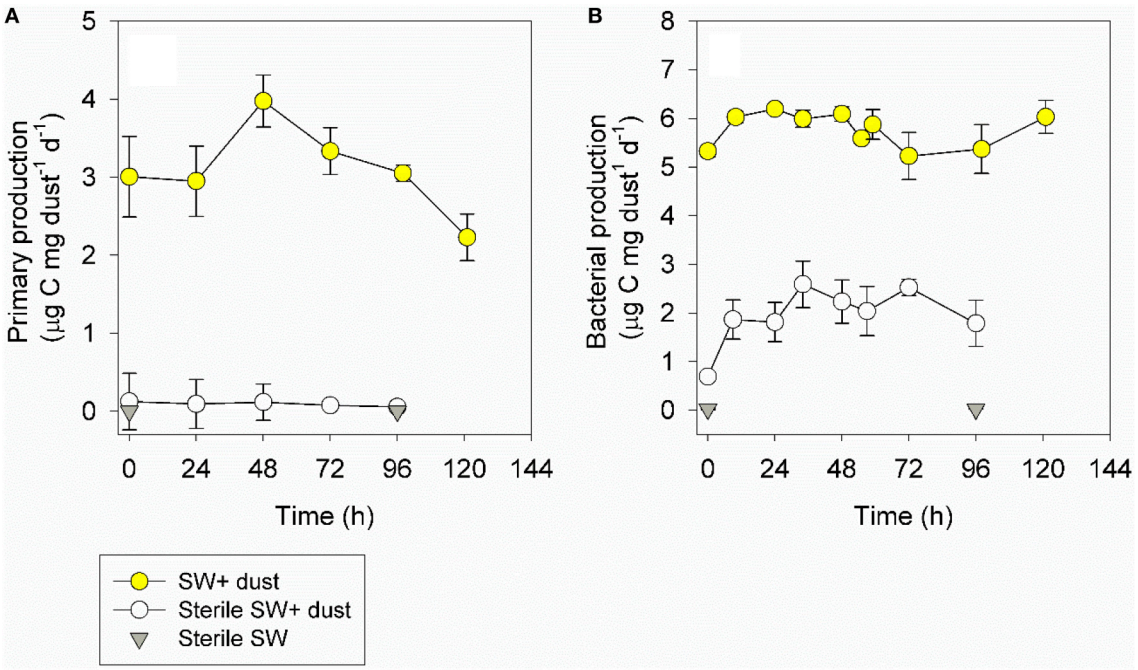

FIGURE 4 | The temporal dynamics of primary production (A) and bacterial production (B) during a dust storm event (*in situ* measurements, 1.05 mg L^{-1}, yellow) off the SEMS between the 8th and 13th of September 2015. The contribution of airborne microbes was tested between the 16th and 20th of September 2015 in sterile seawater, either supplemented with 1.5 mg L^{-1} of the same particles deposited the previous week (white) or without any aerosol addition (gray). Values (as averages and standard deviations, $n = 3$) are normalized to the amount of aerosols added. The un-normalized values are presented in Figure S2.

TABLE 3 | Leached nutrients derived from the aerosols collected in September 8, 2015 and the subsequent values following the dust storm in the SEMS water.

Variable	Leached element conc. (nmole mg^{-1})[a]	Amount deposited (nM)[b]	Amount added in bioassay (nM)[c]
NO_3+NO_2	175.95	184.75	263.93
NH_4	5.37	5.64	8.06
PO_4	1.46	1.53	2.19
$Si(OH)_4$	2.05	2.15	3.08

[a] *Leaching experiments were performed as described in Chen et al. (2006, 2007).*
[b] *Assuming a 1.05 mg L^{-1} dust deposition in the upper mixed layer (5 m).*
[c] *Addition of 1.5 mg L^{-1} dust.*

carbon (Rahav et al., 2016b) can also stimulate heterotrophic bacterial activity. Thus, assuming a C to chl-*a* ratio of ~80 (e.g., Behrenfeld et al., 2005; Wang et al., 2009) and a 106:1 C:P ratio (Redfield, 1934), the addition of the dust-derived P could explain a chl-*a* enhancement of ~0.05 mg m^{-3} above the ambient levels. The chl-*a* enhancement calculated based on the added P is lower than the overall chl-*a* change measured following the dust examined here (~0.08 mg m^{-3}, Figure S1 and see Discussion below). One of the possible explanations for this difference between the actual increase in chl-*a* (~0.08 mg m^{-3}) and the dust-P derived chl-*a* (~0.05 mg m^{-3}) may be chl-*a* associated with airborne microbes (algae and cyanobacteria).

Indeed, both autotrophic and heterotrophic microbes were delivered with the Syrian aerosol studied here (**Figure 2**). These include commonly isolated bacteria from marine, freshwater, and terrestrial environments (e.g., Hervas and Casamayor, 2009; Cho and Hwang, 2011; Seifried et al., 2015), as well as from the surroundings of the SEMS (Katra et al., 2014; Rahav et al., 2016a). It should be noted, that based on the 16S rRNA gene, we cannot rule out that in addition to heterotrophic microbes, chemolithotrophic bacteria were also part of the aerosol collection (Gat et al., 2016). More specific assays should be carried out in future studies to fully understand whether these chemolithotrophic microbes were actually transported with the aerosol particles. Such chemolithotrophic bacteria may play an important role e in the biogeochemistry of nitrogen, sulfur, and iron (e.g., Saeed and Sun, 2012). In contrast to this broad airborne microbial heterotroph biodiversity, only few algal families associated with the aerosol particles were observed based on the 18S rRNA gene. This may be due to the high settling velocities of large eukaryotic particles (such as those of microphytoplankton). Most of the large-size algae and other terrestrial plants were probably deposited along the dust's route (above land) rather than being suspended over long distances and, therefore, were rarely found in our sample. It is possible, however, that aerosols from different origins would contain different amounts of marine/freshwater autotrophic organisms, and particularly small-size cyanobacteria (Cho and Hwang, 2011; Lang-Yona et al., 2014; Seifried et al., 2015). Thus, a more typical atmospheric deposition event coming from the southwest (e.g., Herut et al., 2005) rather than from the northeast (**Figure 1**) would potentially carry more algae or small-size cyanobacteria,

and, therefore, airborne autotrophs could be more abundant than what we have observed in this study.

In situ Dynamics of Autotrophic and Heterotrophic Microbial Populations Following Aerosol Deposition and the Relative Contribution of Airborne Microbes

A moderate change in the *in situ* chl-*a* level and picophytoplankton abundance was observed following the aerosol deposition event of early September 2015 (**Figures 3A–C**). This is consistent with the expected change derived from the PO_4^{3-} addition (∼1.5 nM) and its subsequent carbon addition based on the C to chl-*a* ratio (see above). The relatively limited change in picophytoplankton abundance implies a possible top-down control of small-size autotrophs by grazers (Billen, 1990), dominance of larger-size algae such as microphytoplankton that utilized most of the leached nutrients/trace metals and compete with the picophytoplankton (Duarte et al., 2000), or toxicity of small-size autotrophs (Mann et al., 2002; Paytan et al., 2009). It may also hint at interactions between the ambient population and the airborne microbes that affect the abundance of small-size autotrophs. In contrast, the heterotrophic bacterial abundance was immediately enhanced (**Figure 3D**), suggesting that the leached nutrients and trace metals, and possibly the addition of airborne microbes, favored heterotrophy. A similar response was recorded by Herut et al. (2005) in the SEMS water following a desert-dust storm event that triggered a slight increase in the chl-*a* and heterotrophic bacterial abundance and a decrease in cyanobacterial abundance (*Prochlorococcus* sp.). The similarity in trends observed during these two distinct events lends credibility to the observations.

The temporal dynamics of the *in situ* primary and bacterial production (**Figure 4**, Figure S2) are consistent with observed autotrophic and heterotrophic bacterial abundances (**Figure 3**, Figure S1). The overall low impact of the dust on autotrophic biomass and production is similar to the response reported from an onboard microcosm experiment in the open SEMS (Herut et al., 2005), and was most likely a result of the relatively low nutrient and trace metal amounts added from the dust (**Tables 2, 3**). It may also suggest the likely control of grazing pressure, and/or possible toxicity effects of the dust (Paytan et al., 2009). Alternatively, it is possible that airborne microbes delivered with the dust interacted with the ambient microbial populations and, in some circumstances, outcompeted them, resulting in the decline of abundance and production rates.

The airborne chl-*a* (up to 0.03 mg m^{-3}) measured in sterile SEMS water reached 5–30% (biomass per gram of dry deposition particles added) of the total chl-*a* measured *in situ* during the event (**Figure 3A**, Figure S1). This airborne contribution to the total chl-*a* (∼0.03 mg m^{-3}), along with the increase in the chl-*a* level calculated based on that expected from the uptake of the leached P (∼0.05 mg m^{-3}, see above), is consistent with the overall increase measured *in situ* 55 h post-deposition (∼0.08 mg m^{-3}, Figure S1). The contribution of airborne heterotrophic bacteria measured here (abundance per gram of aerosol added) to the total bacterial abundance in the water is lower than the values recently reported for aerosols collected in the SEMS during 2006–2015, representing different source origins and seasons (Rahav et al., 2016a). This highlights the importance of biogeographical aspects in introducing not only a different diversity of airborne microbes but possibly also different quantities of cells with potentially different activities and functions. However, it should be noted that the presence of autotrophic and heterotrophic bacteria, regardless of their fraction of the total abundance measured *in situ*, is no evidence for their viability in the receiving seawater. It is possible that inactive/dormant cells were leached off the aerosol particles along with viable microbes and were counted using flow cytometry. This issue necessitates additional studies implementing techniques designed to estimate the microbial abundance of active cells.

Another method for estimating whether the retrieved cells are viable upon deposition in seawater is to measure metabolic parameters, such as primary production and bacterial production of the airborne microbes. Our results suggest that airborne primary production was low overall (**Figure 4**, Figure S2), which is consistent with the low contribution of airborne chl-*a* and the negligible fraction of small-size airborne photosynthetic microorganisms (**Figures 3A–C**). On the other hand, airborne bacterial production was more important and immediately responded to the aerosol addition, suggesting that airborne heterotrophs can rapidly interact with the ambient populations. The nature of such interactions can be diverse, depending on the species of the microbes that are associated with the aerosol particles (Rahav et al., 2016a). It is possible that under some circumstances airborne microbes can negatively affect certain microbial groups in seawater (competition, allelopathic affects, cell lysis, etc.), or that they can affect certain ambient populations positively (serving as unique food, relieving N-stress via N_2 fixation, etc.). Rahav et al. (2016a) reported airborne heterotrophic bacterial production rates similar to changes observed following dry deposition aerosol amendments in seawater, potentially accounting for 100% of the change. In this study, however, the contribution of airborne heterotrophic bacterial production rates was lower than that reported by Rahav et al. (2016a) and accounted for a maximum of 42% of the ambient-typical production levels in the SEMS (e.g., Raveh et al., 2015), once again highlighting the importance of the aerosol's origin and associated numbers and taxa of airborne microbes.

To the best of our knowledge, this is one of only few attempts to estimate the role of airborne microbes in seawater following a major dust storm. If the results from this dust storm event are representative, the small contribution of airborne autotrophs (in terms of both abundance and C fixation) may suggest that the increase in primary production and chl-*a* usually observed following dust events (e.g., Herut et al., 2005; Ternon et al., 2011; Gallisai et al., 2014) results from the beneficial impacts of nutrient and/or trace metal additions from the aerosols. However, we postulate that the contribution of airborne microbes to the ambient autotrophic community's chl-*a* in the SEMS water may occasionally be higher if the dust's route prior to deposition went over marine areas of higher productivity rather than over land, which would be more likely to contain a higher abundance of

viable autotrophic organisms that will be viable upon deposition in seawater.

CONCLUSIONS

We determine the role of autotrophic and heterotrophic airborne microbes in seawater during a specific dust storm event. Our results demonstrate that in this case, where the dust arrived from an atypical continental source (**Figure 1**), only a few groups of eukaryotic-autotrophic microbes were transported (**Figure 2B**) and their overall impact in the surface ocean was thus negligible (**Figure 4**). In contrast, a higher diversity of prokaryotes (both heterotrophs and possibly autotrophs such as cyanobacteria and chemolitotrophs) was contained within the dry deposition particles (**Figure 2A**), and at least some of these microbes exhibited immediate activity upon deposition (**Figure 4**). It should be noted that the open SEMS is an ultra-oligotrophic environment (Kress et al., 2014), much more than our coastal study site (Bar-Zeev and Rahav, 2015; Raveh et al., 2015). We postulate that airborne microbes (along with aerosol-derived nutrients) are likely to have a more profound affect in such oligotrophic provinces.

To date, we cannot say what mechanisms and strategies are used by airborne organisms once deposited in seawater to successfully compete with ambient microbes that are already acclimated in their habitat. It is possible that some chemical components derived from aerosols are toxic to specific groups of organisms (Paytan et al., 2009) or have negative biologically impacts via viral lysis (Vardi et al., 2012; Sharoni et al., 2015), allelopathy, or other mechanisms that may be at play. It is also possible that airborne microbes will synergistically interact with ambient populations. Dedicated studies aimed at filling these knowledge gaps are needed, including investigations of dust-derived allelopathic affects and a comparison between the nutrient uptake rates of airborne bacteria and those of *in situ* communities. Addressing these aspects will be particularly important in the near future, since climate and anthropogenic changes may increase aerosol deposition (including mineral dust). This, in turn, will also upsurge airborne microbes transfer and deposition in seawater and could, subsequently, impact surface ocean carbon and nitrogen cycles (Rahav et al., 2016a) as well as other biochemical and ecological aspects.

AUTHOR CONTRIBUTIONS

Conceived and designed the experiment: ER and BH. Performed the experiment: ER, GO, CC, TK, and AP. Analyzed the data: ER, AP, TK, and BH. Contributed reagents/materials/analysis tools: ER, TK, and AP. Wrote the paper: ER, CC, AP, TK, and BH.

ACKNOWLEDGMENTS

We would like to thank Lilach Baumer and Kimberley Bitterwolf for English editing, Dr. Yana Yudkovsky for the XRF analysis and four reviewers that greatly improved the manuscript. This study was supported by a grants awarded by the Ministry of National infrastructures, Energy and Water Resources (grant 3-11519) to ER, by the Ministry of environmental Protection (145–1–2) to ER, by the PERSEUS project's (EC contract 287600) contribution to BH, partially by the ENVIMED MERMEX TRACOMED project's contribution to BH and by the NSF-OCE (grant 0850467) to AP. The authors gratefully acknowledge the NOAA Air Resources Laboratory (ARL) for the provision of the HYSPLIT transport and dispersion model used in this publication.

SUPPLEMENTARY MATERIAL

The Supplementary Material for this article can be found online at: http://journal.frontiersin.org/article/10.3389/fmars.2016.00127

REFERENCES

Bar-Zeev, E., and Rahav, E. (2015). Microbial metabolism of transparent exopolymer particles during the summer months along a eutrophic estuary system. *Front. Microbiol.* 6:403. doi: 10.3389/fmicb.2015.00403

Behrenfeld, M. J., Boss, E., Siegel, D. A., and Shea, D. M. (2005). Carbon-based ocean productivity and phytoplankton physiology from space. *Glob. Biogeochem. Cycles* 19, 1–14. doi: 10.1029/2004GB002299

Billen, G. (1990). Dynamics of bacterioplankton in oligogtrophic and eutrophic aquatic environments: bottom-up or top-down control? *Hydrobiologia* 207, 37–42. doi: 10.1007/BF00041438

Buck, K. N., Moffett, J., Barbeau, K., Bundy, R., Kondo, Y., and Wu, J. (2012). The organic complexation of iron and copper : an intercomparison of competitive ligand exchange – adsorptive cathodic stripping voltammetry (CLE-ACSV) techniques. *Limnol. Oceanogr. Methods* 10, 496–515. doi: 10.4319/lom.2012.10.496

Chen, Y., Mills, S., Street, J., Golan, D., Post, A., Jacobson, M., et al. (2007). Estimates of atmospheric dry deposition and associated input of nutrients to Gulf of Aqaba seawater. *J. Geophys. Res. Atmos.* 112, 1–14. doi: 10.1029/2006JD007858

Chen, Y., Street, J., and Paytan, A. (2006). Comparison between pure-water- and seawater-soluble nutrient concentrations of aerosols from the Gulf of Aqaba. *Mar. Chem.* 101, 141–152. doi: 10.1016/j.marchem.2006.02.002

Cho, B. C., and Hwang, C. Y. (2011). Prokaryotic abundance and 16S rRNA gene sequences detected in marine aerosols on the East Sea (Korea). *FEMS Microbiol. Ecol.* 76, 327–341. doi: 10.1111/j.1574-6941.2011.01053.x

Chow, C.-E. T., and Suttle, C. A. (2015). Biogeography of viruses in the sea. *Annu. Rev. Virol.* 2, 41–66. doi: 10.1146/annurev-virology-031413-085540

Christaki, U., Van-Wambeke, F., Lefevre, D., Lagaria, A., Prieur, L., Pujo-Pay, M., et al. (2011). Microbial food webs and metabolic state across oligotrophic waters of the Mediterranean Sea during summer. *Biogeosciences* 8, 1839–1852. doi: 10.5194/bg-8-1839-2011

Cvetkovic, A., Menon, A. L., Thorgersen, M. P., Scott, J. W., Poole, F. L., Jenney F. E. Jr., et al. (2010). Microbial metalloproteomes are largely uncharacterized. *Nature* 466, 779–782. doi: 10.1038/nature09265

Dannemiller, K. C., Reeves, D., Bibby, K., Yamamoto, N., and Peccia, J. (2014). Fungal high-throughput taxonomic identification tool for use with next-generation sequencing (FHiTINGS). *J. Basic Microbiol.* 54, 315–321. doi: 10.1002/jobm.201200507

Després, V. R., Alex Huffman, J., Burrows, S. M., Hoose, C., Safatov, A. S., Buryak, G., et al. (2012). Primary biological aerosol particles in the

atmosphere: a review. *Tellus Series B Chem. Phys. Meteorol.* 64, 1–40. doi: 10.3402/tellusb.v64i0.15598

Duarte, C. M., Agustí, S., and Agawin, N. S. R. (2000). Response of a Mediterranean phytoplankton community to increased nutrient inputs: a mesocosm experiment. *Mar. Ecol. Prog. Ser.* 195, 61–70. doi: 10.3354/meps195061

Falkowski, P. (1997). Evolution of the nitrogen cycle and its influence on the biological sequestration of CO2 in the ocean. *Nature* 387, 272–275. doi: 10.1038/387272a0

Gallisai, R., Peters, F., Volpe, G., Basart, S., and Baldasano, J. M. (2014). Saharan dust deposition may affect phytoplankton growth in the Mediterranean Sea at ecological time scales. *PLoS ONE* 9:e110762. doi: 10.1371/journal.pone.0110762

Ganor, E., and Mamane, Y. (1982). Transport of Saharan dust across the eastern Mediterranean. *Atmos. Environ.* 16, 581–587. doi: 10.1016/0004-6981(82)90167-6

Ganor, E., Osetinsky, I., Stupp, A., and Alpert, P. (2010). Increasing trend of African dust, over 49 years, in the eastern Mediterranean. *J. Geophys. Res. Atmos.* 115, 1–7. doi: 10.1029/2009JD012500

Gat, D., Zeev, E., and Tsesarsky, M. (2016). Soil bacteria population dynamics following stimulation for ureolytic microbial-induced CaCO3 precipitation. *Environ. Sci. Technol.* 50, 616–624. doi: 10.1021/acs.est.5b04033

Gorbushina, A. A., Kort, R., Schulte, A., Lazarus, D., Schnetger, B., Brumsack, H. J., et al. (2007). Life in Darwin's dust: intercontinental transport and survival of microbes in the nineteenth century. *Environ. Microbiol.* 9, 2911–2922. doi: 10.1111/j.1462-2920.2007.01461.x

Goudie, A. S., and Middleton, N. J. (2001). Saharan dust storms: nature and consequences. *Earth Sci. Rev.* 56, 179–204. doi: 10.1016/S0012-8252(01)00067-8

Griffin, D. W. (2007). Atmospheric movement of microorganisms in clouds of desert dust and implications for human health. *Clin. Microbiol. Rev.* 20, 459–477. doi: 10.1128/CMR.00039-06

Guerzoni, S., Chester, R., Dulac, F., Herut, B., Loÿe-Pilot, M. D., Measures, C., et al. (1999). The role of atmospheric deposition in the biogeochemistry of the Mediterranean Sea. *Prog. Oceanogr.* 44, 147–190. doi: 10.1016/S0079-6611(99)00024-5

Guieu, C., Aumont, O., Paytan, A., Bopp, L., Law, S. C., Mahowald, N., et al. (2014). Global biogeochemical cycles deposition to low nutrient low chlorophyll regions. *Glob. Biogeochem. Cycles* 28, 1179–1198. doi: 10.1002/2014GB004852

Herut, B., Almogi-Labin, A., and Jannink, N. (2000). The seasonal dynamics of nutrient and chlorophyll a concentrations on the SE Mediterranean shelf-slope. *Oceanol. Acta* 23, 771–782. doi: 10.1016/S0399-1784(00)01118-X

Herut, B., Kress, N., and Tibor, G. (2002). The use of hyper-spectral remote sensing in compliance monitoring of water quality (phytoplankton and suspended particles) at "hot spot" areas (Mediterranean coast of Israel). *Fresenius Environ. Bull.* 11, 782–787.

Herut, B., Krom, M. D., Pan, G., and Mortimer, R. (1999). Atmospheric input of nitrogen and phosphorus to the southeast Mediterranean: sources, fluxes, and possible impact, Limnology and Oceanography. 44, 1683–1692. doi: 10.4319/lo.1999.44.7.1683

Herut, B., Nimmo, M., Medway, A., Chester, R., and Krom, M. D. (2001). Dry atmospheric inputs of trace metals at the Mediterranean coast of Israel (SE Mediterranean): sources and fluxes. *Atmos. Environ.* 35, 803–813. doi: 10.1016/S1352-2310(00)00216-8

Herut, B., Zohary, T., Krom, M. D., Mantoura, R. F. C., Pitta, P., Psarra, S., et al. (2005). Response of East Mediterranean surface water to Saharan dust: on-board microcosm experiment and field observations. *Deep Sea Res. Part II Top. Stud. Oceanogr.* 52, 3024–3040. doi: 10.1016/j.dsr2.2005.09.003

Hervas, A., Camarero, L., Reche, I., and Casamayor, E. O. (2009). Viability and potential for immigration of airborne bacteria from Africa that reach high mountain lakes in Europe. *Environ. Microbiol.* 11, 1612–1623. doi: 10.1111/j.1462-2920.2009.01926.x

Hervas, A., and Casamayor, E. O. (2009). High similarity between bacterioneuston and airborne bacterial community compositions in a high mountain lake area. *FEMS Microbiol. Ecol.* 67, 219–228. doi: 10.1111/j.1574-6941.2008.00617.x

Huertas, M. J., López-Maury, L., Giner-Lamia, J., Sánchez-Riego, A. M., and Florencio, J. F. (2014). Metals in cyanobacteria: analysis of the copper, nickel, cobalt and arsenic homeostasis mechanisms. *Life* 4, 865–886. doi: 10.3390/life4040865

Ilaiwi, M. D. (1985). *Soil Map of Arab Countries. Soil Map of Syria and Lebanon.* Damascus.

Katra, I., Arotsker, L., Krasnov, H., Zaritsky, A., Kushmaro, A., and Ben-Dov, E. (2014). Richness and diversity in dust stormborne biomes at the southeast Mediterranean. *Sci. Rep.* 4:5265. doi: 10.1038/srep05265

Kellogg, C. A., and Griffin, D. W. (2006). Aerobiology and the global transport of desert dust. *Trends Ecol. Evol.* 21, 638–644. doi: 10.1016/j.tree.2006.07.004

Kocak, M., Kubilay, N., Herut, B., and Nimmo, M. (2005). Dry atmospheric fluxes of trace metals (Al, Fe, Mn, Pb, Cd, Zn, Cu) over the Levantine Basin: a refined assessment. *Atmos. Environ.* 39, 7330–7341. doi: 10.1016/j.atmosenv.2005.09.010

Kress, N., Frede Thingstad, T., Pitta, P., Psarra, S., Tanaka, T., Zohary, T., et al. (2005). Effect of P and N addition to oligotrophic Eastern Mediterranean waters influenced by near-shore waters: a microcosm experiment. *Deep Res. Part II Top. Stud. Oceanogr.* 52, 3054–3073. doi: 10.1016/j.dsr2.2005.08.013

Kress, N., Gertman, I., and Herut, B. (2014). Temporal evolution of physical and chemical characteristics of the water column in the easternmost Levantine Basin (Eastern Mediterranean Sea) from 2002 to 2010. *J. Mar. Syst.* 135, 6–13. doi: 10.1016/j.jmarsys.2013.11.016

Kress, N., and Herut, B. (2001). Spatial and seasonal evolution of dissolved oxygen and nutrients in the southern Levantine Basin (Eastern Mediterranean Sea): chemical characterization of the water masses and inferences on the N:P ratios. *Deep Sea Res. Part I Oceanogr. Res. Pap.* 48, 2347–2372. doi: 10.1016/S0967-0637(01)00022-X

Krom, M. D., Cliff, R. A., Eijsink, L. M., Herut, B., and Chester, R. (1999). The characterisation of Saharan dusts and Nile particulate matter in surface sediments from the Levantine basin using Sr isotopes. *Mar. Geol.* 155, 319–330. doi: 10.1016/S0025-3227(98)00130-3

Lagaria, A., Psarra, S., Lefèvre, D., Van-Wambeke, F., Courties, C., Pujo-Pay, M., et al. (2011). The effects of nutrient additions on particulate and dissolved primary production in surface waters of three Mediterranean eddies. *Biogeosciences* 8, 2595–2607. doi: 10.5194/bg-8-2595-2011

Lang-Yona, N., Lehahn, Y., Herut, B., Burshtein, N., and Rudich, Y. (2014). Marine aerosol as a possible source for endotoxins in coastal areas. *Sci. Total Environ.* 499, 311–318. doi: 10.1016/j.scitotenv.2014.08.054

Lawrence, C. R., and Neff, J. C. (2009). The contemporary physical and chemical flux of aeolian dust: a synthesis of direct measurements of dust deposition. *Chem. Geol.* 267, 46–63. doi: 10.1016/j.chemgeo.2009.02.005

Mackey, K. R. M., Labiosa, R. G., Calhoun, M., Street, J. H., Post, A. F., and Paytan, A. (2007). Phosphorus availability, phytoplankton community dynamics, and taxon-specific phosphorus status in the Gulf of Aqaba, Red Sea. *Limnol. Oceanogr.* 52, 873–885. doi: 10.4319/lo.2007.52.2.0873

Mann, E. L., Ahlgren, N., Moffett, J. W., and Chisholm, S. W. (2002). Copper toxicity and cyanobacteria ecology in the Sargasso Sea. *Limnol. Oceanogr.* 47, 976–988. doi: 10.4319/lo.2002.47.4.0976

Margalef, R. (1958). Information theory in ecology. *Int. J. Gen. Syst.* 3, 36–71.

Marshall, W. A., and Chalmers, M. O. (1997). Airborne dispersal of antarctic terrestrial algae and cyanobacteria. *Ecography* 20, 585–594. doi: 10.1111/j.1600-0587.1997.tb00427.x

Massana, R., Murray, A. E., Preston, C. M., and Delong, E. (1997). Vertical distribution and phylogenetic characterization of marine planktonic archaea in the Santa Barbara Channel. *Appl. Environ. Microbiol.* 63, 50–56.

Mayol, E., Jiménez, M. A., Herndl, G. J., Duarte, C. M., and Arrieta, J. M. (2014). Resolving the abundance and air-sea fluxes of airborne microorganisms in the North Atlantic Ocean. *Front. Microbiol.* 5:557. doi: 10.3389/fmicb.2014.00557

Mills, M. M., Ridame, C., Davey, M., La-Roche, J., and Geider, R. (2004). Iron and phosphorus co-limit nitrogen fixation in the eastern tropical North Atlantic. *Nature* 429, 292–294. doi: 10.1038/nature02550

Paytan, A., Mackey, K. R. M., Chen, Y., Lima, I. D., Doney, S. C., and Mahowald, N. (2009). Toxicity of atmospheric aerosols on marine phytoplankton. *Proc. Natl. Acad. Sci. U.S.A.* 106, 4601–4605. doi: 10.1073/pnas.0811486106

Peter, H., Hörtnagl, P., Reche, I., and Sommaruga, R. (2014). Bacterial diversity and composition during rain events with and without Saharan dust influence reaching a high mountain lake in the Alps. *Environ. Microbiol. Rep.* 6, 618–624. doi: 10.1111/1758-2229.12175

Pitta, P., Nejstgaard, J. C., Tsagaraki, T. M., Zervoudaki, S., Egge, J. K., Frangoulis, C., et al. (2016). Confirming the "Rapid phosphorus transfer from microorganisms to mesozooplankton in the Eastern Mediterranean Sea"

scenario through a mesocosm experiment. *J. Plankton Res.* 38, 502–521. doi: 10.1093/plankt/fbw010

Polymenakou, P. N. (2012). Atmosphere: a source of pathogenic or beneficial microbes? *Atmosphere* 3, 87–102. doi: 10.3390/atmos3010087

Polymenakou, P. N., Mandalakis, M., Stephanou, E. G., and Tselepides, A. (2008). Particle size distribution of airborne microorganisms and pathogens during an intense African dust event in the Eastern Mediterranean. *Environ. Health Perspect.* 116, 292–296. doi: 10.1289/ehp.10684

Prospero, J. M., Blades, E., Mathison, G., and Naidu, R. (2005). Interhemispheric transport of viable fungi and bacteria from Africa to the Caribbean with soil dust. *Aerobiologia* 21, 1–19. doi: 10.1007/s10453-004-5872-7

Pulido-Villena, E., Wagener, T., and Guieu, C. (2008). Bacterial response to dust pulses in the western Mediterranean: implications for carbon cycling in the oligotropic ocean. *Glob. Biogeochem. Cycles* 22, 1–12. doi: 10.1029/2007GB003091

Rahav, E., Giannetto, M., and Bar-Zeev, E. (2016b). Contribution of mono and polysaccharides to heterotrophic N2 fixation at the eastern Mediterranean coastline. *Sci. Rep.* 6:27858. doi: 10.1038/srep27858

Rahav, E., Ovadia, G., Paytan, A., and Herut, B. (2016a). Contribution of airborne microbes to bacterial production and N2 fixation in seawater upon aerosol deposition. *Geophys. Res. Lett.* 43, 1–9. doi: 10.1002/2015GL066898

Raveh, O., David, N., Rilov, G., and Rahav, E. (2015). The temporal dynamics of coastal phytoplankton and bacterioplankton in the Eastern Mediterranean Sea. *PLoS ONE* 10:e0140690. doi: 10.1371/journal.pone.0140690

Reche, I., Ortega-Retuerta, E., Romera, O., Pulido-Villena, E., Morales-Baquero, R., and Casamayor, E. O. (2009). Effect of Saharan dust inputs on bacterial activity and community composition in Mediterranean lakes and reservoirs. *Limnol. Oceanogr.* 54, 869–879. doi: 10.4319/lo.2009.54.3.0869

Redfield, A. C. (1934). "On the proportions of organic derivatives in sea water and their relation to the composition of plankton," in *James Johnstone Memorial Volume*, ed R. J. Daniel (Liverpool: Liverpool University Press), 176–192.

Saeed, T., and Sun, G. (2012). A review on nitrogen and organics removal mechanisms in subsurface flow constructed wetlands: dependency on environmental parameters, operating conditions and supporting media. *J. Environ. Manag.* 112, 429–448. doi: 10.1016/j.jenvman.2012.08.011

Seifried, J. S., Wichels, A., and Gerdts, G. (2015). Spatial distribution of marine airborne bacterial communities. *MicrobiologyOpen* 25, 475–490. doi: 10.1002/mbo3.253

Sharoni, S., Trainic, M., Schatz, D., Lahahn, Y., Flores, M. J., Bidle, K. D., et al. (2015). Infection of phytoplankton by aerosolized marine viruses. *Proc. Natl. Acad. Sci. U.S.A.* 112, 6643–6647. doi: 10.1073/pnas.1423667112

Simon, M., Alldredge, A., and Azam, F. (1990). Bacterial carbon dynamics on marine snow. *Mar. Ecol. Prog. Ser.* 65, 205–211. doi: 10.3354/meps065205

Sohm, J. A., Webb, E. A., and Capone, D. G. (2011). Emerging patterns of marine nitrogen fixation. *Nat. Rev. Microbiol.* 9, 499–508. doi: 10.1038/nrmicro2594

Steemann-Nielsen, E. (1952). On the determination of the activity for measuring primary production. *J. Cons. Int. Explor. Mer.* 18, 117–140.

Sunda, W. G. (2012). Feedback interactions between trace metal nutrients and phytoplankton in the ocean. *Front. Microbiol.* 3:204. doi: 10.3389/fmicb.2012.00204

Ternon, E., Guieu, C., Ridame, C., L'Helguen, S., and Catala, P. (2011). Longitudinal variability of the biogeochemical role of Mediterranean aerosols in the Mediterranean Sea. *Biogeosciences* 8, 1067–1080. doi: 10.5194/bg-8-1067-2011

Thingstad, T. F., Krom, M. D., Mantoura, R. F. C., Flaten, G. A., Groom, S., Herut, B., et al. (2005). Nature of phosphorus limitation in the ultraoligotrophic eastern Mediterranean. *Science* 309, 1068–1071. doi: 10.1126/science.1112632

Vardi, A., Haramaty, L., Mooy, B. A. S., Van Fredricks, H. F., Kimmance, S. A., Larsen, A., et al. (2012). Host-virus dynamics and subcellular controls of cell fate in a natural coccolithophore population. *Proc. Natl. Acad. Sci. U.S.A.* 109, 19327–19332. doi: 10.1073/pnas.1208895109

Vaulot, D., and Marie, D. (1999). Diel variability of photosynthetic picoplankton in the equatorial Pacific. *Appl. Environ. Microbiol.* 104, 3297–3310. doi: 10.1029/98jc01333

Wang, X. J., Behrenfeld, M., Le-Borgne, R., Murtugudde, R., and Boss, E. (2009). Regulation of phytoplankton carbon to chlorophyll ratio by light, nutrients and temperature in the Equatorial Pacific Ocean : a basin-scale model. *Biogeosciences* 6, 391–404. doi: 10.5194/bg-6-391-2009

Welschmeyer, N. A. (1994). Fluorometric analysis of chlorophyll a in the presence of chlorophyll b and pheopigments. *Limnol. Oceanogr.* 39, 1985–1992. doi: 10.4319/lo.1994.39.8.1985

Zohary, T., Herut, B., Krom, M. D., Mantoura, R. F. C., Pitta, P., Psarra, S., et al. (2005). P-limited bacteria but N and P co-limited phytoplankton in the Eastern Mediterranean—a microcosm experiment. *Deep Sea Res. Part II Top Stud. Oceanogr.* 52, 3011–3023. doi: 10.1016/j.dsr2.2005.08.011

Conflict of Interest Statement: The authors declare that the research was conducted in the absence of any commercial or financial relationships that could be construed as a potential conflict of interest.

The reviewer CP and handling Editor declared their shared affiliation, and the handling Editor states that the process nevertheless met the standards of a fair and objective review.

frontiers in Marine Science

ORIGINAL RESEARCH
published: 16 November 2016
doi: 10.3389/fmars.2016.00222

The Impact of Dry Atmospheric Deposition on the Sea-Surface Microlayer in the SE Mediterranean Sea: An Experimental Approach

Peleg Astrahan[1], Barak Herut[2], Adina Paytan[3] and Eyal Rahav[2]**

[1] Israel Oceanographic and Limnological Research, The Kinneret Limnological Laboratory, Migdal, Israel, [2] Israel Oceanographic and Limnological Research, National Institute of Oceanography, Haifa, Israel, [3] Institute of Marine Science, University of California, Santa Cruz, CA, USA

The oligotrophic southeastern Mediterranean Sea (SEMS) is frequently exposed to desert-dust deposition which supplies nutrients, trace metals and a wide array of viable airborne microorganisms. In this study, we experimentally examined the impact of aerosol addition, collected during an intense dust storm event in early September 2015, on the biomass and activity of pico-phytoplankton and heterotrophic bacterial populations at the sea-surface micro layer (SML) relative to the sub surface layer (SSL). Aerosol (1.5 mg L^{-1}) was added to SML and SSL water samples in microcosms (4.5 L) and the water was frequently sampled over a period of 48 h. While the aerosol amendment triggered a moderate 1.5–2-fold increase in primary production in both the SML and the SSL, bacterial production increased by ~3 and ~7-folds in the SSL and SML, respectively. Concurrently, the abundance and flow-cytometric characteristics (green fluorescence and side scatter signals) of high nucleic acid (HNA) and low nucleic acid (LNA) bacterial cells showed a significant increase in the %HNA, in both SML and SSL samples following aerosol amendment. This shift in nucleic acid content took place at a much faster rate in the SML, suggesting a more active heterotrophic community. These changes were likely a result of higher rates of carbon utilizations in the SML following the dust addition, as assessed by a selected hydrocarbons and saccharides analysis. Additionally, a high absorption rate of hydrocarbons by the aerosol particles was measured following the additions, leaving less than 10% of these molecules available for potential heterotrophic microbial utilization. Our results suggest that the heterotrophic microbial community inhabiting the SML is more efficient in utilizing aerosol associated constituents than the community in the SSL.

Keywords: microlayer, aerosols, microcosms, mediterranean region, bacterial productivity

OPEN ACCESS

Edited by:
Stelios Katsanevakis, University of the Aegean, Greece

Reviewed by:
Ashley Ballantyne, University of Montana, USA
Antoni Tovar-Sanchez, Spanish National Research Council, Spain
Maria Montserrat Sala, Spanish National Research Council, Spain

****Correspondence:***
Peleg Astrahan
peleg.astrahan@ocean.org.il
Eyal Rahav
eyal.rahav@ocean.org.il

Specialty section:
This article was submitted to Marine Ecosystem Ecology, a section of the journal Frontiers in Marine Science

Received: *24 August 2016*
Accepted: *26 October 2016*
Published: *16 November 2016*

Citation:
Astrahan P, Herut B, Paytan A and Rahav E (2016) The Impact of Dry Atmospheric Deposition on the Sea-Surface Microlayer in the SE Mediterranean Sea: An Experimental Approach. Front. Mar. Sci. 3:222. doi: 10.3389/fmars.2016.00222

INTRODUCTION

The sea-surface microlayer (SML) is the uppermost layer of the oceans (20–400 μm thick), located between the subsurface layer (SSL) waters and the atmosphere (Liss and Duce, 1997). The SML is a unique physiochemical and biological habitat that covers ~70% of Earth's surface. This boundary layer may play a significant role in many biogeochemical processes including air-sea gas and heat

exchange (Liss and Duce, 1997) and the cycling of various elements (Wurl and Holmes, 2008). Its chemical content is different from the one usually found in the SSL. For example, higher concentrations of saccharides, hydrocarbons, amino acids, and polysaccharides were detected at the SML compared to the SSL (Engel et al., 2004). Hydrocarbons in the form of alkyl chains (i.e., n-alkanes) are highly enriched in the microlayer due to their hydrophobic character and low density (Marty and Saliot, 1976). It is assumed that high concentrations of organic matter in the SML may aggregate with sticky Transparent Exopolymer Particles (TEP) that are also enriched in the SML, resulting in gel-like particulate matter (Cunliffe et al., 2010). These aggregates may also include bacteria cells (Passow and Alldredge, 1994) and potentially various other molecules. In addition bacteria cells embedded in these particles may use these hydrocarbon molecules in the aggregates as an energy source (Grossi et al., 2007; Yakimov et al., 2007; Sevilla et al., 2015). Unsaturated alkyl chain like molecules as in the case of α-olefins (1-alkenes), might show elevated photo-oxidation rates and as a result light induced degradation (Mouzdahir et al., 2001). These differences may affect microbial activity (Reinthaler et al., 2008; Sarmento et al., 2015), enhance/reduce extracellular enzymatic activity (Kuznetsova and Lee, 2001; Engel and Galgani, 2016) and affect microbial diversity and abundance (Reinthaler et al., 2008; Vila-costa et al., 2013).

The SML communities (frequently termed "Neuston") are composed of diverse groups of phytoneuston (autotrophs) and bacterioneuston (heterotrophs) (Liss and Duce, 1997; Cunliffe et al., 2010), which thrive on the relatively enriched organic matrix (Guitart et al., 2013; Engel and Galgani, 2016). One of the main external sources of nutrients to the SML is wet or dry atmospheric depositions (Cunliffe et al., 2010; Guieu et al., 2014). Deposited aerosols first interact with the SML and then sink through the SSL to deeper waters, supplying nutrients such as N, P, and Fe (e.g., Herut et al., 1999, 2002; Chien et al., 2016). They may also introduce viable airborne microbes (Griffin, 2010; Peter et al., 2014; Rahav et al., 2016a,b). Therefore, any dry or wet deposition has the potential of changing the diversity and activity of the phytoneuston and bacterioneuston communities.

The southeastern Mediterranean Sea (SEMS) is a low nutrients low chlorophyll marine province (Berman et al., 1984; Krom et al., 1991; Yacobi et al., 1995; Rahav et al., 2013; Kress et al., 2014) dominated by small-size microbes with low productivity (Yacobi et al., 1995; Bar-zeev and Rahav, 2015; Raveh et al., 2015). Recent studies showed that these autotrophic microorganisms are primarily limited by N or co-limited by N&P, whereas heterotrophic bacteria are P or C limited during summertime (Kress et al., 2005; Zohary et al., 2005; Rahav et al., 2016c). Previous studies emphasized the significant role of atmospheric deposition in supplying limiting nutrients to the SEMS (Herut et al., 1999, 2002; Guieu et al., 2014). While these studies have assessed the impact of atmospheric dust deposition on surface phytoplankton and heterotrophic bacterial communities in the SEMS (e.g., Ridame et al., 2011; Rahav et al., 2016b), none of these studies distinguished between the SML and the SSL.

In this study, we present a microcosm experimental assay that examines the response of the neuston and bulk bacterioplankton communities, collected from the SML and SSL respectively to the addition of dry deposition of aerosol including desert dust (1.5 mg L^{-1}). Temporal dynamics of the autotrophic and heterotrophic microbial abundances and activity were recorded for 48 h at high temporal resolution (every 4–8 h). High nucleic acid (HNA) concentration per bacterial cell, was reported as an efficient measure for bacterial activity (Lebaron et al., 2001; Talarmin et al., 2011; Van Wambeke et al., 2011) and thus was included in this study in addition to bacterial productivity. Chemical analyses of saccharides and selected hydrocarbons were also examined. We hypothesized that due to the physiochemical and biological differences between the SML and SSL, any external atmospheric addition that delivers micro and macro-nutrients may trigger distinct responses in these two layers.

MATERIALS AND METHODS

SML and SSL Sampling

SML water samples were collected on December 15, 2015 by using a custom made rotating drum sampler as described in Harvey (1966) with minor changes: the rotating drum used was a glass tube ($r = 18$ cm; $l = 60$ cm). The drum was pre-cleaned with a concentrated HCl solution and washed with sample water for a few min prior collection. No silicon or plastic tubes were used. The collector includes an indurated non-contaminating silicon blade (0.5 m) fixed on an aluminum grip holder, collecting the water into a pre-combusted glass bottle. These changes are consistent with the glass plate collection procedure (Harvey and Burzell, 1972) by using similar materials. In addition, these improvements allow for a fast cleaning procedure, avoiding the contamination caused by reusing materials such as plastics and silicon tubing. The SML sample (23 L in total) was collected by connecting the sampler in parallel to a small boat (rotating speed ∼5 RPM). SML thickness was approximately 75 μm thick, and collection time was 90 min. Sampling starting point selected was 1 km offshore (32°49′34N, 34°57′20E); collection ended 560 m northeast of the starting point. The study area is a coastal oligotrophic water zone (see discussion below); with low influence of urban runoff. The port of Haifa is located a few kilometers north of our study area; however, the general water circulation carries most of the bulk water away from our study zone. The average bottom depth along the sampling was 13 m. SSL water sample (23 L in total) was collected from 1 m depth along the same cruise-track. Samples were kept in acid prewashed sealed containers until processed at the Israel Oceanographic and Limnological Research (IOLR) institute. The wind speed was <3.5 knots, with waves of up to 0.3 m, and the seawater surface temperature was 18°C. Though waves in the same magnitude showed no impact on SML surfactants tension and spreading rates (Hale and Mitchell, 1997), it is possible that the SML collection may include minor amounts of SSL water and thus the results presented here may be an underestimation of the trends observed (i.e., dilution of the microlayer water with sub-surface water).

Aerosol Collection and Experimental Design

A dry deposition sample was collected on September 8–9, 2015, using a pre-clean 2 m^2 glass plate (more details in Rahav

et al., 2016b). The pre cleaned glass plate was exposed for 48 h during an extreme dust storm arriving from the north-east (**Supplementary Figure S1**). Over this time 1 gr m^{-2} of aerosol was deposited of plate area. Assuming a deposition rate of up to 50 g dust m^{-2} yr^{-1} in the Mediterranean Sea (Lawrence and Neff, 2009), the accumulated aerosol in this time period corresponds to ∼2–3% of the annual dust deposition in this system. We added 1.5 mg L^{-1} of the collected aerosol (in triplicate) to acid-cleaned 4.5 L transparent High-density polyethylene Nalgene bottles containing either SML or SSL water (6.7–6.8 mg aerosol in total to each bottle). This addition is equivalent to the concentration reported for the upper mixed layer (top 5 m) during a heavy dust storm (Herut et al., 2002, 2005; Rahav et al., 2016b), and is similar to the amounts tested in other studies from the SEMS (Ridame et al., 2011; Herut et al., 2016). Samples were incubated in an outdoor pool with seawater flow-through to maintain ambient seawater temperature. The bottles used allowed the penetration of most of the light spectrum, excluding UV light. Blank treatments of SML or SSL water without an aerosol addition were also carried out in parallel. SSL bottles were submerged to a depth of 1 m in the pool by using weights. Subsamples of seawater from each incubation bottle were collected for *Synechococcus* abundance, pico-eukaryotes abundance, nano-eukaryotic abundance, heterotrophic bacterial abundance, primary production, and bacterial production measurements at 0, 1.5, 5, 9, 17, 21, 26, and 44 h after the aerosol addition.

Pico-Phytoplankton and Bacterial Abundance

Water samples (1.8 mL) were fixed with 50% glutaraldehyde (6 µl, Sigma-Aldrich G7651), frozen in liquid nitrogen and stored at −80°C until analyzed. Pico-phytoplankton abundance (namely *Synechococcus* and autotrophic eukaryotes algae) was determined using an Attune® Acoustic Focusing Flow Cytometer (Applied Biosystems) equipped with a syringe-based fluidic system and 488 and 405-nm lasers at a flow rate of 100 µL min^{-1} (Bar-zeev and Rahav, 2015). For heterotrophic bacterial abundance determination, subsamples (100 µl) were separately incubated at room temperature for 15 min with the nucleic acid stain SYTO9 (1:10^5 vol:vol) and then run at a low flow rate of 25 µL min^{-1} (Vaulot and Marie, 1999). Low nucleic acid (LNA) and HNA bacteria were differentiated by coupling their green fluorescence and side-scatter (Lebaron et al., 2001; Talarmin et al., 2011; Van Wambeke et al., 2011). For more details, see (Rahav et al., 2016b).

Primary Production

Photosynthetic carbon fixation rates were estimated using the ^{14}C incorporation method (Nielsen, 1952). For more details, see (Rahav et al., 2016b).

Bacterial Production

Bacterial production was estimated using the [4,5-^{3}H]-leucine incorporation method (Simon et al., 1990). A conversion factor of 3 kg C mol^{-1} leucine incorporated was used, assuming an isotopic dilution of 2.0 (Simon and Azam, 1989). For more details, see (Rahav et al., 2016b).

Dissolved Monosaccharides Concentration

SML and SSL samples (10 ml) were filtered using 0.22 µm polycarbonate membranes (Osmonics INC). The dissolved monosaccharides' (no hydrolysis) concentration was determined using the 2,4,6-Tripyridyl-s-Triazine (TPTZ) reagent (Sigma-Aldrich) method according to Myklestad et al. (1997). All samples were analyzed using an Uvikon 9100/9400 spectrophotometer (SECOMAM).

GC/MS Analysis

Samples (200 ml) were filtered using 0.22 µm non-absorbing membrane, followed by the extraction of dissolved n-alkanes and α-olefins from the water samples by liquid:liquid extraction, using 3 × 30 ml n-hexane extraction repeats, followed by 3 × 30 ml dichloromethane. The organic extracts were combined, concentrated to 1 ml via rotary evaporation and dried by passing through an $MgSO_4$ column. Samples were analyzed using an Agilent 6890 gas chromatograph coupled with a 5973 Agilent mass spectrometer. Identification of the hydrocarbons was based on ions analysis (alkane ions = 43, 57, 71... α-olefins = 41, 55, 69...) in addition to library matching (NIST 2) and external standards R.T as described next. Quantification of the results was achieved by using C_8-C_{30} external standards of n-alkanes (Sigma-Aldrich) and α-olefins (AccuStandard®, Inc). Alkanes and α-olefins adsorption to the membrane and to the experiment flasks was lower than 10%, method quantitation level = 10 ng L^{-1}.

Statistical Analyses

The different variables presented in the figures and tables are averages and standard deviation (biological replicates, $n = 3$). Changes in primary production, bacterial production, the abundance of *Synechococcus*, pico/nano-eukaryotes, and heterotrophic bacteria throughout the experiments (0–44 h) were evaluated using a one-way analysis of variance (ANOVA), followed by a Fisher LSD multiple comparison *post hoc*-test with a confidence level of 95% ($\alpha = 0.05$). Prior analyses, the ANOVA assumptions were examined. The statistical analyses were carried out using the XLSTAT software.

RESULTS

Initial SML and SSL Characteristics Prior to Aerosol Addition

The SML at the study site was characterized by a higher concentration of n-alkanes (52.5 ng L^{-1}) and olefins, also termed "1-alkenes" (1.12 mg L^{-1}), relative to the SSL (46.4 ng n-alkanes L^{-1} and 0.70 mg α-olefins L^{-1}). Similarly, the SML contained a higher concentration of monosaccharides relative to the SSL, 890 µg L^{-1} vs. 613 µg L^{-1}, respectively (**Table 1**). The total α-olefins (1-alkenes) concentration in the SML was more than 3 orders of magnitude higher than the alkanes and monosaccharides, suggesting α-olefins were a dominant source of carbon (**Table 1**).

TABLE 1 | Dissolved Σ [alkanes$_{(C8-C30)}$], Σ [α-olefins$_{(C11-C32)}$] and monosaccharides in the SML and SSL, prior (T0) and 44 h after (T44) aerosol addition.

Variable	Unit	Prior aerosol addition (0 h)			End of incubations (44 h)		
		SML	SSL	EF	SML	SSL	EF
Total n-alkanes (C_8-C_{30})	ng L^{-1}	52.5	46.4	1.13	23.7	n.d	>2.37
Total α olefins (C_8-C_{30})	mg L^{-1}	1.12	0.70	1.60	0.01	n.d	>1000
Monosaccharides	μg L^{-1}	890	613	1.45	472	190	2.48

EF, enrichment factor (SML: SSL ratio).
n.d, not detected- below the quantitation level of 10 ng L^{-1}.

Synechococcus dominated the picophytoplankton in the SML and SSL (∼2.3 × 10^4 cells ml^{-1}), whereas in both layers the pico-eukaryotes abundance was lower by an order of magnitude (1.0 × 10^3 to 1.5 × 10^3 cells ml^{-1}) (**Table 2**). Heterotrophic bacterial abundance was similar in both water layers (∼1.5 × 10^5 cells ml^{-1}), although high nucleic acid bacteria (HNA) accounted for 7% at the SML and ∼15% at the SSL. Primary production (PP) was overall low, with 60% higher rates measured at the SML (0.08 ± 0.00 μg C L^{-1} h^{-1}) compared to the SSL (0.05 ± 0.00 μg C L^{-1} h^{-1}) (**Table 2**). Similarly, bacterial production (BP) was ∼50% higher at the SML (0.06 ± 0.00 μg C L^{-1} h^{-1}) than at the SSL (0.04 ± 0.01 μg C L^{-1} h^{-1}) (**Table 2**). Nevertheless, these activity rates resulted in a similar BP:PP ratio (∼0.75:1), suggesting a weak dominance of autotrophic metabolism (over heterotrophic metabolism) in both water layers.

Aerosol Characteristics

The aerosol sample used in our experiment was collected during an exceptional dust storm event that arrived from the northeast rather than the more common southwest (Saharan desert) sources (**Supplementary Figure S1**). Based on the aluminum (Al) concentration in the collected aerosol, the Al settling velocity, and the weight of the particles collected, we calculated a dry deposition concentration of 1.05 mg L^{-1} at the upper 5 m mixed layer as reported in Rahav et al. (2016b). While such an episodic and strong deposition event is considered high in this system (reviewed in Guieu et al., 2014), it is well in the range previously reported for the Mediterranean Sea (e.g., Herut et al., 2002; Ridame et al., 2011, 2013) and similar to additions tested in previous microcosm bioassays (Herut et al., 2005; Rahav et al., 2016c). The micro and macro solubilized nutrients concentrations that were leached off the added aerosol sample are detailed in Rahav et al. (2016b) and discussed below.

Bacterioplankton Response to Aerosol Addition

Following aerosol addition, the abundances of *Synechococcus* (ranging from ∼2 × 10^4 cells ml^{-1} to ∼7 × 10^4 cells ml^{-1}) and nano-eukaryote (ranging from 250 cells ml^{-1} to 1200 cells ml^{-1}) in both layer samples were similar to the unamended treatments (**Figure 1**) and thus they were not significantly affected by the addition of the aerosols. Pico-eukaryote abundance following the aerosol addition was similar to the unamended control during the first 21 h in both layers (∼1000–2000 cells ml^{-1}, $P > 0.05$), thereafter increased ∼2-fold relative to the unamended controls in the SML microcosms only (5000 cells ml^{-1}, $P < 0.01$) (**Figures 1B,E**, **Table 3**). Heterotrophic bacterial abundance increased ∼2-fold in the SML and SSL following the addition of aerosol (from ∼1.5 × 10^5 cells ml^{-1} to ∼4 × 10^5 cells ml^{-1}, $P < 0.05$), with more profound differences between the treated versus the non-treated sample for the SML (**Figures 2A,C**). These differences were also apparent in the increased relative abundance of HNA over LNA bacteria, with 2-fold higher HNA bacteria ($P = 0.02$) recorded following the aerosol addition at both the SML and the SSL (**Figure 2**, **Table 3**). While the changes in microorganism abundance were relatively modest (**Figures 1**, **2**), more profound differences were recorded for both PP and BP rates following the aerosol addition (**Figure 3**, **Table 3**). PP rates increased by ∼2-fold relative to the untreated control ($P < 0.05$) 17 h post aerosol addition in both the SML and SSL. This enhancement lasted for the experiment's entire duration; 44 h post addition (**Figures 3A,D**, **Table 3**). Simultaneously, BP exhibited a stronger response to the aerosol addition, ∼3-fold higher rates recorded at the SSL (increasing from 0.04 μg C L^{-1} h^{-1} to 0.11 μg C L^{-1} h^{-1}, $P < 0.05$) and up to a ∼7-fold increase at the SML (from 0.06 μg C L^{-1} h^{-1} to 0.44 μg C L^{-1} h^{-1}, $P < 0.05$) relative to the unamended control that showed no change (**Figures 3B,E**, **Table 3**). These differences resulted in a higher BP:PP ratio at both water layers following the aerosol addition relative to the unamended controls (**Figure 3**, $P < 0.05$). Enrichment factors (EF) were calculated as the ratio between the abundance or the activity in the SML divided by those measured in the SSL (0–44 h). The EF-values for *Synechococcus* and nano-eukaryotes were similar in both the unamended and the aerosol addition bioassays (an insignificant change from a 1:1 ratio, $P > 0.05$). In contrast, pico-eukaryotes abundance, heterotrophic bacterial abundance, PP, and BP all exhibited significant higher EF-values (>1) following aerosol addition (**Figure 4**, $P < 0.05$).

Dissolved Hydrocarbons Post Aerosol Addition

Overall, the dissolved n-alkane concentration decreased substantially with time (T0 vs. T44 h) in the SML and to a lower level in the SSL following aerosol additions (**Table 1**). n-alkanes at the SML were reduced by ∼50% at the conclusion of the experiment (reaching 23.7 ng L^{-1}), whereas a decrease to below detection limit was observed in the SSL (**Table 1**). α-olefins, which were the major carbohydrate found, were reduced by two orders of magnitude in the SML and to below detection limit in the SSL at T44 h (**Table 1**). Finally, monosaccharides decreased by ∼50% at the SML (472 μg L^{-1}) and by ∼66% at the SSL (190 μg L^{-1}) (**Table 1**). Based on the BP rates measured

TABLE 2 | Initial biological characteristics of the SML and SSL prior aerosol addition (T0).

Water layer	BP (μg C L^{-1} h^{-1})	PP (μg C L^{-1} h^{-1})	Total bacteria (cells ml^{-1})	*Synechococcus* (cells ml^{-1})	pico-eukaryotes (cells ml^{-1})
SML	0.06 ± 0.00	0.08 ± 0.00	160086	22653	1063
SSL	0.04 ± 0.01	0.05 ± 0.00	151870	24290	1550
EF	1.50	1.60	1.05	0.93	0.68

EF, enrichment factor (SML:SSL ratio).

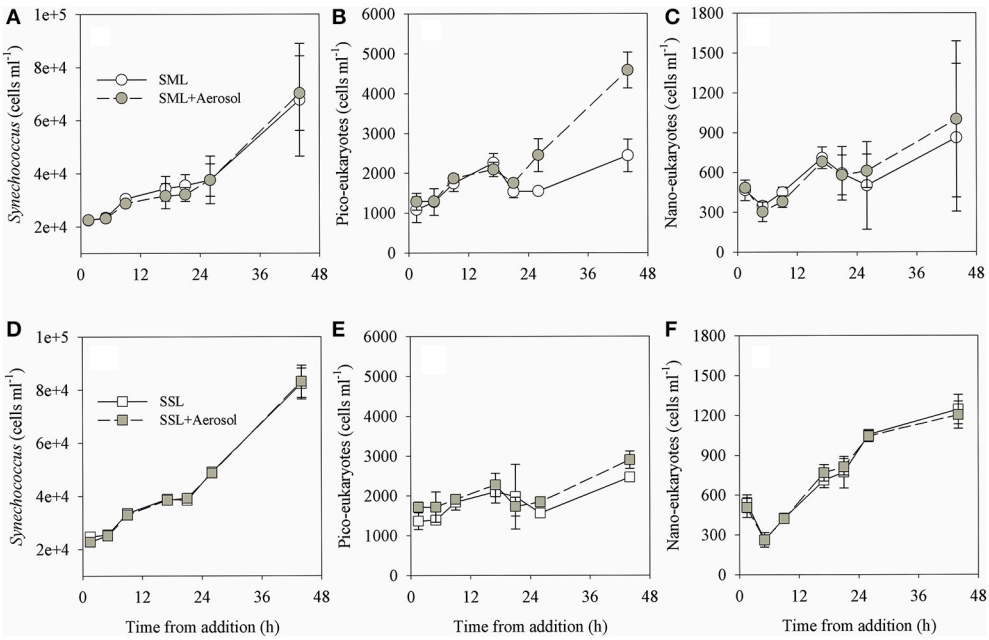

FIGURE 1 | The temporal dynamics of *Synechococcus* (A,D), pico-eukaryotes **(B,E)** and nano-eukaryotes **(C,F)** in the SML (top panels) and SSL (bottom panels) microcosms. Experiments including aerosol additions (1.5 mg L^{-1}) are presented in gray, control experiments (containing no additions) are colored white. Values are the averages and standard deviation from 3 biological replicates ($n = 3$).

TABLE 3 | Summary of the net change (%) observed following aerosol addition (1.5 mg L^{-1}) in the SML and the SSL microcosms relative to unamended controls.

Water sample	Time from aerosol addition (h)	BP	PP	LNA	HNA	*Synechococcus*	pico-eukaryotes	nano-eukaryotes
SML	1.5	126.8	12.2	1.7	87.6	0.6	18.4	3.6
	5	142.6	n.a	49.0	85.5	−1.3	1.1	−12.7
	9	108.9	n.a	16.8	49.2	−5.7	7.3	−15.6
	17	514.6	83.5	−6.8	36.2	−8.0	−7.3	−4.1
	21	643.1	48.6	7.4	40.9	−9.5	13.8	−2.1
	26	757.5	n.a	9.7	14.7	0.0	58.1	21.9
	44	503.3	83.1	20.7	101.8	3.7	87.7	16.0
SSL	1.5	67.3	2.0	−0.1	27.2	−7.8	25.4	−5.7
	5	51.3	n.a	12.6	23.2	−1.3	23.6	−0.5
	9	93.4	n.a	6.5	23.2	−1.9	4.2	−1.1
	17	131.4	72.5	−1.5	49.8	−1.1	8.4	7.7
	21	118.6	50.3	−1.0	31.1	2.2	−12.6	5.2
	26	174.7	n.a	5.6	38.8	−0.8	17.8	−1.1
	44	216.3	60.1	6.8	96.6	1.0	17.7	−3.4

n.a, not available.

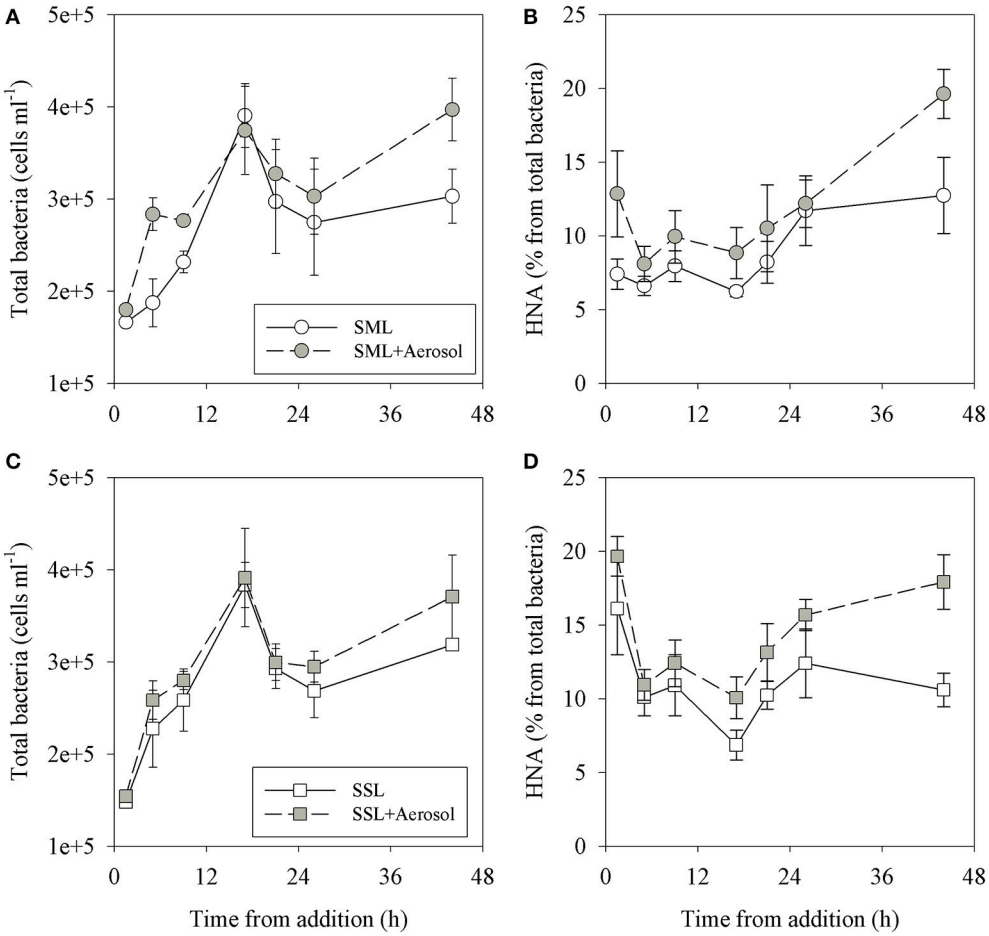

FIGURE 2 | The temporal dynamics of total heterotrophic bacteria (A,C) and the percentage of HNA from the total bacteria **(B,D)** in the SML **(A,B)** and SSL **(C,D)** layers. Experiments including aerosol additions (1.5 mg L^{-1}) are presented in gray, control experiments (containing no additions) are colored white. Values are the averages and standard deviation from 3 biological replicates ($n = 3$).

in the control treatments and the C-rich monosaccharides concentration at the end of the experiment (T44), bacterial activity can account for 2.7 and 2.2 μg C L^{-1} in the SML and SSL unamended microcosms, respectively. Simultaneously, the total consumption of [4,5-^{3}H]-leucine (T44) in the SSL+aerosol can account for 5.4 μg C L^{-1} and up to 15.7 μg C L^{-1} in the SML+aerosol treatments. The concentration (μg/Kg) of hydrocarbons delivered by the aerosol particles only was negligible relative to the ambient concentration in the water.

DISCUSSION

Several studies have examined the effect of dust and aerosols on the marine bacterioplankton biomass and/or activity using model simulations (e.g., Mahowald, 2007; Guieu et al., 2014; Chien et al., 2016) and microcosm/mesocosm bioassays (e.g., Herut et al., 2005; Paytan et al., 2009; Marañón et al., 2010; Guieu et al., 2010; Romero et al., 2011; Rahav et al., 2016a). To the best of our knowledge, none of these studies distinguished between the responses triggered by aerosol additions to the SML and those triggered by such additions to the SSL. In fact, these studies mostly considered the SSL (referred as "surface water" or "surface mixed layer"). Since the SML is the uppermost water layer that interacts with the atmosphere and to which atmospheric particles are directly deposited, its bacteria and plankton (neuston) inhabitants may respond differently than the SSL populations (Cunliffe et al., 2010; Vila-costa et al., 2013). Here we experimentally tested the response of these two water layers to natural dry deposition aerosol addition and compared the responses of the bacterioplankton communities in these two layers at the SEMS.

SML Organic Enrichment

Our measurements demonstrate moderate, yet significant ($P > 0.05$), differences in saccharides and hydrocarbons concentration between the SML and the SSL prior to the aerosol addition, resulting in EF >1 (**Table 1**). Thus, the SML was enriched in dissolved organic carbon, potentially bioavailable for bacterial

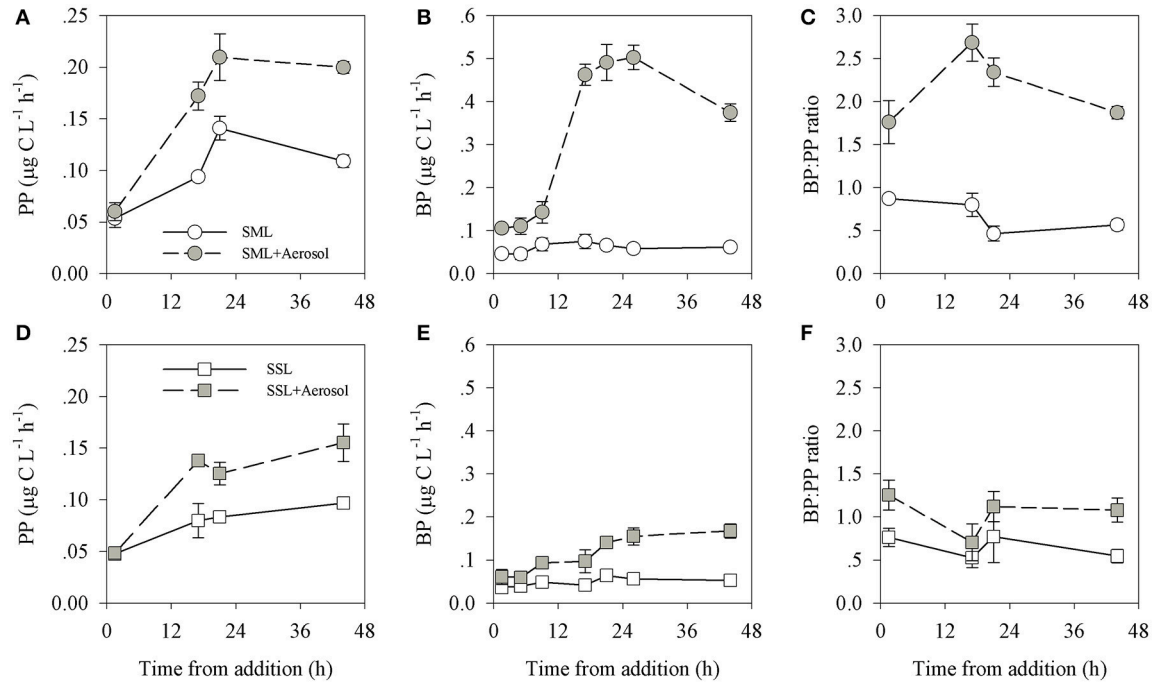

FIGURE 3 | Temporal dynamics of primary production (A,D), bacterial production **(B,E)** and the BP: PP ratio **(C,F)** in the SML **(A–C)** and SSL **(D–F)** layers. Experiments including aerosol additions (1.5 mg L^{-1}) are presented in gray, control experiments (containing no additions) are colored white. Values are the averages and standard deviation from 3 biological replicates ($n = 3$).

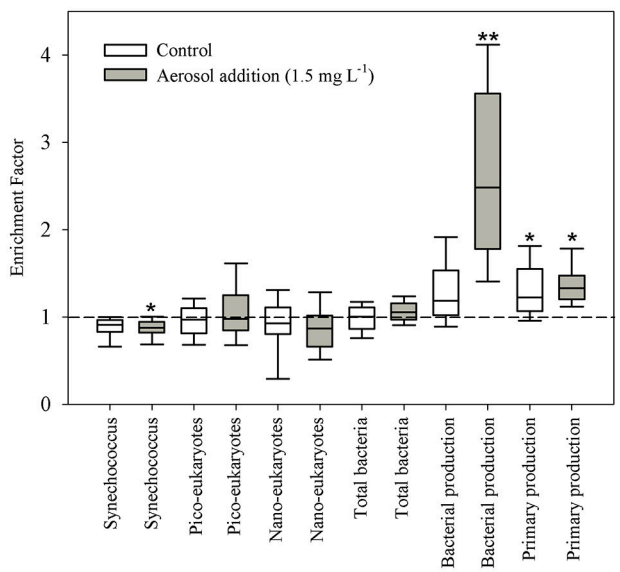

FIGURE 4 | Box-plot distribution of the abundance or activity enrichment factors (SML: SSL ratio). Central line indicates median value. Interquartile box plot of abundance and activity enrichment factors: bottom and top horizontal lines indicate the 10 and 90th percentiles respectively. *$P < 0.05$; **$P < 0.01$.

consumption, as observed in other marine environments (Cincinelli et al., 2001; Guigue et al., 2011; Santos et al., 2011). The major carbon source found in both layers was α-olefins. These hydrocarbons may originate from oil contamination (Riley et al., 1982), phytoplankton (Youngblood and Blumer, 1973) or even aerosol particles downwind to algae bloom (Ovadnevaite et al., 2011). It is possible that in the proximity to Haifa Bay industrial and rural area, aerosol particles, or water runoff could enrich the water with these hydrocarbons. Yet no other sign of such events was observed.

SML Bacterioplankton Enrichment

Heterotrophic bacterial abundances prior to the aerosol addition were similar in the SML and in the underlying SSL water layer (EF ∼1, **Table 2**). These results agree with several studies (Cunliffe et al., 2009, 2010), yet oppose others, which show significantly higher bacterial abundances in the SML (e.g., MacIntyre, 1974; Hardy, 1982). Picophytoplankton abundance at the SML was lower than at the SSL, especially the abundance of pico-eukaryotes (EF < 1). Although studies reported an elevated phyto-neuston abundance relative to the SSL (e.g., Södergren, 1993; Guitart et al., 2013), it is apparent that several eukaryotic phytoplankton species, such as *Chaetoceros*, are less abundant in the SML (Hardy et al., 1984) or are differently effected by high light irradiation levels (Ruiz-González et al., 2012). A low autotrophic abundance in the SML might be explained by the intense radiation levels at this layer (particularly UV), which may cause photo-damage to the cells, especially in environments such as the SEMS in summer where radiation levels may reach >1000 µmol quanta m^{-2} s^{-1} (Dishon et al., 2012).

Activity in the SML and SSL

PP rates were higher at the SML relative to the SSL prior to and after the aerosol addition (**Table 3**, **Figure 3**). In contrast, BP rates were similar in both SML and SSL unamended microcosms and were elevated in both layers following aerosol additions, with a stronger response in the SML+aerosol microcosm. These results reflect higher cell-specific activity (production per cell) in the neuston communities that inhabit the SML relative to the bacterioplankton in the SSL. Relative to the very low concentration of inorganic nutrients characterizing this study area (Azov, 1986; Krom et al., 1991; Yacobi et al., 1995; Raveh et al., 2015), the addition of aerosol leached nutrients (as reported for this aerosol in Rahav et al. (2016b) would result in nearly doubling the levels of nitrate+nitrite (N, ∼550 nM) and in a small increase in phosphorus concentration (P, ∼12 nM). Assuming bacteria in the SEMS as P limited (Krom et al., 2010) and a 10–20 fg C per bacterial cell (Simon and Azam, 1989), the addition of P from the aerosol tested here (using a 106:1 Redfield C:P ratio), could explain an increase in bacterial abundance of up to $\sim 1 \times 10^6$ cells^{-1} mL^{-1}, which is one order of magnitude higher than that measured for both the SML and SSL (net change of $\sim 1 \times 10^5$ cells^{-1} mL^{-1}). It is possible that a great fraction of the added phosphorous was consumed by bacteria cells to fulfill their cellular metabolic needs rather than for growth/cell devision. This is also examplified in the increase in BP rates and the increase in %HNA bacteria following aerosol addition but not in the overall abundance of bacteria (**Figures 2**, **3**). It may also suggest that the added P was taken by other compartments within the food-web (Thingstad et al., 2005; Pitta et al., 2016), or that P is not the limiting nutirent for bacterial activity as recently suggested (Tanaka et al., 2011; Rahav et al., 2016c). Alternativly, phosphorous might have been utilized faster by other microorganisms and transferred through the microbial food web directly to higher trophic levels (e.g., Thingstad et al., 2005), or that heterotrophic bacteria are not primarily limited by this element (e.g., Tanaka et al., 2011; Rahav et al., 2016c). Autotrophic microbes did not exhibit any significant increase in biomass, yet were more active as derived from the elevated PP rate (**Figures 2**, **3**). Further, although relatively higher concentrations of hydrocarbons and saccharides were measured at the SML prior to the aerosol addition (as compared to the SSL), only slightly elevated BP or PP rates were recorded at the SML. Thus, the different carbon concentrations alone cannot explain the elevated BP and PP rates following the aerosol addition. These results are in agreement with a recent study performed in the same area showing a moderate increase in BP rates following the addition of glucose as a single amendment, while a significant enhancement in BP was reached after the addition of glucose, nitrogen and phosphate simultaneously (Rahav et al., 2016c). In addition to the aerosol derived N and P input, other micronutrients from the aerosols may also be limiting factors for microbial activity (e.g., Paytan et al., 2009). Tovar-sánchez et al. (2014) showed that Fe originating from aerosol particles was found to be unevenly distributed between the SML and SSL following a dust storm event. Thus, when considering the results described here and the work presented by Tovar-sánchez and collegues, we assume that aerosol depositions may trigger different impacts in these distinct layers. It is also likely that a high concentration of carbon, along with other aerosol-derived nutrients such as N and P or Fe that are added to a nutrient-poor aquatic system such as the SEMS, may not only alter the total microbial production, but also elevate the activity of specific groups in the SML. The difference in microbial production rates between the SML and SSL measured here are in agreement with a few studies that showed an equal or higher microbial activity in the SML relative to the SSL (e.g., Kuznetsova and Lee, 2001; Obernosterer et al., 2005), yet opposes other studies (Stolle et al., 2009; Santos et al., 2011; Sarmento et al., 2015). It is well-known that diverse bacterial groups have different sensitivities to UV radiation (UVR). SAR11 activity, for example, is known to be inhibited by high UVR, whereas *Gammaproteobacteria* and *Bacteroidetes* show UVR resistance (Alonso-Sáez et al., 2007; Santos et al., 2011). Hence, it is likely that the unique community in the SML in the SEMS is well adapted to the high-light conditions in this environment and can take advantage of the higher carbon and nutrients concentration in the SML, thus grow faster than the SSL microbial communities despite the high radiation. We assume that the bulk microbial activity rate depends on the bacterial species relative abundance, their adaption to the microenvironment and the availability of nutrients in the SML and SSL. The major reduction in dissolved n-alkanes and α-olefins, measured 44 h after the aerosol addition in the SSL and SML, may be attributed to either heterotrophic consumption or adsorption by aerosol particles. So far only a few bacterial strains isolated from polluted aquatic habitats show high uptake rates of α-olefins or alkanes on timescales similar to those examined here (Whyte et al., 1998). Thus, we estimate that in addition to possible heterotrophic utilization of these carbons, the major reduction in soluble alkanes and α-olefins concentration was a result of adsorption to aerosol particles.

Carbons Adsorption to Aerosol Particles

Contrary to alkanes and α-olefins for which concentrations were almost completely reduced following aerosol amendment (T0 vs. T44 h), monosaccharides decreased by only ∼50–60% throughout the experiment's duration (**Table 1**). The monosaccharides' consumption (after 44 h) was almost the same in the SML and the SSL following aerosol additions (∼420 μg L^{-1}), although different initial and end concentrations were recorded in both water layers (**Table 1**). Monosaccharides are considered as the energetically-favored carbon sources for heterotrophic bacterial metabolism (Kirchman, 2012), as opposed to alkanes and α-olefins, which can be utilized only by a few specialized groups (Yakimov et al., 2007; Sevilla et al., 2015). Yet, based on the total leucine C incorporation during the experiment (derived from the BP measurements), less than 10% of the monosaccharides' reduction could be attributed to bacterial consumption in both water layers. We therefore assume that the physical adsorption of saccharides by the aerosol particles was more significant, and accounted for the remaining monosaccharides reduction. Relative to alkanes and α-olefins, monosaccharides are more hydrophilic, we assume that as a result, these saccharides show a reduced adsorption

rate to the surface of the aerosol particles ("preferring" the water phase). Thus, unlike alkanes and α-olefins that are more hydrophobic and were cleared from the soluble fraction following aerosol addition (primarily via adsorption), monosaccharides showed only a low reduction in concentration in the soluble fraction. Considering the abiotic removal via adsorption onto dust particles, a dust storm event such as the one examined here (September 2015), could substantially change the carbons availability to heterotrophic bacteria in the upper water layer and thus shift the PP to BP ratio from being "autotrophic-dominated" to "heterotrophic dominated." Moreover, since considerable amounts of dust and aerosol are usually deposited in the SEMS (Herut et al., 1999, 2002), a chronic adsorption of various carbon substances to aerosol particles and their transfer down the water column may be a mechanism to transfer carbon to the deep water. The different types of carbon containing compounds (polar and hydrophobic) that were possibly adsorbed by the aerosol particles could later be leached off the particles at greater depths such as the deep chlorophyll maxima (usually 100–150 m in the SEMS, Kress et al., 2014) or even at the aphotic layer, thereby contributing to deep-water heterotrophic microbial activity. This adsorption may depend on aerosol concentration, composition, and timing of the deposition, and may thus have significant implications on the microbial loop. This mechanism may contribute to the relatively high metabolic activity of bacteria in the deep waters of the Mediterranean Sea attributed to the relatively warm conditions of this system (Luna et al., 2012). Further work should examine this mechanism of carbon transfer to the aphotic layers, as well as its availability to the subsurface microbial communities in the SEMS.

CONCLUSIONS

We suggest that one of the major differences between the SML and SSL is the higher SML bacterioneuston activity rates that most probably resulted in the higher carbon utilization rate observed. It is possible that in this experiment, the consumption rate of monosaccharides differs between the SML and the SSL, although the same amount was consumed at the experiment end. Vila-costa et al. (2013), who studied freshwater SML's bacteria and archaea communities following two Saharan dust storms, reported that the abundance of these groups did not change significantly following the dust storms. This finding is also supported by other studies in the Mediterranean (e.g., Tovar-sánchez et al., 2014). Yet, Vila Costa's group reported that the composition of these groups was altered following aerosol introduction, resulting in a community shift (Vila-costa et al., 2013). In this study however, we did not characterize bacterial diversity (using molecular approaches such as 16S rRNA or 18S rRNA) and thus we cannot determine whether community shifts occurred following aerosol additions. Nevertheless, the increase in bacterial activity in the SML following aerosol addition and the relative increase in HNA bacterial abundance (**Table 3**), may be an indication of the presence of bacterioneuston that are specifically adapted to take advantage of the constituents supplied by aerosols.

This study demonstrates the opportunistic character of the bacterioneuston community once nutrient-carrying airborne particles are introduced to the SML. Further, studies of the seasonal changes in the biodiversity and physiology of these communities in relation to atmospheric deposition from different sources are needed. Finally, the nature and dynamics of nutrients, metals (and microorganisms) exchange between the SML and SSL is currently unknown and warrants more study. In addition to carbon utilization, physical adsorption of these molecules by the aerosol particles may deliver carbon from the surface into deeper water, from the enriched SML to more oligotrophic layers of the sea.

AUTHOR CONTRIBUTIONS

Conceived and designed the experiment: PA and ER. Performed the experiment: PA and ER. Analyzed the data: PA, AP, BH and ER. Contributed reagents/materials/analysis tools: PA and ER. Wrote the paper: PA, AP, BH and ER.

ACKNOWLEDGMENTS

We would like to thank Lilach Baumer for English editing. This study was supported by a grants awarded by the Ministry of National infrastructures, Energy and Water Resources grants *21317028* to PA, and 3-11519 to ER, by the Ministry of environmental Protection (145–1–2) to ER, by the PERSEUS project's (EC contract 287600) contribution to BH, partially by the ENVIMED MERMEX TRACOMED project's contribution to BH and by the NSF-OCE (grant 0850467) to AP.

SUPPLEMENTARY MATERIAL

The Supplementary Material for this article can be found online at: http://journal.frontiersin.org/article/10.3389/fmars.2016.00222/full#supplementary-material

Supplementary Figure S1 | A three-day back trajectory analysis arriving at 100, 500, and 1000m altitude levels commencing at 10.00 UTC using the HYSPLIT (Hybrid Single-Particle Lagrangian Integrated Trajectory) model from the Air Resources Laboratory. The star represents the study site off the SEMS.

REFERENCES

Alonso-Sáez, L., Arístegui, J., Pinhassi, J., Gómez-Consarnau, L., González, J. M., Vaqué, D., et al. (2007). Bacterial assemblage structure and carbon metabolism along a productivity gradient in the NE Atlantic Ocean. *Aquat. Microbia. Ecol.* 46, 43–53. doi: 10.3354/ame046043

Azov, Y. (1986). Seasonal patterns of phytoplankton productivity and abundance in nearshore oligotrophic waters of the Levant Basin (Mediterranean). *J. Plankton Res.* 8, 41–53. doi: 10.1093/plankt/8.1.41

Bar-zeev, E., and Rahav, E. (2015). Microbial metabolism of transparent exopolymer particles during the summer months along a eutrophic estuary system. *Front. Microbiol.* 6:403. doi: 10.3389/fmicb.2015.00403

Berman, T., Townsend, D. W., ElSayed, S. Z., Trees, C. C., and Azov, Y. (1984). Optical transparency, chlorophyll and primary productivity in the Eastern Mediterranean near the Israeli coast. *Oceanol. Acta* 7, 367–372.

Chien, C.-T., Mackey, K. R. M., Dutkiewicz, S., Mahowald, N. M., Prospero, J. M., and Paytan, A. (2016). Effects of African dust deposition on phytoplankton in the western tropical Atlantic Ocean off Barbados. *Glob. Biogeochem. Cycles* 30, 716–734. doi: 10.1002/2015GB005334

Cincinelli, A., Stortini, A. M., Pergini, M., Checchini, L., and Lepri, L. (2001). Organic pollutants in sea-surface microlayer and aerosol in the coastal environment of Leghorn - (Tyrrhenian Sea). *Mar. Chem.* 76, 77–98. doi: 10.1016/S0304-4203(01)00049-4

Cunliffe, M., Salter, M., Mann, P. J., Whiteley, A. S., Upstill-Goddard, R. C., and Murrell, J. C. (2009). Dissolved organic carbon and bacterial populations in the gelatinous surface microlayer of a Norwegian fjord mesocosm. *FEMS Microbiol. Lett.* 299, 248–254. doi: 10.1111/j.1574-6968.2009.01751.x

Cunliffe, M., Upstill-goddard, R. C., and Murrell, J. C. (2010). Microbiology of aquatic surface microlayers. *FEMS Microbiol. Rev.* 35, 233–246. doi: 10.1111/j.1574-6976.2010.00246.x

Dishon, G., Dubinsky, Z., Caras, T., Rahav, E., Bar-Zeev, E., Tzubery, Y., et al. (2012). Optical habitats of ultraphytoplankton groups in the Gulf of Eilat (Aqaba), Northern Red Sea. *Int. J. Remote Sens.* 33, 2683–2705. doi: 10.1080/01431161.2011.619209

Engel, A., and Galgani, L. (2016). The organic sea-surface microlayer in the upwelling region off the coast of Peru and potential implications for air–sea exchange processes. *Biogeosciences* 13, 989–1007. doi: 10.5194/bg-13-989-2016

Engel, A., Thoms, S., Riebesell, U., Rochelle-Newall, E., and Zondervan, I. (2004). Polysaccharide aggregation as a potential sink of marine dissolved organic carbon. *Nature* 428, 929–932. doi: 10.1038/nature02453

Griffin, D. W. (2010). Atmospheric movement of microorganisms in clouds of desert dust and implications for human health. *Clin. Microbiol. Rev.* 20, 459–477. doi: 10.1128/CMR.00039-06

Grossi, V., Cravo-Laureau, C., Méou, A., Raphel, D., Garzino, F., and Hirschler-Réa, A. (2007). Anaerobic 1-alkene metabolism by the alkane- and alkene-degrading sulfate reducer Desulfatibacillum aliphaticivorans strain CV2803T. *Appl. Environ. Microbiol.* 73, 7882–7890. doi: 10.1128/AEM.01097-07

Guieu, C., Aumont, O., Paytan, A., Bopp, L., Law, C. S., Mahowald, N., et al. (2014). The significance of the episodic nature of atmospheric deposition to Low Nutrient Low Chlorophyll regions. *Glob. Biochem. Cycles* 28, 1179–1198. doi: 10.1002/2014GB004852

Guieu, C., Dulac, F., Desboeufs, K., Wagener, T., Pulido-Villena, E., Grisoni, J. M., et al. (2010). Large clean mesocosms and simulated dust deposition: a new methodology to investigate responses of marine oligotrophic ecosystems to atmospheric inputs. *Biogeosciences* 7, 2765–2784. doi: 10.5194/bg-7-2765-2010

Guigue, C., Tedetti, M., Giorgi, S., and Goutx, M. (2011). Occurrence and distribution of hydrocarbons in the surface microlayer and subsurface water from the urban coastal marine area off Marseilles, Northwestern Mediterranean Sea. *Mar. Pollut. Bull.* 62, 2741–2752. doi: 10.1016/j.marpolbul.2011.09.013

Guitart, C., Murrell, J. C., Cunliffe, M., Engel, A., Frka, S., Salter, M., et al. (2013). Sea surface microlayers: a unified physicochemical and biological perspective of the air – ocean interface. *Progr. Oceanogr.* 109, 104–116. doi: 10.1016/j.pocean.2012.08.004

Hale, M. S., and Mitchell, J. G. (1997). Sea surface microlayer and bacterioneuston spreading dynamics. *Mar. Ecol. Progr. Ser.* 147, 269–276. doi: 10.3354/meps147269

Hardy, J. T. (1982). The sea surface microlayer: biology, chemistry and anthropogenic enrichment. *Progr. Oceanogr.* 11, 307–328. doi: 10.1016/0079-6611(82)90001-5

Hardy, J. T., Apts, C. W., and Marine, B. (1984). The sea-surface microlayer: phytoneuston productivity and effects of atmospheric particulate matter. *Mar. Biol.* 82, 293–300. doi: 10.1007/BF00392409

Harvey, G. (1966). Collection from the sea surface: a new method and initial results. *Limnol. Oceanogr.* 11, 608–613. doi: 10.4319/lo.1966.11.4.0608

Harvey, G. W., and Burzell, L. A. (1972). A simple microlayer method for small samples. *Limnol. Oceanogr.* 17, 156–157. doi: 10.4319/lo.1972.17.1.0156

Herut, B., Collier, R., and Krom, M. D. (2002). The role of dust in supplying nitrogen and phosphorus to the Southeast Mediterranean. *Limnol. Oceanogr.* 47, 870–878. doi: 10.4319/lo.2002.47.3.0870

Herut, B., Krom, M. D., Pan, G., and Mortimer, R. (1999). Atmospheric input of nitrogen and phosphorus to the Southeast Mediterranean: sources, fluxes, and possible impact. *Limnol. Oceanogr.* 44, 1683–1692. doi: 10.4319/lo.1999.44.7.1683

Herut, B., Rahav, E., Tsagaraki, T. M., Giannakourou, A., Tsiola, A., Psarra, S., et al. (2016). The potential impact of Saharan dust and polluted aerosols on microbial populations in the East Mediterranean Sea, an overview of a mesocosm experimental approach. *Front. Mar. Sci.* 3:226. doi: 10.3389/fmars.2016.00226

Herut, B., Zohary, T., Krom, M. D., and Mantoura, R. F. C. (2005). Response of East Mediterranean surface water to Saharan dust: on-board microcosm experiment and field observations. *Deep Sea Res. II* 52, 3024–3040. doi: 10.1016/j.dsr2.2005.09.003

Kirchman, D. L. (2012). *Processes in Microbial Ecology*. New York, NY: Oxford University Press.

Kress, N., Thingstad, T. F., Pitta, P., Psarra, S., Tanaka, T., Zohary, T., et al. (2005). Effect of P and N addition to oligotrophic Eastern Mediterranean waters influenced by near-shore waters: a microcosm experiment. *Deep Sea Res. Part II* 52, 3054–3073.

Kress, N., Gertman, I., and Herut, B. (2014). Temporal evolution of physical and chemical characteristics of the water column in the Easternmost Levantine basin (Eastern Mediterranean Sea) from 2002 to 2010. *J. Mar. Syst.* 135, 6–13. doi: 10.1016/j.jmarsys.2013.11.016

Krom, M. D., Emeis, K.-C., and Van Cappellen, P. (2010). Why is the Eastern Mediterranean phosphorus limited? *Progr. Oceanogr.* 85, 236–244. doi: 10.1016/j.pocean.2010.03.003

Krom, M. D., Kress, N., Brenner, S., and Gordon, L. I. (1991). Phosphorus limitation of primary productivity in the eastern Mediterranean Sea. *Limnol. Oceanogr.* 36, 424–432. doi: 10.4319/lo.1991.36.3.0424

Kuznetsova, M., and Lee, C. (2001). Enhanced extracellular enzymatic peptide hydrolysis in the sea-surface microlayer. *Mar. Chem.* 73, 319–332. doi: 10.1016/S0304-4203(00)00116-X

Lawrence, C. R., and Neff, J. C. (2009). The contemporary physical and chemical flux of aeolian dust: a synthesis of direct measurements of dust deposition. *Chem. Geol.* 267, 46–63. doi: 10.1016/j.chemgeo.2009.02.005

Lebaron, P., Servais, P., Agogué, H., Courties, C., and Joux, F. (2001). Does the high nucleic acid content of individual bacterial cells allow us to discriminate between active cells and inactive cells in aquatic systems? *Appl. Environ. Microbiol.* 67, 1775–1782. doi: 10.1128/AEM.67.4.1775-1782.2001

Liss, P. S., and Duce, R. A. (1997). *The Sea Surface and Global Change*. New York, NY: C*ambridge University Press.*

Luna, G. M., Bianchelli, S., Decembrini, F., De Domenico, E., Danovaro, R., and Dell'Anno, A. (2012). The dark portion of the Mediterranean Sea is a bioreactor of organic matter cycling. *Glob. Biogeochem. Cycles* 26, 1–14. doi: 10.1029/2011GB004168

MacIntyre, F. (1974). The top millimeter of the ocean. *Sci. Am.* 230, 62–77. doi: 10.1038/scientificamerican0574-62

Mahowald, N. M. (2007). Anthropocene changes in desert area: sensitivity to climate model predictions. *Geophys. Res. Lett.* 34, L18817. doi: 10.1029/2007GL030472

Marañón, E., Fernández, A., Mouriño-Carballido, B., MartÍnez-GarcÍa, S., Teira, E., Cermeño, P., et al. (2010). Degree of oligotrophy controls the response of microbial plankton to Saharan dust. *Limnol. Oceanogr.* 55, 2339–2352. doi: 10.4319/lo.2010.55.6.2339

Marty, J. C., and Saliot, A. (1976). Hydrocarbons (normal alkanes) in the surface microlayer of seawater. *Deep Sea Res.* 23, 863–873. doi: 10.1016/0011-7471(76)90853-6

Mouzdahir, A., Grossi, V., Bakkas, S., and Rontani, J.-F. (2001). Visible light-dependent degradation of long-chain alkenes in killed cells of *Emiliania huxleyi* and *Nannochloropsis salina*. *Phytochemistry* 56, 677–684. doi: 10.1016/S0031-9422(00)00468-4

Myklestad, S. M., Skånøy, E., and Hestmann, S. (1997). A sensitive and rapid method for analysis of dissolved mono- and polysaccharides in seawater. *Mar. Chem.* 56, 279–286. doi: 10.1016/S0304-4203(96)00074-6

Nielsen, S. E. (1952). The use of radio-active carbon (C14) for measuring organic production in the sea. *J. Cons. Perm. Ins. Explor. Mer.* 18, 117–140. doi: 10.1093/icesjms/18.2.117

Obernosterer, I., Catala, P., Reinthaler, T., Herndl, G. J., and Lebaron, P. (2005). Enhanced heterotrophic activity in the surface microlayer of the

Mediterranean Sea. *Aquatic Microbial Ecol.* 39, 293–302. doi: 10.3354/ame039293

Ovadnevaite, J., O'Dowd, C., Dall'Osto, M., Ceburnis, D., Worsnop, D. R., and Berresheim, H. (2011). Detecting high contributions of primary organic matter to marine aerosol: a case study. *Geophys. Res. Lett.* 38, L02807. doi: 10.1029/2010GL046083

Passow, U., and Alldredge, A. L. (1994). Distribution, size and bacterial colonization of transparent exopolymer particles (TEP) in the ocean. *Mar. Ecol. Progress Ser.* 113, 185–198. doi: 10.3354/meps113185

Paytan, A., Mackey, K. R. M., Chen, Y., Lima, I. D., Doney, S. C., Mahowald, N., et al. (2009). Toxicity of atmospheric aerosols on marine phytoplankton. *Proc. Natl. Acad. Sci. U.S.A.* 106, 4601–4605. doi: 10.1073/pnas.0811486106

Peter, H., Hörtnagl, P., Reche, I., and Sommaruga, R. (2014). Bacterial diversity and composition during rain events with and without Saharan dust influence reaching a high mountain lake in the Alps. *Environ. Microbiol. Rep.* 6, 618–624. doi: 10.1111/1758-2229.12175

Pitta, P., Nejstgaard, J. C., Tsagaraki, T. M., Zervoudaki, S., Egge, J. K., Frangoulis, C., et al. (2016). Confirming the "Rapid phosphorus transfer from microorganisms to mesozooplankton in the Eastern Mediterranean Sea" scenario through a mesocosm experiment. *J. Plankton Res.* 38, 502–521. doi: 10.1093/plankt/fbw010

Rahav, E., Giannetto, M. J., and Bar-Zeev, E. (2016c). Contribution of mono and polysaccharides to heterotrophic N_2 fixation at the eastern Mediterranean coastline. *Sci. Rep.* 6:27858. doi: 10.1038/srep27858

Rahav, E., Herut, B., Stambler, N., Bar-Zeev, E., Mulholland, M. R., and Berman-frank, I. (2013). Uncoupling between dinitrogen fixation and primary productivity in the eastern Mediterranean Sea. *J. Geophys. Res.* 118, 195–202. doi: 10.1002/jgrg.20023

Rahav, E., Ovadia, G., Paytan, A., and Herut, B. (2016a). Contribution of airborne microbes to bacterial production and N_2 fixation in seawater upon aerosol deposition. *Geophys. Res. Lett.* 43, 719–727. doi: 10.1002/2015GL066898

Rahav, E., Paytan, A., Chien, C.-T., Ovadia, G., Katz, T., and Herut, B. (2016b). The impact of atmospheric dry deposition associated microbes on the Southeastern Mediterranean Sea surface water following an intense dust storm. *Front. Mar. Sci.* 3:127. doi: 10.3389/fmars.2016.00127

Raveh, O., David, N., Rilov, G., and Rahav, E. (2015). The temporal dynamics of coastal phytoplankton and bacterioplankton in the Eastern Mediterranean Sea. *PLoS ONE* 10:e0140690. doi: 10.1371/journal.pone.0140690

Reinthaler, T., Sintes, E., and Herndl, G. J. (2008). Dissolved organic matter and bacterial production and respiration in the sea – surface microlayer of the open Atlantic and the western Mediterranean Sea. *Limnol. Oceanogr.* 53, 122–136. doi: 10.4319/lo.2008.53.1.0122

Ridame, C., Guieu, C., and L'Helguen, S. (2013). Strong stimulation of N_2 fixation in oligotrophic Mediterranean Sea: results from dust addition in large *in situ* mesocosms. *Biogeosciences* 10, 7333–7346. doi: 10.5194/bg-10-7333-2013

Ridame, C., Le Moal, M., Guieu, C., Ternon, E., Biegala, I. C., and Helguen, S. L. (2011). Nutrient control of N_2 fixation in the oligotrophic Mediterranean Sea and the impact of Saharan dust events. *Biogeosciences* 8, 2773–2783. doi: 10.5194/bg-8-2773-2011

Riley, R. G., Garland, T. R., O'Malley, M. L., Mann, D. C., and Wildung, R. E. (1982). 1-Alkenes as potential indicators of sediment shale oil contamination. *Environ. Sci. Technol.* 16, 709–713.

Romero, E., Peters, F., Marrasé, C., Guadayol, Ò., Gasol, J. M., and Weinbauer, M. G. (2011). Coastal Mediterranean plankton stimulation dynamics through a dust storm event: an experimental simulation. *Estuar. Coast. Shelf Sci.* 93, 27–39. doi: 10.1016/j.ecss.2011.03.019

Ruiz-González, C., Lefort, T., Galí, M., Montserrat Sala, M., Sommaruga, R., Simó, R., et al. (2012). Seasonal patterns in the sunlight sensitivity of bacterioplankton from Mediterranean surface coastal waters. *FEMS Microbiol. Ecol.* 79, 661–674. doi: 10.1111/j.1574-6941.2011.01247.x

Santos, L., Santos, A. L., Coelho, F. J. R. C., Gomes, N. C. M., Dias, J. M., Cunha, A., et al. (2011). Relation between bacterial activity in the surface microlayer and estuarine hydrodynamics. *FEMS Microbiol. Ecol.* 77, 636–646. doi: 10.1111/j.1574-6941.2011.01147.x

Sarmento, H., Casamayor, E. O., Auguet, J., Vila-Costa, M., Felip, M., Camarero, L., et al. (2015). Microbial food web components, bulk metabolism, and single-cell physiology of piconeuston in surface microlayers of high-altitude lakes. *Front. Microbiol.* 6:361. doi: 10.3389/fmicb.2015.00361

Sevilla, E., Yuste, L., and Rojo, F. (2015). Marine hydrocarbonoclastic bacteria as whole-cell biosensors for n-alkanes. *Microb. Biotechnol.* 8, 693–706. doi: 10.1111/1751-7915.12286

Simon, M., Alldredge, A. L., and Azam, F. (1990). Bacterial carbon dynamics on marine snow. *Mar. Ecol. Prog. Ser.* 65, 205–211.

Simon, M., and Azam, F. (1989). Protein content and protein synthesis rates of planktonic marine bacteria. *Mar. Ecol. Prog. Ser.* 51, 201–213. doi: 10.3354/meps051201

Södergren, A. (1993). Role of aquatic surface microlayer in the dynamics of nutrients and organic compounds in lakes, with implications for their ecotones. *Hydrobiologia* 251, 217–225. doi: 10.1007/BF00007181

Stolle, C., Nagel, K., Labrenz, M., and Jürgens, K. (2009). Bacterial activity in the sea-surface microlayer : *in situ* investigations in the Baltic Sea and the influence of sampling devices. *Aquatic Microbial Ecol.* 58, 67–78. doi: 10.3354/ame01351

Talarmin, A., Van Wambeke, F., Catala, P., Courties, C., and Lebaron, P. (2011). Flow cytometric assessment of specific leucine incorporation in the open Mediterranean. *Biogeosci.* 8, 253–265. doi: 10.5194/bg-8-253-2011

Tanaka, T., Thingstad, T. F., Christaki, U., Colombet, J., Cornet-Barthaux, V., Courties, C., et al. (2011). Lack of P-limitation of phytoplankton and heterotrophic prokaryotes in surface waters of three anticyclonic eddies in the stratified Mediterranean Sea. *Biogeosci.* 8, 525–538. doi: 10.5194/bg-8-525-2011

Thingstad, T. F., Krom, M. D., Mantoura, R. F. C., Flaten, G. A. F., Groom, S., Herut, B., et al. (2005). Nature of phosphorus limitation in the ultraoligotrophic Eastern Mediterranean. *Science* 309, 1068–1071. doi: 10.1126/science.1112632

Tovar-sánchez, A., Arrieta, J. M., Duarte, C. M., and Sañudo-wilhelmy, S. A. (2014). Spatial gradients in trace metal concentrations in the surface microlayer of the Mediterranean Sea. *Front. Mar. Sci.* 1:79. doi: 10.3389/fmars.2014.00079

Van Wambeke, F., Catala, P., Pujo-Pay, M., and Lebaron, P. (2011). Vertical and longitudinal gradients in HNA-LNA cell abundances and cytometric characteristics in the Mediterranean Sea. *Biogeosciences* 8, 1853–1863. doi: 10.5194/bg-8-1853-2011

Vaulot, D., and Marie, D. (1999). Diel variability of photosynthetic picoplankton in the equatorial Pacific. *J. Geophys. Res. Oceans* 104, 3297–3310. doi: 10.1029/98JC01333

Vila-costa, M., Barberan, A., Auguet, J. C., Sharma, S., Moran, M. A., and Casamayor, E. O. (2013). Bacterial and archaeal community structure in the surface microlayer of high mountain lakes examined under two atmospheric aerosol loading scenarios. *FEMS Microbiol. Ecol.* 84, 387–397. doi: 10.1111/1574-6941.12068

Whyte, L. G., Hawari, J., Zhou, E., Bourbonnie, L. U. C., Inniss, W. E., and Greer, C. W. (1998). Biodegradation of variable-chain-length alkanes at low temperatures by a psychrotrophic *Rhodococcus* sp. *Appl. Environ. Microbiol.* 64, 2578–2584.

Wurl, O., and Holmes, M. (2008). The gelatinous nature of the sea-surface microlayer. *Mar. Chem.* 110, 89–97. doi: 10.1016/j.marchem.2008.02.009

Yacobi, Y. Z., Zohary, T., Kress, N., Hecht, A., Robarts, R. D., Waiser, M., et al. (1995). Chlorophyll distribution throughout the southeastern Mediterranean in relation to the physical structure of the water mass. *J. Mar. Syst.* 6, 179–190. doi: 10.1016/0924-7963(94)00028-A

Yakimov, M. M., Timmis, K. N., and Golyshin, P. N. (2007). Obligate oil-degrading marine bacteria. *Curr. Opin. Biotechnol.* 18, 257–266. doi: 10.1016/j.copbio.2007.04.006

Youngblood, W. W., and Blumer, M. (1973). Alkanes and Alkenes in marine benthic algae. *Mar. Biol.* 21, 163–172. doi: 10.1007/BF00355246

Zohary, T., Herut, B., Krom, M. D., et al. (2005). P-limited bacteria but N and P co-limited phytoplankton in the Eastern Mediterranean - A microcosm experiment. *Deep Sea Research Part II* 52: 3011–3023. doi: 10.1016/j.dsr2.2005.08.011

Conflict of Interest Statement: The authors declare that the research was conducted in the absence of any commercial or financial relationships that could be construed as a potential conflict of interest.

frontiers in Marine Science

ORIGINAL RESEARCH
published: 22 February 2017
doi: 10.3389/fmars.2017.00042

Long Term Flux of Saharan Dust to the Aegean Sea around the Attica Region, Greece

*Vasiliki Vasilatou[1,2], Manousos Manousakas[1], Maria Gini[1], Evangelia Diapouli[1], Michael Scoullos[2] and Konstantinos Eleftheriadis[1]**

[1] Environmental Radioactivity Laboratory, National Centre of Scientific Research "Demokritos," Institute of Nuclear & Radiological Sciences & Technology, Energy & Safety, Agia Paraskevi, Greece, [2] Division III, Environmental Chemistry, Department of Chemistry, University of Athens, Athens, Greece

In this study, Particulate Matter (PM) samples, collected during 2 summer and 2 winter months over a long-term period (1984–2012) at a suburban site in Athens (Greece), were used in order to examine the connection between Sahara dust long range transport events and mass concentrations of the aerosol mineral component, as well as the relative abundance of specific crustal components. As a result, the average deposition flux of dust to the Aegean Sea around the Attica Region, during days with Sahara dust transport events, was calculated. The elemental concentration of aerosol samples was determined by means of ET-AAS, ED-XRF. Mineral dust was chemically reconstructed by using the elemental concentrations of the crustal species based on their common oxides. Two different air mass transport models (HYSPLIT and FLEXTRA) were used for the identification of the days with dust transport events. The dust deposition velocity of the particles was calculated by using Stokes drag law, while the dust deposition flux was calculated taking into account the mean particle size of the aerosol coarse size fraction, which is dominated by the transported crustal component during Sahara dust intrusions. The mineral dust contribution was higher in summer, when dry weather conditions prevail. The Ca/Fe ratio was examined for all years, since this ratio is often used for the identification of Saharan dust events. For the years 1996 and 1998 the Ca/Fe ratio indicates an influence by local urban generated dust. The dust deposition flux per day of a Sahara intrusion event varied from 61 to 199 $\mu g/m^2$ with an average value of 131 $\pm$ 41 $\mu g/m^2$. The total dust deposition over the 4 month measuring period ranged from 237 to 2935 $\mu g/m^2$.

Keywords: surface flux, Sahara dust, elemental composition, deposition, mineral fraction

OPEN ACCESS

Edited by:
Angel Borja, AZTI, Spain

Reviewed by:
Eric Josef Ribeiro Parteli, University of Cologne, Germany
Jose M. Baldasano, Polytechnic University of Catalonia, Spain

****Correspondence:***
Konstantinos Eleftheriadis
eleftheriadis@ipta.demokritos.gr

Specialty section:
This article was submitted to Marine Ecosystem Ecology, a section of the journal Frontiers in Marine Science

Received: *30 September 2016*
Accepted: *06 February 2017*
Published: *22 February 2017*

Citation:
Vasilatou V, Manousakas M, Gini M, Diapouli E, Scoullos M and Eleftheriadis K (2017) Long Term Flux of Saharan Dust to the Aegean Sea around the Attica Region, Greece. Front. Mar. Sci. 4:42. doi: 10.3389/fmars.2017.00042

INTRODUCTION

Dust is primary aerosol arising from mechanical processes and may be generated either naturally or by anthropogenic activities. Natural dust occurs when wind blows over land surfaces, either producing or re-suspending particles, it is mainly coarse in size and dominated by mineral species (silicon, calcium, potassium, magnesium etc.). On the other hand, anthropogenic dust may contain large quantities of carbon and several metals (copper, zinc, iron, magnesium, calcium etc.) contributing to ambient aerosol in both coarse and fine aerosol sizes (Athanasopoulou et al., 2010).

The atmosphere of the Mediterranean region is often affected by long range transport events and aerosol formation through intense photochemical activity (Lazaridis et al., 2005). The aerosols that reach the area originate from areas with different characteristics such as Sahara desert and the industrialized areas of N/NE Europe (Bardouki et al., 2003). Sahara dust transport events frequently occur during spring and autumn, contributing up to 25% of the prevailing air masses which covers Central and Eastern Europe as well as part of the western Turkey (Remoundaki et al., 2011). Annually, 1–3 billion tons of mineral dust is emitted into the atmosphere from arid-semiarid areas and the most important source regions are situated in Northern Africa. Saharan and Sahel sources are responsible for 50–70% of the global dust emission (Escudero et al., 2010; Varga et al., 2014). The increased dust concentrations during heavy dust outbreaks often result in exceedances of the daily PM_{10} limit values set by EU (2008/EC/50) in many countries such as Spain, Italy, and Greece and raise the overall concentration levels of particulate matter (PM) in ambient air (Varga et al., 2014). Dust transport events have been identified as a major type of intense aerosol episodes in the greater Mediterranean basin, accounting for 71.5% of all extreme episodes in the area (Gkikas et al., 2016). Pey et al. (2013) have studied the occurrence of African dust outbreaks in the Mediterranean basin over a 11 year period (2001–2011) and concluded that African dust may be considered the largest PM_{10} source in regional background sites (35–50% of PM_{10}), with peak contributions reaching up to 80% of the PM_{10} mass. According to Querol et al. (2009), African dust contribution to PM_{10} concentrations recorded at regional background sites is higher in the eastern in comparison to the western Mediterranean basin, reaching up to 9–10 $\mu g\ m^{-3}$ on a yearly basis. Similarly, Diapouli et al. (2016) report mean annual African dust contribution to PM_{10} concentrations at urban sites in Southern Europe ranging from 21% (in Athens) to around 2% in the western Mediterranean (Milan, Barcelona, and Porto).

The input of Saharan dust has important effects on the chemistry of the Mediterranean aerosols (Kallos et al., 2006). Depending on the path followed by the air masses, aerosol composition in the different Mediterranean receptor sites may vary (Lazaridis et al., 2006; Semb et al., 2007; Samoli et al., 2011) and have different constituents such as sulfate (Levin et al., 1996) and metals, e.g., Zn, As, and Pb (Sun et al., 2005). For instance, desert dust particles transferred to Barcelona will be probably enriched with elements originating from anthropogenic sources during their path over the Spanish peninsula, compared to dust particles reaching Athens that usually follow a route over the Mediterranean Sea (Samoli et al., 2011).

The Athens Metropolitan area is a large urban center and an important source of anthropogenic pollutants. Athens is located in a climatic sensitive region such as the Mediterranean Sea, where the prevailing air masses may be characterized by diverse aerosol properties such as desert dust from the Sahara and the aged polluted plumes from Western and Eastern Europe (Eleftheriadis et al., 1998, 2014). However, Attica is a peninsula extending into the Aegean Sea and the strong events of dust intrusions observed there, are also characteristic of the surrounding marine area.

The aim of this study was to calculate the average deposition flux of dust to the Aegean Sea around the Attica Region in Greece, during days with Sahara dust transport events. Elemental concentration data from PM samples collected at a suburban site in Athens were used in order to quantify the aerosol mineral component and subsequently the dust deposition flux in the area, during dust transport events. In addition, the relationship between Sahara dust phenomena and the atmospheric concentration of elements such as Calcium and Iron was investigated.

MATERIALS AND METHODS

Sampling

The measurement campaign took place at Demokritos monitoring station which is located at NCSR "Demokritos" campus in Athens, Greece (**Figure 1**). The sampling station is located at the North East corner of the Greater Athens Metropolitan Area in a suburban area on the hillside of Hymettus mountain (270 m a.s.l.) and can be considered as an urban background site (Triantafyllou et al., 2016). The station is away from direct emission sources in a vegetated area (mainly pine trees), partially influenced by the Athens metropolitan area and partially by the incoming air from the North East, which is representative of Regional atmospheric aerosol conditions.

Two long range transport models (HYSPLIT and FLEXTRA) were used to identify the sampling days with Sahara dust events. Only the samples from days with Sahara dust events were used in the current study.

Total Suspended Particles (TSP, Particulate Matter sampled from the ambient air with no threshold in size, except limitations in aspiration efficiency of the sampling head, usually aerodynamic diameters up to 50 μm) samples were collected for many years of the period 1984–2006 (1984, 1986, 1988, 1990, 1992, 1994, 1996, 1998, 2000, 2002, 2006) and specifically during the months January–February for the winter season and June–July for the summer one (4 month sampling period for each year). We consider the measurements for 2011–2012 as 1 year measurements (measurements for the summer period of 2011 and for winter period of 2012). The samples were collected on Whatman 41 cellulose filters, with 47 mm diameter, and by using a low volume sampler with a flow rate of 2.1 m^3/h. In addition, PM_{10} (airborne particles with diameter up 10 μm) samples were collected on PTFE Whatman filters, 47 mm diameter with 1 μm pore size, during summer (June–July) and winter period of 2012 (January–February). The sampler was operating at 23.8 l/min.

All filters were loaded into clean polystyrene Petri dishes after sampling and were stored for subsequent analysis (Manousakas et al., 2013).

Chemical Analyses

Two analytical techniques were used for the elemental analysis of the collected samples, ET-AAS (for the years 1984–1996) and ED-XRF (for the years 1998–2012).

FIGURE 1 | Map of Demokritos station.

Electrothermal Atomic Absorption Spectrometer (ET-AAS)

ET-AAS was used for the determination of the concentration of three elements, Ca, Mg, and Fe (for the years 1984–1996). The instrument used was a Varian 220 spectrometer equipped with a GTA 110 graphite furnace and flame atomic absorption spectrometry. The metal Fe was analyzed using the graphite furnace technique while Mg and Ca were analyzed using flame technique. These metals have been selected because they can be tracers for Saharan dust transport as well as anthropogenic atmospheric pollution. Filter blanks and blank field samples were also prepared and analyzed together with the samples, and the concentrations measured were subtracted from sample measurements (Karanasiou et al., 2005).

Extraction of total metal content was accomplished through microwave assisted digestion of the samples by the use of 2 ml of concentrated HNO_3 65% and 1 ml of HF 40%. All reagents used for the digestion procedures were of analytical grade quality or better (HNO_3 suprapure 65% Merck, HF suprapure 40%Merck; Karanasiou et al., 2005). HNO_3 is usually the first choice for the digestion, because of its strong oxidizing potential. On the other hand, HF has the ability to digest silicon containing compounds (Manousakas et al., 2014). All digestions were performed on a domestic microwave oven. The microwave digestion program settings are presented in **Table 1**. The calibration standards were obtained from Merck and Carlo Erba. Ultrapure water from a Millipore Milli-Q System was used for the preparation of the solutions. Palladium was used as modifier for Pb (as Pd, 10 g/l) and Mg for V [as $Mg(NO_3)_2$, 10 g/l]. For Ca and Mg solutions, La_2O_3 (10% w/v) was added to eliminate interferences, while Caesium Chloride (0.5% w/v) was added to the K solutions. All modifiers were of suprapure grade and were obtained from Merck. Hollow cathode lamps were used as radiation sources for all elements. ET-AAS conditions were carefully optimized for the compensation or elimination of interferences (Karanasiou et al., 2009).

Energy Dispersive X-Ray Fluorescence Spectroscopy (ED-XRF)

The samples of the years 1998–2012 were analyzed for eight elements (Mg, Al, Si, Ca, K, Ti, Fe, Na) by ED-XRF.A secondary target-XRF spectrometer was used (Epsilon 5 by PANanalytical, the Netherlands), which consists of a side-window low power X-ray tube with a W/Sc anode (spot size 1.8–2.1 cm, 100 kV max voltage, 6 mA current, 600 W maximum power consumption). The characteristic X-rays emitted from the sample are detected by a Ge X-ray detector (PAN-32, with 140 eV FWHM at MnKα, 30 mm^2 and 5 mm thick Ge crystal with 8 μm Be window).

For the calibration of the system, both elemental and multi elemental standards were used. In particular, 7 μm thin standards on 6.3 μM (MgF_2, SiO, KCl, CaF_2, Fe, Al, and Zn), and 1 custom made thin target on Kapton (Ti) were used. The calibration was tested using the SRM 2783 by NIST. Each sample was analyzed for 120 min, while laboratory filter blanks were also analyzed to evaluate analytical bias.

Air Mass Trajectories

Two models were used to investigate the transport path of the air masses reaching the sampling site and to identify the sampling days which can be characterized as Sahara dust events: Hybrid Single-Particle Lagrangian Integrated Trajectory model (HYSPLIT; Stein et al., 2015) and FLEXTRA (Stohl et al., 2005). These models simulate the long-range and mesoscale transport of tracers from point or area sources, using interpolated measured

or modeled meteorological fields and accounting for atmospheric processes such as diffusion and dry and wet deposition. They may be used forward in time to simulate the dispersion of tracers from their sources, or backward in time to determine potential source contributions for a given receptor site (Stohl et al., 2005). In the present study, both models were used to gather information about the origin of the observed aerosols. Three dimensional trajectories were computed for the coordinates 38 N, 23.8 E (Demokritos station), at 8:00 and 19:00 UTC by HYSPLIT, and at 0:00, 6:00, 12:00, and 18:00 by FLEXTRA. The calculations by HYSPLIT were made for 300, 700, and 1000 m a.g.l. (above ground level) height and for 180 h backwards, while FLEXTRA model produced 7 day backward air masses trajectories, and at three heights [500, 1000, and 1500 m a.s.l. (above sea level)]. FLEXTRA model can provide information from 1996 onwards. Only African dust transport events verified by both models were identified as such and were used in this study.

Dust Deposition Flux Calculation

Dry deposition refers to the removal of dust particles from the atmosphere in the absence of precipitation. Dry deposition of ambient aerosol particles includes gravitational settling, Brownian diffusion, impaction, and turbulent transfer to the surface (Li et al., 2008; Perez et al., 2011). However, dust particles are in the size range where gravitational settling can be considered as the controlling factor for their deposition velocity (Gao et al., 1997; Schepanski et al., 2009). Gravitational settling is one of the main and most efficient processes of particle removal from the atmospheric environment (Perez et al., 2011). In this study, the dust deposition velocity of the particles was calculated by using Stokes drag law. According to Stokes drag law, the settling of particles is attributed to gravity and the drag forces can be considered as proportional to the relative velocity between particle and fluid, under the assumption that the particles are in spherical shape. The dust deposition velocity (v_d) was defined as:

$$v_d = v_g = \frac{(\rho_p - \rho_a) g d_p^2 C_c}{18 v} \quad (1)$$

Where, v_g is the gravitational settling velocity, d_p is the particle aerodynamic diameter, ρ_a is the air density (g/cm^3), ρ_p is the particle density (g/cm^3), g the gravitational constant (m^3 kg^{-1} s^{-2}), v the air viscosity, and C_c the Cunningham slip correction factor.

As it is presented in Equation (1), the particle density and size are the two key parameters in determining the deposition velocity. When the size distribution of the dust is known, it can be often simulated by a lognormal Gaussian distribution (Eleftheriadis and Colbeck, 2001). The median mass size diameter of the lognormal distribution can be considered as the characteristic parameter to define the mean size of dust particles. In this study, the coarse fraction was approximated as having one mean size, the Mass Median Aerodynamic Diameter (MMAD). As far as for the density of the coarse particles (i.e., dust particles), it can be considered equal to 2.6 g/cm^3 (Schepanski et al., 2009; Chen et al., 2011). However, when the equivalent aerodynamic diameter is used to define the particle size, the density of the particles can be considered equal to 1 g/cm^3.

Then, the dust deposition flux F_d is calculated by multiplying the particle mass concentration C_m by their deposition velocity v_d, as follows (Lin et al., 1994):

$$\mathrm{F_d} = \mathrm{C_m} * \mathrm{V_d} \quad (2)$$

where C_m, is the dust mass concentration in μg/m^3, v_d is the deposition velocity in m/s, and F_d is the flux in μg/m^2/s.

RESULTS AND DISCUSSION

Calculation of Mineral Component

In **Figure 2**, the percentage of the Sahara dust event days (number of event days to total number of sampling days) for the sampling period is presented. According to **Figure 2**, Sahara dust events are more frequent during winter period than during summer period, except for the years 1992 and 2000.

Mineral dust was chemically reconstructed by using the elemental concentrations of the crustal species Al, Si, Ti, and Fe plus non sea salt fraction of Na, Mg, Ca, and K, all multiplied by factors to convert them to their common oxides. More specific soil dust was calculated as: 1.35*Na + 1.66*Mg + 1.89*Al + 2.14*Si + 1.21*K + 1.4 Ca + 1.67*Ti + 1.43*Fe (Nava et al., 2012). Because Al, Si, and Ti concentrations were not determined by ET-AAS, they were estimated from the remaining known mineral components, based on the typical ratios for the site, calculated from XRF measurements. The mean mineral dust contribution during the studied 4 month period ranged from 2 to 13 μg/m^3, with an average value of 8 μg/m^3. The year with the highest mineral dust concentration is 1988 while the lowest is recorded on 1992. Mineral contribution was higher during the summer season, as expected due to drier conditions. The seasonal variability for the different years is presented in **Figure 3**. The intensity of the dust events might also be higher during summer. This is in agreement with other studies (Morales-Baquero et al., 2013).

The Ca/Fe ratio was examined for all years, since this ratio is often used for the identification of Saharan dust events. The typical value of this ratio for Sahara dust identification ranges from 2 to 5 (Guieu et al., 2002; Remoundaki et al., 2011). The average value of the Ca/Fe ratio for all years was 8.5,

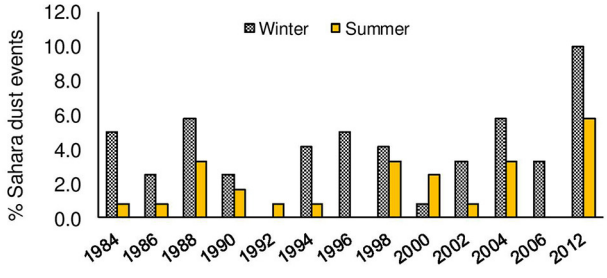

FIGURE 2 | Percentage of Sahara dust event for the two season of the measurement period (1984–2012).

although for most of the years the ratio ranged from 1.5 to 5 (**Figure 4**). Mineral dust concentration is always the product of two different dust sources, transported dust and locally produced or/and resuspended dust. Even though all the samples used in the current study corresponded to days with Sahara dust events, local dust contribution is not always negligible, depending also on the intensity of the dust transport event. The high value of the Ca/Fe ratio for the years 1994 and 1996 indicates higher impact from local soil, which is rich in calcite, as well as from city dust, which often includes Ca-rich dust produced from construction activities (Athanasopoulou et al., 2010). This observation highlights that during days with transport events the contribution from local dust may be equally or even more significant than transported dust, especially during periods with intense construction activity. In these cases, the Ca/Fe ratio may allow us to exclude these data from the long-term impact of the deposited flux to the marine environment. They rather represent the influence of local conditions and dust generation mechanisms.

Total Deposition of Sahara Dust

To calculate the total deposition during the days with Sahara dust events, a mean mass size distribution of ambient aerosol was used, based on size distribution measurements performed in previous studies (Smolık et al., 2003; Athanasopoulou et al., 2010). The measurements for the study of Athanasopoulou et al. (2010) were conducted at the same sampling site, in Ag. Paraskevi, Attica. The measurement campaign in Smolık et al. (2003) took place at the Mediterranean marine background site of Finokalia, Crete. Measurements of size distributions are sparse but the characteristics of dust transport in these cases is very similar. In order to improve the statistics of the most representative size distribution for these dust events, a mean size distribution was calculated from all measurements. The mean distribution was fitted by the sum of log-normal distributions, applying the procedure described by Hussein et al. (2005), also applied in Zwozdziak et al. (2017). The average mass size distribution, normalized by the total mass is presented in **Figure 5**. The size distribution appeared to have two peaks: one in the fine size fraction with Mass Median Aerodynamic Diameter (MMAD) equal to 0.41 μm and standard deviation of 1.47, and one in the coarse size fraction with MMAD equal to 5.00 μm and standard deviation of 2.45. According to the literature in the area (Smolık et al., 2003; Gerasopoulos et al., 2007), the dust mostly contributes to the coarse size fraction, whereas anthropogenic sources mostly contribute to the fine size fraction. Thus, the modal characteristics of the coarse mode were used for the calculation of the dry deposition velocity ($d_p = MMAD$) and dust deposition flux.

The deposition flux was calculated using Equation (2) based on the concentration of the mineral fraction of PM. The dust deposition flux per Sahara day varied from 61 to 199 μg/m^2 with an average value of 131 ± 41 μg/m^2. For most of the years the deposition flux was higher in dry (summer) than in wet period (winter; **Figure 6**). The flux varied from 48 to 1654 μg/m^2/event day in the winter period and from 95 to 364 μg/m^2/event day in summer period. The higher values in the summer period may be expected due to the lack of wet removal process during the long-range transport in the dry period and the additional dust injected locally by resuspension during dry conditions.

Table 2 summarizes the total dust deposition for the winter and summer measuring periods, for every year. The deposition for the 4 months studied period ranged from 237 to 2935 μg/m^2

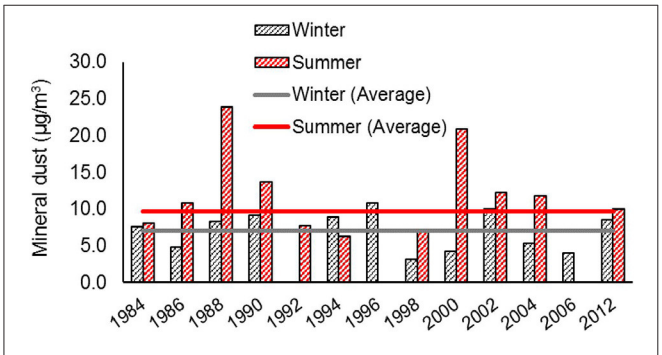

FIGURE 3 | Mineral dust contribution in μg/m^3, for the years 1984–2012 for winter (gray) and summer period (red).

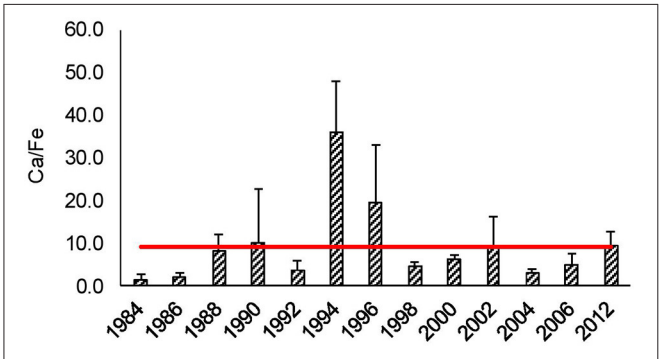

FIGURE 4 | Average Ca/Fe ratio for the years 1984–2012. Red line indicates the mean Ca/Fe ratio.

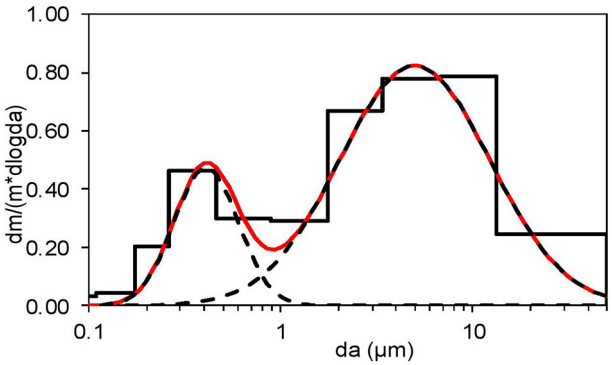

FIGURE 5 | Average mass size distribution of ambient aerosol during Sahara dust events. The mass distribution was normalized by total mass concentration. The red line displays the inverted size distribution assuming a sum of lognormal modes. Black broken line displays these two modes (coarse and fine).

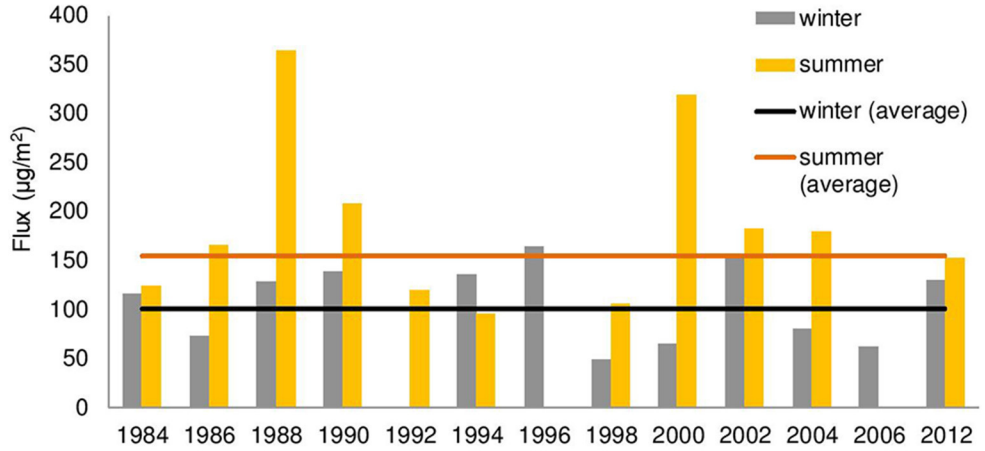

FIGURE 6 | Twenty-four hours dust deposition flux in μg/m^2 for the years 1984–2012 for winter (gray) and summer period (yellow).

TABLE 1 | Program settings of microwave digestion of airborne particulate matter (Karanasiou et al., 2005).

Stage	Power (Watt)	Time (min)
1	300	4
2	450	2
3	600	2

with an average value of 1148 μg/m^2. It is known than in Eastern Mediterranean the maximum of occurrence of Sahara dust event is during spring time (Pey et al., 2013). Therefore, the periods we examine in winter and summer may include only part of the Sahara dust deposition affecting the marine environment annually. From intensive studies where the whole year was examined, we can have a measure of the deposition occurring during the rest of the year. For example for 2013 (Diapouli et al., 2016), the events recorded during January–February and June–July were 30 with a mean 24 h net Saharan dust concentration of 1.8 μg/m^3 while, during the remaining months, 86 events were recorded with a 6.1 μg/m^3 mean net Saharan dust 24 h concentration.

For the years 1996 and 1998 where the Ca/Fe ratio indicates an influence by local urban generated dust, results may not be representative for the deposition in the marine environment.

CONCLUSIONS

In this study, the mineral dust contribution and deposition rate were calculated for Sahara dust event days for a number of years. PM samples were collected during 2 winter and 2 summer months, oven a long-term period (1984–2012). The samples were analyzed for major elements and mineral dust was chemically reconstructed by using the elemental concentrations of the common oxides of the crustal species Al, Si, Ti, and Fe plus non sea salt fraction of Na, Mg, Ca, and K.

TABLE 2 | Total deposition flux of dust in μg/m^2 for the studied winter and summer period of each year.

Year	Season	Deposition (μg/m^2)
1984	Winter	123
	Summer	696
1986	Winter	165
	Summer	219
1988	Winter	1457
	Summer	891
1990	Winter	417
	Summer	417
1992	Winter	118
	Summer	0
1994	Winter	95
	Summer	681
1996	Winter	0
	Summer	989
1998	Winter	423
	Summer	242
2000	Winter	957
	Summer	65
2002	Winter	182
	Summer	608
2004	Winter	716
	Summer	562
2006	Winter	0
	Summer	246
2012	Winter	1070
	Summer	1559

Sahara dust events in the winter period (January–February) are more frequent than in the summer period (June–July) for most of the years of the period under study. However, the mineral dust contribution is higher in summer period because of dry weather conditions which favor the accumulation of dust due to

decreased wet deposition and high resuspension rate. This is an indication that the deposition flux calculated here may be quite representative for the marine environment during winter, while it may be somewhat overestimated for the Saharan dust flux in the marine environment during summer. In addition, the intensity of the dust events might be higher during summer.

The examination of Ca/Fe ratio revealed that occasionally the contribution of local dust may be significant. For instance, the high value of the Ca/Fe ratio for the years 1994 and 1996 indicates higher impact from local soil than from Sahara dust. Local soil is rich in calcite. City dust also, often includes Ca-rich dust produced from construction activities. The flux varied from 48 to 165 $\mu g/m^2$/event day in the winter period and from 95 to 364 $\mu g/m^2$/event day in the summer period. The total dust deposition over the 4 month measuring period ranged from 237 to 2935 $\mu g/m^2$. The year with the highest total dust deposition was 1996 during which the contribution of local dust to the total dust inventory was significant.

According to the results, no clear trend in the annual changes of the number of dust transport events or the dust flux and deposition during the studied period is observed. That fact is another indication that dust transport events are very complex phenomena that are affected by many different factors such as meteorology, which can vary quite significantly every year.

AUTHOR CONTRIBUTIONS

KE, MS, and VV designed the study. VV and MM conducted the trace element analysis performed uncertainty analysis on the data and performed the long range transport study with back trajectory analysis and interpretation. MG provided the size distribution analysis of impactor data evaluated the relevance to Sahara dust and calculated the mean size for deposition calculations. ED evaluated the time series results and assisted with the mass estimation of dust content. KE, VV, and ED edited the manuscript.

ACKNOWLEDGMENTS

This work was funded by EnTeC FP7: Capacities Program (REGPOT -2012-2013-1, FP7, ID:316173).

REFERENCES

Athanasopoulou, E., Tombrou, M., Russel, A. G., Karanasiou, A., Eleftheriadis, K., and Dandou, A. (2010). Implementation of road and soil dust emission parameterizations in the aerosol model CAMx: applications over the greater Athens urban area affected by natural sources. *J. Geophys. Res.* 115:D17301. doi: 10.1029/2009JD013207

Bardouki, H., Liakakou, H., Economou, C., Sciare, J., Smolik, J., Zdimal, V., et al. (2003). Chemical composition of size-resolved atmospheric aerosols in the eastern Mediterranean during summer and winter. *Atmos. Environ.* 37, 195–208. doi: 10.1016/S1352-2310(02)00859-2

Chen, G., Ziemba, L., Chu, D., Thornhill, K., Schuster, G., Winstead, E., et al. (2011). Observations of Saharan dust microphysical and optical properties from the Eastern Atlantic during NAMMA airborne field campaign. *Atmos. Chem. Phys.* 11, 723–740. doi: 10.5194/acp-11-723-2011

Diapouli, E., Manousakas, M., Vratolis, S., Vasilatou, V., Pateraki, S., Bairachtari, K., et al. (2016). Airuse-life+: estimation of natural source contributions to PM_{10} and $PM_{2.5}$ concentration levels in Southern Europe. Implications to compliance with limit values. *Atmos. Chem. Phys. Discuss.* 1–25. doi: 10.5194/acp-2016-781

Eleftheriadis, K., Balis, D., Ziomas, I., Colbeck, I., and Manalis, N. (1998). Atmospheric aerosol and gaseous species in Athens, Greece. *Atmos. Environ.* 32, 2183–2191. doi: 10.1016/S1352-2310(97)00412-3

Eleftheriadis, K., and Colbeck, I. (2001). Coarse atmospheric aerosol: size distributions of trace elements. *Atmos. Environ.* 35, 5321–5330. doi: 10.1016/S1352-2310(01)00304-1

Eleftheriadis, K., Oschenkuhn, K., Lymperopoulou, T., Karanasiou, A., Razos, P., and Ochsenkuhn-Petropoulou, M. (2014). Influence of local and regional sources on the observed spatial and temporal variability of size resolved atmospheric aerosol mass concentrations and water-soluble species in the Athens metropolitan area. *Atmos. Environ.* 97, 252–261. doi: 10.1016/j.atmosenv.2014.08.013

Escudero, M., Stein, A. F., Draxler, R. R., Querol, X., Alastuey, A., Castillo, S., et al. (2010). Source apportionment for African dust over the Western Mediterranean using the HYSPLIT model. *Atmos. Res.* 99, 518–527. doi: 10.1016/j.atmosres.2010.12.002

Gao, Y., Arimoto, R., Duce, R., Zhang, X., Zhang, G., An, Z., et al. (1997). Temporal and spatial distributions of dust and its deposition to the China Sea. *Tellus* 49B, 172–189. doi: 10.3402/tellusb.v49i2.15960

Gerasopoulos, E., Koulouri, E., Kalivitis, N., Kouvarakis, G., Saarikoski, S., Mäkelä, T., et al. (2007). Size-segregated mass distributions of aerosols over Eastern Mediterranean: seasonal variability and comparison with AERONET columnar size-distributions. *Atmos. Chem. Phys.* 7, 2551–2561. doi: 10.5194/acp-7-2551-2007

Gkikas, A., Basart, S., Hatzianastasiou, N., Marinou, E., Amiridis, V., Kazadzis, S., et al. (2016). Mediterranean intense desert dust outbreaks and their vertical structure on remote sensing data. *Atmos. Chem. Phys.* 16, 8609–8642. doi: 10.5194/acp-16-8609-2016

Guieu, C., Loye-Pilot, M. D., Ridame, C., and Thomas, C. (2002). Chemical characterization of the Saharan dust end-member: some biogeochemical implications for the Western Mediterranean Sea. *J. Geophys. Res.* 107, 4258. doi: 10.1029/2001JD000582

Hussein, T., Hameri, K., Aaltoa, P., Paateroa, P., and Kulmala, M. (2005). Modal structure and spatial–temporal variations of urban and suburban aerosols in Helsinki—Finland. *Atmos. Environ.* 39, 1655–1668. doi: 10.1016/j.atmosenv.2004.11.031

Kallos, G., Papadopoulos, A., Katsafados, P., and Nickovic, S. (2006). Transatlantic Saharan dust transport: model simulation and results. *J. Geophys. Res.* 111:D09204. doi: 10.1029/2005JD006207

Karanasiou, A. A., Thomaidis, N. S., Eleftheriadis, K., and Siskos, P. A. (2005). Comparative study of pretreatment methods for the determination of metals in atmospheric aerosol by electrothermal atomic absorption spectrometry. *Talanta* 65, 1196–1202. doi: 10.1016/j.talanta.2004.08.044

Karanasiou, A., Siskos, P., and Eleftheriadis, K. (2009). Assessment of source apportionment by positive matrix factorization analysis on fine and coarse urban aerosol size fractions. *Atmos. Environ.* 43, 3385–3395. doi: 10.1016/j.atmosenv.2009.03.051

Lazaridis, M., Eleftheriadis, K., Smolik, J., Colbeck, I., Kallos, G., Drossinos, Y., et al. (2006). Dynamics of fine particles and photo-oxidants in the Eastern Mediterranean (SUB-AERO). *Atmos. Environ.* 40, 6214–6228. doi: 10.1016/j.atmosenv.2005.06.050

Lazaridis, M., Spyridaki, A., Solberg, S., Smolík, J., Zdímal, V., Eleftheriadis, K., et al. (2005). Mesoscale modeling of combined aerosol and photo-oxidant processes in the Eastern Mediterranean. *Atmos. Chem. Phys.* 5, 927–940. doi: 10.5194/acp-5-927-2005

Levin, Z., Ganor, E., and Gladstein, V. (1996). The effects of desert particles coated with sulfate on rain formation in the Eastern Mediterranean. *J. Appl. Meteorol.* 35, 1511–1523. doi: 10.1175/1520-0450(1996)035<1511:TEODPC>2.0.CO;2

Li, F., Ginoux, P., and Ramaswamy, V. (2008). Distribution, transport, and deposition of mineral dust in the Southern Ocean and Antarctica: contribution of major sources. *J. Geophys. Res.* 113:D10207. doi: 10.1029/2007JD009190

Lin, J. J., Kenneth, E., Noll, T. M., and Holsen, T. N. (1994). Dry deposition velocities as a function of particle size in the ambient atmosphere. *Aerosol Sci. Technol.* 20, 239–252. doi: 10.1080/02786829408959680

Manousakas, M., Eleftheriadis, K., and Papaefthymiou, H. (2013). Characterization of PM_{10} sources and ambient air concentration levels at Megalopolis City (Southern Greece) located in the vicinity of lignite-fired plants. *Aerosol Air Qual. Res.* 13, 804–817. doi: 10.4209/aaqr.2012.09.0239

Manousakas, M., Papaefthymiou, H., Eleftheriadis, K., and Katsanou, K. (2014). Determination of water-soluble and insoluble elements in $PM_{2.5}$ by ICP-MS. *Sci. Total Environ.* 493, 694–700. doi: 10.1016/j.scitotenv.2014.06.043

Morales-Baquero, R., Pulido-Villena, E., and Reche, I. (2013). Chemical signature of Saharan dust on dry and wet atmospheric deposition in the south-western Mediterranean region. *Tellus B: Chem. Phys. Meteorol.* 65, 1–11. doi: 10.3402/tellusb.v65i0.18720

Nava, S., Becagli, S., Calzolai, G., Chiari, M., Lucarelli, F., Prati, P., et al. (2012). Saharan dust impact in central Italy: an overview on three years elemental data records. *Atmos. Environ.* 60, 444–452. doi: 10.1016/j.atmosenv.2012.06.064

Perez, C., Haustein, K., Janjic, Z., Jorba, O., Huneeus, N., Baldasano, J. M., et al. (2011). Atmospheric dust modeling from meso to global scales with the online NMMB/BSC-dust model – part 1: model description, annual simulations and evaluation. *Atmos. Chem. Phys.* 11, 13001–13027. doi: 10.5194/acp-11-13001-2011

Pey, J., Querol, X., Alastuey, A., Forastiere, F., and Stafoggia, M. (2013). African dust outbreaks over the Mediterranean Basin during 2001–2011: PM_{10} concentrations, phenomenology and trends, and its relation with synoptic and mesoscale meteorology. *Atmos. Chem. Phys.* 13, 1395–1410. doi: 10.5194/acp-13-1395-2013

Querol, X., Pey, J., Pandolfi, M., Alastuey, A., Cusack, M., Perez, N., et al. (2009). African dust contributions to mean ambient PM_{10} mass-levels across the Mediterranean Basin. *Atmos. Environ.* 43, 4266–4277. doi: 10.1016/j.atmosenv.2009.06.013

Remoundaki, E., Bourliva, A., Kokkalis, P., Mamouri, R., Papayannis, A., Grigoratos, T., et al. (2011). PM_{10} composition during an intense Saharan dust transport event over Athens (Greece). *Sci. Total Environ.* 409, 4361–4372. doi: 10.1016/j.scitotenv.2011.06.026

Samoli, E., Kougea, E., Kassomenos, P., Analitis, A., and Katsouyanni, K. (2011). Does the presence of desert dust modify the effect of PM_{10} on mortality in Athens. Greece. *Sci. Total Environ.* 409, 2049–2054. doi: 10.1016/j.scitotenv.2011.02.031

Schepanski, K., Tegen, I., and Macke, A. (2009). Saharan dust transport and deposition towards the tropical northern Atlantic. *Atmos. Chem. Phys.* 9, 1173–1189. doi: 10.5194/acp-9-1173-2009

Semb, A., Hanssen, J. E., Francois, F., Maenhaut, W., and Pacyna, J. M. (2007). Long range transport and deposition of mineral matter as a source for base cations. *Water Air Soil Pollut.* 85, 1933–1940. doi: 10.1007/BF01186117

Smolık, J., Zdımal, V., Schwarz, J., Lazaridis, M., Havranek, V., Eleftheriadis, K., et al. (2003). Size resolved mass concentration and elemental composition of atmospheric aerosols over the Eastern Mediterranean area. *Atmos. Chem. Phys.* 3, 2207–2216. doi: 10.5194/acp-3-2207-2003

Stein, A. F., Draxler, R. R., Rolph, G. D., Stunder, B. J. B., Cohen, M. D., and Ngan, F. (2015). NOAA's HYSPLIT atmospheric transport and dispersion modeling system. *Bull. Am. Meteorol. Soc.* 96, 2059–2077. doi: 10.1175/BAMS-D-14-00110.1

Stohl, A., Forster, C., Frank, A., Seibert, P., and Wotawa, G. (2005). Technical note: the Lagrangian particle dispersion model FLEXPART version 6.2. *Atmos. Chem. Phys.* 5, 2461–2474. doi: 10.5194/acp-5-2461-2005

Sun, Y., Zhuang, G., Wang, Y., Zhao, X., Li, J., Wang, Z., et al. (2005). Chemical composition of dust storms in Beijing and implications for the mixing of mineral aerosol with pollution aerosol on the pathway. *J. Geophys. Res.* 110:D24209. doi: 10.1029/2005JD006054

Triantafyllou, E., Diapouli, E., Tsilibari, E. M., Adamopoulos, A. D., Biskos, G., and Eleftheriadis, K. (2016). Assessment of factors influencing PM mass concentration measured by gravimetric & beta attenuation techniques at a suburban site. *Atmos. Environ.* 131, 409–417. doi: 10.1016/j.atmosenv.2016.02.010

Varga, G., Ujvari, G., and Kovacks, J. (2014). Spatiotemporal patterns of Saharan dust outbreaks in the Mediterranean Basin. *Aeolian Res.* 15, 151–160. doi: 10.1016/j.aeolia.2014.06.005

Zwozdziak, A., Gini, M. I., Samek, L., Rogula-Kozlowska, W., Sowka, I., and Eleftheriadis, K. (2017). Implications of the aerosol size distribution modal structure of trace and major elements on human exposure, inhaled dose and relevance to the $PM_{2.5}$ and PM_{10} metrics in a European pollution hotspot urban area. *J. Aerosol. Sci.* 103, 38–52. doi: 10.1016/j.jaerosci.2016.10.004

Conflict of Interest Statement: The authors declare that the research was conducted in the absence of any commercial or financial relationships that could be construed as a potential conflict of interest.

Advantages of publishing in Frontiers

OPEN ACCESS
Articles are free to read, for greatest visibility

COLLABORATIVE PEER-REVIEW
Designed to be rigorous – yet also collaborative, fair and constructive

FAST PUBLICATION
Average 85 days from submission to publication (across all journals)

COPYRIGHT TO AUTHORS
No limit to article distribution and re-use

TRANSPARENT
Editors and reviewers acknowledged by name on published articles

SUPPORT
By our Swiss-based editorial team

IMPACT METRICS
Advanced metrics track your article's impact

GLOBAL SPREAD
5'100'000+ monthly article views and downloads

LOOP RESEARCH NETWORK
Our network increases readership for your article

Frontiers
EPFL Innovation Park, Building I • 1015 Lausanne • Switzerland
Tel +41 21 510 17 00 • Fax +41 21 510 17 01 • info@frontiersin.org
www.frontiersin.org

Find us on